

**DISPERSION AND ABSORPTION PHENOMENA OF  
DIPOLAR LIQUID IN NONPOLAR SOLVENT**

**THE THESIS SUBMITTED FOR THE DEGREE OF DOCTOR  
OF PHILOSOPHY ( SCIENCE ) OF THE  
UNIVERSITY OF NORTH BENGAL**

2007

00000



**ACHINTYA KARMAKAR M. Sc. B. Ed.**

STOCKTAKING-2011

Res. - 537.24  
K18 d

216610  
11 JUN 2009

*Dedicated to my parents*  
*Late Sudhir Chandra Karmakar*  
*&*  
*Smt. Draupadi Karmakar*

## ACKNOWLEDGEMENT

The thesis entitled "Dispersion and absorption phenomena of dipolar liquid in nonpolar solvent" has been submitted to the University of North Bengal for the Ph.D (Sc) degree in Physics under the kind supervision of Dr. Suprakash Acharyya, M.Sc. D.Phil. and Dr. Rabindra Chandra Basak, M.Sc. Ph.D Ex-Reader in Physics of Raiganj College (University College), Raiganj, UttarDinajpur. I am highly grateful to them for their untiring effort to make it success.

I express my heartfelt gratitude to Dr. Koushik Dutta, M.Sc. Ph.D in helping me for his valuable and helpful intellectual suggestions of the thesis works presented.

The author expresses his sincere thanks to Dr. Swapan Kumar Sit, M.Sc. Ph.D, Dr. Nilanjan Ghosh, M.Sc. Ph.D, Sri Uttam Kumar Mitra, M.Sc and Smt. Lipika Dutta, M.Sc. for their involvement in my different publications.

I convey my heartfelt gratitude to all of my family members, my colleagues, friends and well wishers for their encouragement during the progress of the works.

Finally, my deepest thanks to my wife Smt. Anjana Bhadra, M.Sc. B.Ed. and my daughter Manaswita Karmakar (Disha) for their endless support during the work.

*Achintya Karmakar.*

Place: Malda

Date: 16.7.'07

ACHINTYA KARMAKAR M. Sc. (Phys) B. Ed.  
Assistant Head Master  
Malda Umesh Chandra Bastuhara Vidyalaya (HS)  
P.O. & Dist. - Malda

## LIST OF PUBLICATIONS

1. A Karmakar, U K Mitra, K Dutta, S K Sit & S Acharyya, *Indian Journal of Pure & Applied Physics*, **44** 856-866 (2006)
2. K Dutta, A Karmakar, S K Sit & S Acharyya, *Journal of Molecular Liquids*, **128** 161-171 (2006)
3. K Dutta, A Karmakar, Mrs. L Dutta, S K Sit & S Acharyya, *Indian Journal of Pure & Applied Physics*, **40** 801-815 (2002)
4. K Dutta, A Karmakar, S K Sit & S Acharyya, *Indian Journal of Pure & Applied Physics*, **40** 588-596 (2002)
5. N Ghosh, A Karmakar, S K Sit & S Acharyya, *Indian Journal of Pure & Applied Physics*, **38** 574-588 (2000)
6. R C Basak, A Karmakar, S K Sit & S Acharyya, *Indian Journal of Pure & Applied Physics*, **37** 224-233 (1999)
7. A Karmakar, U K Mitra, N Ghosh & S Acharyya, *Indian Journal of Pure & Applied Physics*, (Accepted for publication)

## CONTENTS

<b>Synopsis</b>	..... i-vi
<b>Chapter 1 :</b>	..... 1-33
General introduction and review of the previous works	
1.1. Introduction	
1.2. Dispersion and absorption phenomena in polar non-polar liquid mixture	
1.3. Polarisation	
1.4. Relaxation phenomena	
1.5. The real $\epsilon_{ij}'$ , imaginary $\epsilon_{ij}''$ parts of hf complex relative permittivity $\epsilon_{ij}^*$ and the static permittivity $\epsilon_{oij}$ .	
1.6. Debye equation under static and high frequency (hf) electric field	
1.7. Distribution of relaxation times	
1.8. Macroscopic and microscopic relaxation time	
1.9. Cole – Cole and Cole – Davidson Distribution	
1.10. Debye equation in polar non-polar liquid mixtures	
1.11. Murphy Morgan relation of hf conductivity	
1.12. Onsager's theory under static electric field	
1.13. Kirkwood's theory	
1.14. Frohlich's theory	
1.15. Extrapolation technique	
1.16. Eyring's rate theory	
1.17. Brief review of previous works	
<b>Chapter 2 :</b>	..... 34-54
Scope and objective of the thesis	
2.1. Introduction	
2.2. Debye equation in solution in S.I unit.	
2.3. High frequency complex conductivity, relaxation time and dipole moment.	
2.4. High frequency dielectric susceptibility $\chi_{ij}$	
2.5. Double relaxation phenomena from susceptibility measurement of polar-nonpolar liquid mixture	
2.6. Dipole moment measurement from dielectric susceptibility	
2.7. Material property of relaxation phenomena	
2.8. Substituted polar groups in a dipolar molecule	
2.9. Debye – Pellat's equation	
<b>Chapter 3 :</b>	..... 55-81
Double relaxation phenomena of disubstituted benzenes and anilines in non-polar aprotic solvents under high frequency electric field	
3.1. Introduction	
3.2. Formulations of $c_1$ and $c_2$ for $\tau_1$ and $\tau_2$	

- 3.3. Distribution parameters  $\gamma$  and  $\delta$  related to symmetric and characteristic relaxation times  $\tau_s$  and  $\tau_{cs}$
- 3.4. Theoretical formulation for dipole moments  $\mu_2$  and  $\mu_1$
- 3.5. Dipole moments  $\mu_2$  and  $\mu_1$  from hf conductivity
- 3.6. Results and discussion
- 3.7. Conclusions

**Chapter 4 :**

..... 82-105

Dielectric relaxation of aromatic para substituted derivative polar liquids from dispersion and absorption phenomena under giga hertz electric field

- 4.1. Introduction
- 4.2. Theoretical formulations to measure  $\tau_j$  and  $\mu_j$  of a polar unit
- 4.3. Theoretical formulation of static parameter  $X_{ij}$  to estimate static dipole moment  $\mu_s$
- 4.4. Results and discussion
- 4.5. Conclusions

**Chapter 5 :**

..... 106-129

Dielectric relaxation phenomena of some aprotic polar liquids under giga hertz electric field

- 5.1. Introduction
- 5.2. Symmetric and asymmetric distribution parameters  $\gamma$  and  $\delta$
- 5.3. Dipole moment  $\mu_j$  from susceptibility measurement
- 5.4. Dipole moment  $\mu_j$  from hf conductivity measurement
- 5.5. Results and Discussion
- 5.6. Conclusions

**Chapter 6 :**

..... 130-148

Material properties of dipolar liquid in non-polar solvent through relaxation phenomena under high frequency electric field

- 6.1. Introduction
- 6.2. Theoretical formulations for relaxation times  $\tau_1$ ,  $\tau_2$  and dipole moments  $\mu_1$ ,  $\mu_2$
- 6.3. Results and discussion
- 6.4. Conclusions

**Chapter 7 :**

..... 149-163

Relaxation phenomena in methyl benzenes and ketones from ultra high frequency conductivity

- 7.1. Introduction
- 7.2. High frequency conductivity technique to estimate  $\tau$  and  $\mu$ .
- 7.3. Results and discussion

7.4. Conclusions

**Chapter 8 :**

..... 164-179

High frequency and static relaxation parameters of some polar monosubstituted anilines in benzene.

- 8.1. Introduction
- 8.2. Theoretical formulation to estimate hf dielectric relaxation parameters
- 8.3. Static relaxation parameters
- 8.4. Results and discussion
- 8.5. Conclusions

**Chapter 9 :**

..... 180-199

Structural and associational aspects of dielectropolar straight chain alcohols from relaxation phenomena

- 9.1. Introduction
- 9.2. Static relaxation parameter  $X_{ij}$  and static dipole moment  $\mu_s$
- 9.3. High frequency dipole moment  $\mu_j$  and relaxation time  $\tau_j$
- 9.4. Results and discussion
- 9.5. Conclusions

**Chapter 10 :**

..... 200-206

Summary and conclusions

## Synopsis

The dispersion and absorption phenomena of a polar non-polar liquid mixture consist of variation of  $\epsilon_{ij}'$ ,  $\epsilon_{ij}''$  and  $\epsilon_{oij}$  with the angular frequency  $\omega$  of the applied electric field. This phenomena of liquids and solids represent one of the greatest unresolved problems of physics today. The presence of dispersion and absorption phenomena in the systems under study are related to some form of disorder. There can be no absorption in a perfectly ordered system. Under the alternating electric field in a dipolar liquid molecule each type of polarisation takes some finite time to respond the applied electric field. Thus there exists a considerable lag in the attainment of the equilibrium. This lag in response to the alternation of the applied electric field is commonly known as dielectric relaxation. When the external electric field is withdrawn all types of polarisations decay exponentially with time. The time in which the orientational polarisation is reduced to  $1/e$  times the initial value is called the relaxation time  $\tau$  of a dipolar liquid. In case of static or low frequency electric field all the polarisations are operative. But as the frequency  $\omega$  of the alternating electric field is very high, the polarisation is not able to attain equilibrium before the applied electric field is reversed.

Hence, to study the dielectric dispersion and absorption phenomena in terms of measured dielectric relative permittivities of polar nonpolar liquid mixture under low and high frequency electric fields have attracted the attention of a large number of workers for its wide application in different fields. Scientists are mainly interested to predict shape, size, structure and molecular interaction of the polar molecules. All the information are derived from the relaxation parameters like real  $\epsilon_{ij}'$ , imaginary  $\epsilon_{ij}''$ , parts of complex relative permittivity  $\epsilon_{ij}^*$ , static  $\epsilon_{oij}$  and hf permittivity  $\epsilon_{\infty ij}$  of a dipolar liquid molecule (j) in a nonpolar solvent (i) measured in the effective dispersive region of J-Band ( $\sim 3\text{GHz}$ ), X-Band ( $\sim 10\text{GHz}$ ) and K-Band ( $\sim 24\text{GHz}$ ) electric fields.

These data are generally analysed on the basis of various models like Debye, Kirkwood, Fröhlich, Onsager etc. But Debye and Smyth model is very simpler, straightforward and topical one to apply to almost all rigid non-spherical polar liquid molecules in nonpolar solvents. In such case one polar unit is assumed to be far apart from

the other polar units and remains in the quasi-isolated state to eliminate polar-polar interactions almost completely.

Under the X-Band electric field of nearly 10GHz, the polar molecules are found to absorb electrical energy much more strongly to give rise to what is known as absorption phenomena. Saha et al and Sit et al had already studied the double relaxation phenomena of monosubstituted anilines and benzenes under 9.945 Ghz electric field by their formulations derived within the framework of Debye and Smyth model with the measured permittivities in CGS units to shed more light on the shape, size and structure of the polar molecules. Nowadays it is better to introduce the dielectric terminologies and parameters in terms of SI unit to have a deep insight on the shape, size and structure of the polar molecules. The modern concept to study the dielectric dispersion and absorption phenomena of a polar liquid is to use dimensionless complex relative permittivities. The complex high frequency electrical conductivity  $\sigma_{ij}^*$  of polar nonpolar liquid mixtures is related to  $\sigma_{ij}'$  and  $\sigma_{ij}''$  called the real and imaginary parts of complex conductivity.  $\sigma_{ij}'$  and  $\sigma_{ij}''$  are, however, related to  $\epsilon_{ij}''$  and  $\epsilon_{ij}'$  by the relation  $\sigma_{ij}' = \omega \epsilon_0 \epsilon_{ij}''$  and  $\sigma_{ij}'' = \omega \epsilon_0 \epsilon_{ij}'$  where  $\epsilon_0 =$  absolute permittivity of free space =  $8.854 \times 10^{-12} \text{ F.m}^{-1}$ . The dispersion and absorption phenomena under the heading of relaxation phenomena have already been studied for different polar molecules in terms of hf conductivity measurement to predict the conformational structures and molecular interactions in them.

The author had already applied the dielectric terminologies and parameters to some rigid aromatic molecules like anisidines and toluidines in benzene under X band [9.945 GHz] electric fields at 35°C. The relaxation times  $\tau_j$  and the dipole moments  $\mu_j$  due to rotation of the whole molecules exhibit the rigid nature of the molecules. The molecular associations are supported by the conformational structures of the molecules in which the presence of mesomeric, inductive and electromeric moments are found to play their vital role.

The measured data of  $\epsilon_{ij}'$ ,  $\epsilon_{ij}''$ ,  $\epsilon_{0ij}$  and  $\epsilon_{\infty ij}$  of some straight chain alcohols in solvent benzene at 25°C under 24 GHz electric field were utilised by the author to study the various intra and inter molecular relaxation phenomena. The  $\tau$  of the alcohol molecules were estimated by the slope of the variations  $\sigma_{ij}'' - \sigma_{ij}'$  and also with the ratio of the slopes of the

individual variations of  $\sigma_{ij}''-w_j$  and  $\sigma_{ij}'-w_j$  curves at  $w_j \rightarrow 0$ . In the latter method the polar-polar interactions are fully avoided because here the single polar molecule is surrounded by a large number of solvent molecules.  $\tau_j$ 's from the ratio of the individual slopes at  $w_j \rightarrow 0$  are much more reliable than those of the linear slopes of  $\sigma_{ij}''$  against  $\sigma_{ij}'$  as they are in close agreement with the reported data. The excellent agreement of the measured dipole moment  $\mu_j$ 's in terms of measured  $\tau_j$  and slope  $\beta$  of  $\sigma_{ij}-w_j$  with the reported  $\mu$ 's suggest the basic soundness of the technique of the conductivity measurement used. The polar liquid in a given non-polar solvent behaves as a bound charged species due to polarisation under GHz electric field in order to have very large conductivity  $\sigma_{ij}$  in  $\Omega^{-1}m^{-1}$  for different  $w_j$ 's although they are insulators. The slight disagreement between  $\mu_j$ 's and the theoretical dipole moments  $\mu_{theo}$ 's from the conformational structures reveals the existence of mesomeric, inductive and electromeric effects within the free polar groups attached to the parent molecules. The methodology so far developed is, however, involved with the transfer of bound molecular charges of dipolar molecules in a given solvent.

The author measured the dielectric relaxation time  $\tau_j$  and the hf dipole moment  $\mu_j$  of some dipolar methyl benzenes like toluene; 1,3,5- trimethyl benzene; 1,2,3,4- tetra methyl benzene; 1,2,4,5- tetra methyl benzene; 1,2,3,5- tetra methyl benzene; pentamethyl benzene; trifluoro toluene and p-fluoro toluene in benzene at 25 °C under 9.585 GHz electric field by the conductivity measurement in SI unit. A comparison is made between the hf  $\mu_j$ 's and  $\mu_{theo}$ 's from the available bond angles and bond moments to see the frequency effect on the measured data.

The recent trend is to study the relaxation mechanism of dipolar liquid molecules through hf dielectric orientational susceptibility  $\chi_{ij}^*$  rather than the permittivity  $\epsilon_{ij}^*$  or hf conductivity  $\sigma_{ij}^*$ . The susceptibility parameter is directly linked with the orientational polarisation of the molecule whereas hf or ac conductivity is concerned with the transport of bound molecular charges of the polar species in a non-polar solvent. The susceptibility derived from the measured permittivities of polar non-polar liquid mixtures provides one with only three parameters which are sufficient to predict the relaxation phenomena. The terms are real  $\chi_{ij}' = \epsilon_{ij}' - \epsilon_{\infty ij}$ , imaginary  $\chi_{ij}'' = \epsilon_{ij}''$  parts of complex orientational dielectric susceptibility  $\chi_{ij}^*$  and  $\chi_{oij} = \epsilon_{oij} - \epsilon_{\infty ij}$  is the low frequency dielectric susceptibility which is real.

The simplification in the relaxation formulations could, however, be achieved if the fast polarisation process is excluded. This can be done by working in terms of the orientational hf complex susceptibility  $\chi_{ij}^*$  rather than hf complex permittivity  $\epsilon_{ij}^*$  because,  $\epsilon_{ij}^*$  includes within it all the polarisation processes. The algebra becomes clumsy if the analysis is made in terms of  $\epsilon_{ij}^*$  because  $\epsilon_{\infty ij}$  frequently appears as the subtracted term in the formulations.

Terms corresponding to  $(\epsilon_{ij}' - \epsilon_{\infty ij}) / (\epsilon_{0ij} - \epsilon_{\infty ij})$  and  $\epsilon_{ij}'' / (\epsilon_{0ij} - \epsilon_{\infty ij})$  in Bergmann equations can be replaced by  $\chi_{ij}' / \chi_{0ij}$  and  $\chi_{ij}'' / \chi_{0ij}$  where  $\chi_{0ij}$  is the low frequency susceptibility which is real, appears frequently. The use of  $\chi$ 's forms would simplify the theory considerably. The inclusion of new physical parameters like  $\chi_{ij}$  and its very nature of variations with  $w_j$ 's gives a new insight into the dielectric mechanism involved in the polar liquids.

The present author was, therefore, interested to study some disubstituted benzenes and anilines like o-chloro nitrobenzene; 4-chloro 3 nitro benzotrifluoride; 4-chloro 3-nitro toluene; o-nitro benzo trifluoride; m-nitro benzo trifluoride; 2-chloro 6-methyl aniline; 3-chloro 2-methyl aniline; 3-chloro 4-methyl aniline; 4-chloro 2-methyl aniline and 5-chloro 2-methyl aniline in solvent benzene and carbon tetrachloride at 35 °C under a single high frequency 9.945 GHz electric field. Aniline as well as benzene derivatives are expected to absorb electric energy much more strongly in hf electric field for the presence of their flexible parts such as methyl or other groups attached to the parent molecules. Therefore, they exhibit double relaxation times  $\tau_2$  and  $\tau_1$ . The dipole moments  $\mu_2$  and  $\mu_1$  due to rotations of the whole molecules and the flexible parts were found out. The relaxation time  $\tau_j$ 's are measured from the linear slope of  $\chi_{ij}'' - \chi_{ij}'$  curve as well as from the ratio of the individual slopes of  $\chi_{ij}'' - w_j$  and  $\chi_{ij}' - w_j$  curves at  $w_j \rightarrow 0$ . The hf  $\mu$ 's are then compared with the theoretical dipole moment  $\mu_{\text{theo}}$ 's from the conformational structures.

The corresponding dipole moments  $\mu_2$  and  $\mu_1$  of the whole and the flexible part of the molecule are estimated to compare with the static  $\mu_s$  measured under low frequency electric field and reported  $\mu$ 's. The theoretical dipole moments  $\mu_{\text{theo}}$  is calculated by

applying the vector addition method to the bond moments of the substituent polar groups of the molecules in order to predict their conformational structures.

Thus the subject matter of the thesis is aimed at to study the dispersion and absorption phenomena of polar liquid molecules in different nonpolar solvents under high and low frequency electric field at a single or different temperatures in  $^{\circ}\text{C}$  to predict their conformational structures.

Moreover, the present study through the hf  $\sigma_{ij}$  measurement in terms of modern concept of dielectric terminology and parameter yields the average microscopic  $\tau$  whereas double relaxation phenomena of the molecules offer a better understanding of microscopic as well as macroscopic molecular  $\tau$ . The existence of a double relaxation phenomena reflects the material property of the chemical systems under investigation and is not dependent on the measurement frequency. Likewise, although permittivity and dielectric absorption vary with the frequency, the fundamental dielectric parameters such as dielectric decrement and relaxation time which describe the relaxation properties of the system do not.

Further study of several polar molecules like N,N-dimethyl sulphoxide (DMSO); N,N-dimethyl formamide (DMF); N,N-dimethyl acetamide (DMA) and N,N-diethyl formamide (DEF) in benzene under most effective dispersive region of nearly 10 GHz electric field at 25, 30, 35 and 40  $^{\circ}\text{C}$  for DMSO; 25  $^{\circ}\text{C}$  for DMA and DMF and 30  $^{\circ}\text{C}$  for DEF in terms of orientational susceptibilities  $\chi_{ij}$ 's measured under single frequency electric fields reveals that double relaxation phenomena occurs in them. Also the hf  $\mu_j$  and  $\mu_1$  due to  $\tau_1$  differs from  $\mu_{\text{theo}}$  either by elongation or reduction of bond moments of the substituted polar groups by  $\mu_1/\mu_{\text{theo}}$  in agreement with the measured  $\mu$ 's to take into account of inductive, mesomeric and electromeric effects. Thus the correlation between conformational structures with the observed results increases the scientific contents.

The measured data in terms of  $\epsilon_{ij}'$  and  $\epsilon_{ij}''$  of the complex permittivity  $\epsilon_{ij}^*$  by Dhar et al and Somvanshi et al for some para substituted derivative polar liquid molecules in solvents dioxane and benzene in the temperature range of 17 – 40  $^{\circ}\text{C}$  have been made in terms of modern established symbols of dielectric orientational susceptibilities  $\chi_{ij}'$  and  $\chi_{ij}''$

with weight fraction  $w_j$  in the present study. The Debye-Pellat's equation have been used to find out static  $\epsilon_{0ij}$  and hf  $\epsilon_{\infty ij}$ . They are used in the formulations developed by us to get static dipole moments  $\mu_s$  in order to compare with the  $\mu_1$  and  $\mu_2$  derived from the  $\tau_1$  and  $\tau_2$  by the susceptibility measurements. The information so far gathered is finally compared with  $\mu_{\text{theo}}$ 's in para compounds under considerations.

The analysis of measured data of the polar molecules in terms of dielectric susceptibility  $\chi_{ij}^*$  gives a new dimension and insight into the meaning of the dielectric equations. The errors in estimated  $\tau$ 's and  $\mu$ 's are found to be correct up to  $\pm 10\%$  and  $\pm 5\%$  respectively. A little disagreement between the estimated  $\mu$ 's and the  $\mu_{\text{theo}}$ 's from available bond angles and bond moments suggests the existence of mesomeric, inductive and electromeric effects of the substituent polar groups of the molecules under high and low frequency electric fields.

## *Chapter 1*

### **GENERAL INTRODUCTION AND REVIEW OF THE PREVIOUS WORKS**

## 1.1. Introduction:

The thesis is concerned with the dielectric investigation of nonspherical polar liquid molecules in nonpolar solvents. The principal object of the thesis work is to measure relaxation time  $\tau$ 's, the thermodynamic energy parameters of polar liquids such as free energy of activation  $\Delta F_{\tau}$ , enthalpy of activation  $\Delta H_{\tau}$  and entropy of activation  $\Delta S_{\tau}$  due to dielectric relaxation from the temperature variation of  $\tau_j$ 's and the high frequency (hf) dipole moments  $\mu_j$ 's in terms of measured  $\tau_j$ 's. The  $\mu_1$ ,  $\mu_2$ ,  $\mu_j$ 's and static  $\mu_s$  from the double relaxation method, hf and static or low frequency electric fields are used to arrive at the structural aspects of the polar liquid molecules under investigation.

## 1.2. Dispersion and absorption phenomena of polar nonpolar liquid mixtures:

When a beam of electromagnetic wave propagates through a material medium of a polar-nonpolar liquid mixture, its velocity becomes less than the velocity in vacuum and its intensity gradually decreases as it passes through it. The velocity of the waves varies with the angular frequency  $\omega$  of the waves. As a result the relative permittivity and hence the square of the refractive index of the material changes. This sort of variation is referred to as dispersion. The reduction in the intensity of a beam is partly due to absorption, which goes to generate heat in the medium [1.1]. Let a wave of sinusoidal electric field intensity  $E(t) = E_0 e^{j\omega t}$  pass through a material medium. The electrons of the molecules are displaced from their equilibrium positions. As a result a restoring force  $m\omega_0^2 x$  proportional to the linear displacement  $x$  is called into play. Thus there is a damping force on the electrons. If 'g' represents a damping force per unit mass and per unit velocity, the total damping force for the mass  $m$  of the electron of velocity  $\dot{x}$  is  $mg\dot{x}$ . Thus the equation of motion of the dipole can be written as :

$$m\ddot{x} + mg\dot{x} + m\omega_0^2 x = eE_0 e^{j\omega t} \quad \dots (1.1)$$

The term on the right hand side of Eq. (1.1) is the force on the electron of charge  $e$  and mass  $m$ . Let  $\omega_0$  be the natural frequency of vibration of the electron.

The Eq. (1.1) can be solved by assuming  $x = Ae^{j\omega t}$  and hence  $\dot{x} = Aj\omega e^{j\omega t}$  and  $\ddot{x} = -A\omega^2 e^{j\omega t}$ , where  $j = \sqrt{-1}$  is a complex number.

Hence, Eq. (1.1) becomes,

$$\ddot{x} + g\dot{x} + \omega_0^2 x = \frac{e}{m} E_0 e^{j\omega t} \quad \dots (1.2)$$

$$A[(\omega_0^2 - \omega^2) + jg\omega] = \frac{e}{m} E_0$$

$$A = \frac{\frac{e}{m} E_0}{[(\omega_0^2 - \omega^2) + jg\omega]} \quad \dots (1.3)$$

If  $x$  is the distance of separation between the charges of a molecular dipole we have the oscillating dipole moment  $\mu$  where

$$\mu = x \times e$$

$$\mu = \frac{\frac{e^2}{m} E(t)}{[(\omega_0^2 - \omega^2) + jg\omega]} \quad \dots (1.4)$$

for the sinusoidal electric field of electromagnetic light waves passing through the medium.

If there are  $N_k$  number of electrons per unit volume of the  $k$  th type characterised by the angular frequency  $\omega_k$  and the damping force per unit mass per unit velocity is  $g_k$  then the dipole moment per unit volume is called the polarisation vector  $\vec{P}$  where

$$\vec{P} = \frac{\frac{e^2}{m} \vec{E} \sum N_k}{[(\omega_k^2 - \omega^2) + jg_k \omega]} \quad \dots (1.5)$$

Further more,

$$\vec{D} = \vec{E} + 4\pi\vec{P}$$

$$\epsilon\vec{E} = \vec{E} + 4\pi\vec{P}$$

$$\vec{P} = \frac{\vec{E}}{4\pi} (\epsilon - 1) \quad \dots (1.6)$$

From Eqs. (1.5) and (1.6) ultimately it is found that

$$\begin{aligned} \epsilon &= 1 + 4\pi \frac{e^2}{m} \sum_k \frac{N_k}{[(\omega_k^2 - \omega^2) + jg_k\omega]} \\ &= 1 + 4\pi \frac{e^2}{m} \sum_k \frac{N_k(\omega_k^2 - \omega^2)}{[(\omega_k^2 - \omega^2)^2 + g_k^2\omega^2]} - 4\pi \frac{e^2}{m} j \sum_k \frac{N_k g_k \omega}{[(\omega_k^2 - \omega^2)^2 + g_k^2\omega^2]} \end{aligned} \quad \dots (1.7)$$

Eq. (1.7) shows that the relative permittivity of a medium [here polar liquid (j) in a non-polar solvent (i)] is a complex quantity like

$$\epsilon_{ij}^* = \epsilon'_{ij} - j\epsilon''_{ij} \quad \dots (1.8)$$

and is a function of frequency leading to dispersion and absorption phenomena as well. The variation of real  $\epsilon'_{ij}$  and imaginary  $\epsilon''_{ij}$  parts of the high frequency (hf) complex relative permittivity  $\epsilon_{ij}^*$  as a function of frequency  $\omega$  [1.2] is shown in Fig.1.1.

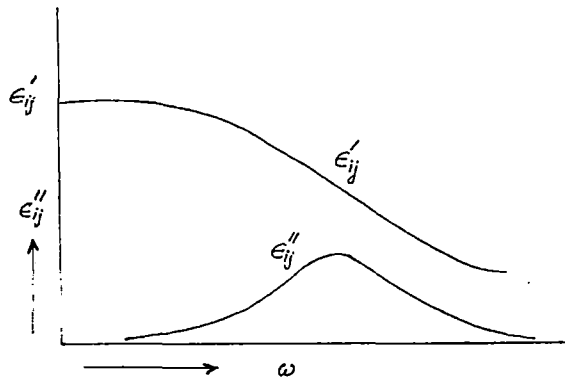


Figure 1.1: Variation of  $\epsilon'$  and  $\epsilon''$  with  $\omega$

Experimentally it is also observed that in some part of the spectrum,  $\epsilon'$  or rather  $n_D^2$  goes on increasing with  $\omega$  and then suddenly drops to a very low value becoming less than unity and begins to increase again. The phenomena of change of  $\epsilon'$  with the frequency is called

the anomalous dispersion. In the region of anomalous dispersion where  $\epsilon''$  goes on increasing and becomes maximum at  $\omega = \omega_0$  giving rise to what is known as absorption of electrical energy of the electromagnetic waves incident on the system of a polar-nonpolar

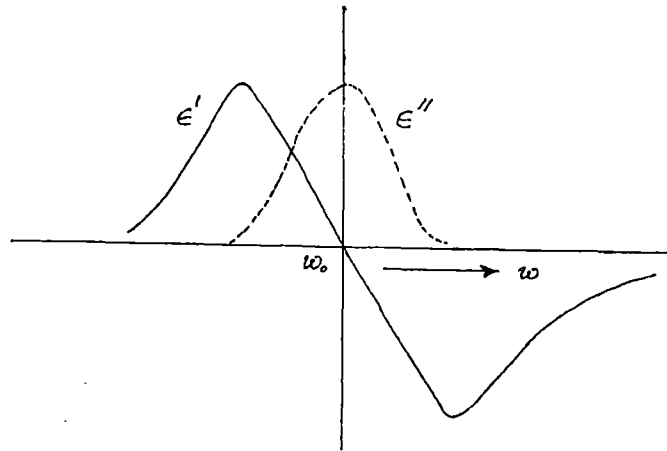


Figure 1.2: Variation of permittivity with angular frequency of electric field

liquid mixture under study is illustrated in Fig. (1.2) by dotted lines. Thus the dispersion and absorption phenomena ultimately yield what is known as the dielectric relaxation processes of polar liquids in non-polar solvents.

### 1.3. Polarisation:

The centres of all the positive and negative charges in each molecule of a substance coincide each other if the substance is a non-polar one. On the other hand, if they do not i.e the centres are separated, it is said to be a polar molecule [1.3]. Under the application of the electric field  $\vec{E}$  these centres get displaced in opposite directions. This sort of relative displacement of the charges for a molecule is called polarisation and the dielectric substance is said to be polarised.

The molecular polarisability  $\alpha$  of a homogeneous or isotropic dielectric is defined as the dielectric polarisation per unit electric field  $\vec{E}$ . The  $\vec{p}$  and  $\vec{E}$  are related as,

$$\bar{p} = \alpha \bar{E} \quad \dots (1.9)$$

In non-polar molecules  $\alpha$  arises in two ways; firstly, due to the displacement of the electrons relative to the nucleus in each atom which is known as electronic polarisation and secondly, for the displacement of the atomic nuclei relative to each other giving rise to the atomic polarisation.

Permanent dipoles of the polar liquid molecules align along the direction of the applied electric field despite the presence of the thermal motions. The polarisation appears is known as orientation polarisation. The total polarisability  $\alpha_T$  of a molecule is finally given by:

$$\begin{aligned} \alpha_T &= \alpha_e + \alpha_a + \alpha_o \\ &= \alpha_d + \alpha_o \end{aligned} \quad \dots (1.10)$$

where  $\alpha_e$ ,  $\alpha_a$  and  $\alpha_o$  are the electronic, atomic and orientation polarisability respectively.  $\alpha_d$  of Eq.(1.10) which is the sum of  $\alpha_e$  and  $\alpha_a$  is called the distortion polarisation.

#### 1.4. Relaxation phenomena:

The polar liquids in non-polar solvents when placed under a hf electric field of frequency in giga hertz (GHz) range the polar units rotate in addition to their thermal agitations and hence the system is not a stable or perfect one. Dielectric relaxation is, therefore, related to some form of disorder present in the systems. There is no relaxation in a perfectly ordered system because nothing can relax from the perfection.

If a polar compound is placed under the alternating electric field, the molecules become polarised. Various types of polarisations are operating in the molecule. Each type of polarisation takes some time to respond to the applied alternating electric field. The considerable lag in response occurs in the attainment of the equilibrium. This lag in response due to the alternations of the applied electric field is commonly known as dielectric relaxation. The external electric field when switched off, all types of polarisations

including the orientation polarisation decay exponentially with time. The time required in which the orientation polarisation is reduced to  $1/e$  times its initial value is known as the relaxation time  $\tau$  of the polar liquid molecule. Under the static or low frequency electric field all types of polarisation exist where as in case of hf electric field all the polarisations do not attain the equilibrium before the electric field is reversed. The dipole moment  $\mu$  of the polar liquid molecule is obtained from the measured  $\tau$  under a hf electric field. Thus  $\tau$  becomes an important molecular parameter in getting the shape, size and structure of the highly non-spherical molecules.

### 1.5. The real $\epsilon_{ij}'$ and imaginary $\epsilon_{ij}''$ parts of hf complex relative permittivity $\epsilon_{ij}^*$ and the static permittivity $\epsilon_{oij}$ :

The force between the two electric charges in a dielectric medium placed at certain distance apart depends upon the medium. The parameter of the medium, arising out of the calculation of forces between two electrical charges of polar molecule is called the static permittivity  $\epsilon_0$  of the medium. If two charges of a polar molecule are placed in a homogeneous or isotropic medium, the forces is, however, reduced by a dimensionless scalar factor  $\epsilon_r$  called the relative dielectric permittivity.  $\epsilon_r$  is the ratio of the capacitances of the condenser, if two charged plates of opposite signs are filled up with dielectric medium and the vacuum respectively i.e,

$$\epsilon_r = \frac{C_m}{C_{vac}} \quad \dots (1.11)$$

Under static electric field there is no absorption of electrical energy and therefore the electric displacement vector  $\vec{D}$  is related to the electric field  $\vec{E}$  by the relation  $\vec{D} = \epsilon \vec{E}$ . When an alternating electric field of  $\vec{E} = \vec{E}_0 \cos \omega t$  is applied on the dielectric material there is always a dissipation of energy due to the absorption of electromagnetic waves. This phenomenon is known as the 'dielectric loss'. A difference of phase between  $\vec{D}$  and  $\vec{E}$  occurs due to various reasons such as

- i) electrical conduction,
- ii) the relaxation effect due to permanent dipoles and

- iii) the resonance effect due to vibration or rotation of atoms, ions or electrons of the dielectric material.

The absorption of energy prompts us to assume the  $\vec{E}$  and  $\vec{D}$  as follows:

$$\begin{aligned}\vec{E} &= \vec{E}_0 e^{j\omega t} \\ \vec{D} &= \vec{D}_0 e^{j(\omega t - \delta)}\end{aligned}$$

where  $\delta$  is the phase difference between  $\vec{E}$  and  $\vec{D}$ ,  $\omega = 2\pi f$ ,  $f$  being the frequency of the applied electric field.

The dielectric response of a system is described by the complex relative permittivity  $\epsilon^*(\omega)$  at the frequency  $\omega$ :

$$\begin{aligned}\epsilon^*(\omega) &= \frac{\vec{D}}{\vec{E}} \\ \epsilon^*(\omega) &= \frac{\vec{D}_0}{\vec{E}_0} (\cos \delta - j \sin \delta) \\ \epsilon^*(\omega) &= \epsilon'(\omega) - j\epsilon''(\omega) \quad \dots (1.12)\end{aligned}$$

where  $\epsilon'(\omega)$  and  $\epsilon''(\omega)$  are the real and imaginary parts of high frequency (hf) complex permittivity  $\epsilon^*(\omega)$ . When a polar liquid (j) is dissolved in nonpolar solvent (i) then the static, real and imaginary parts of permittivities can be expressed respectively as  $\epsilon_{0ij}$ ,  $\epsilon_{ij}'$  and  $\epsilon_{ij}''$ .

### 1.6. Debye equation under static and high frequency (hf) electric field:

The molecular polarisability  $\alpha_d$  of nonpolar molecules due to distortion polarisation does not depend on temperature whereas in case of a polar molecule the orientation polarisation occurs in addition to the distortion polarisation. The polar molecule has a permanent dipole moment  $\vec{\mu}_p$  which is randomly directed due to the thermal agitation resulting out of the net moment to be equal to zero.

Under the application of the electric field the permanent dipole of a polar molecule orients itself along the applied electric field direction. Subsequently, an equilibrium is reached to yield the orientation polarisation  $\bar{P}_o$  which is inversely proportional to the absolute temperature T K. It can be shown that:

$$\begin{aligned}\bar{P}_o &= \frac{n\mu_p^2\bar{E}_{loc}}{3k_B T} \\ &= n\alpha_p\bar{E}_{loc}\end{aligned}\quad \dots (1.13)$$

where  $\alpha_p = \frac{\mu_p^2}{3k_B T}$  is defined as the effective orientation polarisability. Therefore, the total polarisability in case of polar liquid molecule is

$$\begin{aligned}\alpha_T &= \alpha_a + \alpha_e + \frac{\mu_p^2}{3k_B T} \\ \alpha_T &= \alpha_d + \frac{\mu_p^2}{3k_B T}\end{aligned}\quad \dots (1.14)$$

Here  $\alpha_d$  is the polarisability due to distortion polarisation. Thus the Clausius-Mossotti [1.4,1.5] equation becomes:

$$\frac{\epsilon_r - 1}{\epsilon_r + 2} \frac{M}{\rho} = \frac{4}{3} \pi N \left( \alpha_d + \frac{\mu_p^2}{3k_B T} \right) \quad \dots (1.15)$$

The above equation (1.15) is the famous Debye equation [1.3] for polar molecules under static electric field.

In a hf electric field molar polarisation of a dielectric material if expressed in terms of  $\epsilon^*(\omega)$ , the Clausius-Mossotti equation can be written as,

$$\frac{\varepsilon^*(\omega) - 1}{\varepsilon^*(\omega) + 2} \frac{M}{\rho} = \frac{4}{3} \pi N \left( \alpha_d + \frac{\mu_p^2}{3k_B T} \frac{1}{1 + j\omega\tau} \right) \quad \text{..... (1.16)}$$

Now introducing the static and optical relative permittivities  $\varepsilon_0$  and  $\varepsilon_\infty$ , Eq. (1.15) becomes:

$$\frac{\varepsilon_0 - 1}{\varepsilon_0 + 2} \frac{M}{\rho} = \frac{4}{3} \pi N \left( \alpha_d + \frac{\mu^2}{3k_B T} \right) \quad \text{..... (1.17)}$$

and

$$\frac{\varepsilon_\infty - 1}{\varepsilon_\infty + 2} \frac{M}{\rho} = \frac{4}{3} \pi N \alpha_d \quad \text{..... (1.18)}$$

Substituting Eq. (1.17) and (1.18), the Eq. (1.16) can be written as ,

$$\frac{\varepsilon^*(\omega) - 1}{\varepsilon^*(\omega) + 2} = \frac{\varepsilon_\infty - 1}{\varepsilon_\infty + 2} + \left( \frac{\varepsilon_0 - 1}{\varepsilon_0 + 2} - \frac{\varepsilon_\infty - 1}{\varepsilon_\infty + 2} \right) \frac{1}{j\omega\tau} \quad \text{..... (1.19)}$$

The above equation when separated in real and imaginary parts  $\varepsilon'(\omega)$  and  $\varepsilon''(\omega)$  of  $\varepsilon^*(\omega)$  one can obtain,

$$\varepsilon'(\omega) = \varepsilon_\infty + \frac{\varepsilon_0 - \varepsilon_\infty}{1 + x^2} \quad \text{..... (1.20)}$$

$$\varepsilon''(\omega) = \frac{\varepsilon_0 - \varepsilon_\infty}{1 + x^2} x \quad \text{..... (1.21)}$$

where  $x = \frac{\varepsilon_0 + 2}{\varepsilon_\infty + 2} \omega\tau$

The Eqs. (1.20) and (1.21) are the Debye equations under hf electric field.

### 1.7. Distribution of relaxation time:

The dipolar relations are to be satisfied by experimental results according to Cole-Cole [1.6] and Cole-Davidson [1.7]. The experimental curves for most of liquids deviates from the simple Debye curve [1.3]. In addition to Debye semi-circular arc, three types of behaviours were found for different dielectric liquids. A circular arc [1.6] with centre lying below the abscissa as shown in Fig. 1.3 exhibits symmetric distribution of relaxation times.

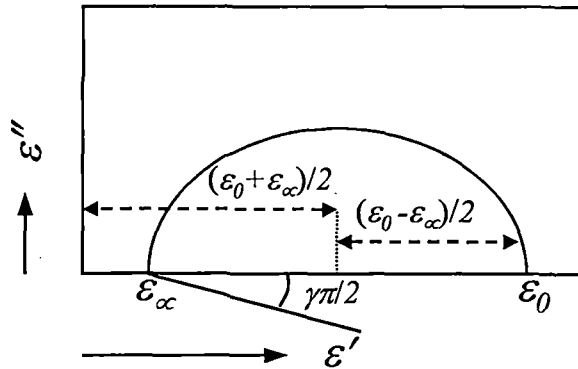


Figure 1.3: Cole-Cole Plot.

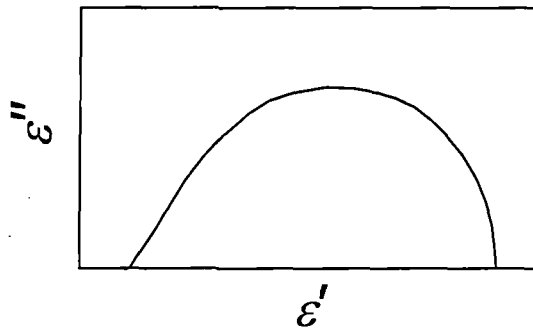


Figure 1.4: Davidson - Cole plot

However, an asymmetric distribution of relaxation times as shown in Fig. 1.4 gives the skewed arc [1.7, 1.8]. A curve is supposed to be made up of a number of Debye semi-circular arc with multiple relaxation times are displayed in Fig.1.5 to understand the asymmetric distribution of relaxation behaviour. Debye equation can also be written for such distribution of relaxation times.

$$\epsilon^* = \epsilon_\infty + (\epsilon_0 - \epsilon_\infty) \int_0^\infty \frac{G(\tau) d\tau}{1 + j\omega\tau} \quad \dots (1.22)$$

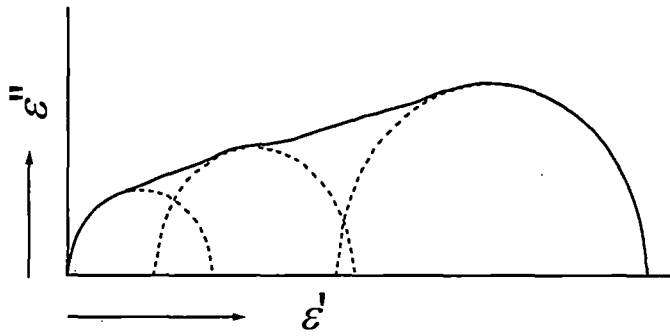


Figure 1.5: Plot of  $\epsilon''$  against  $\epsilon'$  for a number of Debye semicircular arc with multiple relaxation.

where  $G(\tau)d\tau$  is the function of the molecules associated with relaxation times between  $\tau$  and  $\tau+d\tau$  such that the normalisation condition for the distribution function  $G(\tau)$  is

$$\int_0^{\infty} G(\tau)d\tau = 1 \quad \dots (1.23)$$

Now separating the real and imaginary parts of Eq. (1.22) we get,

$$\epsilon' = \epsilon_{\infty} + (\epsilon_0 - \epsilon_{\infty}) \int_0^{\infty} \frac{G(\tau)d\tau}{1 + \omega^2\tau^2} \quad \dots (1.24)$$

$$\epsilon'' = (\epsilon_0 - \epsilon_{\infty}) \int_0^{\infty} \frac{\omega\tau G(\tau)d\tau}{1 + \omega^2\tau^2} \quad \dots (1.25)$$

as Debye equations.

### 1.8. Macroscopic and microscopic relaxation times:

Under the application of the constant alternating electric field an equilibrium is attained with time by the decay function  $f(t)$  where

$$f(t) \propto e^{-t/\tau} \quad \dots (1.26)$$

Here the relaxation time  $\tau$  is a temperature dependent parameter which does not depend on time. If  $E(t)$  is a time dependent electric field and  $E(x)$  is a field which is applied during a time interval  $x$  and  $x+dx$ , the corresponding electric displacement vector  $D(t)$  is written as:

$$D(t) = \epsilon_{\infty} E(t) + \int_{-\infty}^t E(u) f(t-u) du \quad \dots (1.27)$$

The first term on the right hand side of Eq. (1.27) is the instantaneous displacement while the second term is due to absorption of the electric energy by the material.

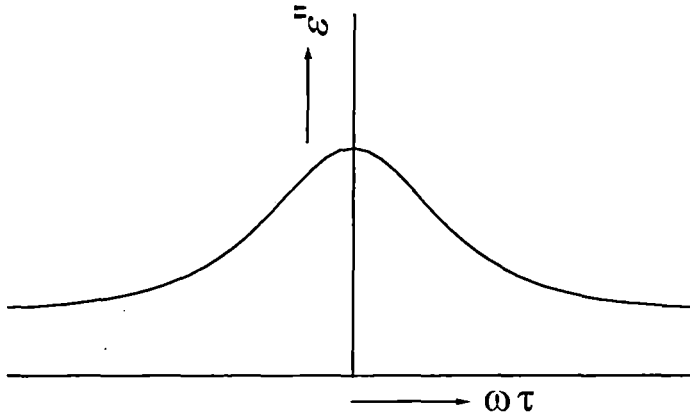


Figure 1.6: Variation of  $\epsilon''$  with  $\omega\tau$

The above equation is simplified by Fröhlich [1.9] as follows:

$$\epsilon^* = \epsilon_{\infty} + \frac{\epsilon_0 - \epsilon_{\infty}}{1 + j\omega\tau} \quad \dots (1.28)$$

Separation of real and imaginary parts results,

$$\frac{\epsilon' - \epsilon_{\infty}}{\epsilon_0 - \epsilon_{\infty}} = \frac{1}{1 + \omega^2\tau^2} \quad \dots (1.29)$$

$$\frac{\varepsilon''}{\varepsilon_0 - \varepsilon_\infty} = \frac{\omega\tau}{1 + \omega^2\tau^2} \quad \dots (1.30)$$

It is evident from Eq.(1.30) that imaginary  $\varepsilon''$  has a maximum value for  $\omega\tau=1$  and approaches zero for both small and high values of  $\omega\tau$  as depicted in Fig. 1.6. The variation

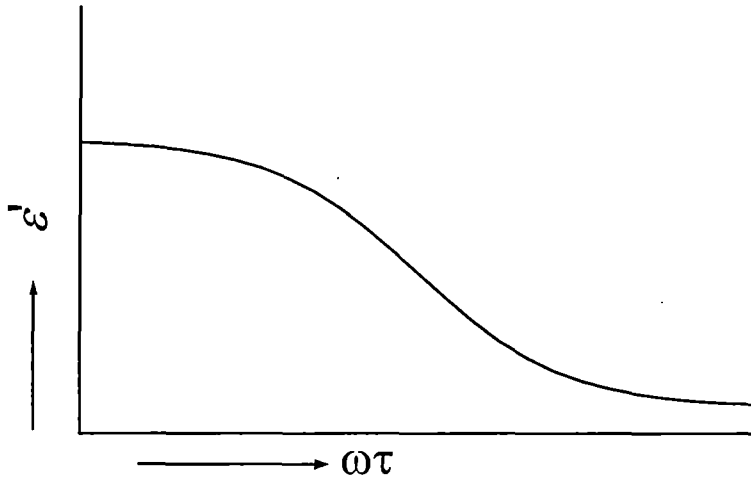


Figure 1.7: Variation of  $\varepsilon'$  with  $\omega\tau$

of  $\varepsilon'$  with  $\omega\tau$  is shown in Fig. 1.7. The Eqs. (1.29) and (1.30) differ from Debye equations (1.24) and (1.25) which contains the quantity  $\tau_0(\varepsilon_0+2)/(\varepsilon_\infty+2)$  instead of  $\tau$ . Comparison of two equations a relation between macroscopic relaxation time  $\tau$  and microscopic relaxation time  $\tau_0$  is obtained as:

$$\tau = \frac{\varepsilon_0 + 2}{\varepsilon_\infty + 2} \tau_0 \quad \dots (1.31)$$

Moreover, the elimination of  $\omega\tau$  from Eqs. (1.29) and (1.30) results,

$$\left( \varepsilon' - \frac{\varepsilon_0 + \varepsilon_\infty}{2} \right)^2 + \varepsilon''^2 = \left( \frac{\varepsilon_0 - \varepsilon_\infty}{2} \right)^2 \quad \dots (1.32)$$

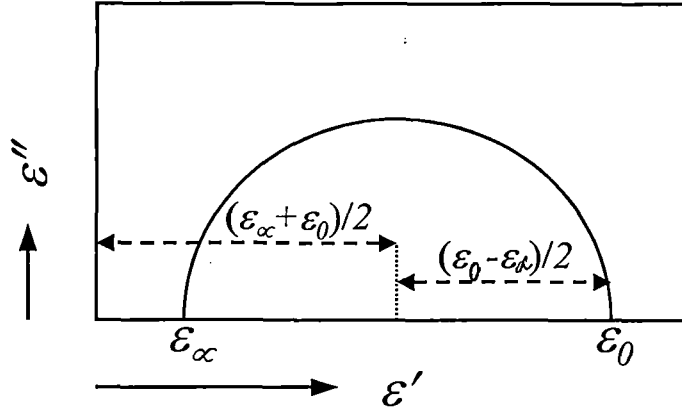


Figure 1.8: Variation of  $\epsilon''$  with  $\epsilon'$  for different angular frequency  $\omega$  (Debye semi-circle)

A plot of  $\epsilon''$  is drawn against  $\epsilon'$  representing the semicircular arc of radius  $(\epsilon_0 - \epsilon_\infty)/2$  and centre lying on abscissa at a distance  $(\epsilon_0 + \epsilon_\infty) / 2$  from the origin as illustrated in Fig. 1.8. This semi-circular arc intersects the abscissa at  $\epsilon' = \epsilon_\infty$  and  $\epsilon' = \epsilon_0$  and is known as the Debye semicircles.

### 1.9. Cole – Cole and Cole – Davidson Distribution:

The behaviour of a dielectric cannot be described by single relaxation time. For a large number of liquid dielectrics the experimental curves deviate from Debye curve showing broader dispersion and lower maximum loss. This is confirmed by Fig. 1.10. Cole – Cole [1.6] plot of  $\epsilon''$  against  $\epsilon'$  for a dielectric material at different frequencies in complex plane shows the relaxation time distribution to be a semi-circular arc. This curve intersects the abscissa axis at two points  $\epsilon_\infty$  and  $\epsilon_0$  and the centre of the semicircle lies below the abscissa axis as evident from Fig.1.11. The radius of the semicircle makes an angle  $\gamma\pi/2$  with  $\epsilon'$  axis where  $\gamma$  is called the symmetric distribution parameter. The modified version of the Cole – Cole of Debye formula is given by,

$$\frac{\epsilon^* - \epsilon_\infty}{\epsilon_0 - \epsilon_\infty} = \frac{1}{1 + (j\omega\tau_s)^{1-\gamma}} \quad \dots (1.33)$$

From Cole – Cole distribution curve of Fig. 1.3 it is observed that the curve is symmetrical about a parallel line of the  $\epsilon''$  axis. However, a skewed arc was obtained by Cole and Davidson [1.7-1.8] by plotting  $\epsilon''$  against  $\epsilon'$  for certain dielectric materials as depicted in Fig. 1.4. The behaviour is represented by the empirical relation:

$$\frac{\epsilon^* - \epsilon_\infty}{\epsilon_0 - \epsilon_\infty} = \frac{1}{(1 + j\omega\tau_{cs})^\delta} \quad \dots (1.34)$$

where  $\delta$  is a asymmetric distribution parameter ( $0 < \delta \leq 1$ ) and is related to characteristic relaxation time  $\tau_{cs}$  of the dipolar molecule.

#### 1.10. Debye equation in polar-nonpolar liquid mixtures:

In pure polar liquids, one polar molecule is surrounded by a large number of similar polar molecules and as a result there exists the polar-nonpolar interactions between the molecules. If one makes a solution of polar liquid in a nonpolar solvent the polar-polar interaction among the molecules is minimised. Again for small concentrations the dissolved dipolar molecules will be far apart on the average from the other similar molecules and thus the interaction of the polar molecule with the surrounding nonpolar molecules of the solvent may occur.

Let a polar liquid (j) is dissolved in a nonpolar solvent (i). Also let  $\alpha_i$  and  $\alpha_j$  be the polarisabilities of solvent and solute of molecular weight  $M_i$  and  $M_j$  respectively. If  $\epsilon_{ij}$  be the relative permittivity of the liquid mixture then Debye equation [1.3] for polar nonpolar liquid mixture is:

$$\begin{aligned} \frac{\epsilon_{ij} - 1}{\epsilon_{ij} + 2} \frac{M_i f_i + M_j f_j}{\rho_{ij}} &= \frac{4\pi N}{3} \left[ \alpha_i f_i + \alpha_j f_j + \frac{\mu_s^2}{3k_B T} f_j \right] \\ &= \frac{4\pi N \alpha_i}{3} + \frac{4\pi N}{3} \frac{\mu_s^2}{3k_B T} f_j \quad \dots (1.35) \end{aligned}$$

$f_i$  and  $f_j$  being the mole fractions of the solvent and solute and these are defined as

$$f_i = \frac{n_i}{n_i + n_j} \quad ; \quad f_j = \frac{n_j}{n_i + n_j}$$

where  $n_i$  and  $n_j$  represent the number of molecules present in 1 cc and  $\alpha_i = \alpha_j$ .

Now Eq. (1.35) becomes:

$$\frac{\epsilon_{ij} - 1}{\epsilon_{ij} + 2} V_{ij} = \frac{\epsilon_i - 1}{\epsilon_i + 2} V_i + \frac{4\pi N}{3} \frac{\mu_s^2}{3k_B T} f_j \quad \dots (1.36)$$

$V_i$  and  $V_{ij}$  of the above equation are the specific volumes of the solvent and solution respectively.

If  $n_{Dij}$  is the refractive index, then for the neutral dielectrics one can have  $\epsilon_{\infty ij} = n_{Dij}^2$ .

With the above substitution the Eq. (1.36) can be written as:

$$\frac{n_{Dij}^2 - 1}{n_{Dij}^2 + 2} V_{ij} = \frac{n_{Di}^2 - 1}{n_{Di}^2 + 2} V_i \quad \dots (1.37)$$

The Eqs. (1.36) and (1.37) when rearranged one gets:

$$\left( \frac{\epsilon_{ij} - 1}{\epsilon_{ij} + 2} - \frac{n_{Dij}^2 - 1}{n_{Dij}^2 + 2} \right) = \left( \frac{\epsilon_i - 1}{\epsilon_i + 2} - \frac{n_{Di}^2 - 1}{n_{Di}^2 + 2} \right) \frac{V_i}{V_{ij}} + \frac{4\pi N}{3} \frac{\mu_s^2}{3k_B T} \frac{f_j}{V_{ij}} \quad \dots (1.38)$$

The above equation can be used to measure the dipole moment of a dipolar liquid by treating it a solute in a solution.

Now if  $C_j$  be the molar concentration i.e.,  $C_j = f_j/V_{ij}$  and for extremely dilute solution  $V_i/V_{ij} \rightarrow 1$ , the Eq. (1.38) can be written as:



216610  
11 JUN 2009

$$\left( \frac{\epsilon_{ij} - 1}{\epsilon_{ij} + 2} - \frac{n_{Dij}^2 - 1}{n_{Dij}^2 + 2} \right) = \left( \frac{\epsilon_i - 1}{\epsilon_i + 2} - \frac{n_{Di}^2 - 1}{n_{Di}^2 + 2} \right) + \frac{4\pi N \mu_s^2}{9k_B T} c_j \quad \dots (1.39)$$

The Eq. (1.39) is an important equation and can be used to determine the static dipole moment  $\mu_s$  of dipolar liquid molecule at infinite dilution. The Eq. (1.39) is known as Debye equation for a polar-nonpolar liquid mixture in cgs units i.e, in Debye units.

### 1.11. Murphy Morgan relation of high frequency (hf) conductivity:

The experimental determination of absorption in a dielectric material is a measure of energy dissipation of electrical energy in a medium. In practice, most systems show energy loss from the process other than dielectric relaxation. Generally these are of smaller in magnitude and related to the d.c conductivity of the medium. If  $\epsilon''$  is a loss factor due to conductivity then at a particular frequency total dielectric loss is:

$$\epsilon''(\text{total}) = \epsilon''(\text{dielectric}) + \epsilon''(\text{conduc tan ce}) \quad \dots (1.40)$$

In an ideal dielectric there would be no free ion conduction, but in actual insulating material Joule heating effect may be developed by the drift of free electrons and ions by the electric field. Therefore, the total heat developed is the sum of dielectric loss and Joule heat.

If a potential  $V$  is established between the parallel plates of condenser having a dielectric material of constant  $\epsilon$  and  $d$  is the distance of separation between the plates of surface area  $A$ , then a charge  $q$  per unit area will appear on each plate and polarisation  $P$  will also be created in the dielectric. If it is assumed that the conductivity due to free ions is of negligible amount, then the conductivity is

$$\sigma = \frac{1}{E} \frac{dq}{dt} \quad \dots (1.41)$$

Where  $E = \frac{V}{d} = \frac{D}{\epsilon}$

Again,  $D = 4\pi q = E + 4\pi p$  and the Eq. (1.41) becomes,

$$\sigma E = \frac{dq}{dt} = \frac{1}{4\pi} \frac{dD}{dt} = \frac{\epsilon}{4\pi d} \frac{dV}{dt}$$

Here, all the parameters are expressed in esu .

If the applied potential is alternating ie,  $V = V_0 e^{j\omega t}$ , the dielectric permittivity is a complex quantity  $\epsilon^*$  where

$$\epsilon^* = \epsilon' - j\epsilon''$$

Now the total current density in the dielectric is,

$$\begin{aligned} I &= \frac{dq}{dt} = \frac{\epsilon^*}{4\pi d} \frac{dV_0 e^{j\omega t}}{dt} \\ &= \frac{\epsilon' - j\epsilon''}{4\pi} \left( j\omega \frac{V_0}{d} e^{j\omega t} \right) \\ I &= \left( \frac{\omega\epsilon''}{4\pi} + j \frac{\omega\epsilon'}{4\pi} \right) E_0 e^{j\omega t} \end{aligned} \quad \dots (1.42)$$

where  $E_0 = V_0/d$

The total current density in the dielectric is the sum of capacitive current and conduction current ie,

$$I = I_{\text{displacement}} + I_{\text{conduction}} \quad \dots (1.43)$$

Murphy and Morgan [1.10] in 1939 deduced an expression of total conductivity  $\sigma^*$  which is a complex quantity and sum of the conductivities due to displacement current  $\sigma''$  and the conduction current  $\sigma'$ .

Therefore,

$$\sigma^* = \sigma' + j\sigma'' \quad \dots (1.44)$$

Comparing Eqs. (1.42) and (1.44) we have:

$$\sigma' = \frac{\omega \varepsilon''}{4\pi} \quad \dots (1.45)$$

and

$$\sigma'' = \frac{\omega \varepsilon'}{4\pi} \quad \dots (1.46)$$

where  $\sigma'$  and  $\sigma''$  are the real and imaginary parts of hf complex conductivity  $\sigma^*$  respectively.

### 1.12. Onsager's theory under static electric field:

Onsager [1.11] considered the polar liquid as a possible dipole at the centre of a spherical cavity of molecular dimensions surrounded by nonpolar medium. If  $\vec{G}$  and  $\vec{R}$  be the cavity field arising out of the external charges and the cavity field arises due to polarisation of the environment medium by the field of dipole then

$$\vec{G} = \frac{3\varepsilon_0}{2\varepsilon_0 + 1} \vec{E} \quad \dots (1.47)$$

$$\vec{R} = \frac{2(\varepsilon_0 - 1)}{(2\varepsilon_0 + 1)a^3} \vec{\mu} \quad \dots (1.48)$$

where 'a' is the radius of the spherical cavity. Thus the total field acting upon spherical polar molecule in a polarised dielectric medium is given by:

$$\begin{aligned} \vec{F} &= \vec{G} + \vec{R} \\ &= \frac{3\varepsilon_0}{2\varepsilon_0 + 1} \vec{E} + \frac{2(\varepsilon_0 - 1)}{(2\varepsilon_0 + 1)a^3} \vec{\mu} \end{aligned} \quad \dots (1.49)$$

Onsager equation for static dielectric constant in case of polar liquids is thus obtained in the following form:

$$\frac{\epsilon_0 - 1}{\epsilon_0 + 2} - \frac{\epsilon_\infty - 1}{\epsilon_\infty + 2} = \frac{\rho}{M} \left( \frac{3\epsilon_0(\epsilon_\infty + 2)}{(2\epsilon_0 + \epsilon_\infty)(\epsilon_0 + 2)} \right) \frac{4\pi N\mu^2}{9k_B T} \quad \dots (1.50)$$

This equation becomes Debye equation when the factor  $\frac{3\epsilon_0(\epsilon_\infty + 2)}{(2\epsilon_0 + \epsilon_\infty)(\epsilon_0 + 2)}$  approaches to unity as  $\epsilon_0$  tends to  $\epsilon_\infty$  for infinitely dilute polar solute in a nonpolar solvent.

The approximate validity of Onsager's Eq. (1.50) is found in case of a large number of unassociated liquids, but the experimental results deviate largely from the theoretical ones for associated liquids like water, alcohols and liquid ammonia. The discrepancies can be interpreted by the following reasons,

- (i) In associated liquids short-range forces arise due to ordered array of neighbouring molecules.
- (ii) Molecules should be spherical in form.
- (iii) The environment of the molecule is treated as homogeneous continuum and the local saturation effects are neglected.

### 1.13. Kirkwood's theory:

The effect of the short range forces was first considered by Kirkwood [1.12] by taking into account the sum of the molecular dipole moment and the moment induced as a result of hindered rotation in the spherical region surrounding the molecules. Kirkwood has derived the following relation:

$$\frac{\epsilon_0 - 1}{\epsilon_0 + 2} - \frac{\epsilon_\infty - 1}{\epsilon_\infty + 2} = \frac{\rho}{M} \left( \frac{3\epsilon_0(\epsilon_\infty + 2)}{(2\epsilon_0 + \epsilon_\infty)(\epsilon_0 + 2)} \right) \frac{4\pi N\mu^2}{9k_B T} g \quad \dots (1.51)$$

where 'g' is a correlation parameter which characterises the inter molecular interactions and short range forces. Kirkwood has pointed out the departure of g from unity and is a measure of hindered relative molecular rotation arising from the short range and intermolecular forces. Thus the unassociated liquids show the value of g approximately equal to unity, while for associated liquids, the g's are far away from unity. Moreover, like Onsager's equation the Kirkwood's equation also contains the approximation involved in treating the polar molecules as a spherical one.

### 1.14. Fröhlich's theory:

Kirkwood's theory has been modified by Fröhlich [1.9] by considering a dipolar dielectric with a number of polarisable units of the same kind within a large spherical region. Each unit has various dipole moment  $\bar{\mu}$  in different directions due to thermal fluctuations with a certain probability. The average moment  $\bar{\mu}^*$  due to such unit within the spherical region is different from  $\bar{\mu}$  because of the short-range interactions between the polarisable units and the deviation of the shape of the molecules from a sphere. An equation for low intensity field has been derived as:

$$\epsilon_o - 1 = \frac{3\epsilon_o}{2\epsilon_o + 1} \frac{4\pi N_o}{3} \frac{\bar{\mu}\bar{\mu}^*}{k_B T} \quad \dots (1.52)$$

where  $N_o$  = number of units per unit volume. The difficulties in Fröhlich's theory are associated with the evaluation of energy of the interaction of the sample with the surrounding medium.

However, as indicated above there are experimental limitations in determining the required parameters involved in various theories lead to Onsager's equation for unassociated liquids when short range forces are absent. So one can use Onsager equation for analysing the experimental data to determine the dipole moment of a polar liquid.

### 1.15. Extrapolation technique:

Large number of workers used the extrapolation technique of different dielectric relaxation parameters for the measurement of dipole moment  $\mu_j$  of a dipolar liquid molecule at infinite dilution. The methods suggested by Hedestrand [1.13], Cohen Henrique [1.14] and Le Fevre [1.15] had some inherent uncertainties in the calculation of  $(\delta\rho_{ij}/\delta x_j)_{x_j \rightarrow 0}$  and  $(\delta n_{Dij}/\delta x_j)_{x_j \rightarrow 0}$  by graphical extrapolation technique.

Higasi [1.16] measured  $\mu_j$  of different polar nonpolar liquid mixtures from the empirical formula of  $\mu_j$  where

$$\mu_j = \beta \left( \frac{\Delta \epsilon}{x_j} \right)^{1/2} \quad \dots (1.53)$$

In Eq. (1.53)  $\Delta \epsilon = \epsilon_{ij} - \epsilon_i$  and the constant  $\beta$  depends upon the solvent used. Guggenheim [1.17], on the other hand, introduced fictitious atomic polarisability to make the solution free from atomic polarisation. The simpler method suggested is to calculate  $\mu_j$  in which the need for measuring densities of liquid mixtures was not necessary. The slope of straight-line equation drawn by experimental parameter  $\frac{3(\epsilon_{ij} - n_{Dij}^2)}{(\epsilon_{ij} + 2)(n_{Dij}^2 + 2)}$  against mole fraction  $C_j$  gave

$\mu_j$  of dipolar liquid molecule dissolved in nonpolar solvent. The quantity  $\Delta$  which is equal to  $[(\epsilon_{ij} - n_{Dij}^2) - (\epsilon_i - n_{Di}^2)]$  was found from the extrapolated value of  $\Delta/C_j$  at infinite dilution to calculate  $\mu_j$  from the following relation,

$$\mu_j^2 = \frac{9k_B T}{4\pi N} \frac{3}{(\epsilon_i + 2)(n_{Di}^2 + 2)} \left( \frac{\Delta}{c_j} \right)_{c_j \rightarrow 0} \quad \dots (1.54)$$

In the mean time many workers suggested different methods to calculate  $\mu_j$  by smoothing the experimental data extrapolated to infinite dilution. Smith [1.18] following Guggenheim [1.17] subsequently introduced the concept of weight fraction  $w_j$  instead of  $C_j$  where,

$$c_j = \frac{\rho_{ij}}{M_j} w_j \quad \dots (1.55)$$

Guggenheim, later on, accepted the idea of extrapolation technique of other workers [1.17, 1.20, 1.21] to modify the Eq. (1.54) for  $\mu_j$ :

$$\mu_j^2 = \frac{9k_B T}{4\pi N} \frac{3}{(\epsilon_i + 2)^2} \frac{M_j}{\rho_i} \left( \frac{\Delta}{w_j} \right)_{w_j \rightarrow 0} \quad \dots (1.56)$$

$M_j$  is the molecular weight of the polar liquid and  $\rho_i$  is the density of the solvent.

Palit and Banerjee [1.22] made an analysis of the error involved in the Guggenheim Smith approximate equation to find how far solution density measurements are necessary for calculation of  $\mu_j$  of polar molecule in nonpolar solvent.

Botcher [1.23], however, calculated  $\mu_j$  for a large number of polar nonpolar liquid mixtures by using different extrapolation technique. Botcher found different  $\mu_j$ . Later on, Krishna and Srivastava [1.24] used the following relation

$$\mu_j = \beta \left( \frac{d\epsilon_{ij}}{dx_j} \right)_{x_j \rightarrow 0}^{1/2} \quad \dots (1.57)$$

to calculate  $\mu_j$  of some polar solute in liquid state. Srivastava and Charandas [1.25] found that the constant  $\beta$  was different for different polar liquids. Therefore, the validity of the Higasi method [1.16] is questionable. Prakash [1.26] showed that the Eq. (1.57) is a special case of Eq. (1.39) when  $\epsilon_{ij}$  is almost equal to unity. As  $\epsilon_{ij} \approx 1$  is not true for any type of polar-nonpolar liquid mixture, Higasi's [1.16] method can not regarded as universal one to compute  $\mu_j$  at all concentrations of the polar solute. The Eq. (1.54) was modified to calculate  $\mu_j$  at  $w_j \rightarrow 0$

$$\mu_j^2 = \frac{27M_j k_B T}{4\pi N \rho_i} \left( \frac{\delta X_{ij}}{\delta w_j} \right)_{w_j \rightarrow 0} \quad \dots (1.58)$$

Here,

$$\left( \frac{\delta X_{ij}}{\delta w_j} \right)_{w_j \rightarrow 0} = \left[ \frac{1}{(\epsilon_i + 2)^2} \left( \frac{\delta \epsilon_{ij}}{\delta w_j} \right)_{w_j \rightarrow 0} - \frac{2n_{Di}}{(n_{Di}^2 + 2)^2} \left( \frac{\delta n_{Dij}}{\delta w_j} \right)_{w_j \rightarrow 0} \right] \quad \dots (1.59)$$

Eq. (1.59) is the famous Guggenheim Eq. (1.56) when  $\epsilon_i = n_{Di}^2$ . Thus in order to estimate  $\mu_j$ 's of dipolar liquid it is necessary to know the extrapolated values at  $w_j \rightarrow 0$  from the measured relaxation parameters of different  $w_j$ 's. Le Fevre and Smyth [1.21] and Guggenheim [1.19] by using different extrapolation technique obtained two different values

of  $\mu_j$  as 0.91 D and 0.83 D for trimethylamine in benzene at 25 °C. This fact suggests a proper extrapolation technique is necessary for the accurate determination of  $\mu_j$  and also  $\tau_j$  for a polar liquid.

Acharyya et al [1.27] tried to develop the dielectric theory within the framework of Debye model by introducing a new concept of weight fraction  $w_j$  instead of molar concentration  $C_j$ . They are related by  $c_j = \rho_{ij} w_j / M_j$  and  $w_i + w_j = 1$ . But  $\rho_{ij}$ , the density of the solution is a function of  $w_j$

$$\rho_{ij} = \frac{\rho_i}{1 - \gamma w_j} \quad \dots (1.60)$$

Here  $\gamma = (1 - \rho_i / \rho_j)$ ,  $\rho_i$  and  $\rho_j$  are the densities of pure solvent and pure solute respectively.

The Eq.(1.39) with the help of Eq. (1.60) can be written as

$$\frac{\epsilon_{ij} - n_{Dij}^2}{(\epsilon_{ij} + 2)(n_{Dij}^2 + 2)} = \frac{\epsilon_i - n_{Di}^2}{(\epsilon_i + 2)(n_{Di}^2 + 2)} + \frac{4\pi N \mu_s^2 \rho_i}{27 k_B T M_j} \frac{w_j}{1 - \gamma w_j}$$

$$X_{ij} = X_i + \frac{4\pi N \mu_s^2}{27 M_j k_B T} \rho_i (w_j + \gamma w_j^2 + \dots) \quad \dots (1.61)$$

The above Eq. (1.61) can be compared with the following type

$$X_{ij} = a + b w_j + c w_j^2 \quad \dots (1.62)$$

where  $X_{ij}$  and  $X_i$  are experimentally derivable static parameters and  $\mu_s$  is the dipole moment of the polar solute under static electric field. The Eq.(1.62) is highly converging in nature at low concentration region of the polar-nonpolar liquid mixture and  $\mu_s$  can be calculated from Eq. (1.61) as

$$\mu_s = \left( \frac{27 k_B T M_j a_1}{4\pi N \rho_i} \right)^{1/2} \quad \dots (1.63)$$

The above theory is applied to large numbers of polar-nonpolar liquid mixtures [1.27-1.29] and  $\mu_s$  were evaluated to observe the validity of the theory so far developed. Suryavanshi and Mehrotra [1.30], on the other hand, suggested the least square extrapolation technique to evaluate  $\tau$  and  $\mu$  of a dipolar liquid using Debye-Smyth model. The results determined by them were in excellent agreement with the reported values. Therefore, one can conclude that the least square extrapolation technique [1.23] is one of the reliable techniques to study the dielectric relaxation phenomena of polar-nonpolar liquid mixtures.

### 1.16. Eyring's Rate Theory:

The study of dielectric relaxation mechanism from the standpoint of chemical rate process has been first pointed out by Eyring et al [1.31]. According to this theory, the dielectric relaxation mechanism may be explained by treating the dipole orientation as a rate process in which the polar molecules rotate from one equilibrium position to other. This process of rotation requires activation energy sufficient to overcome the energy barrier separating the two mean equilibrium positions. The average time required for single rotation is known as relaxation time  $\tau_s$  and is given by

$$\tau_s = \frac{h}{k_B T} \exp(\Delta F_\tau / RT) \quad \dots (1.64)$$

where  $\Delta F_\tau$  = the free energy of activation. If  $\Delta S_\tau$  and  $\Delta H_\tau$  are the entropy of activation and enthalpy of activation respectively then we can have

$$\Delta F_\tau = \Delta H_\tau - T\Delta S_\tau \quad \dots (1.65)$$

Substitution of Eq. (1.65) in Eq. (1.64) results:

$$\tau_s = \frac{h}{k_B T} \exp(-\Delta S_\tau / R) \exp(\Delta H_\tau / RT) \quad \dots (1.66)$$

$$\ln \tau_s T = \ln A + \Delta H_\tau / RT \quad \dots (1.67)$$

Where

$$A = \frac{h}{k_B} \exp\left(\frac{-\Delta S_\tau}{R}\right)$$

Thus  $\Delta H_\tau$  can be evaluated from the slope of linear relation of  $\ln \tau_s T$  against  $1/T$ . From the calculated  $\tau_s$  and  $\Delta H_\tau$  one can easily estimate  $\Delta S_\tau$  and  $\Delta F_\tau$  by using Eqs. (1.66) and (1.65) respectively.

The viscous flow of the liquid may be considered as a rate process like the dielectric relaxation process. The viscous flow is involved with the translational as well as the rotational motion of the liquid with activation energy to pass over a potential barrier. Eyring obtained an expression for the coefficient of viscosity  $\eta$  in terms of reaction rate and is given by:

$$\begin{aligned} \eta &= \frac{Nh}{V} \exp(-\Delta S_\eta / R) \exp(\Delta H_\eta / RT) \\ &= A_1 \exp(\Delta H_\eta / RT) \end{aligned} \quad \dots (1.68)$$

Where  $A_1 = \frac{Nh}{V} \exp(-\Delta S_\eta / R)$ ,  $V$  = the molar volume,  $\Delta S_\eta$  = the entropy of activation,  $\Delta H_\eta$  = the enthalpy of activation respectively for viscous flow of the liquid. Now if  $\Delta F_\eta$  = the free energy of activation of the same then  $\Delta F_\eta$ ,  $\Delta S_\eta$  and  $\Delta H_\eta$  are related as:

$$\Delta F_\eta = \Delta H_\eta - T\Delta S_\eta \quad \dots (1.69)$$

$\Delta H_\eta$  and  $\Delta S_\eta$  are not necessarily the same as those for dipole rotation, since different processes are involved. Eyring, thus concluded that

$$\tau_s T \propto \eta V \quad \dots (1.70)$$

The Eq.(1.70) holds good only if the enthalpies of activation are the same in both the processes. Various workers have made applications to isolated problems in liquid dielectrics.

Eyring's rate theory were critically analysed by Kauzmann [1.32] and he gave a general theory of dielectric relaxation in terms of 'jumps' where 'jumps' stands for the frequency of discontinuous molecular reorientations. Assuming the relaxation process as a chemical reaction it is defined that the relaxation time  $\tau = 1 / k_0$  such that in this time the polarisation will fall to 1/e times of its initial value. Here  $k_0$  is the rate constant for the activation of dipoles and is known as the dielectric relaxation rate.

The reaction rate is:

$$k = K \frac{k_B T}{h} e^{\Delta S_a / R} e^{-\Delta E_a / RT} \quad \dots (1.71)$$

The main importance of the above formulation is that the thermodynamic parameters of the normal and the activated states from the observed reaction rate constant, helps one to infer the stability or the instability of the states, under consideration.

### 1.17. Brief review of previous works:

The relaxation phenomena of dielectropolar liquids and gases was studied by many workers [1.4-1.5, 1.33-1.34] from the concept of dielectric polarisation. Drude [1.35] first observed the anomalous behaviour of dispersion for liquids having -OH or -NH<sub>2</sub> groups under radio frequency electric field, which was later, explained by Debye [1.3]. Rocard [1.36] modified Debye's theory by considering the influence of moment of inertia of the molecules on the relaxation process. Budo [1.37], considering the intra-molecular and inter-molecular rotations of the polar molecules, proposed a new theory of dielectric relaxation. Onsager [1.38], Plumley [1.39] and Pao [1.40] interpreted the origin of ionic conduction in dielectric liquids even in the purest hydrocarbons like hexane. Jackson and Powles [1.41] estimated the relaxation time of polar molecules in benzene and paraffin only to show their dependence on the viscosity of solvents. Schallamach [1.42] studied the relaxation

phenomena of polar liquid molecules under radio frequency (rf) electric field in order to facilitate the rearrangement under single relaxation process. Lane and Saxton [1.43] studied the alcoholic solutions of electrolytes and established that the presence of ions reduces the permittivities of the media more markedly than that of water. Measurement of relaxation parameters of some pure normal alcohols were carried out by Garg and Smyth [1.44] to show three different  $\tau$ 's which are associated with polymetric cluster formation by the strong H-bonding between -OH groups.

Gopalakrishna [1.45] first made the simultaneous determination of  $\tau$  and  $\mu$  of polar molecules dissolved in non-polar solvents which was in excellent agreement with Jayprakash [1.46]. The advantage of this method is to know only the density of the pure solvent. Bergmann et al [1.47] gave a graphical method in complex plane to estimate  $\tau_1$  (smaller) and  $\tau_2$  (larger) that interpreted the intra-molecular and molecular rotations of polar molecules respectively. The experimental data of liquid n-alkyl bromide in terms of distribution of  $\tau$ 's between two limiting  $\tau$  values was analysed by Higasi et al [1.48]. Bhattacharyya et al [1.49] modified Bergmann equations in order to obtain double relaxation time  $\tau_2$  and  $\tau_1$  of phenetole, aniline and orthochloroaniline. Single frequency measurement technique of non-rigid molecules having  $\tau_1$ ,  $\tau_2$  and average  $\tau$  was obtained by Higasi et al [1.50] from Debye model.

The  $\epsilon'$  and  $\epsilon''$  of aliphatic alcohols in nonpolar solvents at different concentrations under hf electric field were measured by various workers [1.51-1.53]. Other group of workers [1.54-1.63] measured relative permittivities  $\epsilon'$ ,  $\epsilon''$ ,  $\epsilon_0$  and  $\epsilon''_\infty = n_D^2$  of some substituted toluidines, paracompounds, diphenylene oxide, chloral, ethyl trichloroacetate, trifluoroethanol, trifluoroacetic acid and a large number of monosubstituted and disubstituted benzene and anilines in different nonpolar solvents at various  $w_j$ 's under nearly 3 cm wavelength electric field to estimate  $\tau$ ,  $\mu$  and thermodynamic energy parameters. The study of relaxation phenomena of some straight chain alcohols, anilines and benzyl chloride from the radio frequency conductivity were made by a number of workers [1.64-1.68].

Dhull, Sharma and Gill [1.69-1.73] measured  $\epsilon'$  and  $\epsilon''$  of NMA, DMF, DMA in benzene, dioxane and carbon tetrachloride in order to obtain different relaxation parameters. Acharyya and Chatterjee [1.74-1.75] estimated  $\tau$ ,  $\mu$  and different energy parameters of some interesting polar molecules in benzene and carbon tetrachloride under rf electric field. Relaxation study of some binary polar liquid mixtures were made by Vyas and Vashisth [1.76] under hf electric field. Murthy et al [1.77] gave a new concept in order to obtain the simultaneous determination of  $\tau$  and  $\mu$  for polar non-polar liquid mixtures under hf electric field. later on, a series of works were done by Saha and Acharyya [1.78-1.79] from the measured relative permittivities based on newly developed methodology. Saha et al [1.80] and Sit et al [1.81-1.82] made a rigorous study of concentration variations of a number disubstituted benzenes, anilines and monosubstituted anilines in benzene and carbon tetrachloride in order to estimate  $\tau_1$ ,  $\tau_2$  and  $\mu_1$ ,  $\mu_2$  due to rotations of the flexible polar groups attached to the parent molecules and the whole molecules. Temperature variation of ethylene glycol–water mixture was carried out by Saha and Ghosh [1.83] under 1 MHz electric field. High values of  $\tau$  were explained by the polymeric cluster formation molecular association. Dutta et al [1.84] studied the dielectric properties of polar non-polar liquid mixture in terms of dielectric orientation susceptibility  $\chi_{ij}$ 's.

#### References:

- [1.1] R S Longhurst, *Geometrical and Physical Optics*, Third Edition (Orient Longman) (1973)
- [1.2] N E Hill, W E Vaughan, A H Price and M Davies, *Dielectric Properties and Molecular Behaviour*, (London) Van Nostrand Reinhold Company, (1969)
- [1.3] P Debye, *Polar Molecules*, Chemical Catalog Co. New York, (1929)
- [1.4] R Clausius, *Die mechanische Wärmttheorie* (Vieweg) 2 62 (1879)
- [1.5] F Mossotti, *Mem. Di Mathe me di fisica in Modena*, 24 II 49 (1850)
- [1.6] K S Cole and R H Cole, *J. Chem. Phys.* 9 341 (1941)
- [1.7] D W Davidson and R H Cole, *J. Chem. Phys.* 18 1417 (1951)
- [1.8] D W Davidson and R H Cole, *J. Chem. Phys.* 19 1484 (1951)
- [1.9] H Fröhlich, *Theory of Dielectrics*, Oxford University press, London (1949)
- [1.10] F J Murphy and S O Morgan, *Bell. Syst. Tech. J.* 18 502 (1939)
- [1.11] L Onsager, *J. Am. Chem. Soc.* 58 1486 (1936)

- [1.12] J G Kirkwood, *J. Chem. Phys.* **7** 911 (1939)
- [1.13] G Z Hedestrand, *J. Phys. Chem.* **32** 428 (1929)
- [1.14] P Cohen Henrique, *Thesis Delft*, **93** (1935)
- [1.15] R J W Le Fevre and H V Vine, *J. Chem. Soc.* 1805 (1937)
- [1.16] K Higasi, *Bull. Inst. Phys. Chem. Res. Tokyo* **22** 805 (1943)
- [1.17] E A Guggenheim, *Trans. Faraday Soc.* **45** 714 (1949)
- [1.18] J W Smith, *Trans. Faraday Soc.* **46** 394 (1950)
- [1.19] E A Guggenheim, *Trans. Faraday Soc.* **47** 573 (1951)
- [1.20] Everard, Hill and Sutton, *Trans. Faraday Soc.* **46** 417 (1950)
- [1.21] Barclay, Le Fevre and Smyth, *Trans. Faraday Soc.* **46** 812 (1950)
- [1.22] S R Palit and B C Banerjee, *Trans. Faraday Soc.* **47** 1299 (1951)
- [1.23] C J F Botcher, *Theory of Electric Polarisation*, Elsevier Publishing Co. New York (1950)
- [1.24] B Krishna and K K Srivastava, *J. Chem. Phys.* **27** 835 (1957)
- [1.25] S C Srivastava and P Charandas, *J. Chem. Phys.* **30** 816 (1959)
- [1.26] J Prakash, *Indian. J. Pure & Appl. Phys.* **11** 901 (1973)
- [1.27] A K Ghosh and S Acharyya, *Indian J. Phys.* **52B** 129 (1978)
- [1.28] A K Guha, D K Das and S Acharyya, *Indian J. Phys.* **51A** 192 (1977)
- [1.29] A K Ghosh and S K Ghosh, *Indian. J. Pure & Appl. Phys.* **20** 743 (1982)
- [1.30] M Suryavanshi and S C Mehrotra, *Indian. J. Pure & Appl. Phys.* **28** 67 (1990)
- [1.31] H Eyring, S Glasstone and J K Laidler, *Theory of Rate Process*, Mc Graw Hill, New York (1941)
- [1.32] W Kauzmann, *Review of Modern Physics* **14** 12 (1942)
- [1.33] H A Lorentz, *Ann. Physik*, **9** 641 (1880)
- [1.34] L V Lorentz, *Ann. Physik*, **11** 70 (1880)
- [1.35] P Drude, *Z. Phys. Chem.*, **23** 267 (1897)
- [1.36] M Y Rocard, *J. Phys. Radium*, **4** 247 (1933)
- [1.37] A Budo, *Phys. Z.*, **39** 706 (1938)
- [1.38] L J Onsager, *J. Chem. Phys.*, **2** 509 (1934)
- [1.39] H J Plumely, *Phys. Rev.*, **59** 200 (1941)
- [1.40] C S Pao, *Phys. Rev.*, **64** 60 (1943)
- [1.41] W Jackson and J G Powles, *Trans. Faraday Soc.*, **42A** 101 (1946)
- [1.42] A Schallamach, *Trans. Faraday Soc.*, **42A** 180 (1946)

- [1.43] J A Lane and J A Saxton, *Proc. R. Soc.*, **214A** 531 (1952)
- [1.44] S K Garg and C P Smyth, *J. Chem. Phys.*, **42** 1397 (1956)
- [1.45] K V Gopalakrishna, *Trans. Faraday Soc.*, **53** 767 (1957)
- [1.46] J Prakash, *Ind. J. Pure. & Appl. Phys.*, **8** 106 (1970)
- [1.47] K Bergmann, D M Roberti and C P Smyth, *J. Phys. Chem.*, **64** 665 (1960)
- [1.48] K Higasi, K Bergmann and C P Smyth, *J. Phy. Chem.*, **64** 880 (1960)
- [1.49] J Bhattacharyya, A Hassan, S B Roy and G S Kastha, *J. Phys. Soc., Japan* **28** 240 (1970)
- [1.50] K Higasi, Y Koga and M Nakamura, *Bull. Chem. Soc., Japan* **44** 988 (1971)
- [1.51] J Crossley, L Glasser and C P Smyth, *J. Chem. Phys.*, **55** 2197 (1971)
- [1.52] H D Purohit and H S Sharma, *Ind. J. Pure & Appl. Phys.*, **9** 450 (1971)
- [1.53] L Glasser, J Crossley and C P Smyth, *J. Chem. Phys.* **57** 3977 (1972)
- [1.54] R L Dhar, A Mathur, J P Shukla and M C Saxena, *Ind. J. Pure & Appl. Phys.*, **11** 568 (1973)
- [1.55] J P Shukla and M C Saxena, *Ind. J. Pure & Appl. Phys.*, **11** 896 (1973)
- [1.56] Y Koga, H Takahasi and H Higasi, *Bull. Chem. Soc. Japan*, **46** 3359 (1973)
- [1.57] H D Purohit, H S Saxena and A D Vyas, *Ind. J. Pure & Appl. Phys.*, **12** 273 (1974)
- [1.58] S C Srivastava and Suresh Chandra, *Ind. J. Pure & Appl. Phys.*, **13** 101 (1975)
- [1.59] S K Srivastava and S L Srivastava, *Ind. J. Pure & Appl. Phys.*, **13** 179 (1975)
- [1.60] M L Arrawatia, P C Gupta and M L Sisodia, *Ind. J. Pure & Appl. Phys.*, **15** 770 (1977)
- [1.61] S K S Somevanshi, S B Misra and N K Mehrotra, *Ind. J. Pure & Appl. Phys.*, **16** 57 (1978)
- [1.62] P C Gupta, M L Arrawatia and M L Sisodia, *Ind. J. Pure & Appl. Phys.*, **16** 934 (1978)
- [1.63] S M Khameshara and M L Sisodia, *Ind. J. Pure & Appl. Phys.*, **18** 110 (1980)
- [1.64] S N Sen and R Ghosh, *J. Phys. Soc., Japan* **36** 743 (1974)
- [1.65] A K Ghosh and S N Sen, *Ind. J. Pure & Appl. Phys.* **18** 588 (1980)
- [1.66] A K Ghosh and S N Sen, *J. Phys. Soc., Japan* **48** 1219 (1980)
- [1.67] R Ghosh and I Chowdhury, *Pramana : J. Phys.*, **16** 319 (1981)
- [1.68] R Ghosh and I Chowdhury, *Ind. J. Pure & Appl. Phys.*, **20** 717 (1982)
- [1.69] J S Dhull and D R Sharma, *J. Phys. D : Appl. Phys.*, **15** 2307 (1982)
- [1.70] J S Dhull and D R Sharma, *Ind. J. Pure & Appl. Phys.*, **21** 694 (1983)

- [1.71] A K Sharma and D R Sharma, *J. Phys. Soc., Japan* **53** 4771 (1984)
- [1.72] A K Sharma and D R Sharma, *Ind. J. Pure & Appl. Phys.*, **23** 418 (1985)
- [1.73] A K Sharma, D R Sharma and D S Gill, *J. Phys. D : Appl. Phys.*, **18** 1199 (1985)
- [1.74] S Acharyya and A K Chatterjee, *Ind. J. pure & Appl. Phys.*, **23** 484 (1985)
- [1.75] C R Acharyya, A K Chatterjee, P K Sanyal and S Acharyya, *Ind. J. Pure & Appl. Phys.*, **24** 234 (1986)
- [1.76] A D Vyas and V M Vashisth, *J. Molecular Liquids*, **38** 11 (1988)
- [1.77] M B R Murthy, R L Patil and D K Deshpande, *Ind. J. Phys.*, **63B** 494 (1989)
- [1.78] U Saha and S Acharyya, *Ind. J. Pure & Appl. Phys.*, **31** 181 (1993)
- [1.79] U Saha and S Acharyya, *Ind. J. Pure & Appl. Phys.*, **32** 346 (1994)
- [1.80] U Saha, S K Sit, R C Basak and S Acharyya, *J. Phys. D : Appl. Phys.*, **27** 596 (1994)
- [1.81] S K Sit, R C Basak, U Saha and S Acharyya, *J. Phys. D : Appl. Phys.* **27** 2194 (1994)
- [1.82] S K Sit, and S Acharyya, *Ind. J. Pure & Appl. Phys.*, **34** 255 (1996)
- [1.83] U Saha and R Ghosh, *J. Phys. D : Appl. Phys.* **32** 820 (1999)
- [1.84] K Dutta, S K Sit and S Acharyya, *Pramana: J. Phys.* **57**, No.4, 775 (2001)

## *Chapter 2*

### **SCOPE AND OBJECTIVE OF THE THESIS**

## 2.1. Introduction:

The aim of this chapter is to suggest simple, straightforward and significant theories of dispersion and absorption phenomena of dipolar liquid in nonpolar solvent. The theories so far developed are on the basis of Debye-Smyth model [2.1] of polar-nonpolar liquid mixtures and the relaxation parameters like dipole moments, energy parameters etc. were determined.

## 2.2. Debye equation in solution in S.I unit:

S.I unit version of dielectric displacement vector  $\vec{D}$  for a homogeneous, isotropic dielectric medium of absolute permittivity  $\epsilon$  in Farad metre<sup>-1</sup> is

$$\vec{D} = \epsilon_r \epsilon_0 \vec{E} \quad \dots (2.1)$$

where  $\epsilon_r$  is the dimensionless relative permittivity defined by  $\epsilon / \epsilon_0$  and  $\epsilon_0 =$  absolute permittivity of free space  $= 8.854 \times 10^{-12} \text{ F.m}^{-1}$ .

The total polarisation  $\vec{P}$  of the medium due to external electric field  $\vec{E}$  are related as :

$$\vec{D} = \epsilon_0 \vec{E} + \vec{P} \quad \dots (2.2)$$

From eqs. (2.1) and (2.2) one gets,

$$\vec{P} = (\epsilon_r - 1) \epsilon_0 \vec{E} \quad \dots (2.3)$$

Again,

$$\vec{P} = n \alpha_T \vec{E}_{loc} \quad \dots (2.4)$$

where  $\vec{E}_{loc}$  is the local electric field within a dielectropolar liquid.

Clausius-Mossotti relation [2.2-2.3] in SI unit for a non-polar liquid molecule is

$$\frac{\epsilon_r - 1}{\epsilon_r + 2} \frac{M}{\rho} = \frac{N\alpha_d}{3\epsilon_0} \quad \dots (2.5)$$

where  $N$  = Avogadro's number =  $6.023 \times 10^{23} \text{ mol}^{-1}$ ,  $M$  = molecular weight and  $\rho$  = the density of the dielectric medium.

Similarly the Debye equation for a polar molecule is given by:

$$\frac{\epsilon_r - 1}{\epsilon_r + 2} \frac{M}{\rho} = \frac{N}{3\epsilon_0} \left( \alpha_d + \frac{\mu_p^2}{3k_B T} \right) \quad \dots (2.6)$$

where  $\alpha_d$  = the polarisability due to distortion polarisation and  $\mu_p$  = the permanent dipole moment of the polar molecule.

Now if a polar liquid (j) is dissolved in a non-polar solvent (i) then the Debye equation for the solution will be:

$$\frac{\epsilon_{ij} - 1}{\epsilon_{ij} + 2} \frac{M_i f_i + M_j f_j}{\rho_{ij}} = \frac{N}{3\epsilon_0} (\alpha_i f_i + \alpha_j f_j) \quad \dots (2.7)$$

The above Eq. (2.7) can be written as

$$\left( \frac{\epsilon_{ij} - 1}{\epsilon_{ij} + 2} - \frac{n_{Dij}^2 - 1}{n_{Dij}^2 + 2} \right) = \left( \frac{\epsilon_i - 1}{\epsilon_i + 2} - \frac{n_{Di}^2 - 1}{n_{Di}^2 + 2} \right) + \frac{N}{3\epsilon_0} \frac{\mu_s^2}{3k_B T} c_j \quad \dots (2.8)$$

The Eq.(2.8) in S.I. unit is used to estimate the static dipole moment  $\mu_s$  of a polar liquid molecule.

### 2.3. High frequency complex conductivity, relaxation time and dipole moment:

Let us consider a dielectropolar material is subjected by an alternating electric field  $E=E_0e^{j\omega t}$  and then if  $I$  be the current density, the relation between  $I$  and  $E$  is given by

$$I = \sigma_{ij}^* E_0 e^{j\omega t} \quad \dots (2.9)$$

where  $\sigma_{ij}^*$  the high frequency complex conductivity.

Now in SI unit the dielectric displacement  $D$  is equal to  $q$  i.e,

$$D = q \quad \dots (2.10)$$

Also the hf complex relative permittivity is given by

$$\epsilon_r^* = \frac{\epsilon^*}{\epsilon_0} \quad \dots (2.11)$$

Here  $\epsilon^*$  and  $\epsilon_0$  are the absolute and free space permittivities of the medium in SI unit respectively.

Again

$$D = \epsilon^* E = \epsilon_0 \epsilon_r^* E \quad \dots (2.12)$$

Now the current density  $I$  is given by

$$\begin{aligned} I &= \frac{dq}{dt} = \frac{dD}{dt} = \frac{d}{dt} (\epsilon_0 \epsilon_r^* E_0 e^{j\omega t}) \\ &= \epsilon_0 \epsilon_r^* j\omega E_0 e^{j\omega t} \quad \dots (2.13) \end{aligned}$$

Comparison of Eqs. (2.9) and (2.13) results:

$$\sigma^* = j\omega\epsilon_0\epsilon_i^* \quad \dots (2.14)$$

For a polar nonpolar solution (ij), the Eq.(2.14) can be written as:

$$\sigma_{ij}^* = j\omega\epsilon_0\epsilon_{ij}^*$$

or,

$$\sigma'_{ij} + j\sigma''_{ij} = j\omega\epsilon_0(\epsilon'_{ij} - j\epsilon''_{ij})$$

Equating the real and imaginary parts we get,

$$\sigma'_{ij} = \omega\epsilon_0\epsilon''_{ij} \quad \dots (2.15a)$$

$$\sigma''_{ij} = \omega\epsilon_0\epsilon'_{ij} \quad \dots (2.15b)$$

where  $\sigma'_{ij}$  and  $\sigma''_{ij}$  are the real and imaginary parts of the hf complex conductivity  $\sigma_{ij}^*$  expressed in  $\Omega^{-1} m^{-1}$ .

In hf region, the total conductivity of a polar non-polar liquid mixture [2.4] is given by,

$$\sigma_{ij} = \sqrt{\sigma'^2_{ij} + \sigma''^2_{ij}} = \omega\epsilon_0\sqrt{\epsilon''^2_{ij} + \epsilon'^2_{ij}} \quad \dots (2.16)$$

In high frequency electric field  $\epsilon_{ij}'$  of a solution is usually very small and nearly equal to optical dielectric constant of the solution. But still  $\epsilon_{ij}' \gg \epsilon_{ij}''$  where  $\epsilon_{ij}''$  is responsible for the absorption of electrical energy by the dielectric medium to offer resistance to polarisation.

Now  $\epsilon_{ij}'$  and  $\epsilon_{ij}''$  are related [2.1] by

$$\epsilon'_{ij} = \epsilon_{\infty ij} + \frac{1}{\omega\tau_j}\epsilon''_{ij} \quad \dots (2.17)$$

where  $\epsilon_{\infty ij}$  = the infinite frequency relative permittivity of the solution and  $\tau_j$  = the relaxation time of the polar solute in nonpolar solvent.

From Eq.(2.17) it can be shown that,

$$\sigma_{ij}'' = \sigma_{\infty ij} + \frac{1}{\omega\tau_j} \sigma_{ij}' \quad \dots (2.18)$$

where  $\sigma_{\infty ij}$  = the constant conductivity at infinite dilution i.e  $w_j \rightarrow 0$ . The Eq.(2.18) on differentiation with respect to  $\sigma_{ij}'$  yields:

$$\frac{d\sigma_{ij}''}{d\sigma_{ij}'} = \frac{1}{\omega\tau_j} \quad \dots (2.19)$$

which provides a convenient method to obtain  $\tau_j$  of a polar molecule [2.5]. It is, however, better to use the ratio of variation of  $\sigma_{ij}''$  and  $\sigma_{ij}'$  with  $w_j$  in order to avoid polar-polar interactions at  $w_j \rightarrow 0$  in a given solvent to get  $\tau_j$  from [2.6]:

$$\left( \frac{d\sigma_{ij}''}{dw_j} \right)_{w_j \rightarrow 0} = \frac{1}{\omega\tau_j} \left( \frac{d\sigma_{ij}'}{dw_j} \right)_{w_j \rightarrow 0} \quad \dots (2.20)$$

In GHz range hf region, it is generally observed that  $\sigma_{ij}'' \approx \sigma_{ij}$ . Therefore, the Eq.(2.18) can be written as [2.7]:

$$\sigma_{ij} = \sigma_{\infty ij} + \frac{1}{\omega\tau_j} \sigma_{ij}'$$

$$\left( \frac{d\sigma_{ij}'}{dw_j} \right)_{w_j \rightarrow 0} = \omega\tau_j \beta \quad \dots (2.21)$$

where  $\beta$  = the slope of  $\sigma_{ij}$  with  $w_j$ . The real  $\sigma_{ij}'$  of a polar nonpolar liquid mixture at T K is given by [2.8]:

$$\sigma'_{ij} = \frac{N\rho_{ij}\mu_j^2}{27M_j k_B T} \left( \frac{\omega^2 \tau_j}{1 + \omega^2 \tau_j^2} \right) (\epsilon_{ij} + 2)^2 w_j$$

$$\left( \frac{d\sigma'_{ij}}{dw_j} \right)_{w_j \rightarrow 0} = \frac{N\rho_i \mu_j^2}{27M_j k_B T} \left( \frac{\omega^2 \tau_j}{1 + \omega^2 \tau_j^2} \right) (\epsilon_i + 2)^2 \quad \dots (2.22)$$

Now comparing Eqs (2.21) and (2.22) one gets hf  $\mu_j$  from

$$\mu_j = \left( \frac{27M_j k_B T \beta}{N\rho_i (\epsilon_i + 2)^2 \omega b} \right)^{1/2} \quad \dots (2.23)$$

where  $b = [1/(1 + \omega^2 \tau_j^2)]$  involved with  $\tau_j$ 's from Eqs (2.19) and (2.20) and is a dimensionless parameter and  $\beta$  is the slope of  $\sigma_{ij}$  against  $w_j$  curves at  $w_j \rightarrow 0$ . The derived formulations in SI units are applied in different solvents at a given experimental temperatures.

#### 2.4. High frequency dielectric susceptibility $\chi_{ij}$ :

The hf complex dielectric orientation susceptibility  $\chi^*$  is related to polarisation P and electric field E by:

$$P = \chi^* E \quad \dots (2.24)$$

From the approximation of  $P \propto E$  and  $D \propto E$ , we define the complex relative dielectric permittivity  $\epsilon^*$  by

$$D = \epsilon^* E \quad \dots (2.25)$$

Now,

$$D = E + 4\pi P \quad \dots (2.26)$$

$$= E + 4\pi \chi^* E$$

$$\varepsilon^* E = (1 + 4\pi\chi^*)E$$

$$\varepsilon^* = (1 + 4\pi\chi^*)$$

Now if it is expressed in SI units we have,

$$\varepsilon^* = 1 + \chi^*$$

$$\chi^* = \varepsilon^* - 1 \quad \dots (2.27)$$

The dielectric susceptibilities are obtained either by subtracting 1 or  $\varepsilon_\infty$  from the high and low frequency relative permittivities  $\varepsilon'$  and  $\varepsilon_0$  [2.9]. If 1 is subtracted from the relative permittivities  $\varepsilon'$  and  $\varepsilon_0$  one gets  $\chi'$  and  $\chi_0$  containing all types of polarisation processes including fast polarisations. When high frequency relative permittivity or optical permittivity  $\varepsilon_\infty$  be subtracted from  $\varepsilon'$  and  $\varepsilon_0$ , the susceptibilities  $\chi'$  and  $\chi_0$  results due to orientation polarisation only [2.10]. It should be distinguished between the fast or rapidly responding component of the polarisation  $\varepsilon_\infty$  representing the processes, which respond to the external field almost instantaneously on the time domain and the frequency dependent component is referred to the dielectric susceptibility.  $\chi^*(\omega)$ 's refers to the delayed processes. The fast component of polarisation  $\varepsilon_\infty$  is purely real and since no energy loss can be involved in this rapid response. But hf dielectric susceptibility has a finite imaginary component and thus  $\chi^*(\omega)$  is a pure complex quantity.

The dielectric relaxation study becomes simpler if the various processes are sufficiently separated with respect to frequency of the applied electric field so that there will be no overlapping amongst them. Thus the dielectric behaviour of a homogeneous medium under hf electric field is well represented in terms of the frequency dependent real and imaginary components of the complex dielectric orientation susceptibility  $\chi^*(\omega)$ :

$$\chi^*(\omega) = \chi'(\omega) - j\chi''(\omega) = \varepsilon^*(\omega) - \varepsilon_\infty \quad \dots (2.28)$$

where,  $j = \sqrt{-1}$  is a complex number.

Now if a polar molecule (j) is dissolved in a non-polar solvent (i), then from Eqs. (2.27) and (2.28) one can have:

$$\chi'_{ij} = \epsilon'_{ij} - \epsilon_{\infty ij} \quad \dots (2.29)$$

$$\chi''_{ij} = \epsilon''_{ij} \quad \dots (2.30)$$

$$\chi_{oij} = \epsilon_{oij} - \epsilon_{\infty ij} \quad \dots (2.31)$$

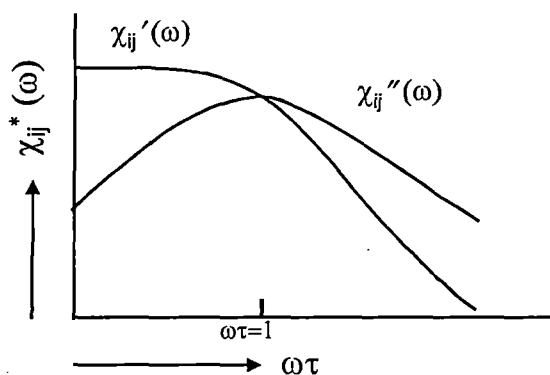


Figure 2.1: Variation of  $\chi'_{ij}$  and  $\chi''_{ij}$  with  $\omega\tau$

The parameters  $\chi'_{ij}$ ,  $\chi''_{ij}$  and  $\chi_{oij}$  of the above equations are the real, imaginary and low frequency susceptibilities respectively.  $\epsilon_{\infty ij}$  is the limit at frequencies of sufficiently high for the particular polarisation mechanism in question which shows negligible loss and dispersion. The hf complex  $\chi_{ij}^*(\omega)$  represents the dielectric response of the solution and it may be due to several independent mechanisms, which may overlap in any given frequency or time domain.

Now for the system of polar-nonpolar liquid mixture the classical Debye relation of  $\chi_{ij}$ 's [2.11] is:

$$\chi_{ij}^*(\omega) = \frac{\chi_{ojj}}{1 + j\omega\tau} \quad \dots (2.32)$$

where  $\tau$  is the temperature dependent relaxation time characterising the Debye process and  $\omega\tau$  is the dimensionless parameter. If we separate the real  $\chi_{ij}'$  and imaginary  $\chi_{ij}''$  parts of complex orientation susceptibility we get:

$$\frac{\chi_{ij}'}{\chi_{ojj}} = \frac{1}{1 + \omega^2\tau^2} \quad \dots (2.33)$$

$$\frac{\chi_{ij}''}{\chi_{ojj}} = \frac{\omega\tau}{1 + \omega^2\tau^2} \quad \dots (2.34)$$

The variations of  $\chi_{ij}'(\omega)$  and  $\chi_{ij}''(\omega)$  against  $\omega\tau$  are depicted in Fig. 2.1 where both the curves show maxima at  $\omega\tau=1$ .

## 2.5. Double relaxation phenomena from susceptibility measurement of polar-nonpolar liquid mixture:

$\tau_1$  and  $\tau_2$  due to rotation of the flexible parts attached to the parent ones as well as the whole molecule can be estimated from  $\chi_{ij}$ 's measured under single frequency electric field [2.12-2.13]. Bergmann et al [2.14] proposed a graphical technique to get  $\tau_1$ ,  $\tau_2$ ,  $c_1$  and  $c_2$  for pure polar liquid at different frequencies of the microwave electric field. In order to avoid fast polarisation processes, the molecular orientational polarisations in terms of established symbols of  $\chi_{ij}$ 's can be written as [2.15].

$$\frac{\chi_{ij}'}{\chi_{ojj}} = c_1 \frac{1}{1 + \omega^2\tau_1^2} + c_2 \frac{1}{1 + \omega^2\tau_2^2} \quad \dots (2.35)$$

$$\frac{\chi_{ij}''}{\chi_{ojj}} = c_1 \frac{\omega\tau_1}{1 + \omega^2\tau_1^2} + c_2 \frac{\omega\tau_2}{1 + \omega^2\tau_2^2} \quad \dots (2.36)$$

assuming two separate broad Debye type dispersions of which  $c_1+c_2=1$ .

Let us assume that  $\alpha_1 = \omega\tau_1$ ,  $\alpha_2 = \omega\tau_2$ ,  $\chi_{ij}'/\chi_{oij} = x$  and  $\chi_{ij}''/\chi_{oij} = y$ . Now with this substitutions from Eqs. (2.35) and (2.36)

$$c_1 = \frac{(x\alpha_2 - y)(1 + \alpha_1^2)}{\alpha_2 - \alpha_1} \quad \dots (2.37)$$

and,

$$c_2 = \frac{(y - x\alpha_1)(1 + \alpha_2^2)}{\alpha_2 - \alpha_1} \quad \dots (2.38)$$

Putting the values of  $x$ ,  $y$ ,  $\alpha_1$  and  $\alpha_2$ , the Eqs. (2.37) and (2.38) become:

$$c_1 = \frac{\left( \frac{\chi_{ij}'}{\chi_{oij}} \omega\tau_2 - \frac{\chi_{ij}''}{\chi_{oij}} \right) (1 + \omega^2\tau_1^2)}{\omega(\tau_2 - \tau_1)} \quad \dots (2.39)$$

and

$$c_2 = \frac{\left( \frac{\chi_{ij}''}{\chi_{oij}} - \frac{\chi_{ij}'}{\chi_{oij}} \omega\tau_1 \right) (1 + \omega^2\tau_2^2)}{\omega(\tau_2 - \tau_1)} \quad \dots (2.40)$$

The experimental values of relative contributions  $c_1$  and  $c_2$  towards dielectric dispersions for a polar-nonpolar liquid mixtures are also obtained graphically by plotting  $\chi_{ij}'/\chi_{oij}$  and  $\chi_{ij}''/\chi_{oij}$  against  $w_j$ 's at  $w_j \rightarrow 0$ .

The polar-nonpolar liquid mixtures under consideration are of complex type. A continuous distribution of  $\tau$  with two discrete values of  $\tau_1$  and  $\tau_2$  could, therefore be expected. Thus Frohlich's Eq.+ [2.16] based on the single frequency distribution of  $\tau$  between two extreme values of  $\tau_1$  and  $\tau_2$  in terms of hf  $\chi_{ij}^*$ 's can be obtained from Debye equation for polar-nonpolar liquid mixtures:

$$\frac{\chi_{ij}^*}{\chi_{oij}} = \int_0^{\infty} \frac{f(\tau)d\tau}{(1 + j\omega\tau)} \quad \dots (2.41)$$

where  $f(\tau)$  is the Fröhlich distribution function for  $\tau$  such that,

$$\begin{aligned} f(\tau) &= \frac{1}{A\tau}; & \tau_1 < \tau < \tau_2 \\ &= 0; & \tau_1 > \tau, \tau_2 < \tau \end{aligned} \quad \dots (2.42)$$

and  $A$  is the Fröhlich parameter given by  $A = \ln(\tau_2 / \tau_1)$ . Now separating the Eq.(2.41) into real and imaginary parts with the substitutions of  $f(\tau)$  of Eq. (2.42) we get,

$$\frac{\chi'_{ij}}{\chi_{oij}} = \frac{1}{A} \int_{\tau_1}^{\tau_2} \frac{d\tau}{\tau(1 + \omega^2 \tau^2)} \quad \dots (2.43)$$

$$\frac{\chi''_{ij}}{\chi_{oij}} = \frac{1}{A} \int_{\tau_1}^{\tau_2} \frac{\omega d\tau}{(1 + \omega^2 \tau^2)} \quad \dots (2.44)$$

Let us consider  $\ln \omega \tau = z$ , then the Eq.(2.43) becomes:

$$\begin{aligned} \frac{\chi'_{ij}}{\chi_{oij}} &= \frac{1}{A} \int_{\ln \omega \tau_1}^{\ln \omega \tau_2} \frac{dz}{1 + e^{2z}} \\ &= 1 - \frac{1}{2A} \ln \frac{1 + \omega^2 \tau_2^2}{1 + \omega^2 \tau_1^2} \end{aligned} \quad \dots (2.45)$$

Similarly, the Eq.(2.44) reduces to

$$\frac{\chi''_{ij}}{\chi_{oij}} = \frac{1}{A} \left[ \tan^{-1}(\omega \tau_2) - \tan^{-1}(\omega \tau_1) \right] \quad \dots (2.46)$$

The Eqs (2.45) and (2.46) are the modified forms of Fröhlich's equations for a distribution of  $\tau$  between two limiting values  $\tau_1$  and  $\tau_2$  in terms of hf  $\chi_{ij}$ .

The relative contributions of  $c_1$  and  $c_2$  towards the dielectric dispersion can be evaluated from Eqs (2.39), (2.40) and (2.45), (2.46) respectively with the estimated  $\tau_1$  and  $\tau_2$ . Now addition of Eqs (2.37) and (2.38) with the approximation  $c_1$  and  $c_2$  yields:

$$\frac{(x\alpha_2 - y)(1 + \alpha_1^2)}{\alpha_2 - \alpha_1} + \frac{(y - x\alpha_1)(1 + \alpha_2^2)}{\alpha_2 - \alpha_1} = 1$$

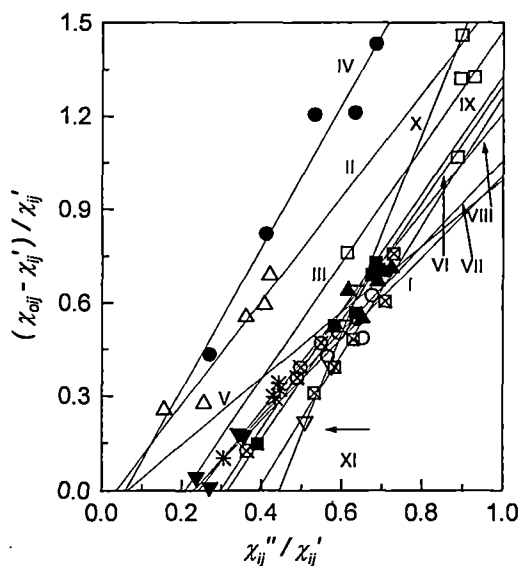


Figure 2.2 : Linear variation of  $(\chi_{oij} - \chi_{ij}')/\chi_{ij}'$  with  $\chi_{ij}''/\chi_{ij}'$  for different  $w_j$ 's at 35°C under 9.945 GHz electric field.

- I. o-chloronitrobenzene in  $C_6H_6$  (-○-); II. 4-chloro 3-nitrobenzotrifluoride in  $CCl_4$  (-△-); III. 4-chloro 3-nitrotoluene in  $C_6H_6$  (-□-); IV. 4-chloro 3-nitrotoluene in  $CCl_4$  (-●-); V. o-nitrobenzotrifluoride in  $C_6H_6$  (-▲-); VI. m-nitrobenzotrifluoride in  $C_6H_6$  (-■-); VII. 2-chloro 6-methyl aniline in  $C_6H_6$  (-▼-); VIII. 3-chloro 2-methyl aniline in  $C_6H_6$  (-\*-); IX. 3-chloro 4-methyl aniline in  $C_6H_6$  (-⊗-); X. 4-chloro 2-methyl aniline in  $C_6H_6$  (-∇-) and XI. 5-chloro 2-methyl aniline in  $C_6H_6$  (-⊗-)

On simplification the above equation reduces to

$$\left(\frac{1}{x} - 1\right) = \frac{y}{x}(\alpha_2 + \alpha_1) - \alpha_1\alpha_2$$

Now putting the values of  $x$ ,  $y$ ,  $\alpha_1$  and  $\alpha_2$ , the above equation becomes:

$$\frac{\chi_{oij} - \chi'_{ij}}{\chi'_{ij}} = \omega(\tau_1 + \tau_2) \frac{\chi''_{ij}}{\chi'_{ij}} - \omega^2 \tau_1 \tau_2 \quad \dots (2.47)$$

The Eq.(2.47) is a linear equation with variables  $(\chi_{oij} - \chi'_{ij})/\chi'_{ij}$  and  $\chi''_{ij}/\chi'_{ij}$ . When  $(\chi_{oij} - \chi'_{ij})/\chi'_{ij}$  are plotted against  $\chi''_{ij}/\chi'_{ij}$  for different weight fractions  $w_j$ 's of solute under a given angular frequency  $\omega$  of the electric field as illustrated in Fig 2.2 [2.13],  $\tau_1$  and  $\tau_2$  can be estimated from the intercept  $\omega(\tau_1 + \tau_2)$  and slope  $-\omega^2 \tau_1 \tau_2$  of Eq.(2.47).

## 2.6. Dipole moment measurement from dielectric susceptibility:

The Clausius Mossotti equation for polar-nonpolar liquid mixture under static or low frequency electric field is given by:

$$\frac{\epsilon_{oij} - 1}{\epsilon_{oij} + 2} \frac{M_i f_i + M_j f_j}{\rho_{ij}} = \frac{N}{3\epsilon_o} (\alpha_i f_i + \alpha_j f_j) + \frac{N}{3\epsilon_o} \frac{f_j \mu^2}{3k_B T} \quad \dots (2.48)$$

and the Lorentz [2.17] equation in case of it at infinitely hf region is

$$\frac{\epsilon_{\infty ij} - 1}{\epsilon_{\infty ij} + 2} \frac{M_i f_i + M_j f_j}{\rho_{ij}} = \frac{N}{3\epsilon_o} (\alpha_i f_i + \alpha_j f_j) \quad \dots (2.49)$$

From Eqs. (2.48) and (2.49) one can write,

$$\frac{\epsilon_{oij} - \epsilon_{\infty ij}}{(\epsilon_{oij} + 2)(\epsilon_{\infty ij} + 2)} = \frac{N}{9\epsilon_o} \frac{\rho_{ij} \mu^2}{3M_j k_B T} w_j \quad \dots (2.50)$$

where  $w_j = M_j f_j / (M_i f_i + M_j f_j)$  and is called the weight fraction of the polar solute.

Now if  $\epsilon_{ij}$  is the relative permittivity of the solution then in hf region it may be assumed that  $\epsilon_{oij} \approx \epsilon_{\infty ij} \approx \epsilon_{ij}$  and  $\mu = \mu_j =$  the dipole moment measured under hf electric field. Then the Eq.(2.50) in terms of dielectric orientational susceptibility becomes:

$$\chi_{oij} = \frac{N\mu_j^2 \rho_{ij} F_{ij}}{3\epsilon_o M_j k_B T} w_j \quad \dots (2.51)$$

where  $F_{ij} = (\epsilon_{ij} + 2)^2/9 =$  the local field of the solution. Now the comparison of Eq.(2.51) with Eq.(2.34) yields,

$$\chi_{ij}'' = \frac{N\mu_j^2 \rho_{ij} F_{ij}}{3\epsilon_o M_j k_B T} \frac{\omega \tau_j}{1 + \omega^2 \tau_j^2} w_j \quad \dots (2.52)$$

Differentiating Eq.(2.52) w.r.to  $w_j$  in the limit  $w_j=0$

$$\left( \frac{d\chi_{ij}''}{dw_j} \right)_{w_j \rightarrow 0} = \frac{N\mu_j^2 \rho_i F_i}{3\epsilon_o M_j k_B T} \frac{\omega \tau_j}{1 + \omega^2 \tau_j^2} \quad \dots (2.53)$$

In Eq.(2.53)  $\rho_{ij} \rightarrow \rho_i$  and  $F_{ij} \rightarrow F_i = (\epsilon_i + 2)^2/9$  in the limit  $w_j=0$  where  $\rho_i$  and  $\epsilon_i$  are the density and relative permittivity of the solvent respectively.

From Eqs (2.33) and (2.34) we have

$$\frac{\chi_{ij}'}{\chi_{ij}''} = \frac{1}{\omega \tau_j} \quad \dots (2.54)$$

or,

$$\left( \frac{d\chi_{ij}''}{dw_j} \right)_{w_j \rightarrow 0} = \omega \tau_j \left( \frac{d\chi_{ij}'}{dw_j} \right)_{w_j \rightarrow 0} = \omega \tau_j \beta \quad \dots (2.55)$$

where  $\beta$  is the slope of the variation of  $\chi_{ij}'$  with  $w_j$  at  $w_j \rightarrow 0$ . The Eq.(2.54) and (2.55) can conveniently be used to measure  $\tau_j$ 's of any polar unit in a non-polar solvent. Now in order

to obtain  $\mu_j$ , i.e the dipole moment of the polar solute in non-polar solvent one can compare Eqs(2.53) and (2.55) to get

$$\mu_j = \left( \frac{27\varepsilon_0 M_j k_B T \beta}{N \rho_i (\varepsilon_i + 2)^2 b} \right)^{1/2} \quad \dots (2.56)$$

In Eq.(2.56),  $b=1/(1+\omega^2\tau_j^2)$  is a dimensionless parameter. The methodology so far developed is used in different chapters of the thesis in getting  $\tau_j$ 's and  $\mu_j$ 's.

## 2.7. Material property of relaxation phenomena :

From the prolonged studies on the relaxation mechanism of dipolar liquids by Raiganj [2.13-2.15] and other groups [2.18-2.19] all over the world, it is appearing that the relaxation phenomena may be the material property of the system under consideration. If any system of polar-nonpolar liquid mixture shows double relaxation times at one frequency  $\omega$  it will show the same  $\tau_1$  and  $\tau_2$  at all the  $\omega$ 's measurements, because  $\tau$ 's are expected to be independent of  $\omega$  of the applied alternating electric field. The Eq.(2.45) can be written as:

$$\begin{aligned} \frac{\chi'_{ij}}{\chi_{\omega ij}} &= \frac{1}{2A} \left( 2A - \ln \frac{1 + \omega^2 \tau_2^2}{1 + \omega^2 \tau_1^2} \right) \\ &= \frac{1}{2A} \left( \ln \frac{\omega^2 \tau_2^2}{\omega^2 \tau_1^2} - \ln \frac{1 + \omega^2 \tau_2^2}{1 + \omega^2 \tau_1^2} \right) \\ &= \frac{1}{2A} \left( \ln \frac{\tau_2^2 (1 + \omega^2 \tau_1^2)}{\tau_1^2 (1 + \omega^2 \tau_2^2)} \right) \end{aligned} \quad \dots (2.57)$$

From Eqs (2.46) and (2.57) one can write:

$$\frac{\chi''_{ij}}{\chi'_{ij}} = \frac{2[\tan^{-1}(\omega\tau_2) - \tan^{-1}(\omega\tau_1)]}{\ln \frac{\tau_2^2 (1 + \omega^2 \tau_1^2)}{\tau_1^2 (1 + \omega^2 \tau_2^2)}} \quad \dots (2.58)$$

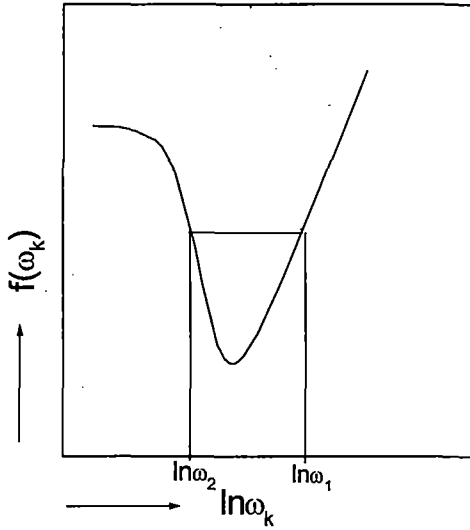


Figure 2.3: Variation of  $f(\omega_k)$  with  $\ln\omega_k$  for a fixed value of  $\omega$

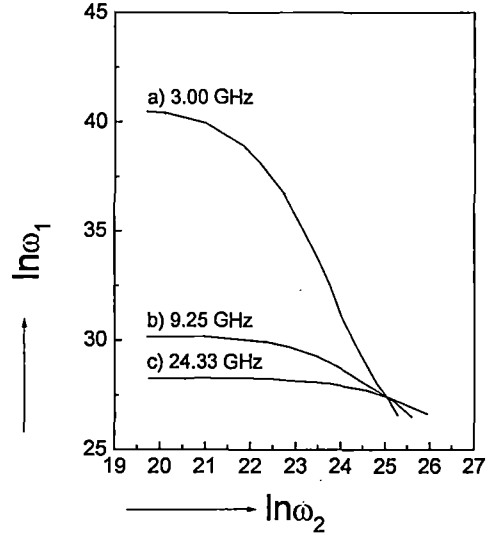


Figure 2.4: Variation of  $\ln\omega_1$  against  $\ln\omega_2$  of 3-methyl 3-heptanol under 3.00, 9.25 and 24.33 GHz electric field.

Assuming  $\tau_1=1/\omega_1$  and  $\tau_2=1/\omega_2$  such that  $\omega\tau = 1$  but  $\omega_2 < \omega_1$  Eq.(2.58), after simplification becomes [2.19]:

$$\frac{\chi''_{ij}}{\chi'_{ij}} \ln(\omega_1^2 + \omega^2) + 2 \tan^{-1} \frac{\omega}{\omega_1} = \frac{\chi''_{ij}}{\chi'_{ij}} \ln(\omega_2^2 + \omega^2) + 2 \tan^{-1} \frac{\omega}{\omega_2} \quad \dots (2.59)$$

The Eq.(2.59) holds good for a number of  $\omega_1, \omega_2, \dots, \omega_k$  i.e.,

$$f(\omega_1) = f(\omega_2) = f(\omega_3) = \dots = f(\omega_k)$$

where,

$$f(\omega_k) = \left[ \frac{\chi''_{ij}}{\chi'_{ij}} \ln(\omega_k^2 + \omega^2) + 2 \tan^{-1} \frac{\omega}{\omega_k} \right] \quad \dots (2.60)$$

The term  $\chi''_{ij}/\chi'_{ij}$  of Eq.(2.60) is a function of  $w_j$  of a polar solute at a temperature  $T$  K and  $\omega$  of the electric field.  $f(\omega_k)$  is, however, made constant for a fixed  $\tau_1$  and  $\tau_2$  of a system at a given  $\omega$  by introducing the least squares fitted extrapolated value of  $(\chi''_{ij}/\chi'_{ij})_{w_j \rightarrow 0}$ . Eq.(2.60) then becomes:

$$f(\omega_k) = \left[ \left( \frac{\chi''_{ij}}{\chi'_{ij}} \right)_{\omega_j \rightarrow 0} \ln(\omega_k^2 + \omega^2) + 2 \tan^{-1} \frac{\omega}{\omega_k} \right] \dots (2.61)$$

A curve of  $f(\omega_k)$  against  $\ln\omega_k$  can be obtained by varying  $\omega_k$  in order to get the arbitrary values of  $\ln\omega_2$  and  $\ln\omega_1$  ( $\omega_2 < \omega_1$ ) for the same  $f(\omega_k)$  as sketched in Fig.2.3. Graphs of  $\ln\omega_1$  vs  $\ln\omega_2$  for different  $\omega$  as shown in Fig.2.4 are used to obtain the points of intersection which yields the values of  $\tau_2$  and  $\tau_1$  of the polar molecular liquids. An attempt has been made in Chapter 6 of the thesis for a large number of alcohols, which are supposed to behave as polymer type molecules due to their H-bonding to show the material property of the systems.

## 2.8. Substituent polar groups in a dipolar molecule:

The measured hf or static dipole moments  $\mu_j$  or  $\mu_s$  of a polar liquid molecule may be compared with the theoretical dipole moments  $\mu_{\text{theo}}$ 's obtained from the vector addition method of bond lengths and bond angles of all the substituent polar groups attached to the parent molecules to get their conformational structures as displayed in different chapters of the thesis. The bond length is the distance between the centres of the two atomic nuclei when two atoms are connected by a covalent bond. The structural conformations of the whole molecule are studied in terms of atomic orbitals, which often overlaps to form hybridised orbitals and this phenomenon is called the hybridisation. The bond due to overlap of two s-orbitals is called  $\sigma$ -bond whereas the sidewise overlap of two half filled p-orbitals having a nodal plane forms a  $\pi$ -bond. The bond angle, on the other hand, is the angle between the dipolar axis of the parent molecule and the bond axis of a flexible polar groups or atoms linked with the parent molecule. The bond angle depends on the nature of hybridisation, the electro-negativity of the atoms or groups and due to size of it. The slight disagreement of  $\mu_j$  and  $\mu_s$  with  $\mu_{\text{theo}}$  is, however, observed for the presence of various effects suffered by the substituent polar groups under low and hf electric fields. The inductive, mesomeric and electromeric effects play the vital role to yield the conformational structure of a dipolar molecule.

The difference in electro-negativity in the atoms of a molecule produces a displacement of electrons towards the more electronegative atoms and hence a certain degree of polarity on the atom is induced. The atoms of the molecule with more electro-negativity acquires negative  $\delta^-$  and less electro-negativity acquires positive  $\delta^+$  charges. The inductive effect (I-effect) is referred to the induced polarity in a molecule as a result of higher electro-negativity of one atom compared to other atom. The functional groups such as  $-\text{NO}_2$ ,  $-\text{F}$ ,  $-\text{Cl}$ ,  $-\text{Br}$ ,  $-\text{I}$ ,  $-\text{OH}$ , etc are electron attracting and thus pull electrons away from C-atom of the polar molecule. They thus produce  $-I$  effect. The electron releasing groups such as  $(\text{CH}_3)_3\text{C}-$ ,  $(\text{CH}_3)_2\text{CH}-$ ,  $\text{CH}_3\text{CH}_2-$ ,  $\text{CH}_3-$  etc, on the other hand, push electrons towards the C-atom and gives rise to  $+I$  effect.

The mesomeric effect (M-effect) refers to the polarity produced in a molecule as a result of interaction between two  $\pi$ -bonds or one  $\pi$ -bond and lone pair of electrons. This effect is a permanent one and is transmitted along the chain of C-atoms linked alternately by single and double bonds in a conjugated component. Atoms or groups such as  $-\text{NO}_2$ ,  $-\text{C}\equiv\text{N}$ ,  $>\text{C}=\text{O}$  etc pull electrons away from C-atom to produce  $-M$  effect whereas  $-\text{F}$ ,  $-\text{Cl}$ ,  $-\text{Br}$ ,  $-\text{I}$ ,  $-\text{NH}_2$ ,  $-\text{OH}$ ,  $-\text{OCH}_3$  etc pushing electrons towards C-atom and are said to have  $+M$  effect.

Electromeric effect unlike mesomeric effect is a temporary effect. It involves with the complete transfer of a shared pair of  $\pi$ -electrons to one or other atoms joined by double or triple bonds like  $>\text{C}=\text{O}$  bond.

Resonance may occur in a polar molecule in which electrons may oscillate from one position to another. The molecule, as a result of this oscillation, may be said to have resonant structure. So far the energy is concerned, each of them does differ significantly. The resonance effect involves with the delocalisation of electron cloud of a molecule by two or more conformations differing only in the arrangement of electrons without shifting any atom.

The inductive, mesomeric, electromeric and resonance effects are taken into consideration to sketch the conformational structures of a large number of dipolar liquid molecules as shown in different chapters of this thesis works. For all the materials concerned due to their aromaticity the resonance effect combined with inductive effect

known as mesomeric effect plays a prominent role to get the required conformations. These are caused by the permanent polarisation of different substituent polar groups acting as pusher or puller of electrons towards or away from atoms attached to the parent molecule. The non-polar solvent  $C_6H_6$  unlike  $CCl_4$ , n-hexane, n-heptane etc is a cyclic planer compound and has three double bonds and six p-electrons on six C atoms. Hence  $\pi$ - $\pi$  interaction or mesomeric effect play the role in calculating  $\mu_{theo}$ 's. The contraction or elongation of bond moments obviously occur in almost all polar liquids by the factor  $\mu_s / \mu_{theo}$  or  $\mu_j / \mu_{theo}$  in order to confirm to the exact  $\mu_s$  or  $\mu_j$  values.

## 2.9. Debye – Pellat's equations:

The available real  $\epsilon_{ij}'$  and imaginary  $\epsilon_{ij}''$  parts of the complex permittivity  $\epsilon_{ij}^*$  at a given experimental temperature under electric field of frequency  $\omega$  can be used to get the low frequency or rather the static permittivity  $\epsilon_{oij}$  and ultra high frequency permittivity  $\epsilon_{\infty ij}$  ( $=n_{Dij}^2$ ) of a polar-nonpolar liquid mixture from

$$\epsilon' = \epsilon_{\infty} + \frac{\epsilon_o - \epsilon_{\infty}}{1 + \omega^2 \tau^2} \quad \dots (2.62)$$

and

$$\epsilon'' = (\epsilon_o - \epsilon_{\infty}) \frac{\omega \tau}{1 + \omega^2 \tau^2} \quad \dots (2.63)$$

which are known as the Debye – Pellat's equations [2.11]. These Eqs (2.62) and (2.63) are used for several para compounds in different solvents of chapter 8 in this thesis to get static  $\mu_s$ .

All these theoretical formulations in Chapter 2, so far derived, have been used to test their validity for a large number of dipolar liquids of different shapes, sizes and structures in all the subsequent chapters of this thesis to enhance the scientific contents of the relaxation phenomena under low and hf electric field.

## References:

- [2.1] C P Smyth, *Dielectric Behaviour and Structure* (McGraw Hill) (1955)
- [2.2] R Clausius, *Die mechanische Wärmttheorie* (Vieweg), **2** 62 (1879)
- [2.3] O F Mossotti, *Mem. di Matheme di fisica in Modena*, **24 II** 49 (1850)
- [2.4] F J Murphy and S O Morgan, *Bull. Syst. Tech. J.* **18** 502 (1939)
- [2.5] M B R Murthy, R L Patil and D K Deshpande, *Ind. J. Phys.*, **63B** 494 (1989)
- [2.6] R C Basak, A Karmakar, S K Sit and S Acharyya, *Indian J. Pure & Appl. Phys.* **37** 224 (1999)
- [2.7] K Dutta, A Karmakar, S K Sit and S Acharyya, *Indian J. Pure & Appl. Phys.* **40** 588 (2002)
- [2.8] K Dutta, R C Basak, S K Sit and S Acharyya, *J. Molecular Liquids* **88** 229 (2000)
- [2.9] A K Jonscher, *Universal Relaxation Law*, Chelsea Dielectrics Press, London (1996)
- [2.10] A K Jonscher, *Inst. Phys. Conf.*, invited papers edited by CHL Goodman, Canterbury (1980)
- [2.11] N E Hill, W E Vaughan, A H Price and M Davies, *Dielectric Properties and Molecular Behaviour*, Van Nostrand Reinhold Co.Ltd. London (1969)
- [2.12] K Dutta, S K Sit and S Acharyya, *Pramana: J. Phys.* **57** 775 (2001)
- [2.13] K Dutta, A Karmakar, L Dutta, S K Sit and S Acharyya, *Indian J. Pure & Appl. Phys.* **40** 801 (2002)
- [2.14] K Bergmann, D M Roberti and C P Smyth, *J. Phys. Chem.* **64** 665 (1960)
- [2.15] N Ghosh, S K Sit, A K Bothra and S Acharyya, *J. Phys. D: Appl. Phys.* **34** 379 (2001)
- [2.16] H Fröhlich, *Theory of Dielectrics*, Oxford University Press, London (1949)
- [2.17] H A Lorentz, *Ann. Physik*, **9** 641 (1880)
- [2.18] K Higasi, Y Koga and M Nakamura, *Bull. Chem. Soc. Japan*, **44** 988 (1971)
- [2.19] A Mansing and P Kumar, *J Phys. Chem.* **69** 4197 (1965)

## *Chapter 3*

### **DOUBLE RELAXATION PHENOMENA OF DISUBSTITUTED BENZENES AND ANILINES IN NONPOLAR APROTIC SOLVENTS UNDER HIGH FREQUENCY ELECTRIC FIELD**

### 3.1. Introduction :

The dielectric relaxation phenomena of nonspherical and rigid polar liquid molecule in different nonpolar solvents at a given temperature, under a high frequency (hf) electric field attracted the attention of a large number of workers [3.1-3.2]. The dipole moment  $\mu$  from the relaxation time  $\tau$  of the polar liquid molecule is of much importance [3.3-3.4] to determine the shape, size, structure and molecular association of a polar molecule. The real  $\epsilon_{ij}'$  and imaginary  $\epsilon_{ij}''$  parts of complex relative permittivity  $\epsilon_{ij}^*$ , static and infinite frequency relative permittivities  $\epsilon_{0ij}$  and  $\epsilon_{\infty ij}$  of a polar liquid molecule (j) in a non-polar solvent (i) at a fixed experimental temperature under a single frequency electric field of GHz range are used to obtain the double relaxation times  $\tau_2$  and  $\tau_1$  due to rotation of the whole molecule as well as the flexible part attached to the parent molecule [3.5].

Khameshara and Sisodia [3.6], Gupta et al [3.7] and Arrawatia et al [3.8] measured the relative permittivities of some disubstituted benzenes and anilines in aprotic nonpolar solvents  $C_6H_6$  and  $CCl_4$  under 9.945 GHz electric field at  $35^\circ C$  to predict the conformation of the molecules in terms of the relaxation time  $\tau$ , based on the single frequency concentration variation method of Gopalakrishna [3.9] and the dipole moment  $\mu$  by Higasi's method [3.10]. The compounds are very interesting for the different functional groups like  $-NH_2$ ,  $-CH_3$ ,  $-NO_2$ ,  $-Cl$  etc. attached to the parent molecules. The samples were of purest quality and supplied by M/s Fluka and M/s E Merck respectively. The solvents  $C_6H_6$  and  $CCl_4$  of M/s BDH were used after double distillation and suitably dried over NaCl and  $CaCl_2$ .  $\epsilon_{0ij}$  at  $35^\circ C$  was measured by heterodyne beat method at 300 KHz.  $\epsilon_{\infty ij} = n_{Dij}^2$ , where the refractive index  $n_{Dij}$  was measured by an Abbe's refractometer. The weight fraction  $w_j$  of the respective solute, which is defined by the weight of the solute per unit weight of the solution was taken up to four decimal place as the accuracy in the measurement was 0.0012 %.  $\epsilon_{ij}'$  and  $\epsilon_{ij}''$  within 1% and 5% accuracies were carried out by using the voltage standing wave ratio in slotted line and short-circuiting plunger, based on the method of Heston et al [3.11]. The possible existence of  $\tau_1$  and  $\tau_2$  of the compounds was, however, detected from the relative permittivity measurements [3.12] under 9.945 GHz electric field at  $35^\circ C$ .

Table 3.1: The real  $\chi_{ij}'$  and imaginary  $\chi_{ij}''$ , parts of the complex dielectric orientational susceptibility  $\chi_{ij}^*$  and static dielectric susceptibility  $\chi_{oij}$  which is real for various weight fraction  $w_j$  of different disubstituted benzenes and anilines in  $C_6H_6$  and  $CCl_4$  at 35 °C under 9.945 GHz electric field.

Weight fraction $w_j$	$\chi_{ij}'$	$\chi_{ij}''$	$\chi_{oij}$	Weight fraction $w_j$	$\chi_{ij}'$	$\chi_{ij}''$	$\chi_{oij}$
(I) o-chloronitrobenzene in $C_6H_6$				(II) 4-chloro 3-nitro benzotrifluoride in $CCl_4$			
0.0109	0.117	0.066	0.167	0.0050	0.122	0.019	0.155
0.0173	0.169	0.100	0.254	0.0101	0.145	0.037	0.185
0.0217	0.197	0.126	0.305	0.0147	0.150	0.054	0.233
0.0280	0.253	0.165	0.376	0.0193	0.167	0.068	0.266
0.0330	0.284	0.192	0.461	0.0231	0.179	0.075	0.302
(III) 4-chloro 3-nitro toluene in $C_6H_6$				(IV) 4-chloro 3-nitro toluene in $CCl_4$			
0.0072	0.075	0.046	0.132	0.0041	0.145	0.039	0.208
0.0144	0.098	0.088	0.241	0.0087	0.173	0.071	0.315
0.0224	0.150	0.133	0.310	0.0128	0.190	0.101	0.419
0.0323	0.200	0.179	0.464	0.0162	0.218	0.138	0.482
0.0453	0.271	0.252	0.630	0.0203	0.241	0.165	0.586
(V) o-nitrobenzotrifluoride in $C_6H_6$				(VI) m-nitrobenzotrifluoride in $C_6H_6$			
0.0085	0.094	0.058	0.154	0.0096	0.082	0.032	0.094
0.0167	0.166	0.108	0.257	0.0173	0.103	0.060	0.157
0.0244	0.226	0.159	0.384	0.0245	0.129	0.082	0.202
0.0335	0.297	0.205	0.495	0.0326	0.157	0.106	0.265
0.0402	0.353	0.255	0.604	0.0380	0.187	0.128	0.323
(VII) 2-chloro 6-methyl aniline in $C_6H_6$				(VIII) 3-chloro 2-methyl aniline in $C_6H_6$			
0.0184	0.072	0.017	0.075	0.0083	0.059	0.018	0.065
0.0305	0.096	0.026	0.097	0.0207	0.099	0.043	0.128
0.0417	0.117	0.040	0.138	0.0270	0.128	0.055	0.166
0.0573	0.163	0.058	0.191	0.0363	0.165	0.073	0.221
0.0636	0.183	0.065	0.214	0.0421	0.193	0.086	0.255
(IX) 3-chloro 4-methyl aniline in $C_6H_6$				(X) 4-chloro 2-methyl aniline in $C_6H_6$			
0.0214	0.088	0.032	0.099	0.0196	0.124	0.063	0.151
0.0374	0.123	0.060	0.167	0.0300	0.157	0.090	0.219
0.0403	0.133	0.066	0.185	0.0417	0.199	0.121	0.304
0.0548	0.166	0.091	0.244	0.0481	0.216	0.138	0.354
(XI) 5-chloro 2-methyl aniline in $C_6H_6$							
0.0194	0.094	0.050	0.123				
0.0249	0.110	0.064	0.153				
0.0307	0.129	0.081	0.191				
0.0480	0.182	0.129	0.292				
0.0569	0.206	0.150	0.362				

Nowadays, the usual practice [3.13] is to study the dielectric relaxation phenomena in terms of dielectric orientational susceptibilities  $\chi_{ij}$ 's.  $\chi_{ij}$ 's are linked with the orientational polarisation of a polar molecule. So it is better to work with  $\chi_{ij}$ 's rather than  $\epsilon_{ij}$ 's or conductivity  $\sigma_{ij}$ 's as the later are involved with all the polarisation processes and the transport of bound molecular charges, respectively [3.14]. The real  $\chi_{ij}'(=\epsilon_{ij}'-\epsilon_{\infty ij})$  and

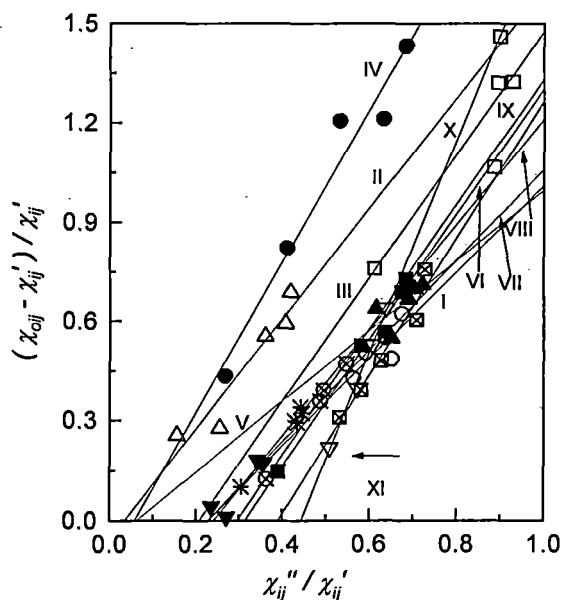


Figure 3.1: Linear variation of  $(\chi_{oij} - \chi_{ij}')/\chi_{ij}'$  with  $\chi_{ij}''/\chi_{ij}'$  for different  $w_j$ 's at 35°C under 9.945 GHz electric field.

I. o-chloronitrobenzene in  $C_6H_6$  (—○—); II. 4-chloro 3-nitrobenzotrifluoride in  $CCl_4$  (—△—); III. 4-chloro 3-nitrotoluene in  $C_6H_6$  (—□—); IV. 4-chloro 3-nitrotoluene in  $CCl_4$  (—●—); V. o-nitrobenzotrifluoride in  $C_6H_6$  (—▲—); VI. m-nitrobenzotrifluoride in  $C_6H_6$  (—■—); VII. 2-chloro 6-methyl aniline in  $C_6H_6$  (—▼—); VIII. 3-chloro 2-methyl aniline in  $C_6H_6$  (—\*—); IX. 3-chloro 4-methyl aniline in  $C_6H_6$  (—⊗—); X. 4-chloro 2-methyl aniline in  $C_6H_6$  (—▽—) and XI. 5-chloro 2-methyl aniline in  $C_6H_6$  (—⊠—)

imaginary  $\chi_{ij}''(=\epsilon_{ij}'')$  parts of the complex dielectric orientational susceptibility  $\chi_{ij}^*(=\epsilon_{ij}^*-\epsilon_{\infty ij})$  and the low frequency susceptibility  $\chi_{oij}(=\epsilon_{oij}-\epsilon_{\infty ij})$  which is real of the disubstituted benzenes and anilines in  $C_6H_6$  and  $CCl_4$  of Table 3.1 are used to obtain their conformational structures in terms of molecular and intra-molecular dipole moments  $\mu_2$  and  $\mu_1$  involved with the estimated  $\tau_2$  and  $\tau_1$ . Disubstituted benzenes and anilines are thought to absorb electric energy

Table 3.2: The relaxation times  $\tau_2$  and  $\tau_1$  from the slope and intercept of straight line Eq.(3.3), correlation coefficients  $r$ 's and % of error in regression technique, measured  $\tau_j$  from the slope of  $\chi_{ij}''$  vs  $\chi_{ij}'$  of Eq.(3.15) and the ratio of the individual slopes of  $\chi_{ij}''$  vs  $w_j$  and  $\chi_{ij}'$  vs  $w_j$  at  $w_j \rightarrow 0$  of Eq.(3.16), reported  $\tau$ , symmetric and characteristic relaxation times  $\tau_s$  and  $\tau_{cs}$  for different disubstituted benzenes and anilines at 35°C under 9.945 GHz electric field.

System with sl.no..	Slope & intercept of Eq.(3.3)		'r'	% of error	Estimated $\tau_2$ and $\tau_1$ in psec		Measured $\tau_j$ in psec from Eqs (3.15) & (3.16)		Rept. $\tau$ in psec	$\tau_s$ in psec	$\tau_{cs}$ in psec
(I) o-chloro nitro benzene in C <sub>6</sub> H <sub>6</sub>	1.310	0.301	0.82	9.88	16.21	4.76	12.08	10.13	13.5	7.87	17.08
(II) 4-chloro 3-nitrobenzotrifluoride in CCl <sub>4</sub>	1.666	0.059	0.95	2.94	26.08	0.58	16.43	22.66	21.1	0.00	--
(III) 4-chloro 3-nitro toluene in C <sub>6</sub> H <sub>6</sub>	1.865	0.389	0.88	6.80	26.02	3.83	16.13	19.89	20.9	10.76	39.65
(IV) 4-chloro 3-nitro toluene in CCl <sub>4</sub>	2.283	0.134	0.98	1.19	35.57	0.96	21.47	22.61	35.0	1.47	38.84
(V) o- nitrobenzo trifluoride in C <sub>6</sub> H <sub>6</sub>	1.063	0.067	0.70	15.38	15.93	1.08	12.09	11.08	13.7	10.89	28.83
(VI) m-nitrobenzotri fluoride in C <sub>6</sub> H <sub>6</sub>	1.898	0.597	0.99	0.60	24.01	6.37	14.33	36.57	19.7	6.20	--
(VII) 2-chloro 6-methyl aniline in C <sub>6</sub> H <sub>6</sub>	1.371	0.313	0.93	4.08	17.31	4.63	7.05	14.55	7.8	4.08	--
(VIII) 3-chloro 2-methyl aniline in C <sub>6</sub> H <sub>6</sub>	1.596	0.386	0.99	0.60	20.79	4.76	7.98	11.49	9.9	4.57	--
(IX) 3-chloro 4- methyl aniline in C <sub>6</sub> H <sub>6</sub>	1.891	0.561	0.99	0.67	24.37	5.90	12.07	13.65	13.6	7.28	--
(X) 4-chloro 2-methyl aniline in C <sub>6</sub> H <sub>6</sub>	3.217	1.428	0.99	0.67	42.97	8.51	12.80	11.04	18.5	7.59	--
(XI) 5-chloro 2-methyl aniline in C <sub>6</sub> H <sub>6</sub>	2.075	0.811	0.97	1.78	24.85	8.36	14.34	14.35	16.6	5.60	4.52

much more strongly in nearly 10 GHz electric field to yield considerable values of  $\tau_1$  and  $\tau_2$ . The 11 polar-nonpolar liquid mixtures under investigation are found to show the double relaxation phenomena. Most of the polar molecules are isomers of aniline and benzene. Some of the polar solutes are dissolved in C<sub>6</sub>H<sub>6</sub> while a few in CCl<sub>4</sub> to observe the solvent

effect too. Moreover, a few of the polar molecules are para-compounds in which a peculiar feature of relaxation phenomena is expected [3.15]. A strong conclusion of double relaxation phenomena of polar molecule in a non-polar solvent based on the single frequency measurement of relaxation parameters can be made only if, the accurate value of  $\chi_{oij}$  ( $\pm 1\%$ ) involved with  $\epsilon_{oij}$  and  $\epsilon_{\infty ij}$  is available. The use of  $n_{Dij}^2$  for  $\epsilon_{\infty ij}$  often introduces [3.6-3.8] an additional error in the calculation, since  $\epsilon_{\infty ij}$  is approximately equal to 1-1.5 times of  $n_{Dij}^2$ .

Bergmann et al [3.16], however, devised a graphical method to obtain  $\tau_1$  and  $\tau_2$  for a pure polar liquid. The respective weighted contributions  $c_1$  and  $c_2$  towards dielectric relaxations were estimated in terms of  $\tau_1$  and  $\tau_2$ . Bhattacharyya et al [3.17] subsequently attempted to simplify the procedure of Bergmann et al [3.16] to get the same for a pure polar molecule with  $\epsilon'$ ,  $\epsilon''$ ,  $\epsilon_0$  and  $\epsilon_\infty$ , measured at two different frequencies in GHz range. The graphical analysis advanced by Higasi et al [3.18] on polar-nonpolar liquid mixture was also a crude one.

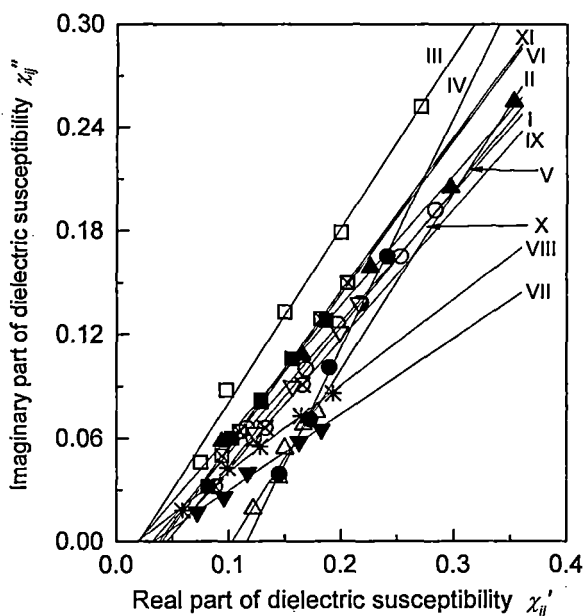


Figure 3.2: Linear variation of  $\chi_{ij}''$  with  $\chi_{ij}'$  for different  $w_j$ 's.

I. o-chloronitrobenzene in  $C_6H_6$  ( $-\circ-$ ); II. 4-chloro 3-nitrobenzotrifluoride in  $CCl_4$  ( $-\triangle-$ ); III. 4-chloro 3-nitrotoluene in  $C_6H_6$  ( $-\square-$ ); IV. 4-chloro 3-nitrotoluene in  $CCl_4$  ( $-\bullet-$ ); V. o-nitrobenzotrifluoride in  $C_6H_6$  ( $-\blacktriangle-$ ); VI. m-nitrobenzotrifluoride in  $C_6H_6$  ( $-\blacksquare-$ ); VII. 2-chloro 6-methyl aniline in  $C_6H_6$  ( $-\blacktriangledown-$ ); VIII. 3-chloro 2-methyl aniline in  $C_6H_6$  ( $-\ast-$ ); IX. 3-chloro 4-methyl aniline in  $C_6H_6$  ( $-\otimes-$ ); X. 4-chloro 2-methyl aniline in  $C_6H_6$  ( $-\nabla-$ ) and XI. 5-chloro 2-methyl aniline in  $C_6H_6$  ( $-\boxtimes-$ )

Thus, the object of the present paper is to detect  $\tau_1$  and  $\tau_2$  and hence, to measure  $\mu_1$  and  $\mu_2$  using  $\chi_{ij}$ 's based on the single frequency measurement technique [3.12, 3.19]. The aspect of molecular orientation polarisation is, however, achieved by introducing  $\chi_{ij}$  because  $\epsilon_{\infty ij}$  which includes fast polarisation, frequently appears as a subtracted term in Bergmann equations. Thus, to avoid the clumsiness of algebra and to exclude the fast polarisation process Bergmann equations [3.16] are simplified by the established symbols of  $\chi'_{ij}$ ,  $\chi''_{ij}$  and  $\chi_{oij}$  of Table 3.1 in SI units:

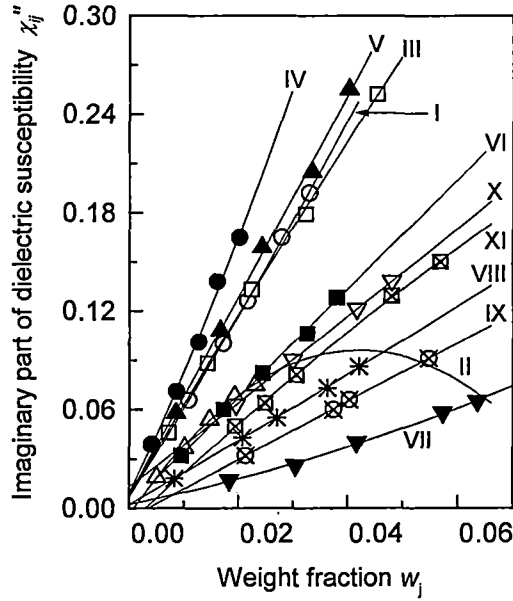


Figure 3.3: Variation of  $\chi''_{ij}$  against  $w_j$  of solutes

I. o-chloronitrobenzene in  $C_6H_6$  (—○—) II. 4-chloro 3-nitrobenzotrifluoride in  $CCl_4$  (—△—); III. 4-chloro 3-nitrotoluene in  $C_6H_6$  (—□—); IV. 4-chloro 3-nitrotoluene in  $CCl_4$  (—●—); V. o-nitrobenzotrifluoride in  $C_6H_6$  (—▲—); VI. m-nitrobenzotrifluoride in  $C_6H_6$  (—■—); VII. 2-chloro 6-methyl aniline in  $C_6H_6$  (—▼—); VIII. 3-chloro 2-methyl aniline in  $C_6H_6$  (—\*—); IX. 3-chloro 4-methyl aniline in  $C_6H_6$  (—⊗—); X. 4-chloro 2-methyl aniline in  $C_6H_6$  (—▽—) and XI. 5-chloro 2-methyl aniline in  $C_6H_6$  (—⊠—)

$$\frac{\chi'_{ij}}{\chi_{oij}} = \frac{c_1}{1 + \omega^2 \tau_1^2} + \frac{c_2}{1 + \omega^2 \tau_2^2} \quad \dots (3.1)$$

$$\frac{\chi''_{ij}}{\chi_{oij}} = c_1 \frac{\omega \tau_1}{1 + \omega^2 \tau_1^2} + c_2 \frac{\omega \tau_2}{1 + \omega^2 \tau_2^2} \quad \dots (3.2)$$

assuming two broad Debye type dispersions for which the sum of  $c_1$  and  $c_2$  is unity. The Eqs.(3.1) and (3.2) are now solved to get:

$$\frac{\chi_{oij} - \chi'_{ij}}{\chi'_{ij}} = \omega(\tau_1 + \tau_2) \frac{\chi''_{ij}}{\chi'_{ij}} - \omega^2 \tau_1 \tau_2 \quad \dots (3.3)$$

The variables  $(\chi_{oij} - \chi'_{ij})/\chi'_{ij}$  and  $\chi''_{ij}/\chi'_{ij}$  are plotted against each other for different  $w_j$ 's of the polar liquid under a single angular frequency  $\omega (=2\pi f)$  of the electric field to get a straight line with intercept  $-\omega^2 \tau_1 \tau_2$  and slope  $\omega(\tau_1 + \tau_2)$ , as shown in Fig.3.1. The intercept and slope of Eq.(3.3) are obtained by linear regression analysis made with the measured  $\chi_{ij}$ 's of solutes in  $\text{CCl}_4$  and  $\text{C}_6\text{H}_6$  to get  $\tau_2$  and  $\tau_1$  as found in the 6<sup>th</sup> and 7<sup>th</sup> columns of Table 3.2. The variables of Eq.(3.3) are extracted from Table 3.1, where all the data are collected together, system-wise, up to three decimals in close agreement with the expected [3.12]  $\tau_2$  and  $\tau_1$  of Table 3.2. Both  $\tau_2$  and  $\tau_1$  were found to deviate significantly, when the data of Table 3.1 were taken up to two decimal places with the claimed accuracy of measurement. The correlation coefficients  $r$ 's and the % of errors were worked out to place them in Table 3.2 only to see how far the variables of Eq.(3.3) are collinear to each other.

The relaxation times  $\tau$ 's due to Debye model are measured from the slope of  $\chi_{ij}''$  vs  $\chi_{ij}'$  curves of Fig.3.2 and the ratio of the individual slopes of  $\chi_{ij}''$  vs  $w_j$  and  $\chi_{ij}'$  vs  $w_j$  curves at  $w_j \rightarrow 0$  of Figs.3.3 and 3.4, respectively.  $\tau$ 's from both the methods are entered in the 8<sup>th</sup> and 9<sup>th</sup> columns of Table 3.2 only to see how far they agree with  $\tau_1$  and  $\tau_2$  due to double relaxation method of Eq.(3.3).

The theoretical values of  $c_1$  and  $c_2$  towards dielectric dispersions for  $\tau_1$  and  $\tau_2$  of different disubstituted benzenes and anilines in  $\text{C}_6\text{H}_6$  and  $\text{CCl}_4$  were calculated from Fröhlich's [3.20] theoretical formulations of  $\chi_{ij}'/\chi_{oij}$  and  $\chi_{ij}''/\chi_{oij}$ . The experimental  $c_1$  and  $c_2$ , on the other hand, were found out from  $(\chi_{ij}'/\chi_{oij})_{w_j \rightarrow 0}$  and  $(\chi_{ij}''/\chi_{oij})_{w_j \rightarrow 0}$  by graphical variations of  $\chi_{ij}'/\chi_{oij}$  and  $\chi_{ij}''/\chi_{oij}$  with  $w_j$ 's of Figs.3.5 and 3.6, in order to place them in Table 3.3 for comparison. The plots of  $\chi_{ij}'/\chi_{oij}$  and  $\chi_{ij}''/\chi_{oij}$  against  $w_j$  of the polar liquids in Figs.3.5 and 3.6 are the least squares fitted curves with the experimental points placed upon them. With the values of the intercepts presented in Table 3.3 from Figs.3.5 and 3.6 and the

graphical plot of  $(1/\phi)\log(\cos\phi)$  against  $\phi$  in degrees given elsewhere [3.4], the symmetric and asymmetric distribution parameters  $\gamma$  and  $\delta$  related to symmetric and characteristic relaxation times  $\tau_s$  and  $\tau_{cs}$  of the molecules were determined. They are seen in Table 3.3. The object of such determinations of  $\gamma$ ,  $\delta$ ,  $\tau_s$  and  $\tau_{cs}$  is to conclude the molecular nonrigidity and distribution of relaxation behaviour as well.

Table 3.3: Fröhlich's parameter  $A$ , theoretical and experimental values of  $\chi_{ij}'/\chi_{oij}$  &  $\chi_{ij}''/\chi_{oij}$  of Fröhlich equations (3.6) and (3.7) and from fitting Eqs. of Figs.3.5 and 3.6 at  $w_j \rightarrow 0$  respectively, theoretical and experimental relative contributions  $c_1$  and  $c_2$  towards dielectric dispersion due to  $\tau_1$  and  $\tau_2$ , symmetric and asymmetric distribution parameters  $\gamma$  and  $\delta$  for polar-nonpolar liquid mixtures of disubstituted benzenes and anilines at 35°C under 9.945 GHz electric field.

System with sl.no	$A$	Theoretical values of $\chi_{ij}'/\chi_{oij}$ & $\chi_{ij}''/\chi_{oij}$ from Eqs (3.6) & (3.7)		Theoretical values of $c_1$ and $c_2$		Expt. values of $\chi_{ij}'/\chi_{oij}$ & $\chi_{ij}''/\chi_{oij}$ at $w_j \rightarrow 0$ of Figs. (3.5) & (3.6)		Expt. values of $c_1$ & $c_2$		Estimated values of $\gamma$ and $\delta$			
(I) o-chloronitro benzene in $C_6H_6$	1.225	0.746	0.410	0.526	0.533	0.733	0.349	0.599	0.371	0.13	0.0095		
(II) 4-chloro 3-nitrobenzotrifluoride in $CCl_4$	3.806	0.830	0.259	0.687	0.525	0.890	0.027	0.894	-0.012	0.82	---		
(III) 4-chloro 3nitro toluene in $C_6H_6$	1.916	0.677	0.409	0.527	0.649	0.600	0.309	0.508	0.435	0.28	0.0070		
(IV) 4-chloro 3-nitro toluene in $CCl_4$	3.612	0.754	0.301	0.638	0.703	0.863	0.144	0.823	0.253	0.38	0.0024		
(V) o-nitrobenzotrifluoride in $C_6H_6$	2.691	0.873	0.266	0.653	0.444	0.616	0.347	0.288	0.655	0.21	0.0084		
(VI) m-nitrobenzotrifluoride in $C_6H_6$	1.327	0.611	0.455	0.485	0.625	1.134	0.261	1.514	-0.561	-0.45	---		
(VII) 2-chloro 6-methyl aniline in $C_6H_6$	1.319	0.737	0.412	0.527	0.544	1.078	0.141	1.402	-0.468	-0.40	---		
(VIII) 3-chloro 2-methyl aniline in $C_6H_6$	1.474	0.693	0.424	0.518	0.585	1.023	0.232	1.192	-0.194	-0.20	---		
(IX) 3-chloro 4- methyl aniline in $C_6H_6$	1.418	0.622	0.449	0.490	0.632	1.244	0.254	1.614	-0.588	-0.62	---		
(X) 4-chloro 2-methyl aniline in $C_6H_6$	1.619	0.427	0.448	0.416	0.842	1.062	0.419	1.449	-0.556	-0.33	---		
(XI) 5-chloro 2-methyl aniline in $C_6H_6$	1.089	0.547	0.475	0.462	0.627	0.907	0.312	1.354	-0.536	-0.03	0.0210		

The dipole moments  $\mu_2$  and  $\mu_1$  were then measured in terms of dimensionless parameters  $b$ 's involved with measured  $\tau$ 's of Table 3.2 and coefficients  $\beta_1$ 's and  $\beta_2$ 's presented in Table 3.4 of the variations of hf  $\chi_{ij}'$  and total hf conductivity  $\sigma_{ij}$  with  $w_j$ 's of Figs.3.4 and 3.7, respectively. The measured  $\mu$ 's are found in Table 3.4 in order to compare with theoretical dipole moment  $\mu_{\text{theo}}$ 's derived from available bond angles and bond moments of the substituent polar groups attached to the parent molecules as sketched in Fig.3.8. The structural aspect of some interesting polar molecules in Fig.3.8 exhibits the prominent mesomeric, inductive and electromeric effects of the substituted polar groups. All these effects are taken into account by the ratio  $\mu_{\text{expt}}/\mu_{\text{theo}}$ , in agreement with the measured  $\mu$ 's [3.6-3.8] of Table 3.4.

### 3.2. Formulations of $c_1$ and $c_2$ for $\tau_1$ and $\tau_2$ :

The Eqs.(3.1) and (3.2) are now solved to get  $c_1$  and  $c_2$  where

$$c_1 = \frac{(\chi'_{ij}\alpha_2 - \chi''_{ij})(1 + \alpha_1^2)}{\chi_{oij}(\alpha_2 - \alpha_1)} \quad \dots (3.4)$$

$$c_2 = \frac{(\chi''_{ij} - \chi'_{ij}\alpha_1)(1 + \alpha_2^2)}{\chi_{oij}(\alpha_2 - \alpha_1)} \quad \dots (3.5)$$

where  $\alpha_1 = \omega\tau_1$  and  $\alpha_2 = \omega\tau_2$  provided  $\alpha_2 > \alpha_1$ . The molecules under consideration are of complex type and only a few data are available under single frequency measurement in the low concentration region. A continuous distribution of  $\tau$  with two discrete values of  $\tau_1$  and  $\tau_2$  could, therefore, be expected. Thus, from Fröhlich's Eq. [3.20] based on distribution of  $\tau$  between the two extreme values of  $\tau_1$  and  $\tau_2$ , one gets:

$$\frac{\chi'_{ij}}{\chi_{oij}} = 1 - \frac{1}{2A} \ln \left( \frac{1 + \omega^2 \tau_2^2}{1 + \omega^2 \tau_1^2} \right) \quad \dots (3.6)$$

$$\frac{\chi''_{ij}}{\chi_{oij}} = \frac{1}{A} \left[ \tan^{-1}(\omega\tau_2) - \tan^{-1}(\omega\tau_1) \right] \quad \dots (3.7)$$

where the Fröhlich parameter A is given by  $A = \ln(\tau_2/\tau_1)$ . The theoretical values of  $\chi_{ij}'/\chi_{oij}$  and  $\chi_{ij}''/\chi_{oij}$  of Eqs.(3.6) and (3.7) were used to get theoretical  $c_1$  and  $c_2$  from Eqs.(3.4) and (3.5) in order to compare them with the experimental values of  $c_1$  and  $c_2$  from the graphical plots of  $\chi_{ij}'/\chi_{oij}$  and  $\chi_{ij}''/\chi_{oij}$  at  $w_j \rightarrow 0$  as seen in Figs.3.5 and 3.6 respectively. Both the theoretical and experimental  $c_1$  and  $c_2$  are presented in Table 3.3 for comparison.

### 3.3. Distribution parameters $\gamma$ and $\delta$ related to symmetric and characteristic relaxation times $\tau_s$ and $\tau_{cs}$ :

The molecules are expected to show either symmetrical circular arc or a skewed arc in addition to other models [3.21] when the values of  $\chi_{ij}''/\chi_{oij}$  are plotted against  $\chi_{ij}'/\chi_{oij}$  at  $w_j \rightarrow 0$  for various frequencies of the electric field to yield:

$$\frac{\chi_{ij}^*}{\chi_{oij}} = \frac{1}{1 + (j\omega\tau_s)^{1-\gamma}} \quad \dots (3.8)$$

$$\frac{\chi_{ij}^*}{\chi_{oij}} = \frac{1}{(1 + j\omega\tau_{cs})^\delta} \quad \dots (3.9)$$

Here,  $\gamma$  and  $\delta$  are the symmetric and asymmetric distribution parameters related to symmetric and characteristic relaxation times  $\tau_s$  and  $\tau_{cs}$ , respectively. Separating the real and imaginary parts of Eq.(3.8) one gets:

$$\gamma = \frac{2}{\pi} \tan^{-1} \left[ \left( 1 - \frac{\chi_{ij}'}{\chi_{oij}} \right) \frac{\chi_{ij}'/\chi_{oij}}{\chi_{ij}''/\chi_{oij}} - \frac{\chi_{ij}''}{\chi_{oij}} \right] \quad \dots (3.10)$$

$$\tau_s = \frac{1}{\omega} \left[ 1 / \left( \frac{\chi_{ij}'/\chi_{oij}}{\chi_{ij}''/\chi_{oij}} \cos \frac{\gamma\pi}{2} - \sin \frac{\gamma\pi}{2} \right) \right]^{\frac{1}{1-\gamma}} \quad \dots (3.11)$$

where  $\chi_{ij}'/\chi_{oij}$  and  $\chi_{ij}''/\chi_{oij}$  are obtained from intercepts of each variable with  $w_j$ 's of Figs.3.5 and 3.6 in the limit  $w_j=0$ . Again  $\delta$  and  $\tau_{cs}$  can be had from Eq.(3.9) as:

$$\tan(\phi\delta) = \frac{(\chi''_{ij}/\chi_{oij})_{w_j \rightarrow 0}}{(\chi'_{ij}/\chi_{oij})_{w_j \rightarrow 0}} \quad \dots (3.12)$$

$$\tau_{cs} = \frac{1}{\omega} \tan \phi \quad \dots (3.13)$$

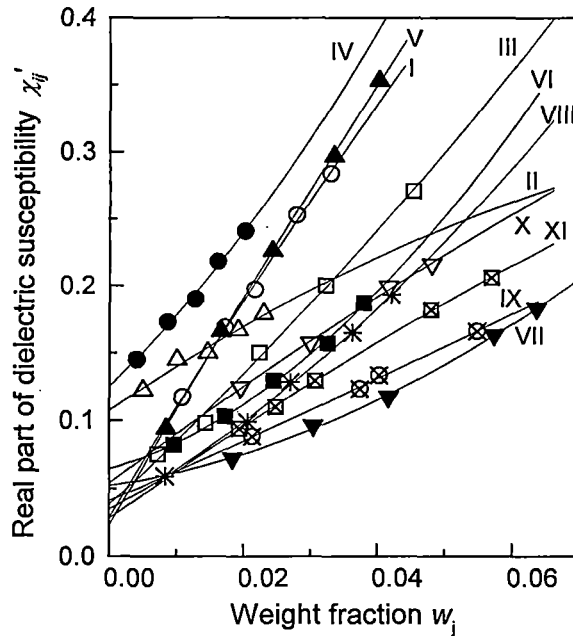


Figure 3.4 : Variation of  $\chi'_{ij}$  against  $w_j$  of solutes

- I. o-chloronitrobenzene in  $C_6H_6$  (-○-); II. 4-chloro 3-nitrobenzotrifluoride in  $CCl_4$  (-△-); III. 4-chloro 3-nitrotoluene in  $C_6H_6$  (-□-); IV. 4-chloro 3-nitrotoluene in  $CCl_4$  (-●-); V. o-nitrobenzotrifluoride in  $C_6H_6$  (-▲-); VI. m-nitrobenzotrifluoride in  $C_6H_6$  (-■-); VII. 2-chloro 6-methyl aniline in  $C_6H_6$  (-▼-); VIII. 3-chloro 2-methyl aniline in  $C_6H_6$  (-\*-); IX. 3-chloro 4-methyl aniline in  $C_6H_6$  (-⊗-); X. 4-chloro 2-methyl aniline in  $C_6H_6$  (-▽-) and XI. 5-chloro 2-methyl aniline in  $C_6H_6$  (-⊠-)

Since,  $\phi$  can not be evaluated directly, a theoretical curve of  $(1/\phi)\log(\cos\phi)$  with  $\phi$  in degrees was drawn as shown elsewhere [3.4], from which:

$\frac{1}{\phi} \log(\cos\phi) = \frac{\log[(\chi'_{ij}/\chi_{oij})/\cos(\phi\delta)]}{\phi\delta}$	$\dots (3.14)$
---	----------------

Table 3.4: Slope  $\beta_1$  of  $\chi_{ij}'$  vs  $w_j$  and  $\beta_2$  of  $\sigma_{ij}$  vs  $w_j$  curves, measured dipole moments  $\mu_j$  from susceptibility measurement technique and  $hf$  conductivity method from Eqs.(3.19) and (3.26) respectively, reported dipole moment, theoretical dipole moment  $\mu_{theo}$  from available bond angles and bond moments expressed in Coulomb.metre (C.m) and the values of  $\mu_{expt}/\mu_{theo}$  for different disubstituted benzenes and anilines at 35 °C under 9.945 GHz electric field.

System with sl.no. & mol.wt.	Slope of $\chi_{ij}'-w_j$ & $\sigma_{ij}-w_j$ curves		Dipole moments $\mu_j$ ( $\times 10^{-30}$ ) in Coulomb.metre								$\mu_{expt}/\mu_{theo}$
	$\beta_1$	$\beta_2$	From Eq (3.19)		From Eq (3.26)		$\mu_j^a$	$\mu_j^b$	$\mu_j^r$	$\mu_{theo}$	
			$\mu_2$	$\mu_1$	$\mu_2$	$\mu_1$					
(I) o-chloronitro benzene in $C_6H_6$ $M_j=0.1575$ Kg	8.326	4.706	16.93	12.41	17.11	12.54	14.90	14.07	14.50	17.60	0.96
(II) 4-chloro3-nitrobenzotrifluoride in $CCl_4$ $M_j=0.2255$ Kg	3.358	1.875	13.02	6.81	13.08	6.84	9.76	11.80	10.57	12.60	1.03
(III) 4-chloro 3-nitro toluene in $C_6H_6$ $M_j=0.1715$ Kg	4.490	2.570	17.39	9.37	17.69	9.53	12.94	14.54	14.97	18.60	0.93
(IV) 4-chloro 3-nitro toluene in $CCl_4$ $M_j=0.1715$ Kg	4.854	3.001	17.40	7.15	18.39	7.56	11.95	12.36	15.60	18.50	0.94
(V) o-nitrobenzotrifluoride in $C_6H_6$ $M_j=0.1910$ Kg	8.598	4.662	18.78	13.34	18.59	13.20	16.68	16.18	16.54	20.60	0.91
(VI) m-nitrobenzotrifluoride in $C_6H_6$ $M_j=0.1910$ Kg	1.426	0.702	9.77	5.83	9.22	5.50	7.27	13.52	12.24	12.47	0.78
(VII) 2-chloro 6-methyl aniline in $C_6H_6$ $M_j=0.1415$ Kg	0.728	0.560	4.91	3.47	5.79	4.09	3.64	4.50	7.73	6.16	0.56
(VIII) 3-chloro 2-methyl aniline in $C_6H_6$ $M_j=0.1415$ Kg	2.674	1.693	10.47	6.66	11.20	7.13	7.14	7.86	10.07	8.27	0.81
(IX) 3-chloro4-methyl aniline in $C_6H_6$ $M_j=0.1415$ Kg	2.128	1.269	10.38	6.07	10.78	6.30	7.14	7.49	8.70	7.33	0.83
(X) 4-chloro2-methyl aniline in $C_6H_6$ $M_j=0.1415$ Kg	3.650	2.063	21.38	8.45	21.61	8.54	9.56	9.07	10.94	10.20	0.83
(XI) 5-chloro2-methyl aniline in $C_6H_6$ $M_j=0.1415$ Kg	3.481	2.196	13.46	8.22	14.37	8.78	9.79	9.79	0.34	9.44	0.87

$\mu_j^a$  = dipole moment by using  $\tau$  from the direct slope of Eq (3.15)

$\mu_j^b$  = dipole moment by using  $\tau$  from the ratio of individual slopes of Eq (3.16)

$\mu_j^r$  = reported dipole moment

$\mu_{theo}$  = theoretical dipole moment from the available bond angles and bond moments.

was found out. The known values of  $(1/\phi)\log(\cos\phi)$  was then used to obtain  $\phi$ . With known  $\phi$  and  $\delta$ ,  $\tau_{cs}$  were obtained from Eqs.(3.12) and (3.13) for each molecule. The estimated  $\gamma$  and  $\delta$  are presented in columns 11 and 12 of Table 3.3. Values of  $\tau_s$  and  $\tau_{cs}$  are entered in columns 11 and 12 of Table 3.2 to conclude symmetric relaxation behaviour for disubstituted anilines and asymmetric relaxation behaviour for disubstituted benzenes, respectively.

#### 3.4. Theoretical formulation for dipole moments $\mu_2$ and $\mu_1$ :

The Debye equation [3.22] for a polar-nonpolar liquid mixture under hf electric field in terms of  $\chi_{ij}$ 's is written as:

$$\frac{d\chi_{ij}''}{d\chi_{ij}'} = \omega\tau \quad \dots (3.15)$$

$$\frac{(d\chi_{ij}''/dw_j)_{w_j \rightarrow 0}}{(d\chi_{ij}'/dw_j)_{w_j \rightarrow 0}} = \omega\tau \quad \dots (3.16)$$

$\tau$ 's of the polar liquids could, however, be estimated from Eqs.(3.15) and (3.16) as seen in 8<sup>th</sup> and 9<sup>th</sup> columns of Table 3.2. Again the imaginary part  $\chi_{ij}''$  of the complex hf susceptibility  $\chi_{ij}^*$  as a function of  $w_j$  of a solute can be written as [3.23-3.24]:

$$\chi_{ij}'' = \frac{N\rho_{ij}\mu_j^2}{27\varepsilon_0 k_B T M_j} \frac{\omega\tau}{1 + \omega^2\tau^2} (\varepsilon_{ij} + 2)^2 w_j$$

which on differentiation with respect to  $w_j$  and at  $w_j \rightarrow 0$  yields:

$$\left( \frac{d\chi_{ij}''}{dw_j} \right)_{w_j \rightarrow 0} = \frac{N\rho_i\mu_j^2}{27\varepsilon_0 k_B T M_j} \frac{\omega\tau}{(1 + \omega^2\tau^2)} (\varepsilon_i + 2)^2 \quad \dots (3.17)$$

where the density of the solution  $\rho_{ij}$  becomes  $\rho_i$ =density of solvent,  $(\varepsilon_{ij}+2)^2$  becomes  $(\varepsilon_i+2)^2$  at  $w_j \rightarrow 0$ ,  $k_B$ =Boltzmann constant,  $N$ =Avogadro's number,  $\varepsilon_i$ =relative permittivity of solvent

and  $\epsilon_0$ =permittivity of free space =  $8.854 \times 10^{-12}$  Farad. metre<sup>-1</sup>. All are expressed in SI units.

Comparing Eqs.(3.16) and (3.17) one gets:

$$\left( \frac{d\chi'_{ij}}{dw_j} \right)_{w_j \rightarrow 0} = \frac{N\rho_i \mu_j^2}{27\epsilon_0 k_B T M_j} \frac{1}{(1 + \omega^2 \tau^2)} (\epsilon_i + 2)^2 = \beta_1 \quad \dots (3.18)$$

where  $\beta_1$  is the slope of  $\chi'_{ij}$  vs  $w_j$  curves of Fig.3.4 at  $w_j \rightarrow 0$ . Here, no approximation in determination of  $\mu_j$  is made, like the conductivity measurement technique [3.4] given below.

After simplification, the hf dipole moment  $\mu_j$  is given by:

$$\mu_j = \left( \frac{27\epsilon_0 k_B T M_j \beta_1}{N\rho_i (\epsilon_i + 2)^2 b} \right)^{\frac{1}{2}} \quad \dots (3.19)$$

where dimensionless parameter  $b$  is given by :

$$b = 1/(1 + \omega^2 \tau^2) \quad \dots (3.20)$$

### 3.5. Dipole moments $\mu_2$ and $\mu_1$ from hf conductivity :

The complex hf conductivity  $\sigma_{ij}^*$  of polar-nonpolar liquid mixture in a GHz electric field is given by [3.25]:

$$\sigma_{ij}^* = \sigma'_{ij} + j\sigma''_{ij} \quad \dots (3.21)$$

where  $\sigma'_{ij}$ (= $\omega\epsilon_0\epsilon_{ij}''$ ) and  $\sigma''_{ij}$ (= $\omega\epsilon_0\epsilon_{ij}'$ ) are the real and imaginary parts of the complex conductivity  $\sigma_{ij}^*$  in  $\Omega^{-1} .m^{-1}$ . The magnitude of the total hf conductivity is:

$$\sigma_{ij} = \omega\epsilon_0 \left( \epsilon_{ij}''^2 + \epsilon_{ij}'^2 \right)^{\frac{1}{2}} \quad \dots (3.22)$$

Although  $\epsilon_{ij}' \gg \epsilon_{ij}''$ , but in the high frequency region,  $\epsilon_{ij}' \cong \epsilon_{ij}''$ .  $\epsilon_{ij}''$  is responsible for absorption of electric energy and offers resistance to polarisation. Hence  $\sigma_{ij}''$  is related to  $\sigma_{ij}'$  by the relation [3.25]:

$$\sigma_{ij}'' = \sigma_{\infty ij} + \frac{1}{\omega\tau} \sigma_{ij}'$$

$$\sigma_{ij}' = \sigma_{\infty ij} + \frac{1}{\omega\tau} \sigma_{ij}'' \quad \dots (3.23)$$

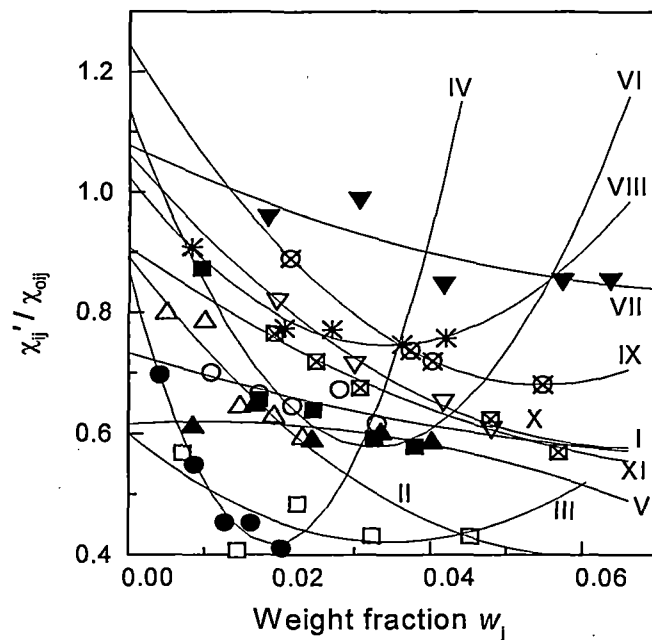


Figure 3.5 : Plot of  $\chi_{ij}''/\chi_{\infty ij}$  with  $w_j$  of solutes

- I. o-chloronitrobenzene in  $C_6H_6$  (—○—); II. 4-chloro 3-nitrobenzo-trifluoride in  $CCl_4$  (—△—); III. 4-chloro 3-nitrotoluene in  $C_6H_6$  (—□—); IV. 4-chloro 3-nitrotoluene in  $CCl_4$  (—●—); V. o-nitrobenzotrifluoride in  $C_6H_6$  (—▲—); VI. m-nitrobenzotrifluoride in  $C_6H_6$  (—■—); VII. 2-chloro 6-methyl aniline in  $C_6H_6$  (—▼—); VIII. 3-chloro 2-methyl aniline in  $C_6H_6$  (—\*—); IX. 3-chloro 4-methyl aniline in  $C_6H_6$  (—⊗—); X. 4-chloro 2-methyl aniline in  $C_6H_6$  (—▽—) and XI. 5-chloro 2-methyl aniline in  $C_6H_6$  (—⊠—)

Here, the approximation  $\sigma_{ij}'' \cong \sigma_{ij}'$  is made. Differentiation of Eq.(3.23) with respect to  $w_j$  at  $w_j \rightarrow 0$  yields:

$$\left(\frac{d\sigma'_{ij}}{dw_j}\right)_{w_j \rightarrow 0} = \omega\tau \left(\frac{d\sigma_{ij}}{dw_j}\right)_{w_j \rightarrow 0} = \omega\tau\beta_2 \quad \dots (3.24)$$

where  $\beta_2$  is the slope of  $\sigma_{ij}$  vs  $w_j$  curves of Fig.3.7 at infinite dilution  $w_j \rightarrow 0$  and placed in Table 3.4.

The real part of hf conductivity  $\sigma'_{ij}$  at T K [3.23] is given by:

$$\sigma'_{ij} = \frac{N\rho_{ij}\mu_j^2}{27k_B TM_j} \frac{\omega^2\tau}{1+\omega^2\tau^2} (\epsilon_{ij} + 2)^2 w_j$$

$$\left(\frac{d\sigma'_{ij}}{dw_j}\right)_{w_j \rightarrow 0} = \frac{N\rho_{ij}\mu_j^2}{27k_B TM_j} \frac{\omega^2\tau}{1+\omega^2\tau^2} (\epsilon_i + 2)^2 \quad \dots (3.25)$$

Comparing Eqs.(3.24) and (3.25) one gets the dipole moment  $\mu_j$  from:

$$\mu_j = \left(\frac{27k_B TM_j \beta_2}{N\rho_{ij} (\epsilon_i + 2)^2 \omega b}\right)^{\frac{1}{2}} \quad \dots (3.26)$$

All the measured dipole moments  $\mu_j$ 's from the susceptibility measurement technique of Eq.(3.19) and hf conductivity method of Eq.(3.26) are entered in the 4<sup>th</sup> -7<sup>th</sup> columns of Table 3.4 respectively.

### 3.6. Results and discussions :

The double relaxation times  $\tau_1$  and  $\tau_2$  for the polar liquid molecules in different solvents are found out from the slope and intercept of Eq.(3.3), as shown in Fig.3.1, in terms of the orientational susceptibility parameters  $\chi_{ij}$ 's of Table 3.1. The  $\chi_{ij}$ 's are, however, derived from the relative permittivities  $\epsilon_{ij}$ 's [3.6-3.8] for different weight fractions  $w_j$ 's of the polar liquids. The variables of Eq.(3.3) i.e  $(\chi_{oij} - \chi_{ij}')/\chi_{ij}'$  and  $\chi_{ij}''/\chi_{ij}'$  are plotted against each other for different  $w_j$ 's of solutes under 9.945 GHz electric field at 35<sup>o</sup>C to get linear equation by regression analysis. From Fig.3.1, it revealed that, the fitting is good for some cases, but poor in other cases. It appears that the linear fit for II (- $\Delta$ -), III (- $\square$ -) and IV (- $\bullet$ -) in Figs.3.1 and 3.2 often passes through two among five data points, others being off

from the fit. Nevertheless, the regression analysis was made on the basis of Eq. (3.3). However, the accuracy of Fig.3.1 is tested by the correlation coefficients  $r$ 's, which were found to be close to unity, indicating the variables are almost collinear.

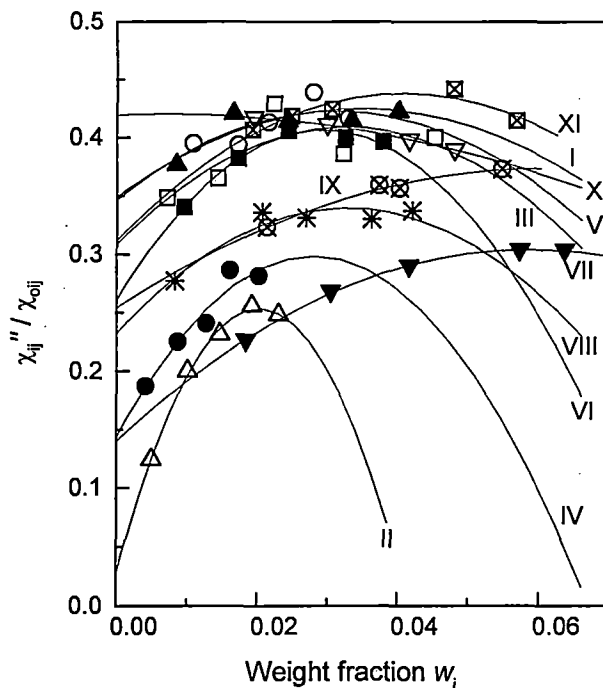


Figure 3.6 : Plot of  $\chi''_{ij}/\chi''_{oij}$  with  $w_j$  of solutes

- I. o-chloronitrobenzene in  $C_6H_6$  (-○-); II. 4-chloro 3-nitrobenzo-trifluoride in  $CCl_4$  (-△-) III. 4-chloro 3-nitrotoluene in  $C_6H_6$  (-□-) IV. 4-chloro 3-nitrotoluene in  $CCl_4$  (-●-) V. o-nitro-benzotrifluoride in  $C_6H_6$  (-▲-) VI. m-nitrobenzotrifluoride in  $C_6H_6$  (-■-) VII. 2-chloro 6-methyl aniline in  $C_6H_6$  (-▼-) VIII. 3-chloro 2-methyl aniline in  $C_6H_6$  (-\*-) IX. 3-chloro 4-methyl aniline in  $C_6H_6$  (-⊗-) X. 4-chloro 2-methyl aniline in  $C_6H_6$  (-▽-) and XI. 5-chloro 2-methyl aniline in  $C_6H_6$  (-⊠-)

The % of errors in terms of  $r$ 's in getting the intercepts and slopes were worked out to find the accuracies of  $\tau_1$  and  $\tau_2$  respectively. In order to locate the double relaxation phenomena of the polar liquid molecules in non-polar aprotic solvents under investigation, accurate measurement of  $\chi_{oij}$  involved with  $\epsilon_{oij}$  and  $\epsilon_{\infty ij}$  is necessary. The refractive index  $n_{Dij}$  measured by Abbe's refractometer often yields  $\epsilon_{\infty i} = n_{Dij}^2$ , although Cole Cole [3.26] and Cole

Davidson [3.27] plots usually give  $\epsilon_{\infty ij} \cong 1.0$  to 1.5 times of  $n_{Dij}^2$ . This often introduces an additional error in the calculations. Nevertheless, the accuracies of  $\chi_{ij}''$ ,  $\chi_{ij}'$  and  $\chi_{oij}$  are of 5% and 1%, respectively derived from measured [3.6-3.8] relative permittivities  $\epsilon_{ij}''$ ,  $\epsilon_{ij}'$ ,  $\epsilon_{oij}$  and  $\epsilon_{\infty ij}$ . The estimated  $\tau_2$  and  $\tau_1$  are placed in Table 3.2, in order to compare them with those of Murthy et al [3.28] of Eq.(3.15) and by the ratio of the individual slopes of the variations of  $\chi_{ij}''$  and  $\chi_{ij}'$  with  $w_j$ 's in the limit  $w_j \rightarrow 0$  of Eq.(3.16). The latter method seems to be better to calculate  $\tau$ , since it eliminates polar-polar interaction almost completely. The linear plot of  $\chi_{ij}''$  against  $\chi_{ij}'$  of Fig.3.2 for different  $w_j$ 's of solute has intercepts although it was expected from Eq.(3.15) that, they should pass through the origin. Nevertheless,  $\tau$ 's are found to be in close agreement with those calculated from the ratio of the individual slopes of the variations of  $\chi_{ij}''$  and  $\chi_{ij}'$  with  $w_j$  at  $w_j \rightarrow 0$  of Eq.(3.16) as shown in Figs.3.3 and 3.4. The experimental points as shown in Figs.3.3 and 3.4 with the fit are presented (Table 3.2) to back up the results of Eq.(3.16) due to Debye model. Values of  $\chi_{ij}''$  increase monotonically with  $w_j$ 's and have a tendency to meet the origin for all the curves. This type of behaviour indicates that  $\chi_{ij}''$  tends to pass through the origin at  $w_j \rightarrow 0$  under 9.945 GHz electric field.

It is evident from Table 3.2 that, all the disubstituted benzenes exhibit the whole molecular rotation while the disubstituted anilines show the rotation of the flexible parts under 10 GHz electric field when  $\tau_1$ 's and  $\tau_2$ 's are compared with the reported data. This indicates the flexible parts are more rigid in the disubstituted benzenes rather than the disubstituted anilines. The assumptions of symmetric and asymmetric relaxation behaviours from Eqs.(3.8) and (3.9) for such non rigid polar molecules yield  $\tau_s$  and  $\tau_{cs}$  from Eqs.(3.11) and (3.13) to place them in the last two columns of Table 3.2. It reveals that the symmetric and asymmetric relaxation processes are more probable since  $\tau_s$  and  $\tau_{cs}$  are almost in agreement with the reported  $\tau$ 's in a solution. The characteristic relaxation times  $\tau_{cs}$  are sometimes very high through asymmetric distribution parameter  $\delta$  and often could not be determined for most of the molecules.

The disubstituted benzenes showed  $\tau_2$ 's in agreement with the reported  $\tau$ 's and  $\tau_{cs}$  except o-nitrobenzotrifluoride in  $C_6H_6$ , which agrees with  $\tau_s$  only. But, 4-chloro 3-nitrobenzotrifluoride in  $CCl_4$  and m-nitrobenzotrifluoride in  $C_6H_6$  yield  $\tau_2$  in close

agreement with reported  $\tau$ 's although they showed  $\tau_s \cong \tau_1$ . Only 2-chloro 6-methyl aniline and 3-chloro 2-methyl aniline in  $C_6H_6$  showed  $\tau_1$ 's in excellent agreement with the calculated  $\tau_s$ 's. For the rest disubstituted anilines  $\tau_1$ 's agree well with the calculated  $\tau_s$ 's, but the agreement is not better with the measured  $\tau$ 's from Eqs.(3.15) and (3.16). It thus reveals that, a part of the disubstituted anilines is rotating, obeying symmetric relaxation behaviour, while most of the disubstituted benzenes showed asymmetric relaxation process for their whole molecular rotations.

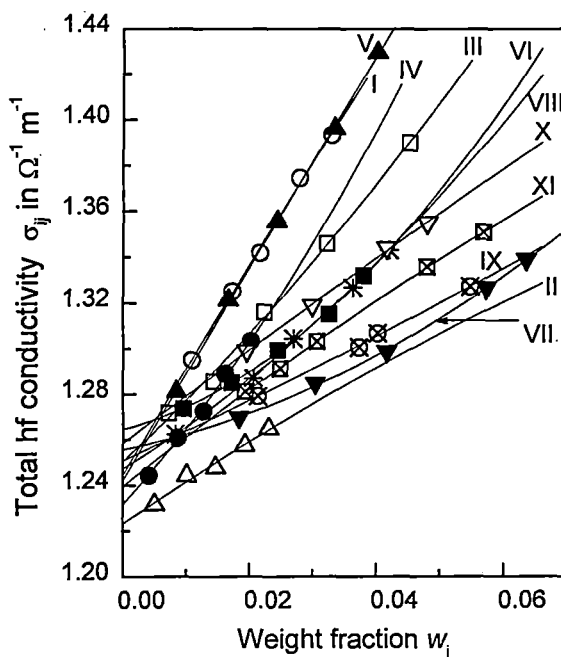


Figure 3.7 : Variation of  $\sigma_{ij}$  against  $w_j$  of solutes

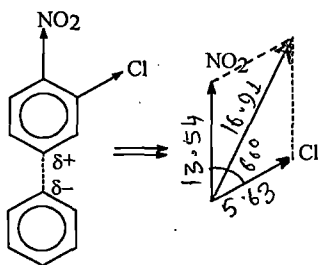
- I. o-chloronitrobenzene in  $C_6H_6$  (-○-); II. 4-chloro 3-nitrobenzo-trifluoride in  $CCl_4$  (-△-); III. 4-chloro 3-nitrotoluene in  $C_6H_6$  (-□-); IV. 4-chloro 3-nitrotoluene in  $CCl_4$  (-●-); V. o-nitro-benzotrifluoride in  $C_6H_6$  (-▲-); VI. m-nitrobenzotrifluoride in  $C_6H_6$  (-■-); VII. 2-chloro 6-methyl aniline in  $C_6H_6$  (-▼-); VIII. 3-chloro 2-methyl aniline in  $C_6H_6$  (-\*-); IX. 3-chloro 4-methyl aniline in  $C_6H_6$  (-⊗-); X. 4-chloro 2-methyl aniline in  $C_6H_6$  (-▽-) and XI. 5-chloro 2-methyl aniline in  $C_6H_6$  (-⊠-)

The relative weighted contributions  $c_1$  and  $c_2$  towards dielectric dispersions due to  $\tau_1$  and  $\tau_2$  are estimated and placed in Table 3.3, by using Fröhlich's Eqs.(3.6) and (3.7). They are compared with the experimental  $c_1$  and  $c_2$  from the fitted curves of  $\chi_{ij}'/\chi_{oij}$  and  $\chi_{ij}''/\chi_{oij}$

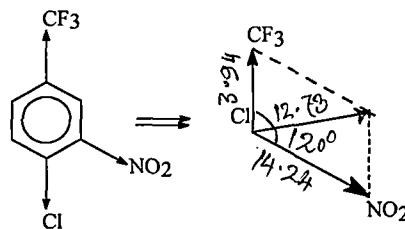
against  $w_j$  in the limit  $w_j \rightarrow 0$  of Figs.3.5 and 3.6. The nonlinear fit with only five points for III ( $-\square-$ ) and IV ( $-\bullet-$ ) of Fig.3.5 appeared to be non-convincing and misleading, but three accurate experimental points are enough for such fit. However, the fit is done with a PC and appropriate software. All the curves of Figs.3.5 and 3.6 vary usually [3.12] except the convex curve V for o-nitrobenzotrifluoride in  $C_6H_6$ . The variations of  $\chi_{ij}'/\chi_{oij}$  with  $w_j$  are, however, concave and convex in nature for all systems as observed elsewhere [3.12]. The left hand sides of Eqs.(3.1) and (3.2) vary with  $w_j$ 's in concave and convex manner according to Figs.3.5 and 3.6 are now fixed for  $\tau_1$  and  $\tau_2$  once estimated from intercept and slope of Eq.(3.3) to yield experimental  $c_1$  and  $c_2$  values from Eqs.(3.4) and (3.5) at  $w_j \rightarrow 0$ .

This study is supposed to yield the accurate values of  $c_1$  and  $c_2$  unlike the earlier one [3.12] based on the graphical extrapolated values of  $(\epsilon_{ij}' - \epsilon_{\infty ij})/(\epsilon_{oij} - \epsilon_{\infty ij})$  and  $\epsilon_{ij}''/(\epsilon_{oij} - \epsilon_{\infty ij})$  at  $w_j \rightarrow 0$  drawn on the basis of scientific judgment. Although, the nature of variations remains unaltered, it is evident from Table 3.3 that,  $c_2$ 's are often negative for 4-chloro 3-nitrobenzotrifluoride in  $CCl_4$ , m-nitrobenzotrifluoride in  $C_6H_6$  and for all the disubstituted anilines unlike other systems. This perhaps signifies that the rotation of the flexible parts of the polar molecules are not in accord with the whole molecular rotation due to inherent inertia of the substituted parts of the molecules under hf electric field. The theoretical values of  $c_1+c_2$  are found to be greater than the sum of the experimental ones as listed in Table 3.3.

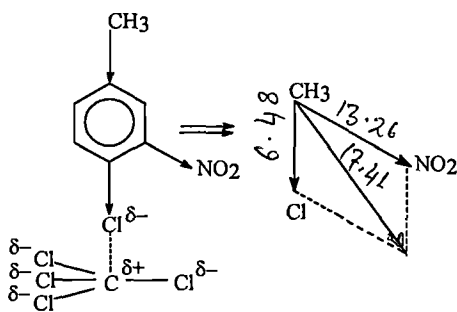
The experimental values show that  $c_1+c_2 \cong 1$  for almost all the non-spherical polar liquid molecules. But (II) 4-chloro 3-nitrobenzo-trifluoride in  $CCl_4$  ( $-\triangle-$ ), (X) 4-chloro 2-methyl aniline ( $-\nabla-$ ) and (XI) 5-chloro 2-methyl aniline ( $-\boxtimes-$ ) in  $C_6H_6$  show considerably lower values of  $c_1+c_2$ . This may indicate the reliability of Eq.(3.3) so far derived for such molecules, although they show high correlation coefficients  $r$ 's and the corresponding very low % of errors to get the intercept and slope of Eq.(3.3). The largest theoretical  $c_1+c_2$  value for (IV) 4-chloro 3-nitro toluene in  $CCl_4$  ( $-\bullet-$ ) is 1.34, showing a deviation of nearly 34%, unlike the other systems. The possible existence of more than two broad Debye type dispersions may be taken into account for such molecules of varying complexities as reported in Tables and Figures.



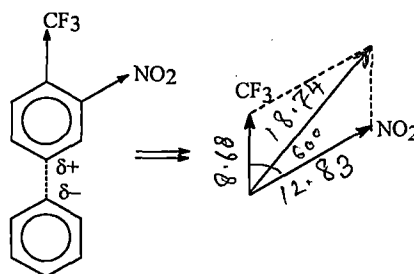
I. o-chloronitrobenzene in  $C_6H_6$



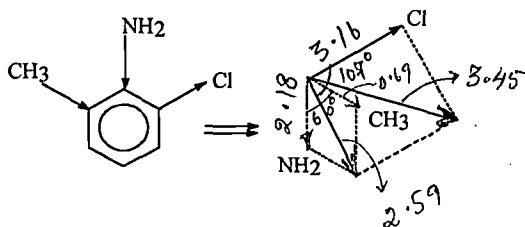
II. 4-chloro 3-nitrobenzotrifluoride in  $CCl_4$



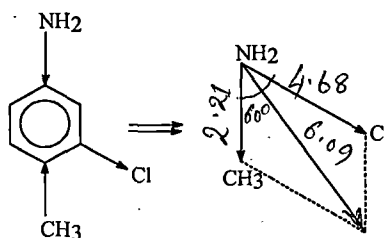
IV. 4-chloro 3-nitro toluene in  $CCl_4$



V. o-nitrobenzotrifluoride in  $C_6H_6$



VII. 2-chloro 6-methyl aniline in  $C_6H_6$



IX. 3-chloro 4-methyl aniline in  $C_6H_6$

Figure 3.8: Conformational structures of solutes from bond angles and bond moments multiplied by  $10^{-30}$  Coulomb. metre (C.m)

Dipole moments  $\mu_2$  and  $\mu_1$  due to rotation of the whole molecule as well as the flexible parts were, however, measured from Eq.(3.19) using dimensionless parameters  $b$ 's involved with  $\tau$ 's by both the methods and slope  $\beta_1$ 's of  $\chi_{ij}'$  vs  $w_j$  curves of Fig.3.4. The

measured values of  $\mu_2$  and  $\mu_1$  are presented in Table 3.4. The variations of all the  $\chi_{ij}'$ 's of polar-nonpolar liquid mixtures are found to be parabolic with  $w_j$ 's of polar compounds as evident from Fig.3.4. They are found to cut the ordinate axis at  $w_j=0$  within  $0.0238 \leq \chi_{ij}' \leq 0.0645$  except 4-chloro 3-nitrobenzotrifluoride in  $\text{CCl}_4$  ( $-\Delta-$ ), 4-chloro 3-nitrotoluene in  $\text{CCl}_4$  ( $-\bullet-$ ). This behaviour probably reflects the solvent effects on the polar compounds under investigation. The interaction of solute on solvent  $\text{CCl}_4$  may occur due to slightly positive charge  $\delta^+$  on C atom of  $\text{CCl}_4$  and negative charge  $\delta^-$  on Cl atom of the substituted group in the benzene ring, as seen in Fig.3.8. All the systems are of similar nature having monotonic increase of  $\chi_{ij}'$  with  $w_j$ .

The dipole moments  $\mu_2$  and  $\mu_1$  are also derived from the conductivity measurement technique of Eq.(3.26) using the slope  $\beta_2$ 's of  $\sigma_{ij}$  vs  $w_j$  curves of Fig.3.7 and are placed in Table 3.4 for comparison. The total hf conductivity  $\sigma_{ij}$  of all the polar-nonpolar liquid mixtures increase monotonically with  $w_j$  and cut the ordinate axis within the range  $1.2233 \leq \sigma_{ij} \leq 1.2646$  at  $w_j=0$  as seen in Fig.3.7. The slight disagreement of  $\mu_1$  and  $\mu_2$  derived from both the methods is due to the fact that the hf conductivity includes the fast polarisation probably for the bound molecular charge associated with the molecule. All  $\mu_2$ 's for disubstituted benzenes and  $\mu_1$ 's for disubstituted anilines are found to agree with the reported  $\mu$ 's placed in Table 3.4. This indicates that, the flexible parts of the disubstituted benzenes are more rigid in comparison to disubstituted anilines.

The hf dipole moment  $\mu_j$ 's are calculated by using  $\tau$  from both the methods of direct slope of Eq.(3.15) and the ratio of the individual slopes of Eq.(3.16) in order to place them in Table 3.4.  $\mu_j$ 's by using  $\tau$  from the ratio of the individual slopes are in close agreement with the reported values suggesting the fact that the latter method to get  $\tau$  is more realistic. In such case one polar molecule is surrounded by a large number of non-polar solvent molecules and remains in a quasi-isolated state.

A special attention is, therefore, paid to obtain the conformational structures of some of the complex molecules as shown schematically in Fig.3.8. The inductive, electromeric and resonance effects combined with mesomeric effect of the substituted polar groups play the key role to yield the theoretical dipole moment  $\mu_{\text{theo}}$ 's depending on the electron affinity

of C-atom of the benzene ring. The molecules have  $C \rightarrow CF_3$ ,  $C \leftarrow NH_2$  ( $\angle 142^\circ$ ),  $C \rightarrow NO_2$ ,  $C \rightarrow Cl$   $C \leftarrow CH_3$  polar groups of bond moments  $9.53 \times 10^{-30}$ ,  $4.93 \times 10^{-30}$ ,  $14.10 \times 10^{-30}$ ,  $5.63 \times 10^{-30}$ ,  $1.23 \times 10^{-30}$  Coulomb.metre (C.m) respectively [3.12,3.19] aligned in different angles in a plane to yield  $\mu_{theo}$ . Out of these, only  $-NO_2$  and  $-NH_2$  groups are in the habit to show resonance effect ( $-R$  or  $+R$ ) in the molecules either by pulling or pushing electrons towards C-atom of the benzene ring. This resonance effect is more stronger than inductive effects ( $+I$  or  $-I$ ) to exhibit the peculiar behaviours as seen in the  $\chi_{ij}'/\chi_{oij}$  vs  $w_j$  and  $\chi_{ij}''/\chi_{oij}$  vs  $w_j$  curves for the disubstituted benzenes II, IV, V, VI including all the disubstituted anilines.

The structure of these polar molecules is of special interest as sketched in Fig.3.8 in view of rearrangement of charge density in them. All the disubstituted anilines include  $-Cl$ ,  $-NH_2$  and  $-CH_3$  polar groups, of which  $-Cl$  and  $-CH_3$  have very weak inductive effects ( $+I$  or  $-I$ ). They are easily influenced by the GHz electric field to show the rotation of their flexible parts. Further, the observed difference in  $\mu$  values for a polar molecule in two aprotic non-polar solvents may arise due to weak polarity of  $CCl_4$  as shown in Fig.3.8. The difference between  $\mu_{theo}$ 's and experimental  $\mu_j$ 's establishes the non consideration of inductive and mesomeric effects. All these effects may be taken into account by the factor  $\mu_{expt}/\mu_{theo}$  to yield the exact  $\mu_1$  and  $\mu_2$  values of the molecules. All the polar molecules have  $sp^2$  hybridized carbon atoms of benzene ring and the substituted parts are associated with  $sp^3$  orbital. The interaction of orbitals may lead to gain knowledge on accumulation of charge on the substituted groups in addition to various effects present in them. The conformational structures of other molecules except six of Fig.3.8 were already shown elsewhere [3.12,3.19].

### 3.7. Conclusions :

The study of relaxation phenomena of disubstituted benzenes and anilines in  $C_6H_6$  and  $CCl_4$  by the modern established symbols of dielectric orientation susceptibilities  $\chi_{ij}$ 's measured under a single frequency electric field is very encouraging. It seems to be more topical, significant and useful contribution to predict the conformational structures and various molecular associations of the molecules at any given temperature. The intercept and

slope of the derived linear Eq.(3.3) by the regression analysis on the measured data of  $\chi_{ij}$ 's of different  $w_j$ 's are used to get  $\tau_2$  and  $\tau_1$ . The methodology so far developed in SI units is superior because of the unified, coherent and rationalised nature of the established symbols of dielectric terminologies and parameters, which are directly linked with orientational polarisation of the molecules. The significant Eqs.(3.15) and (3.16) to obtain  $\tau_j$ 's and hence  $\mu_j$ 's from Eq.(3.19) help the future workers to shed more light on the relaxation phenomena of the complicated non-spherical polar liquids and liquid crystals. The prescribed method to obtain  $\tau_j$ 's from Eq.(3.16) with the use of the ratio of the individual slopes of  $\chi_{ij}''$  vs  $w_j$  and  $\chi_{ij}'$  vs  $w_j$  curves at  $w_j \rightarrow 0$  is a significant improvement over the existing ones, as it eliminates polar-polar interaction almost completely in  $\tau_j$ 's and  $\mu_j$ 's respectively.

$\tau_j$ 's and  $\mu_j$ 's are usually claimed to be accurate within 10% and 5% respectively. But, the correlation coefficient  $r$  and % of errors of Eq.(3.3) demand that,  $\tau$ 's and  $\mu$ 's are more than accurate. The non-spherical disubstituted benzene and aniline molecules absorb electric energy much more strongly, nearly 10 GHz electric field, at which the  $\epsilon''$  for absorption against frequency  $\omega$  showed a peak. This invited the attention to get the double relaxation times  $\tau_2$  and  $\tau_1$  from Eq.(3.3). The corresponding sum of the experimental and theoretical values of weighted contributions  $c_1$  and  $c_2$  towards dielectric dispersions due to estimated  $\tau_2$  and  $\tau_1$  differ significantly to indicate more than two Debye type relaxations in such molecules because of their complexity. The  $\tau$ 's for disubstituted benzenes as seen in Table 3.2 show the whole molecular rotation, while the flexible parts of the disubstituted anilines rotate under 10 GHz electric field.

Disubstituted anilines exhibit the symmetric relaxation behaviour while the asymmetric relaxation behaviour occurs in disubstituted benzenes in  $C_6H_6$  except 4-chloro 3-nitrobenzotrifluoride in  $CCl_4$  and m-nitro benzotrifluoride in  $C_6H_6$  respectively.  $\mu_2$  and  $\mu_1$  due to  $\tau_2$  and  $\tau_1$  are expected to be smaller when they are measured from the susceptibility measurement technique rather than the hf conductivity method, where the approximation of  $\sigma_{ij} \cong \sigma_{ij}''$  is usually made. The difference of  $\mu_2$  for the first six systems and of  $\mu_1$  for the rest five systems of Table 3.4 between conductivity and susceptibility measurement may arise either by elongation or reduction of the bond moments of the substituted polar groups by the factor  $\mu_{\text{expt}}/\mu_{\text{theo}}$  in agreement with the measured  $\mu$ 's to take into account of the inductive,

mesomeric and electromeric effects of the polar groups in the molecules. Thus, the correlation between the conformational structures with the observed results enhances the scientific content to add a new horizon of understanding to the existing knowledge of dielectric relaxation phenomena.

#### References :

- [3.1] J S Dhull and D R Sharma, *J. Phys. D: Appl. Phys.* **15** 2307 (1982)
- [3.2] A K Sharma and D R Sharma, *J. Phys. Soc. Japan* **53** 4771 (1984)
- [3.3] A C Kumbharkhane, S M Puranic, C G Akode and S C Mehrotra, *Indian. J. Phys.* **74A** 471 (2000)
- [3.4] K Dutta, R C Basak, S K Sit and S Acharyya, *J. Molecular Liquids* **88** 229 (2000)
- [3.5] S K Sit, K Dutta, S Acharyya, T Palmajumder and S Roy, *J. Molecular Liquids* **89** 111 (2001)
- [3.6] S M Khameshara and M L Sisodia, *Indian J. Pure & Appl. Phys.* **18** 110 (1980)
- [3.7] P C Gupta, M L Arrawatia and M L Sisodia, *Indian J. Pure & Appl. Phys.* **16** 451 (1978)
- [3.8] M L Arrawatia, P C Gupta and M L Sisodia, *Indian J. Pure & Appl. Phys.* **15** 770 (1977)
- [3.9] K V Gopalakrishna, *Trans. Faraday Soc.* **53** 767 (1957)
- [3.10] K Higasi, *Bull. Chem. Soc. Japan* **39** 2157 (1966)
- [3.11] W M Heston, A D Franklin, E J Henneley and C P Smyth, *J. Am. Chem. Soc.* **72** 3443 (1950)
- [3.12] U Saha, S K Sit, R C Basak and S Acharyya, *J. Phys. D: Appl. Phys.* **27** 596 (1994).
- [3.13] A K Jonscher, *Physics of Dielectric Solids*, invited papers edited by CHL Goodman (1980).
- [3.14] A K Jonscher, *Universal Relaxation Law*, Chelsea Dielectric Press, London (1996)
- [3.15] N Ghosh, R C Basak, S K Sit and S Acharyya, *J. Molecular Liquids* **85** 375 (2000)
- [3.16] K Bergmann, D M Roberti and C P Smyth, *J. Phys. Chem.* **64** 665 (1960)
- [3.17] J Bhattacharyya, A Hasan, S B Roy and G S Kastha, *J. Phys. Soc. Japan* **28** 204 (1970)
- [3.18] K Higasi, Y Koga and M Nakamura, *Bull. Chem. Soc. Japan* **44** 988 (1971)

- [3.19] S K Sit, R C Basak, U Saha and S Acharyya, *J. Phys. D: Appl. Phys.* **27** 2194 (1994)
- [3.20] H Fröhlich, *Theory of Dielectrics*, Oxford University Press (1949)
- [3.21] J G Powles, *J. Molecular Liquids* **56** 35 (1993)
- [3.22] N E Hill, W E Vaughan, A H Price and M Davies, *Dielectric Properties and Molecular Behaviour* (London: Van Nostrand Reinhold Company) (1969).
- [3.23] C P Smyth, *Dielectric Behaviour and Structure* (McGraw Hill, UK) (1955)
- [3.24] K Dutta, S K Sit and S Acharyya, *Pramana: J. of Physics* **57** 775 (2001)
- [3.25] F J Murphy and S O Morgan, *Bell. Syst. Tech. J.* **18** 502 (1939)
- [3.26] K S Cole and R H Cole, *J. Chem. Phys.* **9** 341 (1941)
- [3.27] R H Cole and D W Davidson, *J. Chem. Phys.* **19** 1484 (1951)
- [3.28] M B R Murthy, R L Patil and D K Deshpande, *Indian J. Phys.* **63B** 491 (1989)

*Chapter 4*

**DIELECTRIC RELAXATION OF AROMATIC PARA  
SUBSTITUTED DERIVATIVE POLAR LIQUIDS  
FROM DISPERSION AND ABSORPTION PHENO-  
MENA UNDER GIGA HERTZ ELECTRIC FIELD**

## 4.1. Introduction

Both aliphatic and aromatic polar liquid molecules having substituted polar groups attached to the parent ones are often characterized by more than one relaxation times  $\tau_j$ 's corresponding to rotations of over all molecule and flexible parts attached to it. In long-chain compounds, the molecules having polar flexible parts at their ends may have multiple relaxation processes [4.1-4.2]. It is, of course, possible to measure these  $\tau$ 's while in some cases, the average  $\tau$ 's are, however, determined since the resolution of more than two distinct dispersive regions cannot often be detected. Para-polar aromatic liquid molecules usually, attracted the attention of a large number of workers [4.3-4.5] to study their physico-chemical aspects from the dispersion and absorption phenomena.

Dhar et al [4.6] and Somevanshi et al [4.7] measured real  $\epsilon_{ij}'$  and imaginary  $\epsilon_{ij}''$  parts of hf complex relative permittivity  $\epsilon_{ij}^*$  under 10 GHz electric field, of some interesting para substituted derivative polar liquid molecules in solvent dioxane and benzene respectively in the temperature range of 17 to 40°C as collected in Table 4.1. p-hydroxypropiophenone, p-chloropropiophenone, p-benzyloxybenzaldehyde were available in the purest form from Aldrich Chemicals and p-acetamidobenzaldehyde from Central Drug Research Institute, Lucknow, India. The liquids dioxane, benzene, p-anisidine, p-phenitidine etc. were, however, obtained from M/S BDH. London. The liquids were purified through repeated fractional distillations. The physical constants of the solvents like density  $\rho_i$ , viscosity  $\eta_i$  and the relative permittivities  $\epsilon_i$  at different temperatures in °C were collected from the literature [4.8].

Nowadays, the usual and conventional trend to study the dielectric relaxation phenomena of a polar liquid (DRL) is being advanced with the established symbols of dielectric terminology and parameter of hf complex orientational susceptibility  $\chi_{ij}^*$  of which  $\chi_{ij}'$  ( $= \epsilon_{ij}' - \epsilon_{\infty ij}$ ) and  $\chi_{ij}''$  ( $= \epsilon_{ij}''$ ) are the real and the imaginary parts in S.I. units. If 1 is subtracted from  $\epsilon_{ij}'$  to get the real part  $\chi_{ij}'$  in which all operating processes result, while if infinitely hf permittivity  $\epsilon_{\infty ij}$  is subtracted from hf  $\epsilon_{ij}'$  and static  $\epsilon_{\infty ij}$  one gets  $\chi_{ij}'$  and  $\chi_{oij}$  due to only orientational polarisation process  $\chi_{oij}$  is a real quantity.

Table 4.1: Concentration variation of the real and imaginary parts of dielectric permittivity  $\epsilon_{ij}'$ , static permittivity  $\epsilon_{oij}$ , infinitely high frequency permittivity  $\epsilon_{\infty ij}$ , real and imaginary parts of dielectric susceptibilities  $\chi_{ij}'$  and  $\chi_{ij}''$  of hf complex susceptibility  $\chi_{ij}^*$  and static experimental parameters  $X_{ij}$  of some para polar liquids in non polar solvents at different experimental temperatures under 10 GHz electric field

System with sl. No.	Tem p in °C	Weight fraction $w_j$	Dielectric permittivities				Dielectric susceptibilities		Static expt. Parameter $X_{ij}$
			$\epsilon_{ij}'$	$\epsilon_{ij}''$	$\epsilon_{oij}$	$\epsilon_{\infty ij}$	$\chi_{ij}'$	$\chi_{ij}''$	
1. p-hydroxy-propiofenone in dioxane	17	0.0040	2.0930	0.0320	2.1316	2.0665	0.0265	0.0320	0.00388
		0.0066	2.0970	0.0420	2.1477	2.0665	0.0348	0.0420	0.00507
		0.0089	2.0980	0.0440	2.1511	2.0615	0.0365	0.0440	0.00531
		0.0107	2.0990	0.0470	2.1557	2.0601	0.0389	0.0470	0.00567
	0.0116	2.1210	0.0620	2.1958	2.0695	0.0514	0.0620	0.00739	
	23	0.0040	2.1250	0.0310	2.1663	2.1018	0.0230	0.0310	0.00378
		0.0066	2.1330	0.0470	2.1957	2.0978	0.0352	0.0470	0.00570
		0.0090	2.1410	0.0590	2.2197	2.0968	0.0442	0.0590	0.00711
		0.0117	2.1560	0.0720	2.2520	2.1020	0.0540	0.0720	0.00860
	30	0.0041	2.1490	0.0360	2.2035	2.1252	0.0238	0.0360	0.00451
		0.0067	2.1550	0.0440	2.2216	2.1259	0.0291	0.0440	0.00549
		0.0091	2.1560	0.0470	2.2271	2.1249	0.0311	0.0470	0.00586
		0.0109	2.1570	0.0490	2.2312	2.1246	0.0324	0.0490	0.00610
	0.0118	2.1730	0.0710	2.2805	2.1261	0.0469	0.0710	0.00874	
	37	0.0041	2.1580	0.0350	2.1896	2.1192	0.0388	0.0350	0.00408
		0.0068	2.1750	0.0440	2.2147	2.1263	0.0487	0.0440	0.00509
0.0092		2.1780	0.0510	2.2241	2.1215	0.0565	0.0510	0.00589	
0.0110		2.1840	0.0560	2.2346	2.1220	0.0620	0.0560	0.00645	
0.0119	2.1860	0.0590	2.2393	2.1207	0.0653	0.0590	0.00679		
2. p-chloro-propiofenone in dioxane	19	0.0050	2.1100	0.0280	2.1301	2.0709	0.0391	0.0280	0.00352
		0.0068	2.1200	0.0320	2.1429	2.0754	0.0446	0.0320	0.00400
		0.0080	2.1220	0.0340	2.1464	2.0746	0.0474	0.0340	0.00425
		0.0093	2.1270	0.0400	2.1557	2.0712	0.0558	0.0400	0.00499
		0.0112	2.1330	0.0450	2.1653	2.0702	0.0628	0.0450	0.00561
		0.0123	2.1430	0.0490	2.1781	2.0746	0.0684	0.0490	0.00608
	25	0.0051	2.1230	0.0290	2.1581	2.0990	0.0240	0.0290	0.00347
		0.0069	2.1250	0.0320	2.1637	2.0986	0.0264	0.0320	0.00382
		0.0081	2.1280	0.0340	2.1692	2.0999	0.0281	0.0340	0.00405
		0.0094	2.1290	0.0390	2.1762	2.0968	0.0322	0.0390	0.00464
		0.0113	2.1340	0.0430	2.1861	2.0985	0.0355	0.0430	0.00510
		0.0124	2.1410	0.0500	2.2015	2.0997	0.0413	0.0500	0.00591
	31	0.0051	2.1350	0.0290	2.1817	2.1170	0.0180	0.0290	0.00376
		0.0069	2.1380	0.0330	2.1911	2.1175	0.0205	0.0330	0.00427
		0.0082	2.1390	0.0340	2.1937	2.1179	0.0211	0.0340	0.00439
		0.0095	2.1480	0.0390	2.2108	2.1238	0.0242	0.0390	0.00501
0.0114		2.1490	0.0410	2.2150	2.1235	0.0255	0.0410	0.00526	
0.0125		2.1510	0.0630	2.2524	2.1119	0.0391	0.0630	0.00804	
37	0.0052	2.1450	0.0270	2.1574	2.0861	0.0589	0.0270	0.00419	
	0.0070	2.1680	0.0290	2.1813	2.1048	0.0632	0.0290	0.00446	
	0.0083	2.1730	0.0330	2.1881	2.1011	0.0719	0.0330	0.00507	
	0.0115	2.1740	0.0360	2.1905	2.0955	0.0785	0.0360	0.00553	
	0.0126	2.1790	0.0400	2.1974	2.0918	0.0872	0.0400	0.00615	

System with sl. No.	Tem p in °C	Weight fraction $w_j$	Dielectric permittivities				Dielectric susceptibilities		Static expt. Parameter $X_{ij}$
			$\epsilon_{ij}'$	$\epsilon_{ij}''$	$\epsilon_{oij}$	$\epsilon_{\omega ij}$	$\chi_{ij}'$	$\chi_{ij}''$	
3. p-acetamido benzaldehyde in dioxane	17	0.0023	2.1530	0.0290	2.2024	2.1360	0.0170	0.0290	0.00382
		0.0042	2.1540	0.0380	2.2187	2.1317	0.0223	0.0380	0.00499
		0.0073	2.1600	0.0530	2.2503	2.1289	0.0311	0.0530	0.00692
		0.0078	2.1690	0.0610	2.2729	2.1332	0.0358	0.0610	0.00791
		0.0112	2.1750	0.0670	2.2891	2.1357	0.0393	0.0670	0.00865
	23	0.0023	2.1580	0.0340	2.2031	2.1324	0.0256	0.0340	0.00407
		0.0043	2.1650	0.0440	2.2233	2.1318	0.0332	0.0440	0.00524
		0.0073	2.1710	0.0480	2.2346	2.1348	0.0362	0.0480	0.00570
		0.0078	2.1740	0.0560	2.2482	2.1318	0.0422	0.0560	0.00664
		0.0113	2.1820	0.0670	2.2708	2.1315	0.0505	0.0670	0.00790
	30	0.0154	2.1840	0.0680	2.2741	2.1327	0.0513	0.0680	0.00801
		0.0074	2.1750	0.0350	2.2275	2.1517	0.0233	0.0350	0.00432
		0.0079	2.1860	0.0430	2.2505	2.1573	0.0287	0.0430	0.00527
		0.0098	2.1870	0.0530	2.2665	2.1517	0.0353	0.0530	0.00648
		0.0114	2.1950	0.0590	2.2835	2.1557	0.0393	0.0590	0.00718
37	0.0155	2.2010	0.0710	2.3075	2.1537	0.0473	0.0710	0.00860	
	0.0075	2.2110	0.0370	2.2600	2.1831	0.0279	0.0370	0.00432	
	0.0080	2.2210	0.0470	2.2832	2.1855	0.0355	0.0470	0.00545	
	0.0099	2.2320	0.0550	2.3048	2.1905	0.0415	0.0550	0.00634	
	0.0115	2.2410	0.0730	2.3377	2.1859	0.0551	0.0730	0.00836	
4. p-benzyloxy benzaldehyde in dioxane	20	0.0157	2.2420	0.0760	2.3426	2.1846	0.0574	0.0760	0.00870
		0.0040	2.1450	0.0270	2.1910	2.1292	0.0158	0.0270	0.00358
		0.0066	2.1500	0.0290	2.1994	2.1330	0.0170	0.0290	0.00383
		0.0089	2.1520	0.0310	2.2049	2.1338	0.0182	0.0310	0.00409
		0.0104	2.1530	0.0350	2.2127	2.1325	0.0205	0.0350	0.00461
	25	0.0116	2.1540	0.0360	2.2154	2.1329	0.0211	0.0360	0.00473
		0.0153	2.1560	0.0450	2.2327	2.1296	0.0264	0.0450	0.00590
		0.0041	2.1670	0.0280	2.1947	2.1387	0.0283	0.0280	0.00323
		0.0067	2.1720	0.0340	2.2057	2.1377	0.0343	0.0340	0.00391
		0.0090	2.1740	0.0380	2.2117	2.1357	0.0383	0.0380	0.00436
	30	0.0105	2.1750	0.0390	2.2136	2.1356	0.0394	0.0390	0.00448
		0.0117	2.1800	0.0440	2.2236	2.1356	0.0444	0.0440	0.00504
		0.0154	2.1870	0.0470	2.2336	2.1396	0.0474	0.0470	0.00536
		0.0041	2.1780	0.0310	2.2151	2.1521	0.0259	0.0310	0.00360
		0.0067	2.1920	0.0350	2.2339	2.1627	0.0293	0.0350	0.00404
35	0.0090	2.1930	0.0390	2.2397	2.1604	0.0326	0.0390	0.00449	
	0.0106	2.1940	0.0400	2.2419	2.1606	0.0334	0.0400	0.00461	
	0.0118	2.1960	0.0440	2.2486	2.1592	0.0368	0.0440	0.00506	
	0.0155	2.2060	0.0620	2.2802	2.1542	0.0518	0.0620	0.00709	
	0.0041	2.2030	0.0320	2.2290	2.1636	0.0394	0.0320	0.00371	
5. p-anisidine in benzene	20	0.0091	2.2090	0.0360	2.2382	2.1647	0.0443	0.0360	0.00417
		0.0119	2.2160	0.0420	2.2501	2.1643	0.0517	0.0420	0.00485
		0.0156	2.2190	0.0450	2.2556	2.1636	0.0554	0.0450	0.00519
		0.0071	2.1700	0.0300	2.1854	2.1117	0.0583	0.0300	0.00428
		0.0098	2.1900	0.0350	2.2080	2.1220	0.0680	0.0350	0.00496
0.0121	2.2000	0.0400	2.2206	2.1223	0.0777	0.0400	0.00565		
0.0165	2.2000	0.0440	2.2227	2.1146	0.0854	0.0440	0.00622		
0.0198	2.2100	0.0480	2.2347	2.1168	0.0932	0.0480	0.00676		

System with sl. No.	Tem p in °C	Weight fraction $w_j$	Dielectric permittivities				Dielectric susceptibilities		Static expt. Parameter $X_{ij}$
			$\epsilon_{ij}'$	$\epsilon_{ij}''$	$\epsilon_{oij}$	$\epsilon_{coij}$	$\chi_{ij}'$	$\chi_{ij}''$	
6.p-phenitidine in benzene	30	0.0071	2.1800	0.0300	2.1919	2.1041	0.0759	0.0300	0.00510
		0.0098	2.1900	0.0350	2.2038	2.1014	0.0886	0.0350	0.00594
		0.0121	2.2000	0.0400	2.2158	2.0987	0.1013	0.0400	0.00677
		0.0165	2.2100	0.0450	2.2278	2.0961	0.1139	0.0450	0.00760
		0.0198	2.2200	0.0450	2.2378	2.1061	0.1139	0.0450	0.00757
	40	0.0071	2.1900	0.0400	2.1997	2.0247	0.1653	0.0400	0.01035
		0.0098	2.2000	0.0420	2.2102	2.0265	0.0735	0.0420	0.01084
		0.0121	2.2100	0.0440	2.2206	2.0282	0.1818	0.0440	0.01132
		0.0165	2.2200	0.0460	2.2311	2.0299	0.0901	0.0460	0.01180
		0.0198	2.2300	0.0500	2.2421	2.0234	0.2066	0.0500	0.01281
	20	0.0132	2.3100	0.0300	2.3296	2.2642	0.0458	0.0300	0.00355
		0.0149	2.3200	0.0500	2.3527	2.2436	0.0764	0.0500	0.00591
		0.0168	2.3400	0.0700	2.3858	2.2330	0.1070	0.0700	0.00823
		0.0199	2.3800	0.0800	2.4324	2.2577	0.1223	0.0800	0.00925
		0.0231	2.3900	0.0900	2.4489	2.2525	0.1375	0.0900	0.01038
	30	0.0132	2.3200	0.0300	2.3373	2.2681	0.0519	0.0300	0.00374
		0.0149	2.3700	0.0400	2.3931	2.3008	0.0692	0.0400	0.00489
		0.0168	2.3800	0.0500	2.4089	2.2935	0.0865	0.0500	0.00610
		0.0199	2.4100	0.0600	2.4447	2.3061	0.1039	0.0600	0.00724
		0.0231	2.4100	0.0800	2.4562	2.2715	0.1385	0.0800	0.00970
40	0.0132	2.3400	0.0400	2.3604	2.2615	0.0785	0.0400	0.00532	
	0.0149	2.3400	0.0500	2.3655	2.2419	0.0981	0.0500	0.00668	
	0.0168	2.3600	0.0600	2.3906	2.2422	0.1178	0.0600	0.00796	
	0.0199	2.3900	0.0700	2.4257	2.2526	0.1374	0.0700	0.00920	
	0.0231	2.4100	0.0800	2.4508	2.2530	0.1570	0.0800	0.01045	
7. o-chloro p- nitro aniline in benzene	20	0.0251	2.0700	0.0200	2.0832	2.0398	0.0302	0.0200	0.00264
		0.0293	2.0800	0.0200	2.0932	2.0498	0.0302	0.0200	0.00392
		0.0331	2.0900	0.0300	2.1098	2.0446	0.0454	0.0300	0.00392
		0.0652	2.1000	0.0300	2.1198	2.0546	0.0454	0.0300	0.00390
		0.0851	2.1000	0.0400	2.1265	2.0395	0.0605	0.0400	0.00522
	30	0.0251	2.1000	0.0200	2.1100	2.0600	0.0400	0.0200	0.00300
		0.0293	2.1000	0.0200	2.1100	2.0600	0.0400	0.0200	0.00300
		0.0331	2.1100	0.0250	2.1225	2.0600	0.0500	0.0250	0.00373
		0.0652	2.1100	0.0250	2.1225	2.0600	0.0500	0.0250	0.00373
		0.0851	2.1200	0.0300	2.1350	2.0600	0.0600	0.0300	0.00447
40	0.0251	2.1200	0.0300	2.1344	2.0575	0.0625	0.0300	0.00459	
	0.0293	2.1200	0.0300	2.1344	2.0575	0.0625	0.0300	0.00459	
	0.0331	2.1300	0.0325	2.1456	2.0623	0.0677	0.0325	0.00495	
	0.0652	2.1300	0.0325	2.1456	2.0623	0.0677	0.0325	0.00495	
	0.0851	2.1300	0.0350	2.1468	2.0571	0.0729	0.0350	0.00533	
8. p-bromo - nitrobenzene in benzene	20	0.0162	2.2100	0.0263	2.2267	2.1686	0.0415	0.0263	0.00330
		0.0202	2.2313	0.0302	2.2504	2.1837	0.0476	0.0302	0.00375
		0.0342	2.2352	0.0350	2.2574	2.1801	0.0551	0.0350	0.00434
		0.0375	2.2423	0.0375	2.2661	2.1832	0.0591	0.0375	0.00464
		0.0416	2.2540	0.0400	2.2794	2.1910	0.0630	0.0400	0.00493

System with sl. No.	Tem p in °C	Weight fraction w <sub>j</sub>	Dielectric permittivities				Dielectric susceptibilities		Static expt. Parameter X <sub>ij</sub>
			ε <sub>ij</sub> '	ε <sub>ij</sub> ''	ε <sub>oij</sub>	ε <sub>∞ij</sub>	χ <sub>ij</sub> '	χ <sub>ij</sub> ''	
		0.0162	2.2483	0.0270	2.2634	2.2003	0.0480	0.0270	0.00353
		0.0202	2.2621	0.0320	2.2801	2.2051	0.0570	0.0320	0.00416
	30	0.0342	2.2670	0.0351	2.2867	2.2044	0.0625	0.0351	0.00456
		0.0375	2.2739	0.0441	2.2987	2.1953	0.0786	0.0441	0.00573
		0.0416	2.2880	0.0460	2.3138	2.2061	0.0819	0.0460	0.00594
		0.0162	2.2756	0.0276	2.2898	2.2218	0.0538	0.0276	0.00375
		0.0202	2.2931	0.0332	2.3101	2.2283	0.0648	0.0332	0.00449
	40	0.0342	2.2982	0.0353	2.3162	2.2294	0.0688	0.0353	0.00476
		0.0375	2.3056	0.0463	2.3293	2.2153	0.0903	0.0463	0.00625
		0.0416	2.3220	0.0478	2.3465	2.2287	0.0933	0.0478	0.00641

Ghosh et al [4.9] recently studied all these p-compounds in terms of the complex hf conductivity  $\sigma_{ij}^*$  where [4.10]

$$\sigma_{ij}^* = \sigma'_{ij} + j\sigma''_{ij} = \omega\epsilon_0\epsilon''_{ij} + j\omega\epsilon_0\epsilon'_{ij} \quad \dots (4.1)$$

$\epsilon'_{ij}$  and  $\epsilon''_{ij}$  are the real and imaginary parts of the hf complex relative permittivity  $\epsilon_{ij}^*$  related by

$$\epsilon_{ij}^* = \epsilon'_{ij} - j\epsilon''_{ij} \quad \dots (4.2)$$

$j = \sqrt{-1}$  is a complex number and  $\epsilon_0$  permittivity of free space =  $8.854 \times 10^{-12}$  Farad metre<sup>-1</sup>, to show that all these p-compounds obey Debye- relaxation mechanism. Both  $\sigma_{ij}''$  and  $\sigma_{ij}'$  are related by [4.11]

$$\sigma''_{ij} = \sigma_{\infty ij} + \frac{1}{\omega\tau_j} \sigma'_{ij} \quad \dots (4.3)$$

$$\frac{d\sigma''_{ij}}{d\sigma'_{ij}} = \frac{1}{\omega\tau_j} \quad \dots (4.4)$$

$\tau_j$ 's may, therefore, be determined by the slopes of  $\sigma_{ij}''$  against  $\sigma_{ij}'$  linear curves [4.11]. A better representation of Eq (4.4) can, however, be given by

$$\left(\frac{d\sigma''_{ij}}{dw_j}\right)_{w_j \rightarrow 0} / \left(\frac{d\sigma'_{ij}}{dw_j}\right)_{w_j \rightarrow 0} = \frac{1}{\omega\tau_j} \quad \dots (4.5)$$

to eliminate polar-polar interactions in the solution when  $w_j \rightarrow 0$  to measure  $\tau_j$ 's by Ghosh et al [4.12] by the conductivity method and known  $\omega = 2\pi f$  where  $f$  = frequency of the applied electric field = 10 GHz.. Hence Debye Pellat's Eqs [4.13].

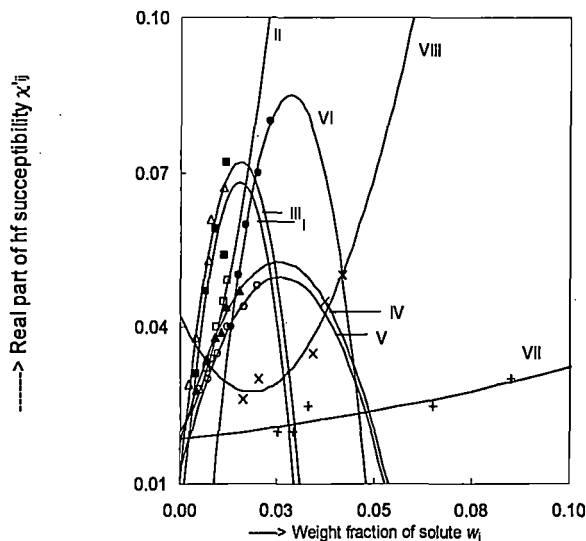


Figure-4.1: Variation of real part  $\chi'_{ij}$  of hf complex orientational susceptibility against weight fraction  $w_j$  of solute of some para compounds at selected temperatures in nonpolar solvents (dioxane and benzene) under 10 GHz electric field frequency  
 I. p-hydroxypopiophenone (--■--) at 23<sup>o</sup> C, II. p-chloropropiophenone (--□--) at 19<sup>o</sup> C, III. P-acetamidobenzaldehyde (--△--) at 17<sup>o</sup> C, IV .p-benzyloxybenzaldehyde (--▲--) at 25<sup>o</sup> C, V. p-anisidine (--o--) at 20<sup>o</sup> C, VI. p-phenitidine (--●--) at 40<sup>o</sup> C, VII. o-chloro-p-nitroaniline (--+--) at 30<sup>o</sup> C, VIII. p-bromonitrobenzene (--x--) at 20<sup>o</sup> C .

$$\epsilon'_{ij} = \epsilon_{\alpha ij} + \frac{\epsilon_{0ij} - \epsilon_{\alpha ij}}{1 + \omega^2 \tau_j^2} \quad \dots (4.6)$$

$$\epsilon''_{ij} = \frac{\epsilon_{0ij} - \epsilon_{\alpha ij}}{1 + \omega^2 \tau_j^2} \omega \tau_j \quad \dots (4.7)$$

can be used to obtain the concentration variation of  $\epsilon_{0ij}$  and  $\epsilon_{\infty ij}$  of any polar liquid in close agreement with the experimentally measured data within  $\pm 1\%$  error as tested. The data are

placed in Table 4.1 together with  $\chi_{ij}' (= \epsilon_{ij}' - \epsilon_{\infty ij})$  and  $\chi_{ij}'' (= \epsilon_{ij}'')$  to measure  $\tau_j$ 's and hf  $\mu_j$ 's and the static parameters  $X_{ij}$  as a function of  $w_j$ 's to get the static  $\mu_s$ 's. The estimated value of  $\mu_s$  confirms the data are much more accurate. This indicates the very soundness of the method so far suggested. Thus a faithful measurement of  $\chi_{ij}'$  and  $\chi_{ij}''$  is possible to study the relaxation phenomena where the orientational polarisation alone plays the important role. In  $\sigma_{ij}$ 's measurements, the transfer of bound molecular charges are responsible to yield hf  $\mu_j$ 's with an approximation that  $\sigma_{ij} \approx \sigma_{ij}''$  where  $\sigma_{ij}$  is the total hf conductivity  $\sigma_{ij} = \omega \epsilon_0 (\epsilon_{ij}''^2 + \epsilon_{ij}'^2)^{1/2}$  as a function of  $w_j$  at each temperature.

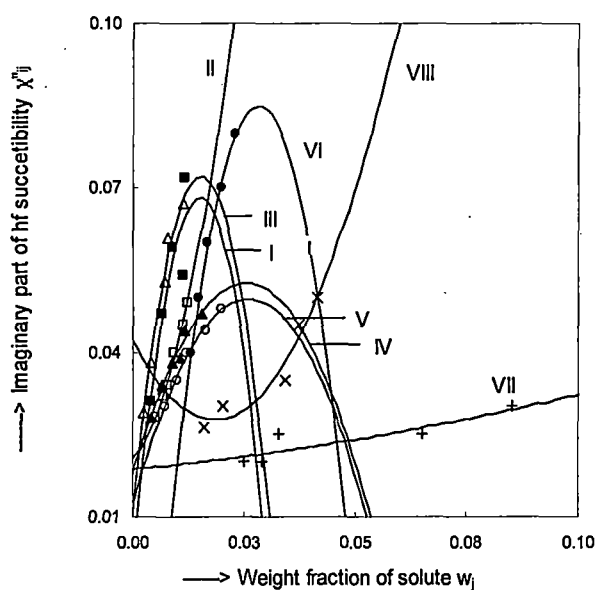


Figure 4.2: Variation of imaginary part  $\chi''_{ij}$  of hf complex orientational susceptibility against weight fraction  $w_j$  of solute of some para compounds at selected temperatures in nonpolar solvents (dioxane and benzene) under 10 GHz electric field frequency. I. p-hydroxypropionophenone (--■--) at 23°C, II. p-chloropropionophenone (--□--) at 19°C, III. P-acetamidobenzaldehyde (--△--) at 17°C, IV. p-benzyloxybenzaldehyde (--▲--) at 25°C, V. p-anisidine (--o--) at 20°C, VI. p-phenitidine (--•--) at 40°C, VII. o-chloro-p-nitroaniline (--+--) at 30°C, VIII. p-bromonitrobenzene (--x--) at 20°C.

Some sample curves of both  $\chi_{ij}'$  and  $\chi_{ij}''$  against  $w_j$ 's are shown in Figs. 4.1 and 4.2 respectively. The linear equations of  $\ln \tau_j T$  against  $1/T$  with  $\tau_j$ 's from the susceptibility measurements are shown graphically in Fig. 4.3 with the experimental points placed upon them. The values of intercepts and slopes are entered in the Table 4.3 to compute

Table 4.2: Measured  $\tau_j$ 's from ratio of slopes of individual variations of  $\chi_{ij}'$  and  $\chi_{ij}''$  with  $w_j$ , estimated relaxation time  $\tau_j$ , reported  $\tau_j$  all are in pico second, estimated dipole moments ( $\mu_j$ ) using  $\tau_j$  of Eq.(4.10), estimated  $\mu_s$ , reported  $\mu_j$  and theoretical dipole moments  $\mu_{theo}$  using bond moments in Coulomb-metre of some para compounds in non-polar solvents at different experimental temperatures under 10 GHz electric field.

System with sl no & molecular weight $M_j$	Temp in $^{\circ}\text{C}$	$\tau_j$ in p-sec using Eq. (4.10)	$\tau_j$ in p-sec by Eq. (4.5)	Reported $\tau_j$ in p-sec	Estimated $\mu_j \times 10^{30}$ in C.m	Estimated $\mu_s \times 10^{30}$ in C.m	Reported $\mu \times 10^{30}$ in C.m	Corrected $\mu_{theo} \times 10^{30}$ in C.m
1. p-hydroxy-propiofenone $M_j=0.150$ Kg	17	19.20	19.20	--	--	--		
	23	21.21	21.21	25.40	14.28	14.65	10.20	14.27
	30	24.08	24.08	24.20	--	--		
	37	14.37	14.37	23.10	10.25	10.16		
2. p-chloro-propiofenone $M_j=0.1685$ Kg	19	11.40	11.40	20.80	5.33	5.61		
	25	19.26	19.26	19.20	--	--	9.84	7.27
	31	25.60	25.60	18.20	--	--		
	37	7.30	7.30	17.10	7.28	6.46		
3. p-aceta-midobenzalde hyde $M_j= 0.163$ Kg	17	27.10	27.10	21.80	15.96	16.07		
	23	21.09	21.09	20.80	12.62	12.60	10.37	12.62
	30	23.86	23.86	19.00	20.57	20.40		
	37	21.07	21.06	18.60	26.85	26.12		
4. p-benzyloxyben zaldehyde $M_j=0.212$ Kg	20	27.13	27.12	20.00	--	--		
	25	15.77	15.77	19.40	10.22	10.34	10.63	10.22
	30	19.03	19.03	18.00	--	--		
	35	12.92	12.92	16.90	6.12	6.05		
5. p-anisidine $M_j=0.123$ Kg	20	8.19	9.21	3.89	9.29	9.38	5.20	
	30	6.28	10.86	3.67	12.43	12.78	10.33	8.56
	40	3.85	11.34	3.17	4.84	4.47	8.87	
6. p-phenitidine $M_j=0.0137$ Kg	20	10.41	9.82	11.08	29.35	29.22	7.47	
	30	9.19	10.17	10.63	11.06	9.55	9.27	29.36
	40	8.10	9.91	9.95	20.32	20.26	10.47	
7. o-chloro p-nitro aniline $M_j=0.1725$ Kg	20	10.52	10.52	10.57	2.41	2.33	8.13	
	30	7.95	20.47	9.89	1.87	1.97	10.93	2.41
	40	7.64	30.59	9.18	1.38	1.17	13.10	
8. p-bromo nitrobenzene $M_j=0.202$ Kg	20	10.10	8.40	--	4.23	4.36	--	
	30	8.93	8.93	--	--	--	--	4.23
	40	8.15	8.16	--	--	--	--	

thermodynamic energy parameters like enthalpy  $\Delta H_r$ , entropy  $\Delta S_r$  and free energy  $\Delta F_r$  of activation due to dielectric relaxation from Eyring's rate process equations [4.14]. The enthalpy of activation  $\Delta H_\eta$  due to viscous flow was estimated from  $\Delta H_r$  and the slope  $\delta$  of

the linear equations of  $\ln\tau_j T$  against  $\ln\eta_i$  where  $\eta_i$  is the coefficient of viscosity of the solvents used. The data as seen in Table 4.2 throw much light on the stability as well as on the physico-chemical properties of the systems. Kalman and Debye factors placed in the Table 4.3 reflect the applicability of Debye model of relaxation for such p-compounds [4.9].

The hf  $\mu_j$ 's of all the para liquid molecules due to orientational prolarisation alone were carefully worked out from the linear coefficients  $\beta$ 's of  $\chi_{ij}'-w_j$  equations and the dimensionless parameters 'b' involved with estimated  $\tau_j$ 's at different temperatures and are placed in Table 4.2. They are compared with the reported hf  $\mu_j$ 's, static  $\mu_s$ 's obtained from linear coefficient  $a_1$  of static  $X_{ij}-w_j$  equations, and  $\mu_{theo}$ 's from the available infrared spectroscopic data of bond moments of the substituted polar groups attached to the parent molecules. The disagreement of measured hf  $\mu_j$  with  $\mu_{theo}$  establishes the existence of inductive and mesomeric moments which in excitd state offers the electromeric effects suffered by the polar groups of the molecules under GHz electric field. The close agreement between  $\mu_j$  with  $\mu_{theo}$  is, however, achieved when the bond moments are corrected by multiplying with  $\mu_j/\mu_{theo}$  and  $\mu_s/\mu_{theo}$  respectively as required.

#### 4.2. Theoretical formulations to measure $\tau_j$ and $\mu_j$ of a polar unit :

The real and imaginary parts of hf complex relative permittivities  $\epsilon_{ij}^*$  are related by

$$\epsilon'_{ij} = \epsilon_{\infty ij} + \frac{1}{\omega\tau_j} \epsilon''_{ij} \quad \dots (4.8)$$

replacing  $(\epsilon_{ij}' - \epsilon_{\infty ij})$  by  $\chi_{ij}'$  and  $\epsilon_{ij}''$  by  $\chi_{ij}''$  we have

$$\chi'_{ij} = \frac{1}{\omega\tau_j} \chi''_{ij}$$

$$\frac{d\chi'_{ij}}{d\chi''_{ij}} = \frac{1}{\omega\tau_j} \quad \dots (4.9)$$

$\chi_{ij}''$  varies linearly with  $\chi_{ij}'$ . The slope of Eq. (4.9) which is used to measure  $\tau_j$  of a polar unit.

But for associative liquids like p-anisidine, p-phenitidine etc the variation of  $\chi_{ij}''$  with  $\chi_{ij}'$  is not strictly linear as claimed elsewhere [4.15]. The ratio of slopes of individual variations of  $\chi_{ij}''$  and  $\chi_{ij}'$  against  $w_j$ 's are found to be a better representation of the slope of Eq. (4.9) in which polar - polar interactions are supposed to be almost eliminated [4.16].

Thus

$$\frac{(d\chi_{ij}''/dw_j)_{w_j \rightarrow 0}}{(d\chi_{ij}'/dw_j)_{w_j \rightarrow 0}} = \omega\tau_j \quad \dots (4.10)$$

The imaginary part  $\chi_{ij}''$  of hf  $\chi_{ij}^*$  is [4.17,4.18].

$$\chi_{ij}'' = \left( \frac{N\rho_{ij}\mu_j^2}{27\varepsilon_0 M_j k_B T} \right) (\varepsilon_i + 2)^2 \cdot \frac{\omega\tau_j}{1 + \omega^2\tau_j^2} w_j \quad \dots (4.11)$$

which on differentiation w.r.t.  $w_j$  and in the limit  $w_j \rightarrow 0$  becomes :

$$\left( \frac{d\chi_{ij}''}{dw_j} \right)_{w_j \rightarrow 0} = \left( \frac{N\rho_{ij}\mu_j^2}{27\varepsilon_0 M_j k_B T} \right) (\varepsilon_i + 2)^2 \cdot \frac{\omega\tau_j}{1 + \omega^2\tau_j^2} \quad \dots (4.12)$$

From Eqs (4.9) and (4.12) one obtains

$$\omega\tau_j \left( \frac{d\chi_{ij}'}{dw_j} \right)_{w_j \rightarrow 0} = \left( \frac{N\rho_{ij}\mu_j^2}{27\varepsilon_0 M_j k_B T} \right) \cdot \frac{\omega\tau_j}{1 + \omega^2\tau_j^2} (\varepsilon_i + 2)^2$$

which at once provides  $\mu_j$  as :

$$\mu_j = \left[ \frac{27\varepsilon_0 M_j k_B T \beta}{N\rho_i (\varepsilon_i + 2)^2 b} \right]^{\frac{1}{2}} \quad \dots (4.13)$$

to measure hf dipole moments  $\mu_j$ 's in terms of  $\tau_j$ 's obtained from Eq.(4.10) where  $\varepsilon_0$ = permittivity of free space =  $8.854 \times 10^{-12}$  Farad metre<sup>-1</sup>

$M_j$  = molecular weight of solute in Kg

$k_B$  = Boltzmann constant =  $1.38 \times 10^{-23}$  J mole<sup>-1</sup>K<sup>-1</sup>

$\beta$  = Linear coefficient of  $\chi_{ij}'$ - $w_j$  curves of Fig. 4.1 at  $w_j \rightarrow 0$

T= temperature in Kelvin

N = Avogadro's number =  $6.023 \times 10^{23}$

$\epsilon_i$  = Dielectric relative permittivity of the solvent and

$b = 1/(1+\omega^2\tau_j^2)$ , a dimensionless parameter involved with estimated  $\tau_j$ 's.

Thus the Eq. (4.13) can be employed to measure hf  $\mu_j$ 's of all para-polar liquid molecules under investigation, in benzene and dioxane at different experimental temperatures. They are presented in Table 4.2. The temperature variations of hf  $\mu_j$ 's are shown graphically in Fig.4.4. It is evident from Fig 4.4 that the temperature variation  $\mu_j$ 's offers a valuable information about the structural aspects in addition to the physico chemical properties of the liquid molecules.

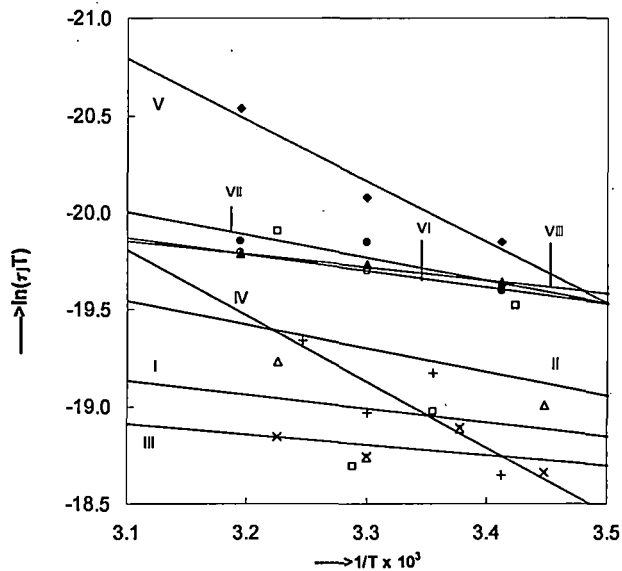


Figure 4.3: Straight line plots of  $\ln\tau_jT$  against  $1/T$  I. p-hydroxypopiophenone (-- $\Delta$ --), II.p-chloropropiophenone (-- $\square$ --), III.P-acetamidobenzaldehyde (--X--), IV .p-benzyloxybenzaldehyde (--+--), V. p-anisidine (-- $\blacklozenge$ --), VI. p-phenitidine (--o--), VII. o-chloro-p-nitroaniline (-- $\bullet$ --), VIII. p-bromonitrobenzene (-- $\blacktriangle$ --)

### 4.3. Theoretical formulation of static parameter $X_{ij}$ to estimate static dipole moment $\mu_s$ :

The static dipole moment  $\mu_s$  of a polar solute (j) in a non-polar solvent (i) at TK is given in terms of  $\epsilon_{0ij}$  and  $\epsilon_{\infty ij}$  of Table 4.1, by [4.12,4.13].

$$\frac{\epsilon_{0ij} - 1}{\epsilon_{0ij} + 2} - \frac{\epsilon_{\infty ij} - 1}{\epsilon_{\infty ij} + 2} = \frac{\epsilon_{0i} - 1}{\epsilon_{0i} + 2} - \frac{\epsilon_{\infty i} - 1}{\epsilon_{\infty i} + 2} + \frac{N\mu_s^2}{9\epsilon_0 k_B T} c_j \quad \dots (4.14)$$

The molar concentration  $c_j$  is expressed by  $w_j$  of the polar solute

$$c_j = \frac{\rho_{ij}}{M_j} w_j$$

The weight  $W_j$  and volume  $V_j$  of a polar solute is dissolved in a non-polar solvent of weight  $W_i$  and volume  $V_i$  to have the solution density  $\rho_{ij}$  where

$$\begin{aligned} \rho_{ij} &= \frac{W_j + W_i}{V_j + V_i} = \frac{W_j + W_i}{(W_j/\rho_j) + (W_i/\rho_i)} \\ &= \frac{\rho_i \rho_j}{\rho_j w_i + \rho_i w_j} = \rho_i (1 - \gamma w_j)^{-1} \\ &= \rho_i (1 + \gamma w_j + \gamma w_j^2 + \dots) \end{aligned} \quad \dots (4.15)$$

The weight fractions  $w_i$  and  $w_j$  of the solvent and solute are

$$w_i = \frac{W_i}{W_i + W_j} \text{ and } w_j = \frac{W_j}{W_i + W_j} \text{ respectively}$$

such that  $w_i + w_j = 1$  and  $\gamma = (1 - \rho_i/\rho_j)$  where  $\rho_i$  and  $\rho_j$  are the densities of pure solvent and pure solute respectively in S.I. units.

Hence Eq. (4.14) becomes:

$$\frac{\epsilon_{0ij} - \epsilon_{\infty ij}}{(\epsilon_{0ij} + 2)(\epsilon_{\infty ij} + 2)} = \frac{\epsilon_{0i} - \epsilon_{\infty i}}{(\epsilon_{0i} + 2)(\epsilon_{\infty i} + 2)} + \frac{N\rho_i \mu_s^2}{27\epsilon_0 M_j k_B T} \times w_j (1 + \gamma w_j + \dots)$$

$$X_{ij} = X_i + \frac{N\rho_i\mu_s^2}{27\varepsilon_0M_jk_B T}w_j + \frac{N\rho_i\mu_s^2}{27\varepsilon_0M_jk_B T}\gamma w_j^2 + \dots \quad (4.16)$$

Since  $0 < w_j \ll 1$ , the above Eq. (4.16) can be expressed by the polynomial equation of  $w_j$  upto the third term only like

$$X_{ij} = a_0 + a_1 w_j + a_2 w_j^2 + \dots \quad (4.17)$$

Comparing the coefficients of first power of  $w_j$  of Eqs. (4.16) and (4.17) one gets the static  $\mu_s$  as:

$$\mu_s = \left[ \frac{27\varepsilon_0M_jk_B T}{N\rho_i} a_1 \right]^{\frac{1}{2}} \quad (4.18)$$

where  $a_1$  is the linear coefficient of  $X_{ij}$ - $w_j$  curves, a few of which are shown in Fig. 4.5 as for example.  $\mu_s$ 's from coefficient of higher powers of  $w_j$  of Eq. (4.16) are not reliable as the term  $\gamma$  is involved with various effects like solute-solute interaction, relative density, macroscopic viscosity, internal field etc. The  $\mu_s$ 's thus obtained establish the very soundness of the methods so far advanced where  $\varepsilon_{oij}$  and  $\varepsilon_{\infty ij}$  are not experimentally measured. The  $\mu_s$ 's thus estimated for the p-compounds are seen in Table 4.2 to compare with hf  $\mu_j$ 's from the orientational susceptibility measurements and theoretical  $\mu_{theo}$ 's from the available bond angles and bond moments of the substituted polar groups attached to the parent molecules.

#### 4.4. Results and Discussion :

The concentration variation of  $\chi_{ij}'$  and  $\chi_{ij}''$  of all the p-compounds in solvents dioxane and benzene respectively at different experimental temperatures in  $^{\circ}C$  are collected in Table 4.1 to show some variations of  $\chi_{ij}'$  and  $\chi_{ij}''$  with  $w_j$ 's in Figs.4.1 and 4.2 respectively as for example. The relaxation times  $\tau_j$ 's have been measured under 3 cm wave length electric field from Eqs. (4.9) and (4.10) by using  $\chi_{ij}'$  and  $\chi_{ij}''$  of Table 4.1.  $\tau$ 's from Eq. (4.10) are presented in the Table 4.2 to compare with those placed in the same Table 4.2

recalculated from Eq.(4.5) by conductivity  $\sigma_{ij}$  method [4.9] and reported ones [4.6, 4.7]. The close agreement between all the  $\tau_j$ 's at once reflects the validity of Eq.(4.10) derived from the susceptibility  $\chi_{ij}$ 's measurements. Thus the method of ratio of slopes of individual variations of  $\chi_{ij}'$  and  $\chi_{ij}''$  with  $w_j$ 's in the limit  $w_j = 0$  to get  $\tau_j$  from Eq.(4.10) is superior one where the effects of fast polarisation in addition to polar-polar interactions are reduced to a large extent [4.16].

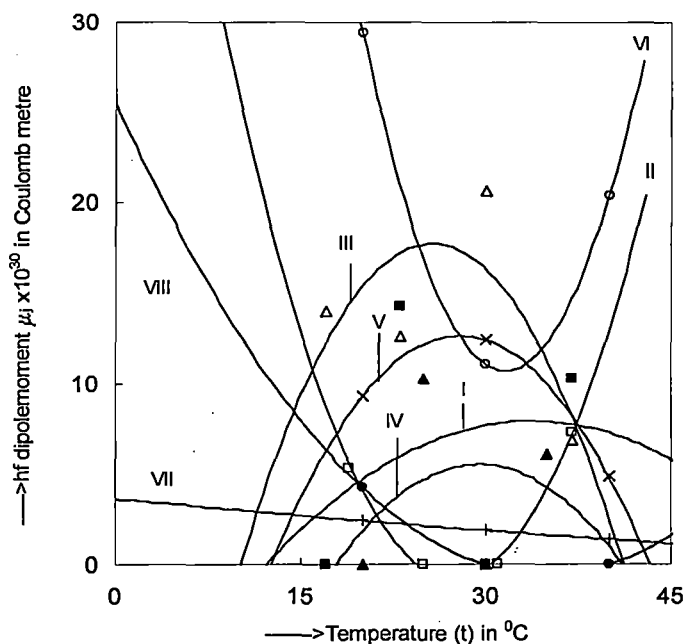


Figure 4. Variation of estimated hf dipolemoments  $\mu_j \times 10^{30}$  in Coulomb metre against  $t$  in  $^{\circ}\text{C}$ . I. p-hydroxy propiophenone (- ■ -) II. p-chloropropiophenone (- □ -) III. p-acetamidobenzaldehyde (- Δ -) IV. p-benzyloxybenzaldehyde (- ▲ -) V. p-anisidine (- x -) VI. p-phenitidine (- o -) VII. o-chloro-p-nitroaniline (- + -) VIII. p-bromonitrobenzene (- • -)

Although not shown in Table 4.2, they were interesting to see that the direct slope of  $\chi_{ij}''$  against  $\chi_{ij}'$  gives rise to almost the same  $\tau_j$ 's with those obtained from the ratio of the individual slopes of  $\chi_{ij}''$  and  $\chi_{ij}'$  against  $w_j$ 's of Eq. (4.10). The  $\tau_j$ 's at all the temperatures

for p-hydroxypropiofenone, p-chloropropiofenone, p-acetamidobenzal dehyde, p-benzyloxy

Table 4.3: The intercepts and slopes of  $\ln\tau_j T$  against  $1/T$  curves of Fig.4.3, thermodynamic energy parameters like enthalpy of activation  $\Delta H_\tau$  in K J mole<sup>-1</sup>, the entropy of activation  $\Delta S_\tau$  in J mole<sup>-1</sup>K<sup>-1</sup>, free energy of activation  $\Delta F_\tau$  in K J mole<sup>-1</sup> for dielectric relaxation process, enthalpy of activation  $\Delta H_\eta$  in K J mole<sup>-1</sup> due to viscous flow,  $\gamma$  as the ratio of  $\Delta H_\tau$  and  $\Delta H_\eta$ , Kalman factor ( $\tau_j T / \eta^\gamma$ ), Debye factor ( $\tau_j T / \eta$ ) at different experimental temperatures in °C and the coefficients of  $\mu_j$ -t equations  $\mu_j = a + bt + ct^2$  of different para compounds in dioxane and benzene under 10 GHz electric field frequency.

System with sl no & molecular weight $M_j$	t in °C	Intercept & slope of $\ln\tau_j T$ against $1/T$		$\Delta H_\tau$	$\Delta S_\tau$	$\Delta F_\tau$	$\gamma$	$\Delta H_\eta$	$\tau_j T / \eta^\gamma$	$\tau_j T / \eta \times 10^6$	Coefficients in $\mu_j \times 10^{30} = a + bt + ct^2$		
											a	b	c
1. p-hydroxy-propiofenone $M_j=0.150$ Kg	17	-21.33	708.00	5.91	-19.29	11.50	0.49	11.99	$1.40 \times 10^{-7}$	3.88	-0.02	1.15	-11.49
	23				-20.71	12.03			$1.66 \times 10^{-7}$	4.83			
	30				-22.42	12.70			$2.06 \times 10^{-7}$	6.40			
	37				-18.74	11.72			$1.30 \times 10^{-7}$	4052			
2. p-chloro-propiofenone $M_j=0.1685$ Kg	19	-23.20	1182.4	9.86	-1.59	10.33	0.92	10.68	$1.48 \times 10^{-6}$	2.40	0.09	-4.8	65.11
	25				-6.81	11.89			$2.81 \times 10^{-6}$	4.57			
	31				-10.01	12.90			$4.22 \times 10^{-6}$	6.95			
	37				-0.33	9.96			$1.38 \times 10^{-6}$	2.30			
3. p-acrtamido-benzaldehyde $M_j=0.163$ Kg	17	-20.56	530.45	4.42	-27.27	12.33	0.30	14.92	$5.48 \times 10^{-8}$	5.48	0.06	-2.06	35.89
	23				-25.66	12.02			$4.48 \times 10^{-8}$	4.80			
	30				-27.23	12.68			$5.40 \times 10^{-8}$	6.34			
	37				-26.71	12.71			$5.09 \times 10^{-8}$	6.63			
4. p-benzyloxy-benzaldehyde $M_j=0.212$ Kg	20	-30.30	3384.2	28.23	53.72	12.49	1.84	15.32	$1.50 \times 10^{-3}$	5.81	-0.04	2.42	30.10
	25				56.49	11.39			$1.04 \times 10^{-3}$	3.74			
	30				53.21	12.10			$1.53 \times 10^{-3}$	5.06			
	35				54.79	11.35			$1.31 \times 10^{-3}$	3.94			
5. p-anisidine $M_j=0.123$ Kg	20	-30.55	3147.2	26.25	56.96	9.56	4.07	6.45	$2.78 \times 10^4$	3.89	-0.05	3.00	29.22
	30				55.93	9.30			$3.24 \times 10^4$	3.39			
	40				56.98	8.42			$2.73 \times 10^4$	2.30			
6. p-phenitidine $M_j=0.0137$ Kg	20	-22.49	844.99	7.05	-10.58	10.15	1.11	6.37	$2.44 \times 10^{-5}$	4.94	0.14	-8.71	148.55
	30				-10.62	10.26			$2.08 \times 10^{-5}$	4.96			
	40				-10.58	10.36			$2.48 \times 10^{-5}$	4.85			
7. o-chloro p-nitro aniline $M_j=0.1725$ Kg	20	-23.65	1177.0	9.82	-1.22	10.17	1.60	6.14	$4.22 \times 10^{-4}$	5.00	0.002	-0.06	3.58
	30				-0.26	9.90			$3.85 \times 10^{-4}$	4.29			
	40				-1.24	10.21			$4.27 \times 10^{-4}$	4.57			
8. p-bromo nitrobenzene $M_j=0.202$ Kg	20	-21.96	678.44	5.66	-15.07	10.07	0.90	6.32	$1.95 \times 10^{-6}$	4.79	0.02	-1.48	25.35
	30				-14.96	10.19			$1.94 \times 10^{-6}$	4.82			
	40				-15.07	10.38			$1.95 \times 10^{-6}$	4.88			

benzaldehyde are of high values probably due to their larger molecular sizes [4.9] while the reverse is true for p-anisidine, p-phenitidine, o-chloroparanitroaniline and p-

bromonitrobenzene. The observation indicates that  $\tau_j$ 's of all the liquids decrease with the rise of temperature in  $^{\circ}\text{C}$  for the lower values of the coefficients of viscosity [4.6] of solution. The variation of some  $\tau_j$ 's with  $t$  in  $^{\circ}\text{C}$  of all the p-liquids were found to be (see Table 4.2) irregular and in disagreement with the Debye relaxation [4.19]. This is, however, explained on the basis of the fact that as the temperature rises the stretching of bond angles and distributions of bond moments of all the flexible polar groups attached to the parent ones lead to either symmetric or asymmetric shapes of the molecules [4.9].

The process of rotation of the rotating molecular dipole requires activation energy sufficient to overcome the energy barrier between two equilibrium positions. Eyring's rate process equation [4.14] can be used with the known  $\tau_j$ 's, where

$$\tau_j = \frac{A}{T} \exp(\Delta F_{\tau} / RT)$$

$$\ln \tau_j T = \ln A' + \frac{\Delta H_{\tau}}{RT} \quad \dots (4.19)$$

( since  $\Delta F_{\tau} = \Delta H_{\tau} - T\Delta S_{\tau}$  and  $A' = Ae^{-\Delta S_{\tau}/R}$  ) to measure thermodynamic energy parameters like  $\Delta F_{\tau}$ ,  $\Delta H_{\tau}$  and  $\Delta S_{\tau}$  usually known as free energy, enthalpy and entropy of activations due to dielectric relaxation processes.

The linear Eq.(4.19) of  $\ln\tau_j T$  against  $1/T$  having intercept and slope are presented in Table 4.3 together with the values of  $\Delta F_{\tau}$ ,  $\Delta H_{\tau}$  and  $\Delta S_{\tau}$  as obtained from Eq. (4.19). The least square fitted linear plots of  $\ln\tau_j T$  against  $1/T$  with the experimental points placed on them have been shown in Fig. 4.3. Some of the experimental points are found not to fall on the smooth curves of Fig. 4.3 due to irregular variations of  $\tau_j$ 's with temperature [4.9] probably due to the fact that the non spherical dipolar molecules are known to be non Debye in their relaxation behaviours. As seen in Table 4.3  $\Delta F_{\tau}$ 's for most of the systems are higher in comparison to  $\Delta H_{\tau}$ 's. This implies that a large number of flexible polar groups surrounding the parent molecules are rotating under GHz electric field [4.6]. The  $-ve \Delta S_{\tau}$  for all the systems except p-benzyloxybenzaldehyde and p-anisidine is due to co-operative orientations of the steric forces [4.20] indicating thereby that the activated states are more ordered [4.4,

4.21] while the +ve  $\Delta S_{\tau}$ 's for other systems refers to the unstability of the activated states. Enthalpy of activation due to viscous flow  $\Delta H_{\eta}$  has been estimated from slope of  $\ln\tau_j T$  with

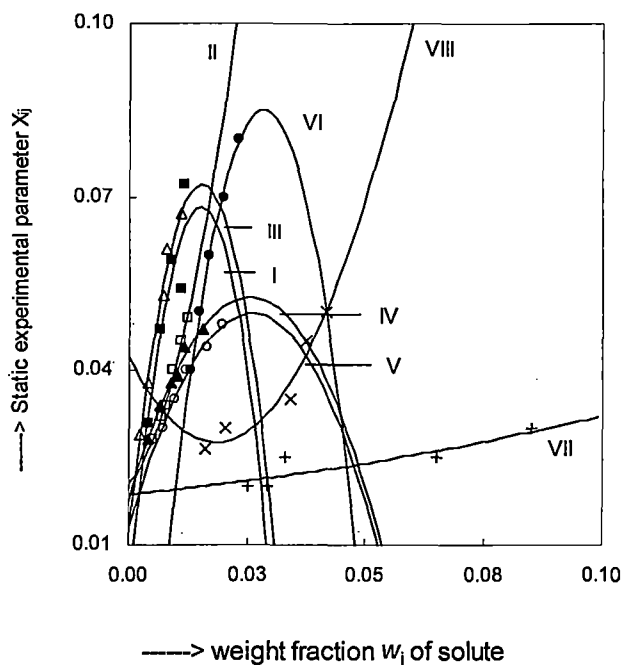


Figure 5: Variation of static experimental parameter  $X_{ij}$  against weight fraction  $w_j$  of solute of some para compounds at temperatures in nonpolar solvents ( dioxane & benzene ) under 10 GHz electric field frequency. I. p-hydroxypropiofenone (—■—) at 23°C, II. p-chloropropiofenone (—□—) at 19°C III. P-acetamidobenzaldehyde (—△—) at 17°C, IV. P-benzyloxybenzaldehyde (—▲—) at 5°C, V p-anisidine (—○—) at 20°C, VI.p-phenitidine (—●—) at 40°C, VII.o-chloro p-nitroaniline (—+—) at 30°C,VIII.p-bromonitrobenzene (—x—) at 20°C

$\ln\eta_i$  fitted linear equation and known  $\Delta H_{\tau}$  in order to place them in Table 4.3.  $\delta$  ( $= \Delta H_{\tau}/\Delta H_{\eta}$ ) for all the molecules  $>0.50$  except p-hydroxypropiofenone and p-acetamidobenzaldehyde indicates the solvent environment around the solute molecules to behave as solid phase rotators [4.9]. Low value of  $\gamma$  for systems as seen in Table 4.3 arises for the weak interaction of the solvent and solute [4.9]. Almost constant values of Debye factor  $\tau_j T/\eta$  rather than Kalman factor  $\tau_j T/\eta^{\gamma}$  at all the temperatures for each molecule implies the applicability of Debye relaxation for such p-liquids [4.9, 4.22].

This at once prompted us to recalculate hf  $\tau_j$ 's from conductivity, measurements in the GHz range. From Eq.(4.3) one gets

$$\beta = \frac{1}{\omega\tau_j} \left( \frac{d\sigma'_{ij}}{dw_j} \right)_{w_j \rightarrow 0} \quad \dots (4.20)$$

where  $\beta$  is the slope of  $\sigma_{ij}$ - $w_j$  curve of a polar-nonpolar liquid mixture at  $w_j \rightarrow 0$ .

The real part of hf complex  $\sigma_{ij}^*$  is [4.12, 4.17]

$$\sigma'_{ij} = \frac{N\rho_i\mu_j^2}{27M_jk_B T} (\epsilon_{ij} + 2)^2 \frac{\omega^2\tau_j}{1 + \omega^2\tau_j^2} w_j$$

$$\left( \frac{d\sigma'_{ij}}{dw_j} \right)_{w_j \rightarrow 0} = \frac{N\rho_i\mu_j^2}{27M_jk_B T} (\epsilon_{ij} + 2)^2 \frac{\omega^2\tau_j}{1 + \omega^2\tau_j^2} \quad \dots (4.21)$$

Comparing Eqs (4.20) and (4.21) the following formula is obtained to get hf  $\mu_j$  from  $\sigma_{ij}$  in  $\Omega^{-1} \cdot m^{-1}$  which takes into account of the contribution of bound molecular charge transfer among the solute molecules.

$$\mu_j = \left[ \frac{27M_jk_B T}{N\rho_i(\epsilon_{ij} + 2)^2} \cdot \frac{\beta}{\omega b} \right]^{\frac{1}{2}} \quad \dots (4.22)$$

where  $b$  is a dimensionless parameter involved with  $\tau_j$ 's measured from Eq.(4.5). The recalculated  $\tau_j$ 's are presented in Table 4.2 for comparison with those measured from Eq. (4.10) and reported ones [4.6, 4.7]. Estimation of  $\tau_j$  by Eq. (4.5) is significant one, as it is useful to obtain  $\epsilon_{oij}$  and  $\epsilon_{\infty ij}$  by Debye-Pellat's equation, to have static  $\mu_s$  as entered in Table 4.2.  $\mu_j$ 's by susceptibility measurements are shown in Table 4.2 to see how far they agree with  $\mu_{theo}$ 's of the bond moments of the flexible parts as calculated in Fig.4.6 and the static  $\mu_s$ 's from Eq.(4.18).  $\mu_s$ 's thus computed from  $\epsilon_{oij}$  and  $\epsilon_{\infty ij}$  data of Table 4.1 show the fact that they are very close to hf  $\mu_j$ . Thus the frequency effect is almost nil in hf  $\mu_j$ 's obtained by susceptibility method. A comparison between hf  $\mu_j$  from Eq.(4.13) and (4.22) may, however, be interesting which is to be studied later on. The values of  $n_{Dij}^2$  ( $\approx \epsilon_{\infty ij}$ ) had been tested from the literature [4.8] where they were available.



$\mu_j - t$  of least square fitted curves of I, III, IV and V of p-hydroxypropiofenone, p-acetamidobenzaldehyde, p-benzyloxybenzaldehyde and p-anisidine initially increases with temperature and then attain the highest value to show maximum asymmetries at different temperatures as seen in Fig. 4.4.  $\mu_j$ 's of those compounds go on decreasing with temperature to attain symmetries. These curves are convex in nature showing  $\mu_j = 0$  at lower and higher temperatures due to strong symmetry attained at those temperatures [4.9]. The curve of VII for o-chloro-p-nitroaniline shows gradual decrease of  $\mu_j$  values with temperature. On the other hand the least square fitted curves of  $\mu_j$  against  $t$  in  $^{\circ}\text{C}$  of II, VI and VIII are concave in nature. The curve VI of p-phenitidine reaches the highest symmetry and then goes on increasing with the rise in temperature. The curve shows 0 (zero) values at lower and higher temperature, as shown by the dotted line to maintain the continuity of the curves. The above nature of  $\mu_j - t$  curves are explained by the rupture of solute-solvent (monomer) and solute-solute (dimer) associations due to stretching of bond angles and bond moments of substituted polar groups at different temperatures [4.4, 4.9].

Ghosh et al [4.9] obtained the  $\mu$ 's of p-compounds i.e. systems I – VIII as 8.27, 9.73, 13.12, 6.23, 6.82, 15.04, 15.93 & 8.40 each multiplied by  $10^{-30}$  in C.m. respectively. A special attention is to be paid to the contributions of the available bond moments and bond angles due to different substituent groups of parent molecules in calculating theoretical dipole moments  $\mu_{\text{theo}}$ 's. But  $\mu_{\text{theo}}$ 's as sketched elsewhere [4.9] are found to be slightly deviated from the measured hf  $\mu_j$ 's and  $\mu_s$ 's because of the existence of the inductive and the mesomeric moments for different flexible groups. The reduced or elongated bond moments of the substituted polar groups are calculated by multiplying the  $\mu_{\text{theo}}$ 's by the factor  $\mu_j / \mu_{\text{theo}}$  around  $20^{\circ}\text{C}$ . The results for systems I to VIII are 14.27, 7.27, 12.62, 10.22, 8.56, 29.36, 2.41 and 4.23 each multiplied by  $10^{-30}$  in C.m. respectively. They are placed in the last column of Table 4.2 and displayed in Fig.4.6. The reduction or elongation in bond moments exhibits the presence of mesomeric, inductive and electromeric effects under static and hf electric fields.

#### 4.5. Conclusions :

Theoretical consideration in S.I units for the effective utilization of the established symbols of dielectric terminologies and parameters in terms of dielectric susceptibilities

obtained from dielectric relative permittivities appears to be more topical, significant and useful one to have valuable information in the study of dispersion and absorption phenomena as they are directly linked with the molecular orientational polarisation. A convenient method is, therefore, suggested to calculate  $\tau_j$  and  $\mu_j$  under GHz electric field along with the static  $\mu_s$  in S.I units of some p-compounds. The ratio of slopes of individual variations of  $\chi_{ij}''$  and  $\chi_{ij}'$  with  $w_j$ 's is a better representation over the previous one of Murthy et al as it eliminates polar-polar interactions almost completely in a given solution. Thermodynamic energy parameters; enthalpy  $\Delta H_\tau$ , entropy  $\Delta S_\tau$  and free energy  $\Delta F_\tau$  of activation due to dielectric relaxation and enthalpy of activation due to viscous flow of solvent provides information about the stability or unstabilities of the states of polar-nonpolar liquid mixture in a given temperature range. The physico-chemical properties could, also be studied in terms of conformations of such p-compounds. The temperature variation of measured  $\mu_j$ 's reveals that the molecules may attain either symmetric or asymmetric shapes with the rise in temperature. The slight difference between experimental  $\mu_j$ 's and theoretical  $\mu_{\text{theo}}$ 's suggests the existence of inductive, mesomeric and electromeric effects of the polar flexible groups of the molecules due to their aromaticity. Theoretical formulations, so far developed, are in S.I. units because of its unified, coherent and rationalised nature. The experimental points in some cases are slightly deviated from the least squares fitted plots indicating that the highly nonspherical polar molecules are slightly non Debye in relaxation behaviour. However, the  $X_{ij} - w_j$  curves used to get  $\mu_s$ , can be used to test the accuracies of the measurements of static  $\epsilon_{0ij}$  and hf  $\epsilon_{\infty ij}$ .

The  $X_{ij}$ 's are involved with the low and infinitely hf permittivities  $\epsilon_{0ij}$  and  $\epsilon_{\infty ij}$  derived from Debye-pellat's equations in terms of measured concentration variation of  $\epsilon_{ij}'$  and  $\epsilon_{ij}''$  of polar-non polar liquid mixtures. The  $\mu_j$ 's and  $\mu_s$ 's are almost equal in some cases only to show that  $\mu_j$ 's are little affected by the applied electric field frequency. The computation of  $\tau_j$ ,  $\mu_j$  and  $\mu_s$  from  $\sigma_{ij}$ ,  $\chi_{ij}$  and  $X_{ij}$  measurements of a polar unit in a given solvent appears to be more simple, straight forward and topical one to locate the accuracies of  $\tau_j$ ,  $\mu_j$  and  $\mu_s$  which are claimed to be accurate within 10% and 5% respectively. The calculated results appear to be of more archival values to reveal some interest in the process of dielectric relaxation. The factors of  $\mu_i / \mu_{\text{theo}}$  and  $\mu_j / \mu_{\text{theo}}$  are almost constant for all the molecules revealing the material property of the systems [4.23]. The correlation between the

conformational structures presented in Fig.4.6 of the p-compounds with the observed results enhances the scientific content and adds a new horizon to understand the existing knowledge of dielectric relaxation from dispersion and absorption phenomena.

#### References :

- [4.1] H D Purohit and H S Sharma, *Bull. Chem. Soc. Japan.* **50** 2606 (1977)
- [4.2] F L Mopisk and R H Cole, *J Chem. Phys.*, **44** 1015 (1966)
- [4.3] S Acharyya, A K Chatterjee, P Acharyya and I L Saha, *Ind J Phys* **56** 291 (1982)
- [4.4] S K Sit, N Ghosh, U Saha and S Acharyya, *Indian J Phys* **71B** 533 (1997)
- [4.5] N Paul, K P Sharma and S Chattopadhyay, *Indian J Phys* **71B** 711 (1997)
- [4.6] R L Dhar, A Mathur, J P Shukla and M C Saxena, *Indian J. Pure & Appl. Phys.* **11** 568 (1973)
- [4.7] S K S Somevanshi, S B I Misra and N K Mehrotra, *Indian J. Pure & Appl. Phys.* **16** 57 (1978)
- [4.8] *Hand Book of Chemistry and Physics*, CRC Press **58th** Edition 1977-78
- [4.9] N Ghosh, R C Basak, S K Sit and S Acharyya, *J. Mol. Liquids (Germany)* **85** 375 (2000)
- [4.10] F J Murphy and S O Morgan, *Bell. Syst. Tech. J.* **18** 502 (1939)
- [4.11] M B R Murthy, R L Patil and D K Deshpande, *Indian J. Phys.* **63B** 491 (1980)
- [4.12] N Ghosh, A Karmakar, S K Sit and S Acharyya, *Indian J. Pure & Appl. Phys.* **38** 574 (2000)
- [4.13] P Debye, *Polar Molecules* (Chemical Catalogue) 1929
- [4.14] H Eyring, S Glasstone and K J Laidler 'The Theory of Rate Process' (Mc Graw Hill: New York) 1941
- [4.15] K Dutta, A Karmakar, L Dutta, S K Sit and S Acharyya, *Indian J. Pure & Appl. Phys.* **40** 801 (2002)
- [4.16] N Ghosh, S K Sit, A K Bothra and S Acharyya, *J. Phys. D : Appl. Phys.* **34** 379 (2001)
- [4.17] C P Smyth, 'Dielectric Behaviour and Structure' (Mc Graw Hill: New York) 1955
- [4.18] N Ghosh, S K Sit and S Acharyya, *J. Mol. Liquids (Germany)* **102** 29 (2003)
- [4.19] S C Srivastava and S Chandra, *Indian J. Pure & Appl. Phys.* **13** 101 (1975)
- [4.20] F H Branin (Jr) and C P Smyth, *J. Chem. Phys.* **02** 1120 (1952)

- [4.21] S K Garg and C P Smyth, *J. Phys. Chem.* **69** 1294 (1965)
- [4.22] K Dutta, S K Sit and S Acharyya, *J. Mol. Liquids*, **92** 263 (2001)
- [4.23] K Dutta, A Karmakar, S K Sit and S Acharyya, *J. Mol. Liquids* **128** 161(2006)

*Chapter 5*

**DIELECTRIC RELAXATION PHENOMENA OF  
SOME APROTIC POLAR LIQUID UNDER GIGA  
HERTZ ELECTRIC FIELD**

## 5.1 Introduction

The relaxation behaviour of polar-nonpolar liquid mixtures under high frequency (hf) electric field is of much importance to study the molecular shapes, sizes as well as associational behaviours [5.1-5.3] in them. Researchers in this field usually analyse the experimental data obtained through relaxation mechanisms involved on the basis of various models [5.4-5.6] applicable to polar liquids. Dhull et al [5.7] and Sharma & Sharma [5.8] had, however, measured the real  $\epsilon_{ijk}'$ ,  $\epsilon_{ij}'$  or  $\epsilon_{ik}'$  and imaginary  $\epsilon_{ijk}''$ ,  $\epsilon_{ij}''$  or  $\epsilon_{ik}''$  parts of relative complex permittivities  $\epsilon_{ijk}^*$ ,  $\epsilon_{ij}^*$  or  $\epsilon_{ik}^*$  of some interesting binary or single polar liquids (jk, j or k) in a nonpolar solvent under X-band electric field at different or fixed temperatures. The purpose of the work was to detect monomer (solute-solvent) or dimer (solute-solute) molecular associations and molecular dynamics of the systems in terms of estimated relaxation time  $\tau_j$  and dipole moment  $\mu_j$ .

The measured [5.9] values of the relative permittivities  $\epsilon_{ij}$ 's of some aprotic polar liquids like N, N-dimethyl sulphoxide (DMSO); N, N-dimethyl formamide (DMF); N, N-dimethyl acetamide (DMA) and N, N-diethyl formamide (DEF) in benzene under the most effective dispersive region of nearly 10 GHz electric field at 25, 30, 35 and 40°C for DMSO; 25°C for DMA and DMF and 30°C for DEF respectively. DMSO is a aprotic dipolar liquid of high penetrating power and wide applications in medicine and industry. It acts as good constituent of binary mixtures because of its associative [5.10] nature. Amides, on the other hand, are the building blocks of proteins and enzymes and have wide biological applications. The liquids usually show two relaxation times  $\tau_2$  and  $\tau_1$  for the rotation of the whole molecules and the flexible parts attached to the parent molecules from the single frequency measurement technique [5.11-5.12].

All these facts inspired us to study  $\tau_2$  and  $\tau_1$  and dipole moments  $\mu_2$  and  $\mu_1$  of these liquids in terms of real  $\chi_{ij}'$  ( $=\epsilon_{ij}'-\epsilon_{\infty ij}$ ) and imaginary  $\chi_{ij}''$  ( $=\epsilon_{ij}''$ ) parts of complex orientational susceptibility  $\chi_{ij}^*$  ( $=\epsilon_{ij}^*-\epsilon_{\infty ij}$ ) in benzene at different temperatures. The low frequency susceptibility  $\chi_{oij}$  ( $=\epsilon_{oij}-\epsilon_{\infty oij}$ ) is, however, real.  $\chi_{ij}'$  can be obtained by subtracting either 1 or  $\epsilon_{\infty oij}$  from the measured  $\epsilon_{ij}$ 's. If 1 is subtracted from the relative permittivity  $\epsilon_{ij}'$  and  $\epsilon_{oij}$  one gets  $\chi_{ij}'$  and  $\chi_{oij}$  containing all types of polarisation processes including fast

Table 5.1: The real  $\chi_{ij}'$  and imaginary  $\chi_{ij}''$ , parts of the complex dielectric orientation susceptibility  $\chi_{ij}^*$  and static dielectric susceptibility  $\chi_{oij}$  which is real for various weight fractions  $w_j$ 's of some aprotic polar liquids in benzenes at different temperatures under hf electric field.

System with sl. no	Temp. in °C	Weight fraction $w_j$	$\chi_{ij}'$	$\chi_{ij}''$	$\chi_{oij}$
I. DMSO	25	0.0022	0.0611	0.0280	0.0731
		0.0043	0.0890	0.0420	0.1094
		0.0047	0.0950	0.0460	0.1181
		0.0069	0.1231	0.0616	0.1594
		0.0086	0.1520	0.0798	0.1982
II. DMSO	30	0.0022	0.0630	0.0274	0.074
		0.0043	0.0915	0.0400	0.1095
		0.0047	0.0980	0.0440	0.1220
		0.0069	0.1155	0.0526	0.1500
		0.0086	0.1340	0.0648	0.1802
III. DMSO	35	0.0022	0.0600	0.0234	0.0693
		0.0043	0.0800	0.0330	0.108
		0.0047	0.0825	0.0360	0.1135
		0.0069	0.1104	0.0496	0.1564
		0.0086	0.1260	0.0580	0.1830
IV. DMSO	40	0.0022	0.0499	0.0170	0.0648
		0.0043	0.0774	0.0282	0.1054
		0.0047	0.0784	0.0286	0.1094
		0.0069	0.1083	0.0420	0.1541
		0.0086	0.1155	0.0500	0.1775
V. DEF	30	0.0023	0.0850	0.0256	0.1137
		0.0042	0.0899	0.0288	0.1335
		0.0079	0.0997	0.0384	0.1822
		0.0095	0.1033	0.0448	0.2053
VI. DMF	25	0.0027	0.0742	0.0256	0.0948
		0.0036	0.0872	0.0302	0.1162
		0.0048	0.1045	0.0386	0.1423
		0.0063	0.1291	0.0484	0.1855
VII. DMA	25	0.0026	0.0818	0.0213	0.1201
		0.0045	0.1046	0.0278	0.1559
		0.0056	0.1198	0.0330	0.1851
		0.0066	0.1370	0.0381	0.2083

polarisations. When high frequency relative permittivity or the optical permittivity  $\epsilon_{\infty ij}$  be subtracted from  $\epsilon_{ij}'$  and  $\epsilon_{oij}$  of the solution at a certain weight fraction  $w_j$ 's of the solute the

susceptibility  $\chi_{ij}'$ ,  $\chi_{ij}''$  and  $\chi_{oij}$  result due to orientational polarisation only. Our earlier study [5.9] was to calculate  $\tau$ 's and  $\mu$ 's in terms of either relative permittivities  $\epsilon_{ij}$ 's or hf conductivities  $\sigma_{ij}$ 's.  $\epsilon_{ij}$ 's are involved with all types of polarisations while  $\sigma_{ij}$ 's are related only to bound molecular charges of polar liquids. Nowadays relaxation mechanisms are studied in terms of  $\chi_{ij}$ 's [5.13] because measurements of  $\mu$ 's in terms of  $\epsilon_{ij}$ 's or  $\sigma_{ij}$ 's include contributions due to all types of polarisations and bound molecular charges, respectively. Moreover, relaxation processes are highly thermally activated to yield  $\tau$  within the framework of Debye–Smith model of polar–nonpolar liquid mixture.

Table 5.2: The relaxation times  $\tau_2$  and  $\tau_1$  from the slope and intercept of straight line Eq. (5.3), measured  $\tau_j$  from different methods of susceptibility and conductivity measurement technique, reported  $\tau$ , symmetric and characteristic relaxation times  $\tau_s$  and  $\tau_{cs}$  for different aprotic polar liquids under effective dispersive region of nearly 10 GHz electric field.

System	Temp °C	Estimated		$\tau_j^a$ in ps	$\tau_j^b$ in ps	$\tau_j^c$ in ps	$\tau_j^d$ in ps	Rep* $\tau_j$ in ps	$\tau_s$ in ps	$\tau_{cs}$ in ps
		$\tau_1$	$\tau_2$							
I. DMSO	25	8.09	21.07	9.91	6.79	8.77	6.01	5.37	4.88	3.69
II. DMSO	30	7.51	52.02	9.07	6.34	8.04	5.86	4.96	4.82	3.05
III. DMSO	35	6.50	59.68	9.08	9.03	7.47	8.95	4.70	4.21	--
IV. DMSO	40	4.51	39.00	8.38	4.90	7.09	4.46	4.33	3.74	22.20
V. DEF	30	3.89	76.41	16.86	1.06	6.64	0.58	2.42	4.16	15.66
VI. DMF	25	4.60	56.24	6.73	6.69	5.87	5.58	5.09	3.02	8.47
VII. DMA	25	2.20	56.61	3.05	6.53	4.96	3.11	6.53	3.90	81.95

$\tau_j^a$  = relaxation time from direct slope of Eq (5.4)

$\tau_j^b$  = relaxation time from ratio of individual slope of Eq (5.5)

$\tau_j^c$  = relaxation time from direct slope of Eq (5.25)

$\tau_j^d$  = relaxation time from ratio of individual slope of Eq (5.26)

\* reported  $\tau_j$  by using Gopalakrishna's [5.16] method.

The purpose of the present work is to assess the contribution of fast polarisation and bound molecular charges in the measurement of  $\mu$ 's when compared with  $\mu$ 's from  $\chi_{ij}$  and

$\sigma_{ij}$  measurements. The variation of  $\mu$ 's with temperature provides knowledge of the state of the system through the measured energy parameters.

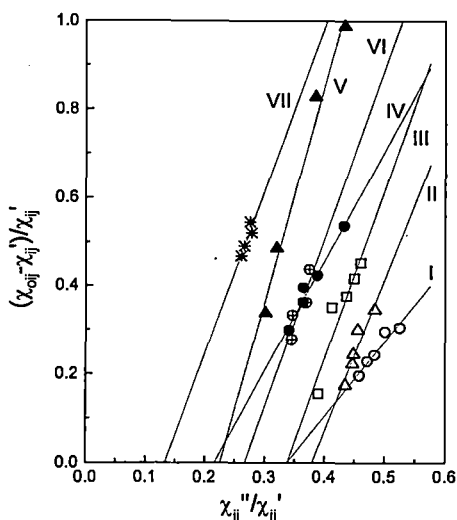


Figure 5.1: Linear Plot of  $(\chi_{\infty ij} - \chi_{ij}') / \chi_{ij}'$  against  $\chi_{ij}'' / \chi_{ij}'$  for different  $w_j$ 's of DMSO, DEF, DMF and DMA in benzene.

(I) DMSO at 25 °C (-o-), (II) DMSO at 30 °C (-Δ-), (III) DMSO at 35 °C (-□-), (IV) DMSO at 40 °C (-●-), (V) DEF at 30 °C (-▲-), (VI) DMF at 25 °C (-⊕-) and (VII) DMA at 25 °C (-\*-).

The detailed experimental technique involved in the measurement of dielectric relaxation parameters of solution has been described elsewhere [5.14]. A Hewlett Packard Impedance Analyser (HP-4192A) measured the capacitance and conductance of the cell containing polar-nonpolar liquid mixtures at different frequencies and temperatures for a fixed  $w_j$  of solute. The real and imaginary parts of relative permittivities  $\epsilon_{ij}^*$  or susceptibility  $\chi_{ij}^*$  are obtained from complex impedances of the cell measured within the range of frequencies from 5 Hz to 13 MHz. The measured  $\epsilon_{ij}$ 's are then plotted in a Cole-Cole semicircular arc to get the values of  $\epsilon_{ij}'$ ,  $\epsilon_{ij}''$ ,  $\epsilon_{\infty ij}$  and  $\epsilon_{\infty ij}$  at nearly 10 GHz electric field (Table 5.1). Again  $\epsilon_{\infty ij}$  is measured at 1 KHz whereas high frequency permittivity  $\epsilon_{\infty ij}$  (=  $n_{\infty ij}^2$ ) is measured by Abbe's Refractometer to compare the values obtained from Cole-Cole plot. The cell containing experimental liquid mixture is then kept in Mettler Hot Stage FP-52 chamber to regulate temperature. Multiply distilled  $C_6H_6$  is used as a solvent in

measurement after several times fractional distillation to get the purest quality of sample. The measured data  $\epsilon_{ij}'$  or  $\chi_{ij}'$ 's are accurate within  $\pm 5\%$ .

Bergmann et al [5.15], however, proposed a graphical technique to get  $\tau_1$ ,  $\tau_2$  and  $c_1$ ,  $c_2$  for a pure polar liquid at different frequencies of the microwave electric field. In order to avoid clumsiness of algebra and fast polarisation processes, the molecular orientational polarisations in terms of established symbols of  $\chi_{ij}$ 's can be written as [5.5]:

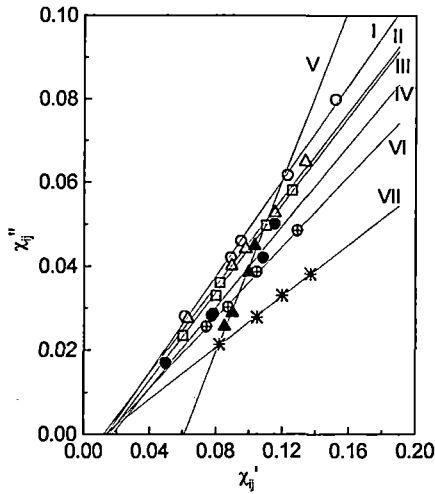


Figure 5.2: Linear variation of imaginary part of dielectric susceptibility  $\chi_{ij}''$  against real part of dielectric susceptibility  $\chi_{ij}'$  for different  $w_j$ 's of DMSO, DEF, DMF and DMA in benzene.

(I) DMSO at 25 °C (-o-), (II) DMSO at 30 °C (-Δ-), (III) DMSO at 35 °C (-□-), (IV) DMSO at 40 °C (-●-), (V) DEF at 30 °C (-▲-), (VI) DMF at 25 °C (-⊕-) and (VII) DMA at 25 °C (-\*-).

$$\frac{\chi'_{ij}}{\chi_{oij}} = \frac{c_1}{1 + \omega^2 \tau_1^2} + \frac{c_2}{1 + \omega^2 \tau_2^2} \quad \dots (5.1)$$

$$\frac{\chi''_{ij}}{\chi_{oij}} = c_1 \frac{\omega \tau_1}{1 + \omega^2 \tau_1^2} + c_2 \frac{\omega \tau_2}{1 + \omega^2 \tau_2^2} \quad \dots (5.2)$$

assuming two separate broad Debye type dispersions of which  $c_1 + c_2 = 1$ .

Saha et al [5.11] and Sit et al [5.12] put forward an analytical technique to measure  $\tau_1$ ,  $\tau_2$  and  $c_1$ ,  $c_2$  of a polar–nonpolar liquid mixture in terms of measured  $\chi_{ij}'$ ,  $\chi_{ij}''$ ,  $\chi_{oij}$  at different  $w_j$ 's of solute under a single frequency electric field and temperature. Eqs (5.1) and (5.2) are solved to get:

$$\frac{\chi_{oij} - \chi_{ij}'}{\chi_{ij}'} = \omega(\tau_1 + \tau_2) \frac{\chi_{ij}''}{\chi_{ij}'} - \omega^2 \tau_1 \tau_2 \quad \dots (5.3)$$

Table 5.3: Fröhlich's parameter A [ $=\ln(\tau_2/\tau_1)$ ], theoretical and experimental values of  $\chi_{ij}'/\chi_{oij}$  &  $\chi_{ij}''/\chi_{oij}$  of Fröhlich equations (5.8) and (5.9) and from fitting equations of Figs 5.5 and 5.6 at  $w_j \rightarrow 0$  respectively, theoretical and experimental relative contributions  $c_1$  and  $c_2$  towards dielectric dispersion due to  $\tau_1$  and  $\tau_2$ , symmetric and asymmetric distribution parameters  $\gamma$  and  $\delta$  for polar-nonpolar liquid mixtures of some aprotic polar liquids under effective dispersion region of nearly 10 GHz electric field.

System	Te mp in °C	A	Theoretical values of $\chi_{ij}'/\chi_{oij}$ & $\chi_{ij}''/\chi_{oij}$ from Eqs (5.8) & (5.9)		Theoretical values of $c_1$ and $c_2$		Experimental values of $\chi_{ij}'/\chi_{oij}$ & $\chi_{ij}''/\chi_{oij}$ at $w_j \rightarrow 0$ of Figs. 5.5 & 5.6		Experimental values of $c_1$ and $c_2$		Estimated values of $\gamma$ and $\delta$	
			$c_1$	$c_2$	$c_1$	$c_2$	$c_1$	$c_2$	$\gamma$	$\delta$		
I. DMSO	25	0.957	0.629	0.466	0.485	0.571	0.874	0.380	1.095	-0.061	-0.07	2.00
II. DMSO	30	1.935	0.449	0.434	0.423	0.933	0.894	0.389	1.049	0.022	-0.08	2.37
III. DMSO	35	2.217	0.454	0.419	0.425	1.043	1.039	0.371	1.192	-0.076	-0.29	--
IV. DMSO	40	2.241	0.611	0.409	0.507	0.794	0.797	0.266	0.803	0.228	0.21	0.36
V. DEF	30	2.978	0.476	0.378	0.443	1.380	0.849	0.247	0.890	0.210	0.17	0.36
VI. DMF	25	2.505	0.497	0.405	0.451	1.086	0.855	0.262	0.921	0.065	0.13	0.61
VII. DMA	25	3.248	0.601	0.357	0.531	1.093	0.724	0.185	0.713	0.338	0.47	0.18

The Eq. (5.3) gives a straight line when  $(\chi_{oij} - \chi_{ij}')/\chi_{ij}'$  is plotted against  $\chi_{ij}''/\chi_{ij}'$  for different  $w_j$ 's of solute for a given angular frequency  $\omega (= 2\pi f)$ ,  $f$  being the frequency of the applied

electric field. The slope  $\omega(\tau_1+\tau_2)$  and intercept  $-\omega^2\tau_1\tau_2$  of straight line of Eq. (5.3) are obtained through linear regression analysis as shown in Fig.5.1. Relaxation times  $\tau_2$  and  $\tau_1$  are calculated from the slopes and intercepts of Eq. (5.3) of Fig.5.1 in terms of measured data of Table 5.1. They are then compared with measured  $\tau_j$ 's from the linear slope of the  $\chi_{ij}''$  against  $\chi_{ij}'$  curve of Fig.5.2 at different  $w_j$ 's of the form:

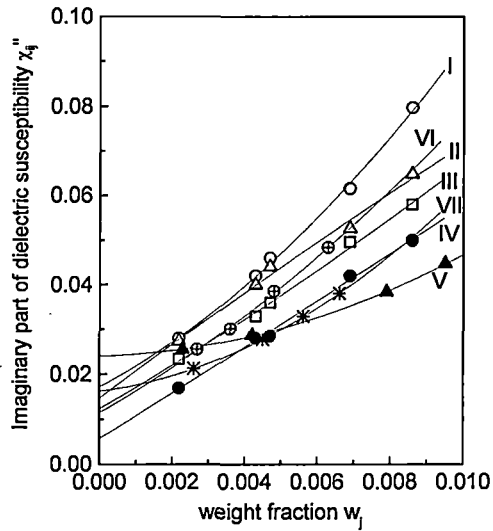


Figure 5.3: Plot of imaginary part of dielectric susceptibility  $\chi_{ij}''$  with weight fraction  $w_j$  of DMSO, DEF, DMF and DMA in benzene.

(I) DMSO at 25 °C (-o-), (II) DMSO at 30 °C (-Δ-), (III) DMSO at 35 °C (-□-), (IV) DMSO at 40 °C (-●-), (V) DEF at 30 °C (-▲-), (VI) DMF at 25 °C (-⊕-) and (VII) DMA at 25 °C (-\*-).

$$\frac{d\chi_{ij}''}{d\chi_{ij}'} = \omega\tau \quad \dots (5.4)$$

Both  $\chi_{ij}''$  and  $\chi_{ij}'$  are functions of  $w_j$ 's of solute. It is better to use the individual slopes  $\chi_{ij}''-w_j$  and  $\chi_{ij}'-w_j$  curves in Figs. 5.3 and 5.4 at  $w_j \rightarrow 0$  to measure  $\tau$  using the following equation:

$$\frac{(d\chi_{ij}''/dw_j)_{w_j \rightarrow 0}}{(d\chi_{ij}'/dw_j)_{w_j \rightarrow 0}} = \omega\tau \quad \dots (5.5)$$

$\tau$ 's from both the methods along with  $\tau$ 's from conductivity measurement technique using Eqs. (5.25) and (5.26) [see later] are placed in Table 5.2 in order to compare with  $\tau$  measured by Gopalakrishna's method [5.16].

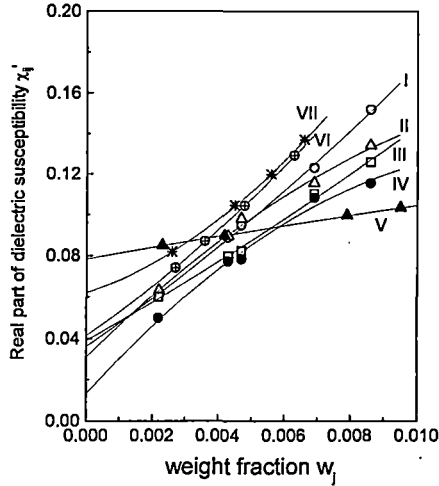


Figure 5.4: Plot of real part of dielectric susceptibility  $\chi_{ij}'$  with weight fraction  $w_j$  of DMSO, DEF, DMF and DMA in benzene.

(I) DMSO at 25 °C (-o-), (II) DMSO at 30 °C (-Δ-), (III) DMSO at 35 °C (-□-), (IV) DMSO at 40 °C (-●-), (V) DEF at 30 °C (-▲-), (VI) DMF at 25 °C (-⊕-) and (VII) DMA at 25 °C (-\*-).

Eqs. (5.1) and (5.2) are solved for  $c_1$  and  $c_2$  to get:

$$c_1 = \frac{(\chi_{ij}'\alpha_2 - \chi_{ij}'')(1 + \alpha_1^2)}{\chi_{oij}(\alpha_2 - \alpha_1)} \quad \dots (5.6)$$

$$c_2 = \frac{(\chi_{ij}'' - \chi_{ij}'\alpha_1)(1 + \alpha_2^2)}{\chi_{oij}(\alpha_2 - \alpha_1)} \quad \dots (5.7)$$

where  $\alpha_1 = \omega \tau_1$  and  $\alpha_2 = \omega \tau_2$ , such that  $\alpha_2 > \alpha_1$ . The values of  $\chi_{ij}'/\chi_{oij}$  and  $\chi_{ij}''/\chi_{oij}$  are also obtained from following Fröhlich's equations [5.17]:

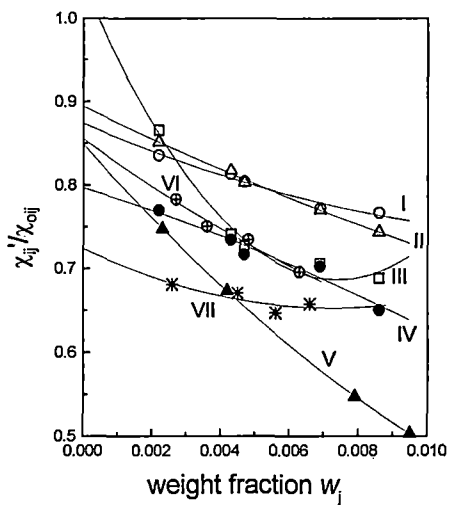


Figure 5.5: Variation of  $\chi_{ij}'/\chi_{oij}$  with  $w_j$ 's of DMSO, DEF, DMF and DMA in benzene. (I) DMSO at 25 °C (-o-), (II) DMSO at 30 °C (-Δ-), (III) DMSO at 35 °C (-□-), (IV) DMSO at 40 °C (-●-), (V) DEF at 30 °C (-▲-), (VI) DMF at 25 °C (-⊖-) and (VII) DMA at 25 °C (-\*-).

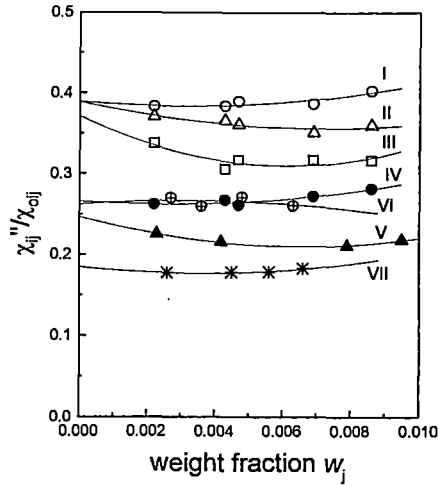


Figure 5.6: Variation of  $\chi''_{ij}/\chi'_{oij}$  with  $w_j$ 's of DMSO, DEF, DMF and DMA in benzene. (I) DMSO at 25 °C (-o-), (II) DMSO at 30 °C (-Δ-), (III) DMSO at 35 °C (-□-), (IV) DMSO at 40 °C (-●-), (V) DEF at 30 °C (-▲-), (VI) DMF at 25 °C (-⊕-) and (VII) DMA at 25 °C (-\*-).

$$\frac{\chi'_{ij}}{\chi'_{oij}} = 1 - \frac{1}{2A} \ln \left( \frac{1 + \omega^2 \tau_2^2}{1 + \omega^2 \tau_1^2} \right) \quad \dots (5.8)$$

$$\frac{\chi''_{ij}}{\chi'_{oij}} = \frac{1}{A} \left[ \tan^{-1}(\omega \tau_2) - \tan^{-1}(\omega \tau_1) \right] \quad \dots (5.9)$$

where  $A = \text{Fröhlich parameter} = \ln(\tau_2 / \tau_1)$ . The theoretical values of relative contributions  $c_1$  and  $c_2$  towards dielectric relaxation processes for  $\tau_1$  and  $\tau_2$  are computed from Eqs.(5.8) and (5.9). They are presented in Table 5.3. The graphical plots of  $\chi'_{ij}/\chi'_{oij}$  and  $\chi''_{ij}/\chi'_{oij}$  curves as a function of  $w_j$  are shown in Figs 5.5 and 5.6 respectively. The experimental values of  $c_1$  and  $c_2$  are also estimated from Eqs (5.1) and (5.2) with the measured values of  $(\chi'_{ij}/\chi'_{oij})_{w_j \rightarrow 0}$  and  $(\chi''_{ij}/\chi'_{oij})_{w_j \rightarrow 0}$  of Figs 5.5 and 5.6. These  $c_1$  and  $c_2$  are finally compared with theoretical ones in Table 5.3.

The symmetric and asymmetric distribution parameters  $\gamma$  and  $\delta$  of the molecules under study are calculated and placed in the last columns of the Table 5.3 along with all the  $c_1$  and  $c_2$ 's in order to see that the relaxation mechanism for such liquids are symmetric. The dipole moments  $\mu_2$  and  $\mu_1$  due to rotation of the whole molecule as well as the flexible parts of the molecules are determined from the slope  $\beta_1$  of  $\chi'_{ij}-w_j$  curve of Fig. 5.4 at  $w_j \rightarrow 0$  in

terms of estimated  $\tau_j$  of Eq. (5.3) as placed in Table 5.4.  $\mu_j$ 's are again calculated from the  $\tau$ 's of Eqs. (5.4) and (5.25) of Murthy et al [5.18] and the ratio of the individual slopes of Eqs. (5.5) and (5.26) from susceptibility and conductivity measurements using slope  $\beta_1$  of  $\chi_{ij}'-w_j$  of Fig 5.4 and  $\beta_2$  of  $\sigma_{ij}-w_j$  curve of Fig. 5.7.  $\mu$ 's from both the measurements are entered in Table 5.4 along with estimated  $\mu$ 's from Gopalakrishna's method [5.16] quoted as reported ones in the Table.

The variations of measured  $\mu_2$  and  $\mu_1$  for DMSO in benzene with temperature in  $^{\circ}\text{C}$  are given by the equations:

$$\begin{aligned}\mu_2 &= -231.61 + 15.597 t - 0.2272 t^2 \\ \mu_1 &= 19.825 - 0.626 t + 0.0108 t^2\end{aligned}\quad \dots (5.10)$$

$\mu_2$  of the parent molecule attains a maximum value of 36 C.m at  $34.32^{\circ}\text{C}$  with zero dipole moments at  $21.72^{\circ}\text{C}$  and  $46.92^{\circ}\text{C}$  respectively due to monomer formation with  $\text{C}_6\text{H}_6$  ring.

Table 5.4: Slope  $\beta_1$  of  $\chi_{ij}'$  vs  $w_j$  and  $\beta_2$  of  $\sigma_{ij}$  vs  $w_j$  curves, measured dipole moments  $\mu_2$  and  $\mu_1$  from susceptibility measurement technique,  $\mu_j$ 's from Eqs.(5.22) and (5.29) respectively, reported dipole moment, theoretical dipole moment  $\mu_{\text{theo}}$  from available bond angles and bond moments expressed in Coulomb.metre (C.m) and the values of  $\mu_1/\mu_{\text{theo}}$  for some aprotic polar liquids in benzene under effective dispersion region of nearly 10 GHz electric field.

System with sl.no. & mol.wt.	Slope of $\chi_{ij}'-w_j$ & $\sigma_{ij}-w_j$ curves		Dipole moments $\mu_j$ ( $\times 10^{-30}$ ) in Coulomb.metre								$\frac{\mu_1}{\mu_{\text{theo}}}$
	$\beta_1$	$\beta_2$	From Eq(5.22)		$\mu_j^a$	$\mu_j^b$	$\mu_j^c$	$\mu_j^d$	$\mu_j^f$	$\mu_{\text{theo}}$	
			$\mu_2$	$\mu_1$							
I.DMSO at $25^{\circ}\text{C}$ $M_j=0.078$ Kg	10.943	6.280	14.69	10.30	10.75	10.03	11.10	10.48	12.65	15.18	0.67
II.DMSO at $30^{\circ}\text{C}$ $M_j=0.078$ Kg	16.440	9.096	36.69	12.64	13.09	12.35	13.31	12.75	12.79	15.18	0.83
III.DMSO at $35^{\circ}\text{C}$ $M_j=0.078$ Kg	8.950	4.621	31.09	9.27	9.79	9.78	9.50	9.82	13.49	15.18	0.61

IV.DMSO at 40°C M <sub>j</sub> = 0.078 Kg	17.646	9.894	30.37	12.69	13.70	12.82	13.94	13.32	13.73	15.18	0.83
V.DEF at 30°C M <sub>j</sub> = 0.101 Kg	2.870	2.922	26.62	5.67	7.91	5.53	8.18	7.58	12.96	13.30	0.42
VI.DMF at 25°C M <sub>j</sub> = 0.073 Kg	10.938	7.282	33.21	9.37	9.81	9.80	10.54	10.48	12.09	12.73	0.74
VII.DMA at 25°C M <sub>j</sub> = 0.087 Kg	5.147	2.792	24.97	6.83	7.07	6.89	7.00	6.81	11.26	13.37	0.51

$\mu_j^a$  = dipole moment by using  $\tau$  from the direct slope of Eq (5.4)

$\mu_j^b$  = dipole moment by using  $\tau$  from the ratio of individual slopes of Eq (5.5)

$\mu_j^c$  = dipole moment by using  $\tau$  from the direct slope of Eq (5.25)

$\mu_j^d$  = dipole moment by using  $\tau$  from the ratio of individual slopes of Eq (5.26)

$\mu_j^r$  = reported dipole moment using Gopalakrishna's [5.16]  $\tau$

$\mu_{\text{theo}}$  = theoretical dipole moment from the available bond moments.

The theoretical dipole moment  $\mu_{\text{theo}}$ 's of the molecules are calculated from the available infrared spectroscopic data of bond moments assuming the molecules are planar as sketched in Fig 5.8. They are found to vary with the measured  $\mu_j$ 's. The difference, however, indicates that the effect of inductive, mesomeric and electromeric moments of the substituent polar groups within the molecules along with temperature in the hf electric field is to be considered to have the conformation of the molecules under interest.

The thermodynamic energy parameters like enthalpy of activation  $\Delta H_\tau$ , free energy of activation  $\Delta F_\tau$  and entropy of activation  $\Delta S_\tau$  were obtained from the slope and intercept of linear equation of  $\ln(\tau_1 T)$  against  $1/T$  for DMSO as given by the equation.

$$\begin{aligned} \ln(\tau_2 T) &= - 4.8353 - 4.088 \times 10^3 (1/T) \\ \ln(\tau_1 T) &= - 30.568 + 3.216 \times 10^3 (1/T) \end{aligned} \quad \dots (5.11)$$

The variation of  $\ln(\tau_1 T)$  or  $\ln(\tau_2 T)$  against  $1/T$  indicate that  $\tau_1$  obeys the Eyring rate process whereas  $\tau_2$  does not.

## 5.2. Symmetric and asymmetric distribution parameters $\gamma$ and $\delta$ :

The polar–nonpolar liquid mixtures under study are nonrigid in nature exhibiting two relaxation times  $\tau_2$  and  $\tau_1$  at a single frequency electric field [5.19]. The measured values of  $\chi_{ij}''/\chi_{oij}$  when plotted against  $\chi_{ij}'/\chi_{oij}$  at  $\omega_j \rightarrow 0$  for different frequency  $\omega$  at a fixed experimental temperature for DMSO may either show Cole–Cole semicircular arc or Cole–Davidson skewed arc having symmetric and asymmetric distribution of relaxation behaviour according to following equations:

$$\frac{\chi_{ij}^*}{\chi_{oij}} = \frac{1}{1 + (j\omega\tau_s)^{1-\gamma}} \quad \dots (5.12)$$

$$\frac{\chi_{ij}^*}{\chi_{oij}} = \frac{1}{(1 + j\omega\tau_{cs})^\delta} \quad \dots (5.13)$$

where  $\tau_s$  and  $\tau_{cs}$  are symmetric and characteristics relaxation times related to symmetric and asymmetric distribution parameters  $\gamma$  and  $\delta$  respectively. On separation the real and imaginary parts of Eq. (5.12) one gets:

$$\gamma = \frac{2}{\pi} \tan^{-1} \left[ \left( 1 - \frac{\chi_{ij}'}{\chi_{oij}} \right) \frac{\chi_{ij}'/\chi_{oij}}{\chi_{ij}''/\chi_{oij}} - \frac{\chi_{ij}''}{\chi_{oij}} \right] \quad \dots (5.14)$$

$$\tau_s = \frac{1}{\omega} \left[ 1 / \left( \frac{\chi_{ij}'/\chi_{oij}}{\chi_{ij}''/\chi_{oij}} \cos \frac{\gamma\pi}{2} - \sin \frac{\gamma\pi}{2} \right) \right]^{\frac{1}{1-\gamma}} \quad \dots (5.15)$$

On simplification of Eq. (5.13) further one gets :

$$\frac{1}{\phi} \log(\cos \phi) = \frac{\log[(\chi_{ij}'/\chi_{oij})/\cos(\phi\delta)]}{\phi\delta} \quad \dots (5.16)$$

$$\tan(\phi\delta) = \frac{(\chi_{ij}''/\chi_{oij})_{\omega_j \rightarrow 0}}{(\chi_{ij}'/\chi_{oij})_{\omega_j \rightarrow 0}} \quad \dots (5.17)$$

where  $\tan\phi = \omega\tau_{cs}$

A theoretical curve of  $(1/\phi)\log(\cos\phi)$  with  $\phi$  in degrees was drawn [5.5] to get the known values of  $\phi$  and  $\delta$  in terms of measured parameter of  $[\log\{(\chi_{ij}'/\chi_{oij})/\cos(\phi\delta)\}] / (\phi\delta)$  of Eqs. (5.16) and (5.17). All the  $\tau_s$ ,  $\tau_{cs}$  and  $\delta$   $\phi$  are given in Tables 5.2 and 5.3 respectively.

### 5.3. Dipole moment $\mu_j$ from susceptibility measurement :

Debye equation [5.20] of relative permittivities of a polar solute (j) dissolved in a nonpolar solvent (i) in terms of complex dielectric orientational susceptibility  $\chi_{ij}^*$  of solution can be written as:

$$\frac{\chi_{ij}^*}{\chi_{oij}} = \frac{1}{1 + j\omega\tau} \quad \dots (5.18)$$

where  $\chi_{ij}' (= \epsilon_{ij}' - \epsilon_{oij})$  and  $\chi_{ij}'' (= \epsilon_{ij}'')$  are the real and imaginary parts of  $\chi_{ij}^* = \chi_{ij}' - j\chi_{ij}''$ .  $j = \sqrt{-1}$  is a complex number  $\chi_{oij} (= \epsilon_{oij} - \epsilon_{oij})$  is the low frequency susceptibility which is real.

Again, the imaginary part of dielectric orientational susceptibility  $\chi_{ij}''$  as a function of  $w_j$  can be written according to Smith [5.21] as:

$$\chi_{ij}'' = \frac{N\rho_{ij}\mu_j^2}{27\epsilon_o k_B T M_j} \frac{\omega\tau}{1 + \omega^2\tau^2} (\epsilon_{ij} + 2)^2 w_j \quad \dots (5.19)$$

On differentiation of Eq. (5.19) w.r. t  $w_j$  at  $w_j \rightarrow 0$  one gets:

$$\left( \frac{d\chi_{ij}''}{dw_j} \right)_{w_j \rightarrow 0} = \frac{N\rho_{ij}\mu_j^2}{27\epsilon_o k_B T M_j} \frac{\omega\tau}{1 + \omega^2\tau^2} (\epsilon_i + 2)^2 \quad \dots (5.20)$$

where  $k_B$  = Boltzmann constant,  $N$  = Avogadro's Number  $\epsilon_i$  = relative permittivity of the solute and  $\epsilon_o$  = Absolute permittivity of free space =  $8.854 \times 10^{-12}$  F.m<sup>-1</sup>, all expressed in S.I. units. Comparing Eqs.(5.4) and (5.20) one gets :

$$\left( \frac{d\chi_{ij}'}{dw_j} \right)_{w_j \rightarrow 0} = \frac{N\rho_i\mu_j^2}{27\epsilon_o k_B T M_j} \frac{1}{1 + \omega^2\tau^2} (\epsilon_i + 2)^2 = \beta_1 \quad \dots (5.21)$$

where  $\beta_1$  is the slope of  $\chi_{ij}'-w_j$  curves at  $w_j \rightarrow 0$ .

From Eq. (5.21) one gets the dipole moment  $\mu_j$  as:

$$\mu_j = \left( \frac{27\epsilon_0 k_B T M_j \beta_1}{N \rho_i (\epsilon_i + 2)^2 b} \right)^{\frac{1}{2}} \quad \dots (5.22)$$

where  $b = 1/(1+\omega^2\tau^2)$  is the dimensionless parameter involved with measured  $\tau_j$  of Table 5.2. All the  $\mu_j$ 's are placed in Table 5.4.

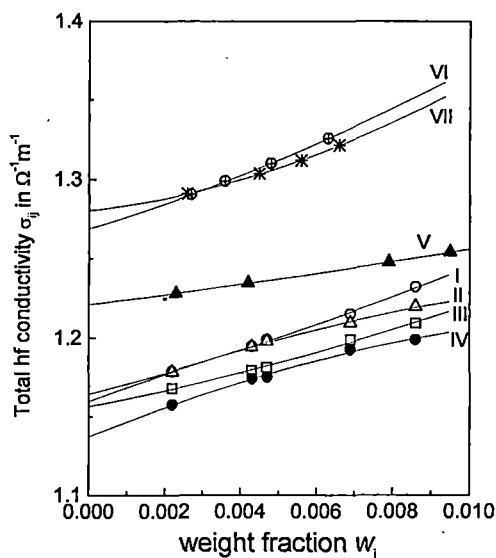


Figure 5.7: Variation of total hf conductivity  $\sigma_{ij}$  with  $w_j$ 's of DMSO, DEF, DMF and DMA in benzene.

(I) DMSO at 25 °C (-o-), (II) DMSO at 30 °C (-Δ-), (III) DMSO at 35 °C (-□-), (IV) DMSO at 40 °C (-●-), (V) DEF at 30 °C (-▲-), (VI) DMF at 25 °C (-⊕-) and (VII) DMA at 25 °C (-\*-).

#### 5.4. Dipole moment $\mu_j$ from hf conductivity measurement :

The hf complex conductivity  $\sigma_{ij}^*$  of a polar–nonpolar liquid mixture is given by:

$$\sigma_{ij}^* = \sigma'_{ij} + j\sigma''_{ij} = \omega\epsilon_0 (\epsilon_{ij}'' + j\epsilon_{ij}') \quad \dots (5.23)$$

the real  $\sigma'_{ij}$  and imaginary  $\sigma''_{ij}$  parts of  $\sigma_{ij}^*$  are related by

$$\sigma''_{ij} = \sigma_{\infty ij} + \frac{1}{\omega\tau_j} \sigma'_{ij} \quad \dots (5.24)$$

where  $\sigma_{\infty ij}$  is the constant conductivity at infinite dilution i.e. at  $w_j \rightarrow 0$ . The Eq. (5.24) on differentiation w.r.t.  $\sigma'_{ij}$  yields:

$$\frac{d\sigma''_{ij}}{d\sigma'_{ij}} = \frac{1}{\omega\tau_j} \quad \dots (5.25)$$

which provides a convenient method to obtain  $\tau_j$  of a polar molecule. It is, however, better to use the ratio of the slopes of variation of  $\sigma''_{ij}$  and  $\sigma'_{ij}$  with  $w_j$  in order to avoid polar–polar interactions at  $w_j \rightarrow 0$  in a given solvent to get  $\tau_j$  from:

$$\frac{(d\sigma''_{ij}/dw_j)_{w_j \rightarrow 0}}{(d\sigma'_{ij}/dw_j)_{w_j \rightarrow 0}} = \frac{1}{\omega\tau_j} \quad \dots (5.26)$$

In hf region of GHz range, it is generally observed that  $\sigma''_{ij} \approx \sigma_{ij}$  the total hf conductivity [5.22] of the solution. Therefore, the Eq. (5.24) can be written as:

$$\sigma_{ij} = \sigma_{\infty ij} + \frac{1}{\omega\tau_j} \sigma'_{ij} \quad \dots (5.27)$$

$$\beta_2 = \frac{1}{\omega\tau_j} \left( \frac{d\sigma'_{ij}}{dw_j} \right)_{w_j \rightarrow 0}$$

where  $\beta_2$  is the slope of  $(d\sigma_{ij}/dw_j)_{w_j \rightarrow 0}$ . The real part  $\sigma'_{ij}$  of a polar-nonpolar liquid mixture is given by [5.5]

$$\sigma'_{ij} = \frac{N\rho_{ij}\mu_j^2}{27k_B TM_j} \frac{\omega^2 \tau_j}{1 + \omega^2 \tau_j^2} (\epsilon_{ij} + 2)^2 w_j$$

$$\left( \frac{d\sigma'_{ij}}{dw_j} \right)_{w_j \rightarrow 0} = \frac{N\rho_{ij}\mu_j^2}{27k_B TM_j} \frac{\omega^2 \tau_j}{1 + \omega^2 \tau_j^2} (\epsilon_{ij} + 2)^2 \quad \dots (5.28)$$

Now comparing Eqs. (5.27) and (5.28) one gets hf  $\mu_j$  from

$$\mu_j = \left( \frac{27k_B TM_j \beta_2}{N\rho_{ij} (\epsilon_{ij} + 2)^2 \omega b} \right)^{\frac{1}{2}} \quad \dots (5.29)$$

where  $b = 1 / (1 + \omega^2 \tau^2)$  is involved with  $\tau_j$ 's from Eqs. (5.25) and (5.26).  $\mu_j$ 's thus obtained from Eq. (5.29) are placed in Table 5.4 along with Gopalakrishna's  $\mu_j$  and  $\mu_{theo}$ 's.

## 5.5. Results and Discussions :

The relaxation parameters in terms of real  $\chi_{ij}' (= \epsilon_{ij}' - \epsilon_{\infty ij})$ , imaginary  $\chi_{ij}'' (= \epsilon_{ij}'')$  and low frequency susceptibility  $\chi_{oij} (= \epsilon_{oij} - \epsilon_{\infty ij})$ , which is real are extracted from the measured relative permittivities  $\epsilon_{ij}$ 's for different  $w_j$ 's of solute at 25, 30, 35 and 40°C for DMSO, 25°C for DMA and DMF and 30°C for DEF under nearly 10 GHz electric field as shown in Table 5.1. The curves of  $(\chi_{oij} - \chi_{ij}')/\chi_{ij}'$  against  $\chi_{ij}''/\chi_{ij}'$  at different  $w_j$ 's of solute are plotted from the measured data in Fig 5.1. All the curves show two relaxation times  $\tau_2$  and  $\tau_1$  due to rotation of the whole molecule and the flexible part attached to the parent ones as evident from Table 5.2. It indicates that the molecules are of non-rigid nature. Unlike  $\tau_2$ 's,  $\tau_1$ 's of DMSO at 25, 30, 35 and 40°C decrease gradually (Table 5.2). This indicates that  $\tau_1$ 's obey the Debye relaxation mechanism. It is also evident from Table 5.2 and Fig.5.1 that the graphs of  $(\chi_{oij} - \chi_{ij}')/\chi_{ij}'$  against  $\chi_{ij}''/\chi_{ij}'$  for different  $w_j$ 's of DMSO shift towards the origin with the increase of temperature.  $\tau_2$ 's of all the liquids are much larger in magnitude than  $\tau_1$ . The parent molecule takes larger time to lag with the electric field frequency for its inertia in comparison to its flexible parts which are supported by the two relaxation model of polar unit under

nearly 10 GHz electric field [5.23].  $\tau_j$ 's are estimated and placed in Table 5.2 from Eqs. (5.4) and (5.5) using linear slope of  $\chi_{ij}''$  against  $\chi_{ij}'$  at different  $w_j$ 's and the ratio of individual slopes of  $\chi_{ij}''-w_j$  and  $\chi_{ij}'-w_j$  curves at  $w_j \rightarrow 0$  of Figs. 5.3 and 5.4 respectively. The values of  $\tau_j$  from Eq. (5.4) are larger than from Eq. (5.5). Reported  $\tau$ 's and  $\tau_j$ 's calculated from both the Gopalakrishna's method [5.16] as well as conductivity measurement technique using Eqs. (5.25) and (5.26) respectively. The agreement is better from the  $\tau_j$ 's due to ratio of the individual slopes of  $\chi_{ij}''-w_j$  and  $\chi_{ij}'-w_j$  curves at  $w_j \rightarrow 0$  of Figs. 5.3 and 5.4 because the polar-polar interactions are almost avoided. They are then compared with the reported  $\tau_s$  and  $\tau_{cs}$  of the molecules assuming symmetric and asymmetric distribution of relaxation processes only to show that the molecules obey symmetric distribution. The curves  $\chi_{ij}''$  against  $\chi_{ij}'$  of Fig. 5.2 of the molecules are found to meet at a point in the region of  $0 < w_j < 0.02$  except DEF the data was measured at 30 °C. The experimental curves of  $\chi_{ij}''-w_j$  and  $\chi_{ij}'-w_j$  are not linear as shown in Figs. 5.3 and 5.4 respectively. Like  $\chi_{ij}'-w_j$  curves all the curves of  $\chi_{ij}''-w_j$  of Fig. 5.3 are parabolic in nature and increase with the  $w_j$ 's of solute. The magnitude of  $\chi_{ij}''$  is, however, maximum in lower temperature region and decrease with the rise of temperature. This indicates the absorption of electric energy in the polar-nonpolar mixture in the lower temperature region.

The relative contributions  $c_1$  and  $c_2$  due to  $\tau_1$  and  $\tau_2$  could, however, be estimated from the  $\chi_{ij}'/\chi_{oij}$  and  $\chi_{ij}''/\chi_{oij}$  of Fröhlich's Eqs. (5.8) and (5.9) and placed in Table 5.3 assuming a continuous distribution of  $\tau$  between limiting values of  $\tau_1$  and  $\tau_2$ .  $c_1$  and  $c_2$  are also calculated in terms of fixed values of  $(\chi_{ij}'/\chi_{oij})_{w_j \rightarrow 0}$  and  $(\chi_{ij}''/\chi_{oij})_{w_j \rightarrow 0}$  of the graphical plots of  $(\chi_{ij}'/\chi_{oij})-w_j$  and  $(\chi_{ij}''/\chi_{oij})-w_j$  curves of Figs. 5.5 and 5.6 respectively. All the curves are extrapolated to get the fixed values of  $(\chi_{ij}'/\chi_{oij})$  and  $(\chi_{ij}''/\chi_{oij})$  at  $w_j \rightarrow 0$ . They are substituted in the Bergmann's Eqs. (5.6) and (5.7) to get  $c_1$  and  $c_2$  for the fixed values of  $\tau_1$  and  $\tau_2$  respectively. All the  $c$ 's are placed in Table 5.3 for comparison with Fröhlich's method. Both  $c_1$  and  $c_2$  from Fröhlich's [5.15] equations are all +ve for all the liquids. But  $c_2$  for DMSO at 25 and 35 °C are -ve from the graphical method. The -ve value of  $c_2$  is physically meaningless as they are considered to be the relative contributions towards dielectric relaxation processes. This may indicate that the rotation of whole molecule under hf electric field is not in accord with the flexible part probably due to inertia as observed elsewhere [5.10-5.11]. The variation of  $\chi_{ij}'/\chi_{oij}$  and  $\chi_{ij}''/\chi_{oij}$  with  $w_j$  as shown in Figs. 5.5 and

5.6 are expected to be concave and convex [5.10-5.11] respectively. All the curves of Figs. 5.5 and 5.6 are, however, concave except systems VI ( $-\oplus-$ ) of Fig. 5.6. This type of anomalous behaviour in the variation of  $\chi_{ij}'/\chi_{oij}$  and  $\chi_{ij}''/\chi_{oij}$  with  $w_j$  invariably demands careful measurement of data in low concentration region.

The dipole moments  $\mu_1$  and  $\mu_2$  are also calculated from the slope  $\beta_1$  of  $\chi_{ij}'-w_j$  curve of Fig. 5.4 and estimated  $\tau_1$  and  $\tau_2$  as shown in Table 5.4. They are compared with  $\mu_j$ 's from  $\tau_j$ 's of Eqs. (5.4) and (5.5) respectively.  $\mu_j$ 's from Gopalakrishna's method [5.16] and conductivity measurement technique [5.9] are also reported and placed in Table 5.4 for comparison among them. The total hf conductivity  $\sigma_{ij}$  is plotted against  $w_j$ 's of the polar-nonpolar liquid mixture as seen in Fig. 5.7 only to show that all the curves are parabolic in nature exhibiting maximum conductivity at lower temperature and higher concentration for

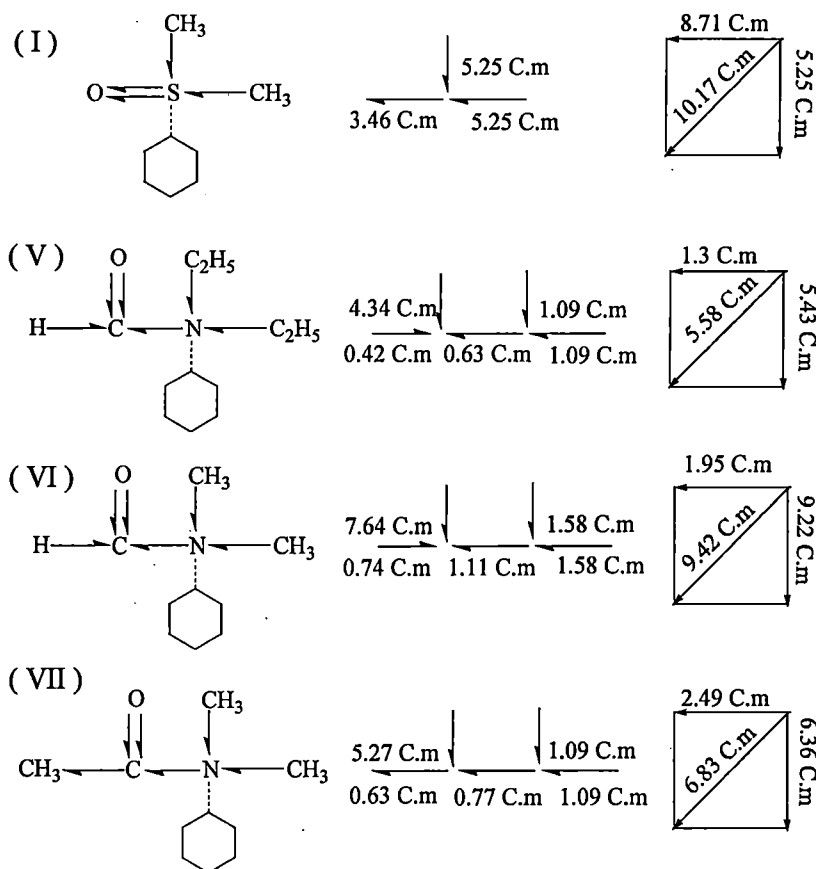


Figure 5.8: Conformational structures of aprotic polar liquids in terms of reduced bond length due to mesomeric and inductive moments in Coulomb metre (C.m.) $\times 10^{30}$  of the substituent polar groups:

(I) DMSO (II) DEF (III) DMF (IV) DMA

DMSO. At  $w_j \rightarrow 0$ , the curves are found to yield different value of  $\sigma_{ij}$  probably due to the term  $1/(M_j T)$  in the Eq. (5.28) as seen in Fig. 5.7. The difference in estimated  $\mu_2$  and  $\mu_1$  from conductivity and susceptibility measurements suggests the involvement of bound molecular charges towards  $\mu$ 's of polar liquid. It is evident from Table 5.4 that  $\mu_1$ 's of the polar liquids are found to be in excellent agreement with the reported  $\mu$ 's. It thus reveals that a part of the molecule is rotating under 10 GHz electric field as observed earlier [5.24]. The variation of  $\mu_1$  and  $\mu_2$  with temperature for DMSO is given by Eq. (5.10). The convex nature of  $\mu_1$ - $t$  equation reveals the fact that the molecule DMSO attains higher asymmetry of larger  $\mu_1$  at a certain temperature. It also shows zero dipole moments at two different temperatures indicating the symmetric nature of the molecule. The variation of  $\mu_1$  with temperature may occur due to elongation of bond moments. This further invites the extensive study of the relaxation phenomena of highly nonspherical dipolar molecules at different experimental temperatures and in different solvents.

The theoretical dipole moment  $\mu_{\text{theo}}$ 's of the polar molecules are calculated assuming the planar structure from the available bond moments of  $7.83 \times 10^{-30}$  C.m.,  $5.17 \times 10^{-30}$  C.m. for polar groups  $S \leftarrow CH_3$ ,  $O \leftarrow S$  in DMSO  $2.13 \times 10^{-30}$  C.m.,  $2.60 \times 10^{-30}$  C.m.,  $1.23 \times 10^{-30}$  C.m. of  $N \leftarrow CH_3$ ,  $N \leftarrow C_2H_5$ ,  $CH_3 \leftarrow C$  in DMF, DEF and DMA respectively. The other bond moments are  $1 \times 10^{-30}$  C.m.,  $1.50 \times 10^{-30}$  C.m.,  $10.33 \times 10^{-30}$  C.m. for  $C \leftarrow H$ ,  $C \leftarrow N$  and  $C \leftarrow O$  in them. The bond moments are, however, reduced by a factor  $\mu_1/\mu_{\text{theo}}$  to yield exact  $\mu$ 's as sketched in Fig. 5.8. The reduction or elongation in bond moments of the substituent polar groups may occur due to inductive, mesomeric and electromeric effects which in turn subsequently act as pusher or puller of electrons in them. The solvent  $C_6H_6$  is a cyclic and planar compound and has three double bonds and six p-electrons on six C-atoms. The dipolar liquid molecules are aliphatic and planar ones. Hence,  $\pi$ - $\pi$  interaction or resonance effect combined with inductive effect commonly known as mesomeric effect in excited state called the electromeric effect may play the vital role in the estimation of  $\mu_{\text{theo}}$ 's of Fig.5.8.

The thermodynamic energy parameters like enthalpy of activation  $\Delta H_\tau$ , entropy of activation  $\Delta S_\tau$  and free energy of activation  $\Delta F_\tau$  of DMSO were calculated from the slope and intercept of  $\ln(\tau_1 T)$  against  $(1/T)$  of Eq. (5.11) on the basis of Eyrings theory considering

the rotation of the polar molecule as a rate process. Unlike  $\ln(\tau_2 T)$  against  $(1/T)$ ;  $\ln(\tau_1 T)$  against  $(1/T)$  of DMSO is in accord with the Eyring's rate theory [5.20]. The value of  $\Delta H_\tau$  for DMSO is 6.85 in KJ mole<sup>-1</sup>  $\Delta S_\tau$  are -8.21, -8.15, -11.65, -11.48 in J mole<sup>-1</sup> K<sup>-1</sup> and  $\Delta F_\tau$  are 9.30, 9.32, 10.43 and 10.45. at 25, 30, 35 and 40°C respectively in KJ mole<sup>-1</sup>. It is observed that  $\Delta S_\tau$  are -ve indicating the activated states are more ordered than the normal states especially for DMSO.

## 5.6. Conclusions :

The study of relaxation phenomena of aprotic polar liquids of amides in C<sub>6</sub>H<sub>6</sub> in terms of the modern established symbols of dielectric terminologies and parameters of orientational susceptibilities  $\chi_{ij}$ 's measured under a single frequency electric field is very encouraging and interesting. It seems to be more topical, significant and useful contribution to predict the conformational structures and various molecular associations of the molecules at any given temperatures. The intercept and slope of derived linear Eq.(5.3) on the measured data of  $\chi_{ij}$  of different  $w_j$ 's are used to get  $\tau_2$  and  $\tau_1$ . The prescribed methodology in S I units is superior because of the unified, coherent and rationalised nature because  $\chi_{ij}$ 's are directly linked only with orientational polarisation of the molecules. The significant Eqs (5.4) and (5.5) to obtain values of  $\tau_j$  and hence values of  $\mu_j$  from Eq. (5.22) help the future workers to shed more light on the relaxation phenomena of complicated non spherical polar liquids and liquid crystals. The present method to obtain values of  $\tau_j$  from Eq.(5.5) with the use of the ratio of the individual slopes of  $\chi_{ij}''$  versus  $w_j$  and  $\chi_{ij}'$  versus  $w_j$  curves at  $w_j \rightarrow 0$  is a significant improvement over the existing ones, as it eliminates polar-polar interaction almost completely in  $\tau_j$ 's and  $\mu_j$ 's respectively.

The values of  $\tau_j$  and  $\mu_j$  are usually claimed to be accurate within 10% and 5% respectively. The tested correlation coefficients  $r$ 's and % of errors of Eq.(5.3) demand that  $\tau$  and  $\mu$  are more than accurate. The DMSO, DMF, DMA and DEF molecules absorb electric energy much more strongly under nearly 10 GHz electric field, at which the variation of  $\chi_{ij}''$  against frequency  $\omega$  seem to be large. This at once indicates the attention to get the double relaxation phenomena from Eq.(5.3). The sum of the experimental and theoretical values of weighted contributions  $c_1$  and  $c_2$  towards dielectric dispersions due to estimated  $\tau_2$  and  $\tau_1$

differ significantly to indicate more than two Debye type relaxations in such molecules because of their complexity. It can, further, be observed that only a part of the molecule is rotating under nearly 10 GHz electric field since  $\ln(\tau_1 T)$  against  $1/T$  obeys the Eyring's rate theory. The values of  $\mu_2$  and  $\mu_1$  due to  $\tau_2$  and  $\tau_1$  are expected to be smaller when they are measured from susceptibility measurement technique rather than the hf conductivity and permittivity methods, where approximation of  $\sigma_{ij} \approx \sigma'_{ij}$  is usually made. The measurement of  $\mu$ 's from hf conductivities  $\sigma_{ij}$ 's and hf permittivities  $\epsilon_{ij}$ 's is involved with the contributions of the bound molecular charges and all types of polarisations including the fast one. The difference of  $\mu_1$  and  $\mu_j$  from  $\mu_{\text{theo}}$  may arise, either by elongation or reduction of the bond moments of the substituted polar groups by factor  $\mu_1/\mu_{\text{theo}}$  in agreement with the measured  $\mu$ 's to take into account of the inductive, mesomeric and electromeric effects of the substituted polar groups in the molecules under investigation. Thus the correlation between the conformational structures with the observed results enhances the scientific content to add a new horizon of understanding the existing knowledge of dielectric relaxation phenomena.

#### References :

- [5.1] S M Puranik,, R Y Ghanabhadur, S N Helambe and S C Mehrotra, *Indian J. Pure & Appl. Phys.* **29** 251 (1991)
- [5.2] M B R Murthy, B S Dayasagar and R L Patil, *Pramana: J. Phys.* **61** 725 (2003)
- [5.3] K K Gupta, A K Bansal, P J Singh and K S Sharma, *Indian J. Pure & Appl. Phys.* **42** 849 (2004)
- [5.4] L Onsager, *J. Am. Chem. Soc.* **58** 1485 (1936)
- [5.5] K Dutta, S K Sit and S Acharyya, *Pramana: J. Phys.* **57** 775 (2001)
- [5.6] N Ghosh, A Karmakar, S K Sit and S Acharyya, *Indian J. Pure & Appl. Phys.* **38** 574 (2000)
- [5.7] J S Dhull, D R Sharma and K N Laxminarayana, *Indian J. Phys.* **56B** 334 (1982)
- [5.8] A Sharma and D R Sharma, *J. Phys. Soc. (Japan)* **61** 1049 (1992)
- [5.9] S K Sit, K Dutta, S Acharyya, T Pal Majumder and S Roy, *J. Mol. Liquids* **89** 111 (2000)
- [5.10] S K Sit, N Ghosh, U Saha and S Acharyya, *Indian J. Phys.* **71B** 533 (1997)

- [5.11] U Saha, S K Sit, R C Basak and S Acharyya, *J. Phys. D: Appl. Phys.* **27** 596 (1994)
- [5.12] S K Sit, R C Basak, U Saha and S Acharyya, *J. Phys. D: Appl. Phys.* **27** 2194 (1994)
- [5.13] A K Jonscher, Inst Phys Conference Serial No 58, Invited paper presented at physics of dielectrics Solids 8 – 11 (1980)
- [5.14] T Pal Majumder, Ph D thesis Jadavpur University, Kolkata, (1996)
- [5.15] K Bergmann, D M Roberti and C P Smyth, *J. Phys. Chem.* **64** 665 (1960)
- [5.16] K V Gopalakrishna, *Trans. Faraday Soc.* **53** 767 (1957)
- [5.17] H Fröhlich, “*Theory of Dielectrics*” (Oxford university press) 1949
- [5.18] M B R Murthy, R L Patil and D K Deshpande, *Indian J. Phys.* **63B** 491 (1989)
- [5.19] K Dutta, A Karmakar, L Dutta, S K Sit and S Acharyya, *Indian J. Pure & Appl. Phys.* **40** 801 (2002)
- [5.20] N E Hill, W E Vaughan, A H Price and M Davis, “*Dielectric properties and Molecular Behaviour*” Van Nostrand Reinhold company Ltd (London), 1969
- [5.21] C P Smyth, “*Dielectric Behaviour and Structure*” (New York; Mc Graw Hill) 1955
- [5.22] K Dutta, A Karmakar, S K Sit and S Acharyya, *Indian J. Pure & Appl. Phys.* **40** 588 (2002)
- [5.23] S K Sit and S Acharyya, *Indian J. Pure & Appl. Phys.* **34** 255 (1996)
- [5.24] R C Basak, S K Sit and S Acharyya, *Indian J. Phys.* **70B** 37 (1996)

*Chapter 6*

**MATERIAL PROPERTIES OF DIPOLAR LIQUID IN  
NONPOLAR SOLVENT THROUGH RELAXATION  
PHENOMENA UNDER HIGH FREQUENCY  
ELECTRIC FIELD**

## 6.1. Introduction:

Relaxation phenomena is one of the most unresolved problems of physics today [6.1]. It is an important tool to measure relaxation time  $\tau_j$ , dipole moment  $\mu_j$ , shape, size as well as molecular interactions of dipolar liquid molecules in a non-polar solvent under high frequency (hf) electric field [6.2-6.3]. It attracted the attention of a large number of workers [6.4-6.5]. There are various techniques [6.6-6.7] like thermally stimulated depolarisation current density (TSDC) and isothermal frequency domain AC spectroscopy (IFDS) with which the present authors are concerned. The later methods are tedious, complicated and often need computer simulations unlike Debye and Smyth model which is simpler, straightforward and more topical to understand the relaxation phenomena. Crossley et al [6.8] and Glasser et al [6.9] showed triple relaxation times for normal and isomeric octyl alcohols under hf electric field of GHz range when they are diluted with non-polar solvent n-heptane. These alcohols showed double relaxation times [6.5]  $\tau_2$  and  $\tau_1$  due to end over end rotation of the whole as well as flexible part of the molecule at all the frequencies of 3.00, 9.25 and 24.33 GHz electric field.  $\tau$ 's are found to vary with frequency of the applied electric field [6.10].

It is, therefore, better to study the alcohols again because of its diverse nature in the identical environment. Alcohols are hydrogen-bonded polymer like molecules. The hydroxyl (-OH) group attached to the saturated hydrogen atom is the functional group of alcohols. Due to highly electro negativity of oxygen atom O-H bond in alcohol is highly polar. Alcohols usually show  $\alpha$ ,  $\beta$  and  $\gamma$  relaxations under hf electric field. It was observed that dipole moment  $\mu_j$ 's of alcohols vary slightly when measurements are done in terms of either relative permittivities  $\epsilon_{ij}$ 's or conductivity  $\sigma_{ij}$ 's [6.10].  $\tau_j$ 's, however, remain the same in both the cases. Nowadays, it is in practice to study the relaxation phenomena in terms of the dielectric orientational susceptibilities  $\chi_{ij}$ 's rather than high frequency relative permittivities  $\epsilon_{ij}$ 's or conductivities  $\sigma_{ij}$ 's [6.11-6.12].  $\epsilon_{ij}$  includes all types of polarisations whereas  $\sigma_{ij}$  is concerned with bound molecular charges. If 1 is subtracted from the relative permittivities the susceptibilities contain all the polarisations including the fast polarisations. But if very hf optical permittivities  $\epsilon_{oij}$  are subtracted from  $\epsilon_{oij}$  and  $\epsilon_{ij}'$  the

Table 6.1: Concentration variation of the real part  $\chi_{ij}'$  and imaginary part  $\chi_{ij}''$  of dimensionless complex dielectric orientation susceptibility  $\chi_{ij}^*$  and the static dielectric orientation susceptibility  $\chi_{oij}$  which is real of some normal and isomeric octyl alcohols in n-heptane under 3.00, 9.25 and 24.33 GHz electric fields at 298 K.

Frequency f in GHz	Weight fraction $w_i$	$\chi_{ij}'$	$\chi_{ij}''$	$\chi_{oij}$	Weight fraction $w_i$	$\chi_{ij}'$	$\chi_{ij}''$	$\chi_{oij}$
		I. 1-Butanol			II. 1-Hexanol			
3.00	0.0451	0.049	0.0114	0.055	0.0459	0.033	0.0065	0.044
	0.0697	0.072	0.0188	0.093	0.0703	0.051	0.0117	0.063
	0.1163	0.123	0.0460	0.197	0.1028	0.070	0.0214	0.094
	0.1652	0.180	0.0782	0.381	0.1688	0.123	0.0446	0.207
	0.2072	0.224	0.1119	0.601	0.2335	0.184	0.0755	0.358
				0.2901	0.232	0.1097	0.562	
9.25	0.0451	0.040	0.0121	0.055	0.0459	0.026	0.0083	0.044
	0.0697	0.057	0.0220	0.093	0.0703	0.038	0.0121	0.063
	0.1163	0.088	0.0416	0.197	0.1028	0.045	0.0226	0.094
	0.1652	0.121	0.0637	0.381	0.1688	0.085	0.0454	0.207
	0.2072	0.152	0.0956	0.601	0.2335	0.126	0.0688	0.358
				0.2901	0.161	0.1000	0.562	
24.33	0.0451	0.036	0.0147	0.055	0.0459	0.024	0.0131	0.044
	0.0697	0.053	0.0236	0.093	0.0703	0.032	0.0190	0.063
	0.1163	0.082	0.0425	0.197	0.1028	0.031	0.0296	0.094
	0.1652	0.105	0.0644	0.381	0.1688	0.048	0.0425	0.207
	0.2072	0.124	0.0818	0.601	0.2335	0.086	0.0569	0.358
				0.2901	0.116	0.0748	0.562	
		III. 1-Heptanol			IV. 1-Decanol			
3.00	0.0735	0.053	0.0111	0.056	0.0572	0.032	0.0051	0.036
	0.1175	0.086	0.0216	0.109	0.1351	0.067	0.0194	0.086
	0.1909	0.128	0.0456	0.236	0.2140	0.098	0.0371	0.157
	0.2465	0.173	0.0651	0.313	0.2640	0.121	0.0496	0.212
	0.2970	0.217	0.0864	0.456	0.3353	0.156	0.0690	0.316
9.25	0.0735	0.040	0.0129	0.056	0.0572	0.028	0.0090	0.036
	0.1175	0.060	0.0232	0.109	0.1351	0.047	0.0228	0.086
	0.1909	0.090	0.0438	0.236	0.2140	0.065	0.0386	0.157
	0.2465	0.112	0.0609	0.313	0.2640	0.069	0.0484	0.212
	0.2970	0.149	0.0774	0.456	0.3353	0.093	0.0656	0.316
24.33	0.0735	0.030	0.0182	0.056	0.0572	0.025	0.0120	0.036
	0.1175	0.050	0.0265	0.109	0.1351	0.039	0.0273	0.086
	0.1909	0.087	0.0482	0.236	0.2140	0.046	0.0400	0.157
	0.2465	0.095	0.0567	0.313	0.2640	0.056	0.0513	0.212
	0.2970	0.118	0.0694	0.456	0.3353	0.067	0.0637	0.316
		V. 2-methyl 3-heptanol			VI. 3-methyl 3-heptanol			
3.00	0.0437	0.040	0.0040	0.041	0.0450	0.040	0.0043	0.040
	0.1299	0.086	0.0137	0.093	0.1334	0.099	0.0131	0.103
	0.2522	0.143	0.0309	0.165	0.2538	0.162	0.0272	0.176
	0.4081	0.215	0.0583	0.276	0.4085	0.242	0.0489	0.277
9.25	0.0437	0.037	0.0088	0.041	0.0450	0.034	0.0103	0.040
	0.1299	0.078	0.0244	0.093	0.1334	0.079	0.0263	0.103
	0.2522	0.108	0.0412	0.165	0.2538	0.126	0.0458	0.176
	0.4081	0.164	0.0710	0.276	0.4085	0.192	0.0766	0.277
24.33	0.0437	0.030	0.0156	0.041	0.0450	0.031	0.0187	0.040
	0.1299	0.056	0.0362	0.093	0.1334	0.061	0.0394	0.103
	0.2522	0.088	0.0565	0.165	0.2538	0.099	0.0674	0.176
	0.4081	0.115	0.0809	0.276	0.4085	0.131	0.0928	0.277

Frequency f in GHz	Weight fraction $w_j$	$\chi_{ij}'$	$\chi_{ij}''$	$\chi_{oij}$	Weight fraction $w_j$	$\chi_{ij}'$	$\chi_{ij}''$	$\chi_{oij}$
		VII. 4-methyl 3-heptanol				VIII. 5-methyl 3-heptanol		
3.00	0.0466	0.039	0.0046	0.040	0.1228	0.084	0.0143	0.092
	0.1326	0.090	0.0147	0.096	0.2489	0.134	0.0337	0.164
	0.2590	0.156	0.0338	0.174	0.3898	0.202	0.0554	0.275
	0.4124	0.224	0.0572	0.287				
9.25	0.0466	0.034	0.0091	0.040	0.1228	0.068	0.0225	0.092
	0.1326	0.076	0.0262	0.096	0.2489	0.095	0.0441	0.164
	0.2590	0.112	0.0472	0.174	0.3898	0.143	0.0706	0.275
	0.4124	0.168	0.0766	0.287				
24.33	0.0466	0.028	0.0146	0.040	0.1228	0.051	0.0297	0.092
	0.1326	0.055	0.0376	0.096	0.2489	0.071	0.0511	0.164
	0.2590	0.093	0.0616	0.174	0.3898	0.107	0.0675	0.275
	0.4124	0.115	0.0849	0.287				
		IX. 2-octanol				X. 4-octanol		
3.00	0.1236	0.078	0.0156	0.065	0.1201	0.081	0.0129	0.092
	0.2479	0.137	0.0419	0.199	0.2445	0.120	0.0302	0.151
	0.3844	0.207	0.0791	0.374	0.3838	0.181	0.0549	0.251
9.25	0.1236	0.061	0.0227	0.065	0.1201	0.063	0.0198	0.092
	0.2479	0.093	0.0467	0.199	0.2445	0.087	0.0397	0.151
	0.3844	0.133	0.0786	0.374	0.3838	0.128	0.0616	0.251
24.33	0.1236	0.047	0.0285	0.065	0.1201	0.052	0.0266	0.092
	0.2479	0.072	0.0513	0.199	0.2445	0.070	0.0449	0.151
	0.3844	0.105	0.0680	0.374	0.3838	0.109	0.0659	0.251

susceptibilities  $\chi_{oij}$  and  $\chi_{ij}'$ , are, however, directly linked with orientation polarisations only. The purpose of the present paper is to study the existence of double relaxation times of alcohols between two limiting  $\tau_2$  and  $\tau_1$  in terms of hf  $\chi_{ij}'$ 's. The chemical systems under consideration are identical in the same environment to show the double relaxation times at one frequency, it will show the same double relaxation times  $\tau_2$  and  $\tau_1$  at all the frequencies because the double relaxation phenomena are the material properties of the system. Saha et al and Sit et al [6.13-6.14] proposed a method to measure double relaxation times  $\tau$ 's of a polar liquid in non-polar solvent at a given experimental temperature under a single frequency electric field. Moreover, varying  $\tau_2$  and  $\tau_1$  at three different frequencies of electric field from a single frequency measurement technique are not so reliable [6.4,6.15].

Mansing and Kumar [6.16] presented a graphical technique to measure  $\tau_2$  and  $\tau_1$  for a pure polar liquid molecule within the framework of Debye and Fröhlich model in terms of measured relative permittivities  $\epsilon$ 's at different frequencies at a single temperature.

However, no such technique has been developed so far to predict  $\tau_2$  and  $\tau_1$  of a polar liquid in a nonpolar solvent at different frequencies of the applied electric field at a single temperature. In this context, it is, however, proposed the almost similar graphical technique to estimate  $\tau_2$  and  $\tau_1$  of alcohols (j) in a non-polar solvent (i) in terms of real  $\chi_{ij}'$  ( $=\epsilon_{ij}' - \epsilon_{\infty ij}$ ) and imaginary  $\chi_{ij}''$  ( $=\epsilon_{ij}''$ ) parts of hf complex dielectric orientational susceptibilities  $\chi_{ij}^*$  under 3.00, 9.25 and 24.33 GHz electric fields as functions of  $\omega_j$ 's.

## 6.2. Theoretical formulations :

### 6.2.1. Relaxation times $\tau_1$ and $\tau_2$ :

The dielectric equation for a polar-nonpolar liquid mixture in terms of the complex hf  $\chi_{ij}^*$  for a distribution of  $\tau$  is [6.1]:

$$\frac{\chi_{ij}^*}{\chi_{oij}} = \int_0^{\infty} \frac{f(\tau) d\tau}{(1 + j\omega\tau)} \quad \dots (6.1)$$

where  $f(\tau)$  is the Fröhlich distribution function for the relaxation time such that :

$$\begin{aligned} f(\tau) &= \frac{1}{A\tau} & \tau_1 < \tau < \tau_2 \\ &= 0 & \tau_1 > \tau; \tau_2 < \tau \end{aligned} \quad \dots (6.2)$$

and  $A = \text{Fröhlich parameter} = \ln(\tau_2/\tau_1)$

Separating the real and imaginary parts of both sides of Eq.(6.1), the following equations are obtained.

$$\frac{\chi_{ij}'}{\chi_{oij}} = \frac{1}{A} \int_{\tau_1}^{\tau_2} \frac{d\tau}{\tau(1 + \omega^2\tau^2)} \quad \dots (6.3)$$

and

$$\frac{\chi_{ij}''}{\chi_{oij}} = \frac{1}{A} \int_{\tau_1}^{\tau_2} \frac{\omega d\tau}{(1 + \omega^2\tau^2)} \quad \dots (6.4)$$

Table 6.2: Intercepts of  $\chi_{ij}''/\chi_{ij}'$  against  $w_j$  curve at  $w_j \rightarrow 0$ , values of  $\ln\omega_2$  and  $\ln\omega_1$  from Fig.6.2 and their average  $\tau_2$  and  $\tau_1$ ,  $\tau_2$  and  $\tau_1$  from single frequency measurement of Eq.(6.8) under 3.00, 9.25 and 24.33 GHz electric fields of some normal and isomeric octyl alcohols in n-heptane at 25°C.

System with sl. no	Frequency f in GHz	Intercept of $\chi_{ij}''/\chi_{ij}'-w_j$ at $w_j \rightarrow 0$	Values of $\ln\omega_2$ and $\ln\omega_1$ from the Fig.6.2	Average $\tau_2$ and $\tau_1$ in psec	$\tau_2$ and $\tau_1$ from single frequency measurement	Average $\tau_2$ and $\tau_1$ in psec
I. 1-Butanol	a) 3.00	0.1262	ab) 23.5015 30.8189	48.41 0.08	211.41 9.10	122.63 4.96
	b) 9.25	0.2120	bc) 24.2051 29.8712		101.87 3.73	
	c) 24.33	0.3231	ca) 23.6737 30.1101		54.60 2.04	
II. 1-Hexanol	a) 3.00	0.1246	ab) 23.2412 31.8059	57.03 0.04	204.26 9.17	110.44 5.01
	b) 9.25	0.1933	bc) 24.1343 30.4314		85.24 3.76	
	c) 24.33	0.2928	ca) 23.5801 30.6780		41.81 2.10	
III. 1-Heptanol	a) 3.00	0.0711	ab) 23.8767 33.6138	18.80 0.91	208.81 9.20	113.91 4.98
	b) 9.25	0.1306	bc) 26.4479 27.0234		83.03 3.30	
	c) 24.33	0.4503	ca) 25.2871 27.7518		49.89 2.43	
IV. 1-Decanol	a) 3.00	0.0438	ab) 25.5281 27.9946	13.12 0.29	135.66 6.89	83.68 5.27
	b) 9.25	0.1620	bc) 24.5801 30.5149		83.14 5.61	
	c) 24.33	0.2631	ca) 25.3244 29.7019		32.25 3.30	
V. 2-methyl 3-heptanol	a) 3.00	0.0700	ab) 24.9650 28.6944	11.19 0.90	73.31 5.41	50.96 4.3
	b) 9.25	0.1974	bc) 25.6712 27.3056		49.61 4.10	
	c) 24.33	0.4952	ca) 25.1384 27.6667		29.96 3.39	
VI. 3-methyl 3-heptanol	a) 3.00	0.0921	25.0098 27.4128	13.75 1.24	73.55 6.17	43.80 4.41
	b) 9.25	0.2882			43.34 4.37	
	c) 24.33	0.5807			14.52 2.68	
VII. 4-methyl 3-heptanol	a) 3.00	0.0892	25.8707 26.9313	5.81 2.01	84.34 6.71	51.61 4.74
	b) 9.25	0.2174			45.08 4.21	
	c) 24.33	0.4932			25.40 3.31	
VIII. 5-methyl 3-heptanol	a) 3.00	0.0358	26.4103 27.3200	3.39 1.36	101.22 6.58	57.13 4.15
	b) 9.25	0.1040			52.36 4.21	
	c) 24.33	0.3276			17.83 1.66	
IX. 2-octanol	a) 3.00	0.0604	24.8271 29.2251	16.51 0.20	160.41 7.83	94.46 4.94
	b) 9.25	0.1964			92.00 5.11	
	c) 24.33	0.3447			30.97 1.89	
X. 4-octanol	a) 3.00	0.0286	26.4780 28.0264	3.17 0.67	85.13 4.72	49.55 3.11
	b) 9.25	0.0699			42.74 2.64	
	c) 24.33	0.2409			20.77 1.97	

where  $\chi_{ij}'=(\epsilon_{ij}'-\epsilon_{\infty ij})$ ,  $\chi_{ij}''=\epsilon_{ij}''$  and  $\chi_{oij}=(\epsilon_{oij}-\epsilon_{\infty oij})$  are the real, imaginary and low frequency dielectric susceptibilities expressed in terms of relative permittivities  $\epsilon_{ij}$ 's.

Dividing Eq. (6.4) by (6.3) and evaluating the integral one gets:

$$\frac{\chi_{ij}''}{\chi_{ij}'} = \frac{2[\tan^{-1}(\omega\tau_2) - \tan^{-1}(\omega\tau_1)]}{\ln \frac{\tau_2^2 (1 + \omega^2\tau_1^2)}{\tau_1^2 (1 + \omega^2\tau_2^2)}} \quad \dots (6.5)$$

On rearrangement of Eq. (6.5) and assuming smaller relaxation time  $\tau_1=1/\omega_1$  and larger relaxation time  $\tau_2=1/\omega_2$  Eq. (6.5) becomes :

$$\frac{\chi_{ij}''}{\chi_{ij}'} \ln(\omega_1^2 + \omega^2) + 2 \tan^{-1} \frac{\omega}{\omega_1} = \frac{\chi_{ij}''}{\chi_{ij}'} \ln(\omega_2^2 + \omega^2) + 2 \tan^{-1} \frac{\omega}{\omega_2}$$

or,  $f(\omega_1) = f(\omega_2) = f(\omega_k)$

where

$$f(\omega_k) = \left[ \left( \frac{\chi_{ij}''}{\chi_{ij}'} \right) \ln(\omega_k^2 + \omega^2) + 2 \tan^{-1} \frac{\omega}{\omega_k} \right] \quad \dots (6.6)$$

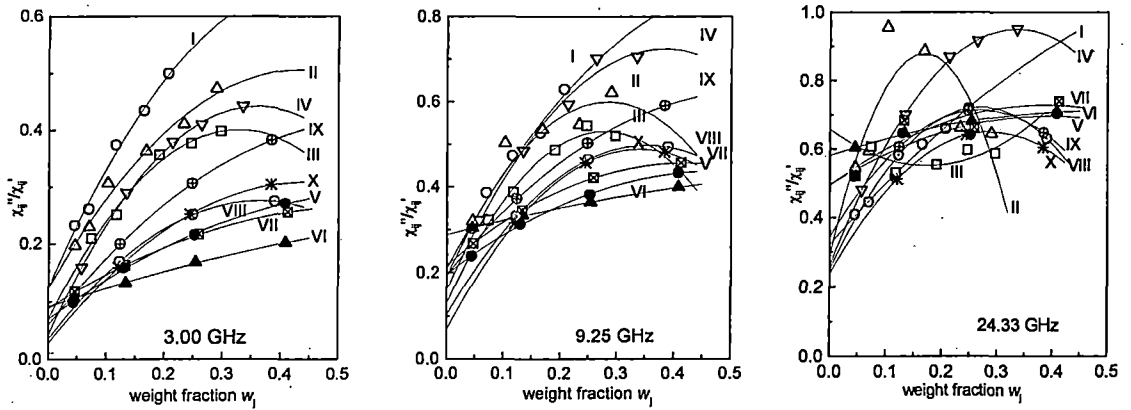


Figure 6.1: Variations of  $\chi_{ij}''/\chi_{ij}'$  with  $w_j$  under 3.00, 9.25 and 24.33 GHz electric fields at 298 K for I. 1-butanol (-O-), II. 1-hexanol (-Δ-), III. 1-heptanol (-□-), IV. 1-decanol (-∇-), V. 2-methyl 3-heptanol (-●-), VI. 3 methyl 3-heptanol (-▲-), VII. 4-methyl 3-heptanol (-⊠-), VIII. 5-methyl 3-heptanol (-⊙-), IX. 2-octanol (-⊗-) and X. 4-octanol (-\*-) in n-heptane.

The term  $\chi_{ij}''/\chi_{ij}'$  of Eq. (6.6) is a function of weight fraction  $w_j$  of polar solute at a given temperature T and angular frequency  $\omega$  of the hf electric field. The factor  $f(\omega_k)$  is, however, made constant for a fixed  $\tau_2$  and  $\tau_1$  at a given angular frequency  $\omega$  by introducing the following term in the Eq.(6.6)

$$f(\omega_k) = \left( \frac{\chi_{ij}''}{\chi_{ij}'} \right)_{w_j \rightarrow 0} \ln(\omega_k^2 + \omega^2) + 2 \tan^{-1} \frac{\omega}{\omega_k} \quad \dots (6.7)$$

where  $(\chi_{ij}''/\chi_{ij}')_{w_j \rightarrow 0}$  is the intercept of  $(\chi_{ij}''/\chi_{ij}')$  against  $w_j$  curve at  $w_j \rightarrow 0$  as shown in Fig.6.1 and are placed in Table 6.2. A curve of  $f(\omega_k)$  against  $\ln \omega_k$  is drawn in Fig.6.2 by varying  $\omega_k$  independently for a given  $\omega$  to get two values of  $\ln \omega_2$  and  $\ln \omega_1$  ( $\omega_2 < \omega_1$ ) for the same  $f(\omega_k)$ . Finally graphs of  $\ln \omega_1$  vs  $\ln \omega_2$  are plotted in Fig.6.3 for three different values of  $\omega (=2\pi f)$ ,  $f$  being the frequency of the electric field of 24.33, 9.25 and 3.00 GHz. The point of intersection of the curves yields  $\tau_2$  and  $\tau_1$  of a polar molecule to place them in Table 6.2.

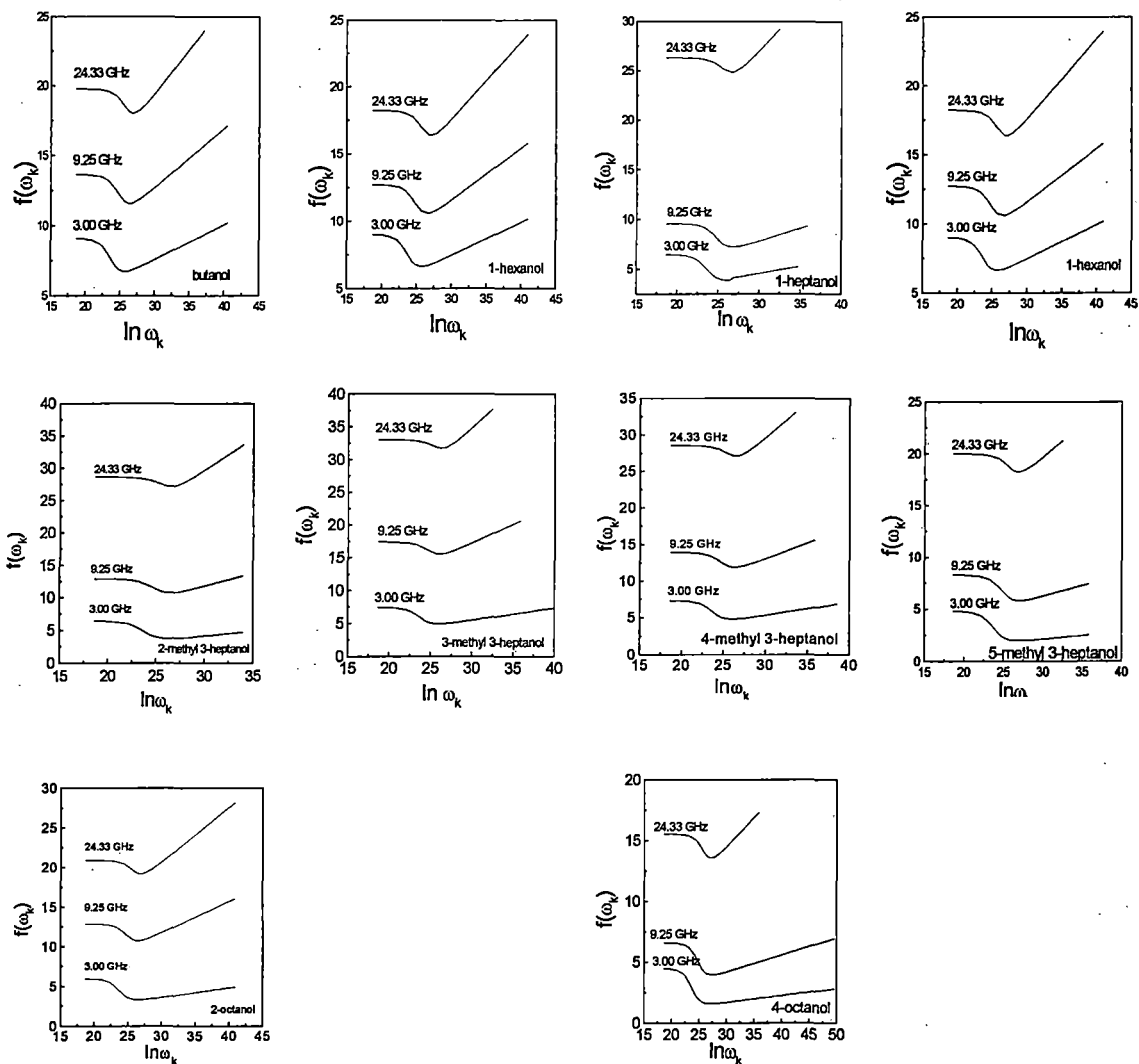


Figure 6.2: Variation of  $f(\omega_k)$  with  $\ln \omega_k$  for 1-butanol, 1-hexanol, 1-heptanol, 1-decanol, 2-methyl 3-heptanol, 3-methyl 3-heptanol, 4-methyl 3-heptanol, 5-methyl 3-heptanol, 2-octanol and 4-octanol in n-heptane under 3.00, 9.25 and 24.33 GHz electric fields at 298 K.

$\tau_2$  and  $\tau_1$  were also estimated from

$$\frac{\chi_{oij} - \chi'_{ij}}{\chi'_{ij}} = \omega(\tau_2 + \tau_1) \frac{\chi''_{ij}}{\chi'_{ij}} - \omega^2 \tau_1 \tau_2 \quad \dots (6.8)$$

based on the single frequency measurement technique [6.12]. The term  $(\chi_{oij} - \chi'_{ij})/\chi'_{ij}$  and  $\chi''_{ij}/\chi'_{ij}$  on both sides of Eq. (6.8) are functions of  $\omega_j$ 's of polar solute at a given angular

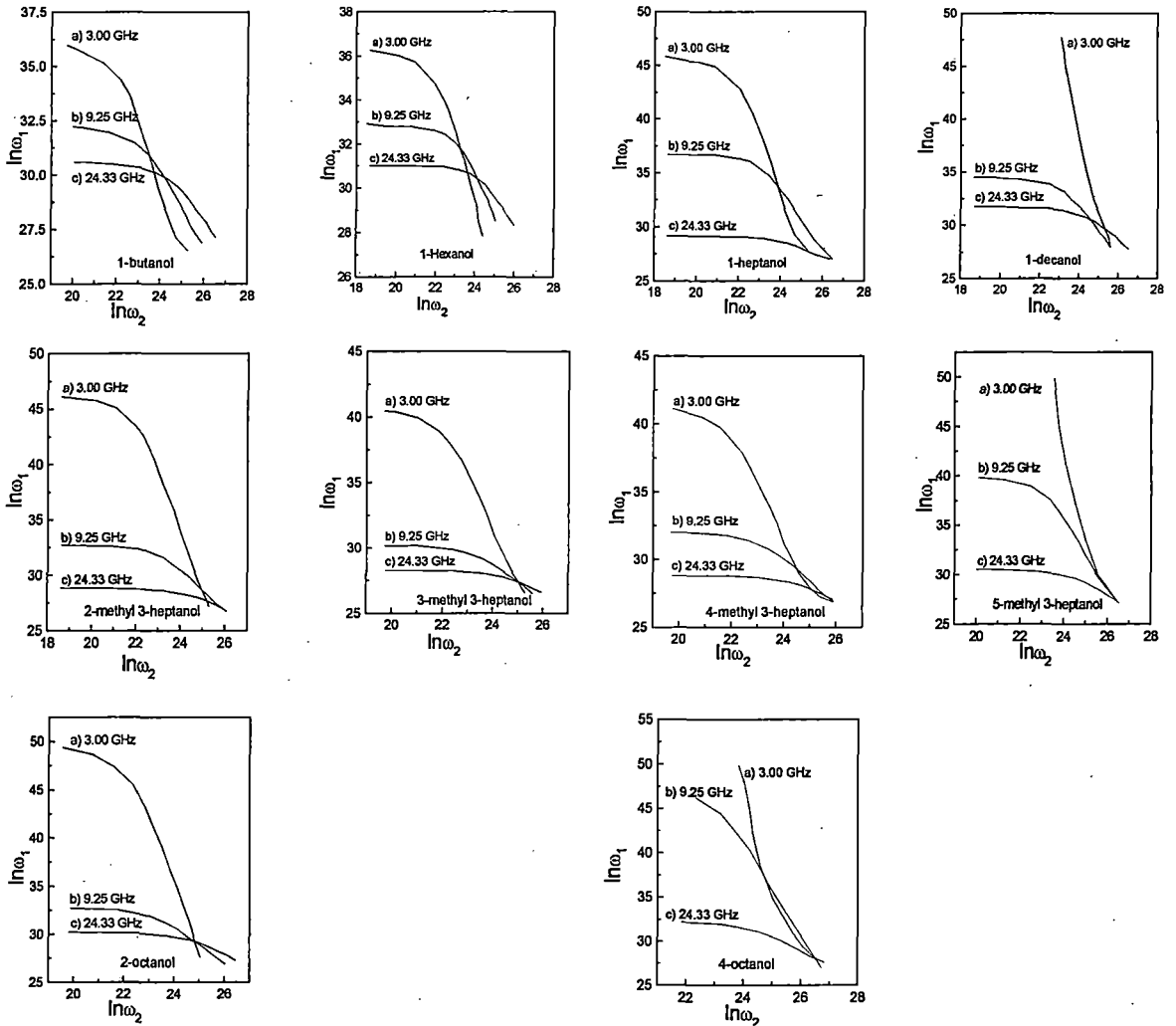


Figure 6.3: plot of  $\ln \omega_1$  against  $\ln \omega_2$  for 1-butanol, 1-hexanol, 1-heptanol, 1-decanol, 2-methyl 3-heptanol, 3-methyl 3-heptanol, 4-methyl 3-heptanol, 5-methyl 3-heptanol, 2-octanol and 4-octanol in n-heptane under 3.00, 9.25 and 24.33 GHz electric fields at 298 K.

frequency  $\omega$  of the electric field. The graphs of  $(\chi_{oij}-\chi_{ij}')/\chi_{ij}'$  against  $\chi_{ij}''/\chi_{ij}'$  are drawn for different  $w_j$ 's at 24.33, 9.25 and 3.00 GHz electric fields to get fixed intercepts and slopes from which  $\tau_1$  and  $\tau_2$  were obtained to get the mean values of  $\tau_1$  and  $\tau_2$  placed in Table 6.2 for comparison with the three sets of  $\tau_1$  and  $\tau_2$  for alcohols at 24.33, 9.25 and 3.00 GHz electric fields respectively.

### 6.2.2. Dipole moments $\mu_1$ and $\mu_2$ from $\tau_1$ and $\tau_2$ :

The Debye equation [6.17] for a polar-nonpolar liquid mixture under hf electric field in terms of  $\chi_{ij}$ 's is now written as :

$$\frac{d\chi_{ij}''}{d\chi_{ij}'} = \omega\tau \quad \dots (6.9)$$

$$\frac{(d\chi_{ij}''/dw_j)_{w_j \rightarrow 0}}{(d\chi_{ij}'/dw_j)_{w_j \rightarrow 0}} = \omega\tau \quad \dots (6.10)$$

Again the imaginary part  $\chi_{ij}''$  of the complex hf susceptibility  $\chi_{ij}^*$  as a function of  $w_j$  of a solute can be written as [6.17]

$$\chi_{ij}'' = \frac{N\rho_{ij}\mu_j^2}{27\varepsilon_o k_B T M_j} \frac{\omega\tau}{1 + \omega^2\tau^2} (\varepsilon_{ij} + 2)^2 w_j$$

which on differentiation with respect to  $w_j$  and at  $w_j \rightarrow 0$  yields :

$$\left( \frac{d\chi_{ij}''}{dw_j} \right)_{w_j \rightarrow 0} = \frac{N\rho_{ij}\mu_j^2}{27\varepsilon_o k_B T M_j} \frac{\omega\tau}{1 + \omega^2\tau^2} (\varepsilon_i + 2)^2 \quad \dots (6.11)$$

where the density of the solution  $\rho_{ij}$  becomes  $\rho_i$  = density of solvent,  $(\varepsilon_{ij}+2)^2$  becomes  $(\varepsilon_i+2)^2$  at  $w_j \rightarrow 0$ ,  $k_B$ =Boltzmann constant =  $1.38 \times 10^{-23}$  J.mole<sup>-1</sup>K<sup>-1</sup>,  $N$ = Avogadro's number =  $6.023 \times 10^{23}$ ,  $\varepsilon_i$ = relative permittivity of solvent,  $\varepsilon_o$ = permittivity of free space =  $8.854 \times$

$10^{-12}$  Farad. metre<sup>-1</sup>,  $M_j$  = alcohol molecular weight and  $\mu_j$  = dipole moment of the alcohol molecule.

Comparing Eqs (6.10) and (6.11) one gets:

$$\left( \frac{d\chi_{ij}'}{dw_j} \right)_{w_j \rightarrow 0} = \frac{N\rho_i\mu_j^2}{27\varepsilon_0 k_B T M_j} \frac{1}{1+\omega^2\tau^2} (\varepsilon_i + 2)^2 = \beta \quad \dots (6.12)$$

where  $\beta$  is the slope of  $\chi_{ij}'$ - $w_j$  curves of Fig.6.5 at  $w_j \rightarrow 0$ . Here no approximation is made in determination of  $\mu_j$  unlike conductivity measurement technique [6.10].

After simplification, the hf  $\mu_j$  due to orientation polarisation alone is given by:

$$\mu_j = \left( \frac{27\varepsilon_0 k_B T M_j \beta}{N\rho_i (\varepsilon_i + 2)^2 b} \right)^{\frac{1}{2}} \quad \dots (6.13)$$

where dimensionless parameter b is given by :

$$b = 1/(1+\omega^2\tau^2) \quad \dots (6.14)$$

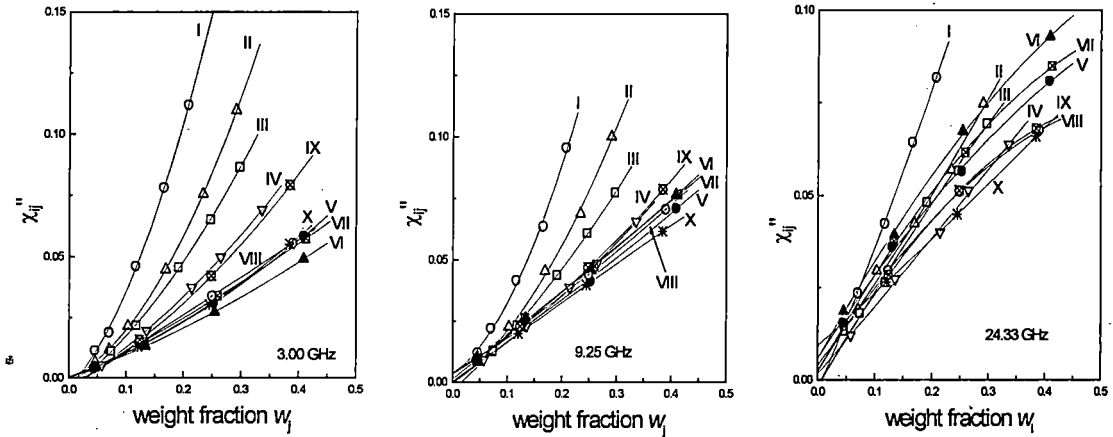


Figure 6.4: Variations of  $\chi_{ij}''$  with  $w_j$  for I. 1-butanol (-○-), II. 1-hexanol (-△-), III. 1-heptanol (-□-), IV. 1-decanol (-▽-), V. 2-methyl 3-heptanol (-●-), VI. 3 methyl 3-heptanol (-▲-), VII. 4-methyl 3-heptanol (-⊠-), VIII. 5-methyl 3-heptanol (-⊙-), IX. 2-octanol (-⊕-) and X. 4-octanol (-\*-) in n-heptane under 3.00, 9.25 and 24.33 GHz electric fields at 298 K.

### 6.3. Results and Discussion :

The data of  $\chi_{ij}'$ ,  $\chi_{ij}''$  and  $\chi_{oij}$  at different  $w_j$ 's of a number of alcohols in n-heptane at 298 K under 24.33, 9.25 and 3.00 GHz electric fields are extracted from the measured permittivities  $\epsilon_{ij}$ 's of Crossley et al [6.8] and Glasser et al [6.9] as presented in Table 6.1. The terms  $\chi_{ij}''/\chi_{ij}'$  for each alcohol are plotted against different  $w_j$ 's for 24.33, 9.25 and 3.00 GHz electric fields at 298 K as seen in Fig. 6.1. So far as Fig.6.1 is concerned, it seems that the variation of  $\chi_{ij}''/\chi_{ij}'$  with weight fraction  $w_j$  for 1-Hexanol in 24.33 GHz electric field exhibits a strange behaviour. The intercept of  $\chi_{ij}''/\chi_{ij}'$  at  $w_j \rightarrow 0$  has been obtained as a polynomial second order least square fitting of the experimental data, but the nature of the curve appears to be surprising. The curves at all the frequencies are convex except system III (-□-) which is concave at 24.33 GHz. It is interesting to see that as the frequency of the applied electric field increases the shape of the curves become more convex. The values of intercepts of  $\chi_{ij}''/\chi_{ij}'$  vs  $w_j$  curves at  $w_j \rightarrow 0$  are placed in column 3 of Table 6.2. The intercepts are found to increase with the frequency of the electric field. For several arbitrary values of angular frequency  $\omega_k$ , three graphs of  $f(\omega_k)$  against  $\ln\omega_k$  according to Eq.(6.7) for the alcohols were drawn for 3.00, 9.25 and 24.33 GHz electric fields in Fig.6.2. The graphs were drawn by using a PC which shows the gradual decrease of  $f(\omega_k)$  with the increase of  $\ln\omega_k$  to exhibit minimum at a certain  $\omega_k$  and then increase afterwards for a fixed  $\omega$  [6.16]. Curves of  $f(\omega_k)$  against  $\ln\omega_k$  at 24.33 and 3.00 GHz electric fields yield the highest and the least values of  $f(\omega_k)$  for a fixed  $\ln\omega_k$ . The  $f(\omega_k)$ - $\ln\omega_k$  curves at 9.25 GHz, however, occupy the intermediate position and are nearer to 3.00 GHz electric field for all the alcohols as observed in Fig.6.2. This is explained on the basis of the fact that  $f(\omega_k)$  is higher for larger intercept of  $\chi_{ij}''/\chi_{ij}'$  against  $w_j$  curve at  $w_j \rightarrow 0$ , in Fig.6.1, according to Eq (6.7). A large number of  $\ln\omega_2$  and  $\ln\omega_1$  ( $\ln\omega_2 < \ln\omega_1$ ) are selected for a fixed  $f(\omega_k)$  in order to draw the graphs of  $\ln\omega_1$  vs  $\ln\omega_2$  at 24.33, 9.25 and 3.00 GHz electric fields from Fig.6.3. The values of  $\ln\omega_2$  and  $\ln\omega_1$  are chosen by drawing horizontal line along the  $\ln\omega_k$  axis in the region of the curve for which  $f(\omega_k)$  is the same in Fig.6.2. It is interesting to see that if  $\ln\omega_2$  is made fixed for all the curves of Fig.6.2 of a polar-nonpolar liquid mixture the values of  $\ln\omega_1$  are the highest and the least for 3.00 and 24.33 GHz respectively in  $\ln\omega_1$  vs  $\ln\omega_2$  curves. This explains the larger magnitudes of  $\ln\omega_1$ 's for 3.00, 9.25 and 24.33 GHz electric fields. The

Table 6.3: Slope of  $\chi_{ij}'-w_j$  curve at  $w_j \rightarrow 0$ , dipole moment  $\mu_2$  and  $\mu_1$  from graphical technique, dipole moments from single frequency measurement, theoretical dipole moment  $\mu_{\text{theo}}$  from the available bond angles and bond moments and the dipole moments using  $\tau$  from Eqs (6.10) and (6.9).

System with sl. no & mol. wt	f in GHz	Slope $\chi_{ij}'-w_j$ at $w_j \rightarrow 0$	$\mu \times 10^{30}$ (C.m) from average $\tau_2$ and $\tau_1$ of Figure 6.3		$\mu \times 10^{30}$ from single frequency measurement		$\mu_{\text{theo}} \times 10^{30}$ in C.m	$\mu_j^a \times 10^{30}$ in C.m	$\mu_j^b \times 10^{30}$ in C.m
			$\mu_2$	$\mu_1$	$\mu_2$	$\mu_1$			
I. 1-Butanol $M_j = 0.074$ Kg	a) 3.00	1.028	4.67	3.45	17.44	4.30	4.95	3.54	3.97
	b) 9.25	0.627	8.04	2.69	22.07	3.77		2.78	3.33
	c) 24.33	0.796	22.69	3.04	29.17	3.63		3.34	3.83
II. 1-Hexanol $M_j = 0.102$ Kg	a) 3.00	0.608	4.57	3.11	16.87	4.30	4.35	3.17	3.50
	b) 9.25	0.330	7.95	2.29	18.77	3.80		2.52	2.75
	c) 24.33	-0.089	--	--	21.20	3.43		--	--
III. 1-Heptanol $M_j = 0.116$ Kg	a) 3.00	0.447	3.02	2.85	17.40	4.33	4.05	3.06	3.15
	b) 9.25	0.213	2.91	1.97	18.40	3.80		2.69	2.31
	c) 24.33	0.588	9.94	3.30	27.01	3.73		3.60	3.80
IV. 1-Decanol $M_j = 0.158$ Kg	a) 3.00	0.383	3.17	3.08	11.94	4.40	3.15	3.29	3.47
	b) 9.25	0.192	2.74	2.18	18.40	3.93		2.76	2.92
	c) 24.33	0.133	4.06	1.81	17.24	3.83		3.10	2.91
V. 2-methyl 3-heptanol $M_j = 0.130$ Kg	a) 3.00	0.530	3.36	3.28	6.93	4.10	5.85	3.33	3.44
	b) 9.25	0.376	3.30	2.77	11.30	3.80		2.95	3.09
	c) 24.33	0.359	5.35	2.73	16.00	3.83		3.24	3.38
VI. 3-methyl 3-heptanol $M_j = 0.130$ Kg	a) 3.00	0.663	3.79	3.67	7.27	4.30	5.85	3.70	3.76
	b) 9.25	0.477	3.99	3.12	10.70	4.07		3.27	3.38
	c) 24.33	0.414	6.75	2.95	8.60	30.83		3.51	3.61
VII. 4-methyl 3-heptanol $M_j = 0.130$ Kg	a) 3.00	0.643	3.64	3.62	7.83	4.20	5.85	3.68	3.76
	b) 9.25	0.413	3.06	2.92	10.64	3.90		3.16	3.25
	c) 24.33	0.424	3.93	3.07	13.90	3.90		3.55	3.72
VIII. 5-methyl 3-heptanol $M_j = 0.130$ Kg	a) 3.00	0.277	2.38	2.37	8.47	3.97	5.85	2.71	2.51
	b) 9.25	0.038	0.90	0.88	11.17	3.60		3.54	1.04
	c) 24.33	0.024	0.79	0.71	9.50	3.37		7.22	0.83
IX. 2-octanol $M_j = 0.130$ Kg	a) 3.00	0.420	3.06	2.92	12.94	4.10	3.58	3.05	3.26
	b) 9.25	0.207	2.84	2.05	18.90	3.63		2.45	2.60
	c) 24.33	0.143	4.63	1.71	16.00	3.43		3.64	2.06
X. 4-octanol $M_j = 0.130$ Kg	a) 3.00	0.142	1.70	1.70	7.10	3.77	3.58	1.99	1.84
	b) 9.25	0.053	1.06	1.04	9.07	3.43		3.39	1.23
	c) 24.33	-0.041	--	--	10.97	3.43		--	--

$\mu_j^a$  = dipole moment using  $\tau$  from Eq (6.10)

$\mu_j^b$  = dipole moment using  $\tau$  from Eq (6.9)

graphs are similar in nature. They cut at a point for almost all the dipolar liquids to yield the significant values of  $\tau_2$  and  $\tau_1$ , respectively. Unlike other systems 1-butanol, 1-hexanol, 1-heptanol, 1-decanol and 2-methyl 3-heptanol the curves meet at three points to exhibit three

different possible values of  $\tau_2$  and  $\tau_1$  [6.8-6.9]. The average values of the points for  $\ln\omega_1$  were, however, selected to get  $\ln\omega_2$  and the recalculated  $\tau_1$  and  $\tau_2$  are placed in the 6<sup>th</sup> and 7<sup>th</sup> column of Table 6.2.

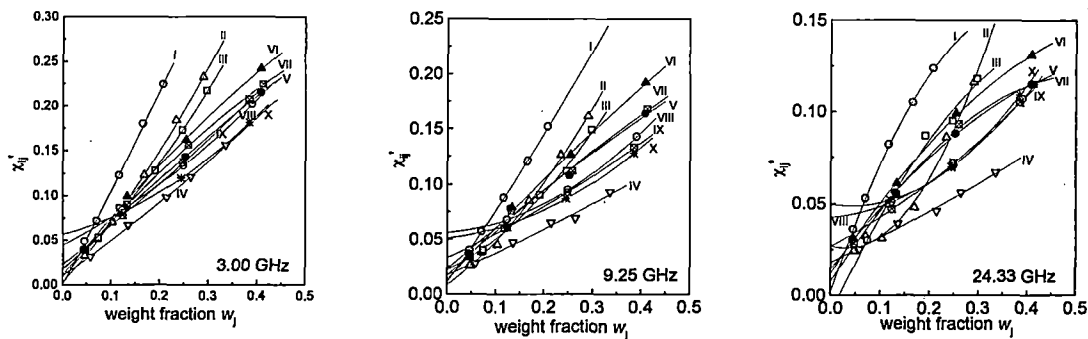


Figure 6.5: Variations of  $\chi_{ij}'$  with  $w_j$  for I. 1-butanol (-O-), II. 1-hexanol (- $\Delta$ -), III. 1-heptanol (- $\square$ -), IV. 1-decanol (- $\nabla$ -), V. 2-methyl 3-heptanol (- $\bullet$ -), VI. 3 methyl 3-heptanol (- $\blacktriangle$ -), VII. 4-methyl 3-heptanol (- $\boxtimes$ -), VIII. 5-methyl 3-heptanol (- $\odot$ -), IX. 2-octanol (- $\otimes$ -) and X. 4-octanol (- $\ast$ -) in n-heptane under 3.00, 9.25 and 24.33 GHz electric fields at 298 K.

$\tau_2$  and  $\tau_1$  are also calculated from the slopes and intercepts of straight line of Eq (6.8) from single frequency measurement technique [6.12]. The estimated  $\tau_2$  and  $\tau_1$  are placed in Table 6.2. They are found to be dependent on the frequency of the applied electric field. The existence of double relaxation phenomena reflects the material property of the chemical systems under investigation and should not depend on the measurement frequency. Although the real part  $\chi_{ij}'$  and the imaginary part  $\chi_{ij}''$  of the hf complex dielectric orientational susceptibility  $\chi_{ij}^*$  vary with the frequency of the applied electric field, the fundamental dielectric parameters such as the dielectric decrement, relaxation time and dipole moment which describe the relaxation property of the system, do not. Therefore, if any alcohol in n-heptane exhibits double relaxation behaviour, this should be reflected at all the three frequencies and the analysis should produce the same value of  $\tau_2$  and  $\tau_1$  at all the

three frequencies. Thus  $\tau$ 's are, therefore, estimated from the ratio of slopes of  $\chi_{ij}''-w_j$  and  $\chi_{ij}'-w_j$  at  $w_j \rightarrow 0$  of Eq. (6.10) and from the slope of linear relation  $\chi_{ij}''-\chi_{ij}'$  curve according to Eq. (6.9). They are placed side by side in the columns 12 and 13 of Table 6.2. The estimated  $\tau_2$  and  $\tau_1$  obtained from present graphical technique are compared with  $\tau$ 's from the single frequency measurement technique [6.13, 6.14] as well as  $\tau$ 's from Eqs (6.10) and (6.9) respectively. It is to be noted that  $\tau$ 's from graphical technique are in agreement with average  $\tau$ 's from Eqs (6.10) and (6.9) respectively for almost all the systems except 1-butanol, 1-hexanol, 5-methyl 3-heptanol and 4-octanol. Average  $\tau_2$  and  $\tau_1$  from Eq (6.8) are, however, higher in magnitude than the graphical technique proposed here.  $\tau_1$ 's are smaller than the reported average  $\tau$  from ratio of slopes as well as direct slopes. This type of behaviour may reveal that double relaxation mechanism of polar-nonpolar liquid mixture is the material property of the chemical systems, which is independent of  $\omega$  of the applied electric field unlike earlier observation [6.12]. The proposed graphical technique seems to be superior to the existing one [6.4, 6.15] as it yields macroscopic and microscopic relaxation times, which are independent of frequency  $\omega$ .

The curves of  $\chi_{ij}''$  against  $w_j$  as seen in Fig.6.4 are all parabolic. They start from origin and increase with  $w_j$  for 3.00, 9.25 and 24.33 GHz electric fields. Unlike the curves at 24.33 GHz, the curves are concave for 9.25 and 3.00 GHz electric fields. The systems V(-●-), VI(-▲-), VII(-⊠-), VIII(-⊙-) and X(-\*-) are found to overlap at 3.00 and 9.25 GHz electric fields exhibiting almost the same absorption of hf electric energy and is maximum at 24.33 GHz. This signifies that the study of relaxation mechanism of alcohols is relevant as observed elsewhere [6.10].

The  $\chi_{ij}'-w_j$  curves of Fig.6.5 are also parabolic in nature at all the frequencies of 3.00, 9.25 and 24.33 GHz. This indicates that the orientation polarisations increase with the  $w_j$ 's and decrease at higher frequency. The dipole moments of the alcohol molecules  $\mu_2$  and  $\mu_1$  from the slope  $\beta$  of  $\chi_{ij}'-w_j$  curve and estimated  $\tau$ 's from  $\chi_{ij}$ 's measurements are calculated to place them in the 4th and 5th columns of Table 6.3.  $\mu_2$ 's and  $\mu_1$ 's from graphical method are found to be in excellent agreement with average reported  $\mu$ 's except 1-butanol, 1-hexanol, 1-heptanol where  $\mu_2$ 's are slightly greater. The slight disagreement

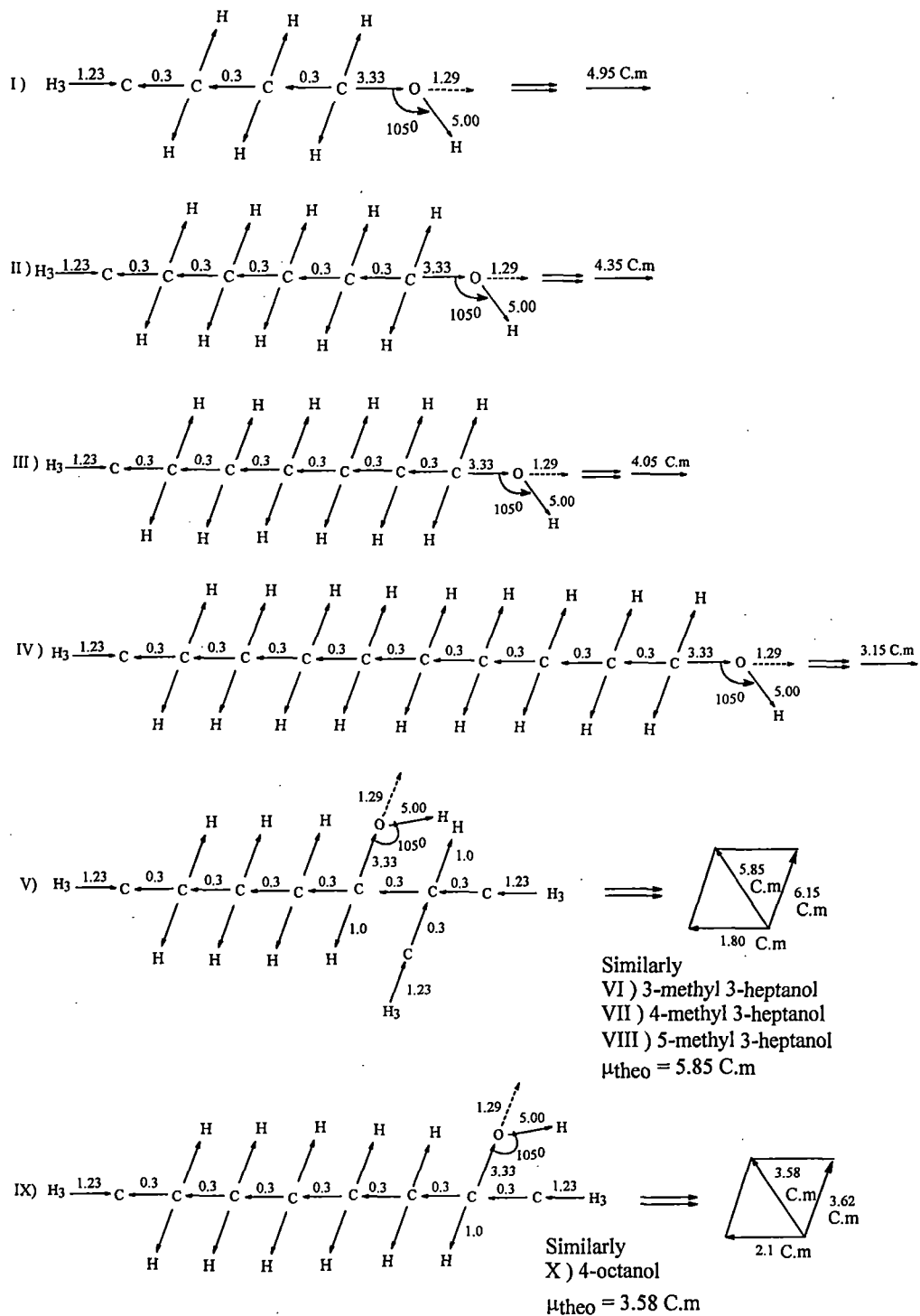


Figure 6.6: Conformational structures of polar molecules in terms of bond angles and bond moments ( $\times 10^{-30}$  Coulomb. metre) of the substituents groups: I.) 1-Butanol, II.) 1-Hexanol, III.) 1-Heptanol, IV.) 1-Decanol, V.) 2-methyl 3-heptanol and IX.) 2-octanol.

between estimated and reported  $\mu$ 's may be due to combined effect of frequency of the applied electric field as well as inductive, electromeric and mesomeric effects existing among polar groups of the molecules. The theoretical dipole moments  $\mu_{\text{theo}}$ 's of the polar alcohols are calculated from the available bond angles and bond moments [6.18] in order to display in Fig.6.6. They are placed in column 8 of Table 6.3. Alcohols are classified as monohydric, dihydric, trihydric and polyhydric compounds in which hydroxyl  $-\text{OH}$  group is attached to the parent molecules. The  $-\text{O}-\text{H}$  bond in them as sketched in Fig.6.6 is highly polar because the  $-\text{O}-$  is highly electronegative carrying a negative charge  $\delta^-$  while the H possesses highly positive charge  $\delta^+$ . The polarity of  $\text{O}-\text{H}$  bond exerts a strong attraction on the other H atoms of the molecules [6.19]. The hydrogen bonding, thus produced, gives rise to theoretical dipole moments  $\mu_{\text{theo}}$ 's for the alcohols under investigation in excellent agreement with  $\mu_1$  measured by graphical and single frequency measurement technique as shown in Table 6.3. This type of study ultimately indicates that  $\mu_1$  of a polar molecule under hf electric field is only due to rotation of the flexible parts attached to the parent ones.

#### 6.4. Conclusions :

The study of relaxation phenomena of a number of alcohols in n-heptane under 3.00, 9.25 and 24.33 GHz electric fields at 298 K is a straightforward, simpler and topical one to establish the material property of the relaxation times. The isomeric type with H-bonding long chained alcohols in n-heptane show  $\tau_2$  and  $\tau_1$  due to the rotations of the whole molecule and the flexible parts attached to the parent molecules. Unlike the other dielectric terminologies and parameters such as the permittivities, dielectric loss etc.  $\tau$ 's are the material property of the chemical system under identical environment.  $\tau$ 's are independent of the electric field frequencies in GHz range.

We are interested only with the susceptibilities  $\chi_{ij}$ 's concerned with the orientation polarisation. Nevertheless the susceptibility measurement is used instead of hf permittivity  $\epsilon_{ij}$  and hf conductivity  $\sigma_{ij}$ .  $\epsilon_{ij}$  includes all types of polarisations while  $\sigma_{ij}$  is concerned with the bound molecular charges of the molecule. A graphical method was, therefore, attempted for to include  $\chi_{ij}$ 's derived from the  $\epsilon_{ij}$ 's measurements of Crossley et al [68] and Glasser et

al [6.9] in order to establish the material property to study the relaxation mechanism of such polar liquids in nonpolar solvent under hf electric fields. Alcohols are supposed to be of polymeric type molecules having strong H-bonding. The variations of  $\chi_{ij}''/\chi_{ij}'$  with  $w_j$ 's in figures and tables showed that the intercepts of  $\chi_{ij}''/\chi_{ij}'$  against  $w_j$  at  $w_j \rightarrow 0$  increase with the applied electric field frequencies. The results of the fixed value of  $\ln\omega_k$  from the values of  $f(\omega_k)$  were larger with the increasing frequency and the potential well like  $f(\omega_k)-\ln\omega_k$  curves assume the highest, intermediate and lowest positions under 24.33, 9.25 and 3.00 GHz electric fields as displayed in Fig.6.2. A number of  $\ln\omega_2$  and  $\ln\omega_1$  values ( $\ln\omega_2 < \ln\omega_1$ ) were selected in Fig.6.2 for a fixed  $f(\omega_k)$  in order to draw  $\ln\omega_1$  vs  $\ln\omega_2$  curves at the three frequencies. All the curves are similar in nature. The  $\ln\omega_1$  decreases gradually with the increase of  $\ln\omega_2$  to cut a point for most of the alcohols while 1-butanol, 1-hexanol, 1-heptanol, 1-decanol and 2-methyl 3-heptanol cut at three points to yield significant values of  $\tau_2$  and  $\tau_1$  respectively. The experimental behaviour may be of the inaccuracies involved with the inapplicability of Fröhlich's model for of the liquid mixtures at different frequencies. The average of the three  $\tau$ 's along with single  $\tau_2$  and  $\tau_1$  for the rest five systems are placed in the respective table to compare with the average values of  $\tau_2$  and  $\tau_1$  from the single frequency technique.  $\tau$ 's are, however, obtained from the ratio of the individual slopes of the variations of  $\chi_{ij}''$  and  $\chi_{ij}'$  with  $w_j$  at  $w_j \rightarrow 0$  of Eq.(6.10) and from the direct slopes of  $\chi_{ij}''-\chi_{ij}'$  curves of Eq.(6.9). The larger values of  $\tau_2$ 's obtained from the method of single frequency measurement of Saha et al and Sit et al and smaller values of  $\tau_1$ 's can be compared with those of the present graphical method. The comparison thus reveals the applicability of both the methods. Moreover, the relaxation times of the graphical technique based on Debye-Fröhlich model may provide with the better understanding to reflect the material property.

The experimental dipole moments  $\mu_2$  and  $\mu_1$  of the whole and flexible parts of the alcohols in terms of  $\tau_2$  and  $\tau_1$  and slope  $\beta$  of  $\chi_{ij}'-w_j$  curves are computed at three different frequencies of GHz range. The identical behaviour of  $\chi_{ij}'-w_j$  curves of the solutions may be due to the almost same polarity of alcohols. The convex or concave nature of the curves reveals the solute-solute molecular associations in the higher concentration region for the formation of hydrogen bonding.  $\mu_2$  and  $\mu_1$  are compared with those by the single frequency

measurement and the  $\mu_{\text{theo}}$ 's from the available bond angles and bond moments. The slight disagreement among  $\mu$ 's may be due to steric hindrances and various effects present in the substituent polar groups attached to the parent ones.

#### References:

- [6.1] A K Jonscher, *Universal Relaxation Law*, Chelsea Dielectric Press, London (1996)
- [6.2] A K Sharma, D R Sharma and D S Gill, *J. Phys. D: Appl. Phys.* **18** 1199 (1985)
- [6.3] A Sharma and D R Sharma, *J. Phys. Soc. Japan* **61** 1049 (1992)
- [6.4] K Higasi, Y Koga and M Nakamura, *Bull. Chem. Soc. Japan* **44** 988 (1971)
- [6.5] S K Sit and S Acharyya, *Indian J. Phys.* **70B** 19 (1996)
- [6.6] M D Migahed, M T Ahmed and A E Kotp, *J. Phys. D: Appl. Phys.* **33** 2108 (2000)
- [6.7] A Bello, E Laredo, M Grimau, A Nogales and T A Ezquerro, *J. Chem. Phys.* **113** 863 (2000)
- [6.8] J Crossley, L Glasser and C P Smyth, *J. Chem. Phys.* **55** 2197 (1971)
- [6.9] L Glasser, J Crossley and C P Smyth, *J. Chem. Phys.* **57** 3977 (1972)
- [6.10] N Ghosh, A Karmakar, S K Sit and S Acharyya, *Indian J. Pure & Appl. Phys.* **38** 574 (2000)
- [6.11] A K Jonscher, Inst. Phys. Conf. (Canterbury) invited papers edited by CHL Goodman(1980)
- [6.12] K Dutta, S K Sit and S Acharyya, *Pramana: J. Phys.* **57** 775 (2001)
- [6.13] U Saha, S K Sit, R C Basak and S Acharyya, *J. Phys. D: Appl. Phys.* **27** 596 (1994)
- [6.14] S K Sit, R C Basak, U Saha and S Acharyya, *J. Phys. D: Appl. Phys.* **27** 2194 (1994)
- [6.15] K Higasi, K Bergmann and C P Smyth, *J. Phys. Chem.* **64** 880 (1960)
- [6.16] A Mansingh and P Kumar, *J. Phys. Chem.* **69** 4197 (1965)
- [6.17] K Dutta, A Karmakar, L Dutta, S K Sit and S Acharyya, *Indian J. Pure & Appl. Phys.* **40** 801 (2002)
- [6.18] *Hand book of Chemistry and Physics* – C.R.C Press 58th edition (1977-1978)
- [6.19] C G Akode, K S Kanse, M P Lokhande, A C Kumbharkhane and S C Mehrotra, *Pramana: J. Phys.* **62** 973 (2004)

*Chapter 7*

**RELAXATION PHENOMENA IN METHYL  
BENZENES AND KETONES FROM ULTRA HIGH  
FREQUENCY CONDUCTIVITY**

## 7.1. Introduction :

Relaxation processes in dielectric polar liquid or solid material (DRL or DRS) are very encouraging to study the molecular behaviours and structures through various experimental techniques [7.1-7.2]. The methods are involved with the high frequency conductivity [7.3] or susceptibility measurements [7.4], thermally stimulated depolarisation current [7.5] (TSDC) and time or frequency domain dielectric AC spectroscopy [7.6] etc. The latter two methods consist of a tedious computer simulated calculation in comparison to others, which are very simple and straightforward within the framework of Debye and Smyth model of dielectric liquid molecule.

Vaish and Mehrotra [7.7-7.8] measured real and imaginary parts  $\epsilon_{ij}'$  and  $\epsilon_{ij}''$  of complex dielectric relative permittivity  $\epsilon_{ij}^*$  of some methyl benzenes and ketones (j) in benzene (i) under 3.13 cm wavelength electric field at 25 °C. They attempted to correlate dielectric relaxation times with those of nuclear magnetic resonance spin lattice relaxation times by using the theory of Bloembergen et al [7.9] in terms of measured relaxation parameters. The relaxation times  $\tau$  of the molecules were calculated on the assumption that dipole-dipole (dimer) interaction occurs between the nuclear spins. The spin lattice relaxation times were obtained to compare with the Gopalakrishna, Debye and other methods. The experimental value differs significantly from those of theoretical one. This study reveals that  $\tau$  plays the main role in inter and intra molecular motions and nuclear magnetic resonance (NMR) spin lattice relaxation etc.

The values of  $\tau$  and dipole moment  $\mu$  of these polar molecules by the conductivity technique have been calculated in the present paper. The procedures employed to get  $\tau$  are those of Murthy et al [7.10] from the direct slope of the linear equation of imaginary  $\sigma_{ij}'' (= \omega \epsilon_0 \epsilon_{ij}'')$  in  $\Omega^{-1} \text{ m}^{-1}$  and real  $\sigma_{ij}' (= \omega \epsilon_0 \epsilon_{ij}')$  in  $\Omega^{-1} \text{ m}^{-1}$  parts of the hf complex conductivity  $\sigma_{ij}^*$  (Fig.7.1) and the ratio of the individual slopes of  $\sigma_{ij}'' - w_j$  and  $\sigma_{ij}' - w_j$  curves [7.11] (Figs.5.2 & 5.3) at  $w_j \rightarrow 0$  respectively. The use of the ratio of individual slopes to estimate  $\tau$  seems to be better as it eliminates the polar-polar interaction almost completely. Hence the purpose of the present paper is to study the success or otherwise of the proposed theory with the existing ones to infer molecular structures and associations. The graphs of  $\sigma_{ij}''$  and  $\sigma_{ij}'$  with  $w_j$ 's in Figs.7.2 & 7.3 are found to be nonlinear to indicate the presence of solute-

Table 7.1 : Slope and intercepts of Eq.(7.2), correlation coefficient  $r$ , ratio of the individual slopes of  $\sigma_{ij}''-w_j$  and  $\sigma_{ij}'-w_j$  curves at  $w_j \rightarrow 0$ , relaxation time  $\tau_j$  from Eqs (7.3) and (7.4) and from Gopalakrishna's method of some methyl benzenes and ketones in benzene at 25°C under 9.585 GHz electric field.

System with sl.no.	Slope and intercepts of Eq.(7.3)		Corrl. coeff. $r$	Ratio of individual slopes of $\sigma_{ij}''-w_j$ and $\sigma_{ij}'-w_j$ at $w_j \rightarrow 0$	Relaxation times $\tau_j$ ( $\times 10^{12}$ ) in sec.		
					$\tau_j^a$	$\tau_j^b$	$\tau_j^c$
(I) toluene	1.8468	1.1385	0.9527	4.3891	8.99	3.78	8.24
(II) 1,3,5 tri methylbenzene	0.7897	1.1844	0.9755	2.8782	21.03	5.77	19.93
(III) 1,2,3,4 tetra methyl benzene	8.3666	1.1992	0.9678	6.5797	1.98	2.52	1.94
(IV) 1,2,4,5 tetra methyl benzene	1.9531	1.1854	0.9890	1.6133	8.50	10.29	8.06
(V) penta methyl benzene	1.3836	1.1770	0.9948	3.8814	12.00	4.28	11.02
(VI) <i>p</i> -fluorotoluene	4.8910	1.2071	0.9941	8.2548	3.39	2.01	3.12
(VII) butyl ethyl ketone	1.0070	1.1878	0.9481	40.3859	16.48	0.41	15.84
(VIII) methyl hexyl ketone	0.8452	1.1737	0.9993	0.6003	19.65	27.66	18.13
(IX) ethyl pentyl ketone	0.8640	1.1713	0.9686	0.6928	19.22	23.97	18.40
(X) heptyl methyl ketone	0.8203	1.1838	0.9859	1.8590	20.24	8.93	19.01

$\tau_j^a$  = Relaxation time from Eq. (7.3)

$\tau_j^b$  = Relaxation time from Eq. (7.4)

$\tau_j^c$  = Relaxation time from Gopalakrishna's method of Eq. (7.9)

solute associations in the mixture.  $\tau$ 's from linear slope are found to agree with the reported  $\tau$ 's from Gopalakrishna's fixed frequency method of Fig.7.4 and are presented in Table 7.1 together with all the measured  $\tau$ 's by different procedures. Further, the polar molecules under investigation are methyl substituted aromatic and ketone substituted aliphatic compounds of highly nonspherical nature. Methyl substituted benzenes and ketones have almost similar characteristics. Some of the methyl benzenes are supposed to have apparently zero dipole moment from bond moment calculation. Moreover, these molecules are supposed to absorb electric energy much more strongly in the effective dispersive region of nearly 10 GHz at which peak of the absorption curve occurs. The ketones, on the other hand, are pleasant smelling liquids and widely used in petroleum industry. These liquids are

used, as good solvents of synthetic rubber, wax etc. The study of the variation of  $\tau$  with respect to various substituted polar groups attached to different positions of the parent molecules may throw much light on the structural conformations of the methyl benzene and ketone molecules. We had already made a detailed investigation on some polysubstituted benzenes [7.12] at various temperatures to get molecular structures by conductivity technique. Dielectric parameters are very much temperature dependent. Calculations at some other temperature may reveal a better picture. Nevertheless, from these studies it may be clear as to what theory is valid for such highly nonspherical aliphatic and aromatic compounds. A systematic comparison of  $\tau$  and  $\mu$  can thus be made from the measured data at 25°C.

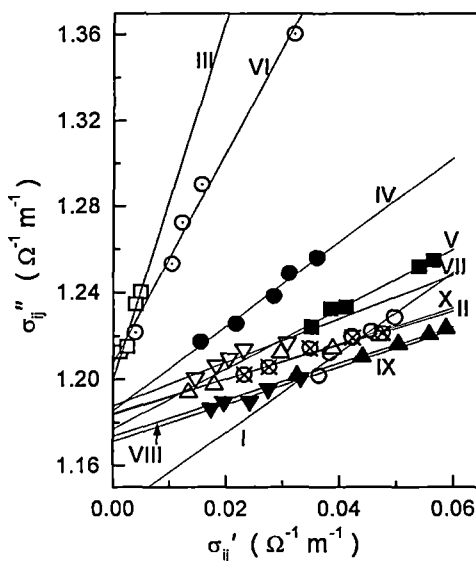


Figure.7.1 : The linear variation of imaginary part  $\sigma_{ij}''$  against real part  $\sigma_{ij}'$  of complex  $hf$  conductivity  $\sigma_{ij}$  at 25°C under 9.585 GHz electric field :

- (I) Toluene (-O-) (II) 1,3,5 tri methyl benzene (-Δ-) (III) 1,2,3,4 tetra methyl benzene (-□-) (IV) 1,2,4,5 tetra methyl benzene (-●-) (V) penta methyl benzene (-■-) (VI) *p*-fluoro toluene (-⊙-) (VII) Butyl ethyl ketone (-▽-) (VIII) Methyl hexyl ketone (-▲-) (IX) Ethyl pentyl ketone (-▼-) (X) heptyl methyl ketone (-⊗-)

The corresponding dipole moments  $\mu_j$ 's of these liquids are obtained from the linear coefficient  $\beta$  of uhf conductivity  $\sigma_{ij}$  curves against  $w_j$ 's of Fig.7.5. All the  $\beta$ 's and  $\mu$ 's are tabulated in Table 7.2 with those from Gopalakrishna and theoretical conformational

calculation of Fig.7.6. The inductive, mesomeric and electromeric effects under 3 cm wavelength electric field play the vital role in determining the theoretical  $\mu_{\text{theo}}$ 's of the molecules of Fig.7.6 in agreement with estimated  $\mu_j$ 's.

## 7.2. High Frequency Conductivity Technique to Estimate $\tau$ and $\mu$ :

The ultra high frequency (uhf) complex conductivity [7.13]  $\sigma_{ij}^*$  is :

$$\sigma_{ij}^* = \sigma'_{ij} + j\sigma''_{ij} \quad \dots (7.1)$$

where  $\sigma'_{ij} = \omega \epsilon_0 \epsilon_{ij}''$  and  $\sigma''_{ij} = \omega \epsilon_0 \epsilon_{ij}'$  are the real and imaginary parts of  $\sigma_{ij}^*$ ,  $\epsilon_0 =$  absolute permittivity of free space  $= 8.854 \times 10^{-12} \text{ F.m}^{-1}$  and  $\omega (= 2\pi f)$  is the angular frequency of the applied electric field of frequency,  $f = 9.585 \times 10^9 \text{ Hz}$ .

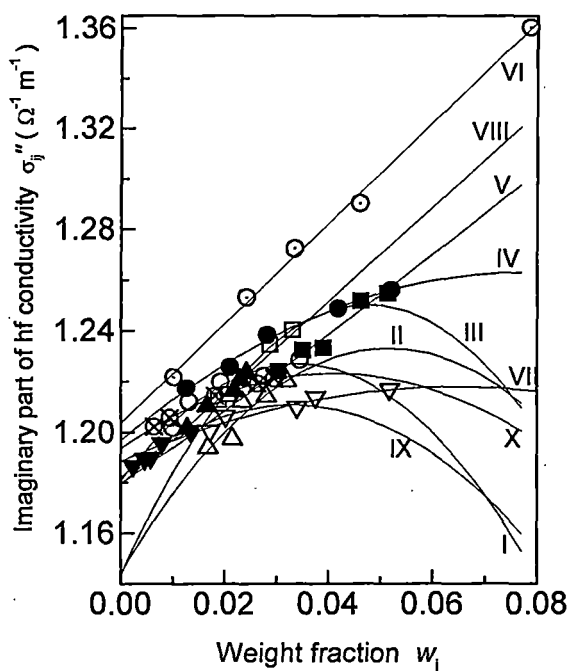


Figure.7.2: Variation of imaginary part of conductivity  $\sigma_{ij}''$  against  $w_1$  at  $25^\circ\text{C}$  under 9.585 GHz electric field :

- (I) Toluene (-O-), (II) 1,3,5 tri methyl benzene (-Δ-), (III) 1,2,3,4 tetra methyl benzene (-□-), (IV) 1,2,4,5 tetra methyl benzene (-●-), (V) penta methyl benzene (-■-), (VI) p-fluoro toluene (-⊙-), (VII) Butyl ethyl ketone (-∇-), (VIII) Methyl hexyl ketone (-▲-), (IX) Ethyl pentyl ketone (-▼-), (X) heptyl methyl ketone (-⊗-)

Table 7.2 : Coefficients of  $\sigma_{ij}-w_j$  curves, dimensionless parameter  $b [=1/(1+\omega^2\tau^2)]$ , dipole moment  $\mu_j$  in Coulomb.metre from  $\tau$ 's of Eq.(7.3), (7.4) and Gopalakrishna's method and the theoretical dipole moment  $\mu_{theo}$  from the available bond angles and bond moments of some methyl benzenes and ketones in benzene at 25°C under 9.585 GHz electric field.

System with sl.no.and mol.wt.	Coefficients of $\sigma_{ij} = \alpha + \beta w_j + \xi w_j^2$			Values of b by using $\tau$ of		Dipole moment ( $\times 10^{-30}$ ) C.m			
	$\alpha$	$\beta$	$\xi$	Eq.(7.3)	Eq.(7.4)	$\mu_j^a$	$\mu_j^b$	$\mu_j^g$	$\mu_{theo}$
(I) toluene $M_j=0.092$ Kg	1.1811	2.7545	-40.2180	0.7733	0.9507	7.93	7.15	7.80	1.23
(II) 1,3,5 tri methylbenzene $M_j= 0.120$ Kg	1.1446	3.4010	-31.2102	0.3840	0.8923	14.27	9.36	13.94	0.00
(III) 1,2,3,4 tetra methyl benzene $M_j=0.134$ Kg	1.1436	4.4952	-47.2133	0.9860	0.9775	10.82	10.87	10.82	0.00
(IV) 1,2,4,5 tetra methyl benzene $M_j=0.134$ Kg	1.1969	1.7313	-11.2125	0.7924	0.7225	7.49	7.84	7.39	0.00
(V) penta methyl benzene $M_j=0.148$ Kg	1.1798	1.4009	2.2168	0.6569	0.9377	7.78	6.51	7.63	1.23
(VI) p- fluoro toluene $M_j=0.110$ Kg	1.2039	1.9329	0.7021	0.9600	0.9856	6.52	6.43	6.53	6.23
(VII) butyl ethyl ketone $M_j=0.114$ Kg	1.1885	0.9115	-6.8748	0.5038	0.9994	6.29	4.46	6.19	8.09
(VIII) methyl hexyl ketone $M_j=0.128$ Kg	1.1790	1.8073	2.1902	0.4166	0.2649	10.32	12.94	10.05	8.14
(IX) ethyl pentyl ketone $M_j=0.128$ Kg	1.1820	1.7921	-27.0543	0.4274	0.3243	10.14	11.64	10.01	8.14
(X) heptyl methyl ketone $M_j=0.142$ Kg	1.1939	1.4569	-17.0797	0.4023	0.7757	9.93	7.15	9.60	8.20

$\mu_j^a$  = Dipole moment from Eq.(7.7) by using  $\tau_j$  of Eq. (7.3)

$\mu_j^b$  = Dipole moment from Eq. (7.7) by using  $\tau_j$  of Eq. (7.4)

$\mu_j^g$  = Dipole moment by Gopalakrishna's method of Eq. (7.10)

$\mu_{theo}$  = Theoretical dipole moment from the available bond angles and bond moments.

Debye equation [7.14] in the GHz region yields:

$$\sigma_{ij}'' = \sigma_{\infty ij} + \frac{1}{\omega\tau} \sigma_{ij}' \quad \dots (7.2)$$

$$\left( \frac{d\sigma_{ij}''}{d\sigma_{ij}'} \right) = \frac{1}{\omega\tau} \quad \dots (7.3)$$

Both  $\sigma_{ij}''$  and  $\sigma_{ij}'$  are functions of  $w_j$ . Their variations are nonlinear in the higher concentration region as seen in Figs.7.2 and 7.3. In this case one can write Eq.(7.2) as:

$$\left( \frac{d\sigma_{ij}''}{dw_j} \right)_{w_j \rightarrow 0} = \frac{1}{\omega\tau} \left( \frac{d\sigma_{ij}'}{dw_j} \right)_{w_j \rightarrow 0} \quad \dots (7.4)$$

$\tau$ 's from both the Eqs.(7.3) and (7.4) were computed and are listed in Table 7.1 for comparison with the reported  $\tau$  recalculated from Gopalakrishna's method.

Since  $\epsilon_{ij}' > \epsilon_{ij}''$ , but in hf region of GHz range  $\epsilon_{ij}' \cong \epsilon_{ij}''$  where  $\epsilon_{ij}''$  offers resistance to polarisation and uhf conductivity  $\sigma_{ij}$  is  $\sigma_{ij} = \omega\epsilon_o (\epsilon_{ij}'^2 + \epsilon_{ij}''^2)^{1/2}$ . We can thus write Eq.(7.2) in the following form:

$$\sigma_{ij} = \sigma_{\infty ij} + \frac{1}{\omega\tau} \sigma_{ij}'$$

$$\left( \frac{d\sigma_{ij}'}{dw_j} \right)_{w_j \rightarrow 0} = \omega\tau\beta \quad \dots (7.5)$$

$\beta$  is the slope of  $\sigma_{ij}$ - $w_j$  curve in the limit  $w_j = 0$  as observed in Fig.7.5 and listed in Table 7.2.

The real part  $\sigma_{ij}'$  of hf complex conductivity  $\sigma_{ij}^*$  is given by [7.12]

$$\sigma_{ij}' = \frac{N\mu_j^2 \rho_{ij}}{27M_j k_B T} \left( \frac{\omega^2 \tau}{1 + \omega^2 \tau^2} \right) (\epsilon_{ij} + 2)^2 w_j$$

$$\left( \frac{d\sigma'_{ij}}{dw_j} \right)_{w_j \rightarrow 0} = \frac{N\mu_j^2 \rho_i}{27M_j k_B T} \left( \frac{\omega^2 \tau}{1 + \omega^2 \tau^2} \right) (\epsilon_i + 2)^2 \quad \dots (7.6)$$

where density  $\rho_{ij}$  and local field  $F_{ij}$  of the solution become  $\rho_i$  and  $F_i = (\epsilon_i + 2)^2 / 9$  of the solvent in the limit  $w_j = 0$ .

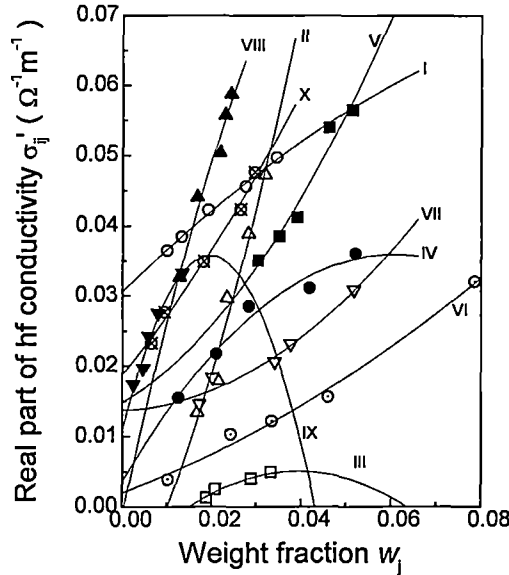


Figure 7.3 : Variation of real part of conductivity  $\sigma'_{ij}$  against  $w_j$  at  $25^\circ\text{C}$  under 9.585 GHz electric field :

(I) Toluene (-○-) (II) 1,3,5 tri methyl benzene (-△-) (III) 1,2,3,4 tetra methyl benzene (-□-) (IV) 1,2,4,5 tetra methyl benzene (-●-) (V) penta methyl benzene (-■-) (VI) p-fluoro toluene (-⊙-) (VII) Butyl ethyl ketone (-▽-) (VIII) Methyl hexyl ketone (-▲-) (IX) Ethyl pentyl ketone (-▼-) (X) heptyl methyl ketone (-⊗-)

From Eqs.(7.5) and (7.6) one gets hf dipole moment  $\mu_j$  as:

$$\mu_j = \left( \frac{27M_j k_B T \beta}{N \rho_i (\epsilon_i + 2)^2 \omega b} \right)^{\frac{1}{2}} \quad \dots (7.7)$$

where,

$N$  = Avogadro's number =  $6.023 \times 10^{23}$

$\rho_i$  = density of solvent benzene at  $25^\circ\text{C}$  =  $874.3 \text{ Kg.m}^{-3}$

$\epsilon_i$  = relative permittivity of solvent benzene at 25°C = 2.274

$M_j$  = molecular weight of solute in Kg.

$k_B$  = Boltzmann constant =  $1.38 \times 10^{-23}$  J.mole<sup>-1</sup>.K<sup>-1</sup> and

$b$  is the dimensionless parameter involved with measured  $\tau$  where  $b=1/(1+\omega^2\tau^2)$

Both the dipole moments  $\mu_j$ 's and dimensionless parameters  $b$ 's are presented in Table 7.2.

### 7.3. Results and Discussion :

The imaginary  $\sigma_{ij}'' (= \omega \epsilon_0 \epsilon_{ij}') \Omega^{-1} \text{ m}^{-1}$  are plotted against real  $\sigma_{ij}' (= \omega \epsilon_0 \epsilon_{ij}'') \Omega^{-1} \text{ m}^{-1}$  parts of hf complex conductivity  $\sigma_{ij}^*$  for different weight fractions  $w_j$ 's of solute according to Eq.(7.2) to get  $\tau$  of polar liquid molecules as shown in Fig.7.1. The variables are found to be almost linearly correlated as evident from the correlation coefficient 'r' of the straight line of Eq.(7.3). It appears from Fig.5.1 that the systems like (I), (II), (III) and (VII) show low values of r (Table 7.1) indicating their departure from perfect linearity of the variables. Perfect linearity is said to be achieved for  $-1 \leq r \leq 1$ . In such cases, the proposed method to determine  $\tau$  from the ratio of the individual slopes of  $\sigma_{ij}''$  and  $\sigma_{ij}'$  against  $w_j$  according to Eq.(7.4) seems to be a better choice and is claimed to be the best improvement over the other two because polar-polar interaction is avoided almost completely in the limit  $w_j = 0$ . The estimated  $\tau$ 's for systems (III), (IV), (VI) and (IX) from Eq.(7.4) are in agreement with those of Murthy et al [7.10] and reported  $\tau$ . For the rest of the systems,  $\tau$ 's are lower from the ratio of individual slopes except methyl hexyl ketone. All the plots of  $\sigma_{ij}''$  and  $\sigma_{ij}'$  against  $w_j$ 's as sketched in Figs.7.2 and 7.3 are parabolic in nature indicating the occurrence of associational aspect of polar liquid molecules in a non-polar solvent. The systems I(-○-), II(-△-), III(-□-), IV(-●-), VII(-▽-), IX(-▼-) and X(-⊗-) exhibit monotonic increase of  $\sigma_{ij}''$  with  $w_j$  like  $\sigma_{ij}-w_j$  curves of Fig.7.5 in order to attain maximum value at a certain concentration ( $w_j$ ) to show the convex nature. This is perhaps due to phase transition occurring in the polar-nonpolar liquid mixture as observed elsewhere [7.12]. Similar variation  $\sigma_{ij}''$  and  $\sigma_{ij}$  in  $\Omega^{-1} \text{ m}^{-1}$  with  $w_j$  as displayed graphically in Figs.7.2 and 7.5 indicates the validity of the approximation of  $\sigma_{ij}'' \cong \sigma_{ij}$  of Eq.(7.5). All the curves of Figs.7.2 and 7.5 have a tendency to cut a point on the  $\sigma_{ij}$ -axis in the limit  $w_j=0$  except systems (II) and (III) probably due to solvation effect [7.15] of the polar-nonpolar liquid mixture. The plots of  $\sigma_{ij}'-w_j$  curves of Fig.7.3 are also parabolic in nature. The variation of  $\sigma_{ij}'$  against  $w_j$ 's for the

III(-□-), IV(-●-) and IX(-▼-) systems show convex shape indicating the maximum absorption of hf electric energy at  $w_j=0.04$ , 0.06 and 0.02 respectively. The rest systems, display gradual increase of  $\sigma_{ij}'$  with  $w_j$  probably due to the fact that absorption of electric energy increases at the higher concentration. This is authenticated by the positive coefficient of the quadratic term in the fitted equations of  $\sigma_{ij}'-w_j$  curves of Fig.7.3. All the  $\tau$ 's of the polar liquid molecules of Table 7.1 agree well with those of Murthy et al [7.10] from Eq.(7.3) and reported value. The reported  $\tau$ 's based on the standard method of Gopalakrishna were found to be much higher [7.7-7.8] which prompted us to recalculate  $\tau$ 's from the following expression [7.16]:

$$x = \frac{\epsilon_{ij}'^2 + \epsilon_{ij}' + \epsilon_{ij}''^2 - 2}{(\epsilon_{ij}' + 2)^2 + \epsilon_{ij}''^2}; y = \frac{3\epsilon_{ij}''}{(\epsilon_{ij}' + 2)^2 + \epsilon_{ij}''^2} \quad \dots (7.8)$$

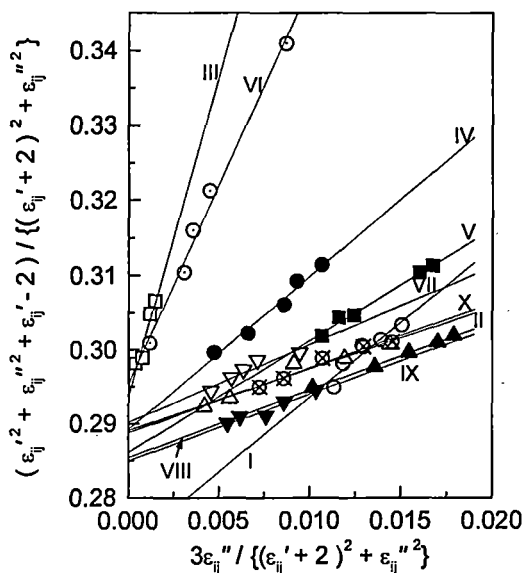


Figure 7.4: Linear plots of x against y for some methyl benzenes and ketones at 25°C under 9.585 GHz electric field:

- (I) Toluene (-○-), (II) 1,3,5 tri methyl benzene (-△-), (III) 1,2,3,4 tetra methyl benzene (-□-), (IV) 1,2,4,5 tetra methyl benzene (-●-), (V) penta methyl benzene (-■-), (VI) p-fluoro toluene (-⊙-), (VII) Butyl ethyl ketone (-▽-), (VIII) Methyl hexyl ketone (-▲-), (IX) Ethyl pentyl ketone (-▼-), (X) heptyl methyl ketone (-⊗-)

The variation of x against y of Eq.(7.8) are linear as seen in Fig.7.4. One can obtain  $\tau$  from:

$$\tau = \frac{1}{\omega(dx/dy)} \quad \dots (7.9)$$

$\mu_j$ 's are recalculated by using Gopalakrishna's equation [7.16] as:

$$\mu = \left[ \frac{9k_B T M_j}{4\pi N \rho_i} \left\{ 1 + \left( \frac{dy}{dx} \right)^2 \right\} \left( \frac{dx}{dw_j} \right)_{w_j \rightarrow 0} \right]^{\frac{1}{2}} \quad \dots (7.10)$$

$\tau$ 's from the ratio of the individual slopes of Eq.(7.4), on the other hand, are found to be in better agreement for the systems: 1,2,3,4 tetramethyl benzene (III); 1,2,4,5 tetramethyl benzene (IV); p-fluoro toluene (VI) and ethyl pentyl ketone (IX) respectively. The other systems exhibit low values of  $\tau$  from the ratio of individual slopes of  $\sigma_{ij}''$  and  $\sigma_{ij}'$  against  $w_j$ 's except methyl hexyl ketone (VIII). This behaviour can be explained on the basis of the fact that the methods of Murthy et al [7.10] and Gopalakrishna yield  $\tau$ 's of either a quasi isolated polar or a dimer (solute-solute association) molecule. The ratio of the individual slopes, on the other hand, takes into account both the processes in addition to  $\tau$  of a dimer molecule. The smaller value of  $\tau$  may be due to formation of monomer supported by low values of r of the systems under investigation.

Dipole moments  $\mu_j$ 's are computed from the slope  $\beta$  of uhf conductivity  $\sigma_{ij}$  against  $w_j$  curves of Fig.7.5 and dimensionless parameters b's of Eq.(7.7) to compare with the results of Eq.(7.10) of Gopalakrishna [7.16]. The  $\mu$ 's are now found to agree well as seen in Table 7.2 with Murthy et al [7.10] and recalculated values of Gopalakrishna for all the systems like  $\tau$ 's indicating the applicability of the methods for such systems under investigation.  $\sigma_{ij}$ 's of polar-nonpolar liquid mixtures are, however, concerned with the bound molecular charges which may be counted by  $\beta$  ( Table 7.2) of  $\sigma_{ij}-w_j$  curves of Fig.7.5. The agreement is better from Eqs.(7.4) and (7.7) with the use of the ratio of individual slopes for systems (I), (III), (IV), (VI) and (IX) respectively unlike other polar liquids where  $\mu$ 's are slightly lower except for methyl hexyl ketone. Low values of  $\mu$ 's may

be due to formation of monomer while high values are responsible for dimer formations. The slight difference between reported and estimated  $\mu$ 's may occur due to existence of steric hindrances among the substituted polar groups.

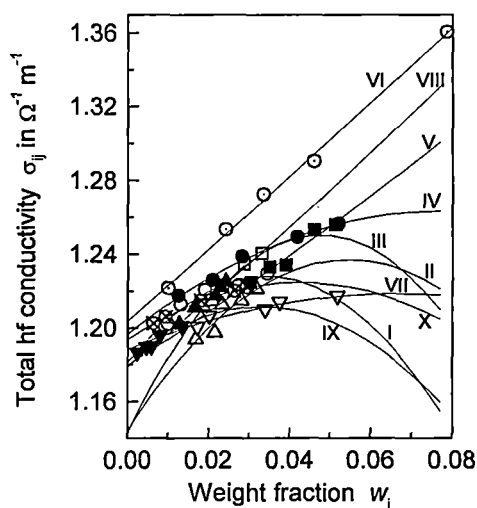


Figure 7.5 : The plot of uhf conductivity  $\sigma_{ij}$  against  $w_j$  :

(I) Toluene (-O-), (II) 1,3,5 tri methyl benzene (- $\Delta$ -), (III) 1,2,3,4 tetra methyl benzene (- $\square$ -), (IV) 1,2,4,5 tetra methyl benzene (- $\bullet$ -), (V) penta methyl benzene (- $\blacksquare$ -), (VI) p-fluoro toluene (- $\odot$ -), (VII) Butyl ethyl ketone (- $\nabla$ -), (VIII) Methyl hexyl ketone (- $\blacktriangle$ -), (IX) Ethyl pentyl ketone (- $\blacktriangledown$ -), (X) heptyl methyl ketone (- $\ominus$ -)

The theoretical dipole moments  $\mu_{\text{theo}}$ 's are calculated on the basis of planar structures for the molecules from the available bond moments of  $\text{CH}_3 \rightarrow \text{C}$ ,  $\text{C} \leftarrow \text{O}$ ,  $\text{C} \leftarrow \text{C}$ ,  $\text{C} \rightarrow \text{F}$  and  $\text{C} \rightarrow \text{H}$  of  $1.23 \times 10^{-30}$ ,  $8 \times 10^{-30}$ ,  $0.3 \times 10^{-30}$ ,  $5.23 \times 10^{-30}$  and  $1 \times 10^{-30}$  in Coulomb-metre (C.m) respectively.  $\text{CH}_3 \rightarrow \text{C}$  makes an angle  $180^\circ$  with the bond axis. The direction of  $\text{C} \leftarrow \text{C}$  bond moment is taken in the reverse direction of bond axis [7.17]. All the substituted polar groups have the usual nature of either pushing or pulling electrons from the adjacent atoms of the parent molecules. Thus there exists a difference in electron affinity within each atom of the substituted polar groups causing inductive, mesomeric and electromeric effects in them, which play a role in the structure of the polar molecules of Fig.7.6. The solvent  $\text{C}_6\text{H}_6$  due to its aromaticity is a cyclic planar compound having three alternate single and double bonds

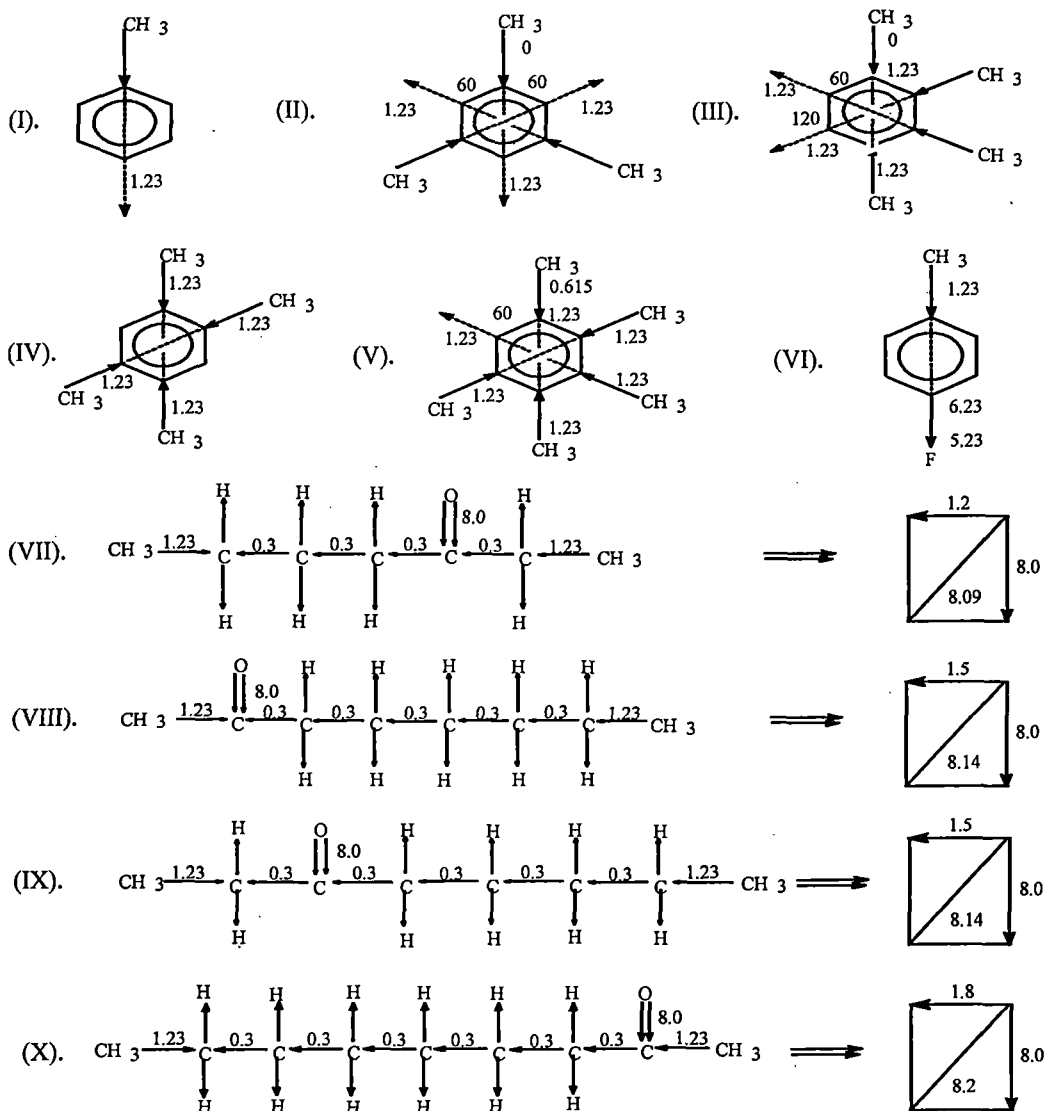


Figure 7.6: Conformational structures of polar molecules in terms of bond angles and bond moments ( $\times 10^{-30}$  Coulomb. metre) of the substituent groups.

(I) Toluene, (II) 1,3,5 tri methyl benzene, (III) 1,2,3,4 tetra methyl benzene (IV), 1,2,4,5 tetra methyl benzene, (V) penta methyl benzene, (VI) p-fluoro toluene, (VII) Butyl ethyl ketone, (VIII) Methyl hexyl ketone, (IX) Ethyl pentyl ketone, (X) heptyl methyl ketone.

and six p-electrons on six C-atoms. The  $sp^2$  hybridised electrons provide delocalised  $\pi$ -electrons to each atom of the substituted polar groups of the molecules.  $CH_3^{\delta+} \rightarrow C^{\delta-}$  is a strong electron pushing (+I effect) while  $>C^{\delta+} \leftarrow O^{\delta-}$  is responsible for both the mesomeric ( $-M$  effect) and electromeric effect. Thus all the substituted polar groups may be

responsible to form either solute-solvent (monomer) or solute-solute (dimer) association to yield lower and higher  $\mu_j$ 's respectively depending upon the solvent used. The difference  $\Delta\mu$  between  $\mu_j$ 's and  $\mu_{\text{theo}}$ 's of Fig.7.6 for the methyl substituted benzenes are 5.92, 9.36, 8.74, 7.84, 5.28 and 0.2 which are multiplied by  $10^{-30}$  C.m for the six systems while the rest of the four ketones have -3.63, 4.8, 3.5 and -1.05 which are multiplied by  $10^{-30}$  C.m respectively. This indicates the mesomeric and electromeric effects which are maximum for 1,3,5 trimethyl benzene and methyl hexyl ketone probably due to presence of strong electron repelling character of  $\text{CH}_3 \rightarrow \text{C}$  group. The  $\mu_{\text{theo}}$  of 1,3,5 tri methyl benzene, 1,2,3,4 tetra methyl benzene and 1,2,4,5 tetra methyl benzene are found to be of zero. The bond moment of  $\text{CH}_3 \rightarrow \text{C}$  group acts in opposite direction in a plane to yield zero value. The molecules may have considerable  $\mu_{\text{theo}}$  values if they are three dimensional structure. All these effects may be taken into account to get exact  $\mu_j$ 's of Table 7.2 from  $\mu_{\text{theo}}$  by the factor  $\mu_{\text{expt}}/\mu_{\text{theo}}$  (5.81, 5.29, 1.03, 0.55, 1.59, 1.43, 0.87 ) except for three molecules.

#### 7.4. Conclusions :

The structural information of some aromatic methyl benzenes and aliphatic ketones are obtained from the conductivity measurement at  $25^\circ\text{C}$  under the most effective dispersive region of 9.585 GHz electric field. Modern internationally accepted symbols of dielectric relaxation terminologies and parameters in SI units seem to be more topical, significant and useful contribution to obtain  $\tau$  and  $\mu$  of a dipolar liquid dissolved in nonpolar solvent.  $\tau_j$ 's measured from the slope of the linear  $\sigma_{ij}'' - \sigma_{ij}'$  curves are not in agreement for all cases with those from the ratio of the individual slopes of  $\sigma_{ij}'' - w_j$  and  $\sigma_{ij}' - w_j$  in the limit  $w_j = 0$  for all cases. The latter method is more significant because in this case one polar molecule is surrounded by a large number of non-polar molecules and thus polar-polar interactions are supposed to be completely eliminated. This method is thus supposed to yield monomeric or often dimeric structure of polar molecules.  $\mu_j$ 's are measured from the linear coefficient  $\beta$  of  $\sigma_{ij} - w_j$  curve at  $w_j \rightarrow 0$ .  $\sigma_{ij}$  or  $\sigma_{ij}''$  in  $\Omega^{-1} \text{ m}^{-1}$  for some systems increase gradually in order to attain the maximum value for a certain concentration of solute and then decrease. This indicates the change of phase of the systems under investigation. Similar nature of variation of  $\sigma_{ij}''$  with  $w_j$  indicates maximum absorption of hf electric energy for some systems.  $\tau_j$ 's and  $\mu_j$ 's claimed to be accurate within 10% and 5% are also compared with those from Gopalakrishna's fixed frequency method. The slight disagreement between experimental  $\mu_j$

with the theoretical dipole moment  $\mu_{\text{theo}}$  for some molecules reveals different associational aspects of dipolar liquid molecules in a non-polar solvent from the frequency dependence of relaxation parameters. This study also exhibits the presence of mesomeric, inductive and electromeric effects of the substituent polar groups of the molecules. The theoretical  $\mu_{\text{theo}}$  for systems II, III and IV are zero although they possess a considerable  $\mu_j$ . This invariably rules out the planar structure of the molecules and establish a three dimensional formation.

#### References :

- [7.1] N Paul, K P Sharma and S Chattopadhyay, *Indian J. Phys.*, **71B** 71 (1997)
- [7.2] S N Sen and R Ghosh, *J. Phys. Soc. (Japan)*, **33** 838 (1972)
- [7.3] K Dutta, R C Basak, S K Sit and S Acharyya, *J. Molecular Liquids*, **88** 229 (2000)
- [7.4] N Ghosh, S K Sit, A K Bothra and S Acharyya, *J. Phys. D: Appl. Phys.*, **34** 379 (2001)
- [7.5] M D Migahed, M T Ahmed and A E Kotp, *J. Phys. D: Appl. Phys.*, **33** 2108 (2000)
- [7.6] A Bello, E Laredo, M Grimau, A Nogales and T A Ezquerria, *J. Chem. Phys.*, **113** 863 (2000)
- [7.7] S K Vaish and N K Mehrotra, *Indian J. Pure. & Appl. Phys.*, **37** 881 (1999)
- [7.8] S K Vaish and N K Mehrotra, *Indian J. Pure. & Appl. Phys.*, **37** 778 (1999)
- [7.9] N Bloembergen, E M Purcel and R V Pound, *Physical Review*, **73** 673 (1948)
- [7.10] M B R Murthy, R L Patil and D K Deshpande, *Indian J. Phys.*, **63B** 491 (1989)
- [7.11] R C Basak, S K Sit, N Nandi and S Acharyya, *Indian J. Phys.*, **70B** 37 (1996)
- [7.12] K Dutta, S K Sit and S Acharyya, *J. Molecular Liquid*, **92** 263 (2001)
- [7.13] F J Murphy and S O Morgan, *Bell. Syst. Tech. J.*, **18** 502 (1939)
- [7.14] N E Hill, W E Vaughan, A H Price and M Davies, *Dielectric Properties and Molecular Behaviour* (Van Nostrand Reinhold Company, London) 1969
- [7.15] S K Sit, R C Basak, U Saha and S Acharyya, *J. Phys. D : Appl. Phys.*, **27** 2194 (1994)
- [7.16] K V Gopalakrishna, *Trans. Faraday. Soc.*, **53** 767 (1957)
- [7.17] S K Sit and S Acharyya, *Indian J. Phys.*, **70B** 19 (1996)

*Chapter 8*

**HIGH FREQUENCY AND STATIC RELAXATION  
PARAMETERS OF SOME POLAR MONO-  
SUBSTITUTED ANILINES IN BENZENE**

## 8.1. Introduction :

The dielectric relaxation behaviour of disubstituted benzenes and anilines in a nonpolar solvent is very interesting, because they usually show the double relaxation phenomena under high frequency (hf) electric fields [8.1]. Monosubstituted anilines, on the other hand, possess either single or double relaxation times ( $\tau_j$ 's) at three different hf electric fields of Giga hertz (GHz) range [8.2]. But they always showed double relaxation times at 9.945 GHz electric field, which seems to be the most effective dispersive region for such polar molecules [8.3]. They were also found to obey the symmetric relaxation behaviour under such electric field [8.3].

An attempt is, therefore, made to get the dimensionless dielectric relaxation parameters like real  $k_{ij}'$ , imaginary  $k_{ij}''$  parts of complex dielectric constant  $k_{ij}^*$  as well as static and infinite frequency-dielectric constants  $k_{0ij}$  and  $k_{\infty ij}$  of solution (ij) as shown in Table 8.1, from the measured [8.3] permittivities of  $\epsilon_{ij}'$ ,  $\epsilon_{ij}''$ ,  $\epsilon_{0ij}$  and  $\epsilon_{\infty ij}$  respectively, of three isomers of anisidines and toluidines at 35 °C under 9.945 GHz electric field at different weight fractions  $w_j$ 's of solute (j). The purpose of such consideration is to get static dipole moment  $\mu_s$  at any stage of dilution as well as the relaxation times ( $\tau_j$ 's) and hence hf dipole moments ( $\mu_j$ 's) derived from hf conductivities  $\sigma_{ij}$ 's as functions of  $k_{ij}'$  and  $k_{ij}''$  at different  $w_j$ 's.

The ratio of individual slopes of the concentration variation of the imaginary  $\sigma_{ij}''$  and the real  $\sigma_{ij}'$  parts of complex hf conductivity  $\sigma_{ij}^*$  as well as the slope of linear variation of  $\sigma_{ij}''$  with  $\sigma_{ij}'$  were simultaneously used [8.4] to estimate  $\tau_j$ 's of a polar liquid. The  $\tau_j$  obtained by the former method provides a significant improvement over the latter one [8.5], as it eliminates the polar-polar interaction in the solution. It is better to use the ratio of slopes of concentration variations of  $k_{ij}''$  and  $k_{ij}'$  instead of  $\sigma_{ij}''-w_j$  and  $\sigma_{ij}'-w_j$  curves to get  $\tau_j$ , because  $k_{ij}'$  and  $k_{ij}''$  can be obtained directly from experimental measurements of  $\epsilon_{ij}'$  and  $\epsilon_{ij}''$ .

But, the variation of  $k_{ij}''$  with  $w_j$  is not always linear with a constant intercept [8.6-8.7]. In this paper, a comparison of static  $\mu_s$  from the slope of  $X_{ij}-w_j$  curve and hf  $\mu_j$  in

terms of  $\tau_j$  using hf conductivities of solution under 9.945 GHz electric field is also made with  $\mu_2$  and  $\mu_1$  due to rotations of the whole as well as the flexible part attached to the parent ring of the molecule from the dielectric relaxation parameters of Table 8.1 obtained by careful graphical interpolation of measured data [8.8] used earlier [8.3]. The comparison of all these seems to be an interesting phenomenon only to see how far they agree with  $\mu_2$  and  $\mu_1$  as obtained elsewhere [8.3]. This study farther observes the effect of inductive and mesomeric moments of polar groups of the molecules as well as the frequency of the alternating electric field on  $\mu_j$ 's in comparison to  $\mu_s$ . Moreover, the present method of study in terms of modern internationally accepted units and symbols appears to be superior because of its unified, coherent and rationalized nature.

As is evident from Table 8.2, hf  $\mu_j$ 's of the polar liquids were computed in terms of  $\tau_j$  and the slopes ( $\beta$ 's) of  $\sigma_{ij} - w_j$  curves of Fig.8.1 under 9.945 GHz electric field at 35°C.  $\tau_j$  being an important parameter for obtaining  $\mu_j$  of a polar liquid estimated from the ratio of slopes of individual variation of  $\sigma_{ij}''$  and  $\sigma_{ij}'$  with  $w_j$ . The nature of variations of  $\sigma_{ij}'' - w_j$  and  $\sigma_{ij}' - w_j$  curves are presented in Figs 8.2 and 8.3 respectively. In place of using  $\tau_j$  from the ratio of the slopes of  $\sigma_{ij}'' - w_j$  and  $\sigma_{ij}' - w_j$  curves, one may use the linear slope of  $\sigma_{ij}'' - \sigma_{ij}'$  curve to get  $\tau_j$  and hence  $\mu_j$  as suggested by Murthy et al [8.5]. All the  $\mu_j$ 's and  $\tau_j$ 's from both the methods are reported in Table 8.2.

The static dipole moment  $\mu_s$  under static or low frequency electric field was also calculated from the linear coefficient of  $X_{ij} - w_j$  curve of Fig.8.4 for each polar-nonpolar liquid mixture. The correlation coefficient  $r$  of the linear curve as well as the % error are presented in Table 8.3 along with  $\mu_s$  and coefficients  $a_0, a_1$  of  $X_{ij} - w_j$  curve. The theoretical dipole moment  $\mu_{theo}$ 's from available bond angles and bond moments [8.3] are found to be deviated from static  $\mu_s$ 's and hf  $\mu_j$ 's, because of the existence of the inductive and mesomeric moments of the different polar groups in them. As the variation of  $\mu_s$  compared to  $\mu_j$  is very little, conformational structures of the polar molecules are predicted by  $\mu_{cal}$  values, which are in agreement with  $\mu_s$  from the reduced bond moments of the substituent groups by a factor  $\mu_s / \mu_{theo}$  presented in Table 8.3 and illustrated in Fig.8.5.

Table 8.1. Experimental dielectric relaxation parameters of three isomers of anisidines and toluidines at 35 °C under 9.945 GHz electric field for different weight fractions  $w_j$ 's of solutes.

System with sl no & mol wt. $M_j$ in kg	Weight fraction $w_j$	$\epsilon_{ij}'$	$\epsilon_{ij}''$	$\epsilon_{oij}$	$\epsilon_{\infty ij}$
1. o-anisidine in $C_6H_6$ $M_j = 0.123$ kg	0.0326	2.3104	0.0148	2.336	2.239
	0.0604	2.3520	0.0244	2.404	2.247
	0.0884	2.4064	0.0340	2.459	2.255
	0.1135	2.4416	0.0400	2.538	2.262
	0.1361	2.4672	0.0512	2.588	2.267
2. m-anisidine in $C_6H_6$ $M_j = 0.123$ kg	0.0160	2.2720	0.0234	2.315	2.235
	0.0336	2.3040	0.0390	2.384	2.241
	0.0579	2.3904	0.0618	2.477	2.246
	0.0823	2.4544	0.0744	2.553	2.253
	0.1109	2.5344	0.1056	2.675	2.261
3. p-anisidine in $C_6H_6$ $M_j = 0.123$ kg	0.0319	2.3104	0.0252	2.373	2.237
	0.0597	2.3904	0.0474	2.442	2.246
	0.0848	2.5088	0.0642	2.539	2.250
	0.1106	2.5376	0.0840	2.638	2.262
	0.1396	2.6272	0.1086	2.745	2.269
4. o-toluidine in $C_6H_6$ $M_j = 0.107$ kg	0.0137	2.2752	0.0162	2.301	2.241
	0.0459	2.3648	0.0408	2.392	2.250
	0.0622	2.4032	0.0570	2.457	2.255
	0.1048	2.5376	0.0900	2.577	2.264
	5. m-toluidine in $C_6H_6$ $M_j = 0.107$ kg	0.0264	2.3136	0.0150	2.337
0.0538		2.3552	0.0342	2.413	2.248
0.0781		2.4576	0.0402	2.470	2.252
0.1015		2.3840	0.0618	2.526	2.258
0.1225		2.5280	0.0732	2.591	2.262
6. p-toluidine in $C_6H_6$ $M_j = 0.107$ kg	0.0213	2.3100	0.0102	2.319	2.237
	0.0428	2.3040	0.0204	2.367	2.244
	0.0616	2.3904	0.0276	2.413	2.249
	0.0916	2.4704	0.0384	2.483	2.254
	0.1048	2.4960	0.0582	2.523	2.260

## 8.2. Theoretical formulation to estimate hf dielectric relaxation parameters :

Under hf electric field of GHz range the dimensionless complex dielectric constant  $\epsilon_{ij}^*$  is written as

$$\epsilon_{ij}^* = \epsilon_{ij}' - j\epsilon_{ij}'' \quad \dots (8.1)$$

Where  $\epsilon_{ij}'$  and  $\epsilon_{ij}''$  are the real and imaginary parts of complex permittivities  $\epsilon_{ij}^*$  having dimension of Farad meter<sup>-1</sup> (F.m<sup>-1</sup>) and  $\epsilon_0$  = permittivity of the free space =  $8.854 \times 10^{-12}$  F.m<sup>-1</sup>. Hence Murphy Morgan [8.9] relation for the complex hf conductivity  $\sigma_{ij}^*$  of a solution of  $w_j$  is given by

$$\sigma_{ij}^* = \omega \epsilon_0 \epsilon_{ij}'' + j \omega \epsilon_0 \epsilon_{ij}' \quad \dots (8.2)$$

where  $\sigma_{ij}' (= \omega \epsilon_0 \epsilon_{ij}'')$  and  $\sigma_{ij}'' (= \omega \epsilon_0 \epsilon_{ij}')$  are the real and imaginary parts of complex conductivity, and  $j$  is a complex number =  $\sqrt{-1}$

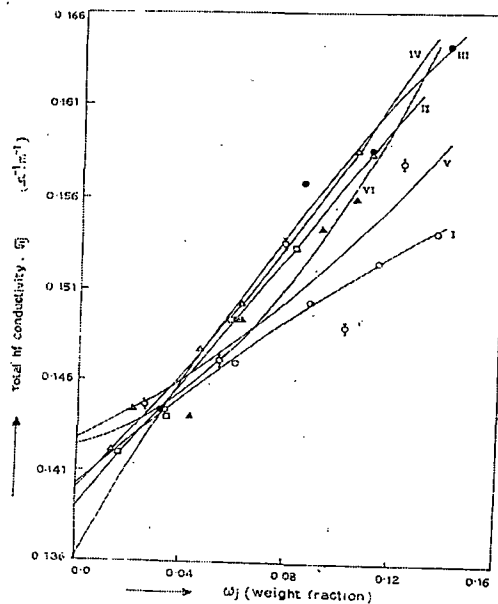


Figure 8.1: The variation of total conductivity  $\sigma_{ij}$  with different  $w_j$ 's of solutes under 9.945 GHz electric field at 35°C.  
 (I) o-anisidine (-○-), (II) m-anisidine (-□-), (III) p-anisidine (-●-), (IV) o-toluidine (-△-), (V) m-toluidine (-◇-), (VI) p-toluidine (-▲-)

The total hf conductivity  $\sigma_{ij}$ , is, however, obtained from

$$\sigma_{ij} = \omega \epsilon_0 \sqrt{\epsilon_{ij}''^2 + \epsilon_{ij}'^2} \quad \dots (8.3)$$

Again, the imaginary part of hf conductivity  $\sigma_{ij}''$  related to the real part of hf conductivity  $\sigma_{ij}'$  by

$$\sigma_{ij}'' = \sigma_{\infty ij} + \frac{1}{\omega\tau} \sigma_{ij}' \quad \dots (8.4)$$

where  $\sigma_{\infty ij}$  is the constant conductivity in the limit of  $w_j=0$  and  $\tau$  is the relaxation time of a polar unit. Differentiating Eq. (8.4) with respect to  $\sigma_{ij}'$  one gets:

$$\left( \frac{d\sigma_{ij}''}{d\sigma_{ij}'} \right) = \frac{1}{\omega\tau} \quad \dots (8.5)$$

In higher concentration region, the variation of the individual  $\sigma_{ij}''$  and  $\sigma_{ij}'$  with  $w_j$  may not be linear due to polar-polar interactions, it is better to use the following relation to get  $\tau_j$  as

$$\left( \frac{d\sigma_{ij}''}{dw_j} \right)_{w_j \rightarrow 0} = \frac{1}{\omega\tau} \left( \frac{d\sigma_{ij}'}{dw_j} \right)_{w_j \rightarrow 0}$$

or  $\frac{x}{y} = \frac{1}{\omega\tau_j} \quad \dots (8.6)$

Under hf alternating electric field, it is also observed experimentally that  $\sigma_{ij}'' \approx \sigma_{ij}$

Hence Eq.(8.4) becomes

$$\sigma_{ij} = \sigma_{\infty ij} + \frac{1}{\omega\tau_j} \sigma_{ij}' \quad \dots (8.7)$$

$$\beta = \frac{1}{\omega\tau_j} \left( \frac{d\sigma_{ij}'}{dw_j} \right)_{w_j \rightarrow 0} \quad \dots (8.8)$$

Where  $\beta$  =slope of  $\sigma_{ij}$ -  $w_j$  curve at  $w_j \rightarrow 0$  as presented in Table 8.2 for all the liquids under investigation. The real part of hf conductivity  $\sigma_{ij}'$  at T K is related with imaginary part of dielectric constant or dielectric loss [8.10] of a given solution of  $w_j$  by

Table 8.2. Ratio of slopes  $\sigma_{ij}''-w_j$  and  $\sigma_{ij}'-w_j$  curves at  $w_j \rightarrow 0$ , linear slope of  $\sigma_{ij}''-\sigma_{ij}'$  curve, computed relaxation time  $\tau_j$  and hence  $\mu_j$  for both the methods and reported  $\mu_2$  and  $\mu_1$  in C.m. from double relaxation method.

System with sl no & mol wt.	Ratio of slope	Slope of $\sigma_{ij}''-\sigma_{ij}'$ Eq. 8.5	Corr. Coeff. r	% of error	Estimated $\tau_j \times 10^{12}$ sec from		Slope $\beta$ in $\Omega^{-1} m^{-1}$	Computed $\mu_j \times 10^{30}$ in C.m from		Reported $\mu_j \times 10^{30}$ in C.m	
					Eq. (8.6)	Eq. (8.5)		Eq.(8.6) &Eq.(8.11)	Eq.(8.5) &Eq.(8.11)	$\mu_2$	$\mu_1$
1. o-anisidine in $C_6H_6$ $M_j = 0.123$ kg	7.5813	4.5290	0.988	0.71	2.11	3.53	0.1302	5.38	5.38	31.11	6.40
2. m-ani sidinein $C_6H_6$ $M_j = 0.123$ kg	3.3015	3.3521	0.993	0.40	4.85	4.77	0.1732	6.33	6.33	24.57	7.55
3. p-anisidine in $C_6H_6$ $M_j = 0.123$ kg	5.4869	3.8143	0.983	0.99	2.92	4.20	0.2621	7.58	7.71	52.74	9.00
4. o-toluidine in $C_6H_6$ $M_j = 0.107$ kg	2.9380	3.5123	0.997	0.31	5.45	4.56	0.1500	5.44	5.47	29.87	7.70
5. m-tolui dine in $C_6H_6$ $M_j = 0.107$ kg	1.9562	2.9025	0.783	11.69	8.18	5.51	0.0732	4.13	3.89	17.07	5.20
6. p-toluidine in $C_6H_6$ $M_j = 0.107$ kg	10.2048	4.4801	0.929	4.12	1.57	3.57	0.0428	2.82	2.88	18.54	4.03

$$\sigma'_{ij} = \frac{N\rho_i\mu_j^2}{27k_B TM_j} \left( \frac{\omega^2\tau}{1+\omega^2\tau^2} \right) (\epsilon_{ij} + 2)^2 w_j \quad \dots (8.9)$$

Which on differentiation with respect to  $w_j$  and at  $w_j \rightarrow 0$  yields

$$\left( \frac{d\sigma'_{ij}}{dw_j} \right)_{w_j \rightarrow 0} = \frac{N\rho_i\mu_j^2}{3k_B TM_j} \left( \frac{\epsilon_i + 2}{3} \right)^2 \left( \frac{\omega^2\tau}{1+\omega^2\tau^2} \right) \quad \dots (8.10)$$

Here  $N$ =Avogadro's number,  $\rho_i$ = density of solvent,  $\epsilon_i$  = dielectric permittivities of the solvent,  $M_j$ = molecular weight of solute and  $k_B$ = Boltzmann constant. All the parameters are, however, expressed in SI units. From Eqs.(8.8) and (8.10) one gets hf dipole moment  $\mu_j$  from

$$\mu_j = \left[ \frac{27M_j k_B T \beta}{N \rho_i (\epsilon_i + 2)^2 \omega b} \right]^{1/2} \quad \dots (8.11)$$

In terms of  $b$ , which is a dimensionless parameter, given by

$$b = \frac{1}{1 + \omega^2 \tau^2} \quad \dots (8.12)$$

All the  $\mu_j$ 's in terms of  $\beta$ 's and  $b$ 's involved with  $\tau_j$ 's are, however, placed in Table 8.2, in order to compare with the static  $\mu_s$  as presented in Table 8.3.

### 8.3. Static relaxation parameters :

Under static or low frequency electric field,  $\mu_s$  of a polar liquid (j) in a non polar solvent (i) may be written from Debye's equation [8.11] as

$$\frac{\epsilon_{oij} - 1}{\epsilon_{oij} + 2} - \frac{\epsilon_{\infty ij} - 1}{\epsilon_{\infty ij} + 2} = \frac{\epsilon_{oi} - 1}{\epsilon_{oi} + 2} - \frac{\epsilon_{\infty oi} - 1}{\epsilon_{\infty oi} + 2} + \frac{N \mu_s^2 c_j}{9 \epsilon_o k_B T} \quad \dots (8.13)$$

where  $\epsilon_{oij}$  and  $\epsilon_{\infty ij}$  are the dimensionless static and infinite frequency relative permittivity of solution.  $c_j$  is the molar concentration given by  $c_j = \rho_{ij} W_j / M_j$  and other symbols carry usual meanings [8.4, 8.12-8.13].

A polar liquid of weight  $W_j$  and of volume  $V_j$  is mixed with a non polar solvent of weight  $W_i$  and of volume  $V_i$  to get the solution density  $\rho_{ij}$  where

$$\rho_{ij} = \frac{\rho_i \rho_j}{\rho_j W_i + \rho_i W_j} = \rho_i (1 - \gamma W_j)^{-1} \quad \dots (8.14)$$

Here, weight fractions  $w_j$  and  $w_i$  of solute and solvent are given by  $w_j = W_j / (W_i + W_j)$  and  $w_i = W_i / (W_i + W_j)$  such that  $w_i + w_j = 1$  and  $\gamma = (1 - \rho_i / \rho_j)$  and  $\rho_i$  and  $\rho_j$  are densities of pure solvent and solute respectively.

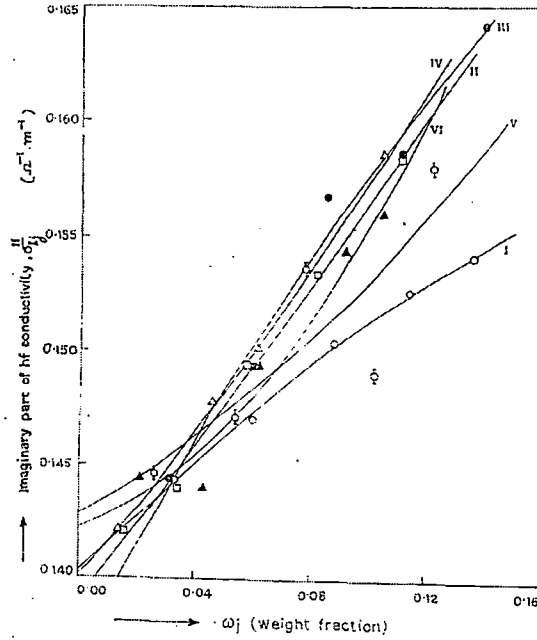


Figure 8.2: The plot of imaginary part of conductivity  $\sigma_{ij}''$  with weight fractions  $w_j$ 's of anisidines and toluidines at  $35^{\circ}\text{C}$  under 9.945 GHz electric field.

(I) o-anisidine ( $-\circ-$ ), (II) m-anisidine ( $-\square-$ ), (III) p-anisidine ( $-\bullet-$ ), (IV) o-toluidine ( $-\triangle-$ ), (V) m-toluidine ( $-\Phi-$ ), (VI) p-toluidine ( $-\blacktriangle-$ )

Now Eq.(8.13) may be written as

$$\frac{\epsilon_{oij} - \epsilon_{\infty ij}}{(\epsilon_{oij} + 2)(\epsilon_{\infty ij} + 2)} = \frac{\epsilon_{oi} - \epsilon_{\infty oi}}{(\epsilon_{oi} + 2)(\epsilon_{\infty oi} + 2)} + \frac{N\rho_i\mu_s^2}{27\epsilon_o M_j k_B T} w_j (1 - \gamma w_j)^{-1}$$

$$X_{ij} = X_i + \frac{N\rho_i\mu_s^2}{27\epsilon_o M_j k_B T} w_j + \frac{N\rho_i\mu_s^2}{27\epsilon_o M_j k_B T} \gamma w_j^2 \quad \dots (8.15)$$

Since the left hand side of Eq.(8.15) is a function of  $w_j$ , the usual variation of  $X_{ij}$  with  $w_j$  can, however, be represented by

$$X_{ij} = a_o + a_1 w_j + a_2 w_j^2 \quad \dots (8.16)$$

Now, comparing the linear coefficients of  $w_j$  of Eqs.(8.15) and (8.16) one gets  $\mu_s$  from

$$\mu_s = \left( \frac{27\epsilon_o M_j k_B T a_1}{N \rho_i} \right)^{1/2} \dots (8.17)$$

where  $a_1$  is the slope of  $X_{ij} - w_j$  curve. But  $\mu_s$  from higher coefficients of Eqs (8.15) or (8.16), which are involved with different factors like solvent effect, relative density effect, solute-solute associations, etc are not reliable. The estimated  $\mu_s$  alongwith the slope  $a_1$  are placed in Table 8.3 in order to compare with hf  $\mu_j$ 's presented in Table 8.2.

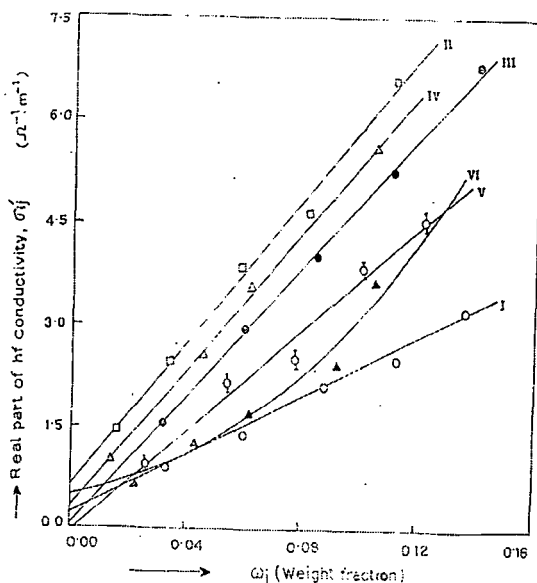


Figure 8.3: The variation of real part of conductivity  $\sigma'_{ij}$  against  $w_j$ 's of solutes at 35<sup>o</sup>C under 9.945 GHz electric field.

(I) o-anisidine (-O-), (II) m-anisidine (-□-), (III) p-anisidine (-●-), (IV) o-toluidine (-△-), (V) m-toluidine (-Φ-), (VI) p-toluidine (-▲-)

#### 8.4. Results and discussion :

The hf dipole moments  $\mu_j$ 's of all the isomers of anisidines and toluidines at different  $w_j$ 's of solutes from the measured data of Table 8.1 are calculated in terms of slope

$\beta$  of  $\sigma_{ij}$ -  $w_j$  curve and  $\tau_j$  estimated from Eqs (8.5) and (8.6) of the methods suggested. The variations of  $\sigma_{ij}$  with  $w_j$  of solutes are parabolic, having almost same intercept and slope as seen in Fig 8.1.

Table 8.3.: Coefficients  $a_0$ ,  $a_1$  in the equation  $X_{ij}=a_0+a_1w_j$ , correlation coefficient ( $r$ ), % of error in fitting technique, static dipole moment  $\mu_s$  in Coulomb metre, theoretical dipole moment  $\mu_{theo}$  from bond angles and bond moments, reduced bond moments of substituent groups,  $\mu_{cal}$  from reduced bond moments of anisidines and toluidines under static electric field at 35 °C.

System with sl no & mol wt.	Intercepts and slopes of $X_{ij}=a_0+a_1w_j$		Corr. Coeff. $r$	% of error	$\mu_s \times 10^{30}$ & $\mu_{theo} \times 10^{30}$ in C.m.		Reduced bond moments $\times 10^{30}$ of			$\mu_{cal} \times 10^{30}$ in C.m
	$a_0$	$a_1$			-OCH <sub>3</sub>	-CH <sub>3</sub>	-NH <sub>2</sub>			
1. o-anisidine in C <sub>6</sub> H <sub>6</sub> Mj= 0.123 kg	0.0193	1.2196	0.9976	0.14	2.94	3.40	2.07	--	-3.36	2.94
2. m-anisidine in C <sub>6</sub> H <sub>6</sub> Mj= 0.123 kg	0.0211	1.9208	0.9988	0.07	3.69	5.50	1.61	--	-2.60	3.68
3. p-anisidine in C <sub>6</sub> H <sub>6</sub> Mj= 0.123 kg	0.0219	1.7353	0.9977	0.14	3.51	6.30	1.33	--	-2.16	3.49
4. o-toluidine in C <sub>6</sub> H <sub>6</sub> Mj= 0.107 kg	0.0158	1.5942	0.9981	0.13	3.13	4.63	--	0.83	-2.63	3.13
5. m-toluidine in C <sub>6</sub> H <sub>6</sub> Mj= 0.107 kg	0.0240	1.3430	0.9988	0.08	2.88	3.43	--	1.03	-3.25	2.88
6. p-toluidine in C <sub>6</sub> H <sub>6</sub> Mj= 0.107 kg	0.0230	1.2393	0.9996	0.02	2.76	5.13	--	0.66	-2.09	2.75

This is probably due to same polarity of the molecules as observed earlier [8.3]. They also meet at a point within  $0.02 \leq w_j \leq 0.045$  indicating solute-solute (dimer) or solute-solvent (monomer) molecular associations under 9.945 GHz electric field [8.3].  $\tau_j$ 's of polar liquids were, estimated from the linear slope of  $\sigma_{ij}'' - \sigma_{ij}'$  curve [8.5] as well as the ratio of slopes of individual variations of  $\sigma_{ij}'' - w_j$  and  $\sigma_{ij}' - w_j$  curves of Figs 8.2 and 8.3. Both  $\sigma_{ij}''$  and  $\sigma_{ij}'$  are

functions of  $w_j$ . Their variations with  $w_j$ 's were not linear as shown in Figs 8.2 and 8.3. The latter method appears to be a significant improvement over the other [8.5], as it eliminates polar-polar interactions at  $w_j \rightarrow 0$ . The correlation coefficients ( $r$ 's) and the % errors in measurement of  $\tau_j$ 's from Eq. (8.4) were calculated and presented in Table 8.2.  $\tau_j$ 's are found to agree well for both the methods and the % error involved in them are very low except m-toluidine, perhaps due to experimental uncertainty in the measurement of the relaxation parameters. It is interesting to note that unlike  $\sigma_{ij}' - w_j$  curve, the variation of  $\sigma_{ij}''$  with  $w_j$  is identical with  $\sigma_{ij} - w_j$  curve.

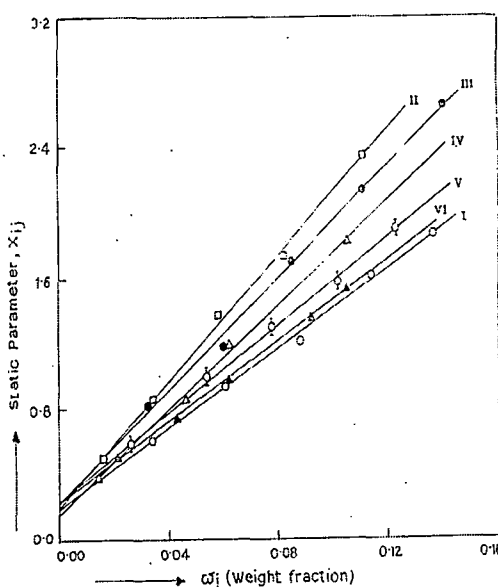


Figure 8.4: The linear variation of static experimental parameter  $X_{ij}$  for different  $w_j$ 's of anisidines and toluidines at  $35^\circ\text{C}$ .  
 (I) o-anisidine ( $-\circ-$ ), (II) m-anisidine ( $-\square-$ ), (III) p-anisidine ( $-\bullet-$ ), (IV) o-toluidine ( $-\triangle-$ ), (V) m-toluidine ( $-\Phi-$ ), (VI) p-toluidine ( $-\blacktriangle-$ )

This fact suggests the applicability of the approximation of  $\sigma_{ij}'' \approx \sigma_{ij}$  in Eq. (8.7). The plot of  $\sigma_{ij}'$  with  $w_j$  is, however, linear except p-toluidine in  $\text{C}_6\text{H}_6$  when fitted with the measured data of  $\epsilon_{ij}''$  for different  $w_j$ 's of solutes under 9.945 GHz electric field as displayed in Fig.8.3. This type of behaviour reveals the fact that the data presented in Table 8.1 are

very accurate. The  $\mu_j$ 's as obtained from slope  $\beta$  of  $\sigma_{ij}-w_j$  curves of Fig.8.1 and the dimensionless parameters  $b$  of Eq. (8.12) involved with  $\tau_j$  measured by both the methods are shown in Table 8.2. The excellent agreement of  $\mu_j$ 's in both cases implies that the method suggested is a correct one.

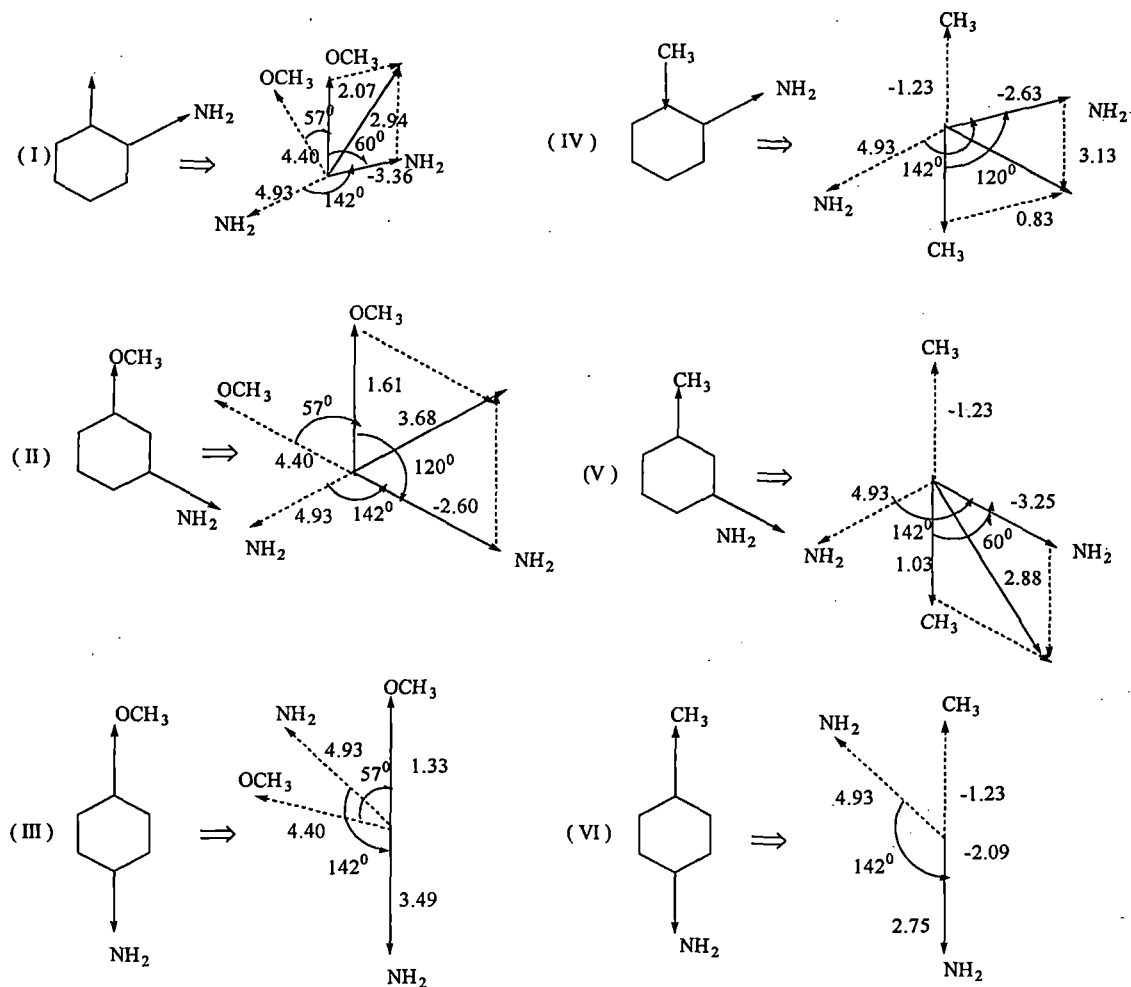


Figure 8.5: Conformational structures of isomers of anisidine and toluidine in terms of reduced bond moments ( $\times 10^{-30}$  Coulomb. metre) of their substituted groups.

(I) o-anisidine, (II) m-anisidine, (III) p-anisidine, (IV) o-toluidine, (V) m-toluidine, (VI) p-toluidine

These  $\mu_j$ 's are again compared with the hf dipole moments  $\mu_2$  and  $\mu_1$  due to whole and the flexible part of the molecule attached to the parent ring as presented earlier [8.3].

$\mu_j$ 's are found to be in agreement with  $\mu_1$  suggesting the fact that a part of the molecule is rotating under nearly 10 GHz electric field [8.4]. The gradual increase of  $\mu_j$ 's from o-to p-anisidines and from p- to o-toluidenes like  $\mu_1$  is probably due to the same polarity of the molecules as supported by the slopes ( $\beta$ 's) as observed earlier [8.3].

The static or low frequency dipole moment  $\mu_s$  at 35 °C are computed from the linear coefficients  $a_1$  of  $X_{ij}$ - $w_j$  curves of Fig.8.4. All the  $\mu_s$ 's are entered in Table 8.3. The variation of  $X_{ij}$  with  $w_j$  is almost linear as evident from the correlation coefficient  $r$  and % error involved in getting the coefficients  $a_0$  and  $a_1$  which are placed in Table 8.3. The curves are found to increase with the addition of solute and show a tendency to meet at a common point on the ordinate axis at  $w_j=0$ . This reveals the fact that static polarisability increases with  $w_j$ 's of solute and yields static experimental parameter  $X_i$  of solvent  $C_6H_6$  for all the polar liquids under investigation at infinite dilution. This indicates the basic soundness of the method adopted here as well as the reliability of the experimental data of  $X_{ij}$  involved with  $\epsilon_{0ij}$  and  $\epsilon_{\infty ij}$  of the solutions. The  $\mu_j$ 's are, however, little smaller than  $\mu_j$ 's. They are seen to increase from o- to p- anisidines and p- to o-toluidines like  $\mu_s$ 's establishing the fact that  $\mu$ 's are very little influenced by the frequency of the applied alternating electric field of GHz range.

The theoretical dipole moments  $\mu_{theo}$ 's of the polar molecules are calculated assuming their planar structures, from the vector addition of available bond moments of  $4.40 \times 10^{-30}$ ,  $1.25 \times 10^{-30}$ ,  $4.93 \times 10^{-30}$  in Coulomb-meter (C.m) for respective  $-OCH_3$ ,  $-CH_3$  and  $-NH_2$  groups, which make angles  $57^\circ$ ,  $180^\circ$  And  $142^\circ$  with the C-atoms of parent benzene ring as placed in Table 8.3.  $\mu_{theo}$ 's are found to differ from  $\mu_s$  probably due to existence of inductive and mesomeric moments of the substituent polar groups arising out of difference in electron affinity of two adjacent atoms. For all the polar compounds as referred to Tables 8.1 to 8.3 are planar ones and have the property of cyclic delocalized  $\pi$ -electrons on each carbon atom of the rings. The solvent  $C_6H_6$  is also a cyclic and planar compound and has three double bonds and six p-electrons on its six carbon atoms. Hence due to their aromaticity, the resonance effect combined with inductive effect known as mesomeric effect are playing an important role among the substituent polar groups attached to the parent ring under static and hf electric field. The so called mesomeric moment is,

however, caused by the permanent polarization of different substituent groups acting as pusher or puller of electrons towards or away from p-electrons of C-atoms attached to the parent rings. Thus a special attention is to be paid to get the conformational structures of the molecules of Fig.8.5 by  $\mu_{cal}$  in terms of reduced bond moments by a factor  $\mu_s/\mu_{theo}$  in agreement with  $\mu_s$  to take into account of the mesomeric effects in them. Similar effects may also be observed in those molecules in the hf electric field. They are not calculated because they were found not to depend strongly on the frequency ( $f$ ) of the alternating hf electric field of 10 GHz.

### 8.5. Conclusions :

A convenient method for the determination of  $\tau_j$  of a polar liquid from the ratio of slopes of the individual variations of imaginary  $\sigma_{ij}''$  and real  $\sigma_{ij}'$  with  $w_j$  of solutes in a non-polar solvent is suggested in terms of measured data to avoid polar-polar interactions. The estimated  $\tau_j$  when compared with the existing method using the slope of  $\sigma_{ij}''$  with  $\sigma_{ij}'$  for different  $w_j$ 's reveals the soundness of the method suggested.  $\tau_j$ 's are reliable and claimed to be accurate up to  $\pm 10\%$ . The computed  $\mu_j$ 's ( $\pm 5\%$ ) in terms of the slopes  $\beta$ 's of  $\sigma_{ij}-w_j$  curves and  $\tau_j$ 's are found to agree with the static  $\mu_s$  excellently. The static  $\mu_s$  as calculated from  $X_{ij}-w_j$  curves are used to test the accuracies of permittivities of  $\epsilon_{oij}$  and  $\epsilon_{\infty ij}$  measured in the static or low frequency electric field. The curves of  $X_{ij}$  with  $w_j$  vary linearly and have a tendency to meet at a common point in the ordinate axis at  $w_j=0$  signifying the accuracy of the measured relaxation data once again. The % errors in terms of correlation coefficients  $r$ 's of  $\sigma_{ij}-w_j$  and  $X_{ij}-w_j$  curves are very easy, simple and straightforward to compute. The deviations of the static  $\mu_s$  and hf  $\mu_j$  from  $\mu_{theo}$  as obtained from the available bond moments and bond angles of the substituent polar groups attached to the parent molecule imply the existence of mesomeric and inductive moments in the molecules. The comparison of  $\mu_j$  with  $\mu_2$  and  $\mu_1$  obtained from double relaxation method provides important information, that under the 10GHz electric field only a part of the molecule is rotating. Thus the present method of study in terms of measured dimensionless dielectric constants of Table 8.1 seems to give a new insight of the molecular interactions in relaxation phenomena.

## References :

- [8.1] U Saha, S K Sit, R C Basak and S Acharyya, *J. Phys. D: Appl. Phys.* **27** 596 (1994).
- [8.2] S K Sit, R C Basak, U Saha and S Acharyya, *J. Phys. D: Appl. Phys.* **27** 2194 (1994)
- [8.3] S K Sit and S Acharyya, *Indian J. Pure & Appl. Phys.* **34** 255 (1996)
- [8.4] R C Basak, S K Sit, N Nandi and S Acharyya, *Indian J. Phys.* **70B** 37 (1996)
- [8.5] M B R Murthy, R L Patil and D K Deshpande, *Indian J. Phys.* **63B** 491 (1989)
- [8.6] K Higasi, Y Koga and M Nakamura, *Bull. Chem. Soc. Japan* **44** 988 (1971)
- [8.7] S Chandra and J Prakash, *J. Phys. Soc. Japan* **35** 876 (1973)
- [8.8] S C Srivastava and Suresh Chandra, *Indian J. Pure & Appl. Phys.* **13** 101 (1975)
- [8.9] F J Murphy and S O Morgan, *Bull. Syst. Tech. J.* **18** 502 (1939)
- [8.10] C P Smyth, *Dielectric Behaviour and Structure* (McGraw Hill) (1955)
- [8.11] P Debye, *Polar Molecules* (Chemical Catalog) 1929
- [8.12] A K Guha, S Acharyya and D K Das, *Indian J. Phys.* **51A** 192 (1977)
- [8.13] A K Ghosh, K K Sarkar and S Acharyya, *Acta Ciencia Indica.* **3** 49 (1977)

*Chapter 9*

**STRUCTURAL AND ASSOCIATIONAL ASPECTS  
OF DIELECTROPOLAR STRAIGHT CHAIN ALCO-  
HOLS FROM RELAXATION PHENOMENA**

## 9.1. Introduction :

The relaxation phenomenon of a dielectropolar liquid in a solvent has attracted the attention of a large number of workers [9.1-9.3] as it is a very sensitive and useful tool to ascertain the shape, size and structure of a polar molecule. The technique provides one with much information about the stability [9.4] of the system undergoing relaxation phenomena. It also offers valuable insight into the solute-solute i.e. dimer and solute-solvent i.e. monomer formations [9.4]. Structural and associational aspects of a polar liquid in a nonpolar solvent can, however, be gained by measured static dipole moment  $\mu_s$  and high frequency (hf) dipole moment  $\mu_j$  in terms of relaxation time  $\tau_j$  and slope  $\beta$  of hf conductivity  $\sigma_{ij}$  with weight fraction  $w_j$ .

Alcohols behaving like almost polymers have  $\alpha$ ,  $\beta$  and  $\gamma$  etc. dispersion regions. The strong dipole of  $-OH$  group rotates about  $\equiv C-O-$  bond without disturbing  $CH_3$  or  $CH_2$  groups and thus they have possibility to exhibit intramolecular as well as intermolecular rotations. Sit and Acharyya [9.5] and Sit et al [9.6] studied the straight long chain alcohols like 1-butanol, 1-hexanol, 1-heptanol, 1-decanol in n-heptane [9.7], ethanol and methanol in benzene [9.8] (9.84GHz) and 2-methyl-3-heptanol, 3-methyl-3-heptanol, 4-methyl-3 heptanol, 5-methyl-3-heptanol, 4-octanol and 2-octanol, in n-heptane [9.9] at 25<sup>o</sup>C to observe that all the alcohols except methanol showed the double relaxation times  $\tau_1$  and  $\tau_2$  at all the frequencies in GHz range. The alcohols were again expected to exhibit the triple relaxation phenomena [9.7] for different frequencies of electric field in GHz range. Such long chain liquids under investigation have wide applications in the fields of biological research, medicine and industry. Moreover, the study of alcohols in terms of modern internationally accepted units and symbols appears to be superior for the unified, coherent and rationalized nature of the SI unit used.

The  $\mu_s$  of all the associated dielectropolar molecules under static electric field was derived from static experimental parameter  $X_{ij}$ .  $X_{ij}$  is again involved with the dimensionless dielectric constants  $k_{oij}$  and  $k_{\infty ij}$  of Table 9.1 from the measured relaxation permittivities static  $\epsilon_{oij}$  and  $\epsilon_{\infty ij}$  of dimensions Farad metre<sup>-1</sup> (F.m<sup>-1</sup>) based on Debye model[9.10]. The

Table 9.1. Measured dielectric permittivities  $\epsilon_{ij}'$ ,  $\epsilon_{ij}''$ ,  $\epsilon_{oij}$  and  $\epsilon_{\infty ij}$  in Farad metre<sup>-1</sup> of some dielectropolar alcohols at 25 °C for different weight fractions  $w_j$ 's of solutes.

System with sl no & mol wt. $M_j$ in kg	Weight fraction $w_j$	$\epsilon_{ij}'$	$\epsilon_{ij}''$	$\epsilon_{oij}$	$\epsilon_{\infty ij}$
1. 1-butanol $M_j = 0.074$ kg	0.0291	1.957	0.0079	1.971	1.928
	0.0451	1.981	0.0147	2.000	1.945
	0.0697	2.011	0.0236	2.050	1.958
	0.1163	2.060	0.0425	2.175	1.978
	0.1652	2.105	0.0644	2.381	2.000
2. 1-hexanol $M_j = 0.102$ kg	0.2072	2.144	0.0818	2.621	2.020
	0.0458	1.968	0.0131	1.988	1.944
	0.0703	1.984	0.0190	2.015	1.952
	0.1028	2.001	0.0296	2.064	1.970
	0.1687	2.037	0.0425	2.196	1.989
3. 1-heptanol $M_j = 0.116$ kg	0.2335	2.088	0.0569	2.360	2.002
	0.2901	2.134	0.0748	2.580	2.018
	0.0564	1.968	0.0147	1.985	1.932
	0.0735	1.975	0.0182	2.008	1.945
	0.1175	2.007	0.0265	2.066	1.957
4. 1-decanol $M_j = 0.158$ kg	0.1909	2.076	0.0482	2.195	1.989
	0.2465	2.097	0.0567	2.315	2.002
	0.2970	2.126	0.0693	2.464	2.008
	0.0572	1.965	0.0120	1.976	1.940
	0.0857	1.979	0.0223	2.003	1.952
5. ethanol $M_j = 0.046$ kg	0.1351	2.003	0.0273	2.050	1.964
	0.2140	2.036	0.0449	2.147	1.990
	0.2640	2.064	0.0513	2.220	2.008
	0.3353	2.097	0.0637	2.346	2.030
	0.0664	2.450	0.0082	3.330	2.262
6. methanol $M_j = 0.032$ kg	0.1393	2.483	0.0124	4.300	2.190
	0.2077	2.500	0.0208	5.400	2.120
	0.2953	2.550	0.0297	7.000	2.062
	0.3638	2.567	0.0342	8.200	2.016
	0.0514	2.467	0.0082	4.800	2.214
7. 2-methyl 3- heptanol $M_j = 0.130$ kg	0.0930	2.500	0.0083	6.500	2.155
	0.1495	2.517	0.0168	8.600	2.085
	0.2266	2.550	0.0298	11.400	2.016
	0.3049	2.583	0.0387	13.700	1.960
	0.0437	1.960	0.0156	1.971	1.930
7. 2-methyl 3- heptanol $M_j = 0.130$ kg	0.1299	2.022	0.0361	2.059	1.966
	0.2522	2.095	0.0565	2.172	2.007
	0.4081	2.169	0.0809	2.330	2.054

System with sl no & mol wt. $M_j$ in kg	Weight fraction $w_j$	$\epsilon_{ij}'$	$\epsilon_{ij}''$	$\epsilon_{oij}$	$\epsilon_{\infty ij}$
8. 3-methyl 3- heptanol $M_j = 0.130$ kg	0.0450	1.965	0.0137	1.974	1.934
	0.1334	2.028	0.0393	2.069	1.966
	0.2538	2.103	0.0674	2.180	2.004
	0.4085	2.188	0.0928	2.334	2.057
9. 4-methyl 3- heptanol $M_j = 0.130$ kg	0.0466	1.964	0.0146	1.976	1.936
	0.1326	2.025	0.0375	2.065	1.969
	0.2590	2.104	0.0616	2.185	2.011
	0.4124	2.180	0.0849	2.352	2.065
10. 5-methyl 3-heptanol $M_j = 0.130$ kg	0.1228	2.008	0.0296	2.048	1.956
	0.2489	2.075	0.0511	2.168	2.004
	0.3898	2.148	0.0676	2.315	2.040
11. 4-octanol $M_j = 0.130$ kg	0.1201	2.000	0.0265	2.040	1.948
	0.2445	2.067	0.0449	2.148	1.997
	0.3838	2.140	0.0659	2.282	2.031
12. 2-octanol $M_j = 0.130$ kg	0.1236	2.001	0.0245	2.049	1.954
	0.2479	2.068	0.0513	2.195	1.996
	0.3844	2.141	0.0680	2.410	2.036

linear coefficients of the expected nonlinear experimental  $X_{ij}$  curves against  $w_j$  graphically shown in Fig. 9.1, of alcohols were conveniently used to estimate  $\mu_s$  at a given temperature.

The  $\tau_j$  of all the alcohols were, however, estimated from the slope of linear variation of imaginary  $\sigma_{ij}''$  against real  $\sigma_{ij}'$  parts [9.11] of hf complex conductivity  $\sigma_{ij}^*$  for different  $w_j$ 's as seen in Fig. 9.2. The hf  $\sigma_{ij}''$  did not vary linearly with hf  $\sigma_{ij}'$  at higher or even lower concentrations [9.12]. It is therefore, better to use the ratio of slopes of individual variations of  $\sigma_{ij}''$  and  $\sigma_{ij}'$  both in  $\Omega^{-1} m^{-1}$  with  $w_j$ 's of Figs 9.3 and 9.4 to get the exact and accurate value of  $d\sigma_{ij}''/d\sigma_{ij}'$  in the limit  $w_j = 0$  to evaluate  $\tau_j$  [9.13-9.14].  $\tau_j$ 's thus obtained by both the methods are placed in Table 9.3 to see how for they are close in agreements.  $\tau_j$ 's of such dielectropolar molecules were, however, estimated at 1.233 cm for molecules like 1-butanol, 1-hexanol, 1-decanol, 2-methyl 3-heptanol, 3-methyl 3-heptanol, 4-methyl-3-heptanol, 5-methyl 3-heptanol, 4-octanol, 2-octanol and at 1.249 cm wavelength electric field for 1-heptanol at which measured  $\epsilon_{ij}''$  of a given  $w_j$  of the solute when were graphically

plotted against the electric field frequency “ $f$ ” showed peak indicating the most effective dispersive region for such liquids.

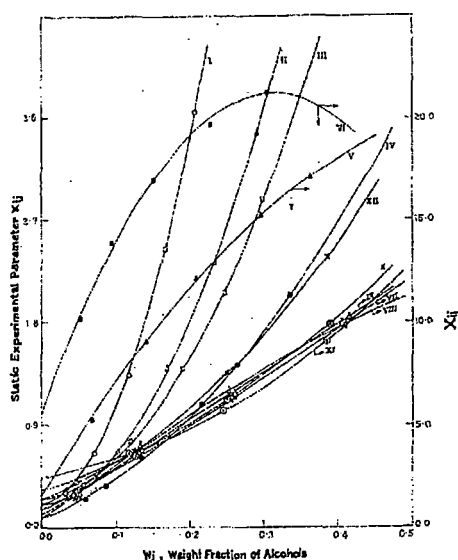


Figure 9.1: Variation of static experimental parameter  $X_{ij}$  against weight fraction  $w_j$  of solute at 25 °C under nearly 24 GHz electric field (ethanol and methanol at 9.84 GHz).

I. 1-butanol (—○—), II. 1-hexanol (—△—), III. 1-heptanol (—□—), IV. 1-decanol (—●—), V. ethanol (—▲—), VI. methanol (—■—), VII. 2-methyl 3-heptanol (—Φ—), VIII. 3-methyl 3-heptanol (—⚠—), IX. 4-methyl 3-heptanol (—⚡—), X. 5-methyl 3-heptanol (—⊗—), XI. 4-octanol (—⊖—), XII. 2-octanol (—✕—).

The formulation to measure  $\mu_j$ 's of all the alcohols involves with the slopes  $\beta$ 's of the expected  $\sigma_{ij} - w_j$  nonlinear curves of Fig. 9.5 and dimensionless parameter  $b$  in terms of  $\tau_j$ 's obtained by both the methods as  $\tau_j$ 's were not found to agree excellently in Table 9.3. The  $\sigma_{ij}''$  and  $\sigma_{ij}'$  in  $\Omega^{-1} \text{ m}^{-1}$  are not linear with  $w_j$  as evident from Figs 9.3 and 9.4.  $\mu_j$ 's thus obtained are finally compared with  $\mu_{\text{theo}}$ 's from available bond angles and bond moments of the substituent polar groups attached to parent ones. The slight disagreement between the measured  $\mu_j$ 's and  $\mu_s$ 's from  $\mu_{\text{theo}}$ 's indicates the existence of inductive and mesomeric moments of different substituent polar groups present in such dielectropolar molecules in addition to strong hydrogen bonding in them as displayed by the molecular conformations of Fig 9.6.

Table 9.2: Coefficients  $a_0$ ,  $a_1$  of the static experimental parameter  $X_{ij}=a_0+a_1w_j+a_2w_j^2$ , correlation coefficients ( $r$ ), % of error in getting  $X_{ij}$ , static or low frequency dipole moment  $\mu_s \times 10^{30}$  in C.m, Corrected theoretical dipole moments  $\mu_{theo} \times 10^{30}$  in C.m from reduced bond moments by  $\mu_s/\mu_{theo}$  and  $\mu_1$ ,  $\mu_2$  by double relaxation method.

System with sl no & mol wt.	Intercepts and slopes of $X_{ij}=a_0+a_1w_j$		Corr. Coeff $r$	% of error	$\mu_s \times 10^{30}$ in C.m Eq.(9.5)	Corrected $\mu_{theo} \times 10^{30}$ in C.m	$\mu_1$ and $\mu_2$ in C.m from double relaxation method	
	$a_0$	$a_1$					$\mu_1$	$\mu_2$
1. 1-butanol in n-heptane Mj= 0.074 kg	0.2047	1.0852	0.9824	0.96	3.74	4.97x0.7525 =3.74	3.63	29.17
2. 1-hexanol in n-heptane Mj= 0.102kg	0.1951	1.0710	0.9896	0.57	3.49	4.37x0.7986 =3.49	3.43	21.20
3. 1-heptanol in n-heptane Mj= 0.116 kg	0.2533	0.8932	0.9867	0.73	3.73	4.07x0.9165 =3.73	3.73	27.00
4. 1-decanol in n-heptane Mj= 0.158 kg	0.0901	2.3826	0.9924	0.42	3.68	3.17x1.1609 =3.68	3.83	17.24
5. ethanol in benzene Mj= 0.046 kg	1.6141	59.189	0.9919	0.49	1.41	5.57x0.2531 =1.41	1.70	490.73
6. methanol in benzene Mj= 0.032 kg	5.6331	99.809	0.9672	1.94	1.25	5.87x0.2129 =1.25	--	293.96
7. 2-methyl 3-heptanol in n-heptane Mj= 0.130 kg	0.1372	3.7778	0.9997	0.02	1.86	5.87x0.3168 =1.86	3.83	16.00
8. 3-methyl 3-heptanol in n-heptane Mj= 0.130 kg	0.0830	4.8577	0.9986	0.09	2.11	5.87x0.3594 =2.11	3.83	8.60
9. 4-methyl 3-heptanol in n-heptane Mj= 0.130 kg	0.1032	4.1481	0.9998	0.01	1.95	5.87x0.3322 =1.95	3.90	13.90
10. 5-methyl 3-heptanol in n-heptane Mj= 0.130 kg	0.3270	2.1113	0.9972	0.22	1.39	5.87x0.2368 =1.39	3.37	9.50
11. 4-octanol in n-heptane Mj= 0.130 kg	0.4402	1.1341	0.9946	0.42	1.11	3.60x0.3083 =1.11	3.43	10.97
12. 2-octanol in n-heptane Mj= 0.130 kg	0.2591	2.2977	0.9955	0.35	1.45	3.60x0.4028 =1.45	3.43	16.00

The solvent  $C_6H_6$  unlike *n*-heptane is a cyclic compound with three double bonds and six  $p$ -electrons on six carbon atoms. Hence  $\pi$ - $\pi$  interaction or resonance effect combined with inductive effect known as mesomeric effect is expected to play an important role in the measured  $\mu_j$ 's under hf electric field. A special attention is to be paid to have the

conformational structures of the alcohols to evaluate  $\mu_{\text{theo}}$ 's as seen in Fig 9.6 and Table 9.2 from the reduction of the available bond moments [9.5-9.6] of different substituent polar groups by the ratio of  $\mu_s/\mu_{\text{theo}}$ . This takes into account of H-bonding, in addition to inductive effect in them. Thus the conclusion regarding the molecular association of such long chain associated aliphatic alcohols may also be the reason to yield higher dipole moments.

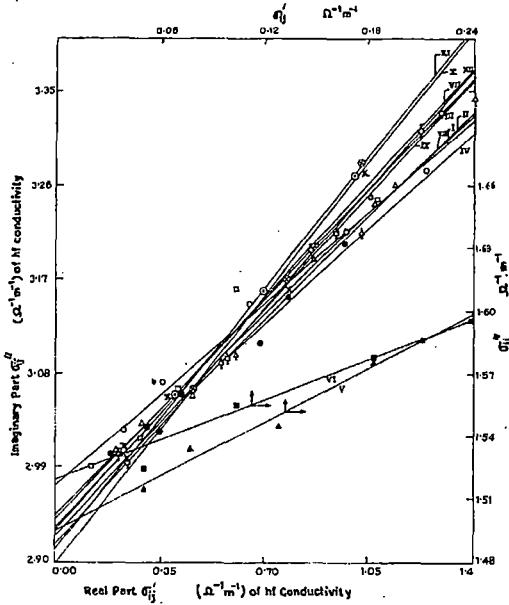


Figure 9.2: Variation of imaginary part of conductivity  $\sigma_{ij}''$  in  $\Omega^{-1}\text{m}^{-1}$  against real part of conductivity  $\sigma_{ij}'$  in  $\Omega^{-1}\text{m}^{-1}$ .

- I. 1-butanol (-O-), II. 1-hexanol (-Δ-), III. 1-heptanol (-□-), IV. 1-decanol (-●-), V. ethanol (-▲-), VI. methanol (-■-), VII. 2-methyl 3-heptanol (-Φ-), VIII. 3-methyl 3-heptanol (-△-), IX. 4-methyl 3-heptanol (-⊥-), X. 5-methyl 3-heptanol (-⊗-), XI. 4-octanol (-⊙-), XII. 2-octanol (-✕-).

## 9.2. Static relaxation parameter $X_{ij}$ and static dipole moment $\mu_s$ :

Under Static electric field  $\mu_s$  of a dielectropolar molecule (j) in a non-polar solvent (i) may be obtained from the following equation [9.10].

$$\frac{\epsilon_{oij} - 1}{\epsilon_{oij} + 2} - \frac{\epsilon_{\infty ij} - 1}{\epsilon_{\infty ij} + 2} = \frac{\epsilon_{oi} - 1}{\epsilon_{oi} + 2} - \frac{\epsilon_{\infty oi} - 1}{\epsilon_{\infty oi} + 2} + \frac{N\mu_s^2 c_j}{9\epsilon_o k_B T} \quad \dots (9.1)$$

Table 9.3: Intercept and slope of  $\sigma_{ij}'' - \sigma_{ij}'$  equation (Fig.9.2), correlation coefficient (r), % of error, relaxation time  $\tau_j$  in psec Eq. (9.10), ratio of slope of  $\sigma_{ij}''$  and  $\sigma_{ij}'$  with  $w_j$ , relaxation time  $\tau_j$  in psec from Eq.(9.11), calculated relaxation time  $\tau_j$  in psec from Gopalakrishna's method for some dielectropolar alcohols under nearly 24 GHz electric field (Q-Band Microwave) at 25 °C.

System with sl no & mol wt.	Intercepts and slopes of $\sigma_{ij}'' - \sigma_{ij}'$		Corr. Coeff r	% of error	$\tau_j$ in psec from Eq (9.10)	Ratio of slope of $\sigma_{ij}''$ & $\sigma_{ij}'$ with $w_j$	$\tau_j$ in psec from Eq (9.11)	$\tau_j^G$ in psec
1. 1-butanol in n-heptane Mj= 0.074 kg	2.9731	2.4816	0.9959	0.22	2.64	3.6215	1.81	2.47
2. 1-hexanol in n-heptane Mj= 0.102kg	2.9457	2.7315	0.9959	0.22	2.40	1.7859	3.66	2.25
3. 1-heptanol in n-heptane Mj= 0.116 kg	2.9414	2.9898	0.9973	0.15	2.19	4.0080	1.65	2.07
4. 1-decanol in n-heptane Mj= 0.158 kg	2.9465	2.5881	0.9925	0.41	2.53	2.0163	3.24	2.39
5. ethanol in benzene Mj= 0.046 kg	1.4952	4.2872	0.9880	0.72	3.77	4.5412	3.56	3.62
6. methanol in benzene Mj= 0.032 kg	1.5188	3.2088	0.9633	2.17	5.04	6.7005	2.41	4.87
7. 2-methyl 3-heptanol in n-heptane Mj= 0.130 kg	2.9162	3.2340	0.9994	0.04	2.02	3.3248	1.97	1.86
8. 3-methyl 3-heptanol in n-heptane Mj= 0.130 kg	2.9361	2.8021	0.9976	0.16	2.33	2.1826	3.00	2.26
9. 4-methyl 3-heptanol in n-heptane Mj= 0.130 kg	2.9254	3.0946	0.9988	0.08	2.11	2.7666	2.36	1.95
10. 5-methyl 3-heptanol in n-heptane Mj= 0.130 kg	2.8973	3.6562	0.9949	0.40	1.79	2.2461	2.91	1.63
11. 4-octanol in n-heptane Mj= 0.130 kg	2.9129	3.5515	0.9999	0.01	1.84	3.8763	1.69	1.68
12. 2-octanol in n-heptane Mj= 0.130 kg	2.9320	3.1511	0.9875	0.97	2.08	1.5646	4.18	1.93

$\tau_j^G$  = Relaxation time estimated from Gopalakrishna's method

where  $\epsilon_{oij}$  and  $\epsilon_{\infty ij}$  are the static and infinite frequency relative permittivities of solution (ij).  $\epsilon_0$  is the permittivities of free space =  $8.854 \times 10^{-12}$  F.m<sup>-1</sup>,  $c_j$  is the molar concentration of the solute where  $c_j = \rho_{ij}w_j/M_j$  and the other symbols carry usual meanings.

A polar liquid of weight  $W_j$  and volume  $V_j$  is mixed with a non-polar solvent of weight  $W_i$  and volume  $V_i$  to get the solution density  $\rho_{ij}$  where

$$\rho_{ij} = \frac{W_i + W_j}{V_i + V_j} = \frac{W_i + W_j}{W_i/\rho_i + W_j/\rho_j}$$

$$= \frac{\rho_i \rho_j}{w_i \rho_j + w_j \rho_i} = \frac{\rho_i}{1 - (1 - \rho_i/\rho_j)w_j} = \rho_i (1 - \gamma w_j)^{-1} \quad \dots (9.2)$$

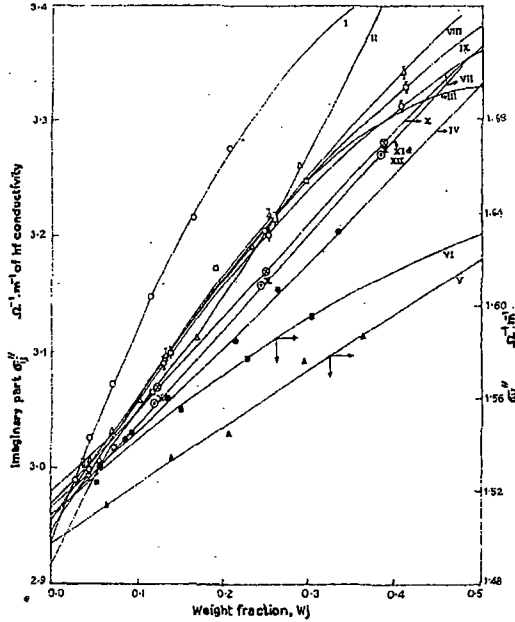


Figure 9.3: Plot of imaginary part of conductivity  $\sigma_{ij}''$  in  $\Omega^{-1}m^{-1}$  against weight fraction  $w_j$  of solute at  $25^\circ$  under 24 GHz electric field (ethanol and methanol at 9.84 GHz).

- I. 1-butanol (-O-), II. 1-hexanol (-Δ-), III. 1-heptanol (-□-), IV. 1-decanol (-●-), V. ethanol (-▲-), VI. methanol (-■-), VII. 2-methyl 3-heptanol (-Φ-), VIII. 3-methyl 3-heptanol (-⊕-), IX. 4-methyl 3-heptanol (-⊖-), X. 5-methyl 3-heptanol (-⊗-), XI. 4-octanol (-⊙-), XII. 2-octanol (-✕-).

The weight fractions  $w_j$  and  $w_i$  of solute and solvent are given by:

$$w_j = \frac{W_j}{W_i + W_j} \quad \text{and} \quad w_i = \frac{W_i}{W_i + W_j}$$

such that  $w_i + w_j = 1$  and  $\gamma = (1 - \rho_i/\rho_j)$ ,  $\rho_i$  and  $\rho_j$  are densities of pure solvent and solute respectively.

Now Eq.(9.1) may be written as :

$$\frac{\epsilon_{oij} - \epsilon_{\infty ij}}{(\epsilon_{oij} + 2)(\epsilon_{\infty ij} + 2)} = \frac{\epsilon_{oi} - \epsilon_{\infty oi}}{(\epsilon_{oi} + 2)(\epsilon_{\infty oi} + 2)} + \frac{N\rho_i\mu_s^2}{27\epsilon_o M_j k_B T} (1 - \gamma w_j)^{-1} w_j$$

$$X_{ij} = X_i + \frac{N\rho_i\mu_s^2}{27\epsilon_o M_j k_B T} w_j + \frac{N\rho_i\mu_s^2}{27\epsilon_o M_j k_B T} \gamma w_j^2 + \dots \dots \dots \quad \dots \dots (9.3)$$

The right hand side of Eq.(9.3) is obviously a polynomial equation of  $w_j$  like

$$X_{ij} = a_o + a_1 w_j + a_2 w_j^2 + \dots \dots \dots \quad \dots \dots (9.4)$$

Now comparing the linear coefficients of Eqs (9.3) and (9.4) one gets  $\mu_s$  from:

$$\mu_s = \left( \frac{27\epsilon_o M_j k_B T a_1}{N\rho_i} \right)^{1/2} \quad \dots \dots (9.5)$$

where  $a_1$  is the slope of  $X_{ij}-w_j$  curve of Fig.9.1. But  $\mu_s$  from higher coefficients of Eqs(9.3) or (9.4) are not reliable as they are involved with various effects of solvent, relative density, solute – solute association, internal field, macroscopic viscosity etc.  $\mu_s$ 's from Eq.(9.5) along with  $a_1$  are placed in Table 9.2 to compare with hf  $\mu_j$ 's presented in Table 9.4.

**9.3. High frequency dipole moment  $\mu_j$  and relaxation time  $\tau_j$  :**

Under hf electric field of GHz range the dimensionless complex dielectric constant  $\epsilon_{ij}^*$  is :

$$\epsilon_{ij}^* = \epsilon'_{ij} - j\epsilon''_{ij} \quad \dots \dots (9.6)$$

Table 9.4: Coefficients  $\alpha$  and  $\beta$  of  $\sigma_{ij}$  against  $w_j$  curve (Fig.9.5), correlation coefficients ( $r$ ), % of error, dimensionless parameter  $b$  using  $\tau_j$  from Eq. (9.10) and (9.11), computed  $\mu_j \times 10^{30}$  in C.m from Eqs (9.10) and (9.16) and Eqs (9.11) and (9.16), estimated  $\mu_j \times 10^{30}$  in C.m from Gopalakrishna's method for some dielectropolar alcohols under nearly 24 GHz electric field (Q-Band microwave) at 25 °C.

System with sl no & mol wt.	Coeff of $\sigma_{ij} - w_j$ equation		Corr. Coeff $r$	% of error	Dimensionless parameter $b=1/(1+\omega^2\tau^2)$		$\mu_j \times 10^{30}$ in C.m		$\mu_j^G \times 10^{30}$ in C.m
	$\alpha$	$\beta$			$\tau_j$ from Eq(9.10)	$\tau_j$ from Eq(9.11)	from Eq(9.10) & (9.16)	from Eq(9.11) & (9.16)	
1. 1-butanol in n-heptane Mj= 0.074 kg	2.9351	2.0769	0.9978	0.12	0.8601	0.9289	4.28	4.11	3.58
2. 1-hexanol in n-heptane Mj= 0.102kg	2.9807	0.5846	0.9961	0.21	0.8815	0.7618	2.63	2.83	3.35
3. 1-heptanol in n-heptane Mj= 0.116 kg	2.9173	1.5312	0.9928	0.39	0.9016	0.9417	4.52	4.42	3.59
4. 1-decanol in n-heptane Mj= 0.158 kg	2.9639	0.6848	0.9995	0.03	0.8699	0.8032	3.57	3.71	3.55
5. ethanol in benzene Mj= 0.046 kg	1.4970	0.2584	0.9927	0.44	0.9485	0.9538	1.44	1.43	1.33
6. methanol in benzene Mj= 0.032 kg	1.5098	0.3444	0.9928	0.43	0.9116	0.9783	1.41	1.36	1.18
7. 2-methyl 3-heptanol in n-heptane Mj= 0.130 kg	2.9437	1.2203	0.9958	0.28	0.9130	0.9169	4.22	4.21	3.42
8. 3-methyl 3-heptanol in n-heptane Mj= 0.130 kg	2.9515	1.1644	0.9985	0.10	0.8875	0.8264	4.18	4.33	3.54
9. 4-methyl 3-heptanol in n-heptane Mj= 0.130 kg	2.9454	1.2172	0.9970	0.02	0.9058	0.8849	4.23	4.28	3.48
10. 5-methyl 3-heptanol in n-heptane Mj= 0.130 kg	2.9658	0.8446	0.9999	0.01	0.9304	0.8349	3.47	3.67	3.24
11. 4-octanol in n-heptane Mj= 0.130 kg	2.9546	0.8544	0.9999	0.01	0.9267	0.9375	3.56	3.48	3.27
12. 2-octanol in n-heptane Mj= 0.130 kg	2.9542	0.8399	0.9999	0.01	0.9083	0.7103	3.51	3.97	3.32

$\mu_j^G$  = Estimated dipole moment from Gopalakrishna's method.

where  $\epsilon_{ij}'$  and  $\epsilon_{ij}''$  are the real the imaginary parts of complex permittivity  $\epsilon_{ij}^*$  in  $F. m^{-1}$  and  $\epsilon_0$  = permittivity of free space =  $8.854 \times 10^{-12} F. m^{-1}$ . The hf complex conductivity  $\sigma_{ij}^*$  of a polar-nonpolar liquid mixture of [9.15] weight fraction  $w_j$  is :

$$\sigma_{ij}^* = \omega \epsilon_0 \epsilon_{ij}'' + j \omega \epsilon_0 \epsilon_{ij}' \quad \dots (9.7)$$

where  $\sigma_{ij}' = \omega \epsilon_0 \epsilon_{ij}''$  and  $\sigma_{ij}'' = \omega \epsilon_0 \epsilon_{ij}'$  are real and imaginary parts of complex conductivity and  $j$  is a complex number =  $\sqrt{-1}$ .

The hf conductivity  $\sigma_{ij}$  is, however, obtained from:

$$\sigma_{ij} = \omega \epsilon_0 \sqrt{\epsilon_{ij}''^2 + \epsilon_{ij}'^2} \quad \dots (9.8)$$

$\sigma_{ij}''$  is related to  $\sigma_{ij}'$  by

$$\sigma_{ij}'' = \sigma_{\infty ij} + \frac{1}{\omega \tau} \sigma_{ij}' \quad \dots (9.9)$$

where  $\sigma_{\infty ij}$  is the constant conductivity at  $w_j \rightarrow 0$  and  $\tau_j$  is the relaxation time of a polar molecule.

Eq.(9.9) on differentiation with respect to  $\sigma_{ij}'$  becomes [9.11]

$$\left( \frac{d\sigma_{ij}''}{d\sigma_{ij}'} \right) = \frac{1}{\omega \tau} \quad \dots (9.10)$$

to yield  $\tau_j$ . It is often better to use the ratio of slopes of individual variation of  $\sigma_{ij}''$  and  $\sigma_{ij}'$  with  $w_j$  at  $w_j \rightarrow 0$  to avoid polar-polar interaction in a given solvent to get  $\tau_j$  from:

$$\left( \frac{d\sigma_{ij}''}{dw_j} \right)_{w_j \rightarrow 0} = \frac{1}{\omega \tau} \left( \frac{d\sigma_{ij}'}{dw_j} \right)_{w_j \rightarrow 0}$$

$$\text{or } \frac{x}{y} = \frac{1}{\omega \tau_j} \quad \dots (9.11)$$

where  $\omega = 2\pi f$ ,  $f$  being the frequency of alternating electric field.

In the region of GHz range, it is often observed that  $\sigma_{ij}'' \approx \sigma_{ij}$  and Eq.(9.9) becomes:

$$\sigma_{ij} = \sigma_{\infty ij} + \frac{1}{\omega \tau_j} \sigma'_{ij} \quad \dots (9.12)$$

$$\beta = \frac{1}{\omega \tau_j} \left( \frac{d\sigma'_{ij}}{dw_j} \right)_{w_j \rightarrow 0} \quad \dots (9.13)$$

where  $\beta$  is the slope of  $\sigma_{ij} - w_j$  curve at  $w_j \rightarrow 0$ .

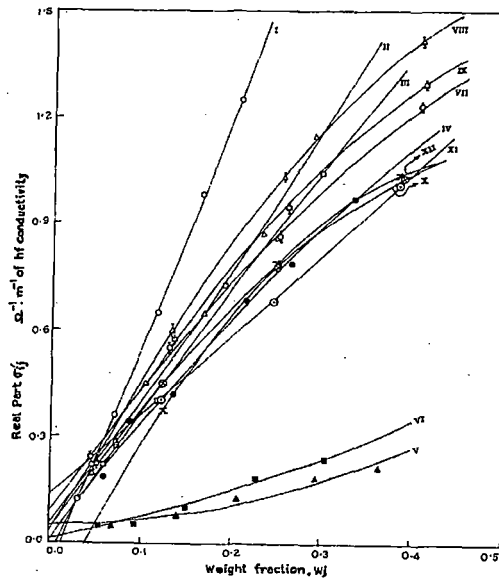


Figure 9.4: Plot of real part of conductivity  $\sigma'_{ij}$  in  $\Omega^{-1}m^{-1}$  against weight fraction  $w_j$  of solute at  $25^\circ$  under 24 GHz electric field (ethanol and methanol at 9.84 GHz).

I. 1-butanol ( $-\circ-$ ), II. 1-hexanol ( $-\triangle-$ ), III. 1-heptanol ( $-\square-$ ), IV. 1-decanol ( $-\bullet-$ ), V. ethanol ( $-\blacktriangle-$ ), VI. methanol ( $-\blacksquare-$ ), VII. 2-methyl 3-heptanol ( $-\oplus-$ ), VIII. 3-methyl 3-heptanol ( $-\boxplus-$ ), IX. 4-methyl 3-heptanol ( $-\boxminus-$ ), X. 5-methyl 3-heptanol ( $-\otimes-$ ), XI. 4-octanol ( $-\ominus-$ ), XII. 2-octanol ( $-\times-$ ).

The  $\sigma'_{ij}$  of a solution of weight fraction  $w_j$  of a polar molecule at TK is given by Smyth [9.14, 9.16] as:

$$\sigma'_{ij} = \frac{N\rho_{ij}\mu_j^2}{27\epsilon_0 k_B T M_j} \left( \frac{\omega^2 \tau}{1 + \omega^2 \tau^2} \right) (\epsilon_0 k_{oij} + 2)(\epsilon_0 k_{\infty ij} + 2) w_j \quad \dots (9.14)$$

Eq (9.14) on differentiation with respect to  $w_j$  and at  $w_j \rightarrow 0$  yields:

$$\left( \frac{d\sigma'_{ij}}{dw_j} \right)_{w_j \rightarrow 0} = \frac{N\rho_j\mu_j^2}{3\epsilon_0 k_B T M_j} \left( \frac{\epsilon_i + 2}{3} \right)^2 \left( \frac{\omega^2 \tau}{1 + \omega^2 \tau^2} \right) \quad \dots (9.15)$$

where  $N$  = Avogadro's number,  $\rho_j$  = density of solvent,  $\epsilon_i$  = permittivities of solvent,  $M_j$  = molecular weight of solute and  $k_B$  = Boltzmann constant.

From Eqs (9.13) and (9.15) one gets hf  $\mu_j$  as:

$$\mu_j = \left[ \frac{27M_j k_B T \beta}{N\rho_j (\epsilon_i + 2)^2 \omega b} \right]^{1/2} \quad \dots (9.16)$$

Where,

$$b = \frac{1}{1 + \omega^2 \tau_j^2} \quad \dots (9.17)$$

is a dimensionless parameter involved with estimated  $\tau_j$  from Eqs (9.10) and (9.11). All the computed hf  $\mu_j$  in terms of slopes  $\beta$ 's and  $b$ 's are placed in Table 9.4 in order to compare with  $\mu_{\text{theo}}$ 's,  $\mu_s$  and  $\mu_1$ ,  $\mu_2$  of the flexible part and end-over-end rotation of the whole molecule [9.5, 9.6] presented in Table 9.2.

#### 9.4. Results and discussion :

The dimensionless real  $\epsilon_{ij}'$  and imaginary  $\epsilon_{ij}''$  of the complex dielectric constants  $\epsilon_{ij}^*$  as well as the static  $\epsilon_{oij}$  and infinite frequency  $\epsilon_{\infty ij}$  of dielectric constants for different  $w_j$ 's of alcohols in different solvents at 25°C are placed in Table 9.1. The static experimental solution parameters  $X_{ij}$ 's involved with  $\epsilon_{oij}$  and  $\epsilon_{\infty ij}$  of Table 9.1 are shown in Fig. 9.1, for different  $w_j$  of alcohols. The nature of variation of  $X_{ij}$  with  $w_j$  are parabolic in nature satisfying a polynomial equation:  $X_{ij} = a_0 + a_1 w_j + a_2 w_j^2$ . The coefficients of  $X_{ij} - w_j$  curves i.e.  $a_0$ ,  $a_1$  and  $a_2$  are placed in the 2nd, 3rd and 4th columns of Table 9.2. As evident from Fig. 9.1, the  $X_{ij} - w_j$  curves for methanol, ethanol and 3-methyl-3-heptanol are convex in nature as their coefficients of quadratic terms in Table 9.2 are negative. The remaining  $X_{ij}$ 's on the other hand, showed a gradual increase with  $w_j$ 's for all the coefficients of the curves

are positive as seen in Table 9.2. The anomalous behaviour of  $X_{ij} - w_j$  curves from linearity for all the alcohols in different solvents at a given temperature in  $^{\circ}\text{C}$  may rouse an interesting relaxation mechanism in such long chain associated liquids. In comparison to octyl alcohols, the curves of normal alcohols in higher concentrations are highly concave having a tendency to meet at a common point on the  $X_{ij}$  axis at  $w_j \rightarrow 0$ .

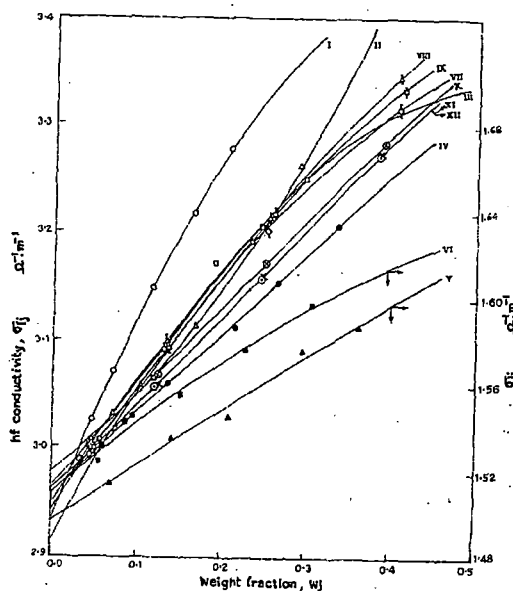


Figure 9.5: Variation of total hf conductivity  $\sigma_{ij}$  in  $\Omega^{-1}\text{m}^{-1}$  with weight fraction  $w_j$  of solute at  $25^{\circ}$  under 24 GHz electric field (ethanol and methanol at 9.84 GHz).

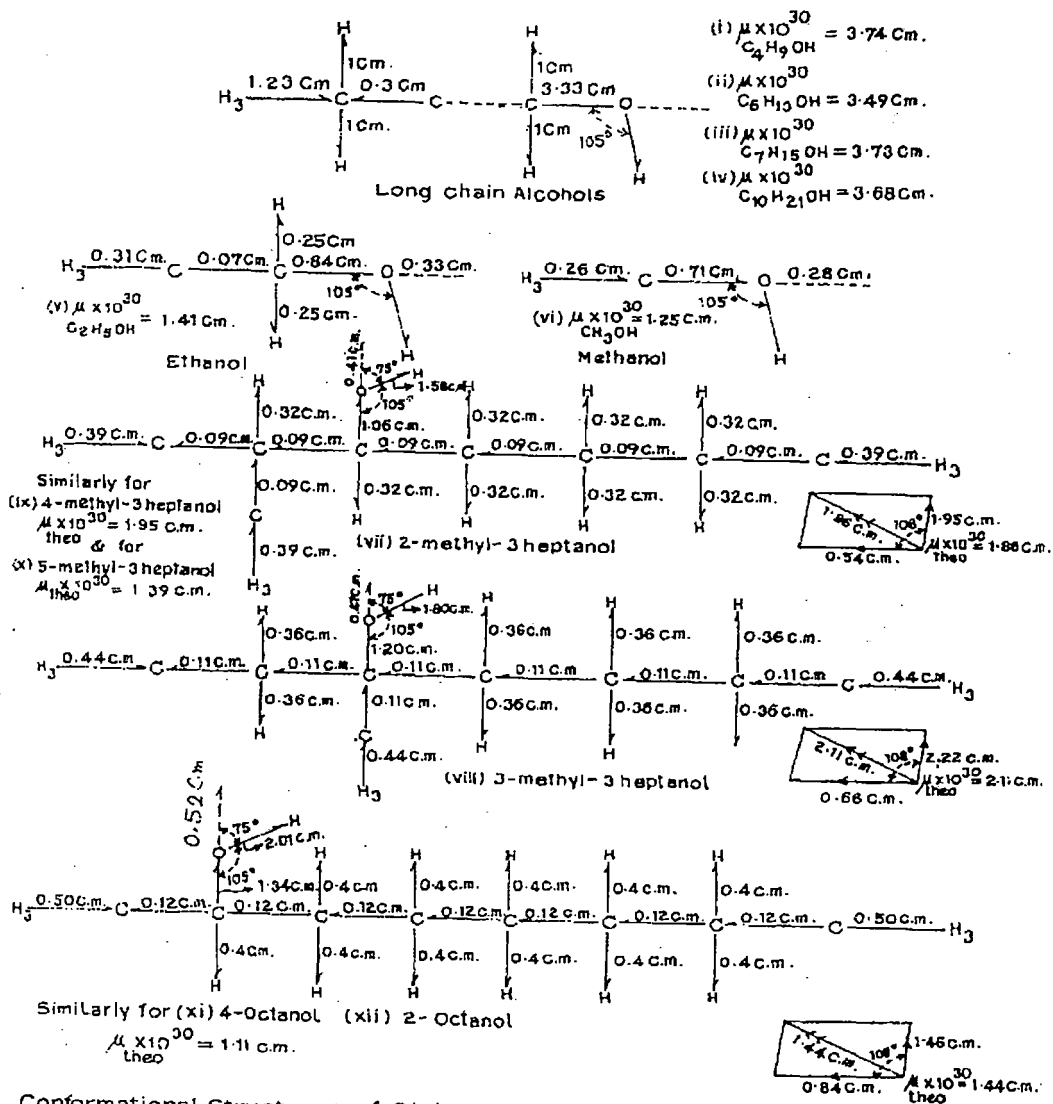
I. 1-butanol ( $-\text{O}-$ ), II. 1-hexanol ( $-\Delta-$ ), III. 1-heptanol ( $-\square-$ ), IV. 1-decanol ( $-\bullet-$ ), V. ethanol ( $-\blacktriangle-$ ), VI. methanol ( $-\blacksquare-$ ), VII. 2-methyl 3-heptanol ( $-\Phi-$ ), VIII. 3-methyl 3-heptanol ( $-\nabla-$ ), IX. 4-methyl 3-heptanol ( $-\ddagger-$ ), X. 5-methyl 3-heptanol ( $-\otimes-$ ), XI. 4-octanol ( $-\ominus-$ ), XII. 2-octanol ( $-\times-$ ).

This sort of behaviour of  $X_{ij} - w_j$  curves of Fig. 9.1 arises either due to solute-solute i.e. dimer or solute-solvent i.e. monomer formations in comparatively high concentrations. The convex shape of ethanol and methanol occurs for the probable experimental uncertainty in their  $\epsilon_{0ij}$  and  $\epsilon_{\infty ij}$  measurements. The identical nature of variations of all the octyl alcohols have almost the same slope, but of different intercepts as a result of salvation effect. Their  $X_{ij}$ 's have tendency to become closer within  $0.1 \leq w_j \leq 0.2$  indicating various molecular association in them.

In case of non-associated liquids  $a_2$ 's were found to be vanishingly small in comparison to  $a_0$  and  $a_1$  to yield almost linear variation of  $X_{ij}$  against  $w_j$ . The estimated correlation coefficient ( $r$ ) and the percentage of error (%) entered in 5<sup>th</sup> and 6<sup>th</sup> columns of Table 9.2 for all the alcohols are such that one may rely on the linear term of  $X_{ij} - w_j$  curve to compute  $\mu_j$ 's from Eq. (9.5).  $\mu_s$ 's thus computed are placed in the 7<sup>th</sup> column of Table 9.2 to compare with  $\mu_{\text{theo}}$ 's obtained from bond angles and bond moments of the substituent polar groups, as presented in Fig. 9.6 and  $\mu_1$  and  $\mu_2$  of the flexible part and the whole molecule by the double relaxation method [9.5,9.6] at nearly 24 GHz electric field. The smaller and larger deviations of  $X_{ij}$ 's from linearity with  $w_j$ 's as seen in Fig.9.1, confirm the molecular associations of such associated dielectropolar liquids in different solvents.

The relaxation times  $\tau_j$ 's are, however, derived from the slope of linear [9.11] variation of  $\sigma_{ij}''$  with  $\sigma_{ij}'$  of Fig. 9.2 for all the alcohols. Although, the experimental data, on the other hand, did not strictly fall on the fitted linear curves of  $\sigma_{ij}''$  and  $\sigma_{ij}'$  both in  $\Omega^{-1}\text{m}^{-1}$  as drawn in Fig. 9.2, the slope of  $\sigma_{ij}''$  against  $\sigma_{ij}'$  of Fig. 9.2 was, however, used to obtain  $\tau_j$  from Eq. (9.10). The 2<sup>nd</sup>, 3<sup>rd</sup> and 6<sup>th</sup> columns of Table 9.3 contain all the estimated intercepts and slopes together with the measured  $\tau_j$ 's. The linearity of  $\sigma_{ij}''$  curves against  $\sigma_{ij}'$  as shown graphically in Fig. 9.2 is again tested by correlation coefficients  $r$ 's and % of errors. They are entered in the 4<sup>th</sup> and 5<sup>th</sup> columns of Table 9.3 only to see how far  $\sigma_{ij}''$  and  $\sigma_{ij}'$  are correlated to each other. But it is often better to use the ratio of the individual slopes of variation of  $\sigma_{ij}''$  and  $\sigma_{ij}'$  with  $w_j$  at  $w_j \rightarrow 0$  to get  $\tau_j$  by using Eq. (9.11) are not in close agreement with those obtained from Eq. (9.10) and by freshly calculated Gopalakrishna's method, as seen in Table 9.3. Figs (9.3) and (9.4) showed that both  $\sigma_{ij}''$  and  $\sigma_{ij}'$  vary nonlinearly with  $w_j$ . The nonlinear behaviour of  $\sigma_{ij}''$  and  $\sigma_{ij}'$  as seen in Figs 9.3 and 9.4 with  $w_j$ 's invites the associational and structural aspects of such long chain dielectropolar associated molecules. The latter method to measure  $\tau_j$ 's thus appears to be a significant improvement [9.12,9.13] over the former one [9.11] as it eliminates the polar-polar interaction in a given solvent.

The hf  $\mu_j$  from Eq. (9.16) was obtained from the slope  $\beta$  of the nonlinear variation of  $\sigma_{ij}$  in  $\Omega^{-1}\text{m}^{-1}$  with  $w_j$  of Fig. 9.5 and dimensionless parameter  $b$  of Eq. (9.17) in terms of  $\tau_j$  obtained by both the methods. The intercept  $\alpha$  and slope  $\beta$  of hf  $\sigma_{ij}$  with  $w_j$  curves of Fig.9.5



**Conformational Structures of Dielectropolar Alcohols :-**

[Bond moment  $\times 10^{30}$  coulomb-metre (c.m.) (given in figures)]

Figure 9.6: Conformational structures of dielectropolar alcohols (theoretical dipole moments  $\mu_{\text{theo}}$  from bond angles and reduced bond moments)

are entered in the 2<sup>nd</sup> and 3<sup>rd</sup> columns of Table 9.3. It is interesting to note that the curves of  $\sigma_{ij} - w_j$  variation of Fig 9.5 are almost identical with  $\sigma_{ij}'' - w_j$  curves of Fig. 9.3. This fact at once confirms the applicability of the approximation that  $\sigma_{ij}' \approx \sigma_{ij}$  as done in Eqs (9.9) and (9.12). The imaginary  $\sigma_{ij}''$  and total hf  $\sigma_{ij}$  in case of normal alcohols in Figs 9.3 and 9.5 decrease gradually with  $w_j$ 's of 1-butanol to methanol except ethanol. This can be explained

on the basis of the fact that the polarity of the molecules decreases from 1-butanol to methanol. Both  $\sigma_{ij}''$  and  $\sigma_{ij}$  in Figs 9.3 and 9.5 of all the octyl alcohols are found to be closer only to show their nearly same polarity. The almost coincident curves of 4-octanol ( $-\ominus-$ ) and 2-octanol ( $-\times-$ ) arise due to their identical polarity as estimated in Fig 9.6.

The estimated  $\mu_s$ 's and  $\mu_j$ 's in Table 9.2 and 9.4 are then compared with the  $\mu_1$  and  $\mu_2$  in Table 9.2 by double relaxation method [9.5,9.6] and those by freshly calculated Gopalakrishna's method. For all the normal alcohols  $\mu_j$ 's and  $\mu_s$ 's are in excellent agreement with Gopalakrishna's  $\mu_j$ 's (reported data) and  $\mu_1$ . The estimated  $\mu_j$ 's for octyl alcohols agree with reported  $\mu_j$ 's and  $\mu_1$ . All these discussions made above establish the fact that a part of the molecule is rotating under GHz electric field. Slight disagreement in  $\mu$ 's and the reported ones arises due to steric hindrances of the substituent polar units of their structural configurations of Fig. 9.6 and the existence of associative nature for their hydrogen bonding. Unlike normal alcohols,  $\mu_s$ 's are always lower than  $\mu_j$ 's and  $\mu_1$ 's for octyl alcohols. This at once reveals under static electric field the possible formation of dimmers which undergo to rupture into the solute solvent association i.e. monomer in the hf electric field to increase  $\mu$ 's. It is also evident that dimmer formation is favourable in octyl alcohols than normal alcohols due to existence of strong inductive effect for their  $-\text{OH}$  groups at the end of the molecular chains.

The theoretical dipole moments  $\mu_{\text{theo}}$ 's of all the alcohols under study were calculated from the available bond angles and bond moments of the substituent polar groups like  $\text{H}_3\text{-C}$ ,  $\text{C-H}$ ,  $\text{C-O}$ ,  $\text{O-H}$  ( $\angle 105^\circ$ ) and  $\text{C-C}$  of  $1.23 \times 10^{-30}$  Coulomb-meter (C.m.) as presented elsewhere [9.5,9.6]. The values thus estimated are then made closer with the measured static  $\mu_s$ 's or even  $\mu_j$ 's by reducing the available bond moments by a factor  $\mu_s/\mu_{\text{theo}}$  which takes into account of the inductive and mesomeric effects of the substituent polar groups as shown in Fig. 9.6. An inductive effect of polar unit acts along the chain of the molecular axis of the normal alcohols to make them strongly polar due to presence of  $-\text{OH}$  group at their ends of the axis. The comparatively lower  $\mu_{\text{theo}}$ 's in octyl alcohols is probably due to screening effect of their  $-\text{OH}$  groups by other polar groups like  $\text{H}_3\text{-C}$ ,  $\text{C-H}$  which favour the dimmer formation of these alcohols through H-bonding to make their  $\mu_s$ 's and  $\mu_j$ 's lower than the normal alcohol as seen in Fig. 9.6.

## 9.5. Conclusions :

The modern internationally accepted symbols of dielectric terminologies and parameters in SI unit are conveniently used to obtain static and hf dipole moments  $\mu_s$  and  $\mu_j$  in terms of relaxation time  $\tau_j$  of a polar molecule.  $\tau_j$ 's measured from the slope of imaginary  $\sigma_{ij}''$  against real  $\sigma_{ij}'$  of complex hf conductivity  $\sigma_{ij}^*$  for different  $w_j$  are not in agreement with those measured from the ratio of the individual slopes  $\sigma_{ij}''-w_j$  and  $\sigma_{ij}'-w_j$  curves at  $w_j \rightarrow 0$  indicating the applicability of the latter method in long chain dielectropolar alcohols. This method of determination of  $\tau_j$  is a significant improvement over the previous one as it eliminates polar-polar interactions in a given solvent. The comparison of  $\mu_j$ 's and  $\mu_s$ 's with  $\mu_1$  and  $\mu_2$  of the flexible part and the whole molecule by double relaxation method and  $\mu_{theo}$ 's from bond angles and bond moments seems to be an interesting phenomenon to have deep insight into relaxation mechanism of dielectropolar alcohols.

The results indicate that a part of the molecule is rotating under GHz electric field. The slight departure among the measured  $\mu_s$ ,  $\mu_j$  and  $\mu_{theo}$  reveals different associational aspects of dielectropolar alcohols in different solvents through the frequency dependence of relaxation parameters. It also shows the strong polar nature of normal alcohols which favour solute-solvent association due to the presence of -OH group at the end of their bond axis. But the comparatively lower values of  $\mu_j$ 's in octyl alcohols indicates the solute-solute association due to -H bonding supported by the fact that -OH being screened by -CH<sub>3</sub> and a large number of >CH<sub>2</sub> polar groups. The  $\mu_s/\mu_{theo}$ 's are almost constant for all the alcohols to take into account of all these facts in addition to their material property of the system. This study further supports the rotation of -OH group along the  $\equiv C-O-$  bond of all the alcohols under static and hf electric fields. Moreover, the methodology so far developed within the framework of Debye and Smyth model appears to be sound, simple, straightforward and useful to arrive at associational and structural aspects of alcohols which are thought to be non-Debye in relaxation behaviour.

## References :

- [9.1] K V Gopalakrishna, *Trans Farad Soc*, **33** 767 (1957).
- [9.2] G S Kastha, J Dutta, J Bhattacharyya & S B Roy, *Indian J Phys*, **43** 14 (1969)
- [9.3] S K Dutta, C R Acharyya & S Acharyya, *Indian J Phys*, **55B** 140 (1981).
- [9.4] S K Sit, N Ghosh, U Saha & S Acharyya, *Indian J Phys*, **71B** 533 (1997).
- [9.5] S K Sit & S Acharyya, *Indian J Phys*, **70B** 19 (1996).
- [9.6] S K Sit, N Ghosh & S Acharyya, *Indian J Pure & Appl Phys*, **35** 329 (1997).
- [9.7] L Glasser, J Crossley & C P Smyth, *J Chem Phys*, **57** 3977 (1972).
- [9.8] A K Ghosh, *PhD Dissertation*, NBU, (1981).
- [9.9] J Crossley, L Glasser & C P Smyth, *J Chem Phys*, **55** 2197 (1971).
- [9.10] P Debye, *Polar Molecules* (Chemical Catalogue), 1929.
- [9.11] M B R Murthy, R L Patil & D K Deshpande, *Indian J Phys*, **63B** 491(1989).
- [9.12] N Ghosh, R C Basak, S K Sit & S Acharyya, *J Molecular Liquid*, (Accepted for publication), 2000.
- [9.13] R C Basak, S K Sit, N Nandi & S Acharyya, *Indian J Phys*, **70B** 37 (1996).
- [9.14] R C Basak, A Karmakar, S K Sit & S Acharyya, *Indian J Pure & Appl Phys*, **37** 224 (1999).
- [9.15] F J Murphy & S O Morgan, *Bell Syst Tech J*, **18** 502 (1939).
- [9.16] C P Smyth, *Dielectric behaviour and structure*, (McGrawHill, New York), 1955.

## *Chapter 10*

### **SUMMARY AND CONCLUSIONS**

The subject matter of the thesis entitled "Dispersion and absorption phenomena of dipolar liquid in nonpolar solvent" has been divided into the following chapters. The Chapter1 entitled "General introduction and review of the previous works" contains the research works done by a large number of workers in dispersion and absorption phenomena of dipolar liquid in non-polar solvent developed chronologically from 1912 onwards. The present author in this chapter collects them. The Chapter2 under the caption of "Scope and objective of the present work" includes the different theoretical formulae developed by the present worker in order to apply them in a large number of polar-nonpolar liquid mixtures. Thus an important conclusion was, however, reached by the present research worker in order to publish them in reputed Indian and foreign journals.

The Chapter3 presents a derived linear equation  $(\chi_{oij} - \chi_{ij}')/\chi_{ij}' = \omega(\tau_1 + \tau_2) \chi_{ij}''/\chi_{ij}' - \omega^2 \tau_1 \tau_2$  for different weight fractions  $w_j$ 's of disubstituted benzenes and anilines (j) in aprotic and nonpolar solvents (i)  $C_6H_6$  and  $CCl_4$  under 9.945 GHz electric field are obtained from the available measured dielectric relative permittivities at  $35^\circ C$ . The double relaxation times  $\tau_1$  and  $\tau_2$  of the flexible part and the whole molecule are estimated from the slope and intercept of the above equation.  $\chi_{ij}'$  and  $\chi_{ij}''$  are the real and imaginary parts of the high frequency complex orientational dielectric susceptibility  $\chi_{ij}^*$  and  $\chi_{oij}$  is the low frequency dielectric susceptibility which is real. They are, however, related with the measured relative permittivities.  $\tau_j$ 's are calculated from the ratio of the individual slope of the variation of  $\chi_{ij}''$  and  $\chi_{ij}'$  with  $w_j$ 's at  $w_j \rightarrow 0$  assuming single Debye like dispersion and compared with Murthy et al ( Ind. J. Phys. 1989 63B 491 ) and Gopalakrishna (Trans. Faraday Soc. 1957 53 767 ). The weighted contributions  $c_1$  and  $c_2$  towards dielectric relaxations for  $\tau_1$  and  $\tau_2$  can, however, be obtained from Fröhlich's theoretical formulations of  $\chi_{ij}'/\chi_{oij}$  and  $\chi_{ij}''/\chi_{oij}$  and compared with those from the experimentally measured values of  $(\chi_{ij}'/\chi_{oij})_{w_j \rightarrow 0}$  and  $(\chi_{ij}''/\chi_{oij})_{w_j \rightarrow 0}$ . The latter measured values are employed to get symmetric distribution parameter  $\gamma$  to yield symmetric relaxation time  $\tau_s$ . The curve of  $(1/\phi)\log(\cos\phi)$  against  $\phi$  in degrees together with the values of  $(\chi_{ij}'/\chi_{oij})_{w_j \rightarrow 0}$  and  $(\chi_{ij}''/\chi_{oij})_{w_j \rightarrow 0}$  experimentally obtained, give the asymmetric distribution parameter  $\delta$  to get the characteristic relaxation time  $\tau_{cs}$ . All these findings ultimately establish the different types of relaxation behaviours for such complex molecules. The dipole moments  $\mu_1$  and  $\mu_2$  for the flexible part and the whole molecule are ascertained from  $\tau_1$  and  $\tau_2$  and the linear coefficients  $\beta_1$  of  $\chi_{ij}' - w_j$  and

$\beta_2$  of  $\sigma_{ij} - w_j$  curves respectively where  $\sigma_{ij}$  is the hf conductivity. The  $\mu$ 's are finally compared with the reported  $\mu$ 's and  $\mu_{\text{theo}}$ 's derived from available bond angles and bond moments of the substituted polar groups of disubstituted anilines to conclude a part of the molecule is rotating while the whole molecular rotation occurs for disubstituted benzenes. The slight disagreement between measured  $\mu$ 's and  $\mu_{\text{theo}}$ 's can, however, be interpreted by the inductive, mesomeric and electromeric effects of the polar groups of the parent molecules.

The ratio of the linear coefficients of the fitted individual equations of  $\chi_{ij}'' - w_j$  and  $\chi_{ij}' - w_j$  of some para substituted derivative polar liquid molecules in solvents dioxane and benzene, are used to get their relaxation times  $\tau_j$ 's under 10 GHz electric field at various experimental temperatures in  $^{\circ}\text{C}$ .  $\chi_{ij}'$  and  $\chi_{ij}''$  are the real and imaginary parts of the high frequency (hf) complex dielectric susceptibility  $\chi_{ij}^*$  as a function of weight fractions  $w_j$ 's of polar solutes at each experimental temperature. The measured  $\tau_j$ 's of solutes at different temperatures, by Eyring's rate process equations, yield thermodynamic energy parameters: enthalpy of activation  $\Delta H_{\tau}$ , entropy of activation  $\Delta S_{\tau}$ , and free energy of activation  $\Delta F_{\tau}$ , due to dielectric relaxation to study stability and physico chemical properties of the systems. The parameter  $\delta$  from the slope of linear variation of  $\ln\tau_j T$  with  $\ln\eta_i$  provides the information of the solvent environment around the solute molecules and also gives  $\Delta H_{\eta}$ , the enthalpy of activation due to viscous flow of the solvent.  $\eta_i$  is the coefficient of viscosity of the solvent used. The estimated Debye and Kalman factors  $\tau_j T / \eta$  and  $\tau_j T / \eta^{\delta}$  confirm Debye relaxation mechanism in such para compounds. Debye-Pellat's equations are, therefore, used to obtain static as well as infinitely hf permittivities  $\epsilon_{0ij}$  and  $\epsilon_{\infty ij}$  respectively to get static parameter  $X_{ij}$  where  $X_{ij}$  vs  $w_j$  equations are used to get static dipole moments  $\mu_s$ 's while the slopes  $\beta$ 's of  $\chi_{ij}' - w_j$  equations to yield hf  $\mu_j$ 's in terms of estimated  $\tau_j$ 's. They are, however, compared with the theoretical  $\mu_{\text{theo}}$ 's from the available bond moments of the substituted flexible polar groups attached to the parent molecules to show the existence of the inductive, mesomeric and often electromeric effects in them. All these factors are presented in Chapter4 of this thesis.

The Chapter5 reports the two relaxation times  $\tau_1$  and  $\tau_2$  due to rotations of the flexible parts and the whole molecules of some aprotic polar liquids (j) like N, N – dimethyl

sulphoxide (DMSO); N, N – dimethyl formamide (DMF), N, N – dimethyl acetamide (DMA) and N, N – diethyl formamide (DEF) in benzene (i) which are estimated from the measured real  $\chi_{ij}'$  and imaginary  $\chi_{ij}''$  part of hf complex dielectric orientational susceptibility  $\chi_{ij}^*$  and low frequency susceptibility  $\chi_{oij}$  at different weight fractions  $w_j$ 's of the solutes at various experimental temperatures [Saha et al J Phys. D: Appl. Phys. 27 (1994) 596]. The relative contributions  $c_1$  and  $c_2$  due to  $\tau_1$  and  $\tau_2$  are calculated from Fröhlich's equations and graphical technique. All the  $c$ 's are positive from Fröhlich's equations while some  $c_2$ 's are negative from graphical method. The dipole moments  $\mu_2$  &  $\mu_1$  in Coulomb-metre (C.m) measured from the slope  $\beta$ 's of  $\chi_{ij}'-w_j$  curves are compared with those of conductivity  $\sigma_{ij}$  measurements using  $\tau$ 's from the ratio of individual slope of  $(d\chi_{ij}''/dw_j)_{w_j \rightarrow 0}$  and  $(d\chi_{ij}'/dw_j)_{w_j \rightarrow 0}$ , linear slope of  $\chi_{ij}''-\chi_{ij}'$  along with Gopalakrishna's method [Trans. Faraday Soc. 53 (1957) 767]. The estimated  $\mu_1$ 's agree with the measured and reported  $\mu$ 's to indicate that the flexible part of the molecule is rotating under GHz electric field. The theoretical dipole moment  $\mu_{theo}$ 's are obtained in terms of available bond moments of the substituent polar groups attached to the parent molecules acting as pusher or puller of electrons due to inductive, mesomeric and electromeric effects in them under hf electric field. The variation of  $\mu_1$  with temperature suggests the elongation of bond moments. The energy parameters such as enthalpy of activation  $\Delta H_\tau$ , free energy of activation  $\Delta F_\tau$  and entropy of activation  $\Delta S_\tau$ 's are obtained for DMSO only assuming dielectric relaxation as a rate process to know the molecular dynamics. The variation of  $\ln(\tau_1 T)$  against  $1/T$  of DMSO reveals that it obeys Eyring rate theory unlike  $\ln(\tau_2 T)$  against  $1/T$  curve.

The Chapter 6 is concerned with a graphical method to measure the double relaxation times  $\tau_2$  and  $\tau_1$  for the rotations of the flexible part and the whole molecule of some long-chain alcohols in n-heptane under 24.33 GHz (K-Band), 9.25 GHz (X-Band) and 3.00 GHz (J-Band) electric fields on the basis of Debye and Fröhlich models. The fixed  $\tau_1$  and  $\tau_2$  at those frequencies are compared with the average  $\tau_1$  and  $\tau_2$  measured by the single frequency method of Saha et al (1994) and reported average  $\tau$ 's. This reveals the material property of the chemical systems in identical environments.  $\tau$ 's thus obtained agree well with the reported average  $\tau$ 's at three different experimental frequencies for most of the alcohols. This at once indicates the whole molecular rotation of the dipolar molecules at those

frequencies. The dipole moments  $\mu_1$  and  $\mu_2$  are, however, measured from the linear coefficients  $\beta$ 's of hf susceptibilities  $\chi_{ij}$ 's curves against weight fractions  $w_j$ 's of the alcohols at all the frequencies in terms of the graphically obtained  $\tau_1$  and  $\tau_2$  and the reported  $\tau$ 's by the existing methods. Theoretical dipole moments  $\mu_{\text{theo}}$ 's from the available bond angles and bond moments are also determined. The slight disagreement among the  $\mu_{\text{theo}}$ 's, reported and estimated  $\mu$ 's indicates the existence of the inductive, electromeric and mesomeric effects of the substituent polar group  $-\text{OH}$  attached to the parent ones.

The relaxation time  $\tau$  and dipole moment  $\mu$  of some methyl benzenes and ketones (j) in a nonpolar solvent benzene (i) at  $25^\circ\text{C}$  under 9.585 GHz electric field are obtained from the measured real and imaginary parts  $\epsilon_{ij}'$  and  $\epsilon_{ij}''$  of hf complex relative permittivity  $\epsilon_{ij}^*$  at various weight fractions  $w_j$ 's of a polar liquid. The methodology to get  $\tau$  from the ratio of the individual slopes of real  $\sigma_{ij}' (= \omega \epsilon_0 \epsilon_{ij}'')$  and imaginary  $\sigma_{ij}'' (= \omega \epsilon_0 \epsilon_{ij}')$  of complex hf conductivity  $\sigma_{ij}^*$  curve against  $w_j$ 's, seems to be a significant improvement over the existing one like the linear slope of  $\sigma_{ij}'' - \sigma_{ij}'$  curve. The variation of  $\sigma_{ij} - w_j$  curve like  $\sigma_{ij}'' - w_j$  curve is often convex indicating the probable occurrence of phase change in the polar-nonpolar liquid mixture after a certain concentration. The convex nature of  $\sigma_{ij}' - w_j$  curves for some systems indicate the maximum absorption of hf electric energy unlike other systems. The estimated  $\mu$ 's from slope  $\beta$  of hf conductivity  $\sigma_{ij} - w_j$  curve and  $\tau$  from both the methods are compared with the work of Gopalakrishna to establish the applicability of the methods. Theoretical dipole moment  $\mu_{\text{theo}}$ 's from available bond angles and bond moments are calculated by considering inductive, mesomeric and electromeric effects of the substituent polar groups of the molecules. All this information is presented in Chapter7.

In Chapter8 the use of slopes of individual variation of the imaginary  $\sigma_{ij}''$  and real  $\sigma_{ij}'$  parts of high frequency (hf) conductivity  $\sigma_{ij}^*$  with the weight fractions  $w_j$ 's of a solute is employed to determine the relaxation times  $\tau_j$ 's of some monosubstituted anilines in  $\text{C}_6\text{H}_6$ . The dipole moments  $\mu_j$ 's of such polar molecules in terms of estimated  $\tau_j$ 's are calculated and compared with those by using the existing methods for  $\tau_j$ ' (Murthy et al 1989). Excellent agreement of  $\mu_j$ 's in all cases except m-toluidine indicates the applicability of both the methods. The hf  $\mu_j$  as well as static  $\mu_s$  differ from  $\mu_{\text{theo}}$ 's as obtained from the available bond angles and bond moments. The reduced bond moments are, however,

calculated from the estimated  $\mu_j$ ,  $\mu_s$  and  $\mu_{\text{theo}}$  to yield the exact  $\mu$ 's in close agreement with  $\mu_s$  and  $\mu_j$  only to establish the presence of inductive and mesomeric moments of the substituent groups, in addition to solute-solute or solute-solvent molecular associations among the molecules in the solution. The  $\mu_j$ 's being little affected by the frequency of the electric field, are finally compared with  $\mu_2$  and  $\mu_1$  (Sit and Acharyya, 1996) due to rotations of the whole and a part of the molecules. They are very close to  $\mu_1$  indicating the fact that a part of the molecule is rotating under the electric field of 10 GHz.

Similarly the Chapter 9 gives the structural and associational aspects of some straight chain alcohols from their static dipole moments  $\mu_s$ 's and high frequency (hf) dipole moments  $\mu_j$ 's in terms of relaxation times  $\tau_j$ 's under effective dispersive region of nearly 24 GHz electric field.  $\tau_j$ 's are estimated from the slope of the linear variation of imaginary part  $\sigma_{ij}''$  with real part  $\sigma_{ij}'$  of hf complex conductivity  $\sigma_{ij}^*$  for different weight fractions  $w_j$  in order to compare with those obtained from the ratio of the individual slopes of  $\sigma_{ij}''$  and  $\sigma_{ij}'$  with  $w_j$ 's of solutes. The linear coefficients of the static experimental parameter  $X_{ij}$  with  $w_j$  are used to obtain  $\mu_s$ . The slopes  $\beta$ 's of  $\sigma_{ij}$  with  $w_j$ 's are employed to get hf  $\mu_j$  in terms of  $\tau_j$ 's obtained by two methods only to see how far they agree with  $\mu_2$  and  $\mu_1$  from double relaxation method (Sit & Acharyya, 1996 and Sit et al 1997). It is observed that -OH bond of alcohols about  $\equiv\text{C}-\text{O}-$  bond rotates under GHz electric field. The slight disagreement of theoretical dipole moments  $\mu_{\text{theo}}$ 's from available bond angles and bond moments with  $\mu_j$ 's and  $\mu_s$ 's suggest the strong hydrogen bonding in them, in addition to mesomeric and inductive moments of the substituent polar groups attached to the parent molecule.

Theories of dispersions and absorptions have been formulated in terms of relative permittivities  $\epsilon_{ij}$ 's. Measurement of  $\tau_j$ 's and  $\mu_j$ 's were carried out in terms of hf conductivity  $\sigma_{ij}$  which is concerned with bound molecular charges of polar molecules. Nowadays, it is preferred to study in terms of dielectric orientation susceptibility  $\chi_{ij}$ 's in SI units.  $\chi_{ij}$ 's are supposed to be involved only with orientation polarisation of molecules. It is to be noted that the dielectric susceptibilities  $\chi$ 's are given by the subtraction of either 1 or  $\epsilon_\infty$  from relative permittivity  $\epsilon_r$ . If 1 is subtracted, the susceptibility due to all operating polarisation processes results, while if  $\epsilon_\infty$  is subtracted from the low frequency value of  $\epsilon_r$ , the susceptibility due only to orientation polarisation processes is given. The methods appear to

be much simpler, straightforward and easy to arrive at the expected conclusion. Moreover, the polar-nonpolar liquid mixtures can be studied by taking into account of the concept of other models like Onsager, Kirkwood, Fröhlich etc. But those models are not so simpler like Debye-Smyth. Recently Thermally Stimulated Depolarisation Current Density (TSDCD) and Isothermal Frequency Domain AC Spectroscopy (IFDS) are used to study the dispersion and absorption phenomena of dielectropolar liquids.

The correlation between the conformational structures obtained from the available bond angles and bond lengths with the observed results enhances the scientific contents and adds a new horizon of understanding to the existing knowledge of dispersion and absorption. The thesis thus provides the future workers in this field to open a new and vast scope to work further in polar-nonpolar liquid mixtures under hf electric field.

## **REPRINTS**

## Dielectric relaxation phenomena of some aprotic polar liquids under giga hertz electric field

A Karmakar, U K Mitra, K Dutta, S K Sit & S Acharyya

Department of Physics, Raiganj College (University College), P.O. Raiganj, Dist: Uttar Dinajpur (West Bengal)

Received 17 October 2005; revised 27 June 2006; accepted 5 July 2006

The two relaxation times  $\tau_1$  and  $\tau_2$  due to rotations of the flexible parts and the whole molecules of some aprotic polar liquids (j) like N, N-dimethyl sulphoxide (DMSO); N, N-dimethyl formamide (DMF), N, N-dimethyl acetamide (DMA) and N, N-diethyl formamide (DEF) in benzene (i) are estimated from the measured real  $\chi_{ij}'$  and imaginary  $\chi_{ij}''$  part of  $hf$  complex dielectric orientational susceptibility  $\chi_{ij}^*$  and low frequency susceptibility  $\chi_{oij}$  at different weight fractions  $w_j$ 's of solute at various experimental temperatures [Saha *et al.*, *J Phys. D: Appl Phys*, 27 (1994) 596]. The relative contributions  $c_1$  and  $c_2$  due to  $\tau_1$  and  $\tau_2$  are calculated from Fröhlich's equations and graphical technique. All the  $c$ 's are positive from Fröhlich's equations while some  $c_2$ 's are negative from graphical method. The dipole moments  $\mu_2$  and  $\mu_1$  in Coulomb-metre (C.m) measured from the slope  $\beta$ 's of  $\chi_{ij}'-w_j$  curves are compared with those of conductivity  $\sigma_{ij}$  measurements using  $\tau$ 's from the ratio of individual slope of  $(d\chi_{ij}''/dw_j)_{w_j \rightarrow 0}$  and  $(d\chi_{ij}'/dw_j)_{w_j \rightarrow 0}$ , linear slope of  $\chi_{ij}''-\chi_{ij}'$  along with Gopalakrishna's method [Trans Faraday Soc, 53 (1957) 767]. The estimated  $\mu_1$ 's agree with the measured and reported  $\mu$ 's to indicate that the flexible part of the molecule is rotating under GHz electric field. The theoretical dipole moment  $\mu_{theo}$ 's are obtained in terms of available bond moments of the substituent polar groups attached to the parent molecules acting as pusher or puller of electrons due to inductive, mesomeric and electromeric effects in them under  $hf$  electric field. The variation of  $\mu_1$  with temperature suggests the elongation of bond moments. The energy parameters such as enthalpy of activation  $\Delta H_\tau$ , free energy of activation  $\Delta F_\tau$  and entropy of activation  $\Delta S_\tau$ 's are obtained for DMSO only assuming dielectric relaxation as a rate process to know the molecular dynamics. The variation of  $\ln(\tau_1 T)$  against  $1/T$  of DMSO reveals that it obeys Eyring rate theory unlike  $\ln(\tau_2 T)$  against  $1/T$  curve.

**Keywords:** Dielectric relaxation, Aprotic polar liquids, Dipole moment

**IPC Code:** G01R27/26

### 1 Introduction

The relaxation behaviour of polar-nonpolar liquid mixtures under high frequency ( $hf$ ) electric field is of much importance to study the molecular shapes, sizes as well as associational behaviour<sup>1-3</sup> in them. Researchers in this field usually analyse the experimental data obtained through relaxation mechanisms involved on the basis of various models<sup>4-6</sup> applicable to polar liquids. Dhull *et al.*<sup>7</sup> and Sharma and Sharma<sup>8</sup> had, however, measured the real  $\epsilon_{ijk}'$ ,  $\epsilon_{ij}'$  or  $\epsilon_{ik}'$  and imaginary  $\epsilon_{ijk}''$ ,  $\epsilon_{ij}''$  or  $\epsilon_{ik}''$  parts of relative complex permittivities  $\epsilon_{ijk}^*$ ,  $\epsilon_{ij}^*$  or  $\epsilon_{ik}^*$  of some interesting binary or single polar liquids (jk, j or k) in a non-polar solvent under X-band electric field at different or fixed temperatures. The purpose of the work was to detect monomer (solute-solvent) or dimer (solute-solute) molecular associations and molecular dynamics of the systems in terms of estimated relaxation time  $\tau_j$  and dipole moment  $\mu_j$ .

The measured<sup>9</sup> values of the relative permittivities  $\epsilon_{ij}$ 's of some aprotic polar liquids like N, N-dimethyl sulphoxide (DMSO); N, N-dimethyl formamide (DMF); N, N-dimethyl acetamide (DMA) and N, N-diethyl formamide (DEF) in benzene under the most effective dispersive region of nearly 10 GHz electric field at 25, 30, 35 and 40°C for DMSO; 25°C for DMA and DMF and 30°C for DEF respectively. DMSO is a aprotic dipolar liquid of high penetrating power and wide applications in medicine and industry. It acts as good constituent of binary mixtures because of its associative<sup>10</sup> nature. Amides, on the other hand, are the building blocks of proteins and enzymes and have wide biological applications. The liquids usually show two relaxation times  $\tau_2$  and  $\tau_1$  for the rotation of the whole molecules and the flexible parts attached to the parent molecules from the single frequency measurement technique<sup>11,12</sup>.

All these facts inspired us to study  $\tau_2$  and  $\tau_1$  and dipole moments  $\mu_2$  and  $\mu_1$  of these liquids in terms of real  $\chi_{ij}'$  ( $=\epsilon_{ij}' - \epsilon_{\infty ij}$ ) and imaginary  $\chi_{ij}''$  ( $=\epsilon_{ij}''$ ) parts of complex orientational susceptibility  $\chi_{ij}^*$  ( $=\epsilon_{ij}' - \epsilon_{\infty ij}$ ) in benzene at different temperatures. The low frequency susceptibility  $\chi_{oij}$  ( $=\epsilon_{oij} - \epsilon_{\infty oij}$ ) is, however, real.  $\chi_{ij}'$  can be obtained by subtracting either 1 or  $\epsilon_{\infty ij}$  from the measured  $\epsilon_{ij}$ 's. If 1 is subtracted from the relative permittivity  $\epsilon_{ij}'$  and  $\epsilon_{oij}$  one gets  $\chi_{ij}'$  and  $\chi_{oij}$  containing all types of polarisation processes including fast polarisations. When high frequency relative permittivity or the optical permittivity  $\epsilon_{\infty ij}$  be subtracted from  $\epsilon_{ij}'$  and  $\epsilon_{oij}$  of the solution at a certain weight fraction  $w_j$ 's of the solute the susceptibility  $\chi_{ij}'$ ,  $\chi_{ij}''$  and  $\chi_{oij}$  result due to orientational polarisation only. Our earlier study<sup>9</sup> was to calculate  $\tau$ 's and  $\mu$ 's in terms of either relative permittivities  $\epsilon_{ij}$ 's or hf conductivities  $\sigma_{ij}$ 's.  $\epsilon_{ij}$ 's are involved with all types of polarisations while  $\sigma_{ij}$ 's are related only to bound molecular charges of polar liquids. Now-a-days relaxation mechanisms are studied in terms<sup>13</sup> of  $\chi_{ij}$ 's because measurements of  $\mu$ 's in terms of  $\epsilon_{ij}$ 's or  $\sigma_{ij}$ 's include contributions due to all types of polarisations and bound molecular charges, respectively. Moreover, relaxation processes are highly thermally activated to yield  $\tau$  within the framework of Debye-Smith model of polar-nonpolar liquid mixture.

The purpose of the present work is to assess the contribution of fast polarisation and bound molecular charges in the measurement of  $\mu$ 's when compared with  $\mu$ 's from  $\chi_{ij}$  and  $\sigma_{ij}$  measurements. The variation of  $\mu$ 's with temperature provides knowledge of the state of the system through the measured energy parameters.

The detailed experimental technique involved in the measurement of dielectric relaxation parameters of solution has been described elsewhere<sup>14</sup>. A Hewlett Packard Impedance Analyser (HP-4192A) measured the capacitance and conductance of the cell containing polar-nonpolar liquid mixtures at different frequencies and temperatures for a fixed  $w_j$  of solute. The real and imaginary parts of relative permittivities  $\epsilon_{ij}$ ' or susceptibility  $\chi_{ij}^*$  are obtained from complex impedances of the cell measured within the range of frequencies from 5 Hz to 13 MHz. The measured  $\epsilon_{ij}$ 's are then plotted in a Cole-Cole semicircular arc to get the values of  $\epsilon_{ij}'$ ,  $\epsilon_{ij}''$ ,  $\epsilon_{oij}$  and  $\epsilon_{\infty oij}$  at nearly 10 GHz electric field (Table 1). Again  $\epsilon_{oij}$  is measured at 1 kHz whereas high frequency permittivity  $\epsilon_{\infty oij}$  ( $=n_{Dij}^2$ ) is

measured by Abbe's refractometer to compare the values obtained from Cole-Cole plot. The cell containing experimental liquid mixture is then kept in Mettler Hot Stage FP-52 chamber to regulate temperature. Multiply distilled  $C_6H_6$  is used as a solvent in measurement after several times fractional distillation to get the purest quality of sample. The measured data  $\epsilon_{ij}'$  or  $\chi_{ij}'$ 's are accurate within  $\pm 5\%$ .

Bergmann *et al.*<sup>15</sup>, however, proposed a graphical technique to get  $\tau_1$ ,  $\tau_2$  and  $c_1$ ,  $c_2$  for a pure polar liquid at different frequencies of the microwave electric field. In order to avoid clumsiness of algebra and fast polarisation processes, the molecular orientational polarisations in terms of established symbols of  $\chi_{ij}$ 's can be written as<sup>5</sup>

$$\frac{\chi_{ij}'}{\chi_{oij}} = \frac{c_1}{1 + \omega^2 \tau_1^2} + \frac{c_2}{1 + \omega^2 \tau_2^2} \quad \dots (1)$$

$$\frac{\chi_{ij}''}{\chi_{oij}} = c_1 \frac{\omega \tau_1}{1 + \omega^2 \tau_1^2} + c_2 \frac{\omega \tau_2}{1 + \omega^2 \tau_2^2} \quad \dots (2)$$

assuming two separate broad Debye type dispersions of which  $c_1 + c_2 = 1$ .

Saha *et al.*<sup>11</sup> and Sit *et al.*<sup>12</sup> put forward an analytical technique to measure  $\tau_1$ ,  $\tau_2$  and  $c_1$ ,  $c_2$  of a polar-nonpolar liquid mixture in terms of measured  $\chi_{ij}'$ ,  $\chi_{ij}''$ ,  $\chi_{oij}$  at different  $w_j$ 's of solute under a single frequency electric field and temperature. Eqs (1) and (2) are solved to get:

$$\frac{\chi_{oij} - \chi_{ij}'}{\chi_{ij}'} = \omega(\tau_1 + \tau_2) \frac{\chi_{ij}''}{\chi_{ij}'} - \omega^2 \tau_1 \tau_2 \quad \dots (3)$$

Eq. (3) gives a straight line when  $(\chi_{oij} - \chi_{ij}')/\chi_{ij}'$  is plotted against  $\chi_{ij}''/\chi_{ij}'$  for different  $w_j$ 's of solute for a given angular frequency  $\omega$  ( $= 2\pi f$ ),  $f$  being the frequency of the applied electric field. The slope  $\omega(\tau_1 + \tau_2)$  and intercept  $-\omega^2 \tau_1 \tau_2$  of straight line of Eq. (3) are obtained through linear regression analysis as shown in Fig. 1. Relaxation times  $\tau_2$  and  $\tau_1$  are calculated from the slopes and intercepts of Eq. (3) of Fig. 1 in terms of measured data of Table 1. They are then compared with measured  $\tau_j$ 's from the linear slope of the  $\chi_{ij}''$  against  $\chi_{ij}'$  curve of Fig. 2 at different  $w_j$ 's of the form:

$$\frac{d\chi_{ij}''}{d\chi_{ij}'} = \omega \tau \quad \dots (4)$$

Both  $\chi_{ij}''$  and  $\chi_{ij}'$  are functions of  $w_j$ 's of solute. It is better to use the individual slopes  $\chi_{ij}''-w_j$  and  $\chi_{ij}'-w_j$

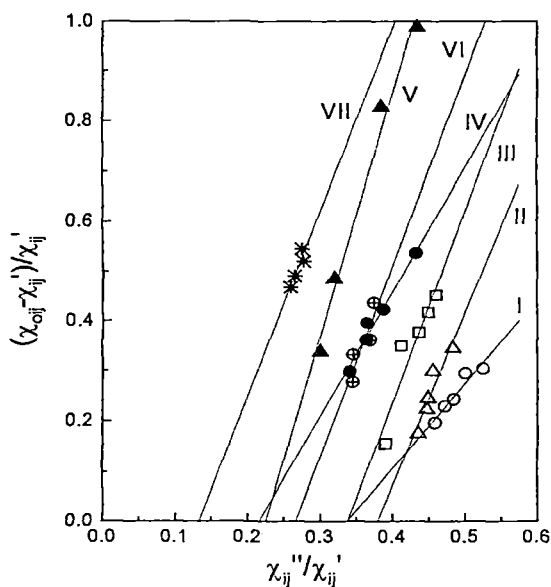


Fig. 1—Linear plot of  $(\chi_{oij}-\chi_{ij})/\chi_{ij}'$  against  $\chi_{ij}''/\chi_{ij}'$  for different  $w_j$ 's of DMSO, DEF, DMF and DMA in benzene (I) DMSO at 25°C (-o-), (II) DMSO at 30°C (-Δ-), (III) DMSO at 35°C (-□-), (IV) DMSO at 40°C (-●-), (V) DEF at 30°C (-▲-), (VI) DMF at 25°C (-⊕-) and (VII) DMA at 25°C (-\*-)

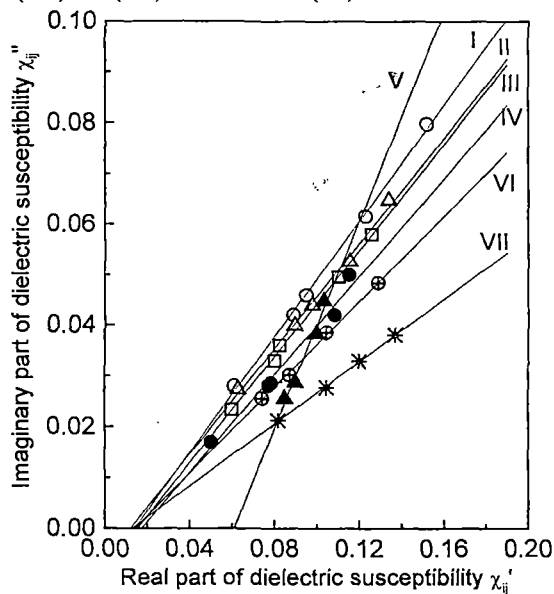


Fig. 2—Linear variation of imaginary part of dielectric susceptibility  $\chi_{ij}''$  against real part of dielectric susceptibility  $\chi_{ij}'$  for different  $w_j$ 's of DMSO, DEF, DMF and DMA in benzene (I) DMSO at 25°C (-o-), (II) DMSO at 30°C (-Δ-), (III) DMSO at 35°C (-□-), (IV) DMSO at 40°C (-●-), (V) DEF at 30°C (-▲-), (VI) DMF at 25°C (-⊕-) and (VII) DMA at 25°C (-\*-)

curves in Figs 3 and 4 at  $w_j \rightarrow 0$  to measure  $\tau$  using the following equation:

$$\frac{(d\chi_{ij}''/dw_j)_{w_j \rightarrow 0}}{(d\chi_{ij}'/dw_j)_{w_j \rightarrow 0}} = \omega\tau \quad \dots (5)$$

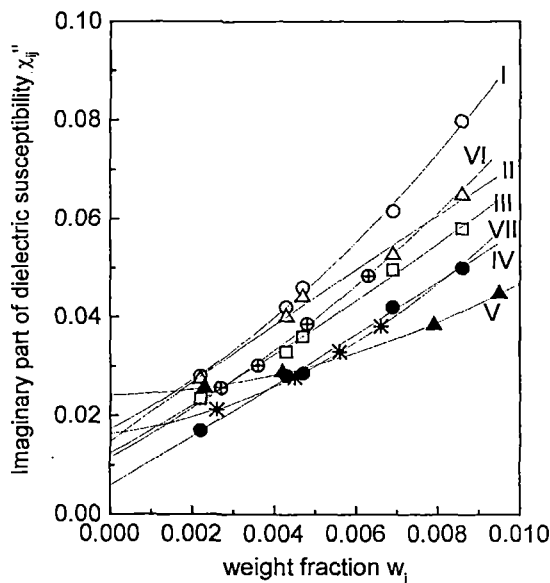


Fig. 3—Plot of imaginary part of dielectric susceptibility  $\chi_{ij}''$  with weight fraction  $w_j$  of DMSO, DEF, DMF and DMA in benzene (I) DMSO at 25°C (-o-), (II) DMSO at 30°C (-Δ-), (III) DMSO at 35°C (-□-), (IV) DMSO at 40°C (-●-), (V) DEF at 30°C (-▲-), (VI) DMF at 25°C (-⊕-) and (VII) DMA at 25°C (-\*-)

$\tau$ 's from both the methods along with  $\tau$ 's from conductivity measurement technique using Eqs (25) and (26) are placed in Table 2 in order to compare with  $\tau$  measured by Gopalakrishna's method<sup>16</sup>.

Eqs (1) and (2) are solved for  $c_1$  and  $c_2$  to get:

$$c_1 = \frac{(\chi_{ij}'\alpha_2 - \chi_{ij}'') (1 + \alpha_1^2)}{\chi_{oij}(\alpha_2 - \alpha_1)} \quad \dots (6)$$

$$c_2 = \frac{(\chi_{ij}'' - \chi_{ij}'\alpha_1) (1 + \alpha_2^2)}{\chi_{oij}(\alpha_2 - \alpha_1)} \quad \dots (7)$$

where  $\alpha_1 = \omega \tau_1$  and  $\alpha_2 = \omega \tau_2$ , such that  $\alpha_2 > \alpha_1$ . The values of  $\chi_{ij}'/\chi_{oij}$  and  $\chi_{ij}''/\chi_{oij}$  are also obtained from following Fröhlich's equations<sup>17</sup>:

$$\frac{\chi_{ij}'}{\chi_{oij}} = 1 - \frac{1}{2A} \ln \left( \frac{1 + \omega^2 \tau_2^2}{1 + \omega^2 \tau_1^2} \right) \quad \dots (8)$$

$$\frac{\chi_{ij}''}{\chi_{oij}} = \frac{1}{A} \left[ \tan^{-1}(\omega\tau_2) - \tan^{-1}(\omega\tau_1) \right] \quad \dots (9)$$

where  $A = \text{Fröhlich parameter} = \ln(\tau_2/\tau_1)$ . The theoretical values of relative contributions  $c_1$  and  $c_2$  towards dielectric relaxation processes for  $\tau_1$  and  $\tau_2$  are computed from Eqs (8) and (9). They are presented in Table 3. The graphical plots of  $\chi_{ij}'/\chi_{oij}$  and  $\chi_{ij}''/\chi_{oij}$  curves as a function of  $w_j$  are shown in Figs 5 and 6, respectively. The experimental values of  $c_1$  and  $c_2$  are

Table 1—Real  $\chi_{ij}'$  and imaginary  $\chi_{ij}''$ , parts of the complex dielectric orientation susceptibility  $\chi_{ij}^*$  and static dielectric susceptibility  $\chi_{oij}$  which are real for various weight fractions  $w_j$ 's of some aprotic polar liquids in benzenes at different temperatures under hf electric field

System	Temp. °C	Weight fraction $w_j$	$\chi_{ij}'$	$\chi_{ij}''$	$\chi_{oij}$
I. DMSO	25	0.0022	0.0611	0.0280	0.0731
		0.0043	0.0890	0.0420	0.1094
		0.0047	0.0950	0.0460	0.1181
		0.0069	0.1231	0.0616	0.1594
		0.0086	0.1520	0.0798	0.1982
II. DMSO	30	0.0022	0.0630	0.0274	0.074
		0.0043	0.0915	0.0400	0.1095
		0.0047	0.0980	0.0440	0.1220
		0.0069	0.1155	0.0526	0.1500
		0.0086	0.1340	0.0648	0.1802
III. DMSO	35	0.0022	0.0600	0.0234	0.0693
		0.0043	0.0800	0.0330	0.108
		0.0047	0.0825	0.0360	0.1135
		0.0069	0.1104	0.0496	0.1564
		0.0086	0.1260	0.0580	0.1830
IV. DMSO	40	0.0022	0.0499	0.0170	0.0648
		0.0043	0.0774	0.0282	0.1054
		0.0047	0.0784	0.0286	0.1094
		0.0069	0.1083	0.0420	0.1541
		0.0086	0.1155	0.0500	0.1775
V. DEF	30	0.0023	0.0850	0.0256	0.1137
		0.0042	0.0899	0.0288	0.1335
		0.0079	0.0997	0.0384	0.1822
		0.0095	0.1033	0.0448	0.2053
VI. DMF	25	0.0027	0.0742	0.0256	0.0948
		0.0036	0.0872	0.0302	0.1162
		0.0048	0.1045	0.0386	0.1423
		0.0063	0.1291	0.0484	0.1855
VII. DMA	25	0.0026	0.0818	0.0213	0.1201
		0.0045	0.1046	0.0278	0.1559
		0.0056	0.1198	0.0330	0.1851
		0.0066	0.1370	0.0381	0.2083

also estimated from Eqs (1) and (2) with the measured values of  $(\chi_{ij}'/\chi_{oij})_{w_j \rightarrow 0}$  and  $(\chi_{ij}''/\chi_{oij})_{w_j \rightarrow 0}$  of Figs 5 and 6. These  $c_1$  and  $c_2$  are finally compared with theoretical ones in Table 3.

The symmetric and asymmetric distribution parameters  $\gamma$  and  $\delta$  of the molecules under study are calculated and placed in the last columns of the Table 3 along with all the  $c_1$  and  $c_2$ 's in order to see that the relaxation mechanism for such liquids are symmetric. The dipole moments  $\mu_2$  and  $\mu_1$  due to rotation of the whole molecule as well as the flexible parts of the molecules are determined from the slope  $\beta_1$  of  $\chi_{ij}'-w_j$  curve of Fig. 4 at  $w_j \rightarrow 0$  in terms of estimated  $\tau_1$  and  $\tau_2$  of Eq. (3) as placed in Table 4.  $\mu_j$ 's are again calculated from the  $\tau$ 's of Eqs (4) and (25) of Murthy *et*

*al.*<sup>18</sup> and the ratio of the individual slopes of Eqs (5) and (26) from susceptibility and conductivity measurements using slope  $\beta_1$  of  $\chi_{ij}'-w_j$  of Fig. 4 and  $\beta_2$  of  $\sigma_{ij}-w_j$  curve of Fig. 7.  $\mu$ 's from both the measurements are entered in Table 4 along with estimated  $\mu$ 's from Gopalakrishna's method<sup>16</sup> quoted as reported ones in the Table 4.

The variations of measured  $\mu_2$  and  $\mu_1$  for DMSO in benzene with temperature in °C are given by the equations:

$$\begin{aligned} \mu_2 &= -231.61 + 15.597 t - 0.2272 t^2 \\ \mu_1 &= 19.825 - 0.626 t + 0.0108 t^2 \end{aligned} \quad \dots (10)$$

$\mu_2$  of the parent molecule attains a maximum value of 36 C.m at 34.32°C with zero dipole moments at 21.72

Table 2—Relaxation times  $\tau_2$  and  $\tau_1$  from the slope and intercept of straight line Eq. (3), measured  $\tau_j$  from different methods of susceptibility and conductivity measurement technique, reported  $\tau$ , symmetric and characteristic relaxation times  $\tau_s$  and  $\tau_{cs}$  for different aprotic polar liquids under effective dispersive region of nearly 10 GHz electric field

System	Temp °C	Estimated $\tau_1$ and $\tau_2$ , ps		$\tau_j^a$ ps	$\tau_j^b$ ps	$\tau_j^c$ ps	$\tau_j^d$ ps	Rept* $\tau_j$ ps	$\tau_s$ ps	$\tau_{cs}$ ps
		$\tau_1$	$\tau_2$							
I. DMSO	25	8.09	21.07	9.91	6.79	8.77	6.01	5.37	4.88	3.69
II. DMSO	30	7.51	52.02	9.07	6.34	8.04	5.86	4.96	4.82	3.05
III. DMSO	35	6.50	59.68	9.08	9.03	7.47	8.95	4.70	4.21	--
IV. DMSO	40	4.51	39.00	8.38	4.90	7.09	4.46	4.33	3.74	22.20
V. DEF	30	3.89	76.41	16.86	1.06	6.64	0.58	2.42	4.16	15.66
VI. DMF	25	4.60	56.24	6.73	6.69	5.87	5.58	5.09	3.02	8.47
VII. DMA	25	2.20	56.61	3.05	6.53	4.96	3.11	6.53	3.90	81.95

$\tau_j^a$  = relaxation time from direct slope of Eq. (4);  $\tau_j^b$  = relaxation time from ratio of individual slope of Eq. (5);  $\tau_j^c$  = relaxation time from direct slope of Eq. (25);  $\tau_j^d$  = relaxation time from ratio of individual slope of Eq. (26) and reported  $\tau_j$  by using Gopalakrishna's<sup>16</sup> method

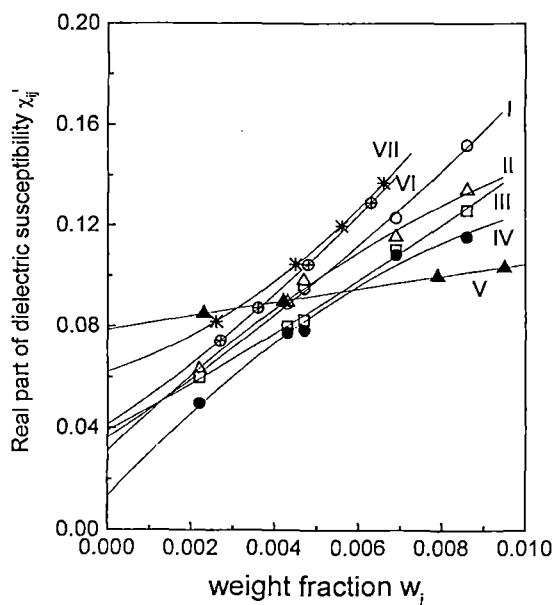


Fig. 4—Plot of real part of dielectric susceptibility  $\chi'_{ij}$  with weight fraction  $w_j$  of DMSO, DEF, DMF and DMA in benzene (I) DMSO at 25°C (-o-), (II) DMSO at 30°C (-Δ-), (III) DMSO at 35°C (-□-), (IV) DMSO at 40°C (-●-), (V) DEF at 30°C (-▲-), (VI) DMF at 25°C (-⊕-) and (VII) DMA at 25°C (-\*-)

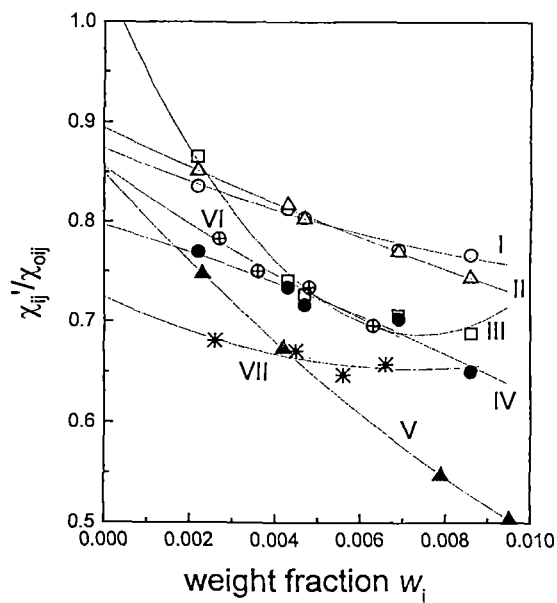


Fig. 5—Variation of  $\chi'_{ij}/\chi_{oij}$  with  $w_j$ 's of DMSO, DEF, DMF and DMA in benzene (I) DMSO at 25°C (-o-), (II) DMSO at 30°C (-Δ-), (III) DMSO at 35°C (-□-), (IV) DMSO at 40°C (-●-), (V) DEF at 30°C (-▲-), (VI) DMF at 25°C (-⊕-) and (VII) DMA at 25°C (-\*-)

and 46.92°C, respectively due to monomer formation with  $C_6H_6$  ring.

The theoretical dipole moment  $\mu_{theo}$ 's of the molecules are calculated from the available infrared spectroscopic data of bond moments assuming the molecules are planar as sketched in Fig. 8. They are found to vary with the measured  $\mu_j$ 's. The difference, how-

ever, indicates that the effect of inductive, mesomeric and electromeric moments of the substituent polar groups within the molecules along with temperature in the  $hf$  electric field is to be considered to have the conformation of the molecules under interest.

The thermodynamic energy parameters like enthalpy of activation  $\Delta H_\tau$  free energy of activation  $\Delta F_\tau$

Table 3—Fröhlich's parameter  $A$  [ $=\ln(\tau_2/\tau_1)$ ], theoretical and experimental values of  $\chi_{ij}'/\chi_{oij}$  and  $\chi_{ij}''/\chi_{oij}$  of Fröhlich Eqs (8) and (9) and from fitting equations of Figs 5 and 6 at  $\omega_j \rightarrow 0$ , respectively, theoretical and experimental relative contributions  $c_1$  and  $c_2$  towards dielectric dispersion due to  $\tau_1$  and  $\tau_2$ , symmetric and asymmetric distribution parameters  $\gamma$  and  $\delta$  for polar-nonpolar liquid mixtures of some aprotic polar liquids under effective dispersion region of nearly 10 GHz electric field

System	Temp °C	A	Theoretical values of $\chi_{ij}'/\chi_{oij}$ and $\chi_{ij}''/\chi_{oij}$ from Eqs (8) and (9)		Theoretical values of $c_1$ and $c_2$		Experimental values of $\chi_{ij}'/\chi_{oij}$ and $\chi_{ij}''/\chi_{oij}$ at $\omega_j \rightarrow 0$ of Figs 5 and 6		Experimental values of $c_1$ and $c_2$		Estimated values of $\gamma$ and $\delta$	
			$c_1$	$c_2$	$c_1$	$c_2$	$c_1$	$c_2$	$\gamma$	$\delta$		
I. DMSO	25	0.957	0.629	0.466	0.485	0.571	0.874	0.380	1.095	-0.061	-0.07	2.00
II. DMSO	30	1.935	0.449	0.434	0.423	0.933	0.894	0.389	1.049	0.022	-0.08	2.37
III. DMSO	35	2.217	0.454	0.419	0.425	1.043	1.039	0.371	1.192	-0.076	-0.29	--
IV. DMSO	40	2.241	0.611	0.409	0.507	0.794	0.797	0.266	0.803	0.228	0.21	0.36
V. DEF	30	2.978	0.476	0.378	0.443	1.380	0.849	0.247	0.890	0.210	0.17	0.36
VI. DMF	25	2.505	0.497	0.405	0.451	1.086	0.855	0.262	0.921	0.065	0.13	0.61
VII. DMA	25	3.248	0.601	0.357	0.531	1.093	0.724	0.185	0.713	0.338	0.47	0.18

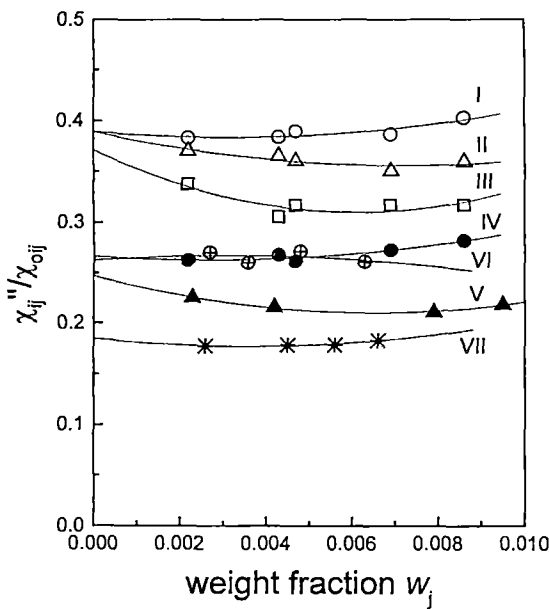


Fig. 6—Variation of  $\chi_{ij}''/\chi_{oij}$  with  $w_j$ 's of DMSO, DEF, DMF and DMA in benzene (I) DMSO at 25°C (-o-), (II) DMSO at 30°C (-Δ-), (III) DMSO at 35°C (-□-), (IV) DMSO at 40°C (-●-), (V) DEF at 30°C (-▲-), (VI) DMF at 25°C (-⊕-) and (VII) DMA at 25°C (-\*-)

and entropy of activation  $\Delta S_\tau$  were obtained from the slope and intercept of linear equation of  $\ln(\tau_1 T)$  against  $1/T$  for DMSO as given by the equation:

$$\begin{aligned} \ln(\tau_2 T) &= -4.8353 - 4.088 \times 10^3 (1/T) \\ \ln(\tau_1 T) &= -30.568 + 3.216 \times 10^3 (1/T) \end{aligned} \quad \dots (11)$$

The variation of  $\ln(\tau_1 T)$  or  $\ln(\tau_2 T)$  against  $1/T$  indicates that  $\tau_1$  obeys the Eyring rate process whereas  $\tau_2$  does not.

## 2 Symmetric and Asymmetric Distribution Parameters $\gamma$ and $\delta$

The polar-nonpolar liquid mixtures under study are non-rigid in nature exhibiting two relaxation times  $\tau_2$  and  $\tau_1$  at a single frequency electric field<sup>19</sup>. The measured values of  $\chi_{ij}''/\chi_{oij}$  when plotted against  $\chi_{ij}'/\chi_{oij}$  at  $\omega_j \rightarrow 0$  for different frequency  $\omega$  at a fixed experimental temperature for DMSO may either show Cole-Cole semicircular arc or Cole-Davidson skewed arc having symmetric and asymmetric distribution of relaxation behaviour according to following equations:

$$\frac{\chi_{ij}^*}{\chi_{oij}} = \frac{1}{1 + (j\omega\tau_s)^{1-\gamma}} \quad \dots (12)$$

$$\frac{\chi_{ij}^*}{\chi_{oij}} = \frac{1}{(1 + j\omega\tau_{cs})^\delta} \quad \dots (13)$$

where  $\tau_s$  and  $\tau_{cs}$  are symmetric and characteristics relaxation times related to symmetric and asymmetric distribution parameters  $\gamma$  and  $\delta$ , respectively. On separation, the real and imaginary parts of Eq. (12), one gets:

$$\gamma = \frac{2}{\pi} \tan^{-1} \left[ \left( 1 - \frac{\chi_{ij}'}{\chi_{oij}} \right) \frac{\chi_{ij}'/\chi_{oij}}{\chi_{ij}''/\chi_{oij}} - \frac{\chi_{ij}''}{\chi_{oij}} \right] \quad \dots (14)$$

$$\tau_s = \frac{1}{\omega} \left[ 1 / \left( \frac{\chi_{ij}'/\chi_{oij}}{\chi_{ij}''/\chi_{oij}} \cos \frac{\gamma\pi}{2} - \sin \frac{\gamma\pi}{2} \right) \right]^{1/(1-\gamma)} \quad \dots (15)$$

Table 4—Slope  $\beta_1$  of  $\chi'_{ij}$  versus  $w_j$  and  $\beta_2$  of  $\sigma_{ij}$  versus  $w_j$  curves, measured dipole moments  $\mu_2$  and  $\mu_1$  from susceptibility measurement technique,  $\mu_j^a$ 's from Eqs (22) and (29), respectively, reported dipole moment, theoretical dipole moment  $\mu_{\text{theo}}$  from available bond angles and bond moments expressed in Coulomb metre (C.m) and the values of  $\mu_1/\mu_{\text{theo}}$  for some aprotic polar liquids in benzene under effective dispersion region of nearly 10 GHz electric field

System mol wt	Slope of $\chi'_{ij}$ - $w_j$ and $\sigma_{ij}$ - $w_j$ curves		Dipole moments $\mu_j$ ( $\times 10^{-30}$ ) in Coulomb.metre							$\frac{\mu_1}{\mu_{\text{theo}}}$	
			From Eq (22)		$\mu_j^a$	$\mu_j^b$	$\mu_j^c$	$\mu_j^d$	$\mu_j^r$		$\mu_{\text{theo}}$
			$\mu_2$	$\mu_1$							
I.DMSO at 25°C $M_j=0.078$ kg	10.943	6.280	14.69	10.30	10.75	10.03	11.10	10.48	12.65	15.18	0.67
II.DMSO at 30°C $M_j=0.078$ kg	16.440	9.096	36.69	12.64	13.09	12.35	13.31	12.75	12.79	15.18	0.83
III.DMSO at 35°C $M_j=0.078$ kg	8.950	4.621	31.09	9.27	9.79	9.78	9.50	9.82	13.49	15.18	0.61
IV.DMSO at 40°C $M_j=0.078$ kg	17.646	9.894	30.37	12.69	13.70	12.82	13.94	13.32	13.73	15.18	0.83
V.DEF at 30°C $M_j=0.101$ kg	2.870	2.922	26.62	5.67	7.91	5.53	8.18	7.58	12.96	13.30	0.42
VI.DMF at 25°C $M_j=0.073$ kg	10.938	7.282	33.21	9.37	9.81	9.80	10.54	10.48	12.09	12.73	0.74
VII.DMA at 25°C $M_j=0.087$ kg	5.147	2.792	24.97	6.83	7.07	6.89	7.00	6.81	11.26	13.37	0.51

$\mu_j^a$  = dipole moment by using  $\tau$  from the direct slope of Eq. (4);  $\mu_j^b$  = dipole moment by using  $\tau$  from the ratio of individual slopes of Eq. (5);  $\mu_j^c$  = dipole moment by using  $\tau$  from the direct slope of Eq. (25);  $\mu_j^d$  = dipole moment by using  $\tau$  from the ratio of individual slopes of Eq. (26);  $\mu_j^r$  = reported dipole moment using Gopalakrishna's<sup>16</sup>  $\tau$  and  $\mu_{\text{theo}}$  = theoretical dipole moment from the available bond moments.

On simplification of Eq. (13) further, one gets :

$$\frac{1}{\phi} \log(\cos \phi) = \frac{\log \left[ \left( \frac{\chi'_{ij}}{\chi_{oij}} \right) / \cos(\phi\delta) \right]}{\phi\delta} \quad \dots (16)$$

$$\tan(\phi\delta) = \frac{\left( \frac{\chi''_{ij}}{\chi_{oij}} \right)_{w_j \rightarrow 0}}{\left( \frac{\chi'_{ij}}{\chi_{oij}} \right)_{w_j \rightarrow 0}} \quad \dots (17)$$

where  $\tan\phi = \omega\tau\epsilon_s$

A theoretical curve of  $(1/\phi) \log(\cos\phi)$  with  $\phi$  in degrees was drawn<sup>5</sup> to get the known values of  $\phi$  and  $\delta$  in terms of measured parameter of  $[\log\{(\chi'_{ij}/\chi_{oij})/\cos(\phi\delta)\}]/(\phi\delta)$  of Eqs (16) and (17). All the  $\tau_s$ ,  $\tau_{cs}$  and  $\delta$   $\phi$  are given in Tables 2 and 3, respectively.

### 3 Dipole Moment $\mu_j$ from Susceptibility Measurement

Debye equation<sup>20</sup> of relative permittivities of a polar solute (j) dissolved in a non-polar solvent (i) in terms of complex dielectric orientational susceptibility  $\chi^*_{ij}$  of solution can be written as:

$$\frac{\chi^*_{ij}}{\chi_{oij}} = \frac{1}{1 + j\omega\tau} \quad \dots (18)$$

where  $\chi'_{ij}$  ( $=\epsilon_{ij}' - \epsilon_{\infty ij}$ ) and  $\chi''_{ij}$  ( $=\epsilon_{ij}''$ ) are the real and imaginary parts of  $\chi^*_{ij} = \chi'_{ij} - j\chi''_{ij}$ .  $j = \sqrt{-1}$  is a complex number  $\chi_{oij}$  ( $=\epsilon_{oij} - \epsilon_{\infty ij}$ ) is the low frequency susceptibility which is real.

Again, the imaginary part of dielectric orientational susceptibility  $\chi''_{ij}$  as a function of  $w_j$  can be written according to Smith<sup>21</sup> as:

$$\chi''_{ij} = \frac{N\rho_{ij}\mu_j^2}{27\epsilon_o k_B T M_j} \frac{\omega\tau}{1 + \omega^2\tau^2} (\epsilon_{ij} + 2)^2 w_j \quad \dots (19)$$

On differentiation of Eq. (19) w.r. t  $w_j$  at  $w_j \rightarrow 0$ , one gets:

$$\left( \frac{d\chi''_{ij}}{dw_j} \right)_{w_j \rightarrow 0} = \frac{N\rho_{ij}\mu_j^2}{27\epsilon_o k_B T M_j} \frac{\omega\tau}{1 + \omega^2\tau^2} (\epsilon_i + 2)^2 \quad \dots (20)$$

where  $k_B$  is the Boltzmann constant,  $N$  the Avogadro's Number  $\epsilon_i$  the relative permittivity of the solute and  $\epsilon_o$

is the absolute permittivity of free space =  $8.854 \times 10^{-12} \text{ F.m}^{-1}$ , all expressed in SI units. Comparing Eqs (4) and (20), one gets:

$$\left( \frac{d\chi'_{ij}}{dw_j} \right)_{w_j \rightarrow 0} = \frac{N\rho_i \mu_j^2}{27\varepsilon_0 k_B T M_j} \frac{1}{1 + \omega^2 \tau_j^2} (\varepsilon_i + 2)^2 = \beta_1 \quad \dots (21)$$

where  $\beta_1$  is the slope of  $\chi'_{ij} - w_j$  curves at  $w_j \rightarrow 0$ .

From Eq. (21), one gets the dipole moment  $\mu_j$  as:

$$\mu_j = \left( \frac{27\varepsilon_0 k_B T M_j \beta_1}{N\rho_i (\varepsilon_i + 2)^2 b} \right)^{\frac{1}{2}} \quad \dots (22)$$

where  $b = 1/(1 + \omega^2 \tau_j^2)$  is the dimensionless parameter involved with measured  $\tau_j$  of Table 2. All the  $\mu_j$ 's are placed in Table 4.

#### 4 Dipole Moment $\mu_j$ from hf Conductivity Measurement

The hf complex conductivity  $\sigma^*_{ij}$  of a polar-non-polar liquid mixture is given by:

$$\sigma^*_{ij} = \sigma'_{ij} + j\sigma''_{ij} = \omega\varepsilon_0 (\varepsilon''_{ij} + j\varepsilon'_{ij}) \quad \dots (23)$$

the real  $\sigma'_{ij}$  and imaginary  $\sigma''_{ij}$  parts of  $\sigma^*_{ij}$  are related by:

$$\sigma''_{ij} = \sigma_{\infty ij} + \frac{1}{\omega\tau_j} \sigma'_{ij} \quad \dots (24)$$

where  $\sigma_{\infty ij}$  is the constant conductivity at infinite dilution i.e. at  $w_j \rightarrow 0$ . The Eq. (24) on differentiation w.r.t.  $\sigma'_{ij}$  yields:

$$\frac{d\sigma''_{ij}}{d\sigma'_{ij}} = \frac{1}{\omega\tau_j} \quad \dots (25)$$

which provides a convenient method to obtain  $\tau_j$  of a polar molecule. It is, however, better to use the ratio of the slopes of variation of  $\sigma''_{ij}$  and  $\sigma'_{ij}$  with  $w_j$  in order to avoid polar-polar interactions at  $w_j \rightarrow 0$  in a given solvent to get  $\tau_j$  from:

$$\frac{(d\sigma''_{ij}/dw_j)_{w_j \rightarrow 0}}{(d\sigma'_{ij}/dw_j)_{w_j \rightarrow 0}} = \frac{1}{\omega\tau_j} \quad \dots (26)$$

In hf region of GHz range, it is generally observed that  $\sigma''_{ij} \equiv \sigma_{ij}$  the total hf conductivity<sup>22</sup> of the solution. Therefore, the Eq. (24) can be written as:

$$\sigma_{ij} = \sigma_{\infty ij} + \frac{1}{\omega\tau_j} \sigma'_{ij} \quad \dots (27)$$

$$\beta_2 = \frac{1}{\omega\tau_j} \left( \frac{d\sigma'_{ij}}{dw_j} \right)_{w_j \rightarrow 0}$$

where  $\beta_2$  is the slope of  $(d\sigma'_{ij}/dw_j)_{w_j \rightarrow 0}$ . The real part  $\sigma'_{ij}$  of a polar-nonpolar liquid mixture is given by<sup>5</sup>:

$$\sigma'_{ij} = \frac{N\rho_i \mu_j^2}{27k_B T M_j} \frac{\omega^2 \tau_j}{1 + \omega^2 \tau_j^2} (\varepsilon_{ij} + 2)^2 w_j$$

$$\left( \frac{d\sigma'_{ij}}{dw_j} \right)_{w_j \rightarrow 0} = \frac{N\rho_i \mu_j^2}{27k_B T M_j} \frac{\omega^2 \tau_j}{1 + \omega^2 \tau_j^2} (\varepsilon_i + 2)^2 \quad \dots (28)$$

Now comparing Eqs (27) and (28), one gets hf  $\mu_j$  from:

$$\mu_j = \left( \frac{27k_B T M_j \beta_2}{N\rho_i (\varepsilon_i + 2)^2 \omega b} \right)^{\frac{1}{2}} \quad \dots (29)$$

where  $b = 1/(1 + \omega^2 \tau_j^2)$  is involved with  $\tau_j$ 's from Eqs (25) and (26).  $\mu_j$ 's thus obtained from Eq. (29) are placed in Table 4 along with Gopalakrishna's  $\mu_j$  and  $\mu_{\text{theo}}$ 's.

#### 5 Results and Discussion

The relaxation parameters in terms of real  $\chi'_{ij}$  ( $=\varepsilon_{ij} - \varepsilon_{\infty ij}$ ), imaginary  $\chi''_{ij}$  ( $=\varepsilon''_{ij}$ ) and low frequency susceptibility  $\chi_{oij}$  ( $=\varepsilon_{oij} - \varepsilon_{\infty ij}$ ), which are real and extracted from the measured relative permittivities  $\varepsilon_{ij}$ 's for different  $w_j$ 's of solute at 25, 30, 35 and 40°C for DMSO, 25°C for DMA and DMF and 30°C for DEF under nearly 10 GHz electric field as shown in Table 1. The curves of  $(\chi_{oij} - \chi'_{ij})/\chi'_{ij}$  against  $\chi''_{ij}/\chi'_{ij}$  at different  $w_j$ 's of solute are plotted from the measured data in Fig. 1. All the curves show two relaxation times  $\tau_2$  and  $\tau_1$  due to rotation of the whole molecule and the flexible part attached to the parent ones as evident from Table 2. It indicates that the molecules are of non-rigid nature. Unlike  $\tau_2$ 's,  $\tau_1$ 's of DMSO at 25, 30, 35 and 40°C decrease gradually (Table 2). This indicates that  $\tau_1$ 's obey the Debye relaxation mechanism. It is also evident from Table 2 and Fig. 1 that the graphs of  $(\chi_{oij} - \chi'_{ij})/\chi'_{ij}$  against  $\chi''_{ij}/\chi'_{ij}$  for different  $w_j$ 's of DMSO shift towards the origin with the increase of temperature.  $\tau_2$ 's of all the liquids are much larger in magnitude than  $\tau_1$ . The parent mole-

cule takes larger time to lag with the electric field frequency for its inertia in comparison to its flexible parts which are supported by the two relaxation model of polar unit under nearly 10 GHz electric field<sup>23</sup>.  $\tau_j$ 's are estimated and placed in Table 2 from Eqs (4) and (5) using linear slope of  $\chi_{ij}''$  against  $\chi_{ij}'$  at different  $w_j$ 's and the ratio of individual slopes of  $\chi_{ij}''-w_j$  and  $\chi_{ij}'-w_j$  curves at  $w_j \rightarrow 0$  of Figs 3 and 4, respectively. The values of  $\tau_j$  from Eq. (4) are larger than from Eq. (5). Reported  $\tau$ 's and  $\tau_j$ 's calculated from both the Gopalakrishna's method<sup>16</sup> as well as conductivity measurement technique using Eqs (25) and (26), respectively. The agreement is better from the  $\tau_j$ 's due to ratio of the individual slopes of  $\chi_{ij}''-w_j$  and  $\chi_{ij}'-w_j$  curves at  $w_j \rightarrow 0$  of Figs 3 and 4 because the polar-polar interactions are almost avoided. They are then compared with the reported  $\tau_s$  and  $\tau_{cs}$  of the molecules assuming symmetric and asymmetric distribution of relaxation processes only to show that the molecules obey symmetric distribution. The curves  $\chi_{ij}''$  against  $\chi_{ij}'$  of Fig. 2 of the molecules are found to meet at a point in the region of  $0 < w_j < 0.02$  except DEF the data was measured at 30°C. The experimental curves of  $\chi_{ij}''-w_j$  and  $\chi_{ij}'-w_j$  are not linear as shown in Figs 3 and 4, respectively. Like  $\chi_{ij}'-w_j$  curves all the curves of  $\chi_{ij}''-w_j$  of Fig. 3 are parabolic in nature and increase with the  $w_j$ 's of solute. The magnitude of  $\chi_{ij}''$  is, however, maximum in lower temperature region and decrease with the rise of temperature. This indicates the absorption of electric energy in the polar-non-polar mixture in the lower temperature region.

The relative contributions  $c_1$  and  $c_2$  due to  $\tau_1$  and  $\tau_2$  could, however, be estimated from the  $\chi_{ij}'/\chi_{oij}$  and  $\chi_{ij}''/\chi_{oij}$  of Fröhlich's Eqs (8) and (9) and placed in Table 3 assuming a continuous distribution of  $\tau$  between limiting values of  $\tau_1$  and  $\tau_2$ .  $c_1$  and  $c_2$  are also calculated in terms of fixed values of  $(\chi_{ij}'/\chi_{oij})_{w_j \rightarrow 0}$  and  $(\chi_{ij}''/\chi_{oij})_{w_j \rightarrow 0}$  of the graphical plots of  $(\chi_{ij}'/\chi_{oij})-w_j$  and  $(\chi_{ij}''/\chi_{oij})-w_j$  curves of Figs 5 and 6 respectively. All the curves are extrapolated to get the fixed values of  $(\chi_{ij}'/\chi_{oij})$  and  $(\chi_{ij}''/\chi_{oij})$  at  $w_j \rightarrow 0$ . They are substituted in the Bergmann's Eqs (6) and (7) to get  $c_1$  and  $c_2$  for the fixed values of  $\tau_1$  and  $\tau_2$ , respectively. All the  $c$ 's are placed in Table 3 for comparison with Fröhlich's method. Both  $c_1$  and  $c_2$  from Fröhlich's<sup>15</sup> equations are all +ve for all the liquids. But  $c_2$  for DMSO at 25 and 35°C are -ve from the graphical method. The -ve value of  $c_2$  is physically

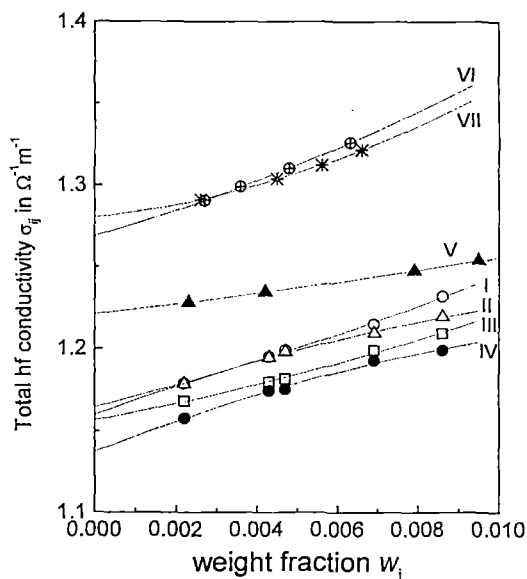


Fig. 7—Variation of total hf conductivity  $\sigma_{ij}$  with  $w_j$ 's of DMSO, DEF, DMF and DMA in benzene (I) DMSO at 25°C (-o-), (II) DMSO at 30°C (-Δ-), (III) DMSO at 35°C (-□-), (IV) DMSO at 40°C (-●-), (V) DEF at 30°C (-▲-), (VI) DMF at 25°C (-⊕-) and (VII) DMA at 25°C (-\*-)

meaningless as they are considered to be the relative contributions towards dielectric relaxation processes. This may indicate that the rotation of whole molecule under *hf* electric field is not in accord with the flexible part probably due to inertia as observed elsewhere<sup>10,11</sup>. The variation of  $\chi_{ij}'/\chi_{oij}$  and  $\chi_{ij}''/\chi_{oij}$  with  $w_j$  as shown in Figs 5 and 6 are expected to be concave and convex<sup>10,11</sup> respectively. All the curves of Figs 5 and 6 are, however, concave except systems VI (-⊕-) of Fig. 6. This type of anomalous behaviour in the variation of  $\chi_{ij}'/\chi_{oij}$  and  $\chi_{ij}''/\chi_{oij}$  with  $w_j$  invariably demands careful measurement of data in low concentration region.

The dipole moments  $\mu_1$  and  $\mu_2$  are also calculated from the slope  $\beta_1$  of  $\chi_{ij}'-w_j$  curve of Fig. 4 and estimated  $\tau_1$  and  $\tau_2$  as shown in Table 4. They are compared with  $\mu_j$ 's from  $\tau_j$ 's of Eqs (4) and (5), respectively.  $\mu_j$ 's from Gopalakrishna's method<sup>16</sup> and conductivity measurement technique<sup>9</sup> are also reported and placed in Table 4 for comparison among them. The total *hf* conductivity  $\sigma_{ij}$  is plotted against  $w_j$ 's of the polar-nonpolar liquid mixture as seen in Fig. 7 only to show that all the curves are parabolic in nature exhibiting maximum conductivity at lower temperature and higher concentration for DMSO. At  $w_j \rightarrow 0$ , the curves are found to yield different value of  $\sigma_{ij}$  probably due to the term  $1/(M_j T)$  in the Eq. (28) as seen in Fig. 7. The difference in estimated  $\mu_2$  and  $\mu_1$  from conductivity and susceptibility measurements

suggests the involvement of bound molecular charges towards  $\mu$ 's of polar liquid. It is evident from Table 4 that  $\mu_1$ 's of the polar liquids are found to be in excellent agreement with the reported  $\mu$ 's. It, thus, reveals that a part of the molecule is rotating under 10 GHz electric field as observed earlier<sup>24</sup>. The variation of  $\mu_1$  and  $\mu_2$  with temperature for DMSO is given by Eq. (10). The convex nature of  $\mu_1-t$  equation reveals the fact that the molecule DMSO attains higher asymmetry of larger  $\mu_1$  at a certain temperature. It also shows zero dipole moments at two different temperatures indicating the symmetric nature of the molecule. The variation of  $\mu_1$  with temperature may occur due to elongation of bond moments. This further invites the extensive study of the relaxation phenomena of highly non-spherical dipolar molecules at different experimental temperatures and in different solvents.

The theoretical dipole moment  $\mu_{\text{theo}}$ 's of the polar molecules are calculated assuming the planar structure from the available bond moments of  $7.83 \times 10^{-30}$  C.m.,  $5.17 \times 10^{-30}$  C.m. for polar groups  $S \leftarrow \text{CH}_3$ ,  $O \leftarrow S$  in DMSO  $2.13 \times 10^{-30}$  C.m.,  $2.60 \times 10^{-30}$  C.m.,  $1.23 \times 10^{-30}$  C.m. of  $N \leftarrow \text{CH}_3$ ,  $N \leftarrow \text{C}_2\text{H}_5$ ,  $\text{CH}_3 \leftarrow \text{C}$  in DMF, DEF and DMA respectively. The other bond moments are  $1 \times 10^{-30}$  C.m.,  $1.5 \times 10^{-30}$  C.m.,  $10.33 \times 10^{-30}$  C.m. for  $\text{C} \leftarrow \text{H}$ ,  $\text{C} \leftarrow \text{N}$  and  $\text{C} \leftarrow \text{O}$  in them. The bond moments are, however, reduced by a factor  $\mu_1/\mu_{\text{theo}}$  to yield exact  $\mu$ 's as sketched in Fig. 8. The reduction or elongation in bond moments of the substituent polar groups may occur due to inductive, mesomeric and electromeric effects which in turn subsequently act as pusher or puller of electrons in them. The solvent  $\text{C}_6\text{H}_6$  is a cyclic and planar compound and has three double bonds and six p-electrons on six C-atoms. The dipolar liquid molecules are aliphatic and planar ones. Hence,  $\pi$ - $\pi$  interaction or resonance effect combined with inductive effect commonly known as mesomeric effect in excited state called the electromeric effect may play the vital role in the estimation of  $\mu_{\text{theo}}$ 's of Fig. 8.

The thermodynamic energy parameters like enthalpy of activation  $\Delta H_\tau$  entropy of activation  $\Delta S_\tau$  and free energy of activation  $\Delta F_\tau$  of DMSO were calculated from the slope and intercept of  $\ln(\tau_1 T)$  against  $(1/T)$  of Eq. (11) on the basis of Eyrings theory considering the rotation of the polar molecule as a rate process. Unlike  $\ln(\tau_2 T)$  against  $(1/T)$ ;  $\ln(\tau_1 T)$  against  $(1/T)$  of DMSO is in accord with the Eyring's rate

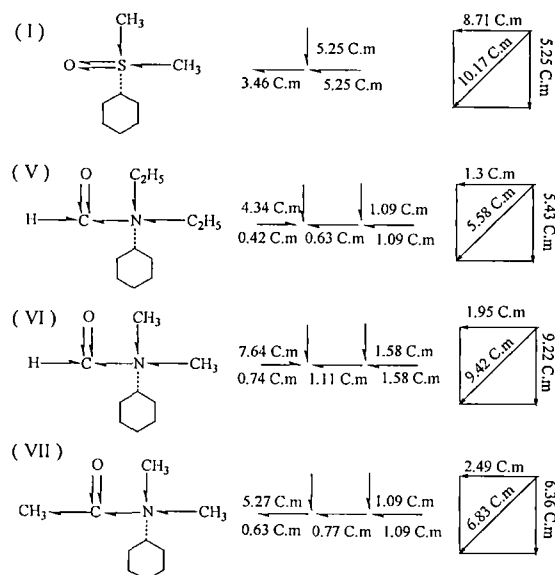


Fig. 8—Conformational structures of aprotic polar liquids in terms of reduced bond length due to mesomeric and inductive moments in Coulomb metre (Cm)  $\times 10^{30}$  of the substituent polar groups: (I) DMSO (II) DEF (III) DMF (IV) DMA

theory<sup>20</sup>. The value of  $\Delta H_\tau$  for DMSO is 6.85 in KJ mole<sup>-1</sup>  $\Delta S_\tau$  are -8.21, -8.15, -11.65, -11.48 in J mole<sup>-1</sup> K<sup>-1</sup> and  $\Delta F_\tau$  are 9.30, 9.32, 10.43 and 10.45. at 25, 30, 35 and 40°C, respectively in KJ. mole<sup>-1</sup>. It is observed that  $\Delta S_\tau$  are -ve indicating the activated states are more ordered than the normal states especially for DMSO.

## 6 Conclusions

The study of relaxation phenomena of aprotic polar liquids of amides in  $\text{C}_6\text{H}_6$  in terms of the modern established symbols of dielectric terminologies and parameters of orientational susceptibilities  $\chi_{ij}$ 's measured under a single frequency electric field is very encouraging and interesting. It seems to be more topical, significant and useful contribution to predict the conformational structures and various molecular associations of the molecules at any given temperatures. The intercept and slope of derived linear Eq. (3) on the measured data of  $\chi_{ij}$  of different  $w_j$ 's are used to get  $\tau_2$  and  $\tau_1$ . The prescribed methodology in SI units is superior because of the unified, coherent and rationalised nature because  $\chi_{ij}$ 's are directly linked only with orientational polarisation of the molecules. The significant Eqs (4) and (5) to obtain values of  $\tau_j$  and hence, values of  $\mu_j$  from Eq. (22) help the future researchers to shed more light on the relaxation phenomena of complicated non-spherical polar liquids and liquid crystals. The present method to obtain val-

ues of  $\tau_j$  from Eq. (5) with the use of the ratio of the individual slopes of  $\chi_{ij}''$  versus  $w_j$  and  $\chi_{ij}'$  versus  $w_j$  curves at  $w_j \rightarrow 0$  is a significant improvement over the existing ones, as it eliminates polar-polar interaction almost completely in  $\tau_j$ 's and  $\mu_j$ 's, respectively.

The values of  $\tau_j$  and  $\mu_j$  are usually claimed to be accurate within 10 and 5%, respectively. The tested correlation coefficients  $r$ 's and % of errors of Eq. (3) demand that  $\tau$  and  $\mu$  are more than accurate. The DMSO, DMF, DMA and DEF molecules absorb electric energy much more strongly under nearly 10 GHz electric field, at which the variation of  $\chi_{ij}''$  against frequency  $\omega$  seem to be large. This at once indicates the attention to get the double relaxation phenomena from Eq. (3). The sum of the experimental and theoretical values of weighted contributions  $c_1$  and  $c_2$  towards dielectric dispersions due to estimated  $\tau_2$  and  $\tau_1$  differ significantly to indicate more than two Debye type relaxations in such molecules because of their complexity. It can, further, be observed that only a part of the molecule is rotating under nearly 10 GHz electric field since  $\ln(\tau_1 T)$  against  $1/T$  obeys the Eyring's rate theory. The values of  $\mu_2$  and  $\mu_1$  due to  $\tau_2$  and  $\tau_1$  are expected to be smaller when they are measured from susceptibility measurement technique rather than the hf conductivity and permittivity methods, where approximation of  $\sigma_{ij} \approx \sigma'_{ij}$  is usually made. The measurement of  $\mu$ 's from hf conductivities  $\sigma_{ij}$ 's and hf permittivities  $\epsilon_{ij}$ 's is involved with the contributions of the bound molecular charges and all types of polarisations including the fast one. The difference of  $\mu_1$  and  $\mu_j$  from  $\mu_{\text{theo}}$  may arise, either by elongation or reduction of the bond moments of the substituted polar groups by factor  $\mu_1/\mu_{\text{theo}}$  in agreement with the measured  $\mu$ 's to take into account of the inductive, mesomeric and electromeric effects of the substituted polar groups in the molecules under investigation. Thus, the correlation between the conformational structures with the observed results enhances the scientific content to add a new horizon of understanding the existing knowledge of dielectric relaxation phenomena.

## References

- 1 Puranik S M, Ghanabhadur R Y, Helambe S N & Mehrotra S C, *Indian J Pure & Appl Phys* 29 (1991) 251.
- 2 Murthy M B R, Dayasagar B S & Patil R L, *Pramana: J Phys*, 61 (2003) 725.
- 3 Gupta K K, Bansal A K, Singh P J & Sharma K S, *Indian J Pure & Appl Phys*, 42 (2004) 849.
- 4 Onsager L, *J American Chem Soc*, 58 (1936) 1485.
- 5 Dutta K, Sit S K & Acharyya S, *Pramana: J Phys*, 57 (2001) 775.
- 6 Ghosh N, Karmakar A, Sit S K & Acharyya S, *Indian J Pure & Appl Phys*, 38 (2000) 574.
- 7 Dhull J S, Sharma D R & Laxminarayana K N, *Indian J Phys B*, 56 (1982) 334.
- 8 Sharma A & Sharma D R, *J Phys Soc (Japan)*, 61 (1992) 1049.
- 9 Sit S K, Dutta K, Acharyya S, Pal Majumder T & Roy S, *J Molecular Liquids*, 89 (2000) 111.
- 10 Sit S K, Ghosh N, Saha U & Acharyya S, *Indian J Phys*, 71B (1997) 533.
- 11 Saha U, Sit S K, Basak R C & Acharyya S, *J Phys D: Appl Phys (London)*, 27 (1994) 596.
- 12 Sit S K, Basak R C, Saha U & Acharyya S, *J Phys D: Appl Phys (London)*, 27 (1994) 2194.
- 13 Jonscher A K, *Inst Phys Conference Serial No 58*, Invited paper presented at physics of dielectrics Solids 8-11 (1980).
- 14 Pal Majumder T, *Ph D thesis* Jadavpur University, Kolkata (1996)
- 15 Bergmann K, Roberti D M & Smyth C P, *J Phys Chem*, 64 (1960) 665.
- 16 Gopalakrishna K V, *Trans Faraday Soc*, 53 (1957) 767.
- 17 Fröhlich H, *Theory of Dielectrics* (Oxford University press) 1949.
- 18 Murthy M B R, Patil R L & Deshpande D K, *Indian J Phys B*, 63 (1989) 491.
- 19 Dutta K, Karmakar A, Dutta L, Sit S K & Acharyya, *Indian J Pure & Appl Phys*, 40 (2002) 801.
- 20 Hill N E, Vaughan W E, Price A H & Davis M *Dielectric properties and Molecular Behaviour* Van Nostrand Reinhold, London, 1969.
- 21 Smyth C P, *Dielectric Behaviour and Structure* (McGraw Hill, New York) 1955.
- 22 Dutta K, Karmakar A, Sit S K & Acharyya, *Indian J Pure & Appl Phys*, 40 (2002) 588.
- 23 Sit S K & Acharyya S, *Indian J Pure & Appl Phys*, 34 (1996) 255.
- 24 Basak R C, Sit S K & Acharyya S, *Indian J Phys B*, 70 (1996) 37.

## Material properties of dipolar liquid in non-polar solvent through relaxation phenomena under high frequency electric field

K. Dutta \*, A. Karmakar, S.K. Sit, S. Acharyya

Department of Physics, Debinagar G.R.U. Vidyapith, P.O.-Debinagar, Raiganj, Dist. Uttar Dinajpur (West Bengal), 733123, India

Received 10 October 2005; accepted 16 January 2006

Available online 17 April 2006

### Abstract

A graphical method is used to determine the double relaxation times  $\tau_2$  and  $\tau_1$  for the rotation of the flexible part and the whole molecule of some long-chain alcohols in *n*-heptane under 24.33 GHz (K-Band), 9.25 GHz (X-Band) and 3.00 GHz (J-Band) electric fields on the basis of Debye and Fröhlich models. The fixed  $\tau_1$  and  $\tau_2$  at those frequencies are compared to the average  $\tau_1$  and  $\tau_2$  measured by the single frequency method of Saha et al. [U. Saha, S.K. Sit, R.C. Basak, S. Acharyya. J. Phys. D: Appl. Phys. 27 (1994) 596.] and reported average  $\tau$ 's. This reveals the material properties of the chemical systems in identical environments.  $\tau$ 's thus obtained agree well with the reported average  $\tau$ 's at three different frequencies for most of the alcohols. This at once indicates the whole molecular rotation of the dipolar molecules at those frequencies. The dipole moments  $\mu_1$  and  $\mu_2$  are, however, measured from the linear coefficients  $\beta$  of hf susceptibilities  $\chi''$  curves against weight fractions  $w_j$  of the alcohols at all the frequencies in terms of the graphically obtained  $\tau_1$  and  $\tau_2$  and the reported  $\tau$  by the existing methods. Theoretical dipole moments  $\mu_{theo}$  from the available bond angles and bond moments are also determined. The slight disagreement among the  $\mu_{theo}$ , reported and estimated  $\mu$  indicates the existence of the inductive, electromeric and mesomeric effects of the substituent polar group –OH attached to the parent ones.

© 2006 Elsevier B.V. All rights reserved.

PACS: 77.22.Gm; 72.80.Le

Keywords: Relaxation time; hf susceptibility; Dipole moment

### 1. Introduction

Relaxation phenomena is one of the most unresolved problems of physics today [1]. It is an important tool to measure relaxation time  $\tau_j$ , dipole moment  $\mu_j$ , shape, size as well as molecular interactions of dipolar liquid molecules in a non-polar solvent under high frequency (hf) electric field [2,3]. It attracted the attention of a large number of workers [4,5]. There are various techniques [6,7] like thermally stimulated depolarization current density (TSDC) and isothermal frequency domain AC spectroscopy (IFDS) with which the present authors are

concerned. The later methods are tedious, complicated and often need computer simulations unlike the Debye and Smyth model which is simpler, straightforward and more topical to understand the relaxation phenomena. Crossley et al. [8] and Glasser et al. [9] showed triple relaxation times for normal and isomeric octyl alcohols under hf electric field of GHz range when they are diluted with non-polar solvent *n*-heptane. These alcohols showed double relaxation times [5]  $\tau_2$  and  $\tau_1$  due to end over end rotation of the whole as well as flexible part of the molecule at all the frequencies of 3.00, 9.25 and 24.33 GHz electric field.  $\tau$  are found to vary with frequency of the applied electric field [10].

It is, therefore, better to study the alcohols again because of their diverse nature in the identical environment. Alcohols are hydrogen-bonded polymer like molecules. The hydroxyl (–OH) group attached to the saturated hydrogen atom is the functional

\* Corresponding author.

E-mail address: koushikduttajsm@rediffmail.com (K. Dutta).

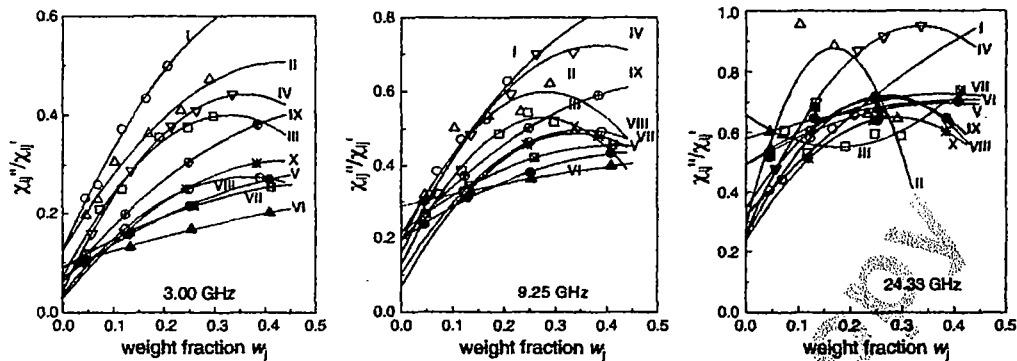


Fig. 1. Variations of  $\chi_{ij}''/\chi_{ij}'$  with  $w_j$  under 3.00, 9.25 and 24.33 GHz electric fields at 298 K for I. 1-butanol (—○—), II. 1-hexanol (—△—), III. 1-heptanol (—□—), IV. 1-decanol (—▽—), V. 2-methyl 3-heptanol (—●—), VI. 3 methyl 3-heptanol (—▲—), VII. 4-methyl 3-heptanol (—■—), VIII. 5-methyl 3-heptanol (—⊙—), IX. 2-octanol (—⊕—) and X. 4-octanol (—★—) in *n*-heptane.

group of alcohols. Due to high electronegativity of oxygen atom O–H bond in alcohol is highly polar. Alcohols usually show  $\alpha$ ,  $\beta$  and  $\gamma$  relaxations under hf electric field. It was observed that dipole moments  $\mu_j$  of alcohols vary slightly when measurements are done in terms of either relative permittivities  $\epsilon_{ij}$  or conductivity  $\sigma_{ij}$  [10].  $\tau_j$ , however, remain the same in both the cases. Nowadays, it is in practice to study the relaxation phenomena in terms of the dielectric orientational susceptibilities  $\chi_{ij}$  rather than high frequency relative permittivities  $\epsilon_{ij}$  or conductivities  $\sigma_{ij}$  [11,12].  $\epsilon_{ij}$  includes all types of polarizations whereas  $\sigma_{ij}$  is concerned with bound molecular charges. If 1 is subtracted from the relative permittivities the susceptibilities contain all the polarizations including the fast polarisations. But if very hf optical permittivities  $\epsilon_{\infty ij}$  are subtracted from  $\epsilon_{oij}$  and  $\epsilon_{ij}$  the susceptibilities  $\chi_{oij}$  and  $\chi_{ij}'$  are, however, directly linked with orientation polarizations only. The purpose of the present paper is to study the existence of double relaxation times of alcohols between two limiting  $\tau_2$  and  $\tau_1$  in terms of hf  $\chi_{ij}$ . The chemical systems under consideration are identical in the same environment to show the double relaxation times at one frequency, it will show the same double relaxation times  $\tau_2$  and  $\tau_1$  at all the frequencies because the double relaxation phenomena are the material properties of the system. Saha et al. and Sit et al. [13,14] proposed a method to measure double relaxation times  $\tau$  of a polar liquid in a non-polar solvent at a given experimental temperature under a single frequency electric field. Moreover, varying  $\tau_2$  and  $\tau_1$  at three different frequencies of electric field from a single frequency measurement technique is not so reliable [4,15].

Mansingh and Kumar [16] presented a graphical technique to measure  $\tau_2$  and  $\tau_1$  for a pure polar liquid molecule within the framework of the Debye and Fröhlich model in terms of measured relative permittivities  $\epsilon$  at different frequencies at a single temperature. However, no such technique has been developed so far to predict  $\tau_2$  and  $\tau_1$  of a polar liquid in a nonpolar solvent at different frequencies of the applied electric field at a single temperature. In this context, however, the almost similar graphical technique is proposed to estimate  $\tau_2$  and  $\tau_1$  of alcohols (j) in a non-polar solvent (i) in terms of real  $\chi_{ij}' (= \epsilon_{ij}' - \epsilon_{\infty ij})$  and imaginary  $\chi_{ij}'' (= \epsilon_{ij}'' - \epsilon_{\infty ij}'')$  parts of hf complex dielectric orientational

susceptibilities  $\chi_{ij}^*$  under 3.00, 9.25 and 24.33 GHz electric fields as functions of  $w_j$ 's.

## 2. Theoretical formulations

### 2.1. Relaxation times $\tau_1$ and $\tau_2$

The dielectric equation for a polar–nonpolar liquid mixture in terms of the complex hf  $\chi_{ij}^*$  for a distribution of  $\tau$  is [1]:

$$\frac{\chi_{ij}^*}{\chi_{oij}} = \int_0^\infty \frac{f(\tau) d\tau}{(1 + j\omega\tau)} \tag{1}$$

where  $f(\tau)$  is the Fröhlich distribution function for the relaxation time such that:

$$f(\tau) = \begin{cases} \frac{1}{A\tau} & \tau_1 < \tau < \tau_2 \\ 0 & \tau_1 > \tau; \tau_2 < \tau \end{cases} \tag{2}$$

and  $A = \text{Fröhlich parameter} = \ln(\tau_2/\tau_1)$ .

Separating the real and imaginary parts of both sides of Eq. (1), the following equations are obtained.

$$\frac{\chi_{ij}'}{\chi_{oij}} = \frac{1}{A} \int_{\tau_1}^{\tau_2} \frac{d\tau}{\tau(1 + \omega^2\tau^2)} \tag{3}$$

and

$$\frac{\chi_{ij}''}{\chi_{oij}} = \frac{1}{A} \int_{\tau_1}^{\tau_2} \frac{\omega d\tau}{(1 + \omega^2\tau^2)} \tag{4}$$

where  $\chi_{ij}' = (\epsilon_{ij}' - \epsilon_{\infty ij})$ ,  $\chi_{ij}'' = \epsilon_{ij}''$  and  $\chi_{oij} = (\epsilon_{oij} - \epsilon_{\infty oij})$  are the real, imaginary and low frequency dielectric susceptibilities expressed in terms of relative permittivities  $\epsilon_{ij}$ .

Dividing Eq. (4) by (3) and evaluating the integral one gets:

$$\frac{\chi_{ij}''}{\chi_{ij}'} = \frac{2[\tan^{-1}(\omega\tau_2) - \tan^{-1}(\omega\tau_1)]}{\ln \frac{\tau_2^2(1 + \omega^2\tau_1^2)}{\tau_1^2(1 + \omega^2\tau_2^2)}} \tag{5}$$

COPY

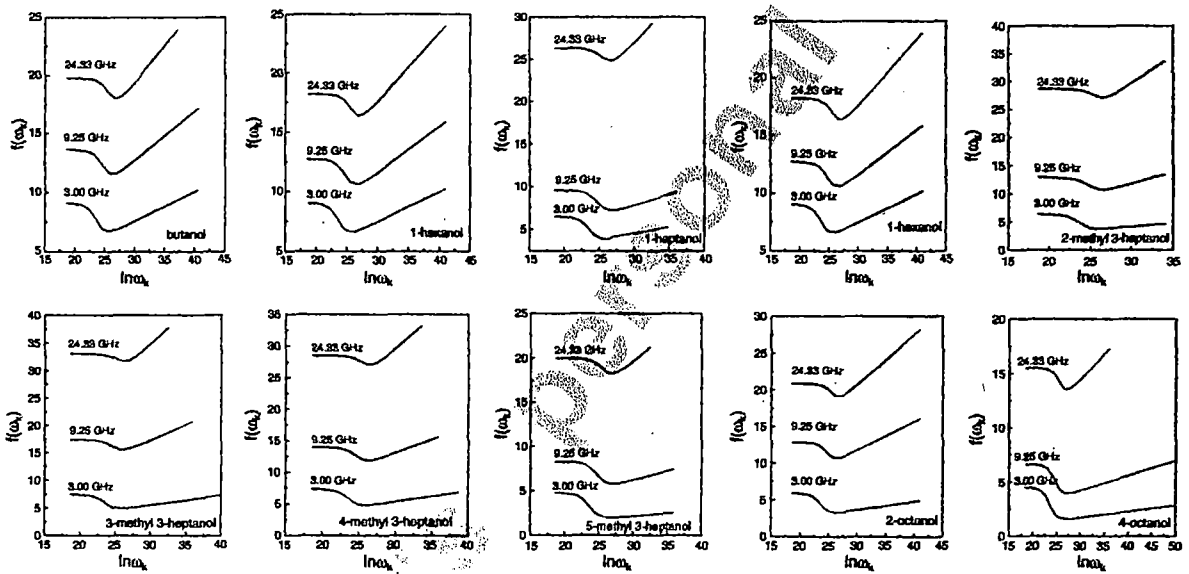


Fig. 2. Variation of  $f(\alpha_x)$  with  $\ln \alpha_x$  for 1-butanol, 1-hexanol, 1-heptanol, 1-decanol, 2-methyl 3-heptanol, 3-methyl 3-heptanol, 4-methyl 3-heptanol, 5-methyl 3-heptanol, 2-octanol and 4-octanol in *n*-heptane under 3.00, 9.25 and 24.33 GHz electric fields at 298 K.

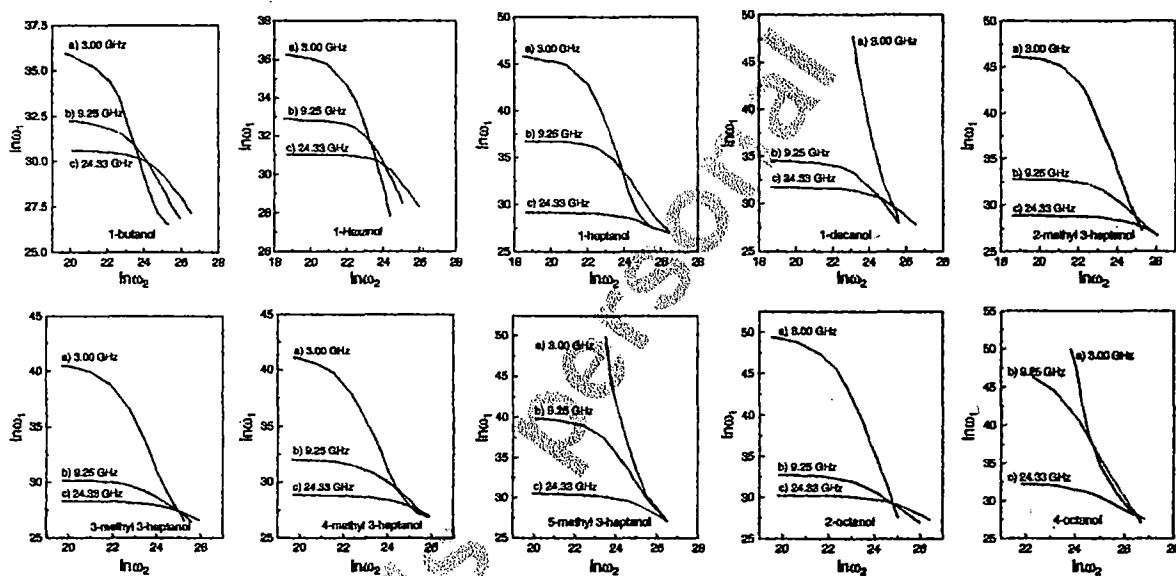


Fig. 3. Plot of  $\ln \omega_1$  against  $\ln \omega_2$  for 1-butanol, 1-hexanol, 1-heptanol, 1-decanol, 2-methyl 3-heptanol, 3-methyl 3-heptanol, 4-methyl 3-heptanol, 5-methyl 3-heptanol, 2-octanol and 4-octanol in *n*-heptane under 3.00, 9.25 and 24.33 GHz electric fields at 298 K.

Table 1

Concentration variation of the real  $\chi'_{ij}$  and imaginary parts  $\chi''_{ij}$  of dimensionless complex dielectric orientation susceptibility  $\chi''_{ij}$  and the static dielectric orientation susceptibility  $\chi_{oij}$  which is real of some normal alcohols and isomeric octyl alcohols in *n*-heptane under 3.00, 9.25 and 24.33 GHz electric fields at 298 K

Frequency <i>f</i> in GHz	Weight fraction $w_j$	$\chi'_{ij}$	$\chi''_{ij}$	$\chi_{oij}$	Weight fraction $w_j$	$\chi'_{ij}$	$\chi''_{ij}$	$\chi_{oij}$
3.00	I. 1-butanol				II. 1-hexanol			
	0.0451	0.049	0.0114	0.055	0.0459	0.033	0.0065	0.044
	0.0697	0.072	0.0188	0.093	0.0703	0.051	0.0117	0.063
	0.1163	0.123	0.0460	0.197	0.1028	0.070	0.0214	0.094
	0.1652	0.180	0.0782	0.381	0.1688	0.123	0.0446	0.207
0.2072	0.224	0.1119	0.601	0.2335	0.184	0.0755	0.358	
9.25	0.0451	0.040	0.0121	0.055	0.0459	0.026	0.0083	0.044
	0.0697	0.057	0.0220	0.093	0.0703	0.038	0.0121	0.063
	0.1163	0.088	0.0416	0.197	0.1028	0.045	0.0226	0.094
	0.1652	0.121	0.0637	0.381	0.1688	0.085	0.0454	0.207
	0.2072	0.152	0.0956	0.601	0.2335	0.126	0.0688	0.358
24.33	0.0451	0.036	0.0147	0.055	0.459	0.024	0.0131	0.044
	0.0697	0.053	0.0236	0.093	0.0703	0.032	0.0190	0.063
	0.1163	0.082	0.0425	0.197	0.1028	0.031	0.0296	0.094
	0.1652	0.105	0.0644	0.381	0.1688	0.048	0.0425	0.207
	0.2072	0.124	0.0818	0.601	0.2335	0.086	0.0569	0.358
3.00	III. 1-heptanol				IV. 1-decanol			
	0.0735	0.053	0.0111	0.056	0.0572	0.032	0.0051	0.036
	0.1175	0.086	0.0216	0.109	0.1351	0.067	0.0194	0.086
	0.1909	0.128	0.0456	0.236	0.2140	0.098	0.0371	0.157
	0.2465	0.173	0.0651	0.313	0.2460	0.121	0.0496	0.212
9.25	0.0735	0.040	0.0129	0.056	0.0572	0.028	0.0090	0.036
	0.1175	0.060	0.0232	0.109	0.1351	0.047	0.0228	0.086
	0.1909	0.090	0.0438	0.236	0.2140	0.065	0.0386	0.157
	0.2465	0.112	0.0609	0.313	0.2640	0.069	0.0484	0.212
	0.2970	0.149	0.0774	0.456	0.3353	0.093	0.0656	0.316
24.33	0.0735	0.030	0.0182	0.056	0.0572	0.025	0.0120	0.036
	0.1175	0.050	0.0265	0.109	0.1351	0.039	0.0273	0.086
	0.1909	0.087	0.0482	0.236	0.2140	0.046	0.0400	0.157
	0.2465	0.095	0.0567	0.313	0.2640	0.056	0.0513	0.212
	0.2970	0.118	0.0694	0.456	0.3353	0.067	0.0637	0.316
3.00	V. 2-methyl 3-heptanol				VI. 3-methyl 3-heptanol			
	0.0437	0.040	0.0040	0.041	0.0450	0.040	0.0043	0.040
	0.1299	0.086	0.0137	0.093	0.1334	0.099	0.0131	0.103
	0.2522	0.143	0.0309	0.165	0.2538	0.162	0.0272	0.176
	0.4081	0.215	0.0583	0.276	0.4085	0.242	0.0489	0.277
9.25	0.0437	0.037	0.0088	0.041	0.0450	0.034	0.0103	0.040
	0.1299	0.078	0.0244	0.093	0.1334	0.079	0.0263	0.103
	0.2522	0.108	0.0412	0.165	0.2538	0.126	0.0458	0.176
	0.4081	0.164	0.0710	0.276	0.4085	0.192	0.0766	0.277
	0.0437	0.030	0.0156	0.041	0.0450	0.031	0.0187	0.040
24.33	0.1299	0.056	0.0362	0.093	0.1334	0.061	0.0394	0.103
	0.2522	0.088	0.0565	0.165	0.2538	0.099	0.0674	0.176
	0.4081	0.115	0.0809	0.276	0.4085	0.131	0.0928	0.277
	VII. 4-methyl 3-heptanol				VIII. 5-methyl 3-heptanol			
	0.0466	0.039	0.0046	0.040	0.1228	0.084	0.0143	0.092
0.1326	0.090	0.0147	0.096	0.2489	0.134	0.0337	0.164	
0.2590	0.156	0.0338	0.174	0.3898	0.202	0.0554	0.275	
0.4124	0.224	0.0572	0.287					
9.25	0.0466	0.034	0.0091	0.040	0.1228	0.068	0.0225	0.092
	0.1326	0.076	0.0262	0.096	0.2489	0.095	0.0441	0.164
	0.2590	0.112	0.0472	0.174	0.3898	0.143	0.0706	0.275
	0.4124	0.168	0.0766	0.287				

Table 1 (continued)

Frequency <i>f</i> in GHz	Weight fraction $w_j$	$\chi'_{ij}$	$\chi''_{ij}$	$\chi_{oij}$	Weight fraction $w_j$	$\chi'_{ij}$	$\chi''_{ij}$	$\chi_{oij}$
24.33	0.0466	0.028	0.0146	0.040	0.1228	0.051	0.0297	0.092
	0.1326	0.055	0.0376	0.096	0.2489	0.071	0.0511	0.164
	0.2590	0.093	0.0616	0.174	0.3898	0.107	0.0675	0.275
	0.4124	0.115	0.0849	0.287				
3.00	IX. 2-octanol				X. 4-octanol			
	0.1236	0.078	0.0156	0.065	0.1201	0.081	0.0129	0.092
	0.2479	0.137	0.0419	0.199	0.2445	0.120	0.0302	0.151
	0.3844	0.207	0.0791	0.374	0.3838	0.181	0.0549	0.251
9.25	0.1236	0.061	0.0227	0.065	0.1201	0.063	0.0198	0.092
	0.2479	0.093	0.0467	0.199	0.2445	0.087	0.0397	0.151
	0.3844	0.133	0.0786	0.374	0.3838	0.128	0.0616	0.251
	0.1236	0.047	0.0285	0.065	0.1201	0.052	0.0266	0.092
24.33	0.2479	0.072	0.0513	0.199	0.2445	0.070	0.0449	0.151
	0.3844	0.105	0.0680	0.374	0.3838	0.109	0.0659	0.251

On rearrangement of Eq. (5) and assuming smaller relaxation time  $\tau_1 = 1/\omega_1$  and larger relaxation time  $\tau_2 = 1/\omega_2$  Eq. (5) becomes :

$$\frac{\chi''_{ij}}{\chi'_{ij}} \ln(\omega_1^2 + \omega^2) + 2 \tan^{-1} \frac{\omega}{\omega_1} = \frac{\chi''_{ij}}{\chi'_{ij}} \ln(\omega_2^2 + \omega^2) + 2 \tan^{-1} \frac{\omega}{\omega_2}$$

or,  $f(\omega_1) = f(\omega_2) = f(\omega_k)$  where

$$f(\omega_k) = \left[ \left( \frac{\chi''_{ij}}{\chi'_{ij}} \right) \ln(\omega_k^2 + \omega^2) + 2 \tan^{-1} \frac{\omega}{\omega_k} \right] \quad (6)$$

The term  $\chi''_{ij}/\chi'_{ij}$  of Eq. (6) is a function of weight fraction  $w_j$  of polar solute at a given temperature  $T$  and angular frequency  $\omega$  of the hf electric field. The factor  $f(\omega_k)$  is, however, made constant for fixed  $\tau_2$  and  $\tau_1$  at a given angular frequency  $\omega$  by introducing the following term in the Eq. (6).

$$f(\omega_k) = \left( \frac{\chi''_{ij}}{\chi'_{ij}} \right)_{w_j \rightarrow 0} \ln(\omega_k^2 + \omega^2) + 2 \tan^{-1} \frac{\omega}{\omega_k} \quad (7)$$

where  $(\chi''_{ij}/\chi'_{ij})_{w_j \rightarrow 0}$  is the intercept of  $(\chi''_{ij}/\chi'_{ij})$  against  $w_j$  curve at  $w_j \rightarrow 0$  as shown in Fig. 1 and are placed in Table 2. A curve of  $f(\omega_k)$  against  $\ln \omega_k$  is drawn in Fig. 2 by varying  $\omega_k$  independently for a given  $\omega$  to get two values of  $\ln \omega_2$  and  $\ln \omega_1$  ( $\omega_2 < \omega_1$ ) for the same  $f(\omega_k)$ . Finally graphs of  $\ln \omega_1$  vs.  $\ln \omega_2$  are plotted in Fig. 3 for three different values of  $\omega (= 2\pi f)$ ,  $f$  being the frequency of the electric field of 24.33, 9.25 and 3.00 GHz. The point of intersection of the curves yields  $\tau_2$  and  $\tau_1$  of a polar molecule to place them in Table 2.

$\tau_2$  and  $\tau_1$  were also estimated from

$$\frac{\chi_{oij} - \chi'_{ij}}{\chi'_{ij}} = \omega(\tau_2 + \tau_1) \frac{\chi''_{ij}}{\chi'_{ij}} - \omega^2 \tau_1 \tau_2 \quad (8)$$

based on the single frequency measurement technique [12]. The terms  $(\chi_{oij} - \chi_{ij}')/\chi_{ij}'$  and  $\chi_{ij}''/\chi_{ij}'$  on both sides of Eq. (8) are functions of  $w_j$  of the polar solute at a given angular frequency  $\omega$  of the electric field. The graphs of  $(\chi_{oij} - \chi_{ij}')/\chi_{ij}'$  against  $\chi_{ij}''/\chi_{ij}'$  are drawn for different  $w_j$  at 24.33, 9.25 and 3.00 GHz electric fields to get fixed intercepts and slopes from which  $\tau_1$  and  $\tau_2$  were obtained to get the mean values of  $\tau_1$  and  $\tau_2$  placed in Table 2 for comparison with the three sets of  $\tau_1$  and  $\tau_2$  for alcohols at 24.33, 9.25 and 3.00 GHz electric fields, respectively.

## 2.2. Dipole moments $\mu_1$ and $\mu_2$ from $\tau_1$ and $\tau_2$

The Debye equation [17] for a polar–nonpolar liquid mixture under hf electric field in terms of  $\chi_{ij}$ 's is now written as :

$$\frac{d\chi_{ij}''}{d\chi_{ij}'} = \omega\tau \quad (9)$$

$$\frac{(d\chi_{ij}''/dw_j)_{w_j \rightarrow 0}}{(d\chi_{ij}'/dw_j)_{w_j \rightarrow 0}} = \omega\tau \quad (10)$$

Again the imaginary part  $\chi_{ij}''$  of the complex hf susceptibility  $\chi_{ij}^*$  as a function of  $w_j$  of a solute can be written as [17]

$$\chi_{ij}'' = \frac{N\rho_{ij}\mu_j^2}{27\epsilon_0 k_B T M_j} \frac{\omega\tau}{1 + \omega^2\tau^2} (\epsilon_{ij} + 2)^2 w_j$$

which on differentiation with respect to  $w_j$  and at  $w_j \rightarrow 0$  yields:

$$\left(\frac{d\chi_{ij}''}{dw_j}\right)_{w_j \rightarrow 0} = \frac{N\rho_{ij}\mu_j^2}{27\epsilon_0 k_B T M_j} \frac{\omega\tau}{1 + \omega^2\tau^2} (\epsilon_i + 2)^2 \quad (11)$$

where the density of the solution  $\rho_{ij}$  becomes  $\rho_i$ =density of solvent,  $(\epsilon_{ij} + 2)^2$  becomes  $(\epsilon_i + 2)^2$  at  $w_j \rightarrow 0$ ,  $k_B$ =Boltzmann constant= $1.38 \times 10^{-23}$  J mole<sup>-1</sup> K<sup>-1</sup>,  $N$ =Avogadro's number= $6.023 \times 10^{23}$ ,  $\epsilon_i$ =relative permittivity of solvent,  $\epsilon_0$ =permittivity of free space= $8.854 \times 10^{-12}$  F m<sup>-1</sup>,  $M_j$ =alcohol molecular weight and  $\mu_j$ =dipole moment of the alcohol molecule.

Comparing Eqs. (10) and (11) one gets:

$$\left(\frac{d\chi_{ij}''}{dw_j}\right)_{w_j \rightarrow 0} = \frac{N\rho_i\mu_j^2}{27\epsilon_0 k_B T M_j} \frac{1}{1 + \omega^2\tau^2} (\epsilon_i + 2)^2 = \beta \quad (12)$$

where  $\beta$  is the slope of  $\chi_{ij}''$ - $w_j$  curves of Fig. 5 at  $w_j \rightarrow 0$ . Here no approximation is made in the determination of  $\mu_j$  unlike conductivity measurement technique [10].

After simplification, the hf  $\mu_j$  due to orientation polarization alone is given by:

$$\mu_j = \left(\frac{27\epsilon_0 k_B T M_j \beta}{N\rho_i(\epsilon_i + 2)^2 b}\right)^{\frac{1}{2}} \quad (13)$$

where the dimensionless parameter  $b$  is given by:

$$b = 1/(1 + \omega^2\tau^2) \quad (14)$$

## 3. Results and discussions

The data of  $\chi_{ij}'$ ,  $\chi_{ij}''$  and  $\chi_{oij}$  at different  $w_j$ 's of a number of alcohols in *n*-heptane at 298 K under 24.33, 9.25 and 3.00 GHz electric fields are extracted from the measured permittivities  $\epsilon_{ij}$  of Crossley et al. [8] and Glasser et al. [9] presented in Table 1. The terms  $\chi_{ij}''/\chi_{ij}'$  for each alcohol are plotted against different  $w_j$  for 24.33, 9.25 and 3.00 GHz electric fields at 298 K as seen in Fig. 1. So far as Fig. 1 is concerned, it seems that the variation of  $\chi_{ij}''/\chi_{ij}'$  with weight fraction  $w_j$  for 1-hexanol in 24.33 GHz electric field exhibits a strange behaviour. The intercept of  $\chi_{ij}''/\chi_{ij}'$  at  $w_j \rightarrow 0$  has been obtained as a polynomial second order least square fitting of the experimental data, but the nature of the curve appears to be surprising. The curves at all the frequencies are convex except system III (–□–) which is concave at 24.33 GHz. It is interesting to see that as the frequency of the applied electric field increases the shape of the curves become more convex. The values of intercepts of  $\chi_{ij}''/\chi_{ij}'$  vs.  $w_j$  curves at  $w_j \rightarrow 0$  are placed in column 3 of Table 2. The intercepts are found to increase with the frequency of the electric field. For several arbitrary values of angular frequency  $\omega_k$ , three graphs of  $f(\omega_k)$  against  $\ln\omega_k$  according to Eq. (7) for the alcohols were drawn for 3.00, 9.25 and 24.33 GHz electric fields in Fig. 2. The graphs were drawn by using a PC which shows the gradual decrease of  $f(\omega_k)$  with the increase of  $\ln\omega_k$  to exhibit minimum at a certain  $\omega_k$  and then increase afterwards for a fixed  $\omega$  [16]. Curves of  $f(\omega_k)$  against  $\ln\omega_k$  at 24.33 and 3.00 GHz electric fields yield the highest and the least values of  $f(\omega_k)$  for a fixed  $\ln\omega_k$ . The  $f(\omega_k)$ - $\ln\omega_k$  curves at 9.25 GHz, however, occupy the intermediate position and are nearer to 3.00 GHz electric field for all the alcohols as observed in Fig. 2. This is explained on the basis of the fact that  $f(\omega_k)$  is higher for larger intercept of  $\chi_{ij}''/\chi_{ij}'$  against  $w_j$  curve at  $w_j \rightarrow 0$ , in Fig. 1, according to Eq. (7). A large number of  $\ln\omega_2$  and  $\ln\omega_1$  ( $\ln\omega_2 < \ln\omega_1$ ) are selected for a fixed  $f(\omega_k)$  in order to draw the graphs of  $\ln\omega_1$  vs.  $\ln\omega_2$  at 24.33, 9.25 and 3.00 GHz electric fields from Fig. 3. The values of  $\ln\omega_2$  and  $\ln\omega_1$  are chosen by drawing a horizontal line along the  $\ln\omega_k$  axis in the region of the curve for which  $f(\omega_k)$  is the same in Fig. 2. It is interesting to see that if  $\ln\omega_2$  is made fixed for all the curves of Fig. 2 of a polar–nonpolar liquid mixture the values of  $\ln\omega_1$  are the highest and the least for 3.00 and 24.33 GHz, respectively, in the  $\ln\omega_1$  vs.  $\ln\omega_2$  curves. This explains the larger magnitudes of  $\ln\omega_1$  for 3.00, 9.25 and 24.33 GHz electric fields. The graphs are similar in nature. They cut at a point for almost all the dipolar liquids to yield the significant values of  $\tau_2$  and  $\tau_1$ , respectively. Unlike other systems 1-butanol, 1-hexanol, 1-heptanol, 1-decanol, 2-methyl 3-heptanol and 4-methyl 3-heptanol the curves meet at three points to exhibit three different possible values of  $\tau_2$  and  $\tau_1$  [8,9]. The average values of the points for  $\ln\omega_1$  were, however, selected to get  $\ln\omega_2$  and the recalculated  $\tau_1$  and  $\tau_2$  are placed in the 6th and 7th column of Table 2.

Table 2

Intercepts of  $\chi''_{ij}/\chi'_{ij}$  against  $w_j$  curve at  $w_j \rightarrow 0$ , values of  $\ln\omega_2$  and  $\ln\omega_1$  from Fig. 3, average  $\tau_2$  and  $\tau_1$  from  $\ln\omega_2$  and  $\ln\omega_1$ ,  $\tau_2$  and  $\tau_1$  from single frequency measurement of Eq. (8) along with their average values,  $\tau$  from the ratio of slopes of  $\chi''_{ij}-w_j$  and  $\chi'_{ij}-w_j$  at  $w_j \rightarrow 0$  of Eq. (10) and from direct slopes of  $\chi''_{ij}-\chi'_{ij}$  of Eq. (9) under 3.00, 9.25 and 24.33 GHz electric fields

System with sl. no	Frequency $f$ in GHz	Intercept of $\chi''_{ij}/\chi'_{ij}-w_j$ at $w_j \rightarrow 0$	Values of $\ln\omega_2$ and $\ln\omega_1$ from Fig. 3	Average $\tau_2$ and $\tau_1$ in ps from Fig. 3	$\tau_2$ and $\tau_1$ in ps from single frequency measurement	Average $\tau_2$ and $\tau_1$	$\tau^a$ in ps	$\tau^b$ in ps
I. 1-butanol	a) 3.00	0.1262	ab) 23.5015 30.8189	46.41 0.08	211.41 9.10	122.63 4.96	12.51	30.37
	b) 9.25	0.2120	bc) 24.2051 29.8712		101.87 3.73		4.28	12.54
	c) 24.33	0.3231	ca) 23.6737 30.1101		54.60 2.04		3.04	5.02
II. 1-hexanol	a) 3.00	0.1246	ab) 23.2412 31.8059	57.03 0.04	204.26 9.17	110.44 5.01	9.79	27.10
	b) 9.25	0.1933	bc) 24.1343 30.4314		85.24 3.76		7.79	11.43
	c) 24.33	0.2928	ca) 23.5801 30.6780		41.81 2.10		—	4.05
III. 1-heptanol	a) 3.00	0.0711	ab) 23.8767 33.6138	18.80 0.91	208.81 9.20	113.91 4.98	20.66	24.87
	b) 9.25	0.1306	bc) 26.4479 27.0234		83.03 3.30		16.10	10.56
	c) 24.33	0.4503	ca) 25.2871 27.7518		49.89 2.43		3.02	3.89
IV. 1-decanol	a) 3.00	0.0438	ab) 25.5281 27.9946	13.12 0.29	135.66 6.89	83.68 5.27	20.18	27.70
	b) 9.25	0.1620	bc) 24.5801 30.5149		83.14 5.61		13.33	15.39
	c) 24.33	0.2631	ca) 25.3244 29.7019		32.25 3.30		9.06	8.21
V. 2-methyl 3-heptanol	a) 3.00	0.0700	ab) 24.9650 28.6944	11.19 0.90	73.31 5.41	50.96 4.3	9.08	16.61
	b) 9.25	0.1974	bc) 25.6712 27.3056		49.61 4.10		6.40	8.54
	c) 24.33	0.4952	ca) 25.1384 27.6667		29.96 3.39		4.35	4.92
VI. 3-methyl 3-heptanol	a) 3.00	0.0921	25.0098 27.4128	13.75 1.24	73.55 6.17	43.80 4.41	6.76	11.83
	b) 9.25	0.2882			43.34 4.37		5.56	7.25
	c) 24.33	0.5807			14.52 2.68		4.45	4.85
VII. 4-methyl 3-heptanol	a) 3.00	0.0892	ab) 24.4955 29.3972	13.40 0.55	84.34 6.71	51.61 4.74	9.87	15.22
	b) 9.25	0.2174	bc) 25.5912 27.4004		45.08 4.21		7.41	8.79
	c) 24.33	0.4932	ca) 25.0210 27.9023		25.40 3.31		4.43	5.09
VIII. 5-methyl 3-heptanol	a) 3.00	0.0358	26.4103 27.3200	3.39 1.36	101.22 6.58	57.13 4.15	29.45	18.39
	b) 9.25	0.1040			52.36 4.21		67.14	10.86
	c) 24.33	0.3276			17.83 1.66		67.32	4.24
IX. 2-octanol	a) 3.00	0.0604	24.8271 29.2251	16.51 0.20	160.41 7.83	94.46 4.94	15.75	26.18
	b) 9.25	0.1964			92.00 5.11		11.25	13.37
	c) 24.33	0.3447			30.97 1.89		12.34	4.40
X. 4-octanol	a) 3.00	0.0286	26.4780 28.0264	3.17 0.67	85.13 4.72	49.55 3.11	32.32	22.21
	b) 9.25	0.0699			42.74 2.64		53.48	10.86
	c) 24.33	0.2409			20.77 1.97		—	4.35

$\tau^a$  = relaxation time from the ratio of slopes of the individual variations of  $\chi''_{ij}-w_j$  and  $\chi'_{ij}-w_j$  at  $w_j \rightarrow 0$  of Eq. (10).

$\tau^b$  = relaxation time from the direct slopes of  $\chi''_{ij}-\chi'_{ij}$  of Eq. (9).

$\tau_2$  and  $\tau_1$  are also calculated from the slopes and intercepts of the straight line of Eq. (8) from single frequency measurement technique [12]. The estimated  $\tau_2$  and  $\tau_1$  are placed in Table 2. They are found to be dependent on the frequency of the applied electric field. The existence of double relaxation phenomena reflects the material property of the chemical systems under investigation and should not depend on the measurement frequency. Although the real part  $\chi'_{ij}$  and the imaginary part  $\chi''_{ij}$  of the hf complex dielectric orientational susceptibility  $\chi_{ij}^*$  vary with the frequency of the applied electric field, the fundamental dielectric parameters such as the dielectric decrement, relaxation time and dipole moment which describe the relaxation property of the system, do not. Therefore, if any alcohol in *n*-heptane exhibits double relaxation behaviour, this should be reflected at all three frequencies and the analysis should produce the same value of  $\tau_2$  and  $\tau_1$  at all three frequencies. Thus  $\tau$  are, therefore, estimated from the ratio of slopes of  $\chi''_{ij}-w_j$  and  $\chi'_{ij}-w_j$  at  $w_j \rightarrow 0$  of Eq. (10) and from the slope of linear relation  $\chi''_{ij}-\chi'_{ij}$  according to Eq. (9). They are placed side by side in the columns 12 and 13 of Table 2. The estimated  $\tau_2$  and  $\tau_1$  obtained

from present graphical technique are compared with  $\tau$  from the single frequency measurement technique [13,14] as well as with  $\tau$  from Eqs. (10) and (9). It is to be noted that  $\tau$  from graphical technique are in agreement with average  $\tau$  from Eqs. (10) and (9) for almost all systems except 1-butanol, 1-hexanol, 5-methyl 3-heptanol and 4-octanol. Average  $\tau_2$  and  $\tau_1$  from Eq. (8) are, however, higher in magnitude than the graphical technique proposed here.  $\tau_1$  are smaller than the reported average  $\tau$  from ratio of slopes as well as direct slopes. This type of behaviour may reveal that double relaxation mechanism of polar-nonpolar liquid mixture is the material property of the chemical systems, which is independent of  $\omega$  of the applied electric field unlike earlier observation [12]. The proposed graphical technique seems to be superior to the existing one [4,15] as it yields macroscopic and microscopic relaxation times, which are independent of frequency  $\omega$ .

The curves of  $\chi''_{ij}$  against  $w_j$  as seen in Fig. 4 are all parabolic. They start from origin and increase with  $w_j$  for 3.00, 9.25 and 24.33 GHz electric fields. Unlike the curves at 24.33 GHz, the curves are concave for 9.25 and 3.00 GHz electric fields.

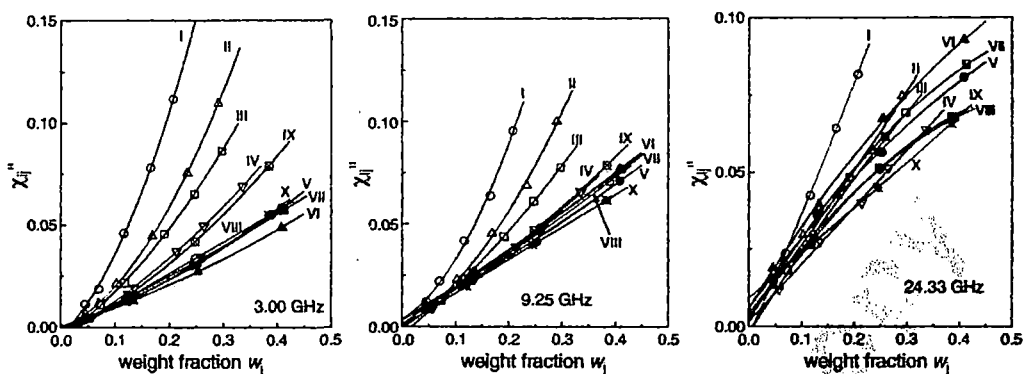


Fig. 4. Variations of  $\chi_{ij}''$  with  $w_j$  for I. 1-butanol (—○—), II. 1-hexanol (—△—), III. 1-heptanol (—□—), IV. 1-decanol (—▽—), V. 2-methyl 3-heptanol (—●—), VI. 3-methyl 3-heptanol (—▲—), VII. 4-methyl 3-heptanol (—⊞—), VIII. 5-methyl 3-heptanol (—⊙—), IX. 2-octanol (—⊕—) and X. 4-octanol (—★—) in *n*-heptane under 3.00, 9.25 and 24.33 GHz electric fields at 298 K.

The systems V(—●—), VI(—▲—), VII(—⊞—), VIII(—⊙—) and X (—★—) are found to overlap at 3.00 and 9.25 GHz electric fields exhibiting almost the same absorption of hf electric energy and are maximum at 24.33 GHz. This signifies that the study of relaxation mechanism of alcohols is relevant as observed elsewhere [10].

The  $\chi_{ij}''-w_j$  curves of Fig. 5 are also parabolic in nature at all the frequencies of 3.00, 9.25 and 24.33 GHz. This indicates that the orientation polarizations increase with the  $w_j$ 's and decrease at higher frequency. The dipole moments of the alcohol molecules  $\mu_2$  and  $\mu_1$  from the slope  $\beta$  of  $\chi_{ij}''-w_j$  curve and estimated  $\tau$  from  $\chi_{ij}''$  measurements are calculated to place them in the 4th and 5th columns of Table 3.  $\mu_2$  and  $\mu_1$  from the graphical method are found to be in excellent agreement with reported average  $\mu$  except 1-butanol, 1-hexanol, 1-heptanol where  $\mu_2$  are slightly greater. The slight disagreement between estimated and reported  $\mu$  may be due to combined effect of frequency of the applied electric field as well as inductive, electromeric and mesomeric effects existing among polar groups of the molecules. The theoretical dipole moments  $\mu_{theo}$  of the polar alcohols are calculated from the available bond

angles and bond moments [18] in order to display in Fig. 6. They are placed in column 8 of Table 3. Alcohols are classified as monohydric, dihydric, trihydric and polyhydric compounds in which the —OH group is attached to the parent molecules. The —O—H bond as sketched in Fig. 6 is highly polar because the —O— is highly electronegative carrying a negative charge  $\delta^-$  while the H possesses highly positive charge  $\delta^+$ . The polarity of O—H bond exerts a strong attraction on the other H atoms of the molecules [19]. The hydrogen bonding, thus produced, gives rise to theoretical dipole moments  $\mu_{theo}$  for the alcohols under investigation in excellent agreement with  $\mu_1$  measured by graphical and single frequency measurement technique as shown in Table 3. This type of study ultimately indicates that  $\mu_1$  of a polar molecule under hf electric field is only due to rotation of the flexible parts attached to the parent ones.

#### 4. Conclusion

The study of relaxation phenomena of a number of alcohols in *n*-heptane under 3.00, 9.25 and 24.33 GHz electric fields at

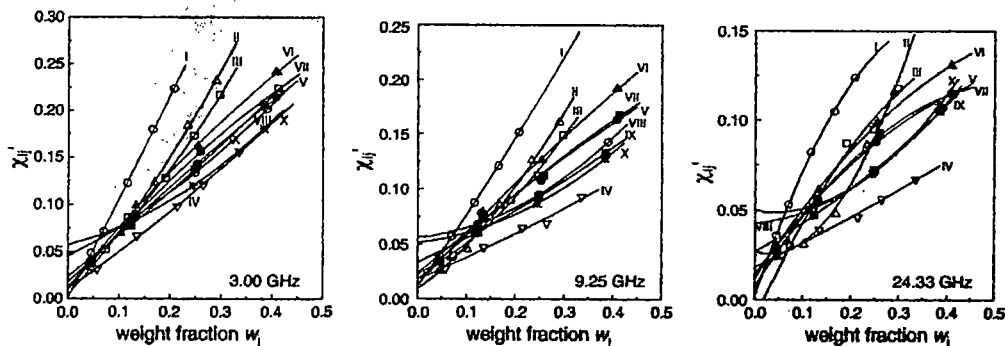


Fig. 5. Variations of  $\chi_{ij}'$  with  $w_j$  for I. 1-butanol (—○—), II. 1-hexanol (—△—), III. 1-heptanol (—□—), IV. 1-decanol (—▽—), V. 2-methyl 3-heptanol (—●—), VI. 3-methyl 3-heptanol (—▲—), VII. 4-methyl 3-heptanol (—⊞—), VIII. 5-methyl 3-heptanol (—⊙—), IX. 2-octanol (—⊕—) and X. 4-octanol (—★—) in *n*-heptane under 3.00, 9.25 and 24.33 GHz electric fields at 298 K.

Table 3

Slope of  $\chi''_{ij}-w_j$  curve at  $w_j \rightarrow 0$ , dipole moment  $\mu_2$  and  $\mu_1$  from graphical technique, dipole moments from single frequency measurement, theoretical dipole moment  $\mu_{theo}$  from the available bond angles and bond moments and the dipole moments using  $\tau$  from Eqs. (10) and (9)

System with sl. no and mol. wt	f in GHz	Slope of $\chi''_{ij}-w_j$ at $w_j \rightarrow 0$	$\mu \times 10^{30}$ (C m) from average $\tau_2$ and $\tau_1$ of Fig. 3		$\mu \times 10^{30}$ from single frequency measurement		$\mu_{theo} \times 10^{30}$ in C m	$\mu_1^a \times 10^{30}$ in C m	$\mu_2^b \times 10^{30}$ in C m
			$\mu_2$	$\mu_1$	$\mu_2$	$\mu_1$			
I. 1-butanol $M_j=0.074$ kg	a) 3.00	1.028	4.67	3.45	17.44	4.30	4.95	3.54	3.97
	b) 9.25	0.627	8.04	2.69	22.07	3.77		2.78	3.33
	c) 24.33	0.796	22.69	3.04	29.17	3.63		3.34	3.83
II. 1-hexanol $M_j=0.102$ kg	a) 3.00	0.608	4.57	3.11	16.87	4.30	4.35	3.17	3.50
	b) 9.25	0.330	7.95	2.29	18.77	3.80		2.52	2.75
	c) 24.33	-0.089	-	-	21.20	3.43		-	-
III. 1-heptanol $M_j=0.116$ kg	a) 3.00	0.447	3.02	2.85	17.40	4.33	4.05	3.06	3.15
	b) 9.25	0.213	2.91	1.97	18.40	3.80		2.69	2.31
	c) 24.33	0.588	9.94	3.30	27.01	3.73		3.60	3.80
IV. 1-decanol $M_j=0.158$ kg	a) 3.00	0.383	3.17	3.08	11.94	4.40	3.15	3.29	3.47
	b) 9.25	0.192	2.74	2.18	18.40	3.93		2.76	2.92
	c) 24.33	0.133	4.06	1.81	17.24	3.83		3.10	2.91
V. 2-methyl 3-heptanol $M_j=0.130$ kg	a) 3.00	0.530	3.36	3.28	6.93	4.10	5.85	3.33	3.44
	b) 9.25	0.376	3.30	2.77	11.30	3.80		2.95	3.09
	c) 24.33	0.359	5.35	2.73	16.00	3.83		3.24	3.38
VI. 3-methyl 3-heptanol $M_j=0.130$ kg	a) 3.00	0.663	3.79	3.67	7.27	4.30	5.85	3.70	3.76
	b) 9.25	0.477	3.99	3.12	10.70	4.07		3.27	3.38
	c) 24.33	0.414	6.75	2.95	8.60	30.83		3.51	3.61
VII. 4-methyl 3-heptanol $M_j=0.130$ Kg	a) 3.00	0.643	3.64	3.62	7.83	4.20	5.85	3.68	3.76
	b) 9.25	0.413	3.06	2.92	10.64	3.90		3.16	3.25
	c) 24.33	0.424	3.93	3.07	13.90	3.90		3.55	3.72
VIII. 5-methyl 3-heptanol $M_j=0.130$ kg	a) 3.00	0.277	2.38	2.37	8.47	3.97	5.85	2.71	2.51
	b) 9.25	0.038	0.90	0.88	11.17	3.60		3.54	1.04
	c) 24.33	0.024	0.79	0.71	9.50	3.37		7.22	0.83
IX. 2-octanol $M_j=0.130$ kg	a) 3.00	0.420	3.06	2.92	12.94	4.10	3.58	3.05	3.26
	b) 9.25	0.207	2.84	2.05	18.90	3.63		2.45	2.60
	c) 24.33	0.143	4.63	1.71	16.00	3.43		3.64	2.06
X. 4-octanol $M_j=0.130$ kg	a) 3.00	0.142	1.70	1.70	7.10	3.77	3.58	1.99	1.84
	b) 9.25	0.053	1.06	1.04	9.07	3.43		3.39	1.23
	c) 24.33	-0.041	-	-	10.97	3.43		-	-

$\mu_1^a$  = dipole moment using  $\tau$  from Eq. (10).

$\mu_2^b$  = dipole moment using  $\tau$  from Eq. (9).

298 K is a straightforward, simpler and topical one to establish the material property of the relaxation times. The isomeric type with H-bonding long chained alcohols in *n*-heptane shows  $\tau_2$  and  $\tau_1$  due to the rotations of the whole molecule and the flexible parts attached to the parent molecules. Unlike the other dielectric terminologies and parameters such as the permittivities, dielectric loss etc.  $\tau$  are the material property of the chemical system under identical environment.  $\tau$  are independent of the electric field frequencies in GHz range.

We are interested only with the susceptibilities  $\chi_{ij}$  concerned with the orientation polarisation. Nevertheless the susceptibility measurement is used instead of hf permittivity  $\epsilon_{ij}$  and hf conductivity  $\sigma_{ij}$ .  $\epsilon_{ij}$  includes all types of polarization while  $\sigma_{ij}$  is concerned with the bound molecular charges of the molecule. A graphical method was, therefore, attempted for to include  $\chi_{ij}$  derived from the  $\epsilon_{ij}$  measurements of Crossley et al. [8] and Glasser et al. [9] in order to establish the material property to study the relaxation mechanism of such polar liquids in nonpolar solvent under hf electric fields. Alcohols are supposed to be molecules of polymeric type having strong H-bonding. The variations of  $\chi''_{ij}/\chi'_{ij}$  with  $w_j$  in figures and tables showed that the intercepts of  $\chi''_{ij}/\chi'_{ij}$  against  $w_j$  at  $w_j \rightarrow 0$  increase with

the applied electric field frequencies. The results of the fixed value of  $\ln\omega_k$  from the values of  $f(\omega_k)$  were larger with the increasing frequency and the potential well like  $f(\omega_k)-\ln\omega_k$  curves assume the highest, intermediate and lowest positions under 24.33, 9.25 and 3.00 GHz electric fields as displayed in Fig. 2. A number of  $\ln\omega_2$  and  $\ln\omega_1$  values ( $\ln\omega_2 < \ln\omega_1$ ) were selected in Fig. 2 for a fixed  $f(\omega_k)$  in order to draw  $\ln\omega_1$  vs.  $\ln\omega_2$  curves at the three frequencies. All the curves are similar in nature. The  $\ln\omega_1$  decreases gradually with the increase of  $\ln\omega_2$  to cut a point for most of the alcohols while 1-butanol, 1-hexanol, 1-heptanol, 1-decanol, 2-methyl 3-heptanol and 4-methyl 3-heptanol cut at three points to yield significant values of  $\tau_2$  and  $\tau_1$ , respectively. The experimental behaviour may be of the inaccuracies involved with the inapplicability of Fröhlich's model for of the liquid mixtures at different frequencies. The average of the three  $\tau$  along with single  $\tau_2$  and  $\tau_1$  for the remaining four systems are placed in the respective table to compare with the average values of  $\tau_2$  and  $\tau_1$  from the single frequency technique.  $\tau$  are, however, obtained from the ratio of the individual slopes of the variations of  $\chi''_{ij}$  and  $\chi'_{ij}$  with  $w_j$  at  $w_j \rightarrow 0$  of Eq. (10) and from the direct slopes of  $\chi''_{ij}-\chi'_{ij}$  curves of Eq. (9). The larger values of  $\tau_2$  obtained from

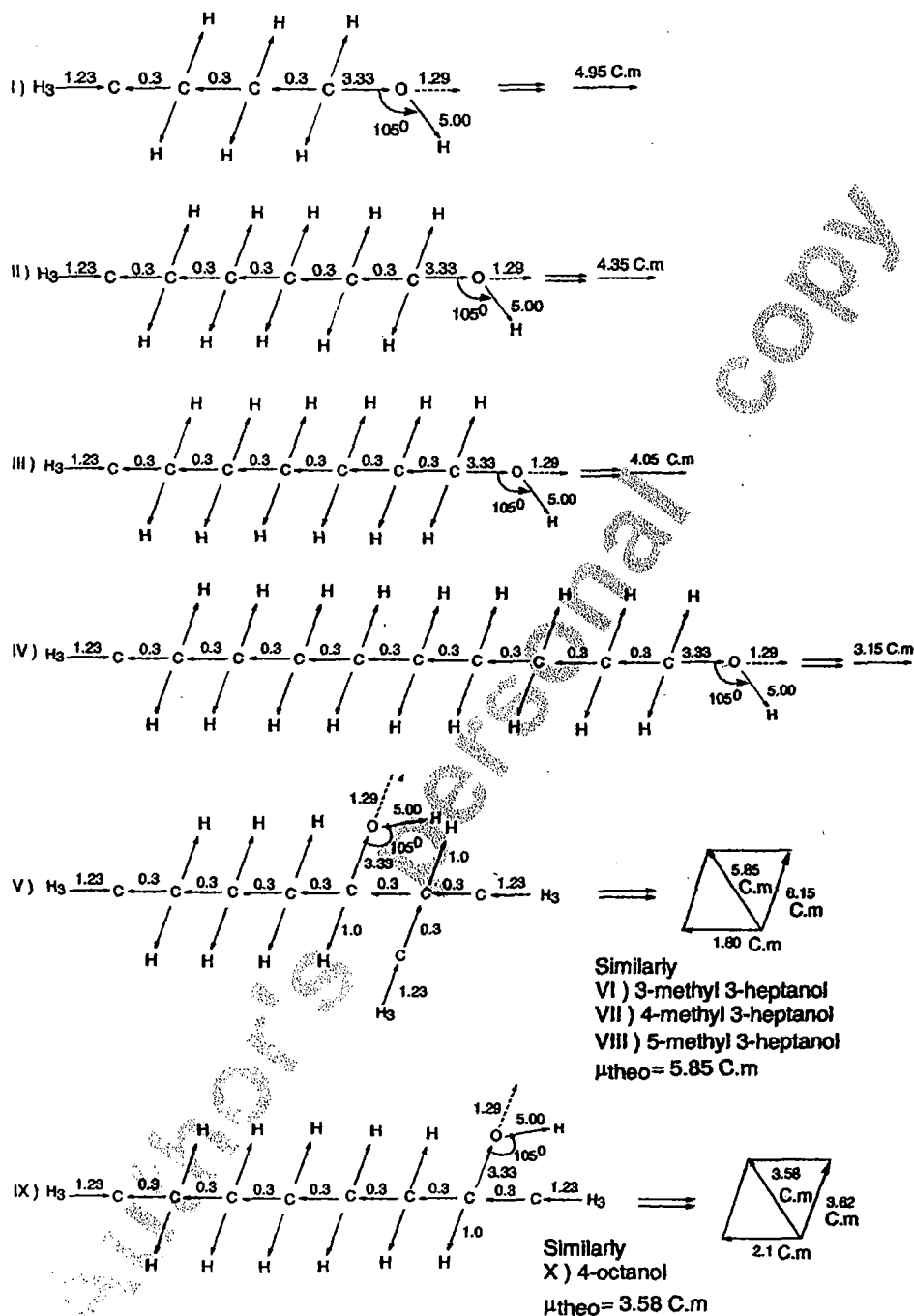


Fig. 6. Conformational structures of polar molecules in terms of bond angles and bond moments ( $\times 10^{-30} \text{ C.m}$ ) of the substituents groups: I.) 1-Butanol, II.) 1-Hexanol, III.) 1-Heptanol, IV.) 1-Decanol, V.) 2-methyl 3-heptanol and IX.) 2-octanol.

the method of single frequency measurement of Saha et al. and Sit et al. and smaller values of  $\tau_1$  can be compared with those of the present graphical method. The comparison thus reveals the applicability of both methods. Moreover, the relaxation times of the graphical technique based on the Debye–Fröhlich model

may provide with the better understanding to reflect the material property.

The experimental dipole moments  $\mu_2$  and  $\mu_1$  of the whole and flexible parts of the alcohols in terms of  $\tau_2$  and  $\tau_1$  and slope  $\beta$  of  $\chi_{ij}^2 - w_j$  curves are computed at three different frequencies of

GHz range. The identical behaviour of  $\chi_{ij}''-w_j$  curves of the solutions may be due to the almost same polarity of alcohols. The convex or concave nature of the curves reveals the solute–solute molecular associations in the higher concentration region for the formation of hydrogen bonding.  $\mu_2$  and  $\mu_1$  are compared with those from the single frequency measurement and the  $\mu_{theo}$  from the available bond angles and bond moments. The slight disagreement among  $\mu$  may be due to steric hindrances and various effects present in the substituent polar groups attached to the parent ones.

## References

- [1] A.K. Jonscher, *Universal Relaxation Law*, Chelsea Dielectric Press, London, 1996.
- [2] A.K. Sharma, D.R. Sharma, D.S. Gill, *J. Phys., D, Appl. Phys.* 18 (1985) 1199.
- [3] A. Sharma, D.R. Sharma, *J. Phys. Soc. Jpn.* 61 (1992) 1049.
- [4] K. Higasi, Y. Koga, M. Nakamura, *Bull. Chem. Soc. Jpn.* 44 (1971) 988.
- [5] S.K. Sit, S. Acharyya, *Indian J. Phys.* 70B (1996) 19.
- [6] M.D. Migahed, M.T. Ahmed, A.E. Kotp, *J. Phys., D, Appl. Phys.* 33 (2000) 2108.
- [7] A. Bello, E. Laredo, M. Grimau, A. Nogales, T.A. Ezquerro, *J. Chem. Phys.* 113 (2000) 863.
- [8] J. Crossley, L. Glasser, C.P. Smyth, *J. Chem. Phys.* 55 (1971) 2197.
- [9] L. Glasser, J. Crossley, C.P. Smyth, *J. Chem. Phys.* 57 (1972) 3977.
- [10] N. Ghosh, A. Karmakar, S.K. Sit, S. Acharyya, *Indian J. Pure Appl. Phys.* 38 (2000) 574.
- [11] A.K. Jonscher, in: C.H.L. Goodman (Ed.), *Inst. Phys. Conf. (Canterbury) Invited Papers*, 1980.
- [12] K. Dutta, S.K. Sit, S. Acharyya, *Pramana: J. Phys.* 57 (2001) 775.
- [13] U. Saha, S.K. Sit, R.C. Basak, S. Acharyya, *J. Phys., D, Appl. Phys.* 27 (1994) 596.
- [14] S.K. Sit, R.C. Basak, U. Saha, S. Acharyya, *J. Phys., D, Appl. Phys.* 27 (1994) 2194.
- [15] K. Higasi, K. Bergmann, C.P. Smyth, *J. Phys. Chem.* 64 (1960) 880.
- [16] A. Mansingh, P. Kumar, *J. Phys. Chem.* 69 (1965) 4197.
- [17] K. Dutta, A. Karmakar, L. Dutta, S.K. Sit, S. Acharyya, *Indian J. Pure Appl. Phys.* 40 (2002) 801.
- [18] *Hand book of Chemistry and Physics*, 58th edition C.R.C. Press, 1977–1978.
- [19] S.G. Akode, K.S. Kanse, M.P. Lokhande, A.C. Kumbarkhane, S.C. Mehrotra, *Pramana: J. Phys.* 62 (2004) 973.

## Double relaxation phenomena of di-substituted benzenes and anilines in non-polar aprotic solvents under high frequency electric field

K Dutta, A Karmakar, (Mrs) L Dutta, S K Sit & S Acharyya

Department of Physics, Raiganj College (University College), PO Raiganj Dist, Uttar Dinajpur 733 134

[e-mail: koushikduttajsm@rediffmail.com]

Received 1 October 2001; revised 12 February 2002; accepted 15 April 2002

The derived linear equation  $(\chi_{oij} - \chi_{ij}')/\chi_{ij}' = \omega(\tau_1 + \tau_2) \chi_{ij}''/\chi_{ij}' - \omega^2\tau_1\tau_2$  for different weight fractions  $w_j$  of di-substituted benzenes and anilines ( $j$ ) in aprotic and non-polar solvents ( $i$ )  $C_6H_6$  and  $CCl_4$  under 9.945 GHz electric field are obtained from the available measured dielectric relative permittivities at 35 °C. The double relaxation times  $\tau_1$  and  $\tau_2$  of the flexible part and the whole molecule are estimated from the slope and intercept of the above equation.  $\chi_{ij}'$  and  $\chi_{ij}''$  are the real and imaginary parts of the high frequency complex orientational dielectric susceptibility  $\chi_{ij}^*$  and  $\chi_{oij}$  is the low frequency dielectric susceptibility, which is real. They are, however, related with the measured relative permittivities. Values of  $\tau_j$  are calculated from the ratio of the individual slopes of the variations of  $\chi_{ij}''$  and  $\chi_{ij}'$  with  $w_j$  at  $w_j \rightarrow 0$ , assuming single Debye-like dispersion and compared with Murthy *et al.* [*Indian J Phys*, 63B (1989) 491] and Gopalakrishna [*Trans Faraday Soc*, 53 (1957) 767]. The weighted contributions  $c_1$  and  $c_2$  towards dielectric relaxations for  $\tau_1$  and  $\tau_2$  can, however, be obtained from Fröhlich's theoretical formulations of  $\chi_{ij}'/\chi_{oij}$  and  $\chi_{ij}''/\chi_{oij}$  and compared with those from the experimentally measured values of  $(\chi_{ij}'/\chi_{oij})_{w_j \rightarrow 0}$  and  $(\chi_{ij}''/\chi_{oij})_{w_j \rightarrow 0}$ . The latter measured values are employed to get symmetric distribution parameter  $\gamma$  to yield symmetric relaxation time  $\tau_s$ . The curve of  $(1/\phi) \log(\cos \phi)$  against  $\phi$  in degrees together with the values of  $(\chi_{ij}'/\chi_{oij})_{w_j \rightarrow 0}$  and  $(\chi_{ij}''/\chi_{oij})_{w_j \rightarrow 0}$  experimentally obtained, gives the asymmetric distribution parameter  $\delta$  to get the characteristic relaxation time  $\tau_{cs}$ . All these findings ultimately establish the different types of relaxation behaviour for such complex molecules. The dipole moments  $\mu_1$  and  $\mu_2$  for the flexible part and the whole molecule are ascertained from  $\tau_1$  and  $\tau_2$  and the linear coefficients  $\beta_1$  of  $\chi_{ij}'$  versus  $w_j$  and  $\beta_2$  of  $\chi_{ij}''$  versus  $w_j$  curves respectively, where  $\sigma_{ij}$  is the hf conductivity. The values of  $\mu$  are finally compared with the reported  $\mu$ 's and  $\mu_{theo}$ 's derived from available bond angles and bond moments of the substituted polar groups of di-substituted anilines to conclude that a part of the molecule is rotating while the whole molecular rotation occurs for di-substituted benzenes. The slight disagreement between measured values of  $\mu$  and  $\mu_{theo}$  can, however, be interpreted by the inductive, mesomeric and electromeric effects of the polar groups of the parent molecules.

### 1 Introduction

The dielectric relaxation phenomena of nonspherical and rigid polar liquid molecule in different non-polar solvents at a given temperature, under a high frequency (hf) electric field attracted the attention of a large number of workers<sup>1,2</sup>. The dipole moment  $\mu$  from the relaxation time  $\tau$  of the polar liquid molecule is of much importance<sup>3,4</sup> to determine the shape, size, structure and molecular association of a polar molecule. The real  $\epsilon_{ij}'$  and imaginary  $\epsilon_{ij}''$  parts of complex relative permittivity  $\epsilon_{ij}^*$ , static and infinite frequency relative permittivities  $\epsilon_{oij}$  and  $\epsilon_{\infty ij}$  of a polar liquid molecule ( $j$ ) in a non-polar solvent ( $i$ ) at a fixed experimental temperature under a single frequency electric field of GHz range are used to obtain the double relaxation times  $\tau_2$  and  $\tau_1$  due to rotation of the

whole molecule as well as the flexible part attached to the parent molecule<sup>5</sup>.

Khameshara & Sisodia<sup>6</sup>, Gupta *et al.*<sup>7</sup> and Arrawatia *et al.*<sup>8</sup> measured the relative permittivities of some di-substituted benzenes and anilines in aprotic non-polar solvents  $C_6H_6$  and  $CCl_4$  under 9.945 GHz electric field at 35 °C to predict the conformation of the molecules in terms of the relaxation time  $\tau$ , based on the single frequency concentration variation method of Gopalakrishna<sup>9</sup> and the dipole moment,  $\mu$  by Higasi's method<sup>10</sup>. The compounds are very interesting for the different functional groups like  $-NH_2$ ,  $-CH_3$ ,  $-NO_2$ ,  $-Cl$ , etc. attached to the parent molecules. The samples were of purest quality and supplied by M/s Fluka and M/s E Merck, respectively. The solvents  $C_6H_6$  and  $CCl_4$  of M/s BDH were used after double distillation and

suitably dried over NaCl and CaCl<sub>2</sub>.  $\epsilon_{oij}$  at 35 °C was measured by heterodyne beat method at 300 kHz  $\epsilon_{\infty ij} = n_{Dij}^2$ , where the refractive index  $n_{Dij}$  was measured by Abbe's refractometer. The weight fraction  $w_j$  of the respective solute, which is defined by the weight of the solute per unit weight of the solution was taken up to four decimal places, as the accuracy in the measurement was 0.0012 %.  $\epsilon_{ij}'$  and  $\epsilon_{ij}''$  within 1 % and 5 % accuracies were carried out by using the voltage standing wave ratio in slotted line and short-circuiting plunger, based on the method of Heston *et al.*<sup>11</sup>. The possible existence of  $\tau_1$  and  $\tau_2$  of the compounds was, however, detected from the relative permittivity measurements<sup>12</sup>, under 9.945 GHz electric field at 35 °C.

Now-a-days, the usual practice<sup>13</sup> is to study the dielectric relaxation phenomena in terms of dielectric orientational susceptibilities  $\chi_{ij}$ .  $\chi_{ij}$ 's are linked with the orientational polarization of a polar molecule. So it is better to work with  $\chi_{ij}$ 's rather than  $\epsilon_{ij}$ 's or conductivity  $\sigma_{ij}$ 's as the latter are involved with all the polarization processes and the transport of bound molecular charges, respectively<sup>14</sup>. The real  $\chi_{ij}' (= \epsilon_{ij}' - \epsilon_{\infty ij})$  and imaginary  $\chi_{ij}'' (= \epsilon_{ij}'')$  parts of the complex dielectric orientational susceptibility  $\chi_{ij}^* (= \epsilon_{ij}^* - \epsilon_{\infty ij})$  and the low frequency susceptibility  $\chi_{oij} (= \epsilon_{oij} - \epsilon_{\infty ij})$  which is real of the di-substituted benzenes and anilines in C<sub>6</sub>H<sub>6</sub> and CCl<sub>4</sub> of Table 1 are used to obtain their conformational structures in terms of molecular and intra-molecular dipole moments  $\mu_2$  and  $\mu_1$  involved with the estimated  $\tau_2$  and  $\tau_1$ . Di-substituted benzenes and anilines are thought to absorb electric energy much more strongly, in nearly 10 GHz electric field yielding considerable values of  $\tau_1$  and  $\tau_2$ . The 11 polar-non-polar liquid mixtures under investigation are found to show the double relaxation phenomena. Most of the polar molecules are isomers of aniline and benzene. Some of the polar solutes are dissolved in C<sub>6</sub>H<sub>6</sub>, while a few in CCl<sub>4</sub> to observe the solvent effect too. Moreover, a few of the polar molecules are para-compounds, in which a peculiar feature of relaxation phenomena is expected<sup>15</sup>. A strong conclusion of double relaxation phenomena of polar molecule in a non-polar solvent, based on the single frequency measurement of relaxation parameters can be made only if, the accurate value of  $\chi_{oij}$  ( $\pm 1$  %) involved with  $\epsilon_{oij}$  and  $\epsilon_{\infty ij}$  is available. The use of  $n_{Dij}^2$  for  $\epsilon_{\infty ij}$  often introduces<sup>6-8</sup> an additional error in the

calculation, since  $\epsilon_{\infty ij}$  is approximately equal to 1-1.5 times of  $n_{Dij}^2$ .

Bergmann *et al.*<sup>16</sup>, however, devised a graphical method to obtain  $\tau_1$  and  $\tau_2$  for a pure polar liquid. The respective weighted contributions  $c_1$  and  $c_2$  towards dielectric relaxations were estimated in terms of  $\tau_1$  and  $\tau_2$ . Bhattacharyya *et al.*<sup>17</sup> subsequently attempted to simplify the procedure of Bergmann *et al.*<sup>16</sup> to get the same for a pure polar molecule with  $\epsilon'$ ,  $\epsilon''$ ,  $\epsilon_0$  and  $\epsilon_{\infty}$ , measured at two different frequencies in GHz range. The graphical analysis advanced by Higasi *et al.*<sup>18</sup> on polar-non-polar liquid mixture was also a crude one.

Thus, the object of the present paper is to detect  $\tau_1$  and  $\tau_2$  and hence, to measure  $\mu_1$  and  $\mu_2$  using values of  $\chi_{ij}$  based on the single frequency measurement technique<sup>12,19</sup>. The aspect of molecular orientational polarization is, however, achieved by introducing  $\chi_{ij}$  because  $\epsilon_{\infty ij}$  which includes fast polarization, frequently appears as a subtracted term in Bergmann equations. Thus, to avoid the clumsiness of algebra and to exclude the fast polarization process, Bergmann equations<sup>16</sup> are simplified by the established symbols of  $\chi_{ij}'$ ,  $\chi_{ij}''$  and  $\chi_{oij}$  of Table 1 in SI units:

$$\frac{\chi_{ij}'}{\chi_{oij}} = \frac{c_1}{1 + \omega^2 \tau_1^2} + \frac{c_2}{1 + \omega^2 \tau_2^2} \quad \dots(1)$$

and

$$\frac{\chi_{ij}''}{\chi_{oij}} = c_1 \frac{\omega \tau_1}{1 + \omega^2 \tau_1^2} + c_2 \frac{\omega \tau_2}{1 + \omega^2 \tau_2^2} \quad \dots(2)$$

assuming two broad Debye-type dispersions for which the sum of  $c_1$  and  $c_2$  is unity.

Eqs (1) and (2) are now solved to get:

$$\frac{\chi_{oij} - \chi_{ij}'}{\chi_{ij}'} = \omega(\tau_1 + \tau_2) \frac{\chi_{ij}''}{\chi_{ij}'} - \omega^2 \tau_1 \tau_2 \quad \dots(3)$$

The variables  $(\chi_{oij} - \chi_{ij}')/\chi_{ij}'$  and  $\chi_{ij}''/\chi_{ij}'$  are plotted against each other for different values of  $w_j$  of the polar liquid under a single angular frequency  $\omega$  ( $=2\pi f$ ) of the electric field to get a straight line with intercept  $-\omega^2 \tau_1 \tau_2$  and slope  $\omega(\tau_1 + \tau_2)$ , as shown in Fig.1. The intercept and slope of Eq. (3) are obtained by linear regression analysis made with the measured values of  $\chi_{ij}$  of solutes in CCl<sub>4</sub> and C<sub>6</sub>H<sub>6</sub> to get  $\tau_2$  and  $\tau_1$  as found in the 6th and 7th columns of

Table 1 — The real  $\chi_{ij}'$  and imaginary  $\chi_{ij}''$ , parts of the complex dielectric orientational susceptibility  $\chi_{ij}^*$  and static dielectric susceptibility  $\chi_{0ij}$  which is real for various weight fraction  $w_j$  of different di-substituted benzenes and anilines at 35 °C under 9.945 GHz electric field

Weight fraction $w_j$	$\chi_{ij}'$	$\chi_{ij}''$	$\chi_{0ij}$	Weight fraction $w_j$	$\chi_{ij}'$	$\chi_{ij}''$	$\chi_{0ij}$
(I) o-chloronitrobenzene in $C_6H_6$				(II) 4-chloro 3-nitro benzotrifluoride in $CCl_4$			
0.0109	0.117	0.066	0.167	0.0050	0.122	0.019	0.155
0.0173	0.169	0.100	0.254	0.0101	0.145	0.037	0.185
0.0217	0.197	0.126	0.305	0.0147	0.150	0.054	0.233
0.0280	0.253	0.165	0.376	0.0193	0.167	0.068	0.266
0.0330	0.284	0.192	0.461	0.0231	0.179	0.075	0.302
(III) 4-chloro 3-nitro toluene in $C_6H_6$				(IV) 4-chloro 3-nitro toluene in $CCl_4$			
0.0072	0.075	0.046	0.132	0.0041	0.145	0.039	0.208
0.0144	0.098	0.088	0.241	0.0087	0.173	0.071	0.315
0.0224	0.150	0.133	0.310	0.0128	0.190	0.101	0.419
0.0323	0.200	0.179	0.464	0.0162	0.218	0.138	0.482
0.0453	0.271	0.252	0.630	0.0203	0.241	0.165	0.586
(V) o-nitrobenzotrifluoride in $C_6H_6$				(VI) m-nitrobenzotrifluoride in $C_6H_6$			
0.0085	0.094	0.058	0.154	0.0096	0.082	0.032	0.094
0.0167	0.166	0.108	0.257	0.0173	0.103	0.060	0.157
0.0244	0.226	0.159	0.384	0.0245	0.129	0.082	0.202
0.0335	0.297	0.205	0.495	0.0326	0.157	0.106	0.265
0.0402	0.353	0.255	0.604	0.0380	0.187	0.128	0.323
(VII) 2-chloro 6-methyl aniline in $C_6H_6$				(VIII) 3-chloro 2-methyl aniline in $C_6H_6$			
0.0184	0.072	0.017	0.075	0.0083	0.059	0.018	0.065
0.0305	0.096	0.026	0.097	0.0207	0.099	0.043	0.128
0.0417	0.117	0.040	0.138	0.0270	0.128	0.055	0.166
0.0573	0.163	0.058	0.191	0.0363	0.165	0.073	0.221
0.0636	0.183	0.065	0.214	0.0421	0.193	0.086	0.255
(IX) 3-chloro 4-methyl aniline in $C_6H_6$				(X) 4-chloro 2-methyl aniline in $C_6H_6$			
0.0214	0.088	0.032	0.099	0.0196	0.124	0.063	0.151
0.0374	0.123	0.060	0.167	0.0300	0.157	0.090	0.219
0.0403	0.133	0.066	0.185	0.0417	0.199	0.121	0.304
0.0548	0.166	0.091	0.244	0.0481	0.216	0.138	0.354
(XI) 5-chloro 2-methyl aniline in $C_6H_6$							
0.0194	0.094	0.050	0.123				
0.0249	0.110	0.064	0.153				
0.0307	0.129	0.081	0.191				
0.0480	0.182	0.129	0.292				
0.0569	0.206	0.150	0.362				

Table 2. The variables of Eq. (3) are extracted from Table 1, where all the data are collected together, system-wise, up to three decimal places in close agreement with the expected<sup>12</sup>  $\tau_2$  and  $\tau_1$  of Table 2. Both  $\tau_2$  and  $\tau_1$  were found to deviate significantly, when the data of Table 1 were taken up to two decimal places with the claimed accuracy of measurement. The values of correlation coefficient

( $r$ ) and the % error were worked out to place them in Table 2, only to see how far the variables of Eq. (3) are collinear to each other.

The relaxation times  $\tau$ 's due to Debye model are measured from the slope of  $\chi_{ij}''$  versus  $\chi_{ij}'$  curves of Fig. 2 and the ratio of the individual slopes of  $\chi_{ij}''$  versus  $w_j$  and  $\chi_{ij}'$  versus  $w_j$  curves at  $w_j \rightarrow 0$  of Figs 3

and 4, respectively. Values of  $\tau$  from both the methods are entered in the 8th and 9th columns of Table 2 only to see how far they agree with  $\tau_1$  and  $\tau_2$  due to double relaxation method of Eq. (3).

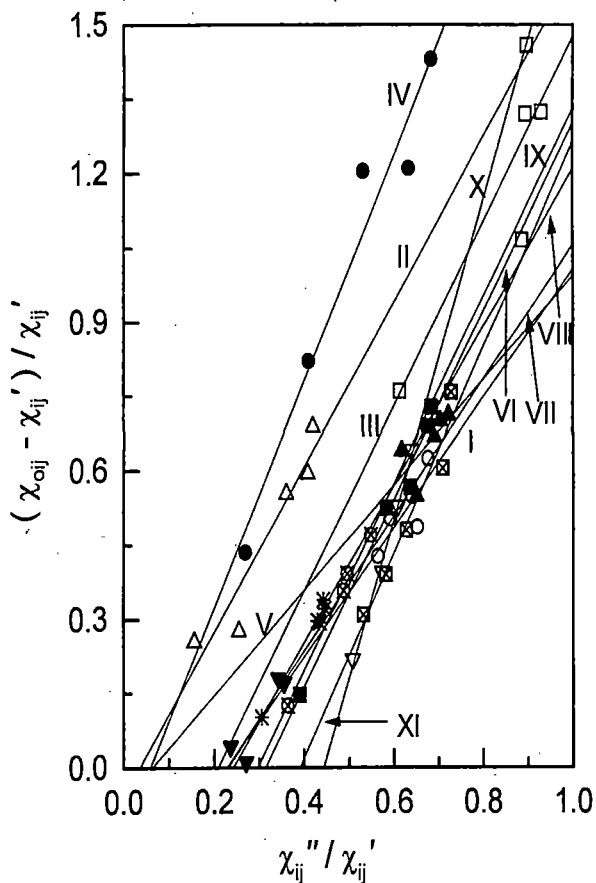


Fig. 1 — Linear variation of  $(\chi_{oij} - \chi_{ij}')/\chi_{ij}'$  with  $\chi_{ij}''/\chi_{ij}'$  for different values of  $w_j$  for: I. o-chloronitrobenzene in  $C_6H_6$  ( $-\circ-$ ); II. 4-chloro 3-nitrobenzotrifluoride in  $CCl_4$  ( $-\triangle-$ ); III. 4-chloro 3-nitrotoluene in  $C_6H_6$  ( $-\square-$ ); IV. 4-chloro 3-nitrotoluene in  $CCl_4$  ( $-\bullet-$ ); V. o-nitrobenzotrifluoride in  $C_6H_6$  ( $-\blacktriangle-$ ); VI. m-nitrobenzotrifluoride in  $C_6H_6$  ( $-\blacksquare-$ ); VII. 2-chloro 6-methyl aniline in  $C_6H_6$  ( $-\blacktriangledown-$ ); VIII. 3-chloro 2-methyl aniline in  $C_6H_6$  ( $-\ast-$ ); IX. 3-chloro 4-methyl aniline in  $C_6H_6$  ( $-\otimes-$ ); X. 4-chloro 2-methyl aniline in  $C_6H_6$  ( $-\nabla-$ ) and XI. 5-chloro 2-methyl aniline in  $C_6H_6$  ( $-\boxtimes-$ ) at 35 °C under 9.945 GHz electric field

The theoretical values of  $c_1$  and  $c_2$  towards dielectric dispersions for  $\tau_1$  and  $\tau_2$  of different di-substituted benzenes and anilines in  $C_6H_6$  and  $CCl_4$  were calculated from Fröhlich's<sup>21</sup> theoretical formulations of  $\chi_{ij}'/\chi_{oij}$  and  $\chi_{ij}''/\chi_{oij}$ . The experimental values of  $c_1$  and  $c_2$ , on the other hand, were found out from  $(\chi_{ij}'/\chi_{oij})_{w_j \rightarrow 0}$  and  $(\chi_{ij}''/\chi_{oij})_{w_j \rightarrow 0}$  by graphical

variations of  $\chi_{ij}'/\chi_{oij}$  and  $\chi_{ij}''/\chi_{oij}$  with values of  $w_j$  of Figs 5 and 6, in order to place them in Table 3 for comparison. The plots of  $\chi_{ij}'/\chi_{oij}$  and  $\chi_{ij}''/\chi_{oij}$  against  $w_j$  of the polar liquids in Figs 5 and 6 are the least square fitted curves with the experimental points placed upon them. With the values of the intercepts presented in Table 3 from Figs 5 and 6 and the graphical plot of  $(1/\phi) \log(\cos \phi)$  against  $\phi$  in degrees given elsewhere<sup>4</sup>, the symmetric and asymmetric distribution parameters  $\gamma$  and  $\delta$  related to symmetric and characteristic relaxation times  $\tau_s$  and  $\tau_{cs}$  of the molecules were determined. They are seen in Table 3. The object of such determinations of  $\gamma$ ,  $\delta$ ,  $\tau_s$  and  $\tau_{cs}$  is to conclude the molecular non-rigidity and distribution of relaxation behaviour as well.

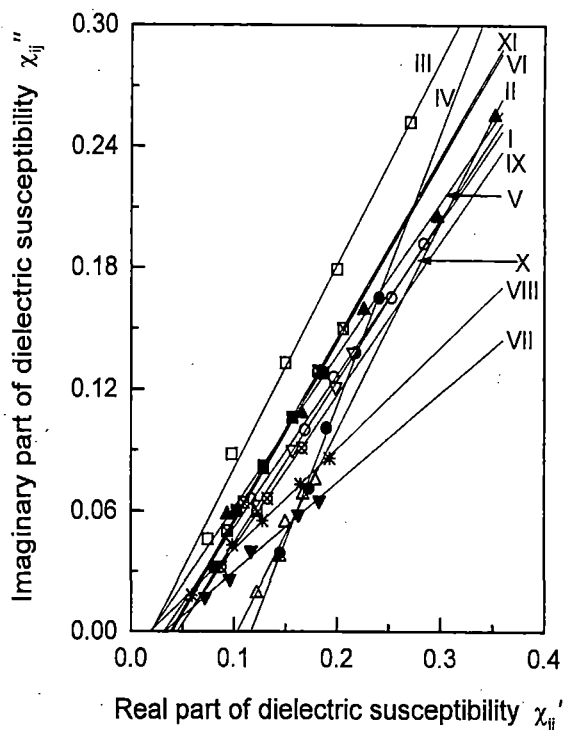


Fig. 2 — Linear variation of  $\chi_{ij}''$  with  $\chi_{ij}'$  for different values of  $w_j$  for: I. o-chloronitrobenzene in  $C_6H_6$  ( $-\circ-$ ); II. 4-chloro 3-nitrobenzotrifluoride in  $CCl_4$  ( $-\triangle-$ ); III. 4-chloro 3-nitrotoluene in  $C_6H_6$  ( $-\square-$ ); IV. 4-chloro 3-nitrotoluene in  $CCl_4$  ( $-\bullet-$ ); V. o-nitrobenzotrifluoride in  $C_6H_6$  ( $-\blacktriangle-$ ); VI. m-nitrobenzotrifluoride in  $C_6H_6$  ( $-\blacksquare-$ ); VII. 2-chloro 6-methyl aniline in  $C_6H_6$  ( $-\blacktriangledown-$ ); VIII. 3-chloro 2-methyl aniline in  $C_6H_6$  ( $-\ast-$ ); IX. 3-chloro 4-methyl aniline in  $C_6H_6$  ( $-\otimes-$ ); X. 4-chloro 2-methyl aniline in  $C_6H_6$  ( $-\nabla-$ ) and XI. 5-chloro 2-methyl aniline in  $C_6H_6$  ( $-\boxtimes-$ ) at 35 °C under 9.945 GHz electric field

Table 2 — The relaxation times  $\tau_2$  and  $\tau_1$  from the slope and intercept of straight line Eq. (3), correlation coefficients  $r$ 's and % of error in regression technique, measured  $\tau_i$  from the slope of  $\chi_{ij}''$  versus  $\chi_{ij}'$  of Eq. (15) and the ratio of the individual slopes of  $\chi_{ij}''$  versus  $w_j$  and  $\chi_{ij}'$  versus  $w_j$  at  $w_j \rightarrow 0$  of Eq. (16), reported  $\tau$ , symmetric and characteristic relaxation times  $\tau_s$  and  $\tau_{cs}$  for different disubstituted benzenes and anilines at 35 °C under 9.945 GHz electric field

System with S.No.	Eq. (3)		Corrl. Coeff ( $r$ )	% of Error	Estimated $\tau_2$ and $\tau_1$ in ps		Measured $\tau_i$ in ps from		Rept. $\tau$ in ps	$\tau_s$ in ps	$\tau_{cs}$ in ps
	Slope/Intercept				Eq. (15)	Eq. (16)					
(I) o-chloro nitro-benzene in $C_6H_6$	1.310	0.301	0.82	9.88	16.21	4.76	12.08	10.13	13.5	7.87	17.08
(II) 4-chloro 3-nitrobenzotrifluoride in $CCl_4$	1.666	0.059	0.95	2.94	26.08	0.58	16.43	22.66	21.1	0.00	--
(III) 4-chloro 3-nitrotoluene in $C_6H_6$	1.865	0.389	0.88	6.80	26.02	3.83	16.13	19.89	20.9	10.76	39.65
(IV) 4-chloro 3-nitrotoluene in $CCl_4$	2.283	0.134	0.98	1.19	35.57	0.96	21.47	22.61	35.0	1.47	38.84
(V) o-nitrobenzotrifluoride in $C_6H_6$	1.063	0.067	0.70	15.38	15.93	1.08	12.09	11.08	13.7	10.89	28.83
(VI) m-nitrobenzotrifluoride in $C_6H_6$	1.898	0.597	0.99	0.60	24.01	6.37	14.33	36.57	19.7	6.20	--
(VII) 2-chloro 6-methyl aniline in $C_6H_6$	1.371	0.313	0.93	4.08	17.31	4.63	7.05	14.55	7.8	4.08	--
(VIII) 3-chloro 2-methyl aniline in $C_6H_6$	1.596	0.386	0.99	0.60	20.79	4.76	7.98	11.49	9.9	4.57	--
(IX) 3-chloro 4-methyl aniline in $C_6H_6$	1.891	0.561	0.99	0.67	24.37	5.90	12.07	13.65	13.6	7.28	--
(X) 4-chloro 2-methyl aniline in $C_6H_6$	3.217	1.428	0.99	0.67	42.97	8.51	12.80	11.04	18.5	7.59	--
(XI) 5-chloro 2-methyl aniline in $C_6H_6$	2.075	0.811	0.97	1.78	24.85	8.36	14.34	14.35	16.6	5.60	4.52

The dipole moments  $\mu_2$  and  $\mu_1$  were then measured in terms of dimensionless parameters ( $b$ ) involved with measured values of  $\tau$  of Table 2 and coefficients  $\beta_1$  and  $\beta_2$  presented in Table 4 of the variations of  $hf \chi_{ij}'$  and total  $hf$  conductivity  $\sigma_{ij}$  with values of  $w_j$  of Figs 4 and 7, respectively. The measured values of  $\mu$  are presented in Table 4 in order to compare with theoretical dipole moment  $\mu_{theo}$  derived from available bond angles and bond moments of the substituent polar groups attached to the parent molecules as sketched in Fig. 8. The structural aspect of some interesting polar molecules presented in Fig. 8 exhibits the prominent mesomeric, inductive and electromeric effects of the substituted polar groups. All these effects are taken into account by the ratio  $\mu_{exp}/\mu_{theo}$ , in agreement with the measured values<sup>6-8</sup> of  $\mu$  presented in Table 4.

## 2 Formulations of $c_1$ and $c_2$ for $\tau_1$ and $\tau_2$

Eqs (1) and (2) are now solved to get  $c_1$  and  $c_2$ , where:

$$c_1 = \frac{(\chi_{ij}'\alpha_2 - \chi_{ij}'')(1 + \alpha_1^2)}{\chi_{oij}(\alpha_2 - \alpha_1)} \quad \dots(4)$$

$$c_2 = \frac{(\chi_{ij}'' - \chi_{ij}'\alpha_1)(1 + \alpha_2^2)}{\chi_{oij}(\alpha_2 - \alpha_1)} \quad \dots(5)$$

where  $\alpha_1 = \omega\tau_1$  and  $\alpha_2 = \omega\tau_2$  provided  $\alpha_2 > \alpha_1$ . The molecules under consideration are of complex type and only little data are available under single frequency measurement in the low concentration region. A continuous distribution of  $\tau$  with two discrete values of  $\tau_1$  and  $\tau_2$  could, therefore, be expected. Thus, from Fröhlich's equations<sup>20</sup> based

on distribution of  $\tau$  between the two extreme values of  $\tau_1$  and  $\tau_2$ , one gets:

$$\frac{\chi'_{ij}}{\chi_{oij}} = 1 - \frac{1}{2A} \ln \left( \frac{1 + \omega^2 \tau_2^2}{1 + \omega^2 \tau_1^2} \right) \quad \dots(6)$$

$$\frac{\chi''_{ij}}{\chi_{oij}} = \frac{1}{A} [\tan^{-1}(\omega\tau_2) - \tan^{-1}(\omega\tau_1)] \quad \dots(7)$$

where the Fröhlich parameter  $A$  is given by  $A = \ln(\tau_2/\tau_1)$ . The theoretical values of  $\chi'_{ij}/\chi_{oij}$  and  $\chi''_{ij}/\chi_{oij}$  of Eqs (6) and (7) were used to get theoretical  $c_1$  and  $c_2$  from Eqs (4) and (5) in order to compare them with the experimental values of  $c_1$  and  $c_2$  from the graphical plots of  $\chi'_{ij}/\chi_{oij}$  and  $\chi''_{ij}/\chi_{oij}$  at  $w_j \rightarrow 0$ , as seen in Figs 5 and 6, respectively. Both the theoretical and experimental values of  $c_1$  and  $c_2$  are presented in Table 3 for comparison.

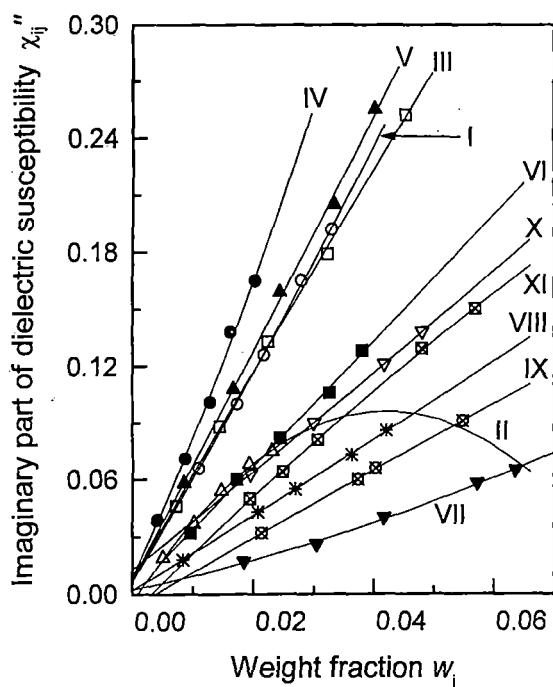


Fig. 3 — Variation of  $\chi''_{ij}$  against  $w_j$  of solutes at 35 °C under 9.945 GHz electric field for: I. o-chloronitrobenzene in  $C_6H_6$  (—○—); II. 4-chloro 3-nitrobenzotrifluoride in  $CCl_4$  (—△—); III. 4-chloro 3-nitrotoluene in  $C_6H_6$  (—□—); IV. 4-chloro 3-nitrotoluene in  $CCl_4$  (—●—); V. o-nitrobenzotrifluoride in  $C_6H_6$  (—▲—); VI. m-nitrobenzotrifluoride in  $C_6H_6$  (—■—); VII. 2-chloro 6-methyl aniline in  $C_6H_6$  (—▼—); VIII. 3-chloro 2-methyl aniline in  $C_6H_6$  (—\*—); IX. 3-chloro 4-methyl aniline in  $C_6H_6$  (—⊗—); X. 4-chloro 2-methyl aniline in  $C_6H_6$  (—▽—) and XI. 5-chloro 2-methyl aniline in  $C_6H_6$  (—⊠—) at 35 °C under 9.945 GHz electric field

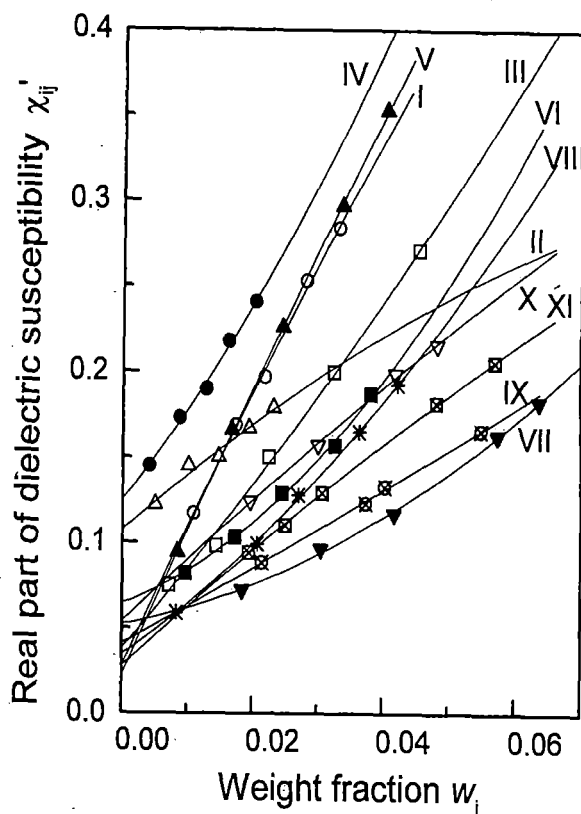


Fig. 4 — Variation of  $\chi'_{ij}$  against  $w_j$  of solutes at 35 °C under 9.945 GHz electric field for: I. o-chloronitrobenzene in  $C_6H_6$  (—○—); II. 4-chloro 3-nitrobenzotrifluoride in  $CCl_4$  (—△—); III. 4-chloro 3-nitrotoluene in  $C_6H_6$  (—□—); IV. 4-chloro 3-nitrotoluene in  $CCl_4$  (—●—); V. o-nitrobenzotrifluoride in  $C_6H_6$  (—▲—); VI. m-nitrobenzotrifluoride in  $C_6H_6$  (—■—); VII. 2-chloro 6-methyl aniline in  $C_6H_6$  (—▼—); VIII. 3-chloro 2-methyl aniline in  $C_6H_6$  (—\*—); IX. 3-chloro 4-methyl aniline in  $C_6H_6$  (—⊗—); X. 4-chloro 2-methyl aniline in  $C_6H_6$  (—▽—) and XI. 5-chloro 2-methyl aniline in  $C_6H_6$  (—⊠—) at 35 °C under 9.945 GHz electric field

### 3 Distribution Parameters Related to Symmetric and Characteristic Relaxation

The molecules are expected to show either symmetrical circular arc or a skewed arc in addition to other models<sup>21</sup> when the values of  $\chi''_{ij}/\chi_{oij}$  are plotted against  $\chi'_{ij}/\chi_{oij}$  at  $w_j \rightarrow 0$  for various frequencies of the electric field to yield

$$\frac{\chi'_{ij}}{\chi_{oij}} = \frac{1}{1 + (j\omega\tau_s)^{1-\gamma}} \quad \dots(8)$$

$$\frac{\chi'_{ij}}{\chi_{oij}} = \frac{1}{(1 + j\omega\tau_{cs})^\delta} \quad \dots(9)$$

Table 3 — Fröhlich's parameter  $A$ , theoretical and experimental values of  $\chi_{ij}'/\chi_{oij}$  and  $\chi_{ij}''/\chi_{oij}$  of Fröhlich equations (6) and (7) and from fitting equations of Figs 5 and 6 at  $\omega_j \rightarrow 0$ , respectively, theoretical and experimental relative contributions  $c_1$  and  $c_2$  towards dielectric dispersion due to  $\tau_1$  and  $\tau_2$  symmetric and asymmetric distribution parameters  $\gamma$  and  $\delta$  for polar-non-polar liquid mixtures of di-substituted benzenes and anilines at 35 °C under 9.945 GHz electric field

System with SI.No.	$A = \ln(\tau_2/\tau_1)$	Theoretical values of $\chi_{ij}'/\chi_{oij}$ & $\chi_{ij}''/\chi_{oij}$ from Eqs (6) & (7)		Theoretical values of $c_1$ and $c_2$		Exptl. values of $\chi_{ij}'/\chi_{oij}$ & $\chi_{ij}''/\chi_{oij}$ at $\omega_j \rightarrow 0$ of Figs 5 & 6		Exptl. values of $c_1$ & $c_2$		Estimated values of $\gamma$ and $\delta$			
(I) o-chloronitrobenzene in $C_6H_6$	1.225	0.746	0.410	0.526	0.533	0.733	0.349	0.599	0.371	0.13	0.010		
(II) 4-chloro 3-nitrobenzotrifluoride in $CCl_4$	3.806	0.830	0.259	0.687	0.525	0.890	0.027	0.894	-0.012	0.82	---		
(III) 4-chloro 3nitrotoluene in $C_6H_6$	1.916	0.677	0.409	0.527	0.649	0.600	0.309	0.508	0.435	0.28	0.007		
(IV) 4-chloro 3-nitrotoluene in $CCl_4$	3.612	0.754	0.301	0.638	0.703	0.863	0.144	0.823	0.253	0.38	0.002		
(V) o-nitrobenzotrifluoride in $C_6H_6$	2.691	0.873	0.266	0.653	0.444	0.616	0.347	0.288	0.655	0.21	0.008		
(VI) m- nitrobenzotrifluoride in $C_6H_6$	1.327	0.611	0.455	0.485	0.625	1.134	0.261	1.514	-0.561	-0.45	---		
(VII) 2-chloro 6-methyl aniline in $C_6H_6$	1.319	0.737	0.412	0.527	0.544	1.078	0.141	1.402	-0.468	-0.40	---		
(VIII) 3-chloro 2-methyl aniline in $C_6H_6$	1.474	0.693	0.424	0.518	0.585	1.023	0.232	1.192	-0.194	-0.20	---		
(IX) 3-chloro 4- methyl aniline in $C_6H_6$	1.418	0.622	0.449	0.490	0.632	1.244	0.254	1.614	-0.588	-0.62	---		
(X) 4-chloro 2-methyl aniline in $C_6H_6$	1.619	0.427	0.448	0.416	0.842	1.062	0.419	1.449	-0.556	-0.33	---		
(XI) 5-chloro 2-methyl aniline in $C_6H_6$	1.089	0.547	0.475	0.462	0.627	0.907	0.312	1.354	-0.536	-0.03	0.021		

Here,  $\gamma$  and  $\delta$  are the symmetric and asymmetric distribution parameters related to symmetric and characteristic relaxation times  $\tau_s$  and  $\tau_{cs}$ , respectively. Separating the real and imaginary parts of Eq. (8) one gets:

$$\gamma = \frac{2}{\pi} \tan^{-1} \left[ \left( 1 - \frac{\chi_{ij}'}{\chi_{oij}} \right) \frac{\chi_{ij}'/\chi_{oij}}{\chi_{ij}''/\chi_{oij}} - \frac{\chi_{ij}''}{\chi_{oij}} \right] \quad \dots(10)$$

and

$$\tau_s = \frac{1}{\omega} \left[ 1 / \left( \frac{\chi_{ij}'/\chi_{oij}}{\chi_{ij}''/\chi_{oij}} \cos \frac{\gamma\pi}{2} - \sin \frac{\gamma\pi}{2} \right) \right]^{1/\gamma} \quad \dots(11)$$

where  $\chi_{ij}'/\chi_{oij}$  and  $\chi_{ij}''/\chi_{oij}$  are obtained from intercepts of each variable with values of  $\omega_j$  of

Figs 5 and 6 in the limit  $\omega_j=0$ . Again  $\delta$  and  $\tau_{cs}$  can be had from Eq. (9) as:

$$\tan(\phi\delta) = \frac{(\chi_{ij}''/\chi_{oij})_{\omega_j \rightarrow 0}}{(\chi_{ij}'/\chi_{oij})_{\omega_j \rightarrow 0}} \quad \dots(12)$$

$$\tau_{cs} = \frac{1}{\omega} \tan \phi \quad \dots(13)$$

Since,  $\phi$  cannot be evaluated directly, a theoretical curve of  $(1/\phi) \log(\cos \phi)$  with  $\phi$  in degrees was drawn as shown elsewhere<sup>4</sup>, from which:

$$\frac{1}{\phi} \log(\cos \phi) = \frac{\log[(\chi_{ij}'/\chi_{oij})/\cos(\phi\delta)]}{\phi\delta} \quad \dots(14)$$

was found out. The known values of  $(1/\phi) \log(\cos \phi)$  was then used to obtain  $\phi$ . With known  $\phi$  and  $\delta$ ,  $\tau_{cs}$  were obtained from Eqs (12) and (13) for each molecule. The estimated  $\gamma$  and  $\delta$  are presented in columns 11 and 12 of Table 3. Values of  $\tau_s$  and  $\tau_{cs}$  are entered in columns 11 and 12 of Table 2 to conclude symmetric relaxation behaviour for di-substituted anilines and asymmetric relaxation behaviour for di-substituted benzenes, respectively.

$$\frac{(d\chi_{ij}''/dw_j)_{w_j \rightarrow 0}}{(d\chi_{ij}'/dw_j)_{w_j \rightarrow 0}} = \omega\tau \quad \dots(16)$$

$\tau$ 's of the polar liquids could, however, be estimated from Eqs (15) and (16) as seen in 8th and 9th columns of Table 2. Again, the imaginary part  $\chi_{ij}''$  of the complex hf susceptibility  $\chi_{ij}^*$  as a function of  $w_j$  of a solute can be written as<sup>23-24</sup>:

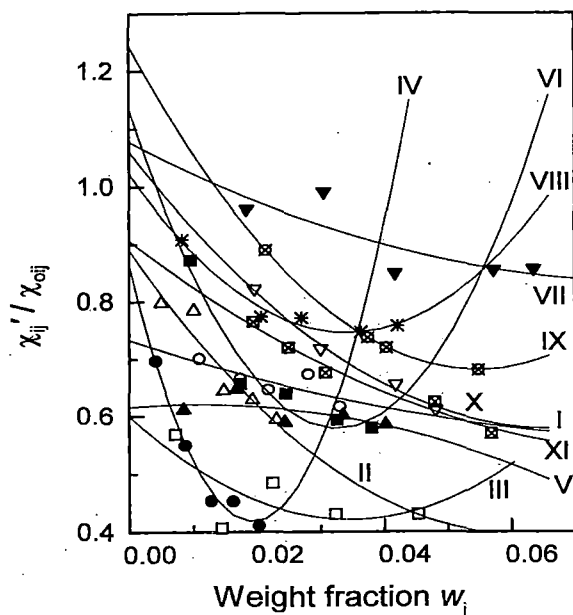


Fig. 5 — Plot of  $\chi_{ij}'/\chi_{oij}'$  with  $w_j$  of solutes at 35 °C under 9.945 GHz electric field for: I. o-chloronitrobenzene in  $C_6H_6$  (—○—); II. 4-chloro 3-nitrobenzotrifluoride in  $CCl_4$  (—△—); III. 4-chloro 3-nitrotoluene in  $C_6H_6$  (—□—); IV. 4-chloro 3-nitrotoluene in  $CCl_4$  (—●—); V. o-nitrobenzotrifluoride in  $C_6H_6$  (—▲—); VI. m-nitrobenzotrifluoride in  $C_6H_6$  (—■—); VII. 2-chloro 6-methyl aniline in  $C_6H_6$  (—▼—); VIII. 3-chloro 2-methyl aniline in  $C_6H_6$  (—\*—); IX. 3-chloro 4-methyl aniline in  $C_6H_6$  (—⊗—); X. 4-chloro 2-methyl aniline in  $C_6H_6$  (—▽—) and XI. 5-chloro 2-methyl aniline in  $C_6H_6$  (—⊠—) at 35 °C under 9.945 GHz electric field

#### 4 Theoretical Formulation for Dipole Moments $\mu_2$ and $\mu_1$

The Debye equation<sup>22</sup> for a polar-nonpolar liquid mixture under hf electric field in terms of  $\chi_{ij}$ 's is written as:

$$\frac{d\chi_{ij}''}{d\chi_{ij}'} = \omega\tau \quad \dots(15)$$

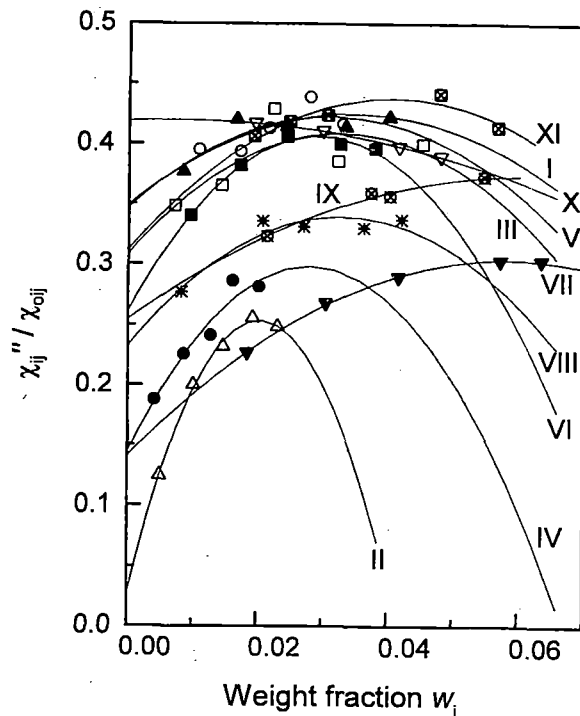


Fig. 6 — Plot of  $\chi_{ij}''/\chi_{oij}''$  with  $w_j$  of solutes at 35 °C under 9.945 GHz electric field for: I. o-chloronitrobenzene in  $C_6H_6$  (—○—); II. 4-chloro 3-nitrobenzotrifluoride in  $CCl_4$  (—△—); III. 4-chloro 3-nitrotoluene in  $C_6H_6$  (—□—); IV. 4-chloro 3-nitrotoluene in  $CCl_4$  (—●—); V. o-nitrobenzotrifluoride in  $C_6H_6$  (—▲—); VI. m-nitrobenzotrifluoride in  $C_6H_6$  (—■—); VII. 2-chloro 6-methyl aniline in  $C_6H_6$  (—▼—); VIII. 3-chloro 2-methyl aniline in  $C_6H_6$  (—\*—); IX. 3-chloro 4-methyl aniline in  $C_6H_6$  (—⊗—); X. 4-chloro 2-methyl aniline in  $C_6H_6$  (—▽—) and XI. 5-chloro 2-methyl aniline in  $C_6H_6$  (—⊠—) at 35 °C under 9.945 GHz electric field

$$\chi_{ij}'' = \frac{N\rho_{ij}\mu_j^2}{27\epsilon_0 k_B T M_j} \frac{\omega\tau}{1 + \omega^2\tau^2} (\epsilon_{ij} + 2)^2 w_j$$

which on differentiation with respect to  $w_j$  and at  $w_j \rightarrow 0$  yields:

$$\left( \frac{d\chi_{ij}''}{dw_j} \right)_{w_j \rightarrow 0} = \frac{N\rho_{ij}\mu_j^2}{27\epsilon_0 k_B T M_j} \frac{\omega\tau}{(1 + \omega^2\tau^2)} (\epsilon_i + 2)^2 \quad \dots(17)$$

Table 4 — Slope  $\beta_1$  of  $\chi_{ij}'$  versus  $w_j$  and  $\beta_2$  of  $\sigma_{ij}$  versus  $w_j$  curves, measured dipole moments  $\mu_j$  from susceptibility measurement technique and hf conductivity method from Eqs (19) and (26), respectively, reported dipole moment, theoretical dipole moment  $\mu_{theo}$  from available bond angles and bond moments expressed in Coulomb-metre (C-m) and the values of  $\mu_{expt}/\mu_{theo}$  for different disubstituted benzenes and anilines at 35 °C under 9.945 GHz electric field

System with Sl. No. & Mol.wt.	Slope of $\chi_{ij}'$ - $w_j$ & $\sigma_{ij}$ - $w_j$ curves		Dipole moments $\mu_j$ ( $\times 10^{-30}$ ) in cm								$\mu_{expt}/\mu_{theo}$
	$\beta_1$	$\beta_2$	From Eq. (19)		From Eq. (26)		$\mu_j^a$	$\mu_j^b$	$\mu_j^r$	$\mu_{theo}$	
			$\mu_2$	$\mu_1$	$\mu_2$	$\mu_1$					
(I)o-chloronitro benzene in $C_6H_6$ $M_j=0.1575$ kg	8.326	4.706	16.93	12.41	17.11	12.54	14.90	14.07	14.50	17.60	0.96
(II)4-chloro3-nitrobenzotrifluoride in $CCl_4$ $M_j=0.2255$ kg	3.358	1.875	13.02	6.81	13.08	6.84	9.76	11.80	10.57	12.60	1.03
(III)4-chloro 3-nitrotoluene in $C_6H_6$ $M_j=0.1715$ kg	4.490	2.570	17.39	9.37	17.69	9.53	12.94	14.54	14.97	18.60	0.93
(IV)4-chloro 3-nitrotoluene in $CCl_4$ $M_j=0.1715$ kg	4.854	3.001	17.40	7.15	18.39	7.56	11.95	12.36	15.60	18.50	0.94
(V)o-nitrobenzotrifluoride in $C_6H_6$ $M_j=0.1910$ kg	8.598	4.662	18.78	13.34	18.59	13.20	16.68	16.18	16.54	20.60	0.91
(VI)m-nitrobenzotrifluoride in $C_6H_6$ $M_j=0.1910$ kg	1.426	0.702	9.77	5.83	9.22	5.50	7.27	13.52	12.24	12.47	0.78
(VII)2-chloro 6-methylaniline in $C_6H_6$ $M_j=0.1415$ kg	0.728	0.560	4.91	3.47	5.79	4.09	3.64	4.50	7.73	6.16	0.56
(VIII)3-chloro 2-methylaniline in $C_6H_6$ $M_j=0.1415$ kg	2.674	1.693	10.47	6.66	11.20	7.13	7.14	7.86	10.07	8.27	0.81
(IX)3-chloro4-methylaniline in $C_6H_6$ $M_j=0.1415$ kg	2.128	1.269	10.38	6.07	10.78	6.30	7.14	7.49	8.70	7.33	0.83
(X)4-chloro2-methylaniline in $C_6H_6$ $M_j=0.1415$ kg	3.650	2.063	21.38	8.45	21.61	8.54	9.56	9.07	10.94	10.20	0.83
(XI)5-chloro2-methylaniline in $C_6H_6$ $M_j=0.1415$ kg	3.481	2.196	13.46	8.22	14.37	8.78	9.79	9.79	10.34	9.44	0.87

$\mu_j^a$  = dipole moment by using  $\tau$  from the direct slope of Eq. (15) ;  $\mu_j^r$  = reported dipole moment

$\mu_j^b$  = dipole moment by using  $\tau$  from the ratio of individual slopes of Eq. (16)

$\mu_{theo}$  = theoretical dipole moment from the available bond angles and bond moments

where the density of the solution  $\rho_{ij}$  becomes  $\rho_i$  = density of solvent,  $(\epsilon_{ij}+2)^2$  becomes  $(\epsilon_i+2)^2$  at  $w_j \rightarrow 0$ ,  $k_B$ =Boltzmann constant,  $N$ = Avogadro's number,  $\epsilon_i$ = relative permittivity of solvent and  $\epsilon_0$ = permittivity

of free space =  $8.854 \times 10^{-12}$  F.m<sup>-1</sup>. All are expressed in SI units.

Comparing Eqs (16) and (17) one gets:

$$\left(\frac{d\chi'_{ij}}{dw_j}\right)_{w_j \rightarrow 0} = \frac{N\rho_i\mu_j^2}{27\varepsilon_0 k_B T M_j} \frac{1}{(1+\omega^2\tau^2)} (\varepsilon_i+2)^2 = \beta_1 \quad \dots(18)$$

where  $\beta_1$  is the slope of  $\chi'_{ij}$  versus  $w_j$  curves of Fig.4 at  $w_j \rightarrow 0$ . Here, no approximation in determination of  $\mu_j$  is made, like the conductivity measurement technique<sup>4</sup> given below. After simplification, the hf dipole moment  $\mu_j$  is given by:

$$\mu_j = \left( \frac{27\varepsilon_0 k_B T M_j \beta_1}{N\rho_i (\varepsilon_i+2)^2 b} \right)^{\frac{1}{2}} \quad \dots(19)$$

where dimensionless parameter  $b$  is given by:

$$b = 1/(1+\omega^2\tau^2) \quad \dots(20)$$

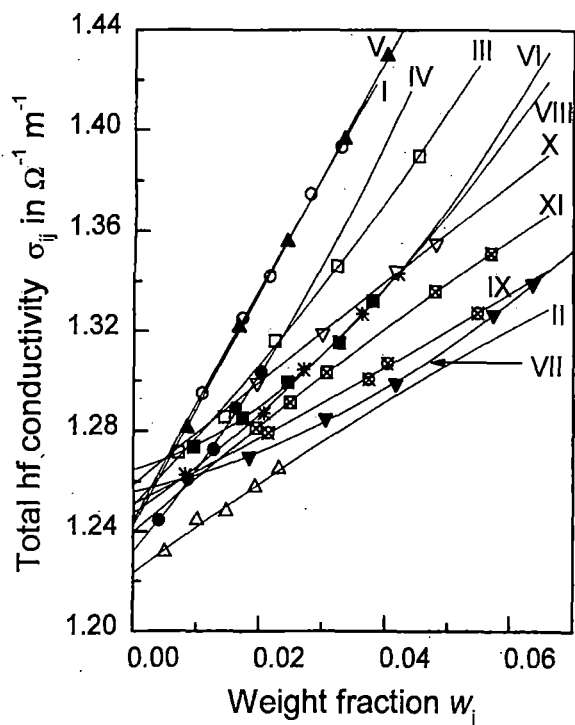


Fig. 7 — Variation of  $\sigma_{ij}$  against  $w_j$  of solutes at 35 °C under 9.945 GHz electric field for: I. o-chloronitrobenzene in  $C_6H_6$  (—○—); II. 4-chloro 3-nitrobenzotrifluoride in  $CCl_4$  (—△—); III. 4-chloro 3-nitrotoluene in  $C_6H_6$  (—□—); IV. 4-chloro 3-nitrotoluene in  $CCl_4$  (—●—); V. o-nitrobenzotrifluoride in  $C_6H_6$  (—▲—); VI. m-nitrobenzotrifluoride in  $C_6H_6$  (—■—); VII. 2-chloro 6-methyl aniline in  $C_6H_6$  (—▼—); VIII. 3-chloro 2-methyl aniline in  $C_6H_6$  (—\*—); IX. 3-chloro 4-methyl aniline in  $C_6H_6$  (—⊗—); X. 4-chloro 2-methyl aniline in  $C_6H_6$  (—▽—) and XI. 5-chloro 2-methyl aniline in  $C_6H_6$  (—⊠—) at 35 °C under 9.945 GHz electric field

## 5 Dipole Moments $\mu_2$ and $\mu_1$ from hf Conductivity

The complex hf conductivity  $\sigma_{ij}^*$  of polar-non-polar liquid mixture in a GHz electric field is given by<sup>25</sup>:

$$\sigma_{ij}^* = \sigma'_{ij} + j\sigma''_{ij} \quad \dots(21)$$

where  $\sigma'_{ij}$  ( $=\omega\varepsilon_0\varepsilon_{ij}'$ ) and  $\sigma''_{ij}$  ( $=\omega\varepsilon_0\varepsilon_{ij}''$ ) are the real and imaginary parts of the complex conductivity  $\sigma_{ij}^*$  in  $\Omega^{-1} m^{-1}$ . The magnitude of the total hf conductivity is:

$$\sigma_{ij} = \omega\varepsilon_0 (\varepsilon_{ij}'^2 + \varepsilon_{ij}''^2)^{\frac{1}{2}} \quad \dots(22)$$

Although  $\varepsilon_{ij}' \gg \varepsilon_{ij}''$ , but in the high frequency region,  $\varepsilon_{ij}' \cong \varepsilon_{ij}''$ .  $\varepsilon_{ij}''$  is responsible for absorption of electric energy and offers resistance to polarization. Hence,  $\sigma_{ij}''$  is related to  $\sigma_{ij}'$  by the relation<sup>26</sup>:

$$\sigma_{ij}'' = \sigma_{\infty ij} + \frac{1}{\omega\tau} \sigma'_{ij}$$

$$\sigma_{ij} = \sigma_{\infty ij} + \frac{1}{\omega\tau} \sigma'_{ij} \quad \dots(23)$$

Here, the approximation  $\sigma_{ij}'' \cong \sigma_{ij}$  is made. Differentiation of Eq. (23) with respect to  $w_j$  at  $w_j \rightarrow 0$  yields:

$$\left(\frac{d\sigma'_{ij}}{dw_j}\right)_{w_j \rightarrow 0} = \omega\tau \left(\frac{d\sigma_{ij}}{dw_j}\right)_{w_j \rightarrow 0} = \omega\tau\beta_2 \quad \dots(24)$$

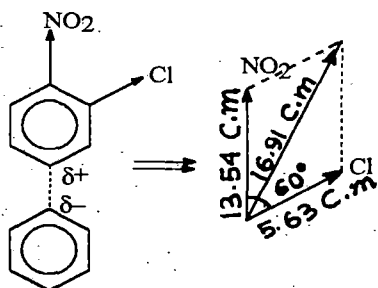
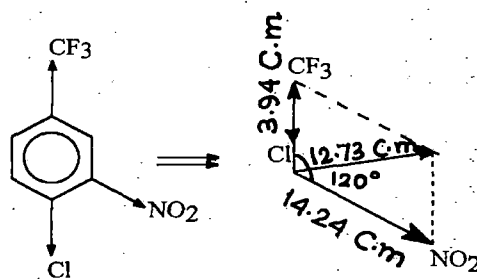
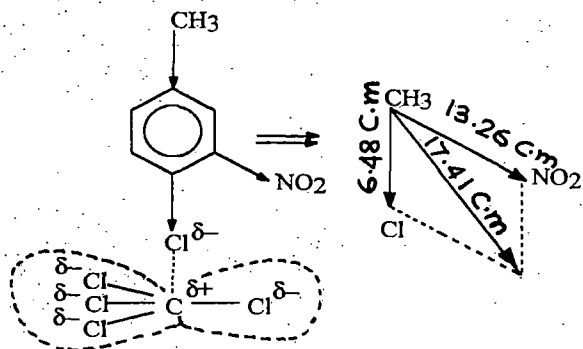
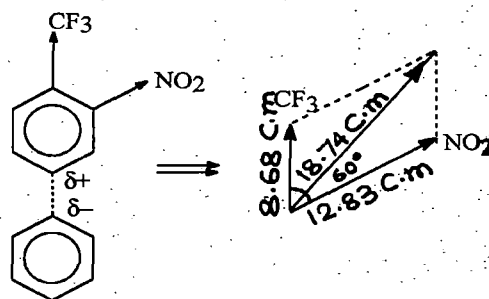
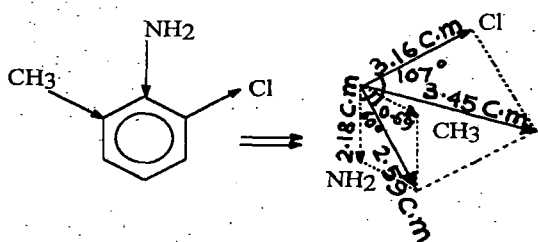
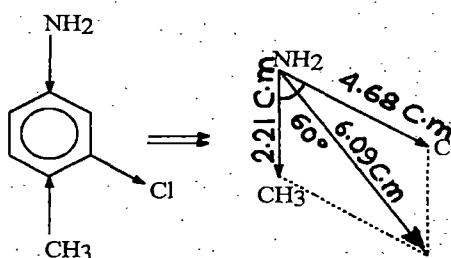
where  $\beta_2$  is the slope of  $\sigma_{ij}$  versus  $w_j$  curves of Fig. 7 at infinite dilution  $w_j \rightarrow 0$  and placed in Table 4. The real part of hf conductivity  $\sigma'_{ij}$  at  $T$  K (Ref. 23) is given by:

$$\sigma'_{ij} = \frac{N\rho_{ij}\mu_j^2}{27k_B T M_j} \frac{\omega^2\tau}{1+\omega^2\tau^2} (\varepsilon_{ij}+2)^2 w_j$$

$$\left(\frac{d\sigma'_{ij}}{dw_j}\right)_{w_j \rightarrow 0} = \frac{N\rho_i\mu_j^2}{27k_B T M_j} \frac{\omega^2\tau}{1+\omega^2\tau^2} (\varepsilon_i+2)^2 \quad \dots(25)$$

Comparing Eqs (24) and (25) one gets the dipole moment  $\mu_j$  from:

$$\mu_j = \left( \frac{27k_B T M_j \beta_2}{N\rho_i (\varepsilon_i+2)^2 \omega b} \right)^{\frac{1}{2}} \quad \dots(26)$$

I. o-chloronitrobenzene in  $C_6H_6$ II. 4-chloro 3-nitrobenzotrifluoride in  $CCl_4$ IV. 4-chloro 3-nitro toluene in  $CCl_4$ V. o-nitrobenzotrifluoride in  $C_6H_6$ VII. 2-chloro 6-methyl aniline in  $C_6H_6$ IX. 3-chloro 4-methyl aniline in  $C_6H_6$ Fig. 8 — Conformational structures of solutes from bond angles and bond moments in multiple  $10^{30}$  C-m

All the measured dipole moments  $\mu_j$  from the susceptibility measurement technique of Eq. (19) and hf conductivity method of Eq. (26) are entered in the 4th to 7th columns of Table 4, respectively.

## Results and Discussion

The double relaxation times  $\tau_1$  and  $\tau_2$  for the polar liquid molecules in different solvents are found out from the slope and intercept of Eq. (3), as

shown in Fig. 1, in terms of the orientational susceptibility parameters  $\chi_{ij}$  of Table 1. The  $\chi_{ij}$  values are, however, derived from the relative permittivities<sup>6-8</sup>  $\epsilon_{ij}$  for different weight fractions  $w_j$  of the polar liquids. The variables of Eq. (3) i.e.  $(\chi_{oij} - \chi_{ij}')/\chi_{ij}'$  and  $\chi_{ij}''/\chi_{ij}'$  are plotted against each other for different values of  $w_j$  of solutes under 9.945 GHz electric field at 35 °C to get linear equation by regression analysis. From Fig. 1, it is revealed that, the fitting is good for some cases, but poor in other cases. It appears that the linear fit for II ( $-\Delta-$ ), III ( $-\square-$ ) and IV ( $-\bullet-$ ) in Figs 1 and 2 often passes through two among five data points, others being off from the fit. Nevertheless, the regression analysis was made on the basis of Eq. (3). However, the accuracy of Fig. 1 is tested by the correlation coefficients ( $r$ ), which were found to be close to unity, indicating that the variables are almost collinear.

The % errors in terms of  $r$ -values in getting the intercepts and slopes were worked out to find the accuracies of  $\tau_1$  and  $\tau_2$ , respectively. In order to locate the double relaxation phenomena of the polar liquid molecules in non-polar aprotic solvents under investigation, accurate measurement of  $\chi_{oij}$  involved with  $\epsilon_{oij}$  and  $\epsilon_{\infty ij}$  is necessary. The refractive index  $n_{Dij}$  measured by Abbe's refractometer often yields  $\epsilon_{\infty ij} = n_{Dij}^2$ , although Cole Cole<sup>27</sup> and Cole Davidson<sup>28</sup> plots usually give  $\epsilon_{\infty ij} \cong 1.0-1.5$  times of  $n_{Dij}^2$ . This often introduces an additional error in the calculations. Nevertheless, the accuracies of  $\chi_{ij}''$ ,  $\chi_{ij}'$  and  $\chi_{oij}$  are of 5 % and 1 %, respectively derived from measured<sup>6-8</sup> relative permittivities  $\epsilon_{ij}''$ ,  $\epsilon_{ij}'$ ,  $\epsilon_{oij}$  and  $\epsilon_{\infty ij}$ . The estimated  $\tau_2$  and  $\tau_1$  are placed in Table 2, in order to compare them with those of Murthy *et al.*<sup>26</sup> of Eq. (15) and by the ratio of the individual slopes of the variations of  $\chi_{ij}''$  and  $\chi_{ij}'$  with  $w_j$  in the limit  $w_j \rightarrow 0$  of Eq.(16). The latter method seems to be better to calculate  $\tau$ , since it eliminates polar-polar interaction almost completely. The linear plot of  $\chi_{ij}''$  against  $\chi_{ij}'$  of Fig. 2 for different  $w_j$  of solute has intercepts, although it was expected from Eq. (15) that, they should pass through the origin. Nevertheless, values of  $\tau$  are found to be in close agreement with those calculated from the ratio of the individual slopes of the variations of  $\chi_{ij}''$  and  $\chi_{ij}'$  with  $w_j$  at  $w_j \rightarrow 0$  of Eq. (16), as shown in Figs 3 and 4. The experimental points as shown in Figs 3 and 4 with the fit are presented

(Table 2) to back up the results of Eq. (16) due to Debye model. Values of  $\chi_{ij}''$  increase monotonically with  $w_j$  and have a tendency to meet the origin for all the curves. This type of behaviour indicates that, under an electric field of 9.945 GHz,  $\chi_{ij}''$  tends to pass through the origin at  $w_j \rightarrow 0$ .

It is evident from Table 2 that, all the di-substituted benzenes exhibit the whole molecular rotation, while the di-substituted anilines show the rotation of the flexible parts under 10 GHz electric field when  $\tau_1$ 's and  $\tau_2$ 's are compared with the reported data. This indicates the flexible parts are more rigid in the di-substituted benzenes rather than the di-substituted anilines. The assumptions of symmetric and asymmetric relaxation behaviour from Eqs (8) and (9) for such non-rigid polar molecules yield  $\tau_s$  and  $\tau_{cs}$  from Eqs (11) and (13) to place them in the last two columns of Table 2. It reveals that the symmetric and asymmetric relaxation processes are more probable since,  $\tau_s$  and  $\tau_{cs}$  are almost in agreement with the reported  $\tau$  values in a solution. The characteristic relaxation times  $\tau_{cs}$  are sometimes very high through asymmetric distribution parameter  $\delta$  and often could not be determined for most of the molecules.

The di-substituted benzenes showed  $\tau_2$ 's in agreement with the reported  $\tau$ 's and  $\tau_{cs}$  except o-nitrobenzotrifluoride in  $C_6H_6$ , which agrees with  $\tau_s$  only. But, 4-chloro 3-nitrobenzotrifluoride in  $CCl_4$  and m-nitro-benzotrifluoride in  $C_6H_6$  yield  $\tau_2$  in close agreement with reported  $\tau$ 's although, they showed  $\tau_s \cong \tau_1$ . Only 2-chloro-6-methyl aniline and 3-chloro 2-methyl aniline in  $C_6H_6$  showed values of  $\tau_1$  in excellent agreement with the calculated values of  $\tau_s$ . For the rest di-substituted anilines values of  $\tau_1$  agree well with the calculated values of  $\tau_s$ , but the agreement is not better with the measured values of  $\tau$  from Eqs (15) and (16). It thus reveals that, a part of the di-substituted anilines is rotating, obeying symmetric relaxation behaviour, while most of the di-substituted benzenes showed asymmetric relaxation process for their whole molecular rotations.

The relative weighted contributions  $c_1$  and  $c_2$  towards dielectric dispersions due to  $\tau_1$  and  $\tau_2$  are estimated and placed in Table 3, by using Fröhlich's Eqs (6) and (7). They are compared with the experimental  $c_1$  and  $c_2$  from the fitted curves of

$\chi_{ij}'/\chi_{oij}$  and  $\chi_{ij}''/\chi_{oij}$  against  $w_j$  in the limit  $w_j \rightarrow 0$  of Figs 5 and 6. The non-linear fit with only five points for III ( $-\square-$ ) and IV ( $-\bullet-$ ) of Fig.5 appeared to be not convincing and in fact misleading, but three accurate experimental points are enough for such a fit. However, the fit is done with a PC and appropriate software. All the curves of Figs 5 and 6 vary usually<sup>12</sup> except the convex curve V for o-nitrobenzotrifluoride in  $C_6H_6$ . The variations of  $\chi_{ij}'/\chi_{oij}$  with  $w_j$  are, however, concave and convex in nature for all systems as observed elsewhere<sup>12</sup>. The left hand sides of Eqs (1) and (2) vary with values of  $w_j$  in concave and convex manner according to Figs 5 and 6 are now fixed for  $\tau_1$  and  $\tau_2$  once estimated from intercept and slope of Eq. (3) to yield experimental  $c_1$  and  $c_2$  values from Eqs (4) and (5) at  $w_j \rightarrow 0$ .

This study is supposed to yield the accurate values of  $c_1$  and  $c_2$  unlike the earlier one<sup>12</sup>, based on the graphical extrapolated values of  $(\epsilon_{ij}' - \epsilon_{\infty ij})/(\epsilon_{oij} - \epsilon_{\infty ij})$  and  $\epsilon_{ij}''/(\epsilon_{oij} - \epsilon_{\infty ij})$  at  $w_j \rightarrow 0$ , drawn on the basis of scientific judgement. Although, the nature of variations remains unaltered, it is evident from Table 3 that,  $c_2$  values are often negative for 4-chloro 3-nitrobenzotrifluoride in  $CCl_4$ , m-nitrobenzotrifluoride in  $C_6H_6$  and for all the di-substituted anilines unlike other systems. This perhaps signifies that the rotation of the flexible parts of the polar molecules are not in accord with the whole molecular rotation due to inherent inertia of the substituted parts of the molecules under hf electric field. The theoretical values of  $c_1+c_2$  are found to be greater than the sum of the experimental ones as listed in Table 3.

The experimental values of  $c_1+c_2 \cong 1$  for almost all the non-spherical polar liquid molecules. But (II) 4-chloro 3-nitrobenzotrifluoride in  $CCl_4$  ( $-\Delta-$ ), (X) 4-chloro 2-methyl aniline ( $-\nabla-$ ) and (XI) 5-chloro 2-methyl aniline ( $-\boxtimes-$ ) in  $C_6H_6$  show considerably lower values of  $c_1+c_2$ . This may indicate the reliability of Eq. (3) so far derived for such molecules, although they show high correlation coefficients ( $r$ ) and the corresponding very low % of errors to get the intercept and slope of Eq. (3). The largest theoretical  $c_1+c_2$  value for (IV) 4-chloro 3-nitro toluene in  $CCl_4$  ( $-\bullet-$ ) is 1.34, showing a deviation of nearly 34 %, unlike the other systems. The possible existence of more than two broad Debye-type dispersions may be taken into account

for such molecules of varying complexities as reported in tables and figures.

Dipole moments  $\mu_2$  and  $\mu_1$  due to rotation of the whole molecule as well as the flexible parts were, however, measured from Eq. (19) using dimensionless parameters ( $b$ ) involved with  $\tau$ 's by both the methods and slope  $\beta_1$ 's of  $\chi_{ij}'$  versus  $w_j$  curves of Fig. 4. The measured values of  $\mu_2$  and  $\mu_1$  are presented in Table 4. The variations of all the  $\chi_{ij}'$  values of polar-nonpolar liquid mixtures are found to be parabolic with values of  $w_j$  of polar compounds as evident from Fig.4. They are found to cut the ordinate axis at  $w_j = 0$  within  $0.0238 \leq \chi_{ij}' \leq 0.0645$  except 4-chloro 3-nitrobenzotrifluoride in  $CCl_4$  ( $-\Delta-$ ), 4-chloro 3-nitrotoluene in  $CCl_4$  ( $-\bullet-$ ). This behaviour probably reflects the solvent effects on the polar compounds under investigation. The interaction of solute on solvent  $CCl_4$  may occur due to slightly positive charge  $\delta^+$  on C atom of  $CCl_4$  and negative charge  $\delta^-$  on Cl atom of the substituted group in the benzene ring, as seen in Fig. 8. All the systems are of similar nature having monotonic increase of  $\chi_{ij}'$  with  $w_j$ .

The dipole moments  $\mu_2$  and  $\mu_1$  are also derived from the conductivity measurement technique of Eq. (26) using the slope  $\beta_2$ 's of  $\sigma_{ij}$  versus  $w_j$  curves of Fig.7 and are placed in Table 4 for comparison. The total hf conductivity  $\sigma_{ij}$  of all the polar-nonpolar liquid mixtures increase monotonically with  $w_j$  and cut the ordinate axis within the range  $1.2233 \leq \sigma_{ij} \leq 1.2646$  at  $w_j=0$  as seen in Fig.7. The slight disagreement of  $\mu_1$  and  $\mu_2$  derived from both the methods is due to the fact that the hf conductivity includes the fast polarization probably for the bound molecular charge associated with the molecule. All values of  $\mu_2$  for di-substituted benzenes and values of  $\mu_1$  for di-substituted anilines are found to agree with the reported values of  $\mu$  presented in Table 4. This indicates that, the flexible parts of the di-substituted benzenes are more rigid in comparison to di-substituted anilines.

The hf dipole moment  $\mu_j$ 's are calculated by using  $\tau$  from both the methods of direct slope of Eq. (15) and the ratio of the individual slopes of Eq. (16) in order to place them in.

Values of  $\mu_j$  by using  $\tau$  from the ratio of the individual slopes are in close agreement with the reported values, suggesting that, the latter method to

obtain  $\tau$  is more realistic. In such a case, one polar molecule is surrounded by a large number of non-polar solvent molecules and remains in a quasi-isolated state.

A special attention is, therefore, paid to obtain the conformational structures of some of the complex molecules as shown schematically in Fig. 8. The inductive, electromeric and resonance effects combined with mesomeric effect of the substituted polar groups play the key role to yield the theoretical dipole moment  $\mu_{\text{theo}}$ , depending on the electron affinity of C-atom of the benzene ring. The molecules have C $\rightarrow$ CF<sub>3</sub>, C $\leftarrow$ NH<sub>2</sub> ( $\angle 142^\circ$ ), C $\rightarrow$ NO<sub>2</sub>, C $\rightarrow$ Cl C $\leftarrow$ CH<sub>3</sub> polar groups of bond moments  $9.53 \times 10^{-30}$ ,  $4.93 \times 10^{-30}$ ,  $14.10 \times 10^{-30}$ ,  $5.63 \times 10^{-30}$ ,  $1.23 \times 10^{-30}$  C-m (Coulomb-metre) respectively<sup>12,19</sup> aligned in different angles in a plane to yield  $\mu_{\text{theo}}$ . Out of these, only -NO<sub>2</sub> and -NH<sub>2</sub> groups are in the habit to show resonance effect (-R or +R) in the molecules either by pulling or pushing electrons towards C-atom of the benzene ring. This resonance effect is stronger than inductive effects (+I or -I) to exhibit the peculiar behaviours as seen in the  $\chi_{ij}''/\chi_{oij}$  versus  $w_j$  and  $\chi_{ij}''/\chi_{oij}$  versus  $w_j$  curves for the di-substituted benzenes II, IV, V, VI including all the di-substituted anilines.

The structure of these polar molecules is of special interest as sketched in Fig. 8 in view of rearrangement of charge-density in them. All the di-substituted anilines include -Cl, -NH<sub>2</sub> and -CH<sub>3</sub> polar groups, of which -Cl and -CH<sub>3</sub> have very weak inductive effects (+I or -I). They are easily influenced by the GHz electric field to show the rotation of their flexible parts. Further, the observed difference in  $\mu$  values for a polar molecule in two aprotic nonpolar solvents may arise due to weak polarity of CCl<sub>4</sub> as shown in Fig. 8. The difference between  $\mu_{\text{theo}}$  and experimental values of  $\mu_j$  establishes the non-consideration of inductive and mesomeric effects. All these effects may be taken into account by the factor  $\mu_{\text{expt}}/\mu_{\text{theo}}$  to yield the exact  $\mu_1$  and  $\mu_2$  values of the molecules. All the polar molecules have  $sp^2$  hybridized carbon atoms of benzene ring and the substituted parts are associated with  $sp^3$  orbital. The interaction of orbitals may lead to gain knowledge on accumulation of charge on the substituted groups in addition to various effects present in them. The conformational structures of

other molecules except six of Fig. 8 were already shown elsewhere<sup>12,19</sup>.

## Conclusions

The study of relaxation phenomena of di-substituted benzenes and anilines in C<sub>6</sub>H<sub>6</sub> and CCl<sub>4</sub> by the modern established symbols of dielectric orientational susceptibilities  $\chi_{ij}$  measured under a single frequency electric field is very encouraging. It seems to be more topical, significant and useful contribution to predict the conformational structures and various molecular associations of the molecules at any given temperature. The intercept and slope of the derived linear Eq. (3) by the regression analysis on the measured data of  $\chi_{ij}$  of different values of  $w_j$  are used to get  $\tau_2$  and  $\tau_1$ . The methodology so far developed in SI units is superior because of the unified, coherent and rationalized nature of the established symbols of dielectric terminologies and parameters, which are directly linked with orientational polarization of the molecules. The significant Eqs (15) and (16) to obtain values of  $\tau_j$  and hence values of  $\mu_j$  from Eq. (19) help the future workers to shed more light on the relaxation phenomena of the complicated non-spherical polar liquids and liquid crystals. The prescribed method to obtain values of  $\tau_j$  from Eq. (16) with the use of the ratio of the individual slopes of  $\chi_{ij}''$  versus  $w_j$  and  $\chi_{ij}'$  versus  $w_j$  curves at  $w_j \rightarrow 0$  is a significant improvement over the existing ones, as it eliminates polar-polar interaction almost completely in  $\tau_j$ 's and  $\mu_j$ 's respectively.

Values of  $\tau_j$  and  $\mu_j$  are usually claimed to be accurate within 10 % and 5 %, respectively. But, the correlation coefficient  $r$  and % errors of Eq. (3) demand that, values of  $\tau$  and  $\mu$  are more than accurate. The non-spherical di-substituted benzene and aniline molecules absorb electric energy much more strongly, nearly 10 GHz electric field, at which the value of  $\epsilon''$  for absorption against frequency  $\omega$  showed a peak. This invited the attention to get the double relaxation times  $\tau_2$  and  $\tau_1$  from Eq. (3). The corresponding sum of the experimental and theoretical values of weighted contributions  $c_1$  and  $c_2$  towards dielectric dispersions due to estimated  $\tau_2$  and  $\tau_1$  differ significantly to indicate more than two Debye type relaxations in such molecules because of their complexity. The values of  $\tau$  for di-substituted benzenes as seen in

Table 2 show the whole molecular rotation, while the flexible parts of the di-substituted anilines rotates under 10 GHz electric field.

Di-substituted anilines exhibit the symmetric relaxation behaviour, while the asymmetric relaxation behaviour occurs in di-substituted benzenes in  $C_6H_6$  except 4-chloro 3-nitrobenzotrifluoride in  $CCl_4$  and m-nitro benzotrifluoride in  $C_6H_6$ , respectively. Values of  $\mu_2$  and  $\mu_1$  due to  $\tau_2$  and  $\tau_1$  are expected to be smaller when they are measured from the susceptibility measurement technique rather than the hf conductivity method, where the approximation of  $\sigma_{ij} \cong \sigma_{ij}''$  is usually made. The difference of  $\mu_2$  for the first six systems and of  $\mu_1$  for the rest five systems of Table 4, between conductivity and susceptibility measurement may arise, either by elongation or reduction of the bond moments of the substituted polar groups by the factor  $\mu_{\text{expt}} / \mu_{\text{theo}}$  in agreement with the measured values of  $\mu$  to take into account of the inductive, mesomeric and electromeric effects of the polar groups in the molecules. Thus, the correlation between the conformational structures with the observed results enhances the scientific content to add a new horizon of understanding to the existing knowledge of dielectric relaxation phenomena.

## References

- Dhull J S & Sharma D R, *J Phys D: Appl Phys*, 15 (1982) 2307.
- Sharma A K & Sharma D R, *J Phys Soc Jpn*, 53 (1984) 4771.
- Kumbharkhane A C, Puranic S M, Akode C G & Mehrotra S C, *Indian J Phys*, 74A (2000) 471.
- Dutta K, Basak R C, Sit S K & Acharyya S, *J Molec Liq*, 88 (2000) 229.
- Sit S K, Dutta K, Acharyya S, Palmajumder T & Roy S, *J Molec Liq*, 89 (2001) 111.
- Khameshara S M & Sisodia M L, *Indian J Pure & Appl Phys*, 18 (1980) 110.
- Gupta P C, Arrawatia M L & Sisodia M L, *Indian J Pure & Appl Phys*, 16 (1978) 451.
- Arrawatia M L, Gupta P C & Sisodia M L, *Indian J Pure & Appl Phys*, 15 (1977) 770.
- Gopalakrishna K V, *Trans Faraday Soc*, 53 (1957) 767.
- Higasi K, *Bull Chem Soc Jpn*, 39 (1966) 2157.
- Heston W M, Franklin A D, Henneley E J & Smyth C P, *J Am Chem Soc*, 72 (1950) 3443.
- Saha U, Sit S K, Basak R C & Acharyya S, *J Phys D: Appl Phys*, 27 (1994) 596.
- Jonscher A K, *Physics of dielectric solids*, invited papers (Ed) C H L Goodman, 1980.
- Jonscher A K, *Universal Relaxation Law* (Chelsea Dielectric Press, London), 1996.
- Ghosh N, Basak R C, Sit S K & Acharyya S, *J Molec Liq*, 85 (2000) 375.
- Bergmann K, Roberti D M & Smyth C P, *J Phys Chem*, 64 (1960) 665.
- Bhattacharyya J, Hasan A, Roy S B & Kastha G S, *J Phys Soc Jpn*, 28 (1970) 204.
- Higasi K, Koga Y & Nakamura M, *Bull Chem Soc Jpn*, 44 (1971) 988.
- Sit S K, Basak R C, Saha U & Acharyya S, *J Phys D: Appl Phys*, 27 (1994) 2194.
- Fröhlich H, *Theory of dielectrics Oxford* (Oxford University Press, Oxford, UK).
- Powles J G, *J Molec Liq*, 56 (1993) 35.
- Hill N E, Vaughan W E, Price A H & Davies M, *Dielectric properties and molecular behaviour* (Van Nostrand Reinhold, London), 1969.
- Smyth C P, *Dielectric behaviour and structure* (McGraw-Hill, UK), 1955.
- Dutta K, Sit S K & Acharyya S, *Pramana: J Phys*, 57 (2001) 775.
- Murphy F J & Morgan S O, *Bell Syst Tech J*, 18 (1939) 502.
- Murthy M B R, Patil R L & Deshpande D K, *Indian J Phys*, 63B (1989) 491.
- Cole K S & Cole R H, *J Chem Phys*, 9 (1941) 341.
- Cole R H & Davidson D W, *J Chem Phys*, 19 (1951) 1484.

# Relaxation phenomena in methyl benzenes and ketones from ultra high frequency conductivity

K Dutta, A Karmakar, S K Sit & S Acharyya

Department of Physics, Raiganj College (University College), PO Raiganj, Dist Uttar Dinajpur (WB) 733 134

e-mail: koushikduttajasm@rediffmail.com

Received 30 August 2001; revised 14 February 2002; accepted 30 May 2002

The relaxation time  $\tau$  and dipole moment  $\mu$  of some methyl benzenes and ketones (j) in a non-polar solvent benzene (i) at 25 °C under 9.585 GHz electric field have been obtained from the measured real and imaginary parts  $\epsilon_{ij}'$  and  $\epsilon_{ij}''$  of hf complex relative permittivity  $\epsilon_{ij}^*$  at various weight fractions  $w_j$ 's of a polar liquid. The methodology to get  $\tau$  from the ratio of the individual slopes of real  $\sigma_{ij}' (= \omega \epsilon_0 \epsilon_{ij}'')$  and imaginary  $\sigma_{ij}'' (= \omega \epsilon_0 \epsilon_{ij}')$  parts of complex hf conductivity  $\sigma_{ij}^*$  curve against  $w_j$ 's, seems to be a significant improvement over the existing one like the linear slope of  $\sigma_{ij}'' - \sigma_{ij}'$  curve. The variation of  $\sigma_{ij} - w_j$  curve like  $\sigma_{ij}'' - w_j$  curve is often convex indicating the probable occurrence of phase change in the polar-nonpolar liquid mixture after a certain concentration. The convex nature of  $\sigma_{ij}' - w_j$  curves for some systems indicate the maximum absorption of hf electric energy unlike other systems. The estimated  $\mu$ 's from slope  $\beta$  of hf conductivity  $\sigma_{ij} - w_j$  curve and  $\tau$  from both the methods are compared with the work of Gopalakrishna to establish the applicability of the methods. Theoretical dipole moments  $\mu_{\text{then}}$ 's from available bond angles and bond moments are calculated by considering inductive, mesomeric and electromeric effects of the substituent polar groups of the molecules.

## 1 Introduction

Relaxation processes in dielectric polar liquid or solid material (DRL or DRS) are very encouraging to study the molecular behaviour and structures through various experimental techniques<sup>1,2</sup>. The methods are involved with the high frequency conductivity<sup>3</sup> or susceptibility measurements<sup>4</sup>, thermally stimulated de-polarisation current<sup>5</sup> (TSDC) and time or frequency domain dielectric ac spectroscopy<sup>6</sup> etc. The latter two methods consist of a tedious computer simulated calculation in comparison to others, which are very simple and straightforward within the framework of Debye & Smyth model of dielectric liquid molecule.

Vaish & Mehrotra<sup>7,8</sup> measured real and imaginary parts ( $\epsilon_{ij}'$  and  $\epsilon_{ij}''$ ) of complex dielectric relative permittivity  $\epsilon_{ij}^*$  of some methyl benzenes and ketones (j) in benzene (i) under 3.13 cm wavelength electric field at 25 °C. They attempted to correlate dielectric relaxation times with those of nuclear magnetic resonance spin lattice relaxation times by using the theory of Bloembergen *et al.*<sup>9</sup> in terms of measured relaxation parameters. The relaxation times  $\tau$  of the molecules were calculated on the assumption that dipole-dipole (dimer)

interaction occurs between the nuclear spins. The spin lattice relaxation times were obtained to compare with the Gopalakrishna, Debye and other methods. The experimental values differ significantly from those of theoretical one. This study reveals that,  $\tau$  plays the main role in inter and intra molecular motions and nuclear magnetic resonance (NMR) spin lattice relaxation etc.

The values of  $\tau$  and dipole moment  $\mu$  of these polar molecules by the conductivity technique have been calculated in the present paper. The procedures employed to get  $\tau$  are those of Murthy *et al.*<sup>10</sup> from the direct slope of the linear equation of imaginary  $\sigma_{ij}'' (= \omega \epsilon_0 \epsilon_{ij}')$  and real  $\sigma_{ij}' (= \omega \epsilon_0 \epsilon_{ij}'')$  in  $\Omega^{-1} \text{ m}^{-1}$  parts of the hf complex conductivity  $\sigma_{ij}^*$  (Fig. 1) and the ratio of the individual slopes of  $\sigma_{ij}'' - w_j$  and  $\sigma_{ij}' - w_j$  curves<sup>11</sup> (Figs 2 and 3) at  $w_j \rightarrow 0$  respectively. The use of the ratio of individual slopes to estimate  $\tau$  seems to be better as it eliminates the polar-polar interaction almost completely. Hence, the purpose of the present paper is to study the success or otherwise of the proposed theory with the existing ones to infer molecular structures and associations. The graphs of  $\sigma_{ij}''$  and  $\sigma_{ij}'$  with  $w_j$ 's in Figs 2 and 3 are found to be non-linear to indicate the presence of solute-solute associations in the mixture. The  $\tau$ 's

from linear slope are found to agree with the reported  $\tau$ 's from Gopalakrishna's fixed frequency method (Fig. 4) and are presented in Table 1 together with all the measured  $\tau$ 's by different procedures. Further, the polar molecules under

synthetic rubber, wax etc. The study of the variation of  $\tau$  with respect to various substituted polar groups attached to different positions of the parent molecules may throw much light on the structural conformations of the methyl benzene and ketone molecules. The authors had already made a detailed investigation on some poly-substituted benzenes<sup>12</sup> at various temperatures to get molecular structures by conductivity technique. Dielectric parameters are very much temperature-dependent. Calculations at some other temperature may reveal a better picture. Nevertheless, from these studies it may be clear as to what theory is valid for such highly non-spherical aliphatic and aromatic compounds. A systematic comparison of  $\tau$  and  $\mu$  can thus be made from the measured data at 25 °C.

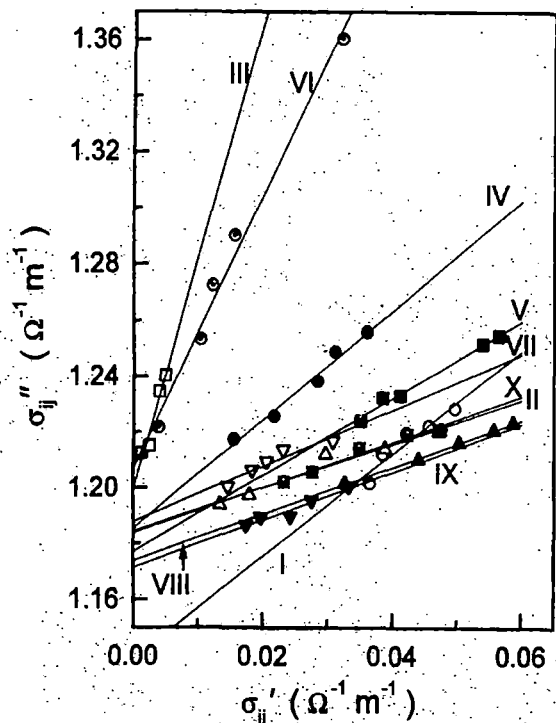


Fig. 1 — The linear variation of imaginary part  $\sigma_{ij}''$  against real part  $\sigma_{ij}'$  of complex hf conductivity  $\sigma_{ij}$  at 25 °C under 9.585 GHz electric field : (I) toluene (-○-); (II) 1,3,5 tri methyl benzene (-△-); (III) 1,2,3,4 tetra methyl benzene (-□-); (IV) 1,2,4,5 tetra methyl benzene (-●-); (V) penta methyl benzene (-■-); (VI) p-fluoro toluene (-⊙-); (VII) butyl ethyl ketone(-∇-); (VIII) methyl hexyl ketone (-▲-); (IX) ethyl pentyl ketone (-▼-); (X) heptyl methyl ketone (-⊗-)

investigation are methyl substituted aromatic and ketone substituted aliphatic compounds of highly non-spherical nature. Methyl substituted benzenes and ketones have almost similar characteristics. Some of the methyl benzenes are supposed to have apparently zero dipole moment from bond moment calculation. Moreover, these molecules are supposed to absorb electric energy much more strongly in the effective dispersive region of nearly 10 GHz at which peak of the absorption curve occurs. The ketones, on the other hand, are pleasant smelling liquids and widely used in petroleum industry. These liquids are used as good solvents of

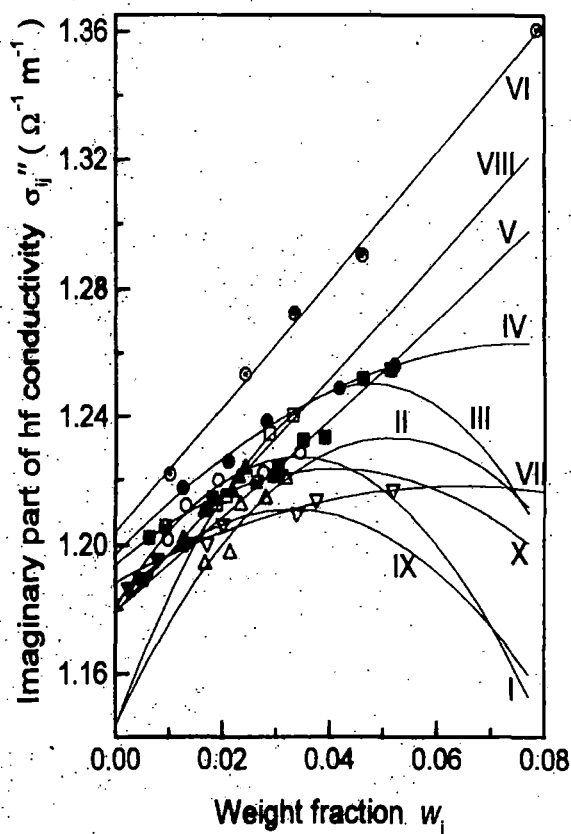


Fig. 2 — Variation of imaginary part of conductivity  $\sigma_{ij}''$  against  $w_j$  at 25 °C under 9.585 GHz electric field : (I) toluene (-○-); (II) 1,3,5 tri methyl benzene (-△-); (III) 1,2,3,4 tetra methyl benzene (-□-); (IV) 1,2,4,5 tetra methyl benzene (-●-); (V) penta methyl benzene (-■-); (VI) p-fluoro toluene (-⊙-); (VII) butyl ethyl ketone(-∇-); (VIII) methyl hexyl ketone (-▲-); (IX) ethyl pentyl ketone (-▼-); (X) heptyl methyl ketone (-⊗-)

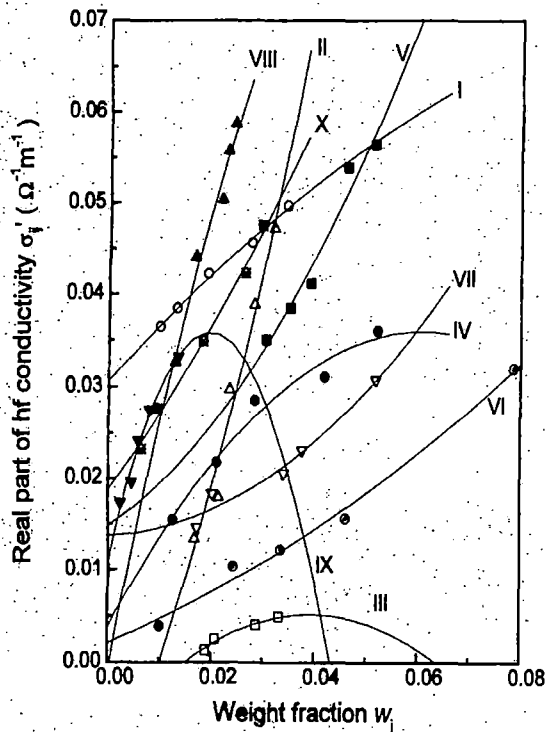


Fig. 3 — Variation of real part of conductivity  $\sigma_{ij}'$  against  $w_j$  at 25 °C under 9.585 GHz electric field: (I) toluene (-○-); (II) 1,3,5 tri methyl benzene (-△-); (III) 1,2,3,4 tetra methyl benzene (-□-); (IV) 1,2,4,5 tetra methyl benzene (-●-); (V) penta methyl benzene (-■-); (VI) p-fluoro toluene (-⊙-); (VII) butyl ethyl ketone (-▽-); (VIII) methyl hexyl ketone (-▲-); (IX) ethyl pentyl ketone (-▼-); (X) heptyl methyl ketone (-⊗-)

The corresponding dipole moments  $\mu_j$ 's of these liquids are obtained from the linear coefficient  $\beta$  of uhf conductivity  $\sigma_{ij}$  curves against  $w_j$ 's (Fig. 5). All the  $\beta$ 's and  $\mu$ 's are tabulated in Table 2 with those from Gopalakrishna and theoretical conformational calculation of Fig. 6. The inductive, mesomeric and electromeric effects under 3 cm wavelength electric field play the vital role in determining the theoretical  $\mu_{\text{theo}}$ 's of the molecules of Fig. 6 in agreement with estimated  $\mu_j$ 's.

## 2 HF Conductivity Technique to Estimate $\tau$ and $\mu$

The ultra high frequency (uhf) complex conductivity<sup>13</sup>  $\sigma_{ij}^*$  is:

$$\sigma_{ij}^* = \sigma_{ij}' + j\sigma_{ij}'' \quad \dots(1)$$

where  $\sigma_{ij}' = \omega \epsilon_0 \epsilon_{ij}''$  and  $\sigma_{ij}'' = \omega \epsilon_0 \epsilon_{ij}'$  are the real and imaginary parts of  $\sigma_{ij}^*$ ,  $\epsilon_0$  is absolute permittivity of free space =  $8.854 \times 10^{-12}$  F.m<sup>-1</sup> and  $\omega (=2\pi f)$  is the angular frequency of the applied electric field of frequency,  $f = 9.585 \times 10^9$  Hz.

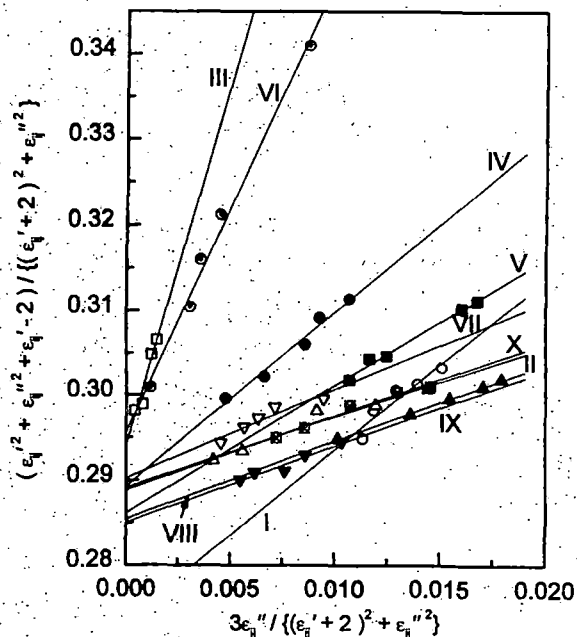


Fig. 4 — Linear plots of  $x$  against  $y$  for some methyl benzenes and ketones at 25 °C under 9.585 GHz electric field: (I) toluene (-○-); (II) 1,3,5 tri methyl benzene (-△-); (III) 1,2,3,4 tetra methyl benzene (-□-); (IV) 1,2,4,5 tetra methyl benzene (-●-); (V) penta methyl benzene (-■-); (VI) p-fluoro toluene (-⊙-); (VII) butyl ethyl ketone (-▽-); (VIII) methyl hexyl ketone (-▲-); (IX) ethyl pentyl ketone (-▼-); (X) heptyl methyl ketone (-⊗-)

Debye equation<sup>14</sup> in the GHz region yields:

$$\sigma_{ij}'' = \sigma_{\infty ij} + \frac{1}{\omega\tau} \sigma_{ij}' \quad \dots(2)$$

$$\left( \frac{d\sigma_{ij}''}{d\sigma_{ij}'} \right) = \frac{1}{\omega\tau} \quad \dots(3)$$

Both  $\sigma_{ij}''$  and  $\sigma_{ij}'$  are functions of  $w_j$ . Their variations are non-linear in the higher concentration region as seen in Figs 2 and 3. In this case, one can write Eq. (2) as:

$$\left( \frac{d\sigma_{ij}''}{dw_j} \right)_{w_j \rightarrow 0} = \frac{1}{\omega\tau} \left( \frac{d\sigma_{ij}'}{dw_j} \right)_{w_j \rightarrow 0} \quad \dots(4)$$

the  $\tau$ 's from both the Eqs (3) and (4) were computed and are listed in Table 1 for comparison with the reported  $\tau$  recalculated from Gopalakrishna's method.

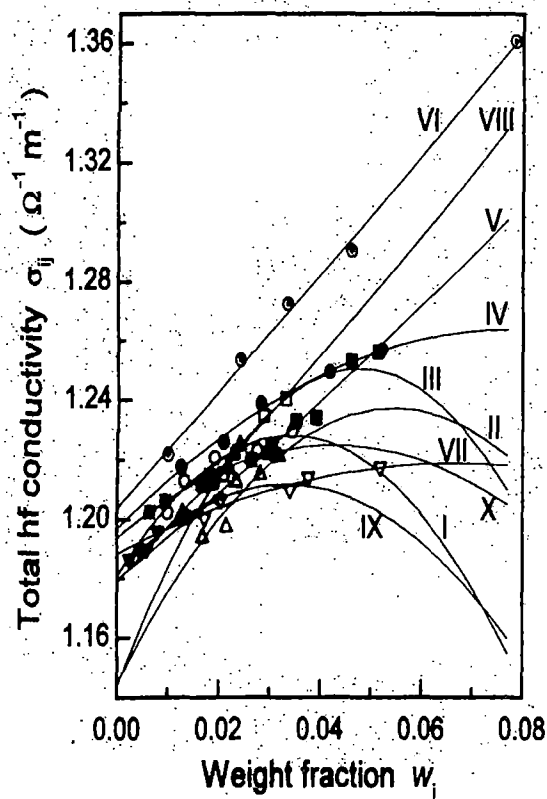


Fig. 5 — The plot of uhf conductivity  $\sigma_{ij}$  against  $w_j$ : (I) toluene (-○-); (II) 1,3,5 tri methyl benzene (-△-); (III) 1,2,3,4 tetra methyl benzene (-□-); (IV) 1,2,4,5 tetra methyl benzene (-●-); (V) penta methyl benzene (-■-); (VI) p-fluoro toluene (-⊙-); (VII) butyl ethyl ketone (-▽-); (VIII) methyl hexyl ketone(-▲-); (IX) ethyl pentyl ketone (-▼-); (X) heptyl methyl ketone (-⊗-)

Since  $\epsilon_{ij}' > \epsilon_{ij}''$ , but in hf region of GHz range  $\epsilon_{ij}' \cong \epsilon_{ij}''$  where  $\epsilon_{ij}''$  offers resistance to polarisation and uhf conductivity  $\sigma_{ij} = \omega\epsilon_0(\epsilon_{ij}'^2 + \epsilon_{ij}''^2)^{1/2}$ . Eq. (2) can thus be written in the following form:

$$\sigma_{ij} = \sigma_{\infty ij} + \frac{1}{\omega\tau} \sigma'_{ij}$$

$$\left( \frac{d\sigma'_{ij}}{dw_j} \right)_{w_j \rightarrow 0} = \omega\tau\beta \quad \dots(5)$$

$\beta$  is the slope of  $\sigma_{ij} - w_j$  curve in the limit  $w_j = 0$  as observed in Fig. 5 and listed in Table 2.

The real part  $\sigma'_{ij}$  of hf complex conductivity  $\sigma_{ij}^*$  is given by<sup>12</sup>:

$$\sigma'_{ij} = \frac{N\mu_j^2 \rho_{ij}}{27M_j k_B T} \left( \frac{\omega^2 \tau}{1 + \omega^2 \tau^2} \right) (\epsilon_{ij} + 2)^2 w_j$$

$$\left( \frac{d\sigma'_{ij}}{dw_j} \right)_{w_j \rightarrow 0} = \frac{N\mu_j^2 \rho_i}{27M_j k_B T} \left( \frac{\omega^2 \tau}{1 + \omega^2 \tau^2} \right) (\epsilon_i + 2)^2 \quad \dots(6)$$

where density  $\rho_{ij}$  and local field  $F_{ij}$  of the solution become  $\rho_i$  and  $F_i = (\epsilon_i + 2)^2/9$  of the solvent in the limit  $w_j=0$ .

From Eqs (5) and (6) one gets hf dipole moment  $\mu_j$  as:

$$\mu_j = \left( \frac{27M_j k_B T \beta}{N \rho_i (\epsilon_i + 2)^2 \omega b} \right)^{1/2} \quad \dots(7)$$

where

$N$  = Avogadro's number =  $6.023 \times 10^{23}$

$\rho_i$  = density of solvent benzene at 25 °C =  $874.3 \text{ Kg.m}^{-3}$

$\epsilon_i$  = relative permittivity of solvent benzene at 25 °C = 2.274

$M_j$  = molecular weight of solute in Kg

$k_B$  = Boltzmann constant =  $1.38 \times 10^{-23} \text{ J.mole}^{-1} \text{ K}^{-1}$  and  $b$  is the dimensionless parameter involved with measured  $\tau$  where  $b = 1 / (1 + \omega^2 \tau^2)$

Both the dipole moments  $\mu_j$ 's and dimensionless parameters  $b$ 's are presented in Table 2.

### 3 Results and Discussion

The imaginary  $\sigma_{ij}'' (= \omega\epsilon_0 \epsilon_{ij}'')$   $\Omega^{-1} \text{ m}^{-1}$  are plotted against real  $\sigma_{ij}' (= \omega\epsilon_0 \epsilon_{ij}')$   $\Omega^{-1} \text{ m}^{-1}$  parts of hf complex conductivity  $\sigma_{ij}^*$  for different weight fractions  $w_j$ 's of solute according to Eq. (2) to get  $\tau$  of polar liquid molecules as shown in Fig. 1. The variables are found to be almost linearly correlated as evident from the correlation coefficient  $r$  of the straight line of Eq. (3). It appears from Fig. 1 that, the systems like (I), (II), (III) and (VII) show low values of  $r$  (Table 1) indicating their departure from perfect linearity of the variables. Perfect linearity is said to

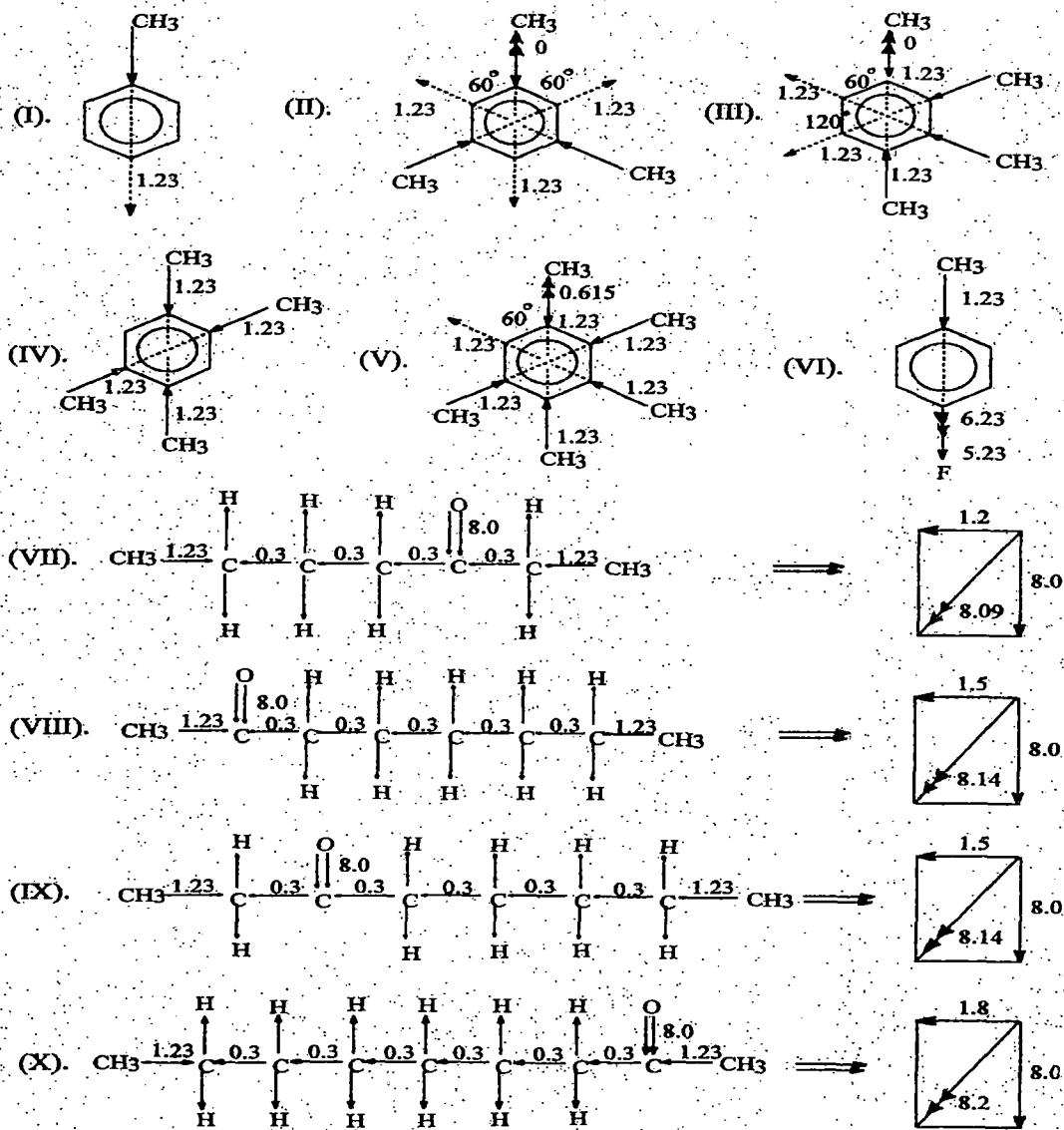


Fig. 6 — Conformational structures of polar molecules in terms of bond angles and bond moments ( $\times 10^{-30}$  Coulomb. metre) of the substituent groups: (I) toluene; (II) 1,3,5 tri methyl benzene; (III) 1,2,3,4 tetra methyl benzene (IV) 1,2,4,5 tetra methyl benzene; (V) penta methyl benzene; (VI) p-fluoro toluene; (VII) butyl ethyl ketone; (VIII) methyl hexyl ketone; (IX) ethyl pentyl ketone; (X) heptyl methyl ketone

be achieved for  $-1 \leq r \leq 1$ . In such cases, the proposed method to determine  $\tau$  from the ratio of the individual slopes of  $\sigma_{ij}''$  and  $\sigma_{ij}'$  against  $w_j$  according to Eq. (4) seems to be a better choice and is claimed to be the best improvement over the other two because polar-polar interaction is avoided almost completely in the limit  $w_j = 0$ . The estimated  $\tau$ 's for systems (III), (IV), (VI) and (IX) from Eq. (4) are in agreement with those of Murthy *et al.*<sup>10</sup>

and reported  $\tau$ . For the rest of the systems,  $\tau$ 's are lower from the ratio of individual slopes, except methyl hexyl ketone. All the plots of  $\sigma_{ij}''$  and  $\sigma_{ij}'$  against  $w_j$ 's as sketched in Figs 2 and 3 are parabolic in nature indicating the occurrence of associational aspect of polar liquid molecules in a non-polar solvent. The systems I(-○-), II(-△-), III(-□-), IV(-●-), VII(-▽-), IX(-▼-) and X(-⊗-) exhibit monotonic increase of  $\sigma_{ij}''$  with  $w_j$  like  $\sigma_{ij}-w_j$  curves

of Fig. 5 in order to attain maximum value at a certain concentration ( $w_j$ ) to show the convex nature. This is perhaps due to phase transition occurring in the polar-non-polar liquid mixture as observed elsewhere<sup>12</sup>. Similar variation  $\sigma_{ij}''$  and  $\sigma_{ij}$  in  $\Omega^{-1} \text{ m}^{-1}$  with  $w_j$  as displayed graphically in Figs 2 and 5 indicates the validity of the approximation of  $\sigma_{ij}'' \cong \sigma_{ij}$  of Eq. (5). All the curves of Figs 2 and 5 have a tendency to cut a point on the  $\sigma_{ij}$ -axis in the limit  $w_j = 0$  except systems (II) and (III) probably due to solvation effect<sup>15</sup> of the polar-non-polar liquid mixture. The plots of  $\sigma_{ij}' - w_j$  curves of Fig. 3 are also parabolic in nature. The variation of  $\sigma_{ij}'$  against  $w_j$ 's for the III(-□-), IV(-●-) and IX(-▼-) systems show convex shape indicating the maximum absorption of hf electric energy at  $w_j = 0.04, 0.06$  and  $0.02$ , respectively. The rest of the systems display gradual increase of  $\sigma_{ij}'$  with  $w_j$  probably due to the fact that absorption of electric energy increases at the higher concentration. This is authenticated by the positive coefficient of the quadratic term in the fitted equations of  $\sigma_{ij}' - w_j$  curves of Fig. 3. All the  $\tau$ 's of the polar liquid molecules of Table 1 agree well with those of Murthy *et al.*<sup>10</sup> from Eq. (3) and reported value. The reported  $\tau$ 's based on the standard method of Gopalakrishna were found to be much higher<sup>7,8</sup> which prompted us to recalculate  $\tau$ 's from the following expression<sup>16</sup>:

$$x = \frac{\epsilon_{ij}'^2 + \epsilon_{ij}' + \epsilon_{ij}''^2 - 2}{(\epsilon_{ij}' + 2)^2 + \epsilon_{ij}''^2}; y = \frac{3\epsilon_{ij}''}{(\epsilon_{ij}' + 2)^2 + \epsilon_{ij}''^2} \quad \dots(8)$$

The variation of  $x$  against  $y$  of Eq. (8) are linear as seen in Fig. 4. One can obtain  $\tau$  from:

$$\tau = 1/\omega \left( \frac{dx}{dy} \right) \quad \dots(9)$$

$\mu_j$ 's are recalculated by using Gopalakrishna's equation<sup>16</sup> as:

$$\mu = \left[ \frac{9k_B T M_j}{4\pi N \rho_i} \left\{ 1 + \left( \frac{dy}{dx} \right)^2 \right\} \left( \frac{dx}{dw_j} \right)_{w_j \rightarrow 0} \right]^{\frac{1}{2}} \quad \dots(10)$$

$\tau$ 's from the ratio of the individual slopes of Eq. (4), on the other hand, are found to be in better agreement for the systems: 1,2,3,4 tetramethyl benzene (III); 1,2,4,5 tetramethyl benzene (IV); p-fluoro toluene (VI) and ethyl pentyl ketone (IX)

respectively. The other systems exhibit low values of  $\tau$  from the ratio of individual slopes of  $\sigma_{ij}''$  and  $\sigma_{ij}'$  against  $w_j$ 's except methyl hexyl ketone (VIII). This behaviour can be explained on the basis of the fact that the methods of Murthy *et al.*<sup>10</sup> and Gopalakrishna yield  $\tau$ 's of either a quasi isolated polar or a dimer (solute-solute association) molecule. The ratio of the individual slopes, on the other hand, takes into account both the processes in addition to  $\tau$  of a dimer molecule. The smaller value of  $\tau$  may be due to formation of monomer supported by low values of  $r$  of the systems under investigation.

Dipole moments  $\mu_j$ 's are computed from the slope  $\beta$  of uhf conductivity  $\sigma_{ij}$  against  $w_j$  curves of Fig. 5 and dimensionless parameters  $b$ 's of Eq. (7) to compare with the results of Eq. (10) of Gopalakrishna<sup>16</sup>. The  $\mu$ 's are now found to agree well as seen in Table 2 with Murthy *et al.*<sup>10</sup> and recalculated values of Gopalakrishna for all the systems like  $\tau$ 's indicating the applicability of the methods for such systems under investigation. The  $\sigma_{ij}$ 's of polar-non-polar liquid mixtures are, however, concerned with the bound molecular charges which may be counted by  $\beta$  (Table 2) of  $\sigma_{ij} - w_j$  curves of Fig. 5. The agreement is better from Eqs (4) and (7) with the use of the ratio of individual slopes for systems (I), (III), (IV), (VI) and (IX) respectively unlike other polar liquids where  $\mu$ 's are slightly lower except for methyl hexyl ketone. Low values of  $\mu$ 's may be due to formation of monomer while high values are responsible for dimer formations. The slight difference between reported and estimated  $\mu$ 's may occur due to existence of steric hindrances among the substituted polar groups.

The theoretical dipole moments  $\mu_{\text{theo}}$ 's are calculated on the basis of planar structures for the molecules from the available bond moments of  $\text{CH}_3 \rightarrow \text{C}$ ,  $\text{C}=\text{O}$ ,  $\text{C} \leftarrow \text{C}$ ,  $\text{C} \rightarrow \text{F}$  and  $\text{C} \rightarrow \text{H}$  of  $1.23 \times 10^{-30}$ ,  $8 \times 10^{-30}$ ,  $0.3 \times 10^{-30}$ ,  $5.23 \times 10^{-30}$  and  $1 \times 10^{-30}$  in Coulomb-metre (C.m) respectively.  $\text{CH}_3 \rightarrow \text{C}$  makes an angle  $180^\circ$  with the bond axis. The direction of  $\text{C} \leftarrow \text{C}$  bond moment is taken in the reverse direction of bond axis<sup>17</sup>. All the substituted polar groups have the usual nature of either pushing or pulling electrons from the adjacent atoms of the parent molecules. Thus, there exists a difference in electron affinity within each atom of the substituted

Table 1 — Slope and intercepts of Eq. (2), correlation coefficient  $r$ , ratio of the individual slopes of  $\sigma_{ij}''-w_j$  and  $\sigma_{ij}'-w_j$  curves at  $w_j \rightarrow 0$ , relaxation time  $\tau$  from Eqs (3) and (4) and from Gopalakrishna's method of some methyl benzenes and ketones in benzene at 25 °C under 9.585 GHz electric field

System	Slope and intercepts of Eq. (3)		Correlation. Coefficient $r$	Ratio of individual slopes of $\sigma_{ij}''-w_j$ and $\sigma_{ij}'-w_j$ at $w_j \rightarrow 0$	Relaxation times $\tau_j (\times 10^{-12})$ in s		
					$\tau_j^a$	$\tau_j^b$	$\tau_j^c$
(I) toluene	1.8468	1.1385	0.9527	4.3891	8.99	3.78	8.24
(II) 1,3,5 tri methylbenzene	0.7897	1.1844	0.9755	2.8782	21.03	5.77	19.93
(III) 1,2,3,4 tetra methyl benzene	8.3666	1.1992	0.9678	6.5797	1.98	2.52	1.94
(IV) 1,2,4,5 tetra methyl benzene	1.9531	1.1854	0.9890	1.6133	8.50	10.29	8.06
(V) penta methyl benzene	1.3836	1.1770	0.9948	3.8814	12.00	4.28	11.02
(VI) p-fluorotoluene	4.8910	1.2071	0.9941	8.2548	3.39	2.01	3.12
(VII) butyl ethyl ketone	1.0070	1.1878	0.9481	40.3859	16.48	0.41	15.84
(VIII) methyl hexyl ketone	0.8452	1.1737	0.9993	0.6003	19.65	27.66	18.13
(IX) ethyl pentyl ketone	0.8640	1.1713	0.9686	0.6928	19.22	23.97	18.40
(X) heptyl methyl ketone	0.8203	1.1838	0.9859	1.8590	20.24	8.93	19.01

$\tau_j^a$  = Relaxation time from Eq. (3)

$\tau_j^b$  = Relaxation time from Eq. (4)

$\tau_j^c$  = Relaxation time from Gopalakrishna's method of Eq. (9)

Table 2 — Coefficients of  $\sigma_{ij}-w_j$  curves, dimensionless parameter  $b [=1/(1+\omega^2\tau^2)]$ , dipole moment  $\mu_j$  in Coulomb.metre from  $\tau$ 's of Eqs (3), (4) and Gopalakrishna's method and the theoretical dipole moment  $\mu_{theo}$  from the available bond angles and bond moments of some methyl benzenes and ketones in benzene at 25 °C under 9.585 GHz electric field

System with mol.wt.	Coefficients of $\sigma_{ij} = \alpha + \beta w_j + \gamma w_j^2$			Values of $b$ by using $\tau$		Dipole moment ( $\times 10^{-30}$ ) C.m			
	$\alpha$	$\beta$	$\gamma$	of Eq. (3)	of Eq. (4)	$\mu_j^a$	$\mu_j^b$	$\mu_j^c$	$\mu_{theo}$
(I) toluene $M_j=0.092$ Kg	1.1811	2.7545	-40.2180	0.7733	0.9507	7.93	7.15	7.80	1.23
(II) 1,3,5 tri methylbenzene $M_j=0.120$ Kg	1.1446	3.4010	-31.2102	0.3840	0.8923	14.27	9.36	13.94	0.00
(III) 1,2,3,4 tetra methyl benzene $M_j=0.134$ Kg	1.1436	4.4952	-47.2133	0.9860	0.9775	10.82	10.87	10.82	0.00
(IV) 1,2,4,5 tetra methyl benzene $M_j=0.134$ Kg	1.1969	1.7313	-11.2125	0.7924	0.7225	7.49	7.84	7.39	0.00
(V) penta methyl benzene $M_j=0.148$ Kg	1.1798	1.4009	2.2168	0.6569	0.9377	7.78	6.51	7.63	1.23
(VI) p- fluoro toluene $M_j=0.110$ Kg	1.2039	1.9329	0.7021	0.9600	0.9856	6.52	6.43	6.53	6.23
(VII) butyl ethyl ketone $M_j=0.114$ Kg	1.1885	0.9115	-6.8748	0.5038	0.9994	6.29	4.46	6.19	8.09
(VIII) methyl hexyl ketone $M_j=0.128$ Kg	1.1790	1.8073	2.1902	0.4166	0.2649	10.32	12.94	10.05	8.14
(IX) ethyl pentyl ketone $M_j=0.128$ Kg	1.1820	1.7921	-27.0543	0.4274	0.3243	10.14	11.64	10.01	8.14
(X) heptyl methyl ketone $M_j=0.142$ Kg	1.1939	1.4569	-17.0797	0.4023	0.7757	9.93	7.15	9.60	8.2

$\mu_j^a$  = dipole moment from Eq.(7) by using  $\tau_j$  of Eq. (3)

$\mu_j^b$  = dipole moment from Eq. (7) by using  $\tau_j$  of Eq. (4)

$\mu_j^c$  = dipole moment by Gopalakrishna's method of Eq. (10)

$\mu_{theo}$  = theoretical dipole moment from the available bond angles and bond moments

polar groups causing inductive, mesomeric and electromeric effects in them, which play a role in the structure of the polar molecules of Fig. 6. The solvent  $C_6H_6$  due to its aromaticity is a cyclic planar compound having three alternate single and double bonds and six *p*-electrons on six C-atoms. The  $sp^2$  hybridised electrons provide de-localised  $\pi$ -electrons to each atom of the substituted polar groups of the molecules.  $CH_3^{\delta+} \rightarrow C^{\delta-}$  is a strong electron pushing (+I effect) while  $>C^{\delta+} \leftarrow O^{\delta-}$  is responsible for both the mesomeric (-M effect) and electromeric effect. Thus all the substituted polar groups may be responsible to form either solute-solvent (monomer) or solute-solute (dimer) association to yield lower and higher  $\mu_j$ 's respectively depending upon the solvent used. The difference  $\Delta\mu$  between  $\mu_j$ 's and  $\mu_{theo}$ 's of Fig. 6 for the methyl substituted benzenes are 5.92, 9.36, 8.74, 7.84, 5.28 and  $0.2 \times 10^{-30}$  C.m for the six systems while the rest of the four ketones have -3.63, 4.8, 3.5 and  $-1.05 \times 10^{-30}$  C.m respectively. This indicates the mesomeric and electromeric effects which are maximum for 1,3,5 trimethyl benzene and methyl hexyl ketone probably due to presence of strong electron repelling character of  $CH_3 \rightarrow C$  group. The  $\mu_{theo}$  of 1,3,5 tri methyl benzene, 1,2,3,4 tetra methyl benzene and 1,2,4,5 tetra methyl benzene are found to be zero. The bond moment of  $CH_3 \rightarrow C$  group acts in opposite direction in a plane to yield zero value. The molecules may have considerable  $\mu_{theo}$  values if they are three dimensional structures. All these effects may be taken into account to get exact  $\mu_j$ 's of Table 2 from  $\mu_{theo}$  by the factor  $\mu_{expt} / \mu_{theo}$  (5.81, 5.29, 1.03, 0.55, 1.59, 1.43, 0.87) except for three molecules.

#### 4 Conclusion

The structural information of some aromatic methyl benzenes and aliphatic ketones is obtained from the conductivity measurement at 25 °C under the most effective dispersive region of 9.585 GHz electric field. Modern internationally accepted symbols of dielectric relaxation terminologies and parameters in S I units seem to be more topical, significant and useful contribution to obtain  $\tau$  and  $\mu$  of a dipolar liquid dissolved in non-polar solvent. The  $\tau_j$ 's measured from the slope of the linear  $\sigma_{ij}'' - \sigma_{ij}'$  curves are not in agreement with those from the ratio of the individual slopes of  $\sigma_{ij}'' - w_j$  and  $\sigma_{ij}' - w_j$

in the limit  $w_j = 0$  for all cases. The latter method is more significant because in this case one polar molecule is surrounded by a large number of non-polar molecules and thus polar-polar interactions are supposed to be completely eliminated. This method is thus supposed to yield monomeric or often dimeric structure of polar molecules. The  $\mu_j$ 's are measured from the linear coefficient  $\beta$  of  $\sigma_{ij} - w_j$  curve at  $w_j \rightarrow 0$ . The  $\sigma_{ij}$  or  $\sigma_{ij}''$  in  $\Omega^{-1} m^{-1}$  for some systems increases gradually in order to attain the maximum value for a certain concentration of solute and then decreases. This indicates the change of phase of the systems under investigation. Similar nature of variation of  $\sigma_{ij}''$  with  $w_j$  indicates maximum absorption of hf electric energy for some systems. The  $\tau_j$ 's and  $\mu_j$ 's claimed to be accurate within 10 and 5 % are also compared with those from Gopalakrishna's fixed frequency method. The slight disagreement between experimental  $\mu_j$  with the theoretical dipole moment  $\mu_{theo}$  for some molecules reveals different associational aspects of dipolar liquid molecules in a non-polar solvent from the frequency dependence of relaxation parameters. This study also exhibits the presence of mesomeric, inductive and electromeric effects of the substituent polar groups of the molecules. The theoretical  $\mu_{theo}$  for systems II, III and IV are zero although they possess a considerable  $\mu_j$ . This invariably rules out the planar structure of the molecules and establish a three dimensional formation.

#### References

- 1 Paul N, Sharma K P & Chattopadhyay S, *Indian J Phys*, 71B (1997) 71.
- 2 Sen S N & Ghosh R, *J Phys Soc Jpn*, 33 (1972) 838.
- 3 Dutta K, Basak R C, Sit S K & Acharyya S, *J Molec Liq*, 88 (2000) 229.
- 4 Ghosh N, Sit S K, Bothra A K & Acharyya S, *J Phys D: Appl Phys*, 34 (2001) 379.
- 5 Migahed M D, Ahmed M T & Kotp A E, *J Phys D: Appl Phys*, 33 (2000) 2108.
- 6 Bello A, Laredo E, Grimau M, Nogales A & Ezquerra T A, *J Chem Phys*, 113 (2000) 863.
- 7 Vaish S K & Mehrotra N K, *Indian J Pure & Appl Phys*, 37 (1999) 881.
- 8 Vaish S K & Mehrotra N K, *Indian J Pure & Appl Phys*, 37 (1999) 778.
- 9 Bloembergen N, Purcel E M & Pound R V, *Phys Rev*, 73 (1948) 673.

- 10 Murthy M B R, Patil R L & Deshpande D K, *Indian J Phys*, 63B (1989) 491.
- 11 Basak R C, Sit S K, Nandi N & Acharyya S, *Indian J Phys*, 70B (1996) 37.
- 12 Dutta K, Sit S K & Acharyya S, *J Molec Liq*, 92 (2001) 263.
- 13 Murphy F J & Morgan S O, *Bell Syst Tech J*, 18 (1939) 502.
- 14 Hill N E, Vaughan W E, Price A H & Davies M, *Dielectric properties and molecular behaviour* (Van Nostrand Reinhold Co, London), 1969.
- 15 Sit S K, Basak R C, Saha U & Acharyya S, *J Phys D: Appl Phys*, 27 (1994) 2194.
- 16 Gopalakrishna K V, *Trans Faraday Soc*, 53 (1957) 767.
- 17 Sit S K & Acharyya S, *Indian J Phys*, 70B (1996) 19.

## Structural and associational aspects of dielectropolar straight chain alcohols from relaxation phenomena

N Ghosh, A Karmakar, S K Sit & S Acharyya

Department of Physics, Raiganj College (University College), PO Raiganj, Dist Uttar Dinajpur, 733 134 (West Bengal)

Received 15 November 1999; revised 27 March 2000; accepted 6 June 2000

The structural and associational aspects of some straight chain aliphatic alcohols are inferred from their static dipole moments  $\mu_s$ 's and high frequency (hf) dipole moments  $\mu_j$ 's in terms of relaxation times  $\tau_j$ 's under effective dispersive region of nearly 24 GHz electric field.  $\tau_j$ 's are estimated from the slope of the linear variation of imaginary part  $\sigma''_{ij}$  with real part  $\sigma'_{ij}$  of hf complex conductivity  $\sigma^*_{ij}$  for different weight fractions  $w_j$  in order to compare with those obtained from the ratio of the individual slopes of  $\sigma''_{ij}$  and  $\sigma'_{ij}$  with  $w_j$ 's of solutes. The linear coefficients of the static experimental parameter  $X_{ij}$  with  $w_j$  are used to obtain  $\mu_s$ . The slopes  $\beta$ 's of  $\sigma_{ij}$  with  $w_j$ 's are employed to get hf  $\mu_j$  in terms of  $\tau_j$ 's obtained by two methods only to see how far they agree with  $\mu_1$  and  $\mu_2$  from double relaxation method (Sit & Acharyya, 1996 and Sit *et al.* 1997). It is observed that -OH bond of alcohols about  $\equiv$  C-O- bond rotates under GHz electric field. The slight disagreement of theoretical dipole moments  $\mu_{\text{theo}}$ 's from available bond angles and bond moments with  $\mu_j$ 's and  $\mu_s$ 's suggest the strong hydrogen bonding in them, in addition to mesomeric and inductive moments of the substituent polar groups attached to the parent molecule.

### 1 Introduction

The relaxation phenomenon of a dielectropolar liquid in a solvent has attracted the attention of a large number of workers<sup>1-3</sup> as it is a very sensitive and useful tool to ascertain the shape, size and structure of a polar molecule. The technique provides one with much information about the stability<sup>4</sup> of the system undergoing relaxation phenomena. It also offers valuable insight into the solute-solute i.e. dimer and solute-solvent i.e. monomer formations<sup>4</sup>. Structural and associational aspects of a polar liquid in a nonpolar solvent can, however, be gained by measured static dipole moment  $\mu_s$  and high frequency (hf) dipole moment  $\mu_j$  in terms of relaxation time  $\tau_j$  and slope  $\beta$  of hf conductivity  $\sigma_{ij}$  with weight fraction  $w_j$ .

Alcohols behaving like almost polymers have  $\alpha$ ,  $\beta$  and  $\gamma$  etc. dispersion regions. The strong dipole of -OH group rotates about  $\equiv$  C-O- bond without disturbing  $\text{CH}_3$  or  $\text{CH}_2$  groups and thus they have possibility to exhibit intramolecular as well as intermolecular rotations. Sit and Acharyya<sup>5</sup> and Sit *et al.*<sup>6</sup> studied the straight long chain alcohols like 1-butanol, 1-hexanol, 1-heptanol, 1-decanol in *n*-heptane<sup>7</sup>, ethanol and methanol in benzene<sup>8</sup> (9.84GHz) and 2-methyl-3-heptanol, 3-methyl-3-heptanol, 4-methyl-3 heptanol, 5-methyl-3-heptanol, 4-octanol and 2-octanol, in *n*-heptane<sup>9</sup> at 25°C

to observe that all the alcohols except methanol showed the double relaxation times  $\tau_1$  and  $\tau_2$  at all the frequencies in GHz range. The alcohols were again expected to exhibit the triple relaxation phenomena<sup>7</sup> for different frequencies of electric field in GHz range. Such long chain liquids under investigation have wide applications in the fields of biological research, medicine and industry. Moreover, the study of alcohols in terms of modern internationally accepted units and symbols appears to be superior for the unified, coherent and rationalized nature of the SI unit used.

The  $\mu_s$  of all the associated dielectropolar molecules under static electric field was derived from static experimental parameter  $X_{ij}$ .  $X_{ij}$  is again involved with the dimensionless dielectric constants  $k_{0ij}$  and  $k_{\infty ij}$  of Table 1. from the measured relaxation permittivities static  $\epsilon_{0ij}$  and hf  $\epsilon_{\infty ij}$  of dimensions Farad metre<sup>-1</sup> (F.m.<sup>-1</sup>) based on Debye model<sup>10</sup>. The linear coefficients of the expected nonlinear experimental  $X_{ij}$  curves against  $w_j$  graphically shown in Fig. 1, of alcohols were conveniently used to estimate  $\mu_s$  at a given temperature.

The  $\tau_j$  of all the alcohols were, however, estimated from the slope of linear variation of imaginary  $\sigma''_{ij}$  against real  $\sigma'_{ij}$  parts<sup>11</sup> of hf complex conductivity  $\sigma^*_{ij}$  for different  $w_j$ 's as seen in Fig. 2. The hf  $\sigma''_{ij}$  did not vary linearly with hf  $\sigma'_{ij}$  at higher or even lower concen-

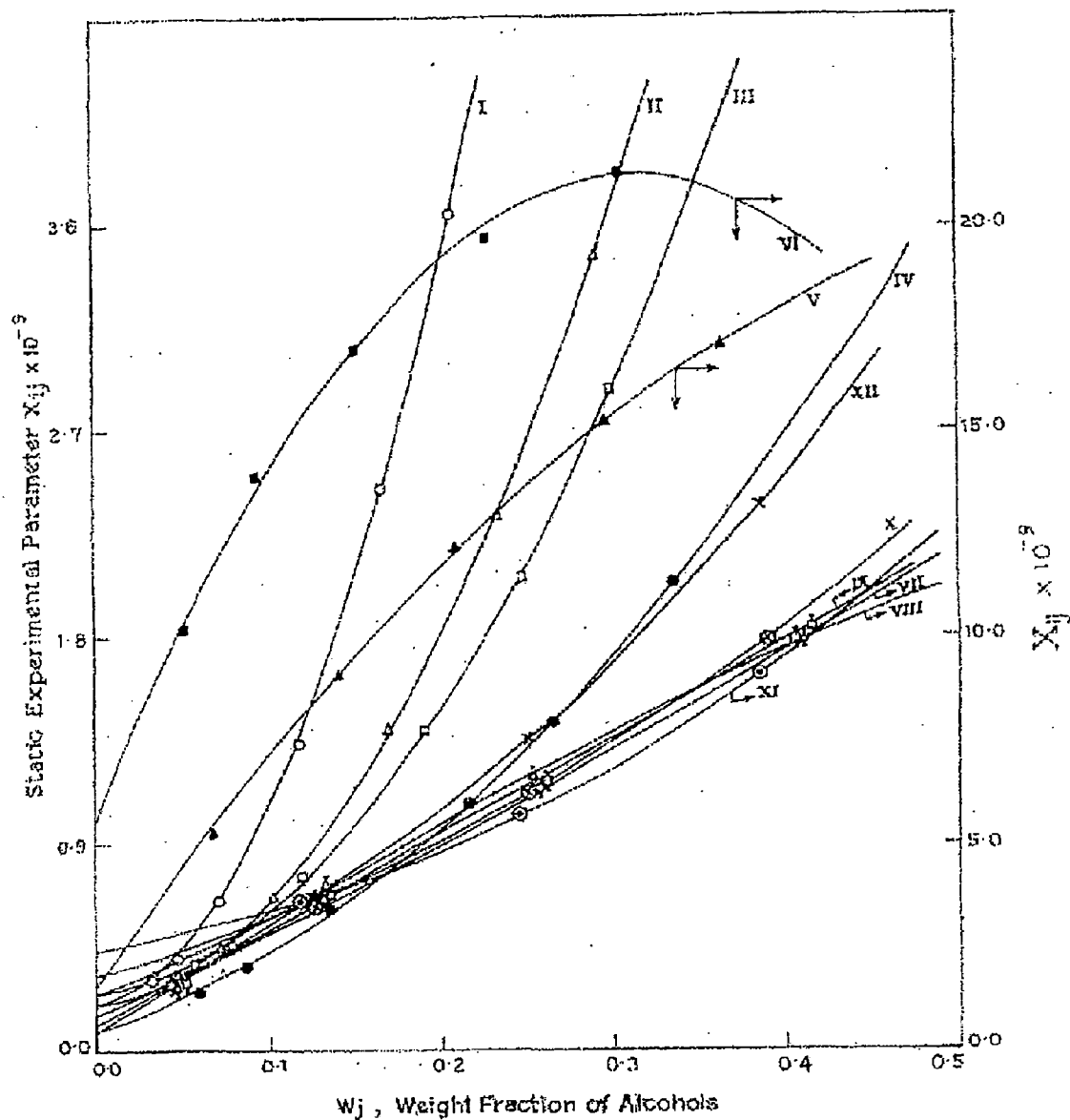


Fig. 1 — Variation of static experimental parameter ( $X_{ij} \times 10^{-9}$ ) against weight fraction  $w_j$  of solute at 25°C under nearly 24 GHz electric field [ethanol and methanol at 9.84 GHz]

System - I 1-butanol (—O—O—);

System - II 1-hexanol (—Δ—Δ—);

System - III 1-heptanol (—□—□—);

System - IV 1-decanol (—●—●—);

System - V ethanol (—▲—▲—);

System - VI methanol (—■—■—);

System - VII 2-methyl - 3 heptanol (—Φ—Φ—);

System - VIII 3-methyl - 3 heptanol (—I—I—);

System - IX 4-methyl - 3 heptanol (—J—J—);

System - X 5-methyl - 3 heptanol (—⊗—⊗—);

System - XI 4-Octanol (—⊙—⊙—);

System - XII 2-Octanol (—x—x—)

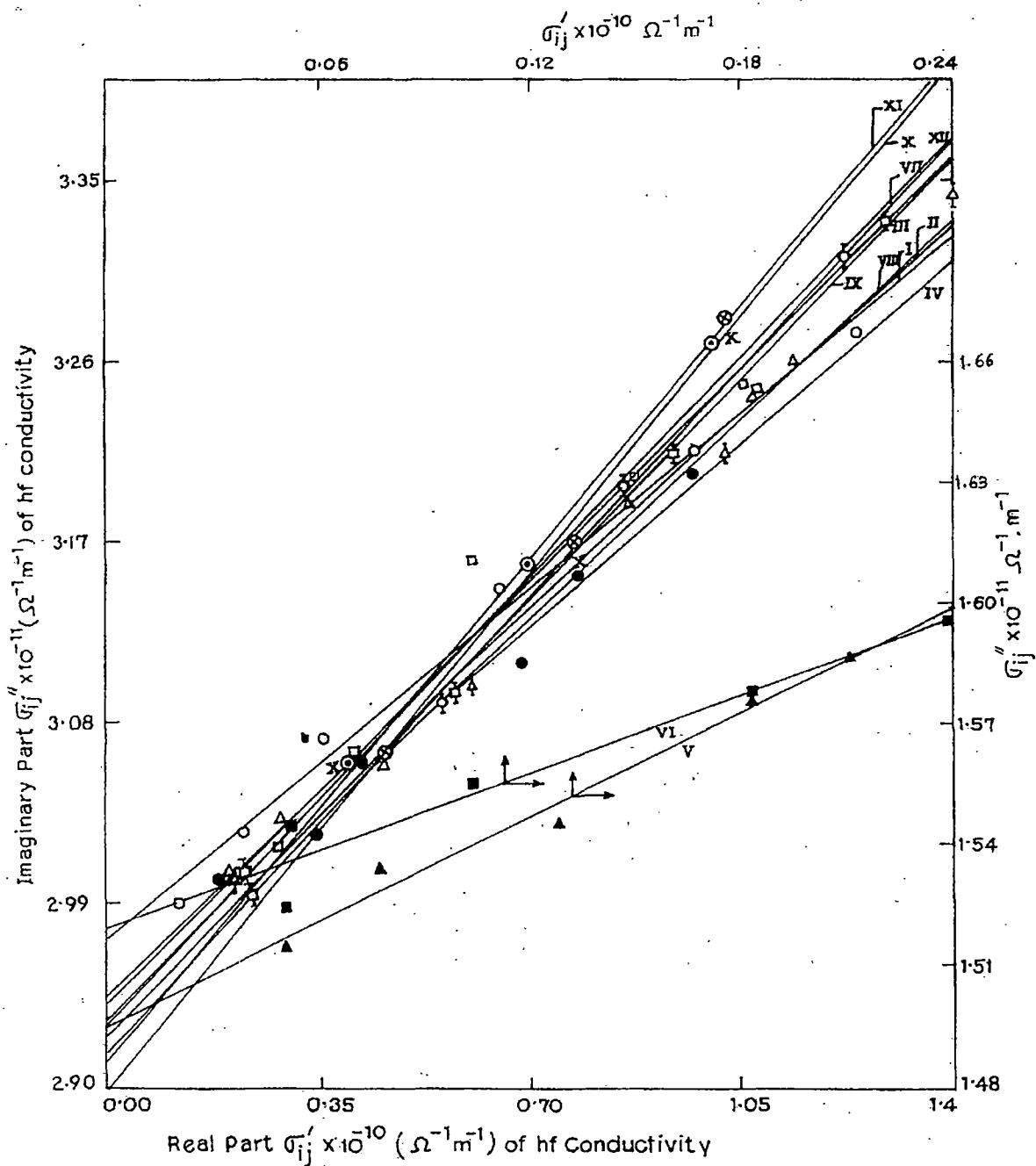


Fig. 2 — Variation of imaginary part of conductivity  $\sigma''_{ij} \times 10^{-11}$  in  $\Omega^{-1} m^{-1}$  against real part of conductivity  $\sigma'_{ij} \times 10^{-10}$  in  $\Omega^{-1} m^{-1}$

- |   |  |
|---|--|
| System - I 1-butanol (— O — O —);                             | System - VII 2-methyl - 3 heptanol (— $\Phi$ — $\Phi$ —);        |
| System - II 1-hexanol (— $\Delta$ — $\Delta$ —);              | System - VIII 3-methyl - 3 heptanol (— $\Lambda$ — $\Lambda$ —); |
| System - III 1-heptanol (— $\square$ — $\square$ —);          | System - IX 4-methyl - 3 heptanol (— $\Gamma$ — $\Gamma$ —);     |
| System - IV 1-decanol (— $\bullet$ — $\bullet$ —);            | System - X 5-methyl - 3 heptanol (— $\otimes$ — $\otimes$ —);    |
| System - V ethanol (— $\blacktriangle$ — $\blacktriangle$ —); | System - XI 4-Octanol (— $\ominus$ — $\ominus$ —);               |
| System - VI methanol (— $\blacksquare$ — $\blacksquare$ —);   | System - XII 2-Octanol (— x — x —)                               |

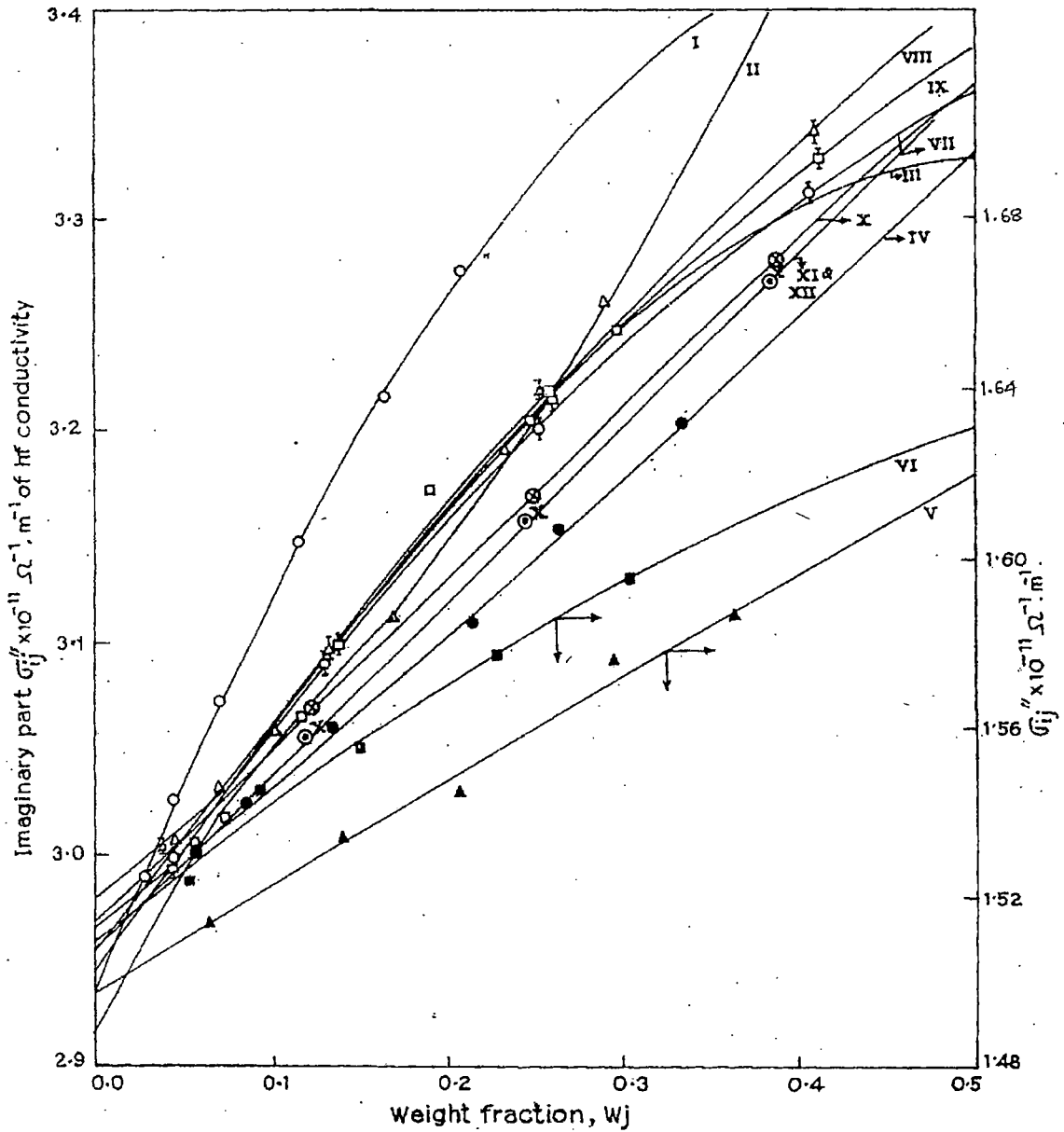


Fig. 3 — Plot of imaginary part of conductivity  $\sigma''_{ij} \times 10^{-11}$  in  $\Omega^{-1} m^{-1}$  against weight fraction  $w_j$  of solute at 25°C under nearly 24 GHz electric field. [ethanol and methanol at 9.84 GHz.]

System - I 1-butanol (—O—O—);

System - II 1-hexanol (—Δ—Δ—);

System - III 1-heptanol (—□—□—);

System - IV 1-decanol (—●—●—);

System - V ethanol (—▲—▲—);

System - VI methanol (—■—■—);

System - VII 2-methyl - 3 heptanol (—Φ—Φ—);

System - VIII 3-methyl - 3 heptanol (—I—I—);

System - IX 4-methyl - 3 heptanol (—H—H—);

System - X 5-methyl - 3 heptanol (—⊗—⊗—);

System - XI 4-Octanol (—⊖—⊖—);

System - XII 2-Octanol (—x—x—)

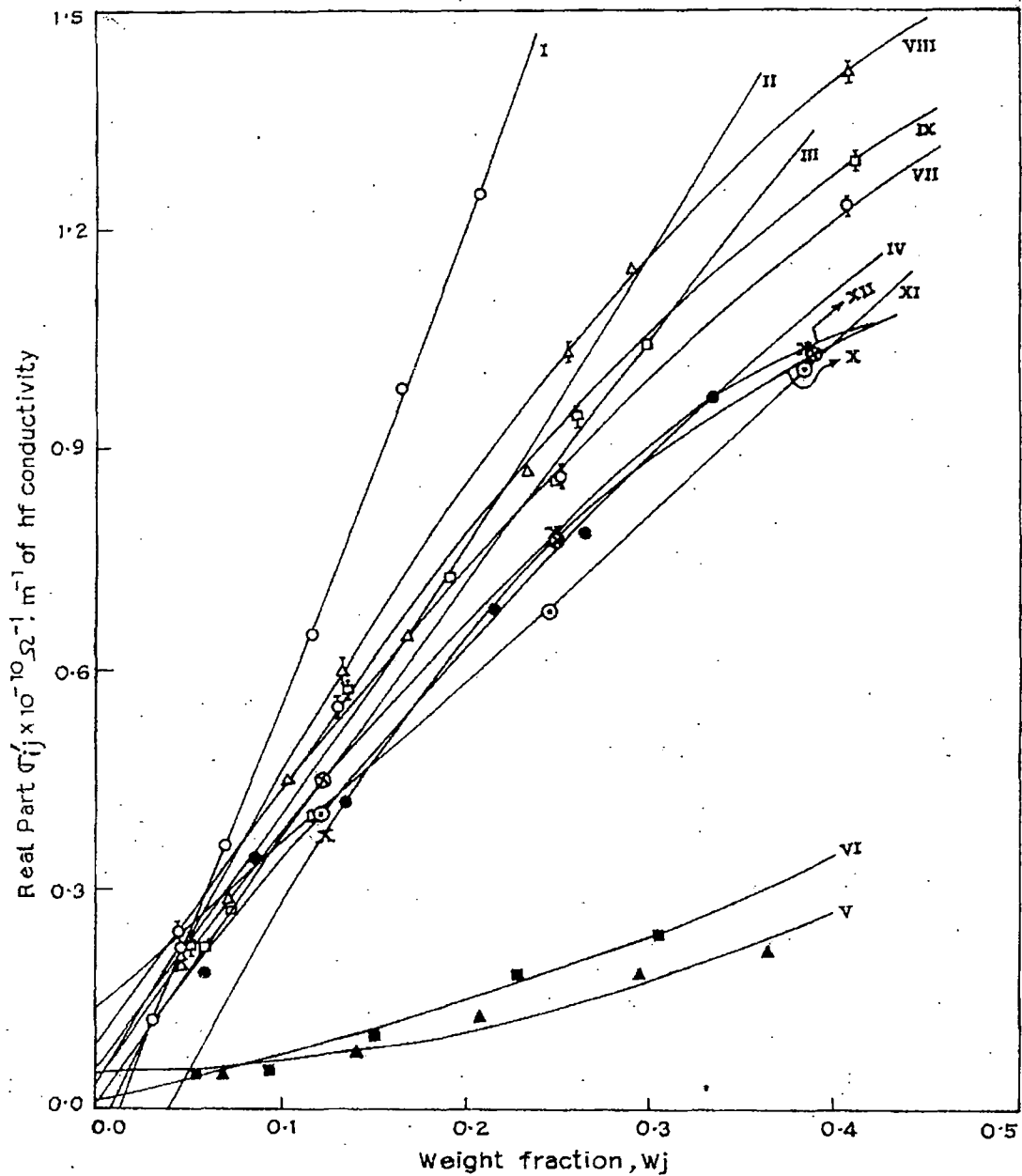


Fig. 4 — Plot of real part of conductivity  $\sigma'_{ij} \times 10^{10}$  in  $\Omega^{-1} \text{ m}^{-1}$  against weight fraction  $w_j$  of solute at  $25^\circ\text{C}$  under nearly 24 GHz electric field [ethanol and methanol at 9.84 GHz]

System - I 1-butanol (—○—○—);

System - II 1-hexanol (—△—△—);

System - III 1-heptanol (—□—□—);

System - IV 1-decanol (—●—●—);

System - V ethanol (—▲—▲—);

System - VI methanol (—■—■—);

System - VII 2-methyl - 3 heptanol (—⊖—⊖—);

System - VIII 3-methyl - 3 heptanol (—⊖—⊖—);

System - IX 4-methyl - 3 heptanol (—⊖—⊖—);

System - X 5-methyl - 3 heptanol (—⊖—⊖—);

System - XI 4-Octanol (—⊖—⊖—);

System - XII 2-Octanol (—x—x—)

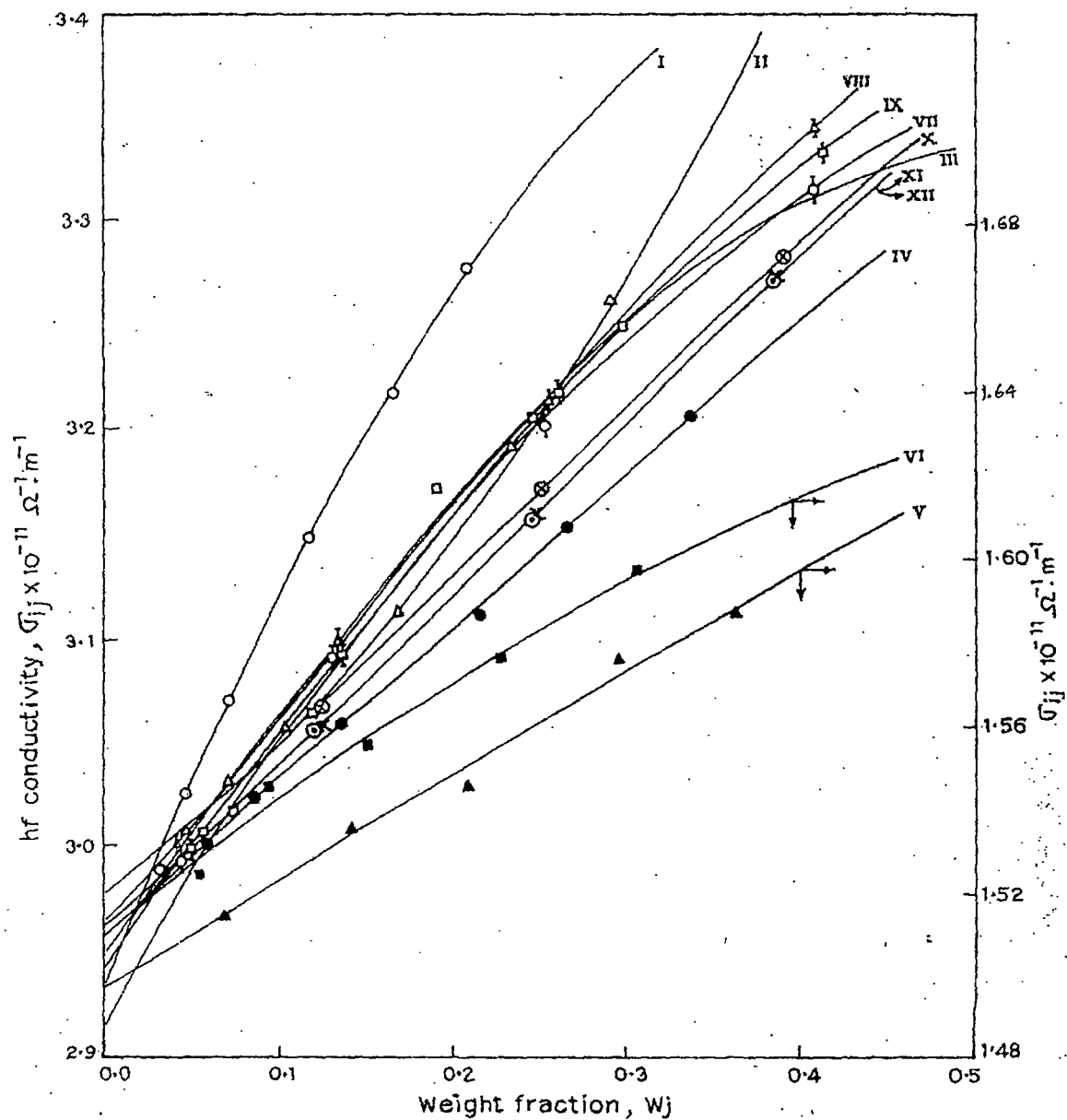


Fig. 5 — Variation of total hf conductivity  $\sigma_{ij} \times 10^{-11}$  in  $\Omega^{-1} \text{m}^{-1}$  against weight fraction  $w_j$  of solute at 25°C under nearly 24 GHz electric field [ethanol and methanol at 9.84 GHz]

System - I 1-butanol (—O—O—);

System - II 1-hexanol (— $\Delta$ — $\Delta$ —);

System - III 1-heptanol (— $\square$ — $\square$ —);

System - IV 1-decanol (— $\bullet$ — $\bullet$ —);

System - V ethanol (— $\blacktriangle$ — $\blacktriangle$ —);

System - VI methanol (— $\blacksquare$ — $\blacksquare$ —);

System - VII 2-methyl - 3 heptanol (— $\Phi$ — $\Phi$ —);

System - VIII 3-methyl - 3 heptanol (— $\text{A}$ — $\text{A}$ —);

System - IX 4-methyl - 3 heptanol (— $\text{I}$ — $\text{I}$ —);

System - X 5-methyl - 3 heptanol (— $\otimes$ — $\otimes$ —);

System - XI 4-Octanol (— $\ominus$ — $\ominus$ —);

System - XII 2-Octanol (—x—x—)

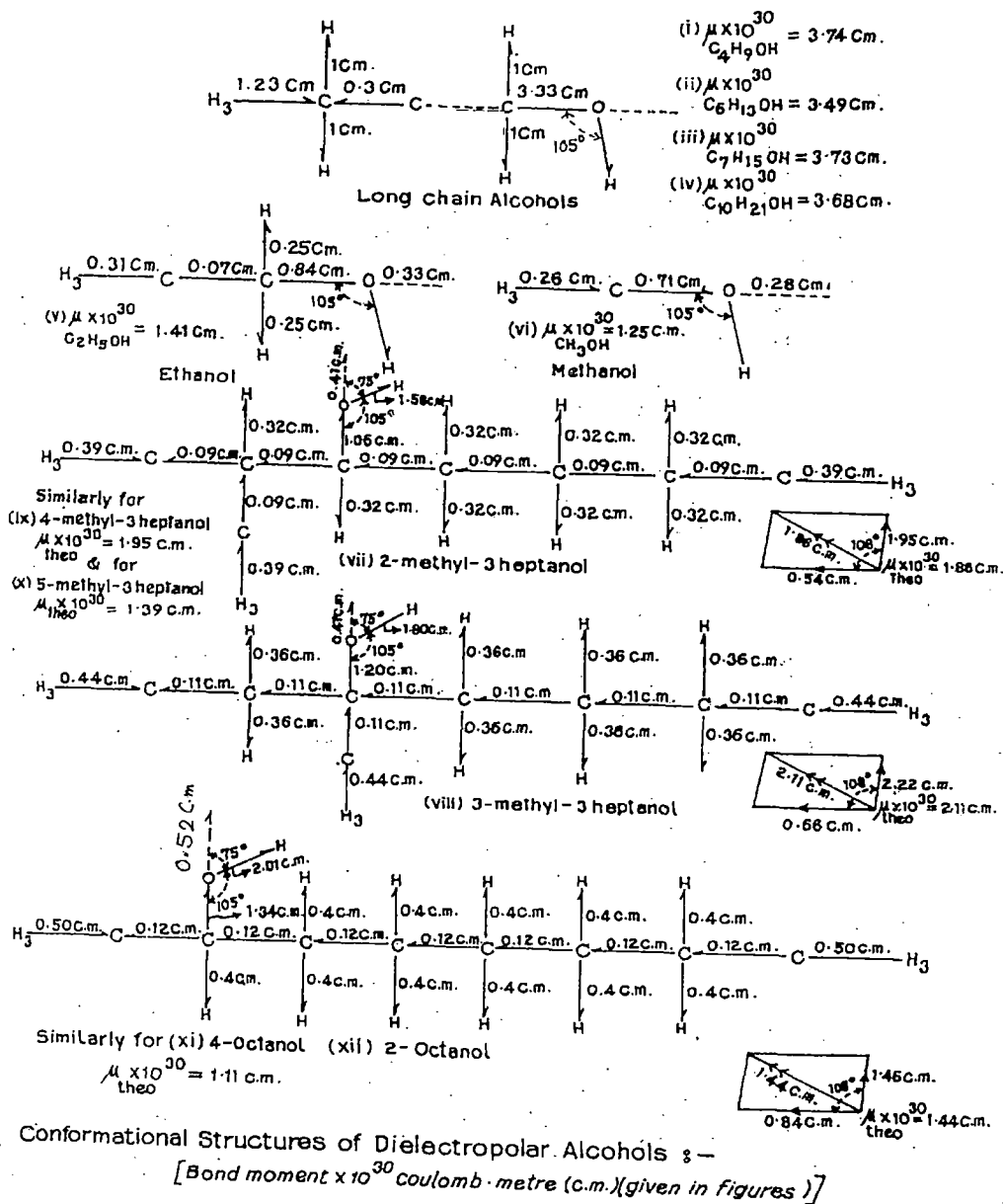


Fig. 6 — Conformational structures of dielectropolar alcohols (theoretical dipole moments  $\mu_{\text{theo}}$  from bond angles and reduced bond moments)

trations<sup>12</sup>. It is therefore, better to use the ratio of slopes of individual variations of  $\sigma''_{ij}$  and  $\sigma'_{ij}$  both in  $\Omega^{-1} \text{ m}^{-1}$  with  $w_j$ 's of Figs 3 and 4 to get the exact and accurate value of  $d\sigma''_{ij}/d\sigma'_{ij}$  in the limit  $w_j = 0$  to evaluate  $\tau_j$ <sup>13,14</sup>.  $\tau_j$ 's thus obtained by both the methods are placed in Table 3 to see how far they are close in agreements.  $\tau_j$ 's of such dielectropolar molecules were, however, estimated at 1.233 cm for molecules like 1-butanol, 1-hexanol, 1-decanol, 2-methyl 3-heptanol, 3-methyl 3-

heptanol, 4-methyl-3-heptanol, 5-methyl 3-heptanol, 4-octanol, 2-octanol and at 1.249 cm wavelength electric field for 1- heptanol at which measured  $\epsilon''_{ij}$  of a given  $w_j$  of the solute when were graphically plotted against the electric field frequency "f" showed peak indicating the most effective dispersive region for such liquids.

The formulation to measure  $\mu_j$ 's of all the alcohols involves with the slopes  $\beta$ 's of the expected  $\sigma_{ij}-w_j$  nonlinear curves of Fig. 5 and dimensionless parameter

Table I — Measured dielectric permittivities  $\epsilon'_{ij}$ ,  $\epsilon''_{ij}$ ,  $\epsilon_{0ij}$ ,  $\epsilon_{\infty ij}$  in farad metre<sup>-1</sup> and dimensionless dielectric constants  $k'_{ij}$ ,  $k''_{ij}$ ,  $k_{0ij}$ ,  $k_{\infty ij}$  of some dielectropolar alcohols at 25°C of different weight fractions  $w_j$ 

Systems with molecular weight $M_j$ in kg	Weight Fraction $w_j$	$\epsilon'_{ij}$ in F.m <sup>-1</sup>	$\epsilon''_{ij}$ in F.m <sup>-1</sup>	$\epsilon_{0ij}$ in F.m <sup>-1</sup>	$\epsilon_{\infty ij}$ in F.m <sup>-1</sup>	Dimensionless dielectric constants			
						$k'_{ij} \times 10^{-11}$	$k''_{ij} \times 10^{-9}$	$k_{0ij} \times 10^{-11}$	$k_{\infty ij} \times 10^{-11}$
(i) 1-butanol $M_j = 0.074$	0.0291	1.957	0.0079	1.971	1.928	2.2103	0.8922	2.2261	2.1775
	0.0451	1.981	0.0147	2.000	1.945	2.2374	1.6603	2.2589	2.1967
	0.0697	2.011	0.0236	2.050	1.958	2.2713	2.6655	2.3153	2.2114
	0.1163	2.060	0.0425	2.175	1.978	2.3266	4.8001	2.4565	2.2340
	0.1652	2.105	0.0644	2.381	2.000	2.3774	7.2735	2.6892	2.2589
	0.2072	2.144	0.0818	2.621	2.020	2.4215	9.2388	2.9602	2.2814
(ii) 1-hexanol $M_j = 0.102$	0.0458	1.968	0.0131	1.988	1.944	2.2227	1.4795	2.2453	2.1956
	0.0703	1.984	0.0190	2.015	1.952	2.2408	2.1459	2.2758	2.2046
	0.1028	2.001	0.0296	2.064	1.970	2.2600	3.3431	2.3311	2.2250
	0.1687	2.037	0.0425	2.196	1.989	2.3006	4.8001	2.4802	2.2464
	0.2335	2.088	0.0569	2.360	2.002	2.3582	6.4265	2.6655	2.2611
(iii) 1-heptanol $M_j = 0.116$	0.0564	1.968	0.0147	1.985	1.932	2.2227	1.6603	2.2419	2.1821
	0.0735	1.975	0.0182	2.008	1.945	2.2306	2.0556	2.2679	2.1967
	0.1175	2.007	0.0265	2.066	1.957	2.2668	2.9930	2.3334	2.2103
	0.1909	2.076	0.0482	2.195	1.989	2.3447	5.4439	2.4791	2.2464
	0.2465	2.097	0.0567	2.315	2.002	2.3684	6.4039	2.6146	2.2611
(iv) 1-decanol $M_j = 0.158$	0.0572	1.965	0.0120	1.976	1.940	2.2193	1.3553	2.2317	2.1911
	0.0857	1.979	0.0223	2.003	1.952	2.2351	2.5186	2.2622	2.2046
	0.1351	2.003	0.0273	2.050	1.964	2.2622	3.0833	2.3153	2.2182
	0.2140	2.036	0.0449	2.147	1.990	2.2995	5.0711	2.4249	2.2476
	0.2640	2.064	0.0513	2.220	2.008	2.3311	5.7940	2.5073	2.2679
(v) ethanol $M_j = 0.046$	0.3353	2.097	0.0637	2.346	2.030	2.3684	7.1945	2.6496	2.2927
	0.0664	2.450	0.0082	3.300	2.262	2.7671	0.9223	3.7271	2.5548
	0.1393	2.483	0.0124	4.300	2.190	2.8047	1.4023	4.8566	2.4734
	0.2077	2.500	0.0208	5.400	2.120	2.8236	2.3529	6.0989	2.3944
(vi) methanol $M_j = 0.032$	0.2953	2.550	0.0297	7.000	2.062	2.8800	3.3600	7.9060	2.3289
	0.3638	2.567	0.0342	8.200	2.016	2.8988	3.8641	9.2613	2.2769
	0.0514	2.467	0.0082	4.800	2.214	2.7858	0.9284	5.4213	2.5006
	0.0930	2.500	0.0083	6.500	2.155	2.8236	0.9408	7.3413	2.4339
(vii) 2-methyl 3-heptanol $M_j = 0.130$	0.1495	2.517	0.0168	8.600	2.085	2.8423	1.8940	9.7131	2.3549
	0.2266	2.550	0.0298	11.400	2.016	2.8800	3.3601	12.8755	2.2769
	0.3049	2.583	0.0387	13.700	1.960	2.9177	4.3765	15.4732	2.2137
	0.0437	1.960	0.0156	1.971	1.930	2.2137	1.7619	2.2261	2.1798
(viii) 3-methyl 3-heptanol $M_j = 0.130$	0.1299	2.022	0.0361	2.059	1.966	2.2847	4.0772	2.3255	2.2205
	0.2522	2.095	0.0565	2.172	2.007	2.3661	6.3813	2.4531	2.2667
	0.4081	2.169	0.0809	2.330	2.054	2.4497	9.1371	2.6316	2.3198
(ix) 4-methyl 3-heptanol $M_j = 0.130$	0.0450	1.965	0.0137	1.974	1.934	2.2193	1.5473	2.2295	2.1843
	0.1334	2.028	0.0393	2.069	1.966	2.2905	4.4387	2.3368	2.2205
	0.2538	2.103	0.0674	2.180	2.004	2.3752	7.6124	2.4622	2.2634
(x) 5-methyl 3-heptanol $M_j = 0.130$	0.4085	2.188	0.0928	2.334	2.057	2.4712	10.4811	2.6361	2.3232
	0.0466	1.964	0.0146	1.976	1.936	2.2182	1.6490	2.2317	2.1866
	0.1326	2.025	0.0375	2.065	1.969	2.2871	4.2354	2.3323	2.2238
(xi) 4-octanol $M_j = 0.130$	0.2590	2.104	0.0616	2.185	2.011	2.3763	6.9573	2.4678	2.2713
	0.4124	2.180	0.0849	2.352	2.065	2.4622	9.5889	2.6564	2.3323
	0.1228	2.008	0.0296	2.048	1.956	2.2679	3.3431	2.3131	2.2092
(xii) 2-octanol $M_j = 0.130$	0.2489	2.075	0.0511	2.168	2.004	2.3436	5.7714	2.4486	2.3634
	0.3898	2.148	0.0676	2.315	2.040	2.4260	7.6350	2.6146	2.3040
	0.1201	2.000	0.0265	2.040	1.948	2.2589	2.9930	2.3040	2.2001
(xiii) 3-heptanol $M_j = 0.130$	0.2445	2.067	0.0449	2.148	1.997	2.3345	5.0711	2.4260	2.2555
	0.3838	2.140	0.0659	2.282	2.031	2.4170	7.4430	2.5764	2.2939
	0.1236	2.001	0.0245	2.049	1.954	2.2600	2.7671	2.3142	2.2069
(xiv) 2-octanol $M_j = 0.130$	0.2479	2.068	0.0513	2.195	1.996	2.3357	5.7940	2.4791	2.2543
	0.3844	2.141	0.0680	2.410	2.036	2.4181	7.6801	2.7219	2.2995

Table 2 — Coefficients  $a_0$ ,  $a_1$  and  $a_2$  of static experimental parameter  $X_{ij} = a_0 + a_1 w_j + a_2 w_j^2$  correlation coefficients ( $r$ ), % of errors in getting  $X_{ij}$ , static or low frequency dipole-moments  $\mu_s \times 10^{30}$  in Coulomb-metre, theoretical dipole-moments  $\mu_{\text{theo}} \times 10^{30}$  in Coulomb-metre from reduced bond moments by  $\mu_s/\mu_{\text{theo}}$  and  $\mu_1, \mu_2$  by double relaxation method

Systems with sl. no. & molecular weight $M_j$	Coefficients $a_0, a_1$ and $a_2$ in Eq. $X_{ij} \times 10^{-9} = a_0 + a_1 w_j + a_2 w_j^2$			Correlation coefficient ( $r$ )	% of error in fitting technique	$\mu_s \times 10^{30}$ in Coulomb-metre from Eq. (5)	Corrected $\mu_{\text{theo}} \times 10^{30}$ in Coulomb metre from bond angle & reduced bond moments	$\mu_1$ and $\mu_2$ in Coulomb metre from double relaxation method	
	$a_0$	$a_1$	$a_2$					$\mu_1 \times 10^{30}$ in Coulomb metre	$\mu_2 \times 10^{30}$ in Coulomb metre
(i) 1-butanol in <i>n</i> -heptane $M_j = 0.074$ kg	0.2047	1.0852	75.2840	0.9824	0.96	3.74	$4.97 \times 0.7525 = 3.74$	3.63	29.17
(ii) 1-hexanol in <i>n</i> -heptane $M_j = 0.102$ kg	0.1951	1.0710	34.8550	0.9896	0.57	3.49	$4.37 \times 0.7986 = 3.49$	3.43	21.20
(iii) 1-heptanol in <i>n</i> -heptane $M_j = 0.116$ kg	0.2553	0.8932	26.4890	0.9867	0.73	3.73	$4.07 \times 0.9165 = 3.73$	3.73	27.00
(iv) 1-decanol in <i>n</i> -heptane $M_j = 0.158$ kg.	0.0901	2.3826	10.1760	0.9924	0.42	3.68	$3.17 \times 1.1609 = 3.68$	3.83	17.24
(v) ethanol in benzene $M_j = 0.046$ kg	1.6141	59.1892	-44.9614	0.9919	0.49	1.41	$5.57 \times 0.2531 = 1.41$	1.70	490.73
(vi) methanol in benzene $M_j = 0.032$ kg.	5.6331	99.8090	-159.9120	0.9672	1.94	1.25	$5.87 \times 0.2129 = 1.25$	—	293.96
(vii) 2-methyl 3-heptanol in <i>n</i> -heptane $M_j = 0.130$ kg.	0.1372	3.7778	0.5639	0.9997	0.02	1.86	$5.87 \times 0.3168 = 1.86$	3.83	16.00
(viii) 3-methyl 3-heptanol in <i>n</i> -heptane $M_j = 0.130$ kg.	0.0830	4.8577	-1.7495	0.9986	0.09	2.11	$5.87 \times 0.3594 = 2.11$	3.83	8.60
(ix) 4-methyl 3-heptanol in <i>n</i> -heptane $M_j = 0.130$ kg.	0.1032	4.1481	0.0885	0.9998	0.01	1.95	$5.87 \times 0.3322 = 1.95$	3.90	13.90
(x) 5-methyl 3-heptanol in <i>n</i> -heptane $M_j = 0.130$ kg.	0.3270	2.1113	4.1567	0.9972	0.22	1.39	$5.87 \times 0.2368 = 1.39$	3.37	9.50
(xi) 4-octanol in <i>n</i> -heptane $M_j = 0.130$ kg.	0.4402	1.1341	5.2073	0.9946	0.42	1.11	$3.60 \times 0.3083 = 1.11$	3.43	10.97
(xii) 2-octanol in <i>n</i> -heptane $M_j = 0.130$ kg.	0.2591	2.2977	8.3285	0.9955	0.35	1.45	$3.60 \times 0.4028 = 1.45$	3.43	16.00

Table 3 — Intercept ( $c$ ) and slope ( $m$ ) of  $\sigma''_{ij} - \sigma'_{ij}$  equation (Fig. 2), correlation coefficient ( $r$ ), percentage of error (%), relaxation time  $\tau_j$  in psec Eq. (10), ratio of slopes of  $\sigma''_{ij}$  and  $\sigma'_{ij}$  with  $w_j (= x/y)$ , relaxation time  $\tau_j$  in psec from (Eq. 11), calculated relaxation time  $\tau_j$  in psec from Gopalakrishana's method for some dielectropolar alcohols under nearly 24 GHz electric field (Q-Band Microwave) at 25 °C

System with sl. no. and molecular weight	Intercept & slope of $\sigma''_{ij} - \sigma'_{ij}$ fitted Equation $c \times 10^{-11}$ m		Correlation coefficient ( $r$ )	% of error	Estimated relaxation time $\tau_j$ in psec from Eq. (10)	Ratio of the slopes of $\sigma''_{ij}$ & $\sigma'_{ij}$ with $w_j$ $x/y = (d \sigma''_{ij} / dw_j) / (d \sigma'_{ij} / dw_j)$	Estimated relaxation time $\tau_j$ in psec from Eq (11)	Relaxation time $\tau_j$ in psec estimated from Gopalakrishna's method
(i) 1-butanol in <i>n</i> -heptane $M_j = 0.074$ kg.	2.9731	2.4816	0.9959	0.22	2.64	$\frac{2.0789 \times 10^{11}}{5.7404 \times 10^{10}} = 3.6215$	1.81	2.47
(ii) 1-hexanol in <i>n</i> -heptane $M_j = 0.102$ kg.	2.9457	2.7315	0.9959	0.22	2.40	$\frac{5.8541 \times 10^{10}}{3.2779 \times 10^{10}} = 1.7859$	3.66	2.25
(iii) 1-heptanol in <i>n</i> -heptane $M_j = 0.116$ kg.	2.9414	2.9898	0.9973	0.15	2.19	$\frac{1.5295 \times 10^{11}}{3.8161 \times 10^{10}} = 4.0080$	1.65	2.07
(iv) 1-decanol in <i>n</i> -heptane $M_j = 0.158$ kg.	2.9465	2.5881	0.9925	0.41	2.53	$\frac{6.8315 \times 10^{10}}{3.3881 \times 10^{10}} = 2.0163$	3.24	2.39
(v) ethanol in benzene $M_j = 0.046$ kg.	1.4952	4.2872	0.9880	0.72	3.77	$\frac{2.5827 \times 10^{10}}{5.6872 \times 10^9} = 4.5412$	3.56	3.62
(vi) methanol in benzene $M_j = 0.032$ kg.	1.5188	3.2088	0.9633	2.17	5.04	$\frac{3.4467 \times 10^{10}}{5.1439 \times 10^9} = 6.7005$	2.41	4.87
(vii) 2-methyl 3-heptanol in <i>n</i> -heptane $M_j = 0.130$ kg.	2.9162	3.2340	0.9994	0.04	2.02	$\frac{1.2112 \times 10^{11}}{3.6429 \times 10^{10}} = 3.3248$	1.97	1.86
(viii) 3-methyl 3-heptanol in <i>n</i> -heptane $M_j = 0.130$ kg.	2.9361	2.8021	0.9976	0.16	2.33	$\frac{1.1146 \times 10^{11}}{5.1067 \times 10^{10}} = 2.1826$	3.00	2.26
(ix) 4-methyl 3-heptanol in <i>n</i> -heptane $M_j = 0.130$ kg.	2.9254	3.0946	0.9988	0.08	2.11	$\frac{1.2125 \times 10^{11}}{4.3826 \times 10^{10}} = 2.7666$	2.36	1.95
(x) 5-methyl 3-heptanol in <i>n</i> -heptane $M_j = 0.130$ kg.	2.8973	3.6562	0.9949	0.40	1.79	$\frac{8.3993 \times 10^{10}}{3.7395 \times 10^{10}} = 2.2461$	2.91	1.63
(xi) 4-octanol in <i>n</i> -heptane $M_j = 0.130$ kg.	2.9129	3.5515	0.9999	0.01	1.84	$\frac{8.5252 \times 10^{10}}{2.1993 \times 10^{10}} = 3.8763$	1.69	1.68
(xii) 2-octanol in <i>n</i> -heptane $M_j = 0.130$ kg.	2.9320	3.1511	0.9875	0.97	2.08	$\frac{8.3278 \times 10^{10}}{5.3226 \times 10^{10}} = 1.5646$	4.18	1.93

Table 4 — Coefficients  $\alpha$ ,  $\beta$ ,  $\gamma$  of hf  $\sigma_{ij}$  against  $w_j$  curves (Fig. 5) correlation coefficients ( $r$ ) percentage of error, dimensionless parameter  $b$  using  $\tau_j$  from Eq. (10) and (11), computed  $\mu_j \times 10^{30}$  in Coulomb metre from Eqs (10) and (16) and Eqs (11) and (16) estimated  $\mu_j \times 10^{30}$  in Coulomb metre from Gopalakrishna's method for some dielectropolar alcohols under nearly 24 GHz electric field (Q-Band micro wave) at 25 ° C

System with sl. no. & molecular weight	Coefficients of $\sigma_{ij}-w_j$ fitted Equation			Correlation coefficient ( $r$ )	% of error	Dimensionless parameter using $\tau_j$ from Eq. (10) $b = 1/(1 + \omega^2 \tau_j^2)$	Dimensionless parameter using $\tau_j$ from Eq. (11) $b = 1/(1 + \omega^2 \tau_j^2)$	Computed $\mu_j \times 10^{30}$ in Coulomb metre		Estimated $\mu_j \times 10^{30}$ in Coulomb metre from Gopalakrishna's method
	$\alpha \times 10^{-11}$	$\beta \times 10^{-11}$	$\gamma \times 10^{-11}$					hf method of Eqs (10) & (16)	hf method of Eqs (11) & (16)	
(i) 1-butanol in <i>n</i> -heptane $M_j = 0.074$ kg.	2.9351	2.0769	-2.0776	0.9978	0.12	0.8601	0.9289	4.28	4.11	3.58
(ii) 1-hexanol in <i>n</i> -heptane $M_j = 0.102$ kg.	2.9807	0.5846	1.3346	0.9961	0.21	0.8815	0.7618	2.63	2.83	3.35
(iii) 1-heptanol in <i>n</i> -heptane $M_j = 0.116$ kg.	2.9173	1.5312	-1.3817	0.9928	0.39	0.9016	0.9417	4.52	4.42	3.59
(iv) 1-decanol in <i>n</i> -heptane $M_j = 0.158$ kg.	2.9639	0.6848	0.1087	0.9995	0.03	0.8699	0.8032	3.57	3.71	3.55
(v) ethanol in benzene $M_j = 0.046$ kg.	1.4970	0.2584	-0.0233	0.9927	0.44	0.9485	0.9538	1.44	1.43	1.33
(vi) methanol in benzene $M_j = 0.032$ kg.	1.5098	0.3444	-0.2046	0.9928	0.43	0.9116	0.9783	1.41	1.36	1.18
(vii) 2-methyl 3-heptanol in <i>n</i> -heptane $M_j = 0.130$ kg.	2.9437	1.2203	-0.7548	0.9958	0.28	0.9130	0.9169	4.22	4.21	3.42
(viii) 3-methyl 3-heptanol in <i>n</i> -heptane $M_j = 0.130$ kg.	2.9515	1.1644	-0.4868	0.9985	0.10	0.8875	0.8264	4.18	4.33	3.54
(ix) 4-methyl 3-heptanol in <i>n</i> -heptane $M_j = 0.130$ kg.	2.9454	1.2172	-0.6697	0.9970	0.02	0.9058	0.8849	4.23	4.28	3.48
(x) 5-methyl 3-heptanol in <i>n</i> -heptane $M_j = 0.130$ kg.	2.9658	0.8446	-0.0754	0.9999	0.01	0.9304	0.8349	3.47	3.67	3.24
(xi) 4-octanol in <i>n</i> -heptane $M_j = 0.130$ kg.	2.9546	0.8544	-0.0762	0.9999	0.01	0.9267	0.9375	3.56	3.48	3.27
(xii) 2-octanol in <i>n</i> -heptane $M_j = 0.130$ kg.	2.9542	0.8399	-0.0280	0.9999	0.01	0.9083	0.7103	3.51	3.97	3.32

$b$  in terms of  $\tau_j$ 's obtained by both the methods as  $\tau_j$ 's were not found to agree excellently in Table 3. The  $\sigma''_{ij}$  and  $\sigma'_{ij}$  in  $\Omega^{-1} \text{ m}^{-1}$  are not linear with  $w_j$  as evident from Figs 3 and 4.  $\mu_j$ 's thus obtained are finally compared with  $\mu_{\text{theo}}$ 's from available bond angles and bond moments of the substituent polar groups attached to parent ones. The slight disagreement between the measured  $\mu_j$ 's and  $\mu_s$ 's from  $\mu_{\text{theo}}$ 's indicates the existence of inductive and mesomeric moments of different substituent polar groups present in such dielectropolar molecules in addition to strong hydrogen bonding in them as displayed by the molecular conformations of Fig 6.

The solvent  $\text{C}_6\text{H}_6$  unlike  $n$ -heptane is a cyclic compound with three double bonds and six  $p$ -electrons on six carbon atoms. Hence  $\pi$ - $\pi$  interaction or resonance effect combined with inductive effect known as mesomeric effect is expected to play an important role in the measured  $\mu_j$ 's under hf electric field. A special attention is to be paid to have the conformational structures of the alcohols to evaluate  $\mu_{\text{theo}}$ 's as seen in Fig 6 and Table 2 from the reduction of the available bond moments<sup>5,6</sup> of different substituent polar groups by the ratio of  $\mu_s/\mu_{\text{theo}}$ . This takes into account of H-bonding, in addition to inductive effect in them. Thus the conclusion regarding the molecular association of such long chain associated aliphatic alcohols may also be the reason to yield higher dipole moments.

## 2 Static Relaxation Parameter $X_{ij}$ and Static Dipole Moment $\mu_s$

Under static electric field  $\mu_s$  of a dielectropolar molecule ( $j$ ) in a non polar solvent ( $i$ ) may be obtained from the following equation<sup>10</sup>.

$$\frac{(\epsilon_0 k_{0ij} - 1)}{(\epsilon_0 k_{0ij} + 2)} - \frac{(\epsilon_0 k_{\infty ij} - 1)}{(\epsilon_0 k_{\infty ij} + 2)} = \frac{(\epsilon_0 k_{0i} - 1)}{(\epsilon_0 k_{0i} + 2)} - \frac{(\epsilon_0 k_{\infty i} - 1)}{(\epsilon_0 k_{\infty i} + 2)} + \frac{N \mu_s^2}{3 \epsilon_0 k_B T} c_j \quad \dots(1)$$

where  $k_{0ij} = \epsilon_{0ij}/\epsilon_0$  and  $k_{\infty ij} = \epsilon_{\infty ij}/\epsilon_0$  are the dimensionless static and infinite frequency dielectric constants of solution ( $ij$ ).  $\epsilon_0$  is the permittivity of free space =  $8.854 \times 10^{-12} \text{ F.m.}^{-1}$ ,  $c_j$  is the molar concentration of the solute where  $c_j = \rho_{ij} w_j / M_j$  and the other symbols carry usual meanings.

A polar liquid of weight  $W_j$  and volume  $V_j$  is mixed with a nonpolar solvent of weight  $W_i$  and volume  $V_i$  to get the solution density  $\rho_{ij}$  where

$$\rho_{ij} = \frac{W_i + W_j}{V_i + V_j} = \frac{W_i + W_j}{W_i/\rho_i + W_j/\rho_j} = \frac{\rho_i \rho_j}{\rho_j W_i / (W_i + W_j) + \rho_i W_j / (W_i + W_j)} = \frac{\rho_i \rho_j}{\rho_j w_i + \rho_i w_j} = \rho_i (1 - \gamma w_j)^{-1} \quad \dots(2)$$

The weight fractions  $w_j$  and  $w_i$  of solute and solvent are given by :

$$w_j = \frac{W_j}{W_i + W_j} \text{ and } w_i = \frac{W_i}{W_i + W_j} \text{ such that } w_i + w_j = 1$$

and  $\gamma = (1 - \rho_i/\rho_j)$ ,  $\rho_i$  and  $\rho_j$  are densities of pure solvent and solute respectively.

Now, Eq. (1) may be written as:

$$\frac{k_{0ij} - k_{\infty ij}}{(\epsilon_0 k_{0ij} + 2)(\epsilon_0 k_{\infty ij} + 2)} = \frac{k_{0i} - k_{\infty i}}{(\epsilon_0 k_{0i} + 2)(\epsilon_0 k_{\infty i} + 2)} + \frac{N \rho_i \mu_s^2}{9 \epsilon_0^2 M_j k_B T} w_j (1 - \gamma w_j)^{-1} X_{ij} = X_i + \frac{N \rho_i \mu_s^2}{9 \epsilon_0^2 M_j k_B T} w_j + \frac{N \rho_i \mu_s^2}{9 \epsilon_0^2 M_j k_B T} \gamma w_j^2 + \dots \quad \dots(3)$$

The right hand side of Eq. (3) is obviously a polynomial equation of  $w_j$  like

$$X_{ij} = a_0 + a_1 w_j + a_2 w_j^2 + \dots \quad \dots(4)$$

Now, comparing the linear coefficients of Eqs (3) and (4) one gets  $\mu_s$  from:

$$\mu_s = \left( \frac{9 \epsilon_0^2 M_j k_B T}{N \rho_i} a_1 \right)^{1/2} \quad \dots(5)$$

where  $a_1$  is the slope of  $X_{ij}$ - $w_j$  curve of Fig. 1. But  $\mu_s$  from higher coefficients of Eqs (3) or (4) are not reliable as they are involved with various effects of solvent, relative density, solute-solute association, internal field, macroscopic viscosity etc.  $\mu_s$ 's from Eq. (5) along with  $a_1$  are placed in Table 2 to compare with hf  $\mu_j$ 's presented in Table 4.

## 3 High Frequency Dipole Moment $\mu_j$ and Relaxation Time $\tau_j$

Under hf electric field of GHz range the dimensionless complex dielectric constant  $k^*_{ij}$  is:

$$k^*_{ij} = k'_{ij} - j k''_{ij} \quad \dots(6)$$

where  $k'_{ij} = \epsilon'_{ij}/\epsilon_0$  and  $k''_{ij} = \epsilon''_{ij}/\epsilon_0$  are the real and imaginary parts of complex dielectric constant.  $\epsilon'_{ij}$  and  $\epsilon''_{ij}$  are the real and imaginary parts of complex permittivity  $\epsilon^*_{ij}$  in F.m.<sup>-1</sup> and  $\epsilon_0 =$  permittivity of free space =  $8.854 \times 10^{-12}$  F.m.<sup>-1</sup>. The hf complex conductivity  $\sigma^*_{ij}$  of a polar-nonpolar liquid mixture of<sup>15</sup> weight fraction  $w_j$  is:

$$\sigma^*_{ij} = \omega \epsilon_0 k''_{ij} + j \omega \epsilon_0 k'_{ij} \quad \dots(7)$$

where  $\sigma'_{ij} = \omega \epsilon_0 k'_{ij}$  and  $\sigma''_{ij} = \omega \epsilon_0 k''_{ij}$  are real and imaginary parts of complex conductivity and  $j$  is a complex number =  $(-1)^{1/2}$

The hf conductivity  $\sigma_{ij}$  is, however, obtained from :

$$\sigma_{ij} = \omega \epsilon_0 (k''_{ij}{}^2 + k'_{ij}{}^2)^{1/2} \quad \dots(8)$$

$\sigma''_{ij}$  is related to  $\sigma'_{ij}$  by

$$\sigma''_{ij} = \sigma_{\infty ij} + (1/\omega \tau_j) \sigma'_{ij} \quad \dots(9)$$

where  $\sigma_{\infty ij}$  is the constant conductivity at  $w_j \rightarrow 0$  and  $\tau_j$  is the relaxation time of a polar molecule.

Eq. (9) on differentiation with respect to  $\sigma'_{ij}$  becomes<sup>11</sup>

$$d\sigma''_{ij}/d\sigma'_{ij} = 1/\omega \tau_j \quad \dots(10)$$

to yield  $\tau_j$

It is often better to use the ratio of slopes of individual variation of  $\sigma''_{ij}$  and  $\sigma'_{ij}$  with  $w_j$  at  $w_j \rightarrow 0$  to avoid polar-polar interaction in a given solvent to get  $\tau_j$  from:  $(d\sigma''_{ij}/dw_j)/(d\sigma'_{ij}/dw_j) = 1/\omega \tau_j$

$$\text{or } x/y = 1/\omega \tau_j \quad \dots(11)$$

where  $\omega = 2\pi f$ ,  $f$  being the frequency of alternating electric field.

In hf region of GHz range, it is often observed that  $\sigma''_{ij} \cong \sigma_{ij}$  and Eq. (9) becomes:

$$\sigma_{ij} = \sigma_{\infty ij} + (1/\omega \tau_j) \sigma'_{ij} \quad \dots(12)$$

$$\beta = 1/\omega \tau_j (d\sigma'_{ij}/dw_j) \quad \dots(13)$$

where  $\beta - (d\sigma_{ij}/dw_j)$  is the slope of  $\sigma_{ij}-w_j$  curve at  $w_j \rightarrow 0$

The  $\sigma'_{ij}$  of a solution of weight fraction  $w_j$  of a polar molecule at  $T$  K is given by Smyth<sup>14,16</sup> as:

$$\sigma'_{ij} = \frac{N \rho_{ij} \mu_j^2}{27 \epsilon_0 M_j k_B T} \left( \frac{\omega^2 \tau}{1 + \omega^2 \tau^2} \right) (\epsilon_0 k_{0ij} + 2) (\epsilon_0 k_{\infty ij} + 2) w_j \quad \dots(14)$$

Eq. (14) on differentiation with respect to  $w_j$  and at  $w_j \rightarrow 0$  yields:

$$(d\sigma'_{ij}/dw_j)_{w_j \rightarrow 0} = \frac{N \rho_i \mu_i^2}{3 \epsilon_0 M_j k_B T} \left( \frac{\epsilon_i + 2}{3} \right)^2 \left( \frac{\omega^2 \tau}{1 + \omega^2 \tau^2} \right) \quad \dots(15)$$

where  $N =$  Avogadro's number,  $\rho_i =$  density of solvent

$\epsilon_i =$  permittivity of solvent;

$M_j =$  Molecular weight of solute and

$k_B =$  Boltzmann constant.

From Eqs (13) and (15) one gets hf  $\mu_j$  as:

$$\mu_j = \left[ \frac{27 \epsilon_0 M_j k_B T}{N \rho_i (\epsilon_i + 2)^2} \frac{\beta}{\omega b} \right]^{1/2} \quad \dots(16)$$

$$\text{where } b = 1/(1 + \omega^2 \tau_j^2) \quad \dots(17)$$

is a dimensionless parameter involved with estimated  $\tau_j$  from Eqs (10) and (11). All the computed hf  $\mu_j$ 's in terms of slopes  $\beta$ 's and  $b$ 's are placed in Table 4 in order to compare with  $\mu_{\text{theo}}$ 's,  $\mu_s$  and  $\mu_1, \mu_2$  of the flexible part and end-over-end rotation of the whole molecule<sup>5,6</sup> presented in Table 2.

#### 4 Results and Discussions

The dimensionless real  $k'_{ij}$  and imaginary  $k''_{ij}$  of the complex dielectric constants  $k^*_{ij}$  as well as the static  $k_{0ij}$  and infinite frequency  $k_{\infty ij}$  of dielectric constants were obtained from the measured relaxation permittivities  $\epsilon'_{ij}, \epsilon''_{ij}, \epsilon_{0ij}$  and  $\epsilon_{\infty ij}$  in F.m.<sup>-1</sup> for different  $w_j$ 's of alcohols in different solvents at 25°C. The data thus obtained are placed in Table 1. The static experimental solution parameters  $X_{ij}$ 's involved with  $k_{0ij}$  and  $k_{\infty ij}$  of Table 1 are shown in Fig. 1, for different  $w_j$  of alcohols. The nature of variation of  $X_{ij}$  with  $w_j$ 's are parabolic in nature satisfying a polynomial equation:  $X_{ij} = a_0 + a_1 w_j + a_2 w_j^2$ . The coefficients of  $X_{ij}-w_j$  curves i.e.  $a_0, a_1$  and  $a_2$  are placed in the 2nd, 3rd and 4th columns of Table 2. As evident from Fig. 1, the  $X_{ij}-w_j$  curves for methanol, ethanol and 3-methyl-3-heptanol are convex in nature as their coefficients of quadratic terms in Table 2 are negative. The remaining  $X_{ij}$ 's on the other hand, showed a gradual increase with  $w_j$ 's for all the coefficients of the curves are positive as seen in Table 2. The anomalous behaviour of  $X_{ij}-w_j$  curves from linearity for all the alcohols in different solvents at a given temperature in °C may rouse an interesting relaxation mechanism in such long chain associated liquids. In comparison to octyl alcohols, the curves of normal alcohols in higher concentrations are highly concave hav-

ing a tendency to meet at a common point on the  $X_{ij}$  axis at  $w_j \rightarrow 0$ . This sort of behaviour of  $X_{ij}$ — $w_j$  curves of Fig. 1 arises either due to solute-solute i.e. dimer or solute-solvent i.e. monomer formations in comparatively high concentrations. The convex shape of ethanol and methanol occurs for the probable experimental uncertainty in their  $\epsilon_{0ij}$  and  $\epsilon_{\infty ij}$  measurements. The identical nature of variations of all the octyl alcohols have almost the same slope, but of different intercepts as a result of solvation effect. Their  $X_{ij}$ 's have tendency to become closer within  $0.1 \leq w_j \leq 0.2$  indicating various molecular association in them.

In case of non-associated liquids  $a_2$ 's were found to be vanishingly small in comparison to  $a_0$  and  $a_1$  to yield almost linear variation of  $X_{ij}$  against  $w_j$ . The estimated correlation coefficient ( $r$ ) and the percentage of error (%) entered in 5th and 6th columns of Table 2 for all the alcohols are such that one may rely on the linear term of  $X_{ij}$ — $w_j$  curve to compute  $\mu_s$ 's from Eq. (5).  $\mu_s$ 's thus computed are placed in the 7th column of Table 2 to compare with  $\mu_{\text{theo}}$ 's obtained from bond angles and bond moments of the substituent polar groups, as presented in Fig. 6 and  $\mu_1$  and  $\mu_2$  of the flexible part and the whole molecule by the double relaxation method<sup>5,6</sup> at nearly 24 GHz electric field. The smaller and larger deviations of  $X_{ij}$ 's from linearity with  $w_j$ 's as seen in Fig. 1, confirm the molecular associations of such associated dielectropolar liquids in different solvents.

The relaxation times  $\tau_j$ 's are, however, derived from the slope of linear<sup>11</sup> variation of  $\sigma''_{ij}$  with  $\sigma'_{ij}$  of Fig. 2 for all the alcohols. Although, the experimental data, on the other hand, did not strictly fall on the fitted linear curves of  $\sigma''_{ij}$  and  $\sigma'_{ij}$  both in  $\Omega^{-1} \text{ m}^{-1}$  as drawn in Fig. 2, the slope of  $\sigma''_{ij}$  against  $\sigma'_{ij}$  of Fig. 2 was, however, used to obtain  $\tau_j$  from Eq. (10). The 2nd, 3rd and 6th columns of Table 3 contain all the estimated intercepts and slopes together with the measured  $\tau_j$ 's. The linearity of  $\sigma''_{ij}$  curves against  $\sigma'_{ij}$  as shown graphically in Fig. 2 is again tested by correlation coefficients  $r$ 's and % of errors. They are entered in the 4th and 5th columns of Table 3 only to see how far  $\sigma''_{ij}$  and  $\sigma'_{ij}$  are correlated to each other. But it is often better to use the ratio of the individual slopes of variation of  $\sigma''_{ij}$  and  $\sigma'_{ij}$  with  $w_j$  at  $w_j \rightarrow 0$  to get  $\tau_j$ .  $\tau_j$ 's by using Eq. (11) are not in close agreement with those obtained from Eq. (10) and by freshly calculated Gopalakrishna's method, as seen in Table 3. Figs (3) and (4) showed that both  $\sigma''_{ij}$  and  $\sigma'_{ij}$  vary nonlinearly with  $w_j$ . The nonlinear behaviour of  $\sigma''_{ij}$

and  $\sigma'_{ij}$  as seen in Figs 3 and 4 with  $w_j$ 's invites the associational and structural aspects of such long chain dielectropolar associated molecules. The latter method to measure  $\tau_j$ 's thus appears to be a significant improvement<sup>12,13</sup> over the former one<sup>11</sup> as it eliminates the polar-polar interaction in a given solvent.

The hf  $\mu_j$  from Eq. (16) was obtained from the slope  $\beta$  of the nonlinear variation of  $\sigma_{ij}$  in  $\Omega^{-1} \text{ m}^{-1}$  with  $w_j$ 's of Fig. 5 and dimensionless parameter  $b$  of Eq. (17) in terms of  $\tau_j$  obtained by both the methods. The intercept  $\alpha$  and slope  $\beta$  of hf  $\sigma_{ij}$  with  $w_j$  curves of Fig. 5 are entered in the 2nd and 3rd columns of Table 3. It is interesting to note that the curves of  $\sigma_{ij}$ — $w_j$  variation of Fig. 5 are almost identical with  $\sigma''_{ij}$ — $w_j$  curves of Fig. 3. This fact at once confirms the applicability of the approximation that  $\sigma''_{ij} \equiv \sigma_{ij}$  as done in Eqs (9) and (12). The imaginary  $\sigma''_{ij}$  and total hf  $\sigma_{ij}$  in case of normal alcohols in Figs 3 and 5 decrease gradually with  $w_j$ 's of 1-butanol to methanol except ethanol. This can be explained on the basis of the fact that the polarity of the molecules decreases from 1-butanol to methanol. Both  $\sigma''_{ij}$ 's and  $\sigma_{ij}$ 's in Figs 3 and 5 of all the octyl alcohols are found to be closer only to show their nearly same polarity. The almost coincident curves of 4-octanol (— $\Theta$ —) and 2-octanol(— $X$ —) arise due to their identical polarity as estimated in Fig. 6.

The estimated  $\mu_s$ 's and  $\mu_j$ 's in Table 2 and 4 are then compared with the  $\mu_1$  and  $\mu_2$  in Table 2 by double relaxation method<sup>5,6</sup> and those by freshly calculated Gopalakrishna's method. For all the normal alcohols  $\mu_j$ 's and  $\mu_s$ 's are in excellent agreement with Gopalakrishna's  $\mu_j$ 's (reported data) and  $\mu_1$ . The estimated  $\mu_j$ 's for octyl alcohols agree with reported  $\mu_j$ 's and  $\mu_1$ . All these discussions made above establish the fact that a part of the molecule is rotating under GHz electric field. Slight disagreement in  $\mu$ 's and the reported ones arises due to steric hindrances of the substituent polar units of their structural configurations of Fig. 6 and the existence of associative nature for their hydrogen bonding. Unlike normal alcohols,  $\mu_s$ 's are always lower than  $\mu_j$ 's and  $\mu_1$ 's for octyl alcohols. This at once reveals under static electric field the possible formation of dimers which undergo to rupture into the solute solvent association i.e. monomer in the hf electric field to increase  $\mu$ 's. It is also evident that dimer formation is favourable in octyl alcohols than normal alcohols due to existence of strong

inductive effect for their  $-OH$  groups at the end of the molecular chains.

The theoretical dipole moments  $\mu_{\text{theo}}$ 's of all the alcohols under study were calculated from the available bond angles and bond moments of the substituent polar groups like  $H_3-C$ ,  $C-H$ ,  $C-O$ ,  $O-H$  ( $\angle 105^\circ$ ) and  $C-C$  of  $1.23 \times 10^{-30}$ ,  $1.0 \times 10^{-30}$ ,  $3.33 \times 10^{-30}$ ,  $1.30 \times 10^{-30}$  and  $0.3 \times 10^{-30}$  Coulomb-meter (C.m.) as presented elsewhere<sup>5,6</sup>. The values thus estimated are then made closer with the measured static  $\mu_s$ 's or even  $\mu_j$ 's by reducing the available bond moments by a factor  $\mu_s/\mu_{\text{theo}}$  which takes into account of the inductive and mesomeric effects of the substituent polar groups as shown in Fig. 6. An inductive effect of polar unit acts along the chain of the molecular axis of the normal alcohols to make them strongly polar due to presence of  $-OH$  group at their ends of the axis. The comparatively lower  $\mu_{\text{theo}}$ 's in octyl alcohols is probably due to screening effect of their  $-OH$  groups by other polar groups like  $H_3-C$ ,  $C-H$  which favour the dimer formation of these alcohols through H-bonding to make their  $\mu_s$ 's and  $\mu_j$ 's lower than the normal alcohol as seen in Fig. 6.

## 5 Conclusion

The modern internationally accepted symbols of dielectric terminologies and parameters in SI unit are conveniently used to obtain static and hf dipole moments  $\mu_s$  and  $\mu_j$  in terms of relaxation time  $\tau_j$  of a polar molecule.  $\tau_j$ 's measured from the slope of imaginary  $\sigma''_{ij}$  against real  $\sigma'_{ij}$  of complex hf conductivity  $\sigma^*_{ij}$  for different  $\omega_j$  are not in agreement with those measured from the ratio of the individual slopes of  $\sigma''_{ij} - \omega_j$  and  $\sigma'_{ij} - \omega_j$  curves at  $\omega_j \rightarrow 0$  indicating the applicability of the latter method in long chain dielectropolar alcohols. This method of determination of  $\tau_j$  is a significant improvement over the previous one as it eliminates polar-polar interactions in a given solvent. The comparison of  $\mu_j$ 's and  $\mu_s$ 's with  $\mu_1$  and  $\mu_2$  of the flexible part and the whole molecule by double relaxation method and  $\mu_{\text{theo}}$ 's from bond angles and bond moments seems to be an interesting phenomenon to have deep insight into relaxation mechanism of dielectropolar alcohols.

The results indicate that a part of the molecule is rotating under GHz electric field. The slight departure among the measured  $\mu_s$ ,  $\mu_j$  and  $\mu_{\text{theo}}$  reveals different associational aspects of dielectropolar alcohols in dif-

ferent solvents through the frequency dependence of relaxation parameters. It also shows the strong polar nature of normal alcohols which favour solute-solvent association due to the presence of  $-OH$  group at the end of their bond axis. But the comparatively lower values of  $\mu_j$ 's in octyl alcohols indicates the solute-solute association due to  $-H$  bonding supported by the fact that  $-OH$  being screened by  $-CH_3$  and a large number of  $>CH_2$  polar groups. The  $\mu_s/\mu_{\text{theo}}$ 's are almost constant for all the alcohols to take into account of all these facts in addition to their material property of the system. This study further supports the rotation of  $-OH$  group along the  $\equiv C-O-$  bond of all the alcohols under static and hf electric fields. Moreover, the methodology so far developed within the frame work of Debye and Smyth model appears to be sound, simple, straightforward and useful to arrive at associational and structural aspects of alcohols which are thought to be non-Debye in relaxation behaviour.

## References

- 1 Gopalakrishna K V, *Trans Farad Soc*, 33 (1957) 767.
- 2 Kastha G S, Dutta J, Bhattacharyya J & Roy S B, *Indian J Phys*, 43 (1969) 14.
- 3 Dutta S K, Acharyya C R & Acharyya S, *Indian J Phys*, 55B (1981) 140.
- 4 Sit S K, Ghosh N, Saha U & Acharyya S, *Indian J Phys*, 71B (1997) 533.
- 5 Sit S K & Acharyya S, *Indian J Phys*, 70B (1996) 19.
- 6 Sit S K, Ghosh N & Acharyya S, *Indian J Pure & Appl Phys*, 35 (1997) 329.
- 7 Glasser L, Crossley J & Smyth C P, *J Chem Phys*, 57 (1972) 3977.
- 8 Ghosh A K, PhD Dissertation, N B U, (1981).
- 9 Crossley J, Glasser L & Smyth C P, *J Chem Phys*, 55 (1971) 2197.
- 10 Debye P, *Polar Molecules* (Chemical Catalogue), 1929.
- 11 Murthy M B R, Patil R L & Deshpande D K, *Indian J Phys*, B63 (1989) 491.
- 12 Ghosh N, Basak R C, Sit S K & Acharyya S, *J Mol Liq*, Germany, (Accepted for publication), 2000.
- 13 Basak R C, Sit S K, Nandi N & Acharyya S, *Indian J Phys*, B70 (1996) 37.
- 14 Basak R C, Karmakar A, Sit S K & Acharyya S, *Indian J Pure & Appl Phys*, 37 (1999) 224.
- 15 Murphy F J & Morgan S O, *Bell Syst Tech J*, 18 (1939) 502.
- 16 Smyth C P, *Dielectric behaviour and structure*, (McGraw-Hill, New York), 1955.

## High frequency and static relaxation parameters of some polar monosubstituted anilines in benzene

R C Basak, A Karmakar, S K Sit & S Acharyya

Department of Physics, Raiganj College (University College),  
P O Raiganj, Dist. Uttar Dinajpur (WB) 733 134

Received 12 January 1998; revised 17 August 1998 ; accepted 22 January 1999

The use of slopes of individual variation of the imaginary  $\sigma''_{ij}$  and real  $\sigma'_{ij}$  parts of high frequency (hf) conductivity  $\sigma^*_{ij}$  with the weight fractions  $W_j$ 's of a solute is employed to determine relaxation times  $\tau_j$ 's of some monosubstituted anilines in  $C_6H_6$ . The dipole moments  $\mu_j$ 's of such polar molecules in terms of estimated  $\tau_j$ 's are calculated and compared with those by using the existing methods for  $\tau_j$  (Murthy et al. 1989). Excellent agreement of  $\mu_j$ 's in all cases except m-toluidine indicates the applicability of both the methods. The hf  $\mu_j$  as well as static  $\mu_s$  differ from  $\mu_{theo}$ 's as obtained from the available bond angles and bond moments. The reduced bond moments are, however, calculated from the estimated  $\mu_j$ ,  $\mu_s$  and  $\mu_{theo}$  to yield the exact  $\mu$ 's in close agreement with  $\mu_s$  and  $\mu_j$  only to establish the presence of inductive and mesomeric moments of the substituent groups, in addition to solute-solute or solute-solvent molecular associations among the molecules in the solution. The  $\mu_j$ 's being little affected by the frequency of the electric field, are finally compared with  $\mu_2$  and  $\mu_1$  (Sit and Acharyya, 1996) due to rotations of the whole and a part of the molecules. They are very close to  $\mu_1$  indicating the fact that a part of the molecule is rotating under the electric field of 10 GHz.

### 1 Introduction

The dielectric relaxation behaviour of disubstituted benzenes and anilines in a nonpolar solvent is very interesting, because they usually show the double relaxation phenomena under high frequency (hf) electric fields<sup>1</sup>. Monosubstituted anilines, on the other hand, possess either single or double relaxation times ( $\tau_j$ 's) at three different hf electric fields of Giga hertz (GHz) range<sup>2</sup>. But they always showed double relaxation times at 9.945 GHz electric field, which seems to be the most effective dispersive region for such polar molecules<sup>3</sup>. They were also found to obey the symmetric relaxation behaviour under such electric field<sup>3</sup>.

An attempt is, therefore, made to get the dimensionless dielectric relaxation parameters like real  $\kappa'_{ij}$ , imaginary  $\kappa''_{ij}$  parts of complex dielectric constant  $\kappa^*_{ij}$  as well as static and infinite frequency-dielectric constants  $\kappa_{0ij}$  and  $\kappa_{\infty ij}$  of solution (ij) as shown in Table 1, from the measured<sup>3</sup> permittivities of  $\epsilon'_{ij}$ ,  $\epsilon''_{ij}$ ,  $\epsilon_{0ij}$  and  $\epsilon_{\infty ij}$  respectively, of three isomers of anisidines and toluidines at 35° C under 9.945 GHz electric field at different weight fractions  $W_j$ 's of solute (j). The purpose of such consideration is to get static dipole moment  $\mu_s$  at any stage of dilution as well as the relaxation times ( $\tau_j$ 's) and hence

hf dipole moments ( $\mu_j$ 's) derived from hf conductivities  $\sigma^*_{ij}$ 's as functions of  $\kappa'_{ij}$  and  $\kappa''_{ij}$  at different  $W_j$ 's.

The ratio of individual slopes of the concentration variation of the imaginary  $\sigma''_{ij}$  and the real  $\sigma'_{ij}$  parts of complex hf conductivity  $\sigma^*_{ij}$  as well as the slope of linear variation of  $\sigma''_{ij}$  with  $\sigma'_{ij}$  were simultaneously used<sup>4</sup> to estimate  $\tau_j$ 's of a polar liquid. The  $\tau_j$  obtained by the former method provides a significant improvement over the latter one<sup>5</sup>, as it eliminates the polar-polar interaction in the solution. It is better to use the ratio of slopes of concentration variations of  $\kappa''_{ij}$  and  $\kappa'_{ij}$  instead of  $\sigma''_{ij} - W_j$  and  $\sigma'_{ij} - W_j$  curves to get  $\tau_j$ , because  $\kappa'_{ij}$  and  $\kappa''_{ij}$  can be obtained directly from experimental measurements of  $\epsilon'_{ij}$  and  $\epsilon''_{ij}$ .

But, the variation of  $\kappa''_{ij}$  with  $W_j$  is not always linear with a constant intercept<sup>6,7</sup>. In this paper, a comparison of static  $\mu_s$  from the slope of  $X_{ij} - W_j$  curve and hf  $\mu_j$  in terms of  $\tau_j$  using hf conductivities of solution under 9.945 GHz electric field is also made with  $\mu_2$  and  $\mu_1$  due to rotations of the whole as well as the flexible part attached to the parent ring of the molecule from the dielectric relaxation parameters of Table 1 obtained by careful graphical interpolation of measured data<sup>8</sup> used earlier<sup>3</sup>. The comparison of all these seems to be an interesting phenomenon only to see how far they agree

Table 1 — Experimental dielectric relaxation parameters of three isomers of anisidines and toluidines at 35 °C under 9.945 GHz electric field for different weigh fractions  $W_j$ 's of solutes

System with Sl. No and molecular wt.	Weight fraction	Real part of permittivity	Dielectric loss factor	Static permittivity	Infinite frequency permittivity	Dimensionless dielectric constants			
						$M_j$ , kg	$W_j$ of solute	$(\epsilon'_{ij})$ F.m <sup>-1</sup>	$(\epsilon''_{ij})$ F.m <sup>-1</sup>
1.o-anisidine in C <sub>6</sub> H <sub>6</sub> $M_j = 0.123$ kg	0.0326	2.3104	0.0148	2.336	2.239	0.2609	0.1672	0.2638	0.2529
	0.0604	2.3520	0.0244	2.404	2.247	0.2656	0.2756	0.2715	0.2538
	0.0884	2.4064	0.0340	2.459	2.255	0.2718	0.3840	0.2777	0.2547
	0.1135	2.4416	0.0400	2.538	2.262	0.2758	0.4578	0.2867	0.2555
	0.1361	2.4672	0.0512	2.588	2.267	0.2786	0.5783	0.2923	0.2560
2.m-anisidine in C <sub>6</sub> H <sub>6</sub> $M_j = 0.123$ kg	0.0160	2.2720	0.0234	2.315	2.235	0.2566	0.2643	0.2615	0.2524
	0.0336	2.3040	0.0390	2.384	2.241	0.2602	0.4405	0.2693	0.2531
	0.0579	2.3904	0.0618	2.477	2.246	0.2700	0.6980	0.2798	0.2537
	0.0823	2.4544	0.0744	2.553	2.253	0.2772	0.8403	0.2883	0.2545
	0.1109	2.5344	0.1056	2.675	2.261	0.2862	1.1927	0.3021	0.2554
3.p-anisidine in C <sub>6</sub> H <sub>6</sub> $M_j = 0.123$ kg	0.0319	2.3104	0.0252	2.373	2.237	0.2609	0.2846	0.2680	0.2527
	0.0597	2.3904	0.0474	2.442	2.246	0.2700	0.5354	0.2758	0.2537
	0.0848	2.5088	0.0642	2.539	2.250	0.2834	0.7251	0.2868	0.2541
	0.1106	2.5376	0.0840	2.638	2.262	0.2866	0.9487	0.2929	0.2555
	0.1396	2.6272	0.1086	2.745	2.269	0.2967	1.2266	0.3100	0.2563
4.o-toluidine in C <sub>6</sub> H <sub>6</sub> $M_j = 0.107$ kg	0.0137	2.2752	0.0162	2.301	2.241	0.2570	0.1830	0.2600	0.2531
	0.0459	2.3648	0.0408	2.392	2.250	0.2671	0.4608	0.2702	0.2541
	0.0622	2.4032	0.0570	2.457	2.255	0.2714	0.6438	0.2775	0.2547
	0.1048	2.5376	0.0900	2.577	2.264	0.2866	1.0165	0.2911	0.2557
	0.1225	2.5280	0.0732	2.591	2.262	0.2855	0.8267	0.2926	0.2555
5.m-toluidine in C <sub>6</sub> H <sub>6</sub> $M_j = 0.107$ kg	0.0264	2.3136	0.0150	2.337	2.243	0.2613	0.1694	0.2639	0.2533
	0.0538	2.3552	0.0342	2.413	2.248	0.2660	0.3863	0.2725	0.2539
	0.0781	2.4576	0.0402	2.470	2.252	0.2776	0.4540	0.2790	0.2543
	0.1015	2.3840	0.0618	2.526	2.258	0.2692	0.6980	0.2853	0.2550
	0.1225	2.5280	0.0732	2.591	2.262	0.2855	0.8267	0.2926	0.2555
6.p-toluidine in C <sub>6</sub> H <sub>6</sub> $M_j = 0.107$ kg	0.0213	2.3100	0.0102	2.319	2.237	0.2609	0.1152	0.2619	0.2527
	0.0428	2.3040	0.0204	2.367	2.244	0.2602	0.2304	0.2673	0.2534
	0.0616	2.3904	0.0276	2.413	2.249	0.2700	0.3117	0.2725	0.2540
	0.0916	2.4704	0.0384	2.483	2.254	0.2790	0.4337	0.2804	0.2646
	0.1048	2.4960	0.0582	2.523	2.260	0.2819	0.6573	0.2850	0.2553

with  $\mu_2$  and  $\mu_1$  as obtained elsewhere<sup>3</sup>. This study farther observes the effect of inductive and mesomeric moments of polar groups of the molecules as well as the frequency of the alternating electric field on  $\mu_j$ 's in comparison to  $\mu_s$ . Moreover, the present method of study in terms of modern internationally accepted units and symbols appears to be superior because of its unified, coherent and rationalised nature.

As is evident from Table 2, hf  $\mu_j$ 's of the polar liquids were computed in terms of  $\tau_j$  and the slopes ( $\beta$ 's) of  $\sigma_{ij} - W_j$  curves of Fig. 1 under 9.945 GHz electric field at 35°C.  $\tau_j$  being an important parameter for obtaining  $\mu_j$  of polar liquid estimated from the ratio of slopes of individual variation of  $\sigma''_{ij}$  and  $\sigma'_{ij}$  with  $W_j$ . The nature of variations of  $\sigma''_{ij} - W_j$  and  $\sigma'_{ij} - W_j$  curves are presented in Figs 2 and 3, respectively. In place of using  $\tau_j$

from the ratio of the slopes of  $\sigma''_{ij} - W_j$  and  $\sigma'_{ij} - W_j$  curves, one may use the linear slope of  $\sigma''_{ij} - \sigma'_{ij}$  curve to get  $\tau_j$  and hence  $\mu_j$  as suggested by Murthy et al<sup>5</sup>. All the  $\mu_j$ 's and  $\tau_j$ 's from both the methods are reported in Table 2.

The static dipole moment  $\mu_s$  under static or low frequency electric field was also calculated from the linear coefficient of  $X_{ij} - W_j$  curve of Fig. 4 for each polar-nonpolar liquid mixture. The correlation coefficient  $r$  of the linear curve as well as the % error are presented in Table 3 along with  $\mu_s$  and coefficients  $a_0, a_1$

of  $X_{ij} - W_j$  curve. The theoretical dipole moment  $\mu_{\text{theo}}$ 's from available bond angles and bond moments<sup>3</sup> are found to be deviated from static  $\mu_s$ 's and hf  $\mu_j$ 's, because of the existence of the inductive and mesomeric moments of the different polar groups in them. As the variation of  $\mu_s$  compared to  $\mu_j$  is very little, conformational structures of the polar molecules are predicted by  $\mu_{\text{cal}}$  values, which are in agreement with  $\mu_s$  from the reduced bond moments of the substituent groups by a factor  $\mu_s / \mu_{\text{theo}}$  presented in Table 3 and illustrated in Fig. 5.

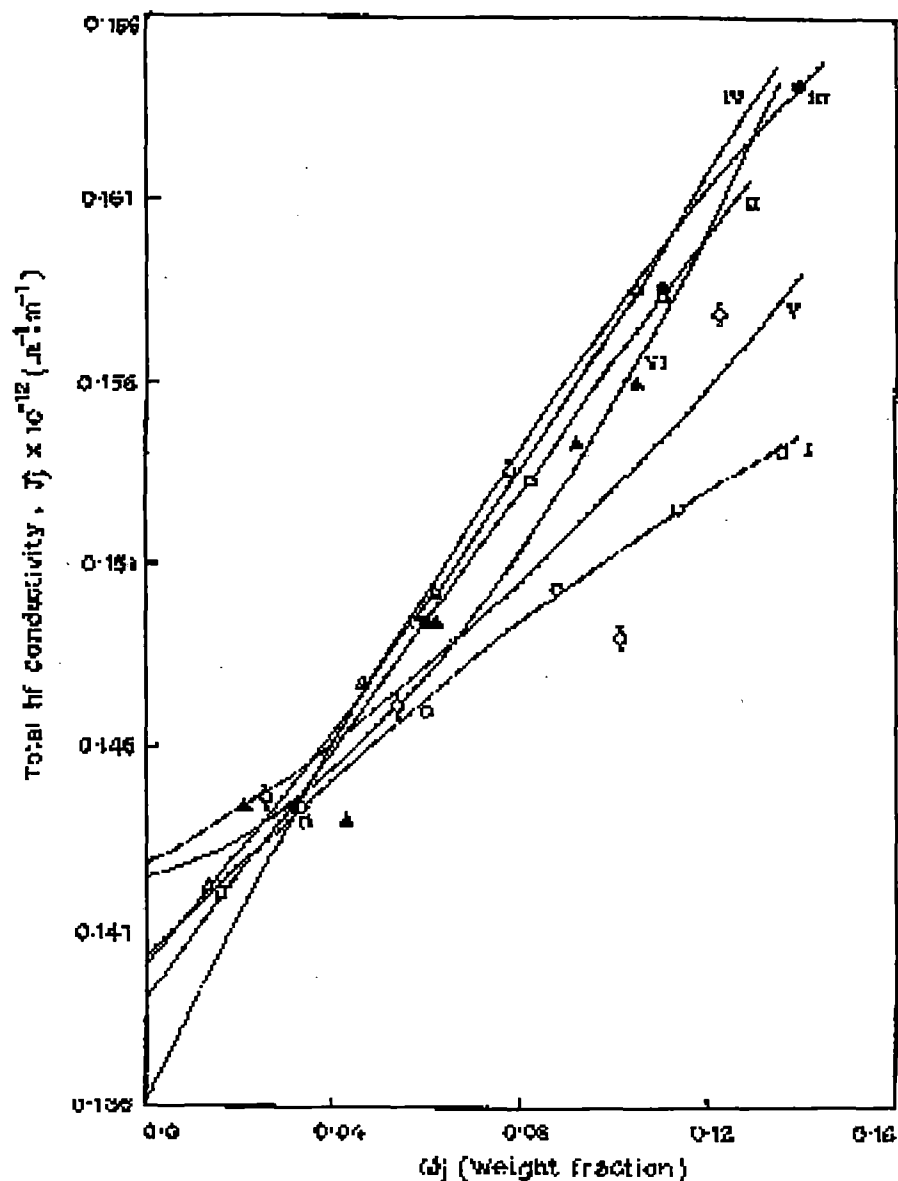


Fig. 1 — The variation of total conductivity  $\sigma_j$  with different  $W_j$ 's of solutes under 9.945 GHz electric field at 35°C [(I) o-anisidine (—○—), (II) m-anisidine (—□—), (III) p-anisidine (—●—), (IV) o-toluidine (—△—), (V) m-toluidine (—◇—), (VI) p-toluidine (—▲—)]

Table 2 — Reports ratio slopes of  $(\sigma''_{ij} - W_j)$  and  $(\sigma'_{ij} - W_j)$  curves at  $W_j \rightarrow 0$ , linear slope of  $(\sigma''_{ij} - \sigma'_{ij})$  curve, computed relaxation time  $\tau_j$  and hence  $\mu_j$  for both the methods and reported  $\mu_2$  and  $\mu_1$  in C.m from double relaxation method

System with Sl.No and molecular wt. $M_j$ in kg.of solute	Ratio of slopes $x/y =$ $\frac{(d \sigma''_{ij}/d w_j)_{w_j \rightarrow 0}}{(d \sigma'_{ij}/d w_j)_{w_j \rightarrow 0}}$	Slope of $(\sigma''_{ij} -$ $\sigma'_{ij})$ curve Eq. (5)	Correlation coefficient ( $r$ )	% of Error	Estimated $\tau_j \times$ $10^{12}$ n sec. from		Slope $\beta \times 10^{-12}$ in $\Omega^{-1}m^{-1}$ of $(\sigma'_{ij} - W_j)$ curve	Computed $\mu_j \times 10^{30}$ in c.m from		Reported $\mu \times 10^{30}$ In c.m	
					Eq. (6)	Eq.(5)		Eq. (6) &	Eq. (5) &	( $\mu_2$ )	( $\mu_1$ )
1.o-anisidine in C <sub>6</sub> H <sub>6</sub> $M_j = 0.123$ kg	$(1.3024 \times 10^{11}) /$ $(1.7179 \times 10^{10})$ $= 7.5813$	4.5290	0.988	0.71	2.11	3.53	0.1302	5.38	5.38	31.11	6.40
2.m-anisidine in C <sub>6</sub> H <sub>6</sub> $M_j = 0.123$ kg	$(1.7305 \times 10^{11}) /$ $(5.2415 \times 10^{10})$ $= 3.3015$	3.3521	0.993	0.40	4.85	4.77	0.1732	6.33	6.33	24.57	7.55
3.p-anisidine in C <sub>6</sub> H <sub>6</sub> $M_j = 0.123$ kg	$(2.6210 \times 10^{11}) /$ $(4.7768 \times 10^{10})$ $= 5.4869$	3.8143	0.983	0.99	2.92	4.20	0.2621	7.58	7.71	52.74	9.00
4.o-toluidine in C <sub>6</sub> H <sub>6</sub> $M_j = 0.107$ kg	$(1.4076 \times 10^{11}) /$ $(5.0973 \times 10^{10})$ $= 2.9380$	3.5123	0.997	0.31	5.45	4.56	0.1500	5.44	5.47	29.87	7.70
5.m-toluidine in C <sub>6</sub> H <sub>6</sub> $M_j = 0.107$ kg	$(7.3263 \times 10^{10}) /$ $(3.7452 \times 10^{10})$ $= 1.9562$	2.9025	0.783	11.69	8.18	5.51	0.0732	4.13	3.89	17.07	5.20
6.p-toluidine in C <sub>6</sub> H <sub>6</sub> $M_j = 0.107$ kg	$(4.3247 \times 10^{10}) /$ $(4.2379 \times 10^9)$ $= 10.2048$	4.4801	0.929	4.12	1.57	3.57	0.0428	2.82	2.88	18.54	4.03

Table 3 — Coefficients  $a_0, a_1$ , in the equation  $X_{ij} = a_0 + a_1 w_j$ , correlation coefficient ( $r$ ), % of error in fitting technique, static dipole moment  $\mu_s$  in coulomb-metre, theoretical dipole moment  $\mu_{theo}$  from bond angles and bond moments, reduced bond moments of substituent groups,  $\mu_{cal}$  from reduced bond moments of anisidines and toluidines under static electric field at 35° C

Systems with Sl.no and molecular wt. $M_j$ in kg. of solutes	Intercepts and slopes of $x_{ij} - w_j$ Eq.		Correlation coefficient ( $r$ )	% of error in fitting technique	$\mu_s \times 10^{30}$ and $\mu_{theo} \times 10^{30}$		Reduced bond moments $\times 10^{30}$ of			$\mu_{cal} \times 10^{30}$ in c.m
	$a_0 \times 10^{-10}$	$a_1 \times 10^{-10}$			in c.m	-OCH <sub>3</sub> (c.m)	-CH <sub>3</sub> (c.m)	-NH <sub>2</sub> (c.m)		
1. o-anisidine in C <sub>6</sub> H <sub>6</sub> $M_j = 0.123$ kg	0.0193	1.2196	0.9976	0.14	2.94	3.40	2.07	-	-3.36	2.94
2. m-anisidine in C <sub>6</sub> H <sub>6</sub> $M_j = 0.123$ kg	0.0211	1.9208	0.9988	0.07	3.69	5.50	1.61	-	-2.60	3.68
3. p-anisidine in C <sub>6</sub> H <sub>6</sub> $M_j = 0.123$ kg	0.0219	1.7353	0.9977	0.14	3.51	6.30	1.33	-	-2.16	3.49
4. o-toluidine in C <sub>6</sub> H <sub>6</sub> $M_j = 0.107$ kg	0.0158	1.5942	0.9981	0.13	3.13	4.63	-	0.83	-2.63	3.13
5. m-toluidine in C <sub>6</sub> H <sub>6</sub> $M_j = 0.107$ kg	0.0240	1.3430	0.9988	0.08	2.88	3.43	-	1.03	-3.25	2.88
6. p-toluidine in C <sub>6</sub> H <sub>6</sub> $M_j = 0.107$ kg	0.0230	1.2393	0.9996	0.02	2.76	5.13	-	0.66	-2.09	2.75

**2 Theoretical Formulation to Estimate hf Dielectric Relaxation Parameters**

Under hf electric field of GHz range the dimensionless complex dielectric constant  $\kappa^*_{ij}$  is written as

$$\kappa^*_{ij} = \kappa'_{ij} - j\kappa''_{ij} \quad \dots(1)$$

where  $\kappa'_{ij} = \epsilon'_{ij} / \epsilon_0 =$  real part of dielectric constant and  $\kappa''_{ij} = \epsilon''_{ij} / \epsilon_0 =$  dielectric loss factor, respectively.  $\epsilon'_{ij}$  and  $\epsilon''_{ij}$  are the real and imaginary parts of complex permittivity  $\epsilon^*_{ij}$  having dimension of Farad meter<sup>-1</sup> (F.m<sup>-1</sup>) and  $\epsilon_0 =$  permittivity of free space =  $8.854 \times 10^{-12}$  F.m<sup>-1</sup>. Hence, Murphy-Morgan<sup>9</sup> relation for the complex hf conductivity  $\sigma^*_{ij}$  of a solution of  $W_j$  is given by

$$\sigma^*_{ij} = \omega\epsilon_0 \kappa''_{ij} + j\omega\epsilon_0 \kappa'_{ij} \quad \dots(2)$$

where  $\sigma'_{ij} (= \omega\epsilon_0 \kappa'_{ij})$  and  $\sigma''_{ij} (= \omega\epsilon_0 \kappa''_{ij})$  are the real and imaginary parts of complex conductivity, and  $j$  is a complex number =  $\sqrt{-1}$ .

The total hf conductivity  $\sigma_{ij}$ , is, however, obtained from

$$\sigma_{ij} = \omega\epsilon_0 \sqrt{\kappa''^2_{ij} + \kappa'^2_{ij}} \quad \dots(3)$$

Again, the imaginary part of hf conductivity  $\sigma''_{ij}$  related to the real part of hf conductivity  $\sigma'_{ij}$  by

$$\sigma''_{ij} = \sigma_{\omega ij} + (1/\omega\tau) \sigma'_{ij} \quad \dots(4)$$

where  $\sigma_{\omega ij}$  is the constant conductivity in the limit of  $W_j = 0$  and  $\tau$  is the relaxation time of a polar unit.

Differentiating Eq. (4) with respect to  $\sigma'_{ij}$  one gets  $d\sigma''_{ij}/d\sigma'_{ij} = 1/\omega\tau_j \quad \dots(5)$

In higher concentration region, the variation of the individual  $\sigma''_{ij}$  and  $\sigma'_{ij}$  with  $W_j$  may not be linear due to

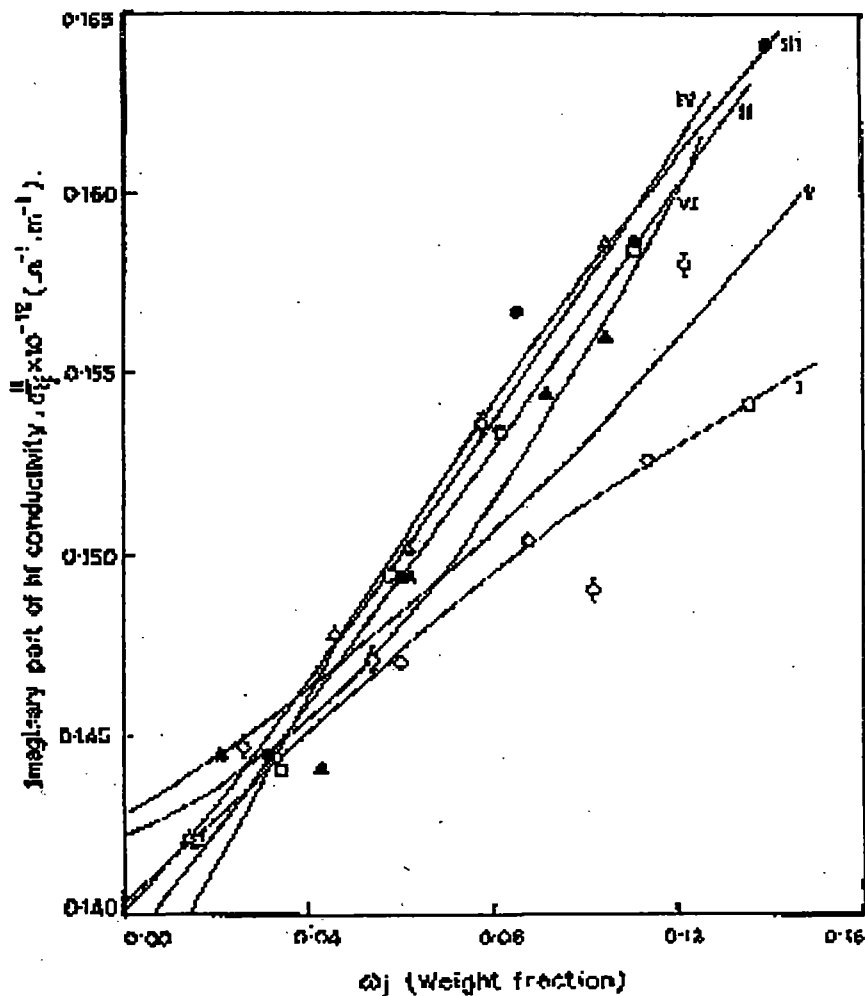


Fig. 2 — The plot of imaginary part of conductivity  $\sigma''_{ij}$  with fractions  $W_j$ 's of anisidines and toluidines at 35°C under 9.945 GHz electric field

[(I) o-anisidine (—○—), (II) m- anisidine (—□—), (III) p- anisidine (—●—), (IV) O- toluidine (—△—), (V) m- toluidine (—◇—), (VI) p-toluidine (—▲—)]

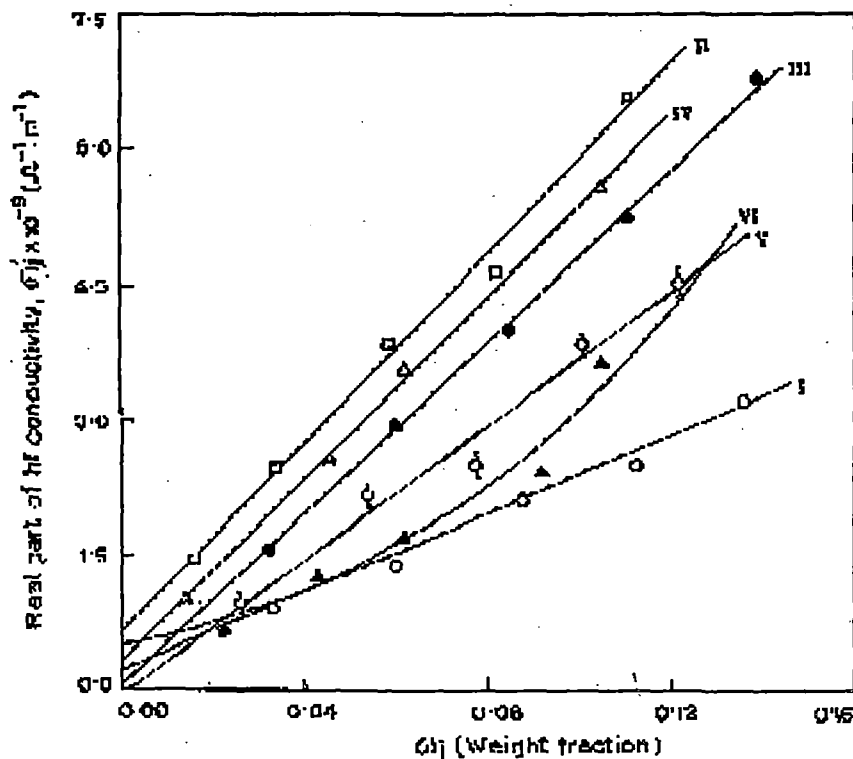


Fig. 3 — The variation of real part of conductivity  $\sigma'_{ij}$  against  $W_j$ 's of solute at 35°C under 9.945 GHz electric field [(I) o-anisidine (—○—), (II) m-anisidine (—□—), (III) p-anisidine (—●—), (IV) o-toluidine (—△—), (V) m-toluidine (—◇—), (VI) p-toluidine (—▲—)]

polar-polar interactions, it is better to use the following relation to get  $\tau_j$  as:

$$\left(\frac{d\sigma'_{ij}}{dW_j}\right)_{W_j \rightarrow 0} / \left(\frac{d\sigma'_{ij}}{dW_j}\right)_{\omega_j \rightarrow 0} = 1 / \omega \tau_j$$

or  $x / y = 1 / \omega \tau_j$  ... (6)

Under hf alternating electric field, it is also observed

experimentally that  $\sigma'_{ij} \approx \sigma_{ij}$

Hence Eq. (4) becomes

$$\sigma_{ij} = \sigma_{\infty ij} + (1 / \omega \tau_j) \sigma'_{ij} \quad \dots (7)$$

$$\text{or } \beta = \frac{1}{\omega \tau_j} \left(\frac{d\sigma'_{ij}}{dW_j}\right)_{W_j \rightarrow 0} \quad \dots (8)$$

where  $\beta$  = slope of  $\sigma_{ij} - W_j$  curve at  $W_j \rightarrow 0$ ; i.e.

$$\left(\frac{d\sigma'_{ij}}{dW_j}\right)_{W_j \rightarrow 0} \text{ as presented in Table 2 for all the liquids}$$

under investigation. The real part of hf conductivity  $\sigma'_{ij}$  at  $T, K$  is related with imaginary part of dielectric constant or dielectric loss<sup>10</sup> of a given solution of  $W_j$  by

$$\sigma'_{ij} = \frac{N \rho_{ij} \mu_j^2}{27 \epsilon_0 k_B T M_j} \left(\frac{\omega^2 \tau}{1 + \omega^2 \tau^2}\right) (\epsilon_0 \kappa_{\infty ij} + 2) (\epsilon_0 \kappa_{\infty ij} + 2) W_j \quad \dots (9)$$

which on differentiation with respect to  $W_j$  and at  $W_j \rightarrow 0$  yields

$$\left(\frac{d\sigma'_{ij}}{dW_j}\right)_{W_j \rightarrow 0} = \frac{N \rho_{ij} \mu_j^2}{3 \epsilon_0 k_B T M_j} \left(\frac{\epsilon_i + 2}{3}\right)^2 \left(\frac{\omega^2 \tau}{1 + \omega^2 \tau^2}\right) \quad \dots (10)$$

Here,  $N$  = Avogadro's number,  $\rho_i$  = density of solvent,  $\epsilon_i$  = dielectric permittivity of the solvent,

$M_j$  = molecular weight of solute and  $k_B$  = Boltzmann constant. All the parameters are, however, expressed in S.I. Units. From Eqs (8) and (10) one gets hf dipole moment  $\mu_j$  from

$$\mu_j = \left(\frac{27 \epsilon_0 k_B T M_j \beta}{N \rho_i (\epsilon_i + 2)^2 \omega b}\right)^{1/2} \quad \dots (11)$$

in terms of  $b$ , which is a dimensionless parameter, given by

$$b = \frac{1}{1 + \omega^2 \tau^2} \quad \dots (12)$$

All the  $\mu_j$ 's in terms of  $\beta$ 's and  $b$ 's involved with  $\tau_j$ 's are, however, placed in Table 2, in order to compare with the static  $\mu_s$  as presented in Table 3.

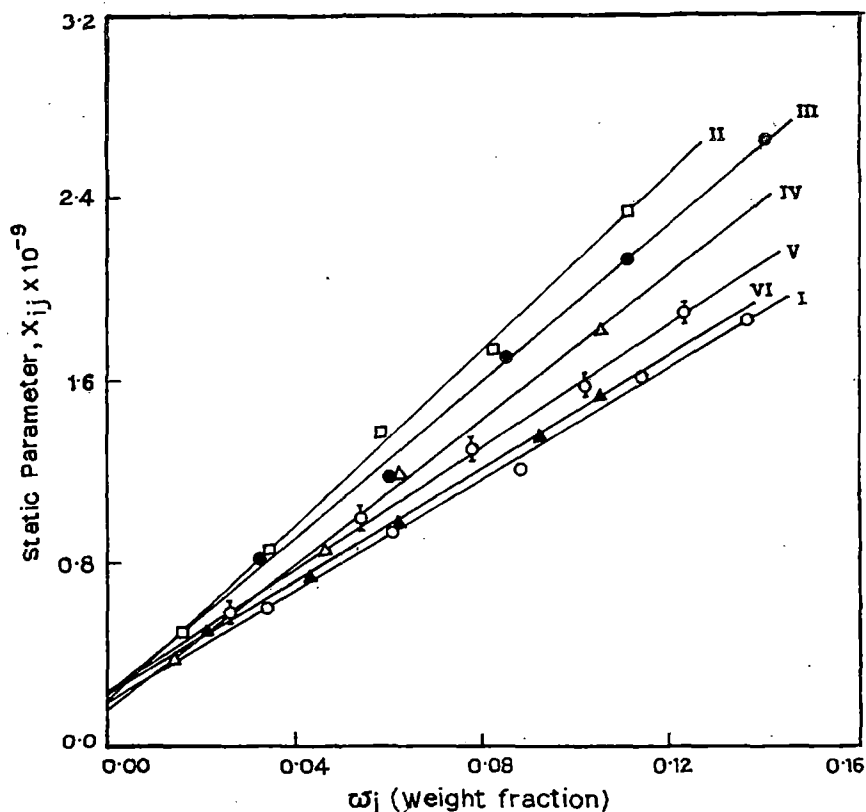


Fig. 4 — The linear variation of static experimental parameter  $X_{ij}$  for different  $W_j$ 's of anisidines and toluidines at 35°C [(I) *o*-anisidine (—○—), (II) *m*-anisidine (—□—), (III) *p*-anisidine (—●—), (IV) *O*-toluidine (—△—), (V) *m*-toluidine (—Φ—), (VI) *p*-toluidine (—▲—)]

### 3 Static Relaxation Parameters

Under static or low frequency electric field,  $\mu_s$  of a polar liquid (*j*) in a non polar solvent (*i*) may be written from Debye's equation<sup>11</sup> as

$$\frac{(\epsilon_0 \kappa_{0ij} - 1)}{(\epsilon_0 \kappa_{0ij} + 2)} - \frac{(\epsilon_0 \kappa_{\infty ij} - 1)}{(\epsilon_0 \kappa_{\infty ij} + 2)} = \frac{(\epsilon_0 \kappa_{0ij} - 1)}{(\epsilon_0 \kappa_{0i} + 2)} - \frac{(\epsilon_0 \kappa_{\infty i} - 1)}{(\epsilon_0 \kappa_{\infty i} + 2)} + \frac{N \mu_s^2}{3 \epsilon_0 k_B T} C_j \quad \dots(13)$$

where  $\kappa_{0ij} (= \epsilon_{0ij} / \epsilon_0)$  and  $\kappa_{\infty ij} (= \epsilon_{\infty ij} / \epsilon_0)$  are the dimensionless static and infinite frequency dielectric constants of solution.  $c_j$  is the molar concentration given by

$$c_j = \rho_j W_j / M_j \quad \text{and other symbols carry usual meanings}^{4,12-13}$$

A polar liquid of weight  $W_j$  and of volume  $V_j$  is mixed with a non-polar solvent of weight  $W_i$  and of volume  $V_i$  to get the solution density  $\rho_{ij}$  where

$$\rho_{ij} = \frac{\rho_i \rho_j}{\rho_j W_i + \rho_i W_j} = \rho_i (1 - \gamma W_j)^{-1} \quad \dots(14)$$

Here, weight fractions  $W_j$  and  $W_i$  of solute and solvent are given by  $W_j = \frac{W_j}{W_i + W_j}$  and  $W_i = \frac{W_i}{W_j + W_i}$ , such that  $W_i + W_j = 1$ ,  $\gamma = \left(1 - \frac{\rho_i}{\rho_j}\right)$

and  $\rho_i$  and  $\rho_j$  are densities of pure solvent and solute, respectively.

Now Eq. (13) may be written as

$$\frac{(\kappa_{0ij} - \kappa_{\infty ij})}{(\epsilon_0 \kappa_{0ij} + 2)(\epsilon_0 \kappa_{\infty ij} + 2)} = \frac{(\kappa_{0i} - \kappa_{\infty i})}{(\epsilon_0 \kappa_{0i} + 2)(\epsilon_0 \kappa_{\infty i} + 2)} + \frac{N \rho_i \mu_s^2}{9 \epsilon_0^2 M_j k_B T} W_j (1 - \gamma W_j)^{-1}$$

$$\text{or } X_{ij} = X_i + \frac{N \rho_i \mu_s^2}{9 \epsilon_0^2 M_j k_B T} W_j + \frac{N \rho_i \mu_s^2}{9 \epsilon_0^2 M_j k_B T} \gamma W_j^2 \quad \dots(15)$$

Since, the left hand side of Eq. (15) is a function of  $W_j$ , the usual variation of  $X_{ij}$  with  $W_j$  can, however, be represented by

$$X_{ij} = a_0 + a_1 W_j + a_2 W_j^2 \quad \dots(16)$$

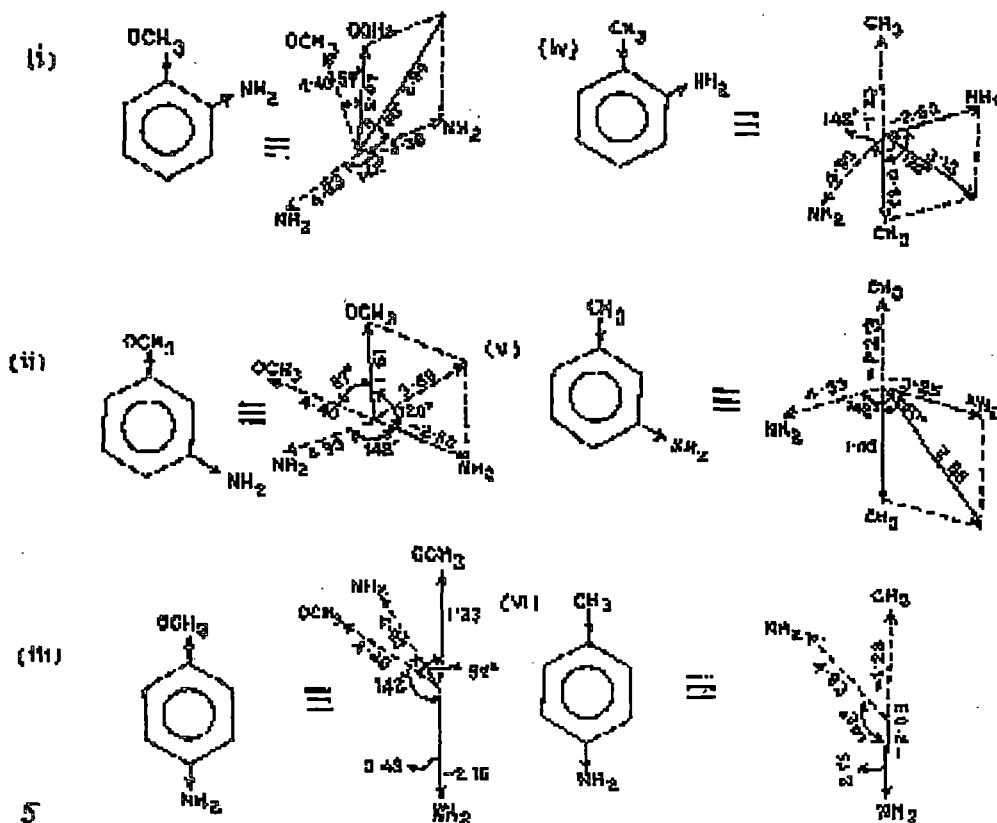


Fig. 5 — Conformational structures of Isomers of anisidine and toluidine in terms of reduced bond moments ( $\times 10^{-30}$  coulomb-metre) of their substituent groups [(I) o-anisidine], (II) m-anisidine, (III) p-anisidine, (IV) o-toluidine, (V) m-toluidine, (VI) p-toluidine]

Now, comparing the linear coefficients of  $W_j$  of Eqs (15) and (16) one gets  $\mu_s$  from

$$\mu_s = \left( \frac{9 \epsilon_0^2 M_j k_B T}{N \rho_i} \times a_1 \right)^{1/2} \quad \dots(17)$$

where  $a_1$  is the slope of  $X_{ij} - W_j$  curve. But  $\mu_s$  from higher coefficients of Eqs (15) or (16), which are involved with different factors like solvent effect, relative density effect, solute-solute associations, etc. are not reliable. The estimated  $\mu_s$  along with the slope  $a_1$  are placed in Table 3 in order to compare with hf  $\mu_j$ 's presented in Table 2.

#### 4 Results and Discussion

The hf dipole moments  $\mu_j$ 's of all the isomers of anisidines and toluidines at different  $W_j$ 's of solutes from the measured data of Table 1 are calculated in terms of slope  $\beta$  of  $\sigma_{ij} - W_j$  curve and  $\tau_j$  estimated from Eqs (5) and (6) of the methods suggested. The variation of  $\sigma_{ij}$  with  $W_j$ 's of solutes are parabolic, having almost same intercept and slope as seen in Fig.1. This is probably due to same polarity of the molecules as observed

earlier<sup>3</sup>. They also meet at a point within  $0.02 \leq W_j \leq 0.045$  indicating solute-solute (dimer) or solute-solvent (monomer) molecular associations under 9.945 GHz electric field<sup>3</sup>.  $\tau_j$ 's of polar liquids were, estimated from the linear slope of  $\sigma''_{ij} - \sigma'_{ij}$  curve<sup>5</sup> as well as the ratio of slopes of individual variations of  $\sigma''_{ij} - W_j$  and  $\sigma'_{ij} - W_j$  curves of Figs 2 and 3. Both  $\sigma''_{ij}$  and  $\sigma'_{ij}$  are functions of  $W_j$ . Their variations with  $W_j$ 's were not linear as shown in Figs 2 and 3. The latter method appears to be a significant improvement over the other<sup>5</sup>, as it eliminates polar-polar interactions at  $W_j \rightarrow 0$ . The correlation coefficients ( $r$ 's) and the % errors in measurement of  $\tau_j$ 's from Eq. (4) were calculated and presented in Table 2.  $\tau_j$ 's are found to agree well for both the methods and the % error involved in them are very low except m-toluidine, perhaps due to experimental uncertainty in the measurement of the relaxation parameters. It is interesting to note that unlike  $\sigma'_{ij} - W_j$  curve, the variation of  $\sigma''_{ij}$  with  $W_j$  is identical with  $\sigma_{ij} - W_j$  curve. This fact suggests the applicability of the approximation of  $\sigma'' \cong \sigma_{ij}$  in Eq.

(7). The plot of  $\sigma'_{ij}$  with  $W_j$  is, however, linear except p-toluidine in  $C_6H_6$  when fitted with the measured data of  $\kappa''_{ij}$  for different  $W_j$ 's of solutes under 9.945 GHz electric field as displayed in Fig. 3. This type of behaviour reveals the fact that the data presented in Table 1 are very accurate. The  $\mu_j$ 's as obtained from slope  $\beta$  of  $\sigma_{ij} - W_j$  curves of Fig. 1 and the dimensionless parameters  $b$  of Eq. (12) involved with  $\tau_j$  measured by both the methods are shown in Table 2. The excellent agreement of  $\mu_j$ 's in both cases implies that the method suggested is a correct one.

These  $\mu_j$ 's are again compared with the hf dipole moments  $\mu_2$  and  $\mu_1$  due to whole and the flexible part of the molecule attached to the parent ring as presented earlier<sup>3</sup>.  $\mu_j$ 's are found to be in agreement with  $\mu_1$  suggesting the fact that a part of the molecule is rotating under nearly 10 GHz electric field<sup>4</sup>. The gradual increase of  $\mu_j$ 's from o- to p-anisidines and from p- to o-toluidenes like  $\mu_1$  is probably due to the same polarity of the molecules as supported by the slopes ( $\beta$ 's) as observed earlier<sup>3</sup>.

The static or low frequency dipole moment  $\mu_s$  at 35°C are computed from the linear coefficients  $a_1$  of  $X_{ij} - W_j$  curves of Fig. 4. All the  $\mu_s$ 's are entered in Table 3. The variation of  $X_{ij}$  with  $W_j$  is almost linear as evident from the correlation coefficient  $r$  and % error involved in getting the coefficients  $a_0$  and  $a_1$  which are placed in Table 3. The curves are found to increase with the addition of solute and show a tendency to meet at a common point on the ordinate axis at  $W_j = 0$ . This reveals the fact that static polarisability increases with  $W_j$ 's of solute and yields static experimental parameter  $X_i$  of solvent  $C_6H_6$  for all the polar liquids under investigation at infinite dilution. This indicates the basic soundness of the method adopted here as well as the reliability of the experimental data of  $X_{ij}$  involved with  $k_{oij}$  and  $k_{\infty ij}$  of the solutions. The  $\mu_j$ 's are, however, little smaller than  $\mu_j$ 's. They are seen to increase from o- to p-anisidines and p- to o-toluidines like  $\mu_j$ 's establishing the fact that  $\mu$ 's are very little influenced by the frequency of the applied alternating electric field of GHz range.

The theoretical dipole moments  $\mu_{theo}$ 's of the polar molecules are calculated assuming their planar structures, from the vector addition of available bond moments of  $4.40 \times 10^{-30}$ ,  $1.25 \times 10^{-30}$ ,  $4.93 \times 10^{-30}$  in Coulomb-meter(C.m) for respective-  $OCH_3$ ,  $-CH_3$  and  $-NH_2$  groups, which make angles  $57^\circ$ ,  $180^\circ$  and  $142^\circ$  with the C-atoms of parent benzene ring as placed in Table 3.  $\mu_{theo}$ 's are found to differ from  $\mu_s$  probably due

to existence of inductive and mesomeric moments of the substituent polar groups arising out of difference in electron affinity of two adjacent atoms. For all the polar compounds as referred to Tables 1 - 3 are planar ones and have the property of cyclic delocalized  $\pi$ -electrons on each carbon atom of the rings. The solvent  $C_6H_6$  is also a cyclic and planar compound and has three double bonds and six p-electrons on its six carbon atoms. Hence due to their aromaticity, the resonance effect combined with inductive effect known as mesomeric effect are playing an important role among the substituent polar groups attached to the parent ring under static and hf electric field. The so called mesomeric moment is, however, caused by the permanent polarisation of different substituent groups acting as pusher or puller of electrons towards or away from p-electrons of C-atoms attached to the parent rings. Thus a special attention is to be paid to get the conformational structures of the molecules of Fig.5 by  $\mu_{cal}$  in terms of reduced bond moments by a factor  $\mu_s / \mu_{theo}$  in agreement with  $\mu_s$  to take into account of the mesomeric effects in them. Similar effects may also be observed in those molecules in the hf electric field. They are not calculated because they were found not to depend strongly on the frequency ( $f$ ) of the alternating hf electric field of 10 GHz.

## 5 Conclusions

A convenient method for the determination of  $\tau_j$  of a polar liquid from the ratio of slopes of the individual variations of imaginary  $\sigma''_{ij}$  and real  $\sigma'_{ij}$  with  $W_j$ 's of solutes in a non-polar solvent is suggested in terms of measured data to avoid polar-polar interactions. The estimated  $\tau_j$  when compared with the existing method using the slope of  $\sigma''_{ij}$  with  $\sigma'_{ij}$  for different  $W_j$ 's reveals the soundness of the method suggested.  $\tau_j$ 's are reliable and claimed to be accurate up to  $\pm 10\%$ . The computed  $\mu_j$ s ( $\pm 5\%$ ) in terms of the slopes  $\beta$ 's of  $\sigma_{ij} - W_j$  curves and  $\tau_j$ 's are found to agree with the static  $\mu_s$  excellently. The static  $\mu_s$  as calculated from  $X_{ij} - W_j$  curves are used to test the accuracies of permittivities of  $\epsilon_{oij}$  and  $\epsilon_{\infty ij}$  measured in the static or low frequency electric field. The curves of  $X_{ij}$  with  $W_j$  vary linearly and have a tendency to meet at a common point in the ordinate axis at  $W_j = 0$ , signifying the accuracy of the measured relaxation data once again. The % errors in terms of correlation coefficients  $r$ 's of  $\sigma_{ij} - W_j$  and  $X_{ij} - W_j$  curves are very easy, simple and straightforward to compute. The deviations of the static  $\mu_s$  and hf  $\mu_j$  from  $\mu_{theo}$  as obtained from the available bond moments and bond angles of the substituent polar groups attached to the parent molecule imply

the existence of mesomeric and inductive moments in the molecules. The comparison of  $\mu_j$  with  $\mu_2$  and  $\mu_1$  obtained from double relaxation method provides an important information, that under the 10GHz electric field only a part of the molecule is rotating. Thus the present method of study in terms of measured dimensionless dielectric constants of Table 1 seems to give a new insight of the molecular interactions in relaxation phenomena.

### References

- 1 Saha U, Sit S K, Basak R C & Acharyya S, *J Phys D (London)*, 27 (1994) 596.
- 2 Sit S K, Basak R C, Saha U & Acharyya S, *J Phys D (London)*, 27 (1994) 2194.
- 3 Sit S K & Acharyya S, *Indian J Pure and Appl Phys*, 34 (1996) 255.
- 4 Basak R C, Sit S K, Nandi N & Acharyya S, *Indian J Phys B*, 70 (1996) 37.
- 5 Murthy M B R, Patil R L & Deshpande D K, *Indian J Phys B*, 63 (1989) 491.
- 6 Higasi K, Koga Y & Nakamura M, *Bull Chem Soc Japan*, 44 (1971) 988.
- 7 Chandra S & Prakash J, *J Phys Soc Japan*, 35 (1973) 876.
- 8 Srivastava S C & Chandra Suresh, *Indian J Pure Appl Phys*, 13 (1975) 101.
- 9 Murphy F J & Morgan S O, *Bull Syst Tech J*, 18 (1939) 502.
- 10 Smyth CP, *Dielectric Behaviour and Structure* (McGraw-Hill, New York), 1955.
- 11 Debye P, *Polar Molecules* (Chemical Catalog, New York), 1929.
- 12 Guha A K, Acharyya S & Das D K, *Indian J Phys*, 51 A (1977) 192.
- 13 Ghosh A K, Sarkar K K & Acharyya S, *Acta Ciencia Indica*, 3 (1977) 49.

# Dielectric relaxation of aromatic para substituted derivative polar liquids from dispersion and absorption phenomena under giga hertz electric field

By

A KARMAKAR\*, U K MITRA, N GHOSH & S ACHARYYA

DEPARTMENT OF PHYSICS

RAIGANJ COLLEGE (UNIVERSITY COLLEGE)

P.O. : RAIGANJ, DIST.: UTTAR DINAJPUR

PIN CODE: 733 134 (W.B.), INDIA

## Abstract

The ratio of the linear coefficients of the fitted individual equations of  $\chi''_{ij}-w_j$  and  $\chi'_{ij}-w_j$  of some para substituted derivative polar liquid molecules in solvents dioxane and benzene, are used to get their relaxation times  $\tau_j$ 's under 10 GHz electric field at various experimental temperatures in  $^{\circ}\text{C}$ .  $\chi'_{ij}$  and  $\chi''_{ij}$  are the real and imaginary parts of the high frequency (hf) complex dielectric susceptibility  $\chi_{ij}^*$  as a function of weight fractions  $w_j$ 's of polar solutes at each experimental temperature. The measured  $\tau_j$ 's of solutes at different temperatures, by Eyring's rate process equations, yield thermodynamic energy parameters: enthalpy of activation  $\Delta H_{\tau}$ , entropy of activation  $\Delta S_{\tau}$  and free energy of activation  $\Delta F_{\tau}$ , due to dielectric relaxation to study stability and physico-chemical properties of the systems. The parameter  $\delta$  from the slope of linear variation of  $\ln \tau_j T$  with  $\ln \eta_i$  provides the information of the solvent environment around the solute molecules and also gives  $\Delta H_{\eta_i}$ , the enthalpy of activation due to viscous flow of the solvent.  $\eta_i$  is the coefficient of viscosity of the solvent used. The estimated Debye and Kalman factors  $\tau_j T / \eta$  and  $\tau_j T / \eta^{\delta}$  confirm Debye relaxation mechanism in such p-compounds. Debye-Pellat's equations are, therefore, used to obtain static as well as infinitely hf permittivities  $\epsilon_{oij}$  and  $\epsilon_{\infty ij}$  respectively to get static parameter  $X_{ij}$  where  $X_{ij}$  vs  $w_j$  equations are used to get static dipole moments  $\mu_s$ 's while the slopes  $\beta$ 's of  $\chi'_{ij}-w_j$  equations to yield hf  $\mu_j$ 's in terms of estimated  $\tau_j$ 's. They are, however, compared with the theoretical  $\mu_{theo}$ 's from the available bond moments of the substituted flexible polar groups attached to the parent molecules to show the existence of the inductive, mesomeric and often electrometric effects in them.

\*Malda Umesh Chandra Bastuhara Vidyalaya (H.S.)

P.O. & Dist. Malda, Pin code- 732101

## 1. Introduction

Both aliphatic and aromatic polar liquid molecules having substituted polar groups attached to the parent ones are often characterized by more than one relaxation times  $\tau_j$ 's corresponding to rotations of over all molecule and flexible parts attached to it. In long-chain compounds, the molecules having polar flexible parts at their ends may have multiple relaxation processes<sup>[1, 2]</sup>. It is, of course, possible to measure these  $\tau$ 's while in some cases, the average  $\tau$ 's are, however, determined since the resolution of more than two distinct dispersive regions cannot often be detected. Para-polar aromatic liquid molecules usually, attracted the attention of a large number of workers<sup>[3-5]</sup> to study their physico-chemical aspects from the dispersion and absorption phenomena.

Dhar et al<sup>[6]</sup> and Somevanshi et al<sup>[7]</sup> measured real  $\epsilon'_{ij}$  and imaginary  $\epsilon''_{ij}$  parts of hf complex relative permittivity  $\epsilon^*_{ij}$  under 10 GHz electric field, of some interesting para substituted derivative polar liquid molecules in solvent dioxane and benzene respectively in the temperature range of 17 to 40°C as collected in Table 1. p-hydroxypropiophenone, p-chloropropiophenone, p-benzyloxybenzaldehyde were available in the purest form from Aldrich Chemicals and p-acetamidobenzaldehyde from Central Drug Research Institute, Lucknow, India. The liquids dioxane, benzene, p-anisidine, p-phenitidine etc. were, however, obtained from M/S BDH. London. The liquids were purified through repeated fractional distillations. The physical constants of the solvents like density  $\rho_i$ , viscosity  $\eta_i$ , and the relative permittivity  $\epsilon_i$ , at different temperatures in °C were collected from the literature<sup>[8]</sup>.

Nowadays, the usual and conventional trend to study the dielectric relaxation phenomena of a polar liquid (DRL) is being advanced with the established symbols of dielectric terminology and parameter of hf, complex orientational susceptibility  $\chi^*_{ij}$  of which  $\chi'_{ij}$  ( $= \epsilon'_{ij} - \epsilon_{\infty ij}$ ) and  $\chi''_{ij}$  ( $= \epsilon''_{ij}$ ) are the real and the imaginary parts in S.I. units. If 1 is subtracted from  $\epsilon'_{ij}$  to get the real part  $\chi'_{ij}$  in which all operating processes result, while if infinitely hf permittivity  $\epsilon_{\infty ij}$  is subtracted from hf  $\epsilon'_{ij}$  and static  $\epsilon_{0ij}$  one gets  $\chi'_{ij}$  and  $\chi_{0ij}$  due to only orientational polarisation process,  $\chi_{0ij}$  is a real quantity.

Ghosh et al <sup>[9]</sup> recently studied all these p-compounds in terms of the complex  $hf$  conductivity  $\sigma^*_{ij}$  where <sup>[10]</sup>

$$\sigma^*_{ij} = \sigma'_{ij} + j\sigma''_{ij} = \omega\epsilon_0\epsilon'_{ij} + j\omega\epsilon_0\epsilon''_{ij} \text{ ----- (1)}$$

$\epsilon'_{ij}$  and  $\epsilon''_{ij}$  are the real and imaginary parts of the  $hf$  complex relative permittivity  $\epsilon^*_{ij}$  related by

$$\epsilon^*_{ij} = \epsilon'_{ij} - j\epsilon''_{ij} \text{ ----- (2)}$$

$j = \sqrt{-1}$  is a complex number and  $\epsilon_0 =$  permittivity of free space  $= 8.854 \times 10^{-12}$  Farad metre<sup>-1</sup>, to show that all these p-compounds obey Debye- relaxation mechanism. Both  $\sigma''_{ij}$  and  $\sigma'_{ij}$  are related by <sup>[11]</sup>

$$\sigma'_{ij} = \sigma_{aij} + \frac{1}{\omega\tau_j} \sigma''_{ij} \text{ ----- (3)}$$

$$\text{or, } \frac{d\sigma''_{ij}}{d\sigma'_{ij}} = \frac{1}{\omega\tau_j} \text{ ----- (4)}$$

$\tau_j$ 's may, therefore, be determined by the slopes of  $\sigma''_{ij}$  against  $\sigma'_{ij}$  linear curves <sup>[11]</sup>. A better representation of Eq (4) can, however, be given by

$$\left( \frac{d\sigma''_{ij}}{d\omega_j} \right)_{\omega_j \rightarrow 0} / \left( \frac{d\sigma'_{ij}}{d\omega_j} \right)_{\omega_j \rightarrow 0} = \frac{1}{\omega\tau_j} \text{ ----- (5)}$$

to eliminate polar-polar interactions in the solution when  $\omega_j \rightarrow 0$  to measure  $\tau_j$ 's by Ghosh et al <sup>[12]</sup> by the conductivity method and known  $\omega = 2\pi f$  where  $f =$  frequency of the applied electric field = 10 GHz.. Hence Debye Pellat's Eqs. <sup>[13]</sup>

$$\epsilon'_{ij} = \epsilon_{aij} + \frac{\epsilon_{0ij} - \epsilon_{aij}}{1 + \omega^2\tau_j^2} \text{ ----- (6)}$$

$$\text{and } \epsilon''_{ij} = \frac{\epsilon_{0ij} - \epsilon_{aij}}{1 + \omega^2\tau_j^2} \omega\tau_j \text{ ----- (7)}$$

can be used to obtain the concentration variation of  $\epsilon_{0ij}$  and  $\epsilon_{\infty ij}$  of any polar liquid in close agreement with the experimentally measured data within  $\pm 1\%$  error as tested. The data are placed in Table 1 together with  $\chi'_{ij} (= \epsilon'_{ij} - \epsilon_{\infty ij})$ ,  $\chi''_{ij} (= \epsilon''_{ij})$  to measure  $\tau_j$ 's and  $hf \mu_j$ 's and the static parameters  $X_{ij}$  as a function of  $w_j$ 's to get the static  $\mu_s$ 's. The estimated value of  $\mu_s$  confirms the data are much more accurate. This indicates the very soundness of the method so far suggested. Thus a faithful measurement of  $\chi'_{ij}$  and  $\chi''_{ij}$  is possible to study the relaxation phenomena where the orientational polarisation alone plays the important role. In  $\sigma_{ij}$ 's measurements, the transfer of bound molecular charges are responsible to yield  $hf \mu_j$ 's with an approximation that  $\sigma_y \approx \sigma''_y$  where  $\sigma_y$  is the total  $hf$  conductivity  $\sigma_{ij} = \omega \epsilon_0 (\epsilon''_{ij}{}^2 + \epsilon'_{ij}{}^2)^{1/2}$  as a function of  $w_j$  at each temperature.

Some sample curves of both  $\chi'_{ij}$  and  $\chi''_{ij}$  against  $w_j$ 's are shown in Figs. 1 and 2 respectively. The linear equations of  $\ln \tau_j T$  against  $1/T$  with  $\tau_j$ 's from the susceptibility measurements are shown graphically in Fig. 3 with the experimental points placed upon them. The values of intercepts and slopes are entered in the Table 3, to compute thermodynamic energy parameters like enthalpy  $\Delta H_r$ , entropy  $\Delta S_r$  and free energy  $\Delta F_r$  of activation due to dielectric relaxation from Eyring's rate process equations [14]. The enthalpy of activation  $\Delta H_\eta$  due to viscous flow was estimated from  $\Delta H_r$  and the slope  $\delta$  of the linear equations of  $\ln \tau_j T$  against  $\ln \eta_i$  where  $\eta_i$  is the coefficient of viscosity of the solvents used. The data as seen in Table 2 throw much light on the stability as well as on the physico-chemical properties of the systems. Kalman and Debye factors placed in the Table 3 reflect the applicability of Debye model of relaxation for such p-compounds [19].

The  $hf \mu_j$ 's of all the para liquid molecules due to orientational prolarisation alone were carefully worked out from the linear coefficients  $\beta$ 's of  $\chi'_{ij} - w_j$  equations and the dimensionless parameters 'b' involved with estimated  $\tau_j$ 's at different temperatures and are placed in Table 2. They are compared with the reported  $hf \mu_j$ 's, static  $\mu_s$ 's obtained from linear coefficient  $a_1$  of static  $X_{ij} - w_j$  equations, and  $\mu_{theo}$ 's from the available infrared spectroscopic data of bond moments of the substituted polar groups

attached to the parent molecules. The disagreement of measured hf  $\mu_j$  with  $\mu_{theo}$  establishes the existence of inductive and mesomeric moments which in excited state offers the electromeric effects suffered by the polar groups of the molecules under GHz electric field. The close agreement between  $\mu_j$  and  $\mu_{theo}$  is, however, achieved when the bond moments are corrected by multiplying with  $\frac{\mu_j}{\mu_{theo}}$  and  $\frac{\mu_s}{\mu_{theo}}$  respectively as required.

## 2. Theoretical formulations to measure $\tau_j$ and $\mu_j$ of a polar unit.

The real and imaginary parts of hf complex relative permittivity  $\epsilon^*_{ij}$  are related by

$$\epsilon'_{ij} = \epsilon_{\omega ij} + \frac{1}{\omega\tau_j} \epsilon''_{ij} \text{-----} (8)$$

replacing  $\epsilon'_{ij} - \epsilon_{\omega ij}$  by  $\chi'_{ij}$  and  $\epsilon''_{ij}$  by  $\chi''_{ij}$  we have

$$\begin{aligned} \chi''_{ij} &= (\omega\tau_j) \chi'_{ij} \\ \text{or } d\chi''_{ij}/d\chi'_{ij} &= (\omega\tau_j) \text{-----} (9) \end{aligned}$$

$\chi''_{ij}$  varies linearly with  $\chi'_{ij}$ . The slope of Eq. (9) which is used to measure  $\tau_j$  of a polar unit.

But for associative liquids like p-anisidine, p-phenitidine etc the variation of  $\chi''_{ij}$  with  $\chi'_{ij}$  is not strictly linear as claimed elsewhere<sup>[15]</sup>. The ratio of slopes of individual variations of  $\chi''_{ij}$  and  $\chi'_{ij}$  against  $w_j$ 's are found to be a better representation of the slope of Eq. (9) in which polar - polar interactions are supposed to be almost eliminated<sup>[16]</sup>.

$$\text{Thus } \frac{(d\chi''_{ij}/dw_j)_{w_j \rightarrow 0}}{(d\chi'_{ij}/dw_j)_{w_j \rightarrow 0}} = \omega\tau_j \text{-----} (10)$$

The imaginary part  $\chi''_{ij}$  of hf  $\chi^*_{ij}$  is<sup>[17, 18]</sup>.

$$\chi''_{ij} = \left( \frac{N\rho_{ij}\mu_j^2}{27\varepsilon_0 M_j k_B T} \right) (\varepsilon_i + 2)^2 \cdot \frac{\omega\tau_j}{1 + \omega^2\tau_j^2} w_j \quad \text{----- (11)}$$

which on differentiation w.r.t.  $w_j$  and in the limit  $w_j \rightarrow 0$  becomes :

$$\left( \frac{d\chi''_{ij}}{dw_j} \right)_{w_j \rightarrow 0} = \left( \frac{N\rho_{ij}\mu_j^2}{27\varepsilon_0 M_j k_B T} \right) (\varepsilon_i + 2)^2 \cdot \frac{\omega\tau_j}{1 + \omega^2\tau_j^2} \quad \text{----- (12)}$$

From Eqs (9) and (12) one obtains

$$\omega\tau_j \left( \frac{d\chi'_{ij}}{dw_j} \right)_{w_j \rightarrow 0} = \left( \frac{N\rho_{ij}\mu_j^2}{27\varepsilon_0 M_j k_B T} \right) \cdot \frac{\omega\tau_j}{1 + \omega^2\tau_j^2} (\varepsilon_i + 2)^2$$

which at once provides  $\mu_j$  as :

$$\mu_j = \left[ \frac{27\varepsilon_0 M_j k_B T \beta}{N\rho_i (\varepsilon_i + 2)^2 b} \right]^{\frac{1}{2}} \quad \text{----- (13)}$$

to measure *hf* dipole moments  $\mu_j$ 's in terms of  $\tau_j$ 's obtained from Eq.(10) where  $\varepsilon_0 =$  permittivity of free space  $= 8.854 \times 10^{-12}$  Farad. metre<sup>-1</sup>.

$M_j$  = molecular weight of solute in Kg

$k_B$  = Boltzmann constant  $= 1.38 \times 10^{-23}$  J mole<sup>-1</sup>K<sup>-1</sup>

$\beta$  = Linear coefficient of  $\chi'_{ij} - w_j$  curves of Fig. 1 at  $w_j \rightarrow 0$

T = temperature in Kelvin

N = Avogadro's number  $= 6.023 \times 10^{23}$

$\varepsilon_i$  = Dielectric relative permittivity of the solvent and

$b = \frac{1}{1 + \omega^2\tau_j^2}$ , a dimensionless parameter involved with estimated  $\tau_j$ 's.

Thus the Eq. (13) can be employed to measure *hf*  $\mu_j$ 's of all para-polar liquid molecules under investigation, in benzene and dioxane at different experimental

temperatures. They are presented in Table 2. The temperature variations of hf  $\mu_j$ 's are shown graphically in Fig. 4. It is evident from Fig 4 that the temperature variation  $\mu_j$ 's offers a valuable information about the structural aspects in addition to the physico chemical properties of the liquid molecules.

3. Theoretical formulation of static parameter  $X_{ij}$  to estimate static dipole moment  $\mu_s$

The static dipole moment  $\mu_s$  of a polar solute (j) in a non-polar solvent (i) at TK is given in terms of  $\epsilon_{0ij}$  and  $\epsilon_{aij}$  of Table 1, by <sup>[12, 13]</sup>

$$\frac{\epsilon_{0ij}-1}{\epsilon_{0ij}+2} - \frac{\epsilon_{aij}-1}{\epsilon_{aij}+2} = \frac{\epsilon_{0i}-1}{\epsilon_{0i}+2} - \frac{\epsilon_{ai}-1}{\epsilon_{ai}+2} + \frac{N\mu_s^2}{9\epsilon_0 k_B T} c_j \text{-----} (14)$$

The molar concentration  $c_j$  is expressed by  $w_j$  of the polar solute

$$c_j = \frac{\rho_j}{M_j} w_j$$

The weight  $W_j$  and volume  $V_j$  of a polar solute is dissolved in a non-polar solvent of weight  $W_i$  and volume  $V_i$  to have the solution density  $\rho_{ij}$  where

$$\begin{aligned} \rho_{ij} &= \frac{W_j + W_i}{V_j + V_i} = \frac{W_j + W_i}{(W_j / \rho_j) + (W_i / \rho_i)} \\ &= \frac{\rho_i \rho_j}{\rho_j w_i + \rho_i w_j} = \rho_i (1 - \gamma w_j)^{-1} \\ &= \rho_i (1 + \gamma w_j + \gamma w_j^2 + \dots) \text{-----} (15) \end{aligned}$$

The weight fractions  $w_i$  and  $w_j$  of the solvent and solute are

$$w_i = \frac{W_i}{W_i + W_j} \quad \text{and} \quad w_j = \frac{W_j}{W_i + W_j} \quad \text{respectively}$$

such that  $w_i + w_j = 1$  and  $\gamma = \left(1 - \frac{\rho_i}{\rho_j}\right)$  where  $\rho_i$  and  $\rho_j$  are the densities of pure solvent and pure solute respectively in S.I. units.

Hence Eq. (14) becomes:

$$\frac{\epsilon_{0ij} - \epsilon_{aij}}{(\epsilon_{0ij} + 2)(\epsilon_{aij} + 2)} = \frac{\epsilon_{oi} - \epsilon_{ai}}{(\epsilon_{oi} + 2)(\epsilon_{ai} + 2)} + \frac{N\rho_i\mu_s^2}{27\epsilon_0M_jk_B T} \times w_j (1 + \gamma w_j + \dots)$$

or,  $X_{ij} = X_i + \frac{N\rho_i\mu_s^2}{27\epsilon_0M_jk_B T} w_j + \frac{N\rho_i\mu_s^2}{27\epsilon_0M_jk_B T} \gamma w_j^2 + \dots$  (16)

Since  $0 < w_j \ll 1$ , the above Eq. (16) can be expressed by the polynomial equation of  $w_j$  upto the third term only like

$$X_{ij} = a_0 + a_1 w_j + a_2 w_j^2 + \dots + \dots \dots \dots (17)$$

Comparing the coefficients of first power of  $w_j$  of Eqs. (16) and (17) one gets the static  $\mu_s$  as:

$$\mu_s = \left[ \frac{27\epsilon_0M_jk_B T}{N\rho_i} a_1 \right]^{\frac{1}{2}} \dots \dots \dots (18)$$

where  $a_1$  is the linear coefficient of  $X_{ij} - w_j$  curves, a few of which are shown in Fig. 5 as for example.  $\mu_s$ 's from coefficient of higher powers of  $w_j$  of Eq. (16) are not reliable as the term  $\gamma$  is involved with various effects like solute-solute interaction, relative density, macroscopic viscosity, internal field etc. The  $\mu_s$ 's thus obtained establish the very soundness of the methods so far advanced where  $\epsilon_{0ij}$  and  $\epsilon_{aij}$  are not experimentally measured. The  $\mu_s$ 's thus estimated for the p-compounds are seen in Table 2 to compare with  $hf \mu_j$ 's from the orientational susceptibility measurements and theoretical  $\mu_{theo}$ 's from the available bond angles and bond moments of the substituted polar groups attached to the parent molecules.

#### 4. Results and Discussion

The concentration variation of  $\chi'_{ij}$  and  $\chi''_{ij}$  of all the p-compounds in solvents dioxane and benzene respectively at different experimental temperatures in  $^{\circ}\text{C}$  are collected in Table 1 to show some variations of  $\chi'_{ij}$  and  $\chi''_{ij}$  with  $w_j$ 's in Figs.1 and 2 respectively as for example. The relaxation times  $\tau_j$ 's have been measured under 3 cm wave length electric field from Eqs. (9) and(10) by using  $\chi'_{ij}$  and  $\chi''_{ij}$  of Table 1.  $\tau$ 's from Eq. (10) are presented in the Table 2 to compare with those placed in the same Table 2 recalculated from Eq.(5) by conductivity  $\sigma_{ij}$  method <sup>[9]</sup> and reported ones <sup>[6, 7]</sup>. The close agreement between all the  $\tau_j$ 's at once reflects the validity of Eq.(10) derived from the susceptibility  $\chi_{ij}$ 's measurements. Thus the method of ratio of slopes of individual variations of  $\chi'_{ij}$  and  $\chi''_{ij}$  with  $w_j$ 's in the limit  $w_j = 0$  to get  $\tau_j$  from Eq.(10) is superior one where the effects of fast polarization in addition to polar -polar interactions are reduced to a large extent <sup>[16]</sup>. Although not shown in Table 2, they were interesting to see that the direct slope of  $\chi''_{ij}$  against  $\chi'_{ij}$  gives rise to almost the same  $\tau_j$ 's with those obtained from the ratio of the individual slopes of  $\chi''_{ij}$  and  $\chi'_{ij}$  against  $w_j$ 's of Eq. (10). The  $\tau_j$ 's at all the temperatures for p-hydroxypropiofenone, p-chloropropiofenone, p-acetamidobenzaldehyde, p-benzyloxy benzaldehyde are of high values probably due to their larger molecular sizes <sup>[9]</sup> while the reverse is true for p-anisidine, p-phenitidine, o-chloroparanitroaniline and p-bromonitrobenzene. The observation indicates that  $\tau_j$ 's of all the liquids decrease with the rise of temperature in  $^{\circ}\text{C}$  for the lower values of the coefficients of viscosity <sup>[6]</sup> of solution. The variation of some  $\tau_j$ 's with  $t^{\circ}\text{C}$  of all the p-liquids were found to be (see Table 2) irregular and in disagreement with the Debye relaxation <sup>[19]</sup>. This is, however, explained on the basis of the fact that as the temperature rises the stretching of bond angles and distributions of bond moments of all the flexible polar groups attached to the parent ones lead to either symmetric or asymmetric shapes of the molecules <sup>[9]</sup>.

The process of rotation of the rotating molecular dipole requires an activation energy sufficient to overcome the energy barrier between two equilibrium positions. Eyrings rate process equation <sup>[14]</sup> can be used with the known  $\tau_j$ 's, where

$$\tau_j = \frac{A}{T} \exp(\Delta F_r / RT)$$

$$\text{or, } \ln \tau_j T = \ln A' + \frac{\Delta H_r}{RT} \text{-----} \quad (19)$$

$$\text{since } \Delta F_r = \Delta H_r - T\Delta S_r \quad \text{and } A' = Ae^{-\Delta S_r / R}$$

to measure thermodynamic energy parameters like  $\Delta F_r$ ,  $\Delta H_r$  and  $\Delta S_r$  usually known as free energy, enthalpy and entropy of activations due to dielectric relaxation processes.

The linear Eq.(19) of  $\ln \tau_j T$  against  $1/T$  having intercept and slope are presented in Table 3 together with the values of  $\Delta F_r$ ,  $\Delta H_r$  and  $\Delta S_r$  as obtained from Eq. (19). The least square fitted linear plots of  $\ln \tau_j T$  against  $1/T$  with the experimental points placed on them have been shown in Fig. 3. Some of the experimental points are found not to fall on the smooth curves of Fig. 3 due to irregular variations of  $\tau_j$ 's with temperature<sup>[9]</sup> probably due to the fact that the non spherical dipolar molecules are known to be non Debye in their relaxation behaviours. As seen in Table 3  $\Delta F_r$ 's for most of the systems are higher in comparison to  $\Delta H_r$ 's. This implies that a large number of flexible polar groups surrounding the parent molecules are rotating under GHz electric field<sup>[6]</sup>. The  $-\Delta S_r$  for all the systems except p-benzyloxybenzaldehyde and p-anisidine is due to cooperative orientations of the steric forces<sup>[20]</sup> indicating thereby that the activated states are more ordered<sup>[4,21]</sup> while the +ve  $\Delta S_r$ 's for other systems refers to the unstability of the activated states. Enthalpy of activation due to viscous flow  $\Delta H_\eta$  has been estimated from slope  $\delta$  of  $\ln \tau_j T$  with  $\ln \eta_i$  fitted linear equation and known  $\Delta H_r$  in order to place them in Table 3.  $\delta (= \Delta H_r / \Delta H_\eta)$  for all the molecules  $>0.50$  except p-hydroxypropiophenone and p-acetamidobenzaldehyde indicates the solvent environment around the solute molecules to behave as solid phase rotators<sup>[9]</sup>. Low value of  $\delta$  for systems as seen in Table 3 arises for the weak interaction of the solvent and solute<sup>[9]</sup>. Almost constant values of Debye factor  $\tau_j T / \eta_i$  rather than Kalman factor  $\tau_j T / \eta_i^\delta$  at all the temperatures for each molecule implies the applicability of Debye relaxation for such p-liquids<sup>[9,22]</sup>.

This at once prompted us to recalculate hf  $\tau_j$ 's from conductivity, measurements in the GHz range. From Eq.(3) one gets

$$\beta = \frac{1}{\omega\tau_j} \left( \frac{d\sigma'_{ij}}{dw_j} \right)_{w_j \rightarrow 0} \text{-----} (20)$$

where  $\beta$  is the slope of  $\sigma_{ij} - w_j$  curve of a polar-nonpolar liquid mixture at  $w_j \rightarrow 0$

The real part of hf complex  $\sigma_{ij}$  \* is [12, 17]

$$\text{Now } \sigma'_{ij} = \frac{N\rho_i\mu_j^2}{27M_jk_B T} (\epsilon_{ij} + 2)^2 \frac{\omega^2\tau_j}{1 + \omega^2\tau_j^2} w_j$$

$$\text{or, } \left( \frac{d\sigma'_{ij}}{dw_j} \right)_{w_j \rightarrow 0} = \frac{N\rho_i\mu_j^2}{27M_jk_B T} (\epsilon_i + 2)^2 \frac{\omega^2\tau_j}{1 + \omega^2\tau_j^2} \text{-----} (21)$$

Comparing Eqs (20) and (21) the following formula is obtained to get hf  $\mu_j$  from  $\sigma_{ij}$  in  $\Omega^{-1}m^{-1}$  which takes into account of the contribution of bound molecular charge transfer among the solute molecules

$$\mu_j = \left[ \frac{27M_jk_B T}{N\rho_i(\epsilon_i + 2)^2} \cdot \frac{\beta}{\omega b} \right]^{\frac{1}{2}} \text{-----} (22)$$

where b is a dimensionless parameter involved with  $\tau_j$ 's measured from Eq.(5). The recalculated  $\tau_j$ 's are presented in Table 2 for comparison with those measured from Eq (10) and reported ones <sup>[6,7]</sup>. Estimation of  $\tau_j$  by Eq. (5) is significant one, as it is useful to obtain  $\epsilon_{0ij}$  and  $\epsilon_{aij}$  by Debye – Pellat's equation, to have static  $\mu_s$  as entered in Table 2.  $\mu_j$ 's by susceptibility measurements are shown in Table 2 to see how far they agree with  $\mu_{theo}$ 's of the bond moments of the flexible parts as calculated in Fig. 6 and the static  $\mu_s$  from Eq. (18).  $\mu_s$ 's thus computed from  $\epsilon_{0ij}$  and  $\epsilon_{aij}$  data of Table 1 show the fact that they are very close to hf  $\mu_j$ . Thus the frequency effect is almost nil in hf  $\mu_j$ 's

obtained by susceptibility method. A comparison between hf  $\mu_j$  from Eq.(13) and (22) may, however, be interesting which is to be studied later on. The values of  $n_{Dij}^2$  ( $\approx \epsilon_{\infty ij}$ ) had been tested from the literature <sup>[8]</sup> where they were available.

$\mu_j - t$  of least square fitted curves of I, III, IV and V of p-hydroxypropiophenone, p-acetamidobenzaldehyde, p-benzyloxybenzaldehyde and p-anisidine initially increases with temperature and then attain the highest value to show maximum asymmetries at different temperatures as seen in Fig. 4.  $\mu_j$ 's of those compounds go on decreasing with temperature to attain symmetries. These curves are convex in nature showing  $\mu_j = 0$  at lower and higher temperatures due to strong symmetry attained at those temperatures <sup>[9]</sup>. The curve of VII for o-chloro-p-nitroaniline shows gradual decrease of  $\mu_j$  values with temperature. On the other hand the least square fitted curves of  $\mu_j$  against t in  $^{\circ}\text{C}$  of II, VI and VIII are concave in nature. The curve VI of p-phenitidine reaches the highest symmetry and then goes on increasing with the rise in temperature. The curve shows 0 (zero) values at lower and higher temperature, as shown by the dotted line to maintain the continuity of the curves. The above nature of  $\mu_j - t$  curves are explained by the rupture of solute-solvent (monomer) and solute-solute (dimer) associations due to stretching of bond angles and bond moments of substituted polar groups at different temperatures. [4,9].

Ghosh et al <sup>[9]</sup> obtained the  $\mu$ 's of p-compounds i.e. systems I – VIII as 8.27, 9.73, 13.12, 6.23, 6.82, 15.04, 15.93 & 8.40 each multiplied by  $10^{-30}$  in C.m. respectively. A special attention is to be paid to the contributions of the available bond moments and bond angles due to different substituent groups of parent molecules in calculating theoretical dipole moments  $\mu_{theo}$ 's. But  $\mu_{theo}$ 's as sketched elsewhere <sup>[9]</sup> are found to be slightly deviated from the measured hf  $\mu_j$ 's and  $\mu_s$ 's because of the existence of the inductive and the mesomeric moments for different flexible groups. The reduced or elongated bond moments of the substituted polar groups are calculated by multiplying the  $\mu_{theo}$ 's by the factor  $\mu_j / \mu_{theo}$  around  $20^{\circ}\text{C}$ . The results for systems I to VIII are 14.27, 7.27, 12.62, 10.22, 8.56, 29.36, 2.41 and 4.23 each multiplied by  $10^{-30}$  in C.m. respectively. They are placed in the last column of Table 2 and displayed in Fig. 6. The reduction or elongation in bond moments exhibits the presence of mesomeric, inductive and electromeric effects under static and hf electric fields.

## 5. Conclusion

Theoretical consideration in S.I units for the effective utilization of the established symbols of dielectric terminologies and parameters in terms of dielectric susceptibilities obtained from dielectric relative permittivities appears to be more topical, significant and useful one to have valuable information in the study of dispersion and absorption phenomena as they are directly linked with the molecular orientational polarisation. A convenient method is, therefore, suggested to calculate  $\tau_j$  and  $\mu_j$  under GHz electric field along with the static  $\mu_s$  in S.I units of some p-compounds. The ratio of slopes of individual variations of  $\chi''_{ij}$  and  $\chi'_{ij}$  with  $w_j$ 's is a better representation over the previous one of Murthy et al as it eliminates polar-polar interactions almost completely in a given solution. Thermodynamic energy parameters ; enthalpy  $\Delta H_\tau$ , entropy  $\Delta S_\tau$ , and free energy  $\Delta F_\tau$  of activation due to dielectric relaxation and enthalpy of activation due to viscous flow of solvent provides information about the stability or unstabilities of the states of polar-nonpolar liquid mixture in a given temperature range. The physico chemical properties could, also be studied in terms of conformations of such p-compounds. The temperature variation of measured  $\mu_j$ 's reveals that the molecules may attain either symmetric or asymmetric shapes with the rise in temperature. The slight difference between experimental  $\mu_j$ 's and theoretical  $\mu_{theo}$ 's suggests the existence of inductive, mesomeric and electromeric effects of the polar flexible groups of the molecules due to their aromaticity. Theoretical formulations, so far developed, are in S.I. units because of its unified, coherent and rationalised nature. The experimental points in some cases are slightly deviated from the least squares fitted plots indicating that the highly nonspherical polar molecules are slightly nonDebye in relaxation behaviour. However, the  $X_{ij} - w_j$  curves used to get  $\mu_s$ , can be used to test the accuracies of the measurements of static  $\epsilon_{oij}$  and hf  $\epsilon_{\omega ij}$ .

The  $X_{ij}$ 's are involved with the low and infinitely hf permittivities  $\epsilon_{oij}$  and  $\epsilon_{\omega ij}$  derived from Debye- pellat's equations in terms of measured concentration variation of  $\epsilon'_{ij}$  and  $\epsilon''_{ij}$  of polar-non polar liquid mixtures. The  $\mu_j$ 's and  $\mu_s$ 's are almost equal in some cases only to show that  $\mu_j$ 's are little affected by the applied electric field frequency. The computation of  $\tau_j$ ,  $\mu_j$  and  $\mu_s$  from  $\sigma_{ij}$ ,  $\chi_{ij}$  and  $X_{ij}$  measurements of a

polar unit in a given solvent appears to be more simple, straight forward and topical one to locate the accuracies of  $\tau_j$ ,  $\mu_j$  and  $\mu_s$  which are claimed to be accurate within 10% and 5% respectively. The calculated results appear to be of more archival values to reveal some interest in the process of dielectric relaxation. The factors of  $\mu_i / \mu_{\text{theo}}$  and  $\mu_j / \mu_{\text{theo}}$  are almost constant for all the molecules revealing the material property of the systems [23]. The correlation between the conformational structures presented in Fig. 6 of the p-compounds with the observed results enhances the scientific content and adds a new horizon to understand the existing knowledge of dielectric relaxation from dispersion and absorption phenomena.

## REFERENCES

1. Purohit, H D and Sharma, H. S. *Bull. Chem. Soc. Japan.* 50 (1977) 2606
2. Mopisk F L and Cole R H, *J Chem. Phys.* 44 (1966) 1015
3. Acharyya S, Chatterjee A K , Acharyya P and Saha I L , *Ind J Phys* 56 (1982) 291
4. Sit S K , Ghosh N, Saha U and Acharyya S , *Indian J Phys* 71B (1997) 533
5. Paul N , Sharma KP and Chattopadhyay S, *Indian J Phys* 71B (1997 ) 711
6. Dhar R L , Mathur A , Shukla JP and Saxena MC ,*Indian J Pure & Appl Phys* 11 (1973) 568
7. Somevanshi S K S, Misra S B I and Mehrotra N K , *Indian J Pure & Appl Phys* 16 (1978)57
8. *Hand Book of Chemistry and Physics'*.CRC Press 58th Edition 1977-78
9. Ghosh N, Basak R C, Sit S K and Acharyya S, *J Mol Liquids (Germany)* 85 (2000) 375
10. Murphy F J and Morgan S O , *Bell Syst Tech J* 18 (1939) 502
11. Murthy M B R , Patil R L and Deshpande D K, *Indian J Phys* 63B (1980) 491
12. Ghosh N, Karmakar A, Sit S K and Acharyya S, *Indian J Pure & Appl Phys* 38 (2000 )574
13. Debye P, *Polar Molecules (Chemical Catalogue)* 1929
14. Eyring H, Glasstone S and Laidler K J 'The Theory of Rate Process' ( Mc Graw Hill: New York) 1941
15. Dutta K, Karmakar A, Dutta L, Sit S K and Acharyya S, *Indian J Pure & Appl Phys* 40 (2002 )801
16. Ghosh N, Sit S K, Bothra A K and Acharyya S, *J Phys D : Appl Phys* 34 (2001) 379
17. Smyth C P, ' *Dielectric Behaviour and Structure* ' ( Mc Graw Hill: New York) 1955
18. Ghosh N, Sit S K, and Acharyya S , *J Mol Liquids (Germany)* 102 (2003) 29
19. Srivastava S C and Chandra S, *Indian J Pure & Appl Phys* 13 (1975) 101
20. Branin (Jr) F H and Smyth C P J, *Chem Phys* 02 (1952) 1120
21. Garg SK and Smyth CP, *J Phys Chem* 69 (1965) 1294
22. Dutta K, Sit S K and Acharyya S, *J Mol liquids* 92 (2001) 263
23. Dutta K, Karmakar A, Sit S K, and Acharyya S, *Pramana J phys* (communicated) 2004

Table 1: Concentration variation of the real and imaginary parts of dielectric permittivity  $\epsilon'_{ij}$ , static permittivity  $\epsilon_{0ij}$ , infinitely high frequency permittivity  $\epsilon_{\alpha ij}$ , real and imaginary parts of dielectric susceptibilities  $\chi'_{ij}$  and  $\chi''_{ij}$  of hf complex susceptibility  $\chi^*_{ij}$  and static experimental parameters  $X_{ij}$ , of some parapolar liquids in non polar solvents at different experimental temperatures under 10 GHz electric field

System with Sl. No.	Temp in °C	Weight fraction $w_j$	Dielectric permittivities				Dielectric susceptibilities		static experimental parameter
			$\epsilon'_{ij}$	$\epsilon''_{ij}$	$\epsilon_{0ij}$	$\epsilon_{\alpha ij}$	$\chi'_{ij}$	$\chi''_{ij}$	$X_{ij}$
1. p-hydroxy-propiofenone ( in dioxane )	17	0.0040	2.0930	0.0320	2.1316	2.0665	0.0265	0.0320	0.00388
		0.0066	2.0970	0.0420	2.1477	2.0622	0.0348	0.0420	0.00507
		0.0089	2.0980	0.0440	2.1511	2.0615	0.0365	0.0440	0.00531
		0.0107	2.0990	0.0470	2.1557	2.0601	0.0389	0.0470	0.00567
		0.0116	2.1210	0.0620	2.1958	2.0696	0.0514	0.0620	0.00739
	23	0.0040	2.1250	0.0310	2.1663	2.1018	0.0232	0.0310	0.00378
		0.0066	2.1330	0.0470	2.1957	2.0978	0.0352	0.0470	0.00570
		0.0090	2.1410	0.0590	2.2197	2.0968	0.0442	0.0590	0.00711
		0.0117	2.1560	0.0720	2.2520	2.1020	0.0540	0.0720	0.00860
	30	0.0041	2.1490	0.0360	2.2035	2.1252	0.0238	0.0360	0.00451
		0.0067	2.1550	0.0440	2.2216	2.1259	0.0291	0.0440	0.00549
		0.0091	2.1560	0.0470	2.2271	2.1249	0.0311	0.0470	0.00586
		0.0109	2.1570	0.0490	2.2312	2.1246	0.0324	0.0490	0.00610
		0.0118	2.1730	0.0710	2.2805	2.1261	0.0469	0.0710	0.00874
	37	0.0041	2.1580	0.0350	2.1896	2.1192	0.0388	0.0350	0.00408
		0.0068	2.1750	0.0440	2.2147	2.1263	0.0487	0.0440	0.00509
		0.0092	2.1780	0.0510	2.2241	2.1215	0.0565	0.0510	0.00589
		0.0110	2.1840	0.0560	2.2346	2.1220	0.0620	0.0560	0.00645
		0.0119	2.1860	0.0590	2.2393	2.1207	0.0653	0.0590	0.00679
	2. p-chloro-propiofenone ( in dioxane )	19	0.0050	2.1100	0.0280	2.1301	2.0709	0.0391	0.0280
0.0068			2.1200	0.0320	2.1429	2.0754	0.0446	0.0320	0.00400
0.0080			2.1220	0.0340	2.1464	2.0746	0.0474	0.0340	0.00425
0.0093			2.1270	0.0400	2.1557	2.0712	0.0558	0.0400	0.00499
0.0112			2.1330	0.0450	2.1653	2.0702	0.0628	0.0450	0.00561
0.0123			2.1430	0.0490	2.1781	2.0746	0.0684	0.0490	0.00608
25		0.0051	2.1230	0.0290	2.1581	2.0990	0.0240	0.0290	0.00347
		0.0069	2.1250	0.0320	2.1637	2.0986	0.0264	0.0320	0.00382
		0.0081	2.1280	0.0340	2.1692	2.0999	0.0281	0.0340	0.00405
		0.0094	2.1290	0.0390	2.1762	2.0968	0.0322	0.0390	0.00464
		0.0113	2.1340	0.0430	2.1861	2.0985	0.0355	0.0430	0.00510
		0.0124	2.1410	0.0500	2.2015	2.0997	0.0413	0.0500	0.00591
31		0.0051	2.1350	0.0290	2.1817	2.1170	0.0180	0.0290	0.00376
		0.0069	2.1380	0.0330	2.1911	2.1175	0.0205	0.0330	0.00427
		0.0082	2.1390	0.0340	2.1937	2.1179	0.0211	0.0340	0.00439
		0.0095	2.1480	0.0390	2.2108	2.1238	0.0242	0.0390	0.00501
		0.0114	2.1490	0.0410	2.2150	2.1235	0.0255	0.0410	0.00526
		0.0125	2.1510	0.0630	2.2524	2.1119	0.0391	0.0630	0.00804
37		0.0052	2.1450	0.0270	2.1574	2.0861	0.0589	0.0270	0.00419
		0.0070	2.1680	0.0290	2.1813	2.1048	0.0632	0.0290	0.00446
	0.0083	2.1730	0.0330	2.1881	2.1011	0.0719	0.0330	0.00507	
	0.0115	2.1740	0.0360	2.1905	2.0955	0.0785	0.0360	0.00553	
	0.0126	2.1790	0.0400	2.1974	2.0918	0.0872	0.0400	0.00615	

System with Sl. No.	Temp in °C	Weight fraction	Dielectric permittivities				Dielectric susceptibilities		static experimental parameter
			$w_j$	$\epsilon'_{ij}$	$\epsilon''_{ij}$	$\epsilon_{o\ ij}$	$\epsilon_{\alpha\ ij}$	$\chi'_{ij}$	$\chi''_{ij}$
3. p-acetamido benzaldehyde ( in dioxane )	17	0.0023	2.1530	0.0290	2.2024	2.1360	0.0170	0.0290	0.00382
		0.0042	2.1540	0.0380	2.2187	2.1317	0.0223	0.0380	0.00499
		0.0073	2.1600	0.0530	2.2503	2.1289	0.0311	0.0530	0.00692
		0.0078	2.1690	0.0610	2.2729	2.1332	0.0358	0.0610	0.00791
		0.0112	2.1750	0.0670	2.2891	2.1357	0.0393	0.0670	0.00865
	23	0.0023	2.1580	0.0340	2.2031	2.1324	0.0256	0.0340	0.00407
		0.0043	2.1650	0.0440	2.2233	2.1318	0.0332	0.0440	0.00524
		0.0073	2.1710	0.0480	2.2346	2.1348	0.0362	0.0480	0.00570
		0.0078	2.1740	0.0560	2.2482	2.1318	0.0422	0.0560	0.00664
		0.0113	2.1820	0.0670	2.2708	2.1315	0.0505	0.0670	0.00790
	30	0.0154	2.1840	0.0680	2.2741	2.1327	0.0513	0.0680	0.00801
		0.0074	2.1750	0.0350	2.2275	2.1517	0.0233	0.0350	0.00432
		0.0079	2.1860	0.0430	2.2505	2.1573	0.0287	0.0430	0.00527
		0.0098	2.1870	0.0530	2.2665	2.1517	0.0353	0.0530	0.00648
		0.0114	2.1950	0.0590	2.2835	2.1557	0.0393	0.0590	0.00718
37	0.0155	2.2010	0.0710	2.3075	2.1537	0.0473	0.0710	0.00860	
	0.0075	2.2110	0.0370	2.2600	2.1831	0.0279	0.0370	0.00432	
	0.0080	2.2210	0.0470	2.2832	2.1855	0.0355	0.0470	0.00545	
	0.0099	2.2320	0.0550	2.3048	2.1905	0.0415	0.0550	0.00634	
	0.0115	2.2410	0.0730	2.3377	2.1859	0.0551	0.0730	0.00836	
4. p-benzyloxy-benzaldehyde ( in dioxane )	20	0.0157	2.2420	0.0760	2.3426	2.1846	0.0574	0.0760	0.00870
		0.004	2.1450	0.027	2.1910	2.1292	0.0158	0.0270	0.00358
		0.0066	2.1500	0.029	2.1994	2.1330	0.0170	0.0290	0.00383
		0.0089	2.1520	0.031	2.2049	2.1338	0.0182	0.0310	0.00409
		0.0104	2.1530	0.035	2.2127	2.1325	0.0205	0.0350	0.00461
	25	0.0116	2.1540	0.036	2.2154	2.1329	0.0211	0.0360	0.00473
		0.0153	2.1560	0.045	2.2327	2.1296	0.0264	0.0450	0.00590
		0.0041	2.167	0.028	2.1947	2.1387	0.0283	0.0280	0.00323
		0.0067	2.172	0.034	2.2057	2.1377	0.0343	0.0340	0.00391
		0.009	2.174	0.038	2.2117	2.1357	0.0383	0.0380	0.00436
	30	0.0105	2.175	0.039	2.2136	2.1356	0.0394	0.0390	0.00448
		0.0117	2.18	0.044	2.2236	2.1356	0.0444	0.0440	0.00504
		0.0154	2.187	0.047	2.2336	2.1396	0.0474	0.0470	0.00536
		0.0041	2.1780	0.0310	2.2151	2.1521	0.0259	0.0310	0.00360
		0.0067	2.1920	0.0350	2.2339	2.1627	0.0293	0.0350	0.00404
35	0.009	2.1930	0.0390	2.2397	2.1604	0.0326	0.0390	0.00449	
	0.0106	2.1940	0.0400	2.2419	2.1606	0.0334	0.0400	0.00461	
	0.0118	2.1960	0.0440	2.2486	2.1592	0.0368	0.0440	0.00506	
	0.0155	2.2060	0.0620	2.2802	2.1542	0.0518	0.0620	0.00709	
	0.0041	2.2030	0.0320	2.2290	2.1636	0.0394	0.0320	0.00371	
5. p-anisidine ( in benzene )	20	0.0091	2.2090	0.036	2.2382	2.1647	0.0443	0.0360	0.00417
		0.0119	2.2160	0.042	2.2501	2.1643	0.0517	0.0420	0.00485
		0.0156	2.2190	0.0450	2.2556	2.1636	0.0554	0.0450	0.00519
		0.0071	2.1700	0.0300	2.1854	2.1117	0.0583	0.0300	0.00428
		0.0098	2.1900	0.0350	2.2080	2.1220	0.0680	0.0350	0.00496
	30	0.0121	2.2000	0.0400	2.2206	2.1223	0.0777	0.0400	0.00565
		0.0165	2.2000	0.0440	2.2227	2.1146	0.0854	0.0440	0.00622
		0.0198	2.2100	0.0480	2.2347	2.1168	0.0932	0.0480	0.00676
		0.0071	2.1800	0.0300	2.1919	2.1041	0.0759	0.0300	0.00510
		0.0098	2.1900	0.0350	2.2038	2.1014	0.0886	0.0350	0.00594
		0.0121	2.2000	0.0400	2.2158	2.0987	0.1013	0.0400	0.00677
		0.0165	2.2100	0.0450	2.2278	2.0961	0.1139	0.0450	0.00760
		0.0198	2.2200	0.0450	2.2378	2.1061	0.1139	0.0450	0.00757

System with SI. No.	Temp in °C	Weight fraction	Dielectric permittivities				Dielectric susceptibilities		static experimental parameter $X_{ij}$
			$w_j$	$\epsilon'_{ij}$	$\epsilon''_{ij}$	$\epsilon_{oij}$	$\epsilon_{\alpha ij}$	$\chi'_{ij}$	
5. p-anisidine ( in benzene )	40	0.0071	2.1900	0.0400	2.1997	2.0247	0.1653	0.0400	0.01035
		0.0098	2.2000	0.0420	2.2102	2.0265	0.1735	0.0420	0.01084
		0.0121	2.2100	0.0440	2.2206	2.0282	0.1818	0.0440	0.01132
		0.0165	2.2200	0.0460	2.2311	2.0299	0.1901	0.0460	0.01180
		0.0198	2.2300	0.0500	2.2421	2.0234	0.2066	0.0500	0.01281
6. p-phenitidine ( in benzene )	20	0.0132	2.3100	0.0300	2.3296	2.2642	0.0458	0.0300	0.00355
		0.0149	2.3200	0.0500	2.3527	2.2436	0.0764	0.0500	0.00591
		0.0168	2.3400	0.0700	2.3858	2.2330	0.1070	0.0700	0.00823
		0.0199	2.3800	0.0800	2.4324	2.2577	0.1223	0.0800	0.00925
		0.0231	2.3900	0.0900	2.4489	2.2525	0.1375	0.0900	0.01038
	30	0.0132	2.3200	0.0300	2.3373	2.2681	0.0519	0.0300	0.00374
		0.0149	2.3700	0.0400	2.3931	2.3008	0.0692	0.0400	0.00489
		0.0168	2.3800	0.0500	2.4089	2.2935	0.0865	0.0500	0.00610
		0.0199	2.4100	0.0600	2.4447	2.3061	0.1039	0.0600	0.00724
		0.0231	2.4100	0.0800	2.4562	2.2715	0.1385	0.0800	0.00970
40	0.0132	2.3400	0.0400	2.3604	2.2615	0.0785	0.0400	0.00532	
	0.0149	2.3400	0.0500	2.3655	2.2419	0.0981	0.0500	0.00668	
	0.0168	2.3600	0.0600	2.3906	2.2422	0.1178	0.0600	0.00796	
	0.0199	2.3900	0.0700	2.4257	2.2526	0.1374	0.0700	0.00920	
	0.0231	2.4100	0.0800	2.4508	2.2530	0.1570	0.0800	0.01045	
7. o-chloro-p-nitro aniline ( in benzene )	20	0.0251	2.0700	0.0200	2.0832	2.0398	0.0302	0.0200	0.00264
		0.0293	2.0800	0.0200	2.0932	2.0498	0.0302	0.0200	0.00262
		0.0331	2.0900	0.0300	2.1098	2.0446	0.0454	0.0300	0.00392
		0.0652	2.1000	0.0300	2.1198	2.0546	0.0454	0.0300	0.00390
		0.0851	2.1000	0.0400	2.1265	2.0395	0.0605	0.0400	0.00522
	30	0.0251	2.1000	0.0200	2.1100	2.0600	0.0400	0.0200	0.00300
		0.0293	2.1000	0.0200	2.1100	2.0600	0.0400	0.0200	0.00300
		0.0331	2.1100	0.0250	2.1225	2.0600	0.0500	0.0250	0.00373
		0.0652	2.1100	0.0250	2.1225	2.0600	0.0500	0.0250	0.00373
		0.0851	2.1200	0.0300	2.1350	2.0600	0.0600	0.0300	0.00447
40	0.0251	2.1200	0.0300	2.1344	2.0575	0.0625	0.0300	0.00459	
	0.0293	2.1200	0.0300	2.1344	2.0575	0.0625	0.0300	0.00459	
	0.0331	2.1300	0.0325	2.1456	2.0623	0.0677	0.0325	0.00495	
	0.0652	2.1300	0.0325	2.1456	2.0623	0.0677	0.0325	0.00495	
	0.0851	2.1300	0.0350	2.1468	2.0571	0.0729	0.0350	0.00533	
8. p-bromo-nitro benzene ( in benzene )	20	0.0162	2.2100	0.0263	2.2267	2.1686	0.0415	0.0263	0.00330
		0.0202	2.2313	0.0302	2.2504	2.1837	0.0476	0.0302	0.00375
		0.0342	2.2352	0.0350	2.2574	2.1801	0.0551	0.0350	0.00434
		0.0375	2.2423	0.0375	2.2661	2.1832	0.0591	0.0375	0.00464
		0.0416	2.2540	0.0400	2.2794	2.1910	0.0630	0.0400	0.00493
	30	0.0162	2.2483	0.0270	2.2634	2.2003	0.0480	0.0270	0.00353
		0.0202	2.2621	0.0320	2.2801	2.2051	0.0570	0.0320	0.00416
		0.0342	2.2670	0.0351	2.2867	2.2044	0.0625	0.0351	0.00456
		0.0375	2.2739	0.0441	2.2987	2.1953	0.0786	0.0441	0.00573
		0.0416	2.2880	0.0460	2.3138	2.2061	0.0819	0.0460	0.00594
40	0.0162	2.2756	0.0276	2.2898	2.2218	0.0538	0.0276	0.00375	
	0.0202	2.2931	0.0332	2.3101	2.2283	0.0648	0.0332	0.00449	
	0.0342	2.2982	0.0353	2.3162	2.2294	0.0688	0.0353	0.00476	
	0.0375	2.3056	0.0463	2.3293	2.2153	0.0903	0.0463	0.00625	
	0.0416	2.3220	0.0478	2.3465	2.2287	0.0933	0.0478	0.00641	

Table-2:- Measured  $\tau_i$ 's from ratio of slopes of individual variations of  $\chi''_{ii}$  and  $\chi''_{ii}$  with  $w_j$ , estimated relaxation time  $\tau_i$ , reported  $\tau_i$  all are in pico second, estimated dipole moments ( $\mu_i$ ) using  $\tau_i$  of equ. (10), estimated  $\mu_s$ , reported  $\mu_i$  and theoretical dipole moment  $\mu_{theo}$  using bond moments in Coulomb - metre of some para compounds in non-polar solvents at different experimental temperatures under 10 GHz electric field.

System with Sl.no. & molecular weight (Mj) in Kg	Temp. in °C	Measured $\tau_i$ in p-sec using eq.(10)	$\tau_i$ in p-sec by eq.(5)	Reported $\tau_i$ in p-sec	Estimated hf $\mu_i \times 10^{30}$ in C.m.	Estimated $\mu_s \times 10^{30}$ in C.m.	Reported $\mu \times 10^{30}$ in C.m.	Corrected $\mu_{theo} \times 10^{30}$ in C.m.
1. p-hydroxy propiophenone Mj = 0.150 Kg	17	19.20	19.20	-	-	-		
	23	21.21	21.21	25.40	14.28	14.65	10.20	14.27
	30	24.08	24.08	24.20		-		
	37	14.37	14.37	23.10	10.25	10.16		
2. P-chloro propiophenone Mj = 0.1685 Kg	19	11.40	11.40	20.80	5.33	5.61	9.84	7.27
	25	19.26	19.26	19.20	-	-		
	31	25.60	25.60	18.20	-	-		
	37	7.30	7.30	17.10	7.28	6.46		
3. P-acetamido benzaldehyde Mj = 0.163 Kg	17	27.10	27.10	21.80	15.96	16.07		
	23	21.09	21.09	20.80	12.62	12.60	10.37	12.62
	30	23.86	23.86	19.00	20.57	20.40		
	37	21.07	21.06	18.60	26.85	26.12		
4. P-benzyloxy benzaldehyde Mj = 0.212 Kg	20	27.13	27.12	20.00	-	-		
	25	15.77	15.77	19.40	10.22	10.34	10.63	10.22
	30	19.03	19.03	18.00	-	-		
	35	12.92	12.92	16.90	6.12	6.05		
5. P-anisidine Mj = 0.123 Kg	20	8.19	9.21	3.89	9.29	9.38	5.20	8.56
	30	6.28	10.86	3.67	12.43	12.78	10.33	
	40	3.85	11.34	3.17	4.84	4.47	8.87	
6. P-phenitidine Mj = 0.0.137 Kg	20	10.41	9.82	11.08	29.35	29.22	7.47	29.36
	30	9.19	10.17	10.63	11.06	9.55	9.27	
	40	8.10	9.91	9.95	20.32	20.26	10.47	
7. O-chloro p-nitro aniline Mj = 0.1725 Kg	20	10.52	10.52	10.57	2.41	2.33	8.13	2.41
	30	7.95	20.47	9.89	1.87	1.97	10.93	
	40	7.64	30.59	9.18	1.38	1.17	13.10	
8. P-bromo nitrobenzene Mj = 0.202 kg	20	10.10	8.40	-	4.23	4.36	-	4.23
	30	8.93	8.93	-	-	-	-	
	40	8.15	8.16	-	-	-	-	

Table-3 :The intercepts and slopes of  $\ln\tau_j T$  against  $1/T$  curves of Fig. 3, thermodynamic energy parameters like enthalpy of activation  $\Delta H\tau$  in Kilo Joule mole<sup>-1</sup>, the entropy of activation  $\Delta S\tau$  in Joule mole<sup>-1</sup> K<sup>-1</sup>, free energy of activation  $\Delta F\tau$  in Kilo Joule mole<sup>-1</sup> for dielectric relaxation process, enthalpy of activation  $\Delta H\eta$  in kilo Joule mole<sup>-1</sup> due to viscous flow,  $\delta$  as the ratio of  $\Delta H\tau$  and  $\Delta H\eta$ , kalman factor  $(\tau_j T/\eta^8)$ , Debye factor  $(\tau_j T/\eta)$  at different experimental temperatures in °C and the coefficients of  $\mu_j - t$  equations  $\mu_j = a + bt + ct^2$  of different para compounds in dioxane and benzene under 10 GHz electric field frequency.

Sample name with weight in Kg	Temp in °C	Intercept & slope of $\ln\tau_j T$ Vs $1/T$ equation		$\Delta H\tau$ in KJ mole <sup>-1</sup>	$\Delta S\tau$ in J mole <sup>-1</sup> K <sup>-1</sup>	$\Delta F\tau$ in KJ mole <sup>-1</sup>	$\gamma = (\Delta H\tau/\Delta H\eta)$	$\Delta H\eta$ in KJ mole <sup>-1</sup>	Kalman factor $(\tau_j T/\eta^8)$	Debye factor $(\tau_j T/\eta) \times 10^6$	Coefficients in the eqs $\mu_j \times 10^{30} = a + bt + ct^2$ equation		
		Intercept	slope								a	b	c
hydroxy phenone 0.150 Kg	17			5.91	-19.29	11.50			$1.40 \times 10^{-7}$	3.88			
	23	-21.33	708.00	5.91	-20.71	12.03	0.49	11.99	$1.66 \times 10^{-7}$	4.83	-0.02	1.15	-11.49
	30				-22.42	12.70			$2.06 \times 10^{-7}$	6.40			
	37				-18.74	11.72			$1.30 \times 10^{-7}$	4.52			
chloro phenone 0.1685	19			9.86	-1.59	10.33			$1.48 \times 10^{-6}$	2.40			
	25	-23.20	1182.4	9.86	-6.81	11.89	0.92	10.68	$2.81 \times 10^{-6}$	4.57	0.0875	-4.8	65.11
	31				-10.01	12.90			$4.22 \times 10^{-6}$	6.95			
	37				-0.33	9.96			$1.38 \times 10^{-6}$	2.30			
amido aldehyde 0.163 Kg	17			4.42	-27.27	12.33			$5.48 \times 10^{-8}$	5.48			
	23	-20.56	530.45	4.42	-25.66	12.02	0.30	14.92	$4.48 \times 10^{-8}$	4.80	0.0595	-2.06	35.89
	30				-27.23	12.68			$5.40 \times 10^{-8}$	6.34			
	37				-26.71	12.71			$5.09 \times 10^{-8}$	6.63			
benzyloxy aldehyde 0.212 Kg	20			28.23	53.72	12.49			$1.50 \times 10^{-3}$	5.81			
	25	-30.30	3384.2	28.23	56.49	11.39	1.84	15.32	$1.04 \times 10^{-3}$	3.74	-0.041	2.42	30.10
	30				53.21	12.10			$1.53 \times 10^{-3}$	5.06			
	35				54.79	11.35			$1.31 \times 10^{-3}$	3.94			
anisidine 0.123 Kg	20			26.25	56.96	9.56			$2.78 \times 10^4$	3.89			
	30	-30.55	3147.2	26.25	55.93	9.30	4.07	6.45	$3.24 \times 10^4$	3.39	-0.054	3.00	29.22
	40				56.98	8.42			$2.73 \times 10^4$	2.30			
tidine Mj 137 Kg	20			7.05	-10.58	10.15			$2.44 \times 10^{-5}$	4.94			
	30	-22.49	844.99	7.05	-10.62	10.26	1.11	6.37	$2.08 \times 10^{-5}$	4.96	0.1377	-8.71	148.55
	40				-10.58	10.36			$2.48 \times 10^{-5}$	4.85			
chloro p-aniline 0.1725	20			9.82	-1.22	10.17			$4.22 \times 10^{-4}$	5.00			
	30	-23.65	1177.0	9.82	-0.26	9.90	1.60	6.14	$3.85 \times 10^{-4}$	4.29	0.0002	-0.06	3.575
	40				-1.24	10.21			$4.27 \times 10^{-4}$	4.57			
bromo benzene 1.202 kg	20			5.66	-15.07	10.07			$1.95 \times 10^{-6}$	4.79			
	30	-21.96	678.44	5.66	-14.96	10.19	0.90	6.32	$1.94 \times 10^{-6}$	4.82	0.0211	-1.48	25.35
	40				-15.07	10.38			$1.95 \times 10^{-6}$	4.88			

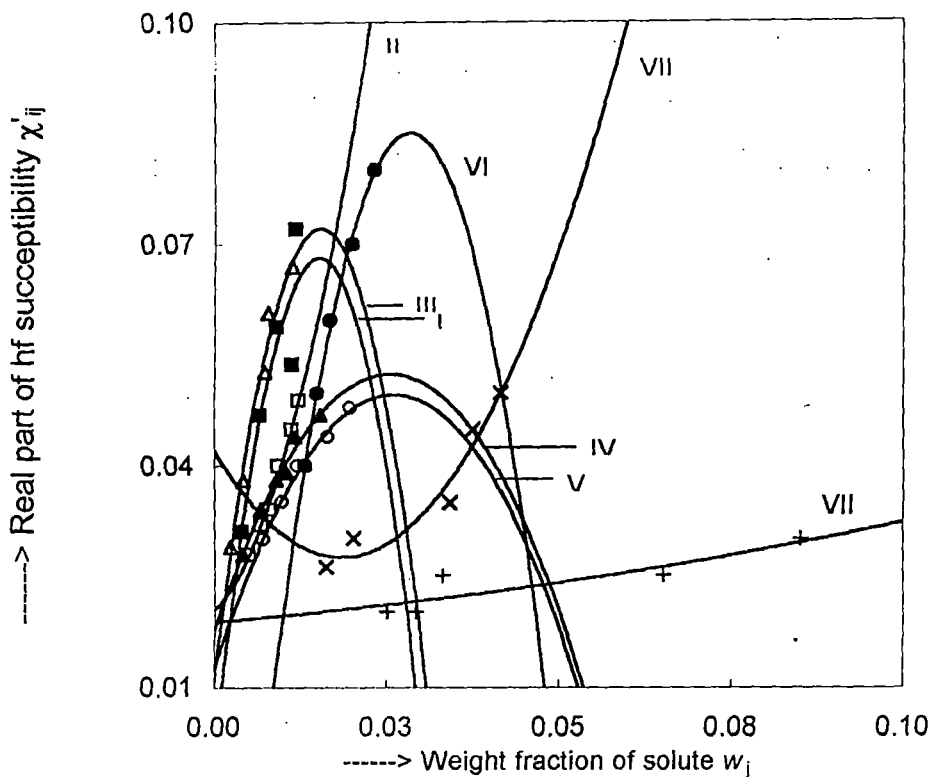


Figure-1: Variation of real part  $\chi'_{ij}$  of hf complex orientational susceptibility against weight fraction  $w_j$  of solute of some para compounds at selected temperatures in nonpolar solvents ( dioxane and benzene ) under 10 GHz electric field frequency I. p-hydroxypropiofenone (--- ■ ---) at 23<sup>o</sup>C, II. p-chloropropiofenone (--- □ ---) at 19<sup>o</sup>C, III. P-acetamidobenzaldehyde (--- Δ ---) at 17<sup>o</sup>C, IV. p-benzyloxybenzaldehyde (--- ▲ ---) at 25<sup>o</sup>C, V. p-anisidine (--- o ---) at 20<sup>o</sup>C, VI. p-phenitidine (--- • ---) at 40<sup>o</sup>C, VII. o-chloro p-nitroaniline (--- + ---) at 30<sup>o</sup>C, VIII. p-bromonitrobenzene (--- x ---) at 20<sup>o</sup>C .

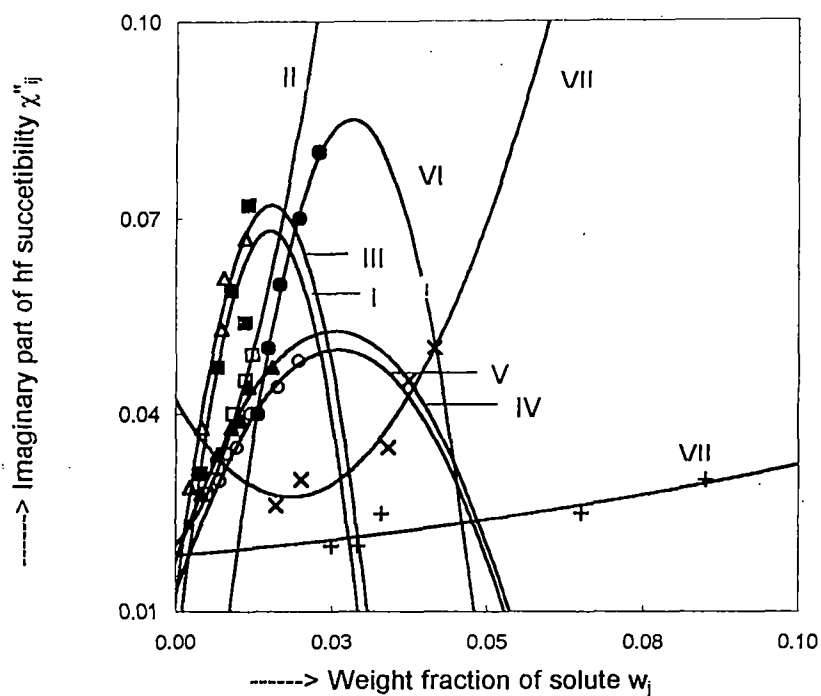


Figure.2: Variation of imaginary part  $\chi''_{ij}$  of hf complex orientational susceptibility against weight fraction  $w_j$  of solute of some para compounds at selected temperatures in nonpolar solvents (dioxane and benzene) under 10 GHz electric field frequency. I. p-hydroxypropiofenone (-- ■ --) at 23°C, II. p-chloropropiofenone (-- □ --) at 19°C, III. P-acetamidobenzaldehyde (-- Δ --) at 17°C, IV. P-benzyloxybenzaldehyde (-- ▲ --) at 25°C V. p-anisidine (-- o --) at 20°C, VI. p-phenitidine (-- ● --) at 40°C, VII. o-chloro p-nitroaniline (-- + --) at 30°C, VIII. p-bromonitrobenzene (-- x --) at 20°C

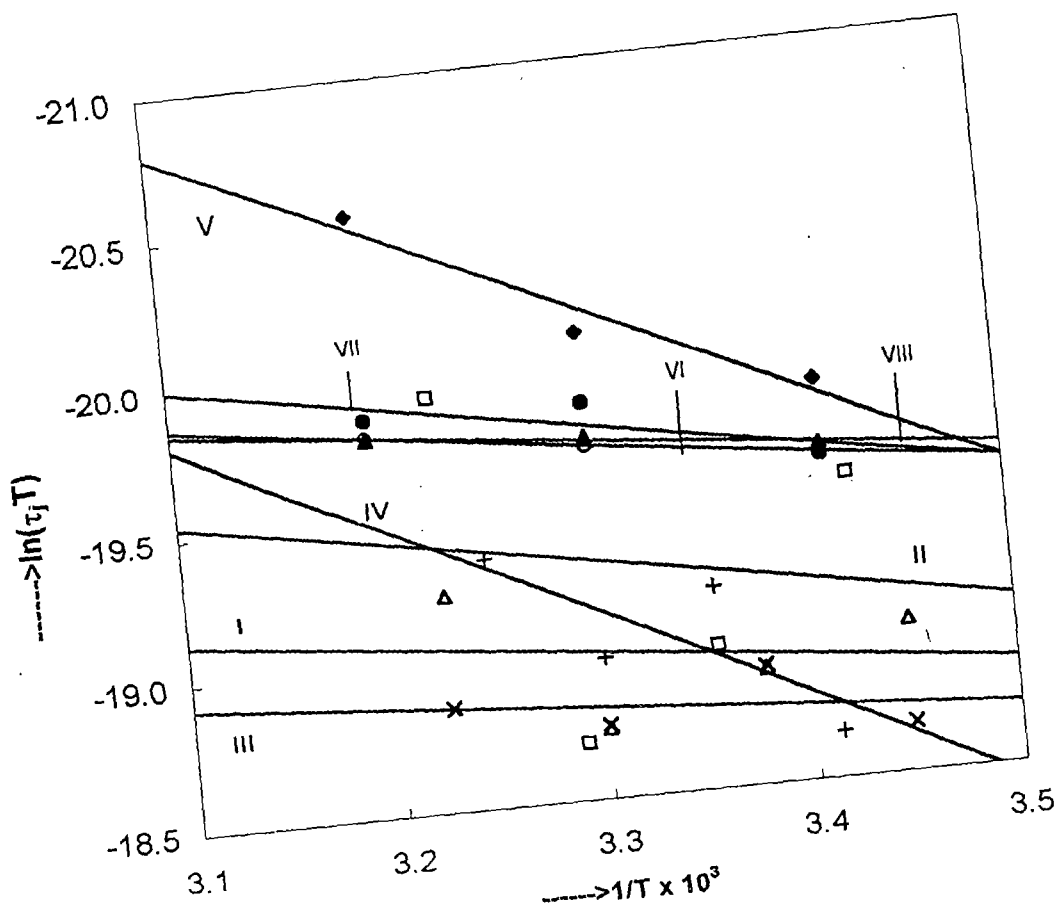


Figure 3. Straight line plots of  $\ln(\tau_j T)$  against  $1/T$  I. p-hydroxypropiophenone (-- $\Delta$ --). II. P-chloroproiohenone (-- $\square$ --). III. P-acetamidobenzaldehyde (-- $\times$ --). IV. P-benzyloxybenzaldehyde (-- $+$ --). V. P-anisidine (-- $\blacklozenge$ --). VI. P-phenitidine (-- $\circ$ --). VII. o-chloro-p-nitroaniline (-- $\bullet$ --). VIII. P-bromonitrobenzene (-- $\blacktriangle$ --).

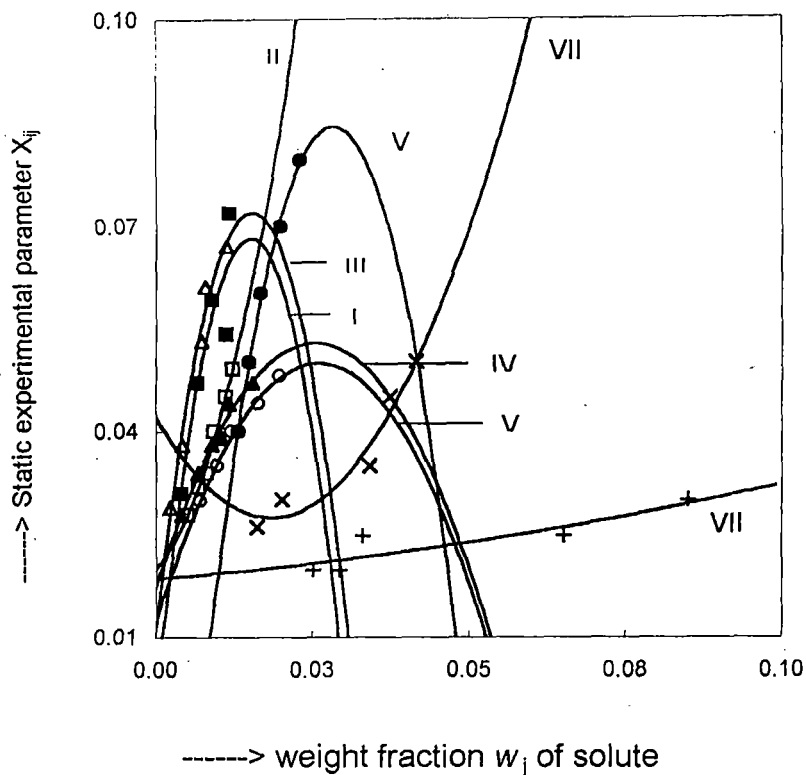


Figure 5: Variation of static experimental parameter  $X_{ij}$  against weight fraction  $w_j$  of solute of some para compounds at temperatures in nonpolar solvents (dioxane & benzene) under 10 GHz electric field frequency. I. p-hydroxypopiophenone (-- ■ --) at 23°C, II. p-chloropropiophenone (-- □ --) at 19°C, III. P-acetamidobenzaldehyde (-- Δ --) at 17°C, IV. P-benzyloxybenzaldehyde (-- ▲ --) at 5°C, V p-anisidine (-- o --) at 20°C, VI. p-phenitidine (-- ● --) at 40°C, VII. o-chloro p-nitroaniline (-- + --) at 30°C, VIII. p-bromonitrobenzene (-- x --) at 20°C

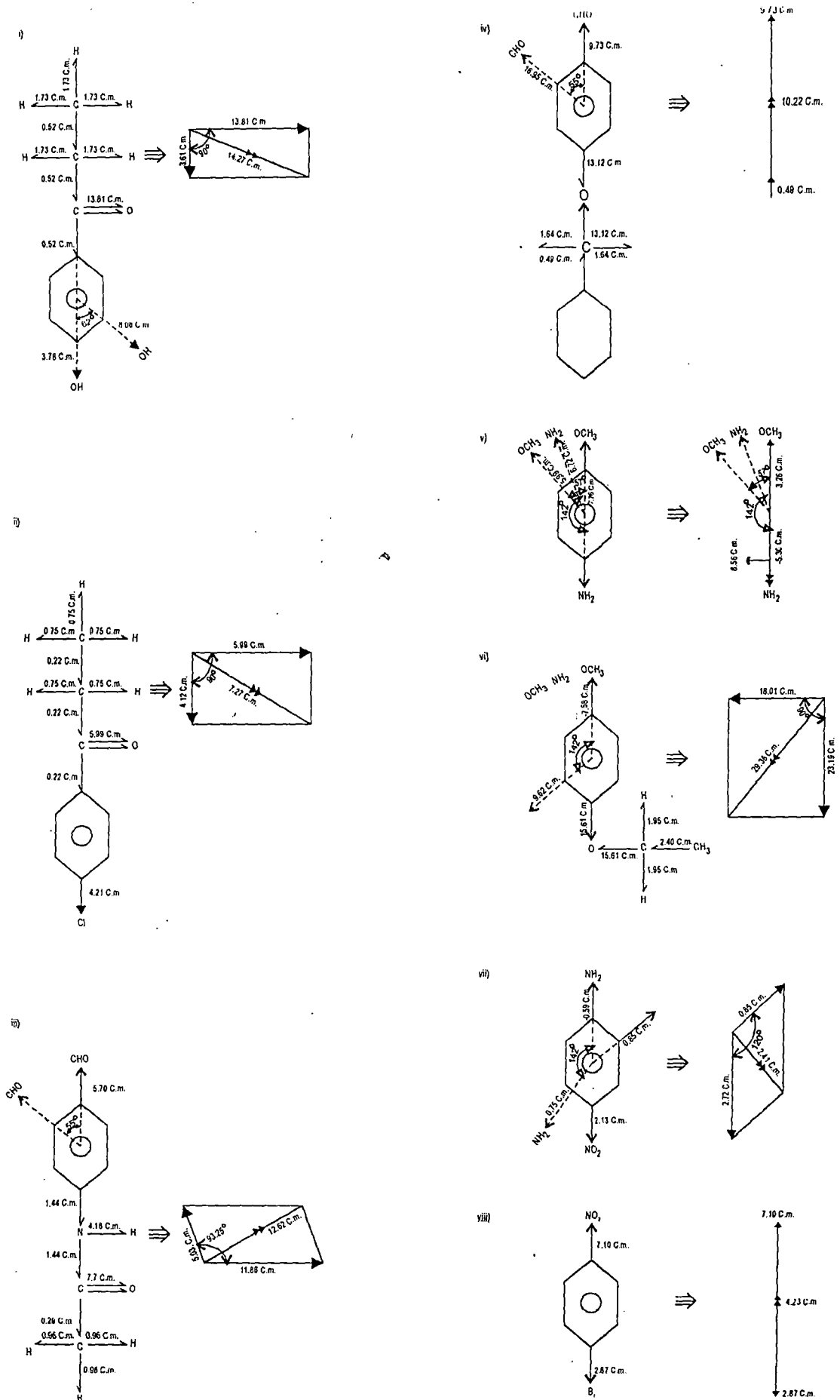


Figure 6 Confrontational structures from available bond moments and bond angles of para compounds: (i) para-hydroxypropiophenone (ii) para-chloropropiophenone (iii) para-acetamidobenzaldehyde (iv) para-benzyloxybenzaldehyde (v) para-anisidine (vi) para-phenitidine (vii) ortho-chloroparanitroaniline and (viii) para-bromonitrobenzene

INDIAN JOURNAL OF PURE & APPLIED PHYSICS  
National Institute of Science Communication & Information  
Resources

(Council of Scientific & Industrial Research)  
Dr K S Krishnan Marg, Pusa Campus, New Delhi 110012, India

---

Editor. Poonam Bhatt [poonam@niscair.res.in](mailto:poonam@niscair.res.in) [ijpap@niscair.res.in](mailto:ijpap@niscair.res.in)  
Phone: 2584301-07; Ext: 247, 321  
Fax: 91-011-25847062  
Advance contents & abstracts of the journal are available on the web <http://www.niscair.res.in>

---

Niscom-3/4(P-1480)/2007

Dated 23.4.07.

Dear Dr Acharya

Ref. Paper entitled "... Dielectric field

Enclosed please find a copy of our referee's report on the above paper. A suitably modified and condensed paper may please be communicated, in duplicate, along with the original manuscript for publication.

While submitting the revised manuscript, a note, in *duplicate*, may please be enclosed indicating which of the modification suggested by the referee have been effected and giving reasons for not complying with such suggestions of the referee which have been considered unacceptable.

The following points, non-compliance of which is likely to delay the publications of the paper, may also be attended to (items *ticked only*):

- (i) Attention may please be given to the corrections or modifications indicated in the enclosed manuscript while typing the revised manuscript.
- (ii) The title of the paper, authors' address, etc., along with the abstract may be typed in separate sheet and furnished in triplicate.
- (iii) The references list may be prepared strictly according to the style followed in the journal and may be typed on a separate sheet.
- (iv) Every effort should be made, particularly in the 'Notes' Section, to keep the number of references included in a paper to the strictly essential minimum; barring exceptional cases, it should *not exceed* 20. A block of references quoted in a reference mentioned in the paper need not be reproduced again.
- (v) Indian ink drawings of the illustrations modified as indicated in the enclosed set of illustrations may please be submitted, along with a set of Xerox copies.
- (vi) Current related papers published in the Indian Journal of Pure & Applied Physics should be included in the reference list.
- (vii) The revised paper may be returned to us within \_\_\_\_\_ months, failing which, you are liable to lose the priority of publication and your paper will only be considered as a fresh paper again.
- (viii) A copy of your revised paper should be sent in floppy form using the software MS Word Version 6, 7 or 8. It is essential, failing which I am afraid may result in enormous delay in the publication of your paper. Please ensure to send the floppy in a Floppy Mailer for its safe posting. Please follow the enclosed instruction sheet while entering the data in the floppy.

Poonam Bhatt  
Mrs Poonam Bhatt  
Editor

**Indian Journal of Pure & Applied Physics**  
**Reviewer's Report**  
**Proforma**

Title of the Paper - 3/4(P- <sup>1480</sup> )2006 "

Points for evaluation of the paper

- 1 Is the paper of sufficient scientific interest and originality in its technical content to merit publication?
- 2 If the paper is generally acceptable, are there any errors of fact, logic or interpretation which need correction(s)?
- 3 Is the paper well written and the presentation clear and concise. If not, which portion or parts including tables and figures, need deletion, recasting or condensation?
- 4 Have the authors cited the relevant literature (ii) Is there any cited document which in your opinion, is superfluous or irrelevant?
- 5 Is the abstract sufficiently informative, concise and clear?
- 6 Suggestions, if any, for improvements in the manuscripts.

In the reviewer's opinion the paper is acceptable: without any change ; with minor changes , only after major revision and reevaluation , not at all

**Detailed Specific Comments**

The above said manuscript reports the dielectric relaxation, dipole moment and thermodynamic energy parameters of some para substituted derivative polar liquids under 10 GHz measurements. The following changes must be considered after which the paper may be published as 'Short Note'

- (i) Introduction must be reduced to page length or less.
- (ii) Theoretical formulations must be deleted from page 4 to 11, because the authors have already published these expressions many times in their all earlier papers (refs). Only the references of earlier work are sufficient for the background of the theoretical formulations.
- (iii) There is no need for the data reported in Table 1. Therefore it must be removed. Further in Table 3, there is no need of the reported values of the intercepts and slopes of  $\ln\tau; T$  against  $1/T$ . Furthermore the notations in Table 3 i.e.  $\Delta H_0$  etc: must be corrected by  $\Delta H_1$ .
- (iv) Authors should remove all the Figs 1-5 of the manuscript.
- (v) Results and discussion part must be condensed. The authors should report and discuss the effect of weakly polar behaviour of dioxane solvent on the studied solutes.
- (vi) Conclusions must be set in a small size paragraph only. The total size of the rewritten manuscript should not exceed 4-5 pages. The revised and condensed paper may be accepted for publication as 'short note' for the record of the results only.